

**THE INFLUENCE OF VARIABLE DISCHARGE REGIMES ON
COLORADO RIVER SAND BARS BELOW GLEN CANYON DAM:
FINAL REPORT**

PRINCIPAL INVESTIGATORS:

Stanley S. Beus and Charles C. Avery

Northern Arizona University

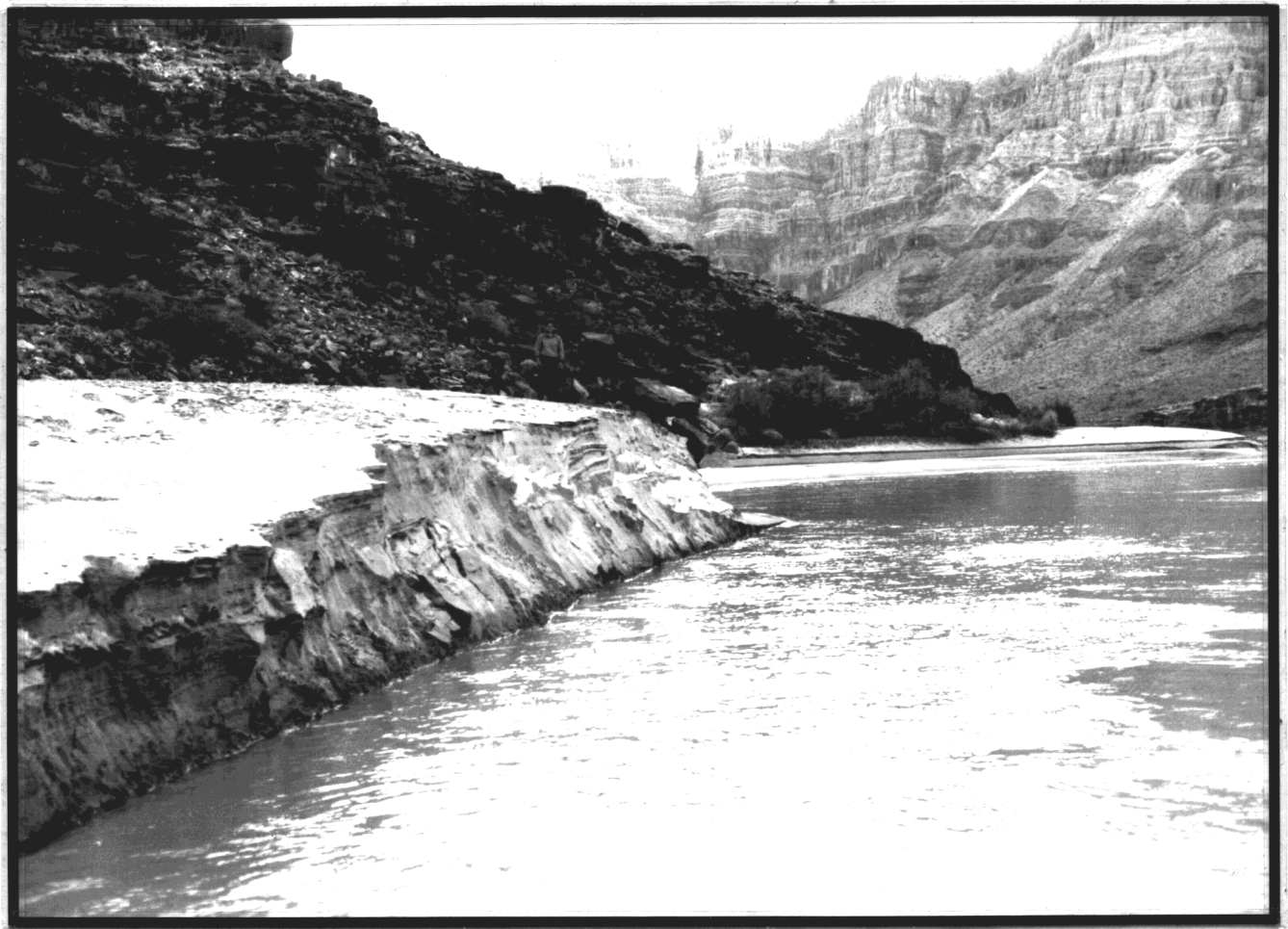


**THE INFLUENCE OF VARIABLE DISCHARGE REGIMES ON
COLORADO RIVER SAND BARS BELOW GLEN CANYON DAM:
FINAL REPORT**

PRINCIPAL INVESTIGATORS:

Stanley S. Beus and Charles C. Avery

Northern Arizona University



**THE INFLUENCE OF VARIABLE DISCHARGE REGIMES ON
COLORADO RIVER SAND BARS BELOW GLEN CANYON DAM:
FINAL REPORT**

PRINCIPAL INVESTIGATORS:

Stanley S. Beus and Charles C. Avery

Northern Arizona University

WITH CONTRIBUTIONS FROM:

**L. Stevens and B. Cluer
(NPS-RMD, Grand Canyon, Arizona)**

**M. Budhu
(Univ. Arizona Civil Engineering Dept, Tucson, AZ)**

**M.C. Carpenter, R.L. Carruth, J.B. Fink and J.K. Boling
(USGS WDR, Tucson, AZ)**

J. Schmidt (Utah State Univ., Logan, UT)

**W. Jackson, R. Inglis, Jr., L. Martin, G. Smillie, D. Tucker and W. Werrell
(NPS-WRD, Ft. Collins, CO)**

**M. Kaplinski, P. Anderson, J. Bennett, C. Brod, J. Courson,
M. Gonzales, J. Hazel, H. Mayes, F. Protiva
(Northern Arizona Univ. Geology Dept., Flagstaff, AZ)**

and

W. Vernieu and J. Korn (Bureau of Reclamation GCES, Flagstaff, AZ)

NPS Cooperative Agreement Number: CA 8006-8-0002

Government Technical representative: Dr. Peter G. Rowlands

Effective Date of Cooperative Agreement: 27 August, 1990

Cooperative Agreement Expiration Date: 1 July, 1992

**Sponsored by: The U.S. Department of Interior National Park Service Cooperative Parks Study Unit
Northern Arizona University Flagstaff, AZ 86011**

TABLE OF CONTENTS

Abstract

Chapter 1: Introduction

Chapter 2: Mechanisms of erosion and a model to predict seepage-driven erosion due to transient flow. M. Budhu.

Chapter 3: Hydrogeology of beaches 43.1L and 172.3L and the implications on flow alternatives along the Colorado River in the Grand Canyon. M.C. Carpenter, R.L. Carruth, J.B. Fink, J.K. Boling and B.L. Cluer.

Chapter 4: Beach face erosion in Grand Canyon National Park: a response to ground water seepage during fluctuating flow releases from Glen Canyon Dam. W. Werrell, R. Inglis, Jr. and L. Martin.

Chapter 5: Daily responses of Colorado River sand bars to Glen Canyon Dam test flows, Grand Canyon, Arizona. B.L. Cluer

Chapter 6: The influence of variable discharge regimes on Colorado River sand bars below Glen Canyon Dam, Arizona. S.S. Beus, C.C. Avery, L.E. Stevens, M.A. Kaplinski, H.B. Mayes and B.L. Cluer.

Chapter 7: Analysis of sand bar response along the Colorado River in Glen and Grand Canyons to test flows from Glen Canyon Dam, using aerial photography. B.L. Cluer.

Chapter 8: Historic changes in sediment deposits in Grand Canyon, 1965-1990. J.C. Schmidt, J.J. Clark, E.L. Kyle and P.E. Grams.

Chapter 9: Colorado River sand budget: Lees Ferry to Little Colorado River including Marble Canyon. G. Smillie, W.L. Jackson and D. Tucker.

Chapter 10: Summary and conclusions of the Glen Canyon Environmental Studies sand bar stability research project, Grand Canyon, Arizona. Prepared by S.S. Beus and all participants.

Glossary

Appendix I: A summary of Glen Canyon Environmental Studies test flow statistics, June 1990 through July 1991. B.L. Cluer, M.A. Kaplinski, L.E. Stevens, W. Vernieu, J. Korn.

Draft Final Administrative Report, 1990-1992. S.S. Beus, C.C. Avery, and K.A. Walters.

ABSTRACT

This study involved evaluation of the effects of 16 experimental discharge test from Glen Canyon Dam on sand bars along the Colorado River in Glen and Grand canyons, Arizona. This series of test flows was designed by the Bureau of Reclamation's Glen Canyon Environmental Studies Phase II (GCES-II) program to bracket the range of discharge parameters that comprise normal dam operations. We collected and analyzed ground-based topographic and bathymetric survey data from 33 sand bars during test flows from September, 1990 through July, 1991. These results may be useful for the GCES-II/ EIS process and for the testing of sediment transport models under development in long-term studies by the U.S. Geological Survey.

Fluctuating discharges from Glen Canyon Dam affected the geomorphology and stability of downstream sediment deposits in Glen and Grand Canyons during the GCES-II test flows. Changes in topography, volume and area occurred on sand bar faces in what we termed the "hydrologically active zone" (HAZ), lying between 142 and 900 m³/sec stage elevations. HAZ volume change rate (%VCR) and HAZ areal change rates varied on a bi-weekly basis between the 29 study sites for which sufficient data were available and between the 16 test flows. From late summer, 1990 through July, 1991, three bars (10.3%) sustained significant net losses of HAZ sand, eleven bars (37.9%) remained relatively unchanged, and 15 bars (51.7%) gained sand. The 29 sand bars under study sustained a mean aggradation of 2.9% by volume (s.e. = 2.6%) between 27 October, 1990 (the first run for which survey coverage was virtually complete) and 31 July, 1991. During that period the total 87,435 m³ of HAZ sand under study decreased by 1,034 m³ (1.2%) because several large losses occurred at a few sites, in contrast with the general condition of near-equilibrium observed on most sites.

Factors influencing sand bar stability included geomorphic setting, distance downstream, season, recreational use intensity and flow regime parameters. Although mean %VCR was approximately equal between reattachment and separation bars (mean %VCR = 0.040 and 0.037 percent/d, respectively), the standard deviation on 13 reattachment bars was 0.072 percent/d, one third greater than that of separation bars (0.054 percent/d). This finding supports the assertion that reattachment bars are less stable than separation bars. Bar instability increased with distance downstream from Glen Canyon Dam, perhaps attributable to sediment supply. Fall and winter flows in 1990-1991 were generally erosive, whereas some spring and summer flows were aggradational; however, this seasonality effect may also reflect sediment contribution by tributaries. Recreational use intensity was not significantly correlated with sand bar erosion or aggradation.

Constant and controlled low-fluctuation test flows resulted in little change or in degradation. Three of five regular, high-fluctuation flows of short duration resulted in system-wide aggradation of HAZ sand volume, while two such flows resulted in system-wide degradation. Each of the three constant flow tests resulted in stable or slight net erosion of HAZ sand volume.

Aggradational events were correlated with regular, highly fluctuating flows coupled with significant tributary sediment input. High stage levels (larger fluctuations) were required to deliver sand to higher elevations. Aggradation was observed following three of the five high-fluctuation flows ("E", "D" and normal summer in June, 1991), whereas one of the high fluctuation flows ("G" in 1991) was strongly degradational and the other ("F" in 1991) resulted in little net change. Two of the three aggradational flows occurred following significant sediment input events from tributaries; however, the normal summer, 1991 flow was not associated with sediment input. In addition, two minor aggradational flows ("Normal Fall" in 1990, and "C" in 1991) were associated with minor pulses of sediment input.

Antecedent conditions exerted an important influence over subsequent %VCR under daily fluctuating flow regimes. A significant pattern of cyclic aggradation and degradation characterized these sand bars. Periods of aggradation tended to be followed by periods of degradation, particularly when large-fluctuation flows were followed by low-fluctuation or constant flows.

INTRODUCTION

Problem Statement

Sand bars (beaches) along the Colorado River downstream of Glen Canyon Dam exist as ephemeral storage sites for (primarily) sand in transport through the Glen and Grand Canyons. Recent concern regarding the stability of sand bars under fluctuating discharges from Glen Canyon Dam prompted interest in research under the Glen Canyon Environmental Studies Phase II program (Bureau of Reclamation 1990). As part of this program, a series of test flow releases from Glen Canyon Dam was conducted from June, 1990 through July, 1991 (Figure 1; Appendix A). This preliminary report presents the results of an interagency research project designed to evaluate role of antecedent conditions, discharge parameters and seepage-driven erosion (a ubiquitous form of erosion) on sand bar stability in this system. Additional sedimentological studies are underway by the U.S. Geological Survey.

Sand bar management along the Colorado River in the Grand Canyon involves three basic concepts (Fig. 1).

1. A long-term sand balance must be maintained in the Colorado River corridor, including critical river reaches. This means that the delivery of sand to the river downstream from Glen Canyon Dam must, over the long term, equal or exceed the transport of sand out of the Grand Canyon.
2. A long-term balance must be maintained between beach erosion (the translocation of sand from beach deposits to the river channel below the low water line) and beach replenishment (the translocation of river-transported sand to sites above the elevation of normal river flows).
3. Maintenance of a natural range of geomorphic features associated with ephemeral sand margin deposits (e.g. bar platforms, backwaters, return channels) is also required.

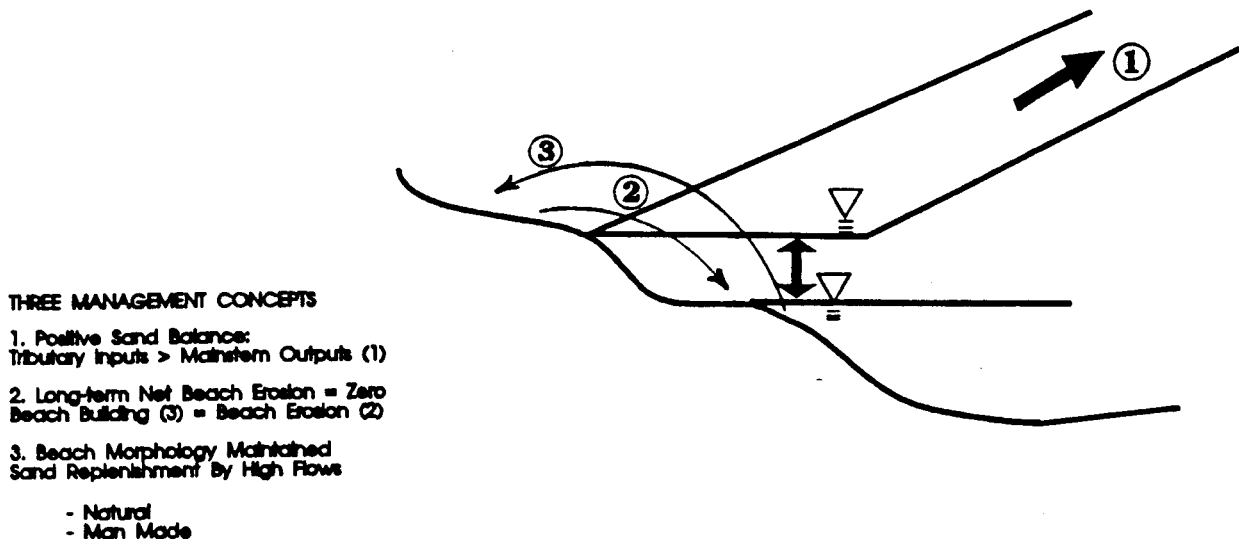


Figure 1. Sediment management in the Grand Canyon.

Although simply stated, the application of these requirements to the management of sand bars in the Grand Canyon is greatly complicated by the array of interacting processes, variables and time scales involved in the delivery, transport, storage, and erosion of sediments along through this structurally controlled river channel. The present project deals primarily with Concept No. 2, the composite erosion and replenishment of sand bars and, specifically, emphasizes the role of groundwater seepage-induced erosion of sand bars. The results of theoretical and empirical studies of seepage erosion and bank stability, sediment storage and sand bar topographic responses to variable flow regimes at different time scales, and includes a model to predict estimated sediment transport in the sediment-limited reach between the confluences of the Paria River and the Little Colorado River (Concept 1).

Background Information

Present knowledge of the stability (aggradation, degradation) of fluvial deposits in the Colorado River downstream from Glen Canyon Dam is based on sporadic profile surveys of about 30 sediment bars since 1973, and occasional aerial photography since 1965 (Howard, 1975; Howard and Dolan, 1981; Beus, et.al, 1985 et subsequ.; Zink, 1989; Schmidt and Graff, 1990; Schmidt, 1989; Schmidt, et.al., in press). These studies documented slight-to-significant instability of sediment deposits under the post-dam fluctuating flow regimes, with bar building reported under the high flows of 1983-1986, and bar erosion both prior and subsequent to that period. However, none of these studies related bar responses to the specific hydrologic conditions and associated processes which caused them. This is especially true during the post-1986 period when annual flows were overlaid by highly variable daily release patterns associated with the operation of Glen Canyon Dam. This makes it very difficult to use historic bar response to annual flows as a basis for evaluating bar response to alternative daily flow release patterns resulting from dam operations.

This project arose from the need to identify what, if any, differences in sand-bar stability result from alternative daily flow release patterns. That information is required to relate dam operations alternatives being evaluated as part of the Glen Canyon Dam EIS process to the management of beach resources in the Grand Canyon. It has been assumed, based upon the results of earlier investigations, that increases in the range and rate of daily flow fluctuations contributed to 1) increased sediment transport, and 2) increased beach erosion due to the seepage of ground water from beach faces (USDI Bureau of Reclamation 1990; Howard and McLane, 1988). However, neither of these assumptions had been effectively demonstrated or quantified in the field during periods of normal (low and fluctuating) daily dam operations. Implementation in 1990, by the Bureau of Reclamation, of a series of alternative research releases from Glen Canyon Dam provided an opportunity to evaluate short-term composite beach response to alternative daily discharge patterns. It also provided an opportunity to investigate the causative processes of beach instability, including seepage-induced erosion. Other investigations conducted as part of the GCES-II Program are investigating other aspects of the sediment management issue, including main-stem sediment transport and sedimentation processes (especially sediment deposition) in recirculation zones.

Objectives

The objective of this project was to evaluate how alternative discharge regimes affect the stability of sand bars (beaches) along the Colorado River downstream from Glen canyon Dam.

The following project tasks were identified:

1. Prepare a site-specific model of the response of beach ground water to fluctuating river stage, and of beach erosion resulting from ground water seepage from saturated beach faces.
2. Quantify the effects of alternative daily flow regimes on sand-bar stability (composite aggradation and erosion).
3. Monitor intensively a sub-set of sand bars to a) develop continuous river stage and ground water table profiles, b) monitor daily erosion, and 3) monitor major failure events.
4. Document, using existing data, the effects of past dam operations on beach distribution and rates of change in beach volume.
5. To the extent possible, assess the effects of alternative dam operations on sand bar stability for management decision making.

Project Design

This study was conducted under the auspices of the National Park Service Cooperative Studies Unit, Flagstaff, Arizona, as part of the Bureau of Reclamation's Glen Canyon Environmental Studies (GCES) Phase II program. This multi-institutional project involved researchers from Northern Arizona University Department of Geology and School of Forestry, the University of Arizona Civil Engineering Department, the National Park Service at Grand Canyon and the Water Resources Division in Ft. Collins, the U.S. Geological Survey Office in Tucson, Arizona, and the Bureau of Reclamation Glen Canyon Environmental Studies Office in Flagstaff, Arizona.

The composite response of sand bars to alternative river discharge regimes was investigated using several approaches (Fig. 2). The investigation of seepage-induced beach erosion is keyed to the development and application of a finite element ground water seepage and sand bar slope failure model.

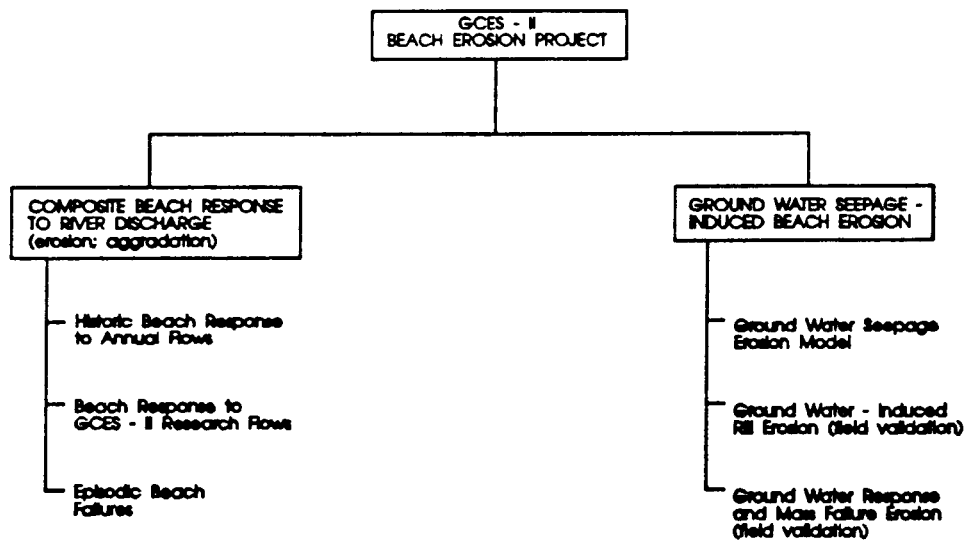


Figure 2. The major research components of the GCES Phase II Cooperative Beach Erosion Project.

The model was developed from basic theory and was calibrated to Grand Canyon beaches based upon a series of detailed studies at three "validation sites" (Colorado River miles -6.5R, 43.1L and 172.1L). Validation studies involved intensive data collection and synthesis during the research flow period, using concurrent data sets of river stage, ground water table response/dynamics, and sand bar face erosion. The validated model permitted a relative comparison of the effects of alternative daily flow patterns on beach erosion rates as caused by the ground water seepage process.

Short-term studies of bank bank movement and seepage erosion provided support for seepage erosion processes and erosion rate estimates. Daily rates of change under fluctuating flow regimes were examined at the Mile 43 site. Detailed topographic changes were monitored on a daily basis and experimental methods were used to reduce rilling erosion. Seven sand bars (including two of the validation sites) were intensively monitored using terrestrial photogrammetry to identify the occurrence of episodic beach failures in relation to daily flow patterns. Daily topographic surveys were conducted at the Mile 45 site under fluctuating and constant discharge regimes.

Medium-term sand bar responses to variable discharge regimes were also studied. Thirty-three characteristic sand bars were surveyed following each of the Glen Canyon Environmental Studies Phase II (GCES-II) research test flows program (Figure 3; Appendix I). This assessment permitted a description of bi-weekly sand bar responses to alternative daily flow release prescriptions. A preliminary aerial photogrammetric study was performed on aerial images of ten sand bars captured immediately after each of the GCES test flows. These results were compared with those of the ground topographic study.

Data from previous sand bar topographic surveys and available photography were reviewed, and the annual or multi-annual responses of sand bars to periods of different flows were evaluated during the post-dam period. Long-term changes in sediment storage and sand bar area were evaluated for the post-dam (post-1963) period. Data from previously conducted sand bar topographic surveys and all available aerial photography were reviewed. The responses of sand bars and sediment storage were then compared with periods with different flow characteristics, including the 1965-1980 reservoir filling phase, the 1983-1986 spillover flooding phase, and the 1987-1990 post-flooding phase.

A synthesis of the conclusions from all studies is presented in relation to the on-going Glen Canyon Dam Environmental Impact Statement.

Since other processes such as wave erosion, tractive-based sand transport, and main channel and eddy zone storage dynamics also influence the responses of sand bars to river discharge, it is beyond the scope of this project to develop a comprehensive, process-based model of composite beach response to alternative flow regimes. However, important insights into the dynamics of beach sand storage during the GCES-II research flow period are provided, and the seepage-induced erosion process is described and modeled. It is intended that when combined with the results of other GCES-II studies, specifically those investigating main-channel sediment transport and recirculation zone sediment dynamics, the composite effects of alternative flows on beaches can be better predicted from the basis of sediment transport and erosion theory.

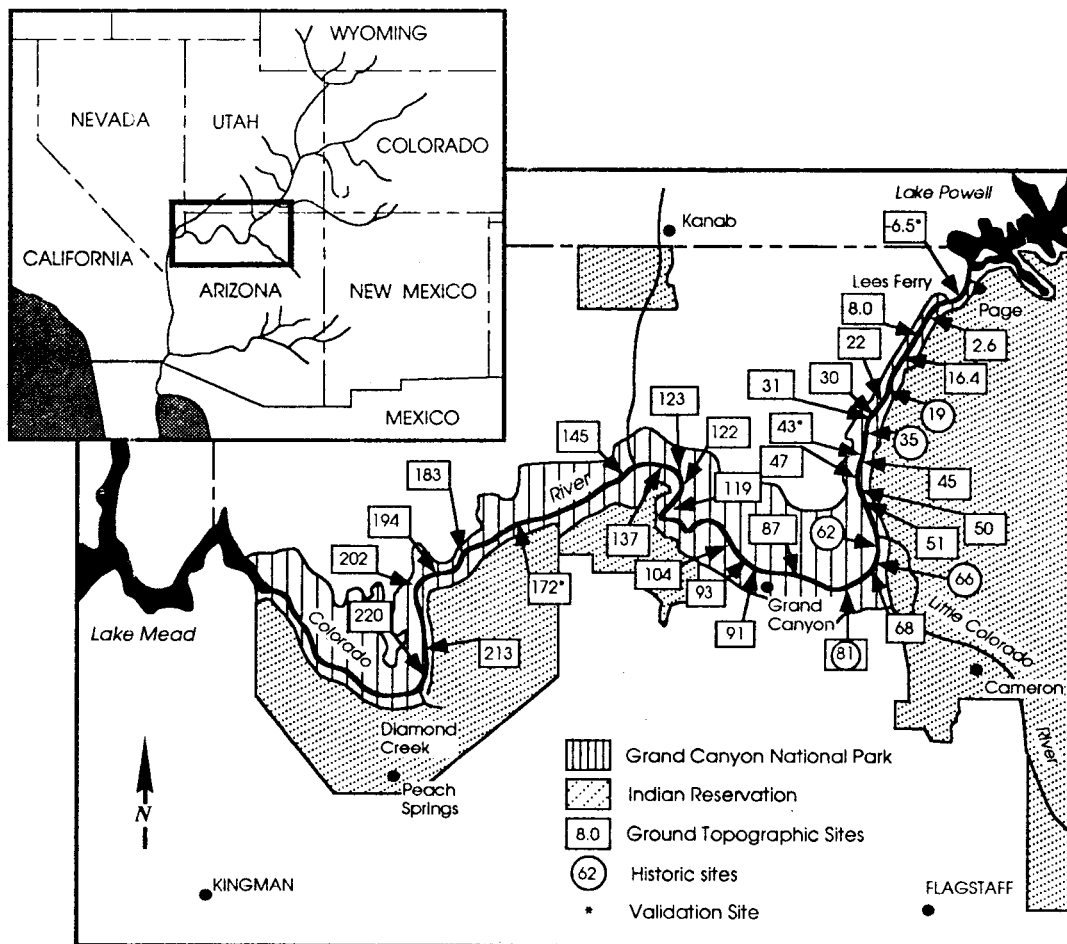


Figure 3. Map of the ground topography, daily photography, historic and groundwater study sites used in the Glen Canyon Environmental Studies sand bar stability research project, Glen and Grand Canyons, Arizona.

Report Organization

This report contains four main components. This chapter introduces the research problem, project objectives, and overall project design. Preliminary research reports are presented in Chapters 2-9 in which the individual research component results are presented objectively. Chapter 10 provides an integrated assessment written by the Project Team regarding patterns identified to date and the extent to which the information developed can be used to evaluate the effects of management alternatives on sand bar stability. Appendix A provides information on the hydrologic regimes implemented as part of the GCES-II Research Flow Program, while appendices provide background information for the various individual studies.

CHAPTER 2

**MECHANISMS OF EROSION AND A MODEL TO PREDICT
SEEPAGE-DRIVEN EROSION DUE TO TRANSIENT FLOW**

**Muniram Budhu
Department of Civil Engineering and Engineering Mechanics
University of Arizona
Tucson, Arizona 85721**

ABSTRACT

The erosion process in the Colorado River downstream from the Glen Canyon Dam comprises three interrelated mechanisms- seepage, traction and wave induced. Under certain hydraulic conditions, one of these mechanisms is predominant at a given sand bar. For most of the sand bars in this study, the dominant erosion mechanism is due to seepage. Seepage driven erosion is responsible for rilling, formation of rivulets, slope failures (bank cuts, mass wasting), piping and tunneling.

A seepage driven finite element model embracing Biot's coupled stress- pore water pressure theory was developed to predict ground water level variations and seepage erosion. The model predictions match the measured ground water level variations and the seepage driven erosion process extremely well. A ground water model using the boundary element method was also developed. The ground water level predictions from this model are also in good agreement with the measured values.

The results from the model show that fast up ramping rates followed by a period of constant peak discharge or slow up ramping rates enable a greater amount of water to be stored in the sand bars than fast up ramping rates. Consequently, to reduce seepage driven erosion under these conditions, a slow down ramping rate is desirable.

For the test site sand bars below the Glen Canyon Dam, there is an equilibrium slope between 11° and 13° in the hydraulically active zone below which slope failures (mass wasting, bank cuts) are unlikely to occur. However, this equilibrium slope is not static but dynamic and depends on the soil type and the local hydraulic conditions. The sediments enclosed by the equilibrium slope and the maximum slope angle (which is between 26° and 30°) will be in a state of flux undergoing aggradation and erosion. Whenever the hydraulic and hydrologic conditions are favorable for accretion, any sediment deposition with a slope angle greater than the equilibrium slope is likely to be eroded by seepage, especially mass wasting, under fluctuating flows.

Interpretation of the field data using the model indicates that any change in dam operation will result in the sand bars acquiring new equilibrium positions. Seepage driven erosion of transient sediments will continue to occur for any dam operation that involves fluctuating discharge in which the down ramping rate is higher than the rate at which the bank stored water can exit the sand bar.

INTRODUCTION

Erosion is an unstoppable process of nature. Wind, water, ice, chemicals, etc. are all agents of this natural process. The banks and bottoms of rivers and streams are continuously scoured by water and ice through tractive, wave, friction and seepage forces. The paths of rivers and streams are then dictated by the immense erosive power of flowing water. The Grand Canyon is a testament to this immense power. Before the construction of Glen Canyon Dam, the Colorado River was laden with sediments; depositing some and gaining some throughout its course. Now, sediments are trapped upstream of the dam in Lake Powell. The water downstream of the dam, though diminished in flood transport capacity, is clear- almost devoid of sediments- with its full (remaining) power for erosion and sediment transport.

Unlike coal fired plants, hydroelectric dams can produce electricity on demand. The discharge from the Glen Canyon Dam then fluctuates depending on the electrical demands of some Western States. Typical fluctuation, on a diurnal basis, is between one to three meters with some narrow river sections reaching four meters. The ground water level in the sand bars then varies according to the transient river stage. Water enters the sand bar during rising river stages and exits when the river stage drops.

PROBLEM STATEMENT

The fluctuating discharge from the Glen Canyon Dam is thought by environmentalists to accelerate the erosion of sand bars. Several questions have arisen about the current operation of the Glen Canyon Dam and its link to the erosion of sand bars. The questions that appear to be technically important to this part of the research effort are:

- (1) What are the mechanisms of erosion in the Colorado River downstream of the Glen Canyon Dam?
- (2) Does current operation of the dam accelerate erosion rates?
- (3) Are there alternative dam discharge regimes that can reduce erosion rates?

OBJECTIVES

The objectives of this study are

- (1) to identify the predominant mechanism(s) of erosion due to current dam operation,
- (2) to develop an analytical/ numerical technique to model the identified mechanism(s),
- (3) to calibrate the analytical/numerical model using data gathered from three test sites under the 'research flows',
- (4) to predict the erosion of a representative sand bar profile for alternative dam discharge regimes.

SCOPE

In this part of the overall project effort, only one mechanism, that of seepage driven erosion, will be studied in detail. However, with some additional work, the algorithm developed here could be used for tractive and wave induced erosion. This study does not involve sediment transport.

EROSION MECHANISMS

Three mechanisms, seepage, traction and wave induced, have been identified as the cause of the erosion of sand bars along the Colorado River below the Glen Canyon Dam. The sequence of events attributed to each of these mechanisms are described below.

Seepage Driven Erosion

The literature is very rich in observations and terms to describe seepage related erosion phenomena. Howard and McLane (1988) summarized many of these early observations and theories concerning the geomorphical changes in river banks, and presented some laboratory evidence of erosion due to seepage stresses. They developed a fluvial transport model and described the physical process of seepage transport of cohesionless materials using the theories developed by geotechnical engineers. They did not consider the combined mechanics of seepage and slope failures. Hagerty (1991a,b) documented several cases where seepage was primarily responsible for river bank erosion and insisted on the need for hydraulic engineers to recognize the importance of 'piping/sapping erosion'.

Some terms that are used to describe erosion by seepage of ground water include artesian sapping, spring sapping, seepage driven erosion, rilling, tunnel scour, seepage-induced transport and seepage weathering. We will use the term seepage erosion as a generalization of the above seepage related phenomena. The mechanics of each of these phenomena may be different. We will differentiate these wherever necessary in this report.

Seepage driven erosion was observed in most of the sand bars downstream of the Glen Canyon Dam. When the river stage falls at a rate greater than the permeability of the soil, the volume of water stored during the rising stage must drain from the bank. The exit hydraulic gradient (i) may become greater than the critical hydraulic gradient [$i_{cr} = (G - 1)/(1 + e)$ where G is the specific gravity and e is the void ratio of the soil] during the falling river stage. The soil fluidizes (quicksand condition) and is then carried in suspension by the outflow of water (Fig. 1). Rivulets and gullies (rilling process) are formed below the exit point along the sand bar as the bank stored water with its sediments rushes down slope towards the river. These rivulets and gullies are scoured deeper as the water picks up sediments along its path to the river. Typical examples of these are shown in Figs. 2 and 3.

Within the river bank deposits and before the exit points, the extrusion of sediments can form tunnels whose walls are supported by the arching action of the sand. These walls can easily collapse or cave in as the tunnel becomes deeper destroying the arching action and/or adjoining erosion segments encroach on one another. During rising river stage, the increase in pore water pressures reduces the shear strength of the soil and the tunnel walls or the free standing walls between rivulets or gullies can collapse with some of the soil carried away with the flow. Typical examples of tunnel formation and subsequent collapse are shown in Figs. 4 and 5.

The permeability and porosity (or void ratio) of the soil are key factors in determining the extent of seepage driven erosion. For soils with low permeabilities, for example, the silty sand on some sand bars along the Colorado River, the water accumulated during the rising river stage cannot drain sufficiently fast. The resulting pore water pressures reduce the shear strength of the soils so that slope failures under undrained conditions occur. A typical example of this is shown in Fig. 6. The mass of material involved in the catastrophic undrained failure of sand bar slopes is often very large - several hundred tons. A substantial area of the sand bar can be lost in a few seconds. On occasions, incipient undrained slope failures may occur during the down ramping river stage. That is, the failure plane develops, but for complete failure a further reduction (by a very small amount) in shear strength is required. The next rising river stage could then easily precipitate complete failure because the shear strength of the soil mass is now reduced by the increase in pore water pressure. It is quite easy to confuse this seepage related failure to a tractive force induced failure or the failure is categorized as caused by a rising river stage. The condition that is predominant in provoking such failures is a rapid, high down ramping stage followed by a constant low stage over a day or more.

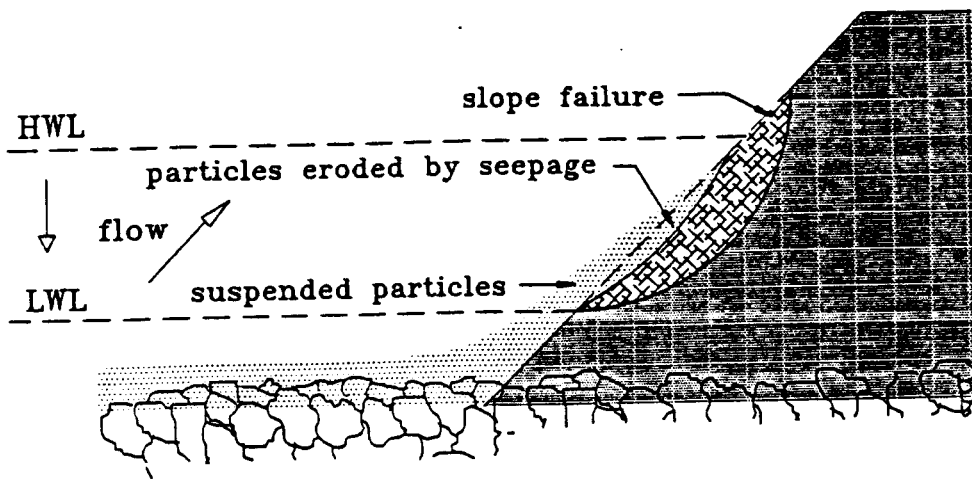


Fig. 1 Mechanism of seepage driven erosion.

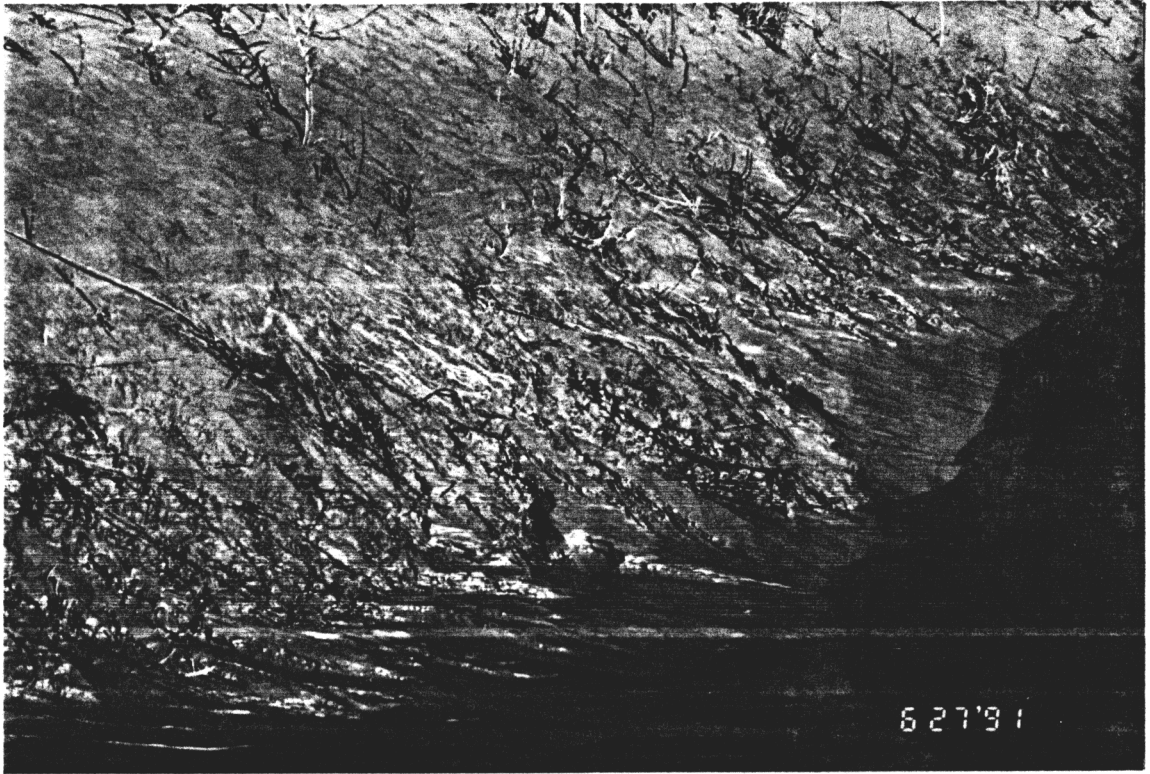


Fig. 2 Rilling due to ground water seepage

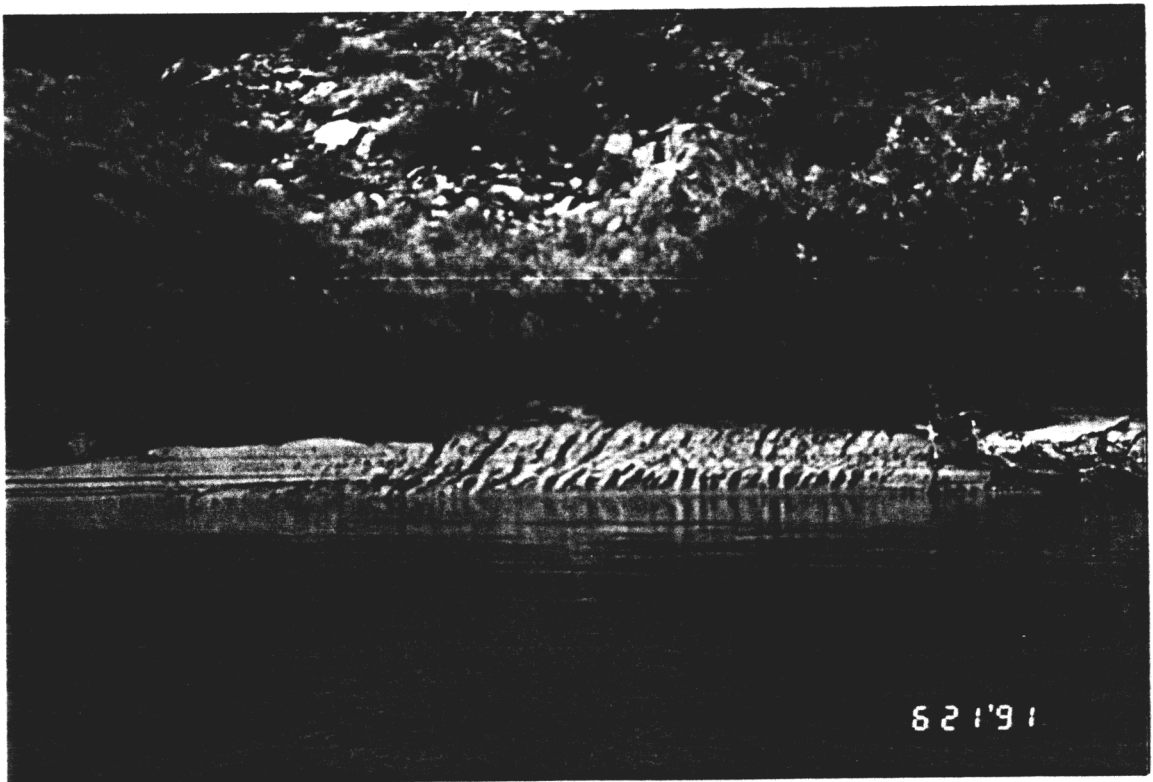


Fig. 3 Rivulets due to ground water seepage

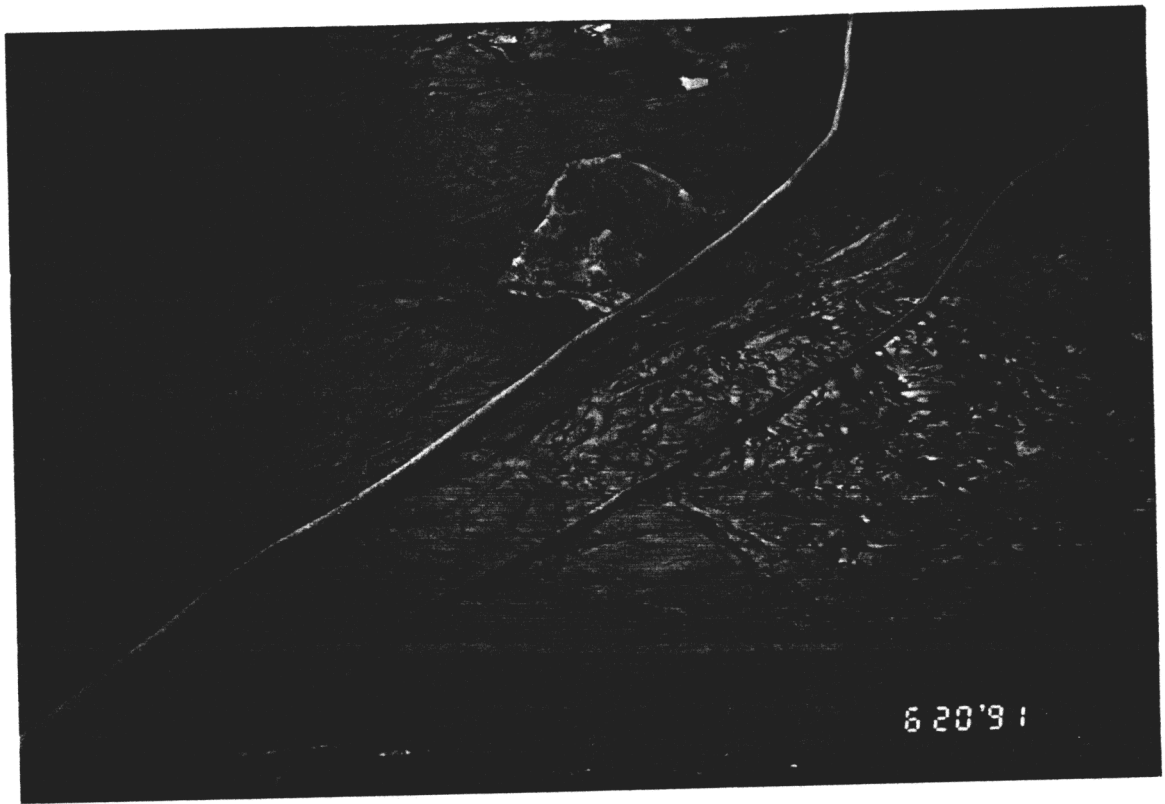


Fig. 4 Tunnelling due to ground water seepage

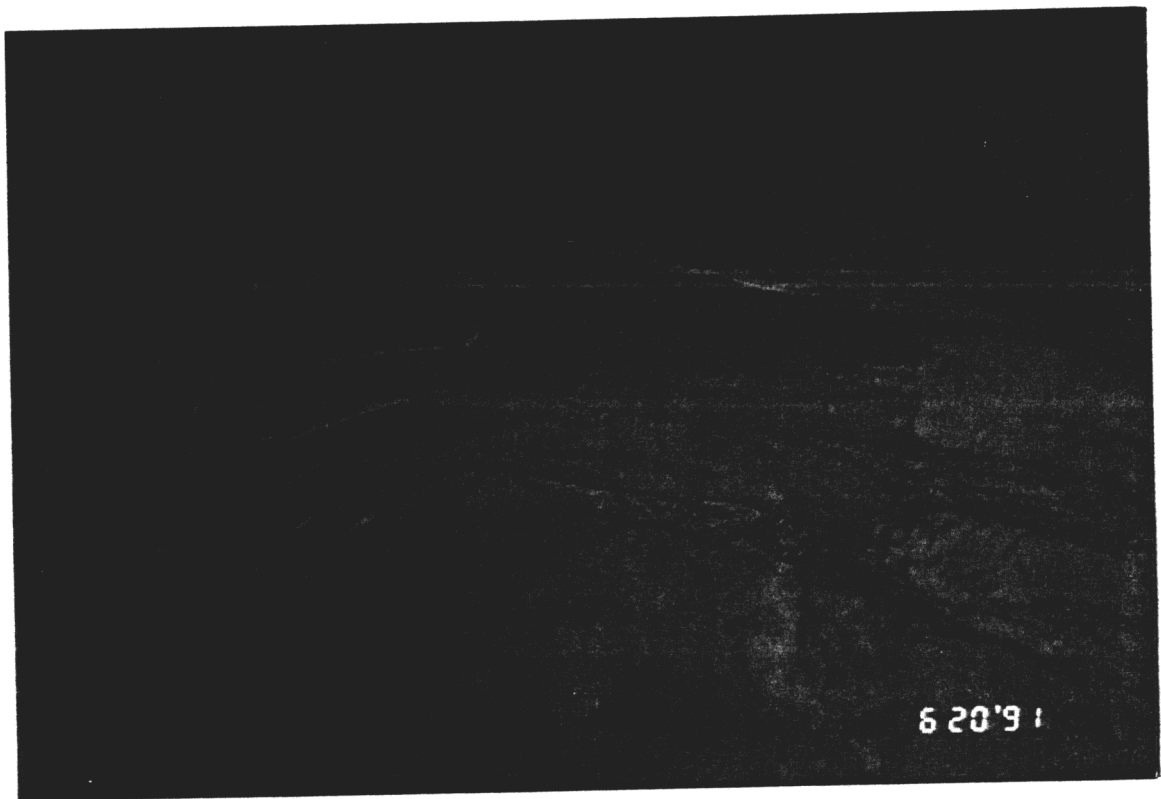


Fig. 5 Flow of sediments from tunnelling

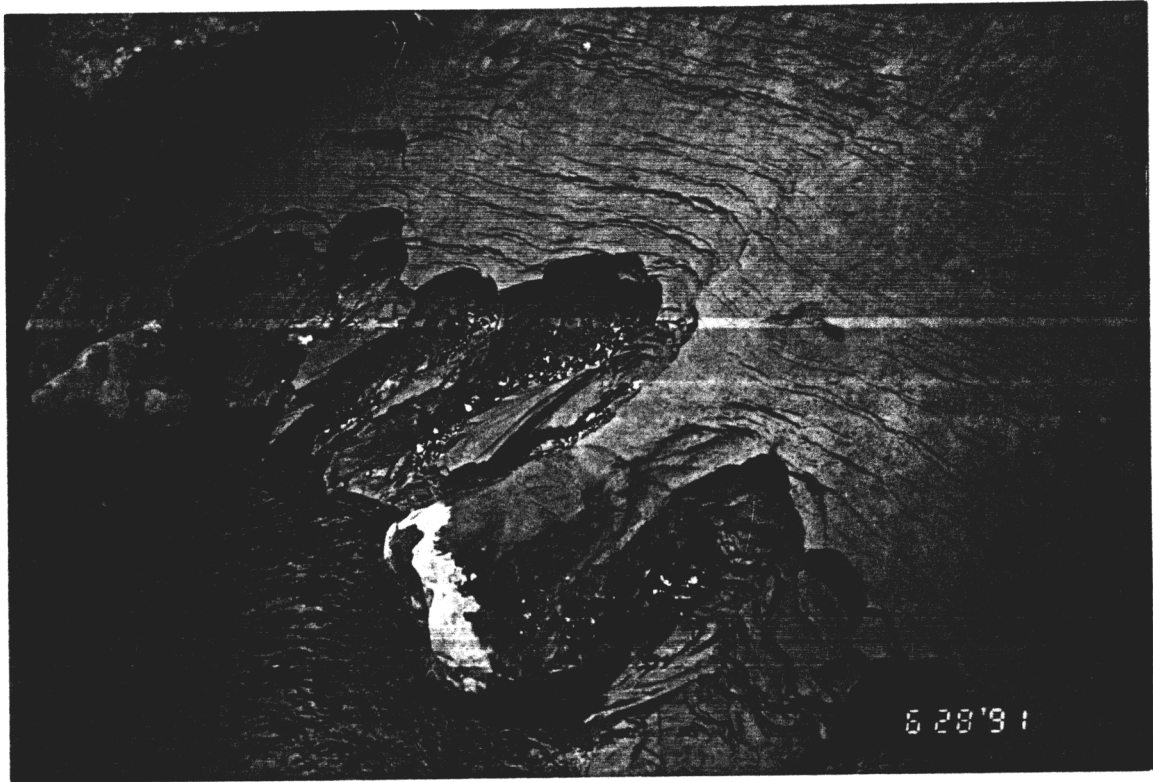


Fig. 6 Slope failures due to seepage and rapid down ramping

Seepage driven erosion also tends to steepen the sand bar slopes with concomitant bank or slope failures. The maximum safe slope angle for a clean, sandy sand bar without seepage is equal to the angle of internal friction of the sand. If seepage were to occur, the maximum safe slope angle reduces to approximately one-half the angle of internal friction of the soil. At this latter angle, the slope is unlikely to fail from ground water seepage. However, the conditions in the Colorado River, like most river systems, are dynamic. The 'equilibrium' slope may become over-steepened by ground water exiting from the sand bar and slope failures reoccur.

Tractive Force Erosion

Tractive erosion is well described in the literature. Most of the reported work dealt with the scouring of river beds due to shearing forces in the direction of flow. Tractive forces erode river banks due to velocity gradients from changes in the geometry of the river system. Fig. 7 shows the predominant tractive force mechanism in the Colorado River downstream of the Glen Canyon Dam. Velocity gradients during rapid rising river stage undercut the bank slopes. The soil directly above collapses into the void of the undercut. If the soil has some cohesion, a tension crack develops at the surface and the soil mass above the undercut rotates about its lower corner at the end of the undercut towards the river. Most of this collapsed soil is then transported downstream with the rising river stage. A typical example of this type of erosion mechanism is shown in Fig. 8.

In some sections of the river where the sand bar slope is shallow, the tractive forces scour the soil in the direction of flow between low water level and high water level. The slope steepens and eventually exceeds its limiting value (the angle of repose of the soil) leading to a slope failure (mass wasting).

Wave induced Erosion

The erosion of sand bars along oceans due to waves have been extensively studied by oceanologists. These ocean waves generally have large amplitudes and wavelengths. The waves in the Colorado river are due to wind, turbulence from rapids, boat wakes and eddies. These waves are of small amplitude and are superimposed on either rising or falling river stages. The action of these waves is to lift the soil grains, place them in suspension and transport them down slope and/or in the direction of flow. A concave erosion strip is carved on the sand bar. The slope at the top half of the strip becomes greater than the angle of repose of the soil and mini slope failures occur (Fig. 9). This is a very rapid sequential process in which a layer of sand bar several centimeters thick can be eroded away in a matter of minutes. A typical example of this process in the Colorado River is shown in Fig. 10.

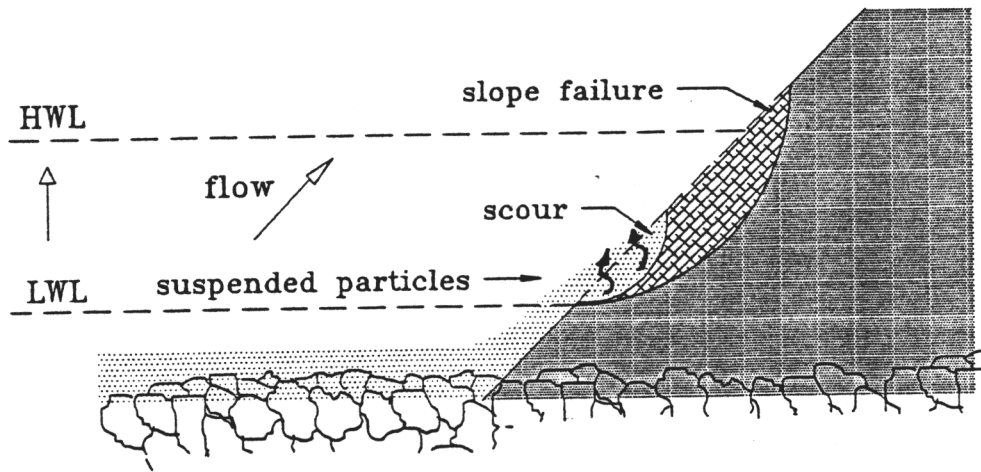


Fig. 7 Mechanism of tractive erosion



Fig. 8 Scouring and bank failure from tractive force

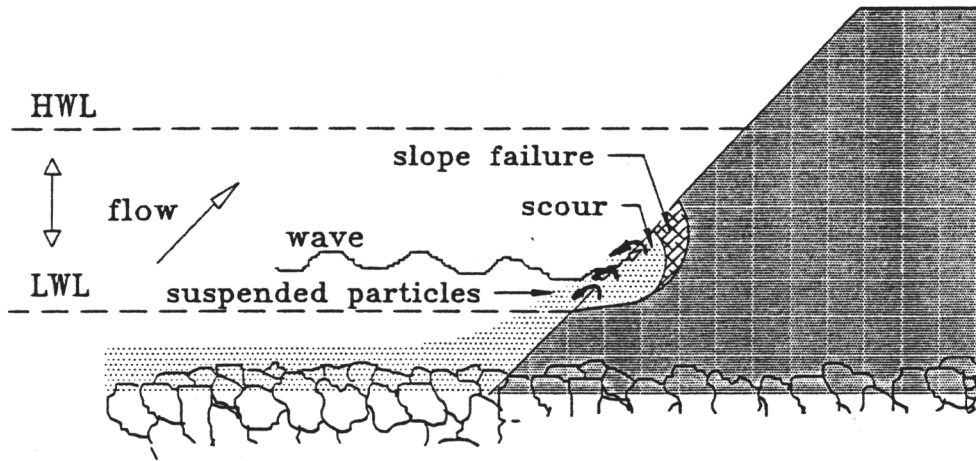


Fig. 9 Mechanism of wave induced erosion

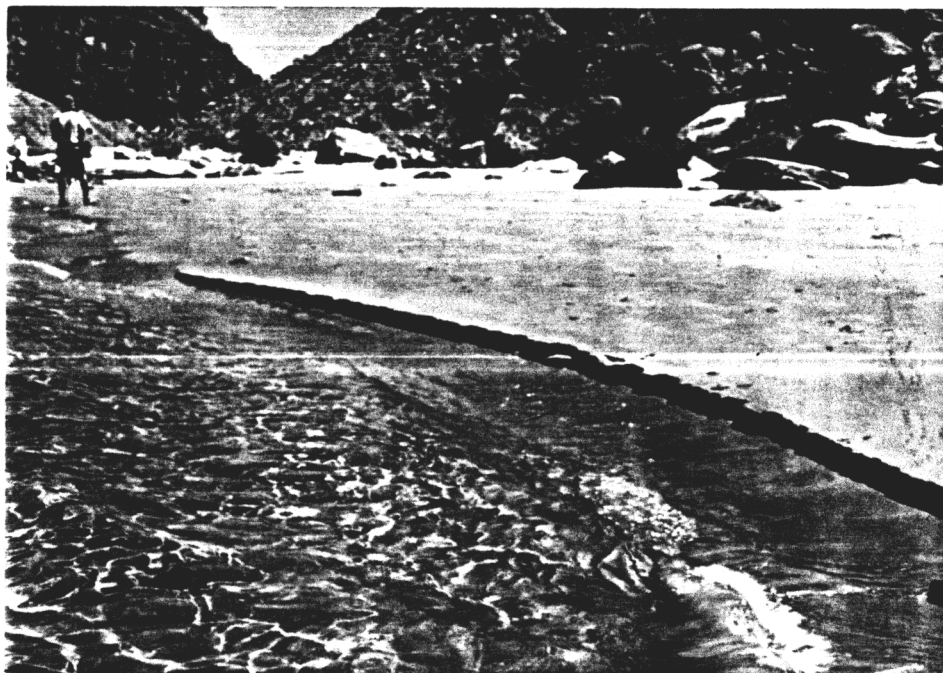


Fig. 10 Scouring and mini slope failures from waves

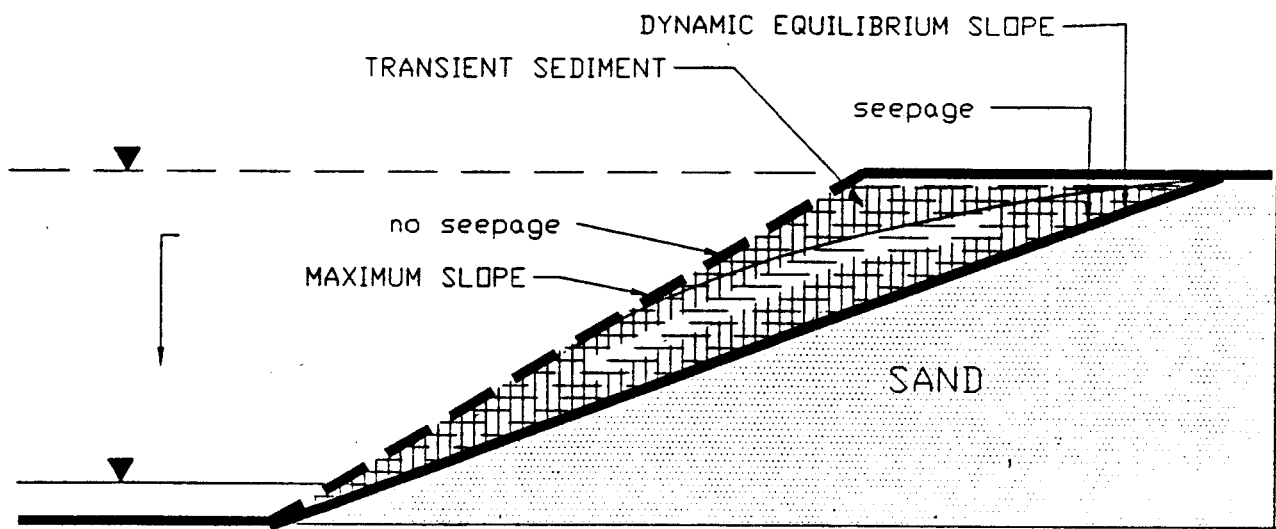


Fig. 11 Equilibrium slope and transient sediment zone.

Stability of Sand Bar Slopes Due to Seepage - An Equilibrium Slope

It is well known to Geotechnical Engineers that seepage forces reduce the stability of slopes. The factor of safety (F) can be reduced to as much as 1/2 of its initial (non-seepage) value. Consider a sand (a cohesionless soil) bar slope of angle α (Fig. 11). If the sand were dry or wet but with no seepage of ground water from the sand bar, the maximum sand bar slope for stability (slope stability) will be the angle of friction or angle of repose (ϕ) of the sand. Typical values of ϕ range between 20° and 45° . If seepage were now to occur in an initial stable wet or dry slope of sand with a slope angle of α , then the slope angle for stability under seepage (α_s) is

$$\alpha_s = \tan^{-1}\left(\frac{\gamma_b}{\gamma} \tan\phi\right) \quad (1)$$

where γ_b is the buoyant unit weight and γ is the bulk unit weight. In the derivation of equation (1), found in many geotechnical text books (for example, Lambe and Whitman, 1969), it is assumed that seepage occurs parallel to the slope of an infinite slope.

Consider a soil of bulk unit weight 17.2 kN/m^3 (an average value for the sand in the Colorado River) with an angle of friction of 30° . If no seepage were to occur, a sand bar comprising of this soil can have a stable slope of 30° . However, with seepage, the slope angle for stability is reduced to 14° which is less than one half the slope angle for no seepage. At this latter slope angle, the sand bar is unlikely to fail through slope instability. Thus, an equilibrium position is established for slope instability due to seepage parallel to the slope. However, water exiting from the sand bar would erode (formation of rivulets etc.) and transport the soil from the sand bar to the river during rapid down ramping river stage. The slope will steepen and slope failures can reoccur. Thus, the equilibrium slope is not static but dynamic; it depends on the soil type and the local hydraulic conditions. The sediments within the maximum slope angle and the dynamic equilibrium seepage slope will undergo cycles of erosion and aggradation. It is postulated here that the dynamic equilibrium slope will not vary much, perhaps only by a few degrees, from the static equilibrium slope. The sediments that accrued above the dynamic equilibrium slope will be unconsolidated and thus easily eroded. Indeed, catastrophic slope failures involving all or part of the enclosed sediments can occur if the stage changes are conducive to seepage driven erosion. For example, if the rate of down ramping is rapid, then an undrained slope failure can occur.

Many of the sand bar deposits along the Colorado River are not clean cohesionless sand. Rather, silts and/or clays in small quantities are mixed with the sand giving the sand bar deposits some cohesion (c). This is one of the reasons, the other important reason being the existence of tree roots, why on some sand bars, we noticed vertical slopes. For the case of sand bar deposits which have cohesion (c) as well as

friction, the critical height of slope, for an infinite slope with seepage parallel to the slope (Lambe and Whitman, 1969) is

$$H_{cr} = \frac{c}{\sin \alpha \cos \alpha (\gamma - \gamma_b \frac{\tan \phi}{\tan \alpha})} \quad (2)$$

where H_{cr} is the critical height of the slope, ϕ is the angle of friction of the soil and α is the slope angle. If there is no seepage, the critical height is given by

$$H_{cr} = \frac{c}{\gamma_b \sin \alpha \cos \alpha [1 - \frac{\tan \phi}{\tan \alpha}]} \quad (3)$$

Typically, for the sand bars below the Glen Canyon Dam, the average angle of repose of the soil is 26° (see Appendix III), the average cohesion is 1 kPa and the average bulk unit weight is 16.3 kN/m^3 for fresh sediments. If there were no seepage, the theoretical critical height of a saturated sand bar, with a slope of 30° , will be 4.3m; but, with seepage the theoretical height will only be 0.22m.

MODEL FORMULATION FOR SEEPAGE DRIVEN EROSION

In order to formulate a model to predict seepage driven erosion and to interpret the field observations, we make use of Biot's coupled stress - pore water pressure (head) theory. The details of the formulation is presented in Appendix I. In developing the model, we considered two factors (a) the geometry of the problems and (b) the constitutive relationship for the soils. One of the major advantages of utilizing Biot's theory is that stress changes, pore water pressures, seepage stresses, seepage driven erosion, slope (bank) stability and the free surface can be solved simultaneously. In addition, one can introduce tractive forces on the sand bar faces. In this contribution, our concerns are with seepage driven erosion and bank or slope stability (mass wasting). Thus, we will only present results that are directly linked to these concerns.

GROUND WATER LEVEL VARIATIONS FROM TRANSIENT DAM FLOW

Any comprehensive model which intends to model seepage driven erosion must be able to predict the changes in ground water levels. Thus, one of the first task of the model developed here for seepage driven erosion is to predict the variation of the free surface in the sand bars. We developed two numerical solutions for free surface determination. One is embedded in the finite element coupled seepage-stress analysis (Appendix I) and the other is a boundary element solution of the Laplace equation for flow

through porous media (Appendix II). The major advantage of the boundary element method over the finite element method is that only the boundaries of the problem need to be discretized. In the finite element method, the whole domain has to be discretized. These two solution techniques allow us to compare the accuracy of the finite element method and the boundary element method with the field data.

The free surface (phreatic surface) in sand bars along the Colorado River varies daily due to the operation of the Glen Canyon Dam. In each excursion, seepage into or out of the banks would incur stress changes and this should be considered in the analysis of such problems. A fall in river stage would cause a decrease in the hydrostatic pressure on the face of the river bank and a decrease in pore water pressure within the bank with a concomitant increase in effective stresses. The soil will consolidate and the permeability will decrease. A rise in river stage would result in the opposite effect. In the seepage-stress model developed here (Appendix I), we account for the stress changes accompanying transient flow conditions.

The prediction of the numerical analyses developed here is evaluated by comparison with a set of field data for changes in the free surface along sand bar -6.5R (Fig 12). The amount of ground water and river stage data gathered at sand bar -6.5R is enormous. We will only use an arbitrarily selected small portion of this data from the original instrumentation program to demonstrate the capability of our numerical analysis for free surface determination under transient flow conditions. A typical set of river stage and ground water level variation over a period of 5 days for the cross section depicted in Fig. 12 for Flows G and E is shown in Fig. 13. We use the approximation illustrated in Fig. 14 in the seepage-stress model to represent the river stage variation.

A comparison of the free surface between the finite element results and the field data from Well #2 for Flows G and E for Day 1 and Day 5 is illustrated in Fig. 15. The concordance in results is very reasonable. The sand bar was subjected to repeated variations in river stages before the installation of the field instruments. Thus, the data used for the analysis do not represent the first and fifth day of river stage fluctuations. A more extensive comparison was carried out using the boundary element method because of the ease of data preparation. Fig. 16 shows the comparison between the boundary element results and the field data over the full five day period. Here again the predictions are in good agreement with the field data.

EFFECTS OF RAMPING RATES ON BANK STORED WATER

Ramping rates are expected to control the amount of bank stored water and the rate of drainage of this water from the bank for a given soil type. Consequently, ramping rates directly influence the rate of seepage driven erosion. The GCSEIS alternatives (Table I), the peak summer flow of 1991 and arbitrarily selected up ramping and down ramping rates were imposed on a sand bar of maximum slope 26° (a typical slope angle down stream of the Glen Canyon Dam for a stable sand bar without seepage). The boundary element method (Appendix II) and the seepage-stress model (Appendix I) were

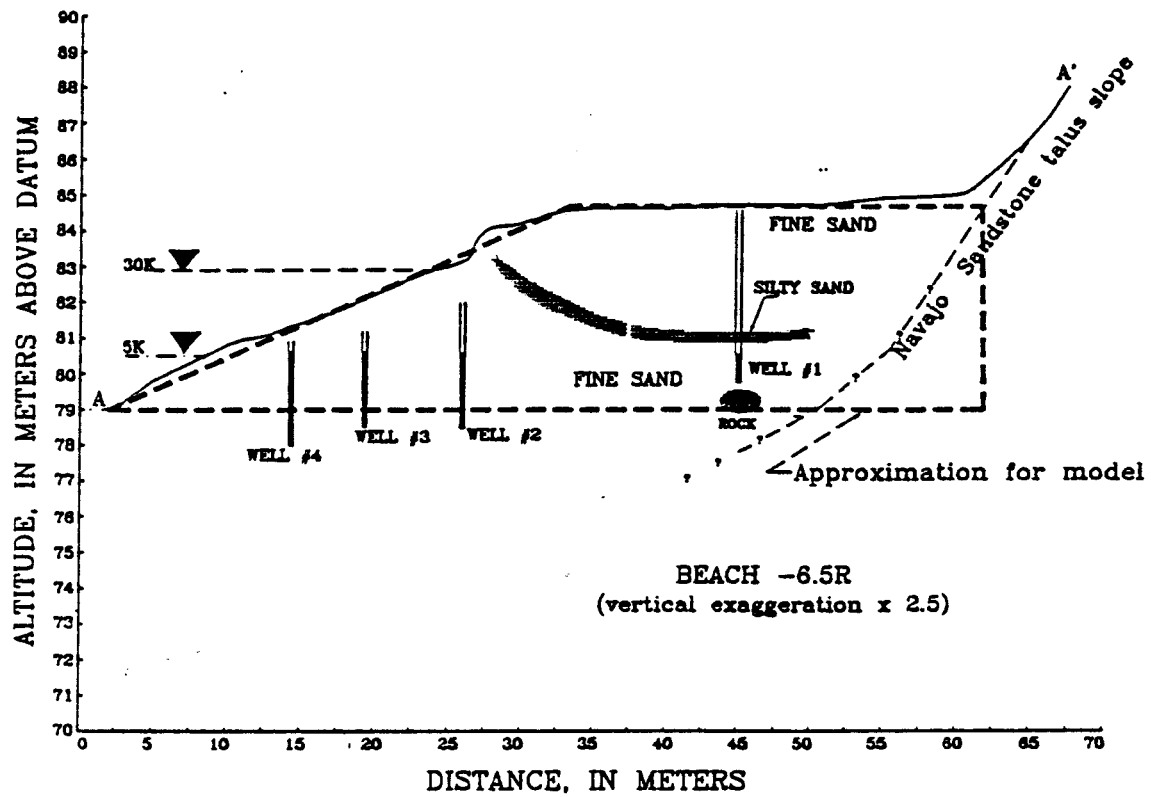


Fig. 12 A cross section of sand bar -6.5R and the approximation used in the seepage-stress model.

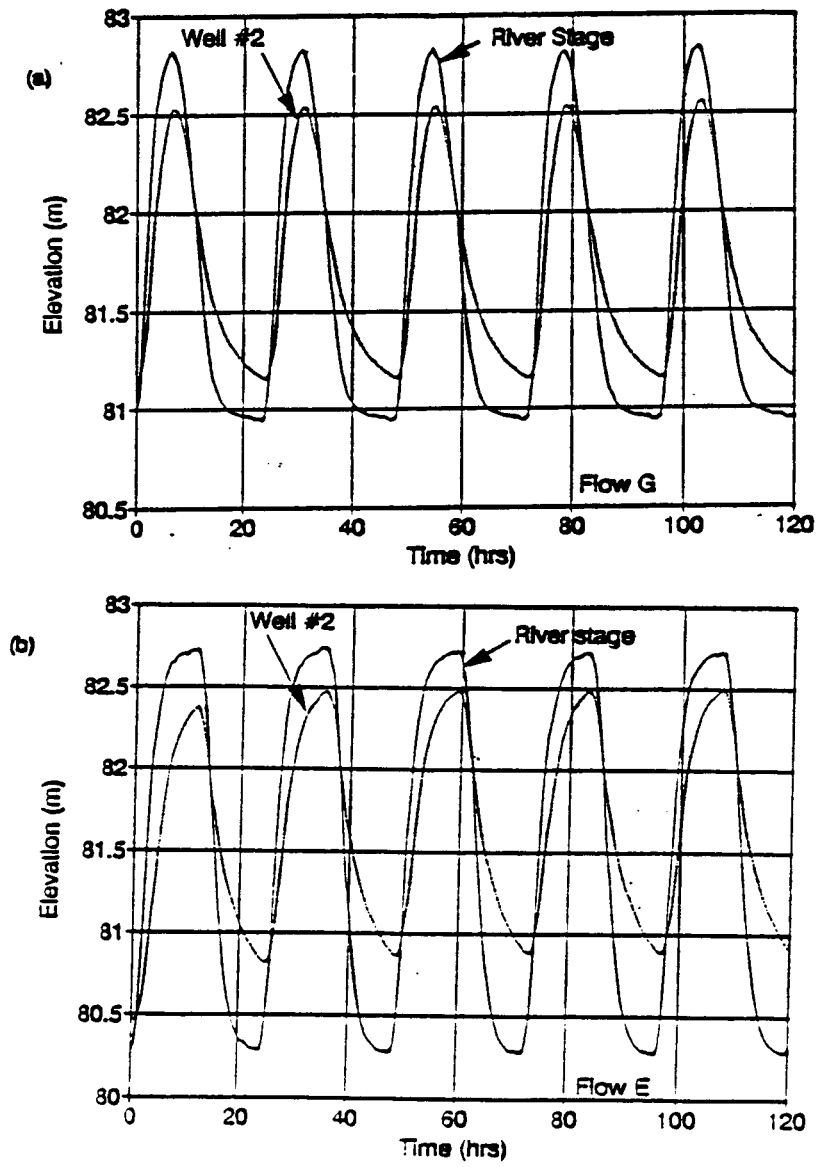


Fig. 13 River stage and well #2 field data for (a) Flow G and (b) Flow E .

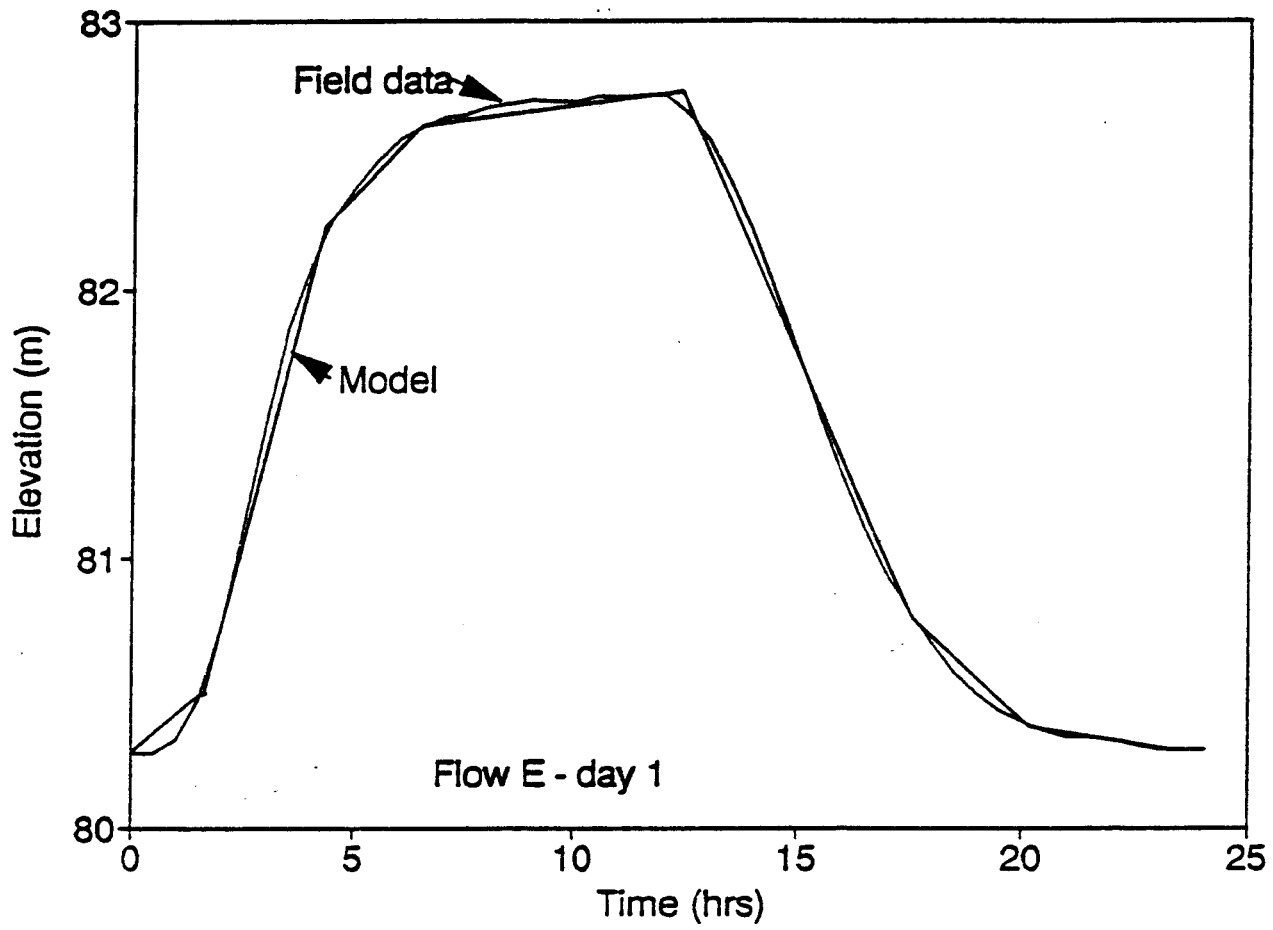


Fig. 14 Approximation of river stage fluctuation for use in the model.

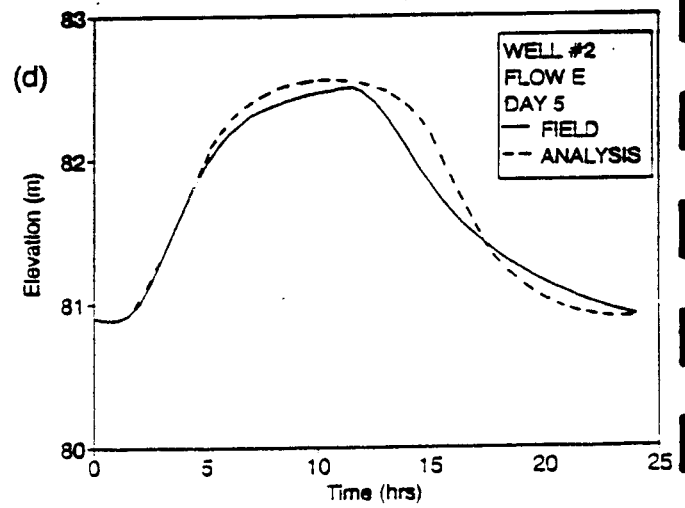
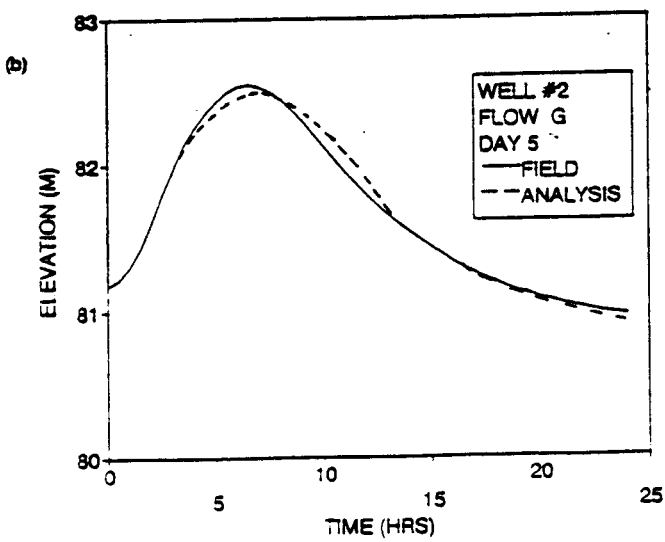
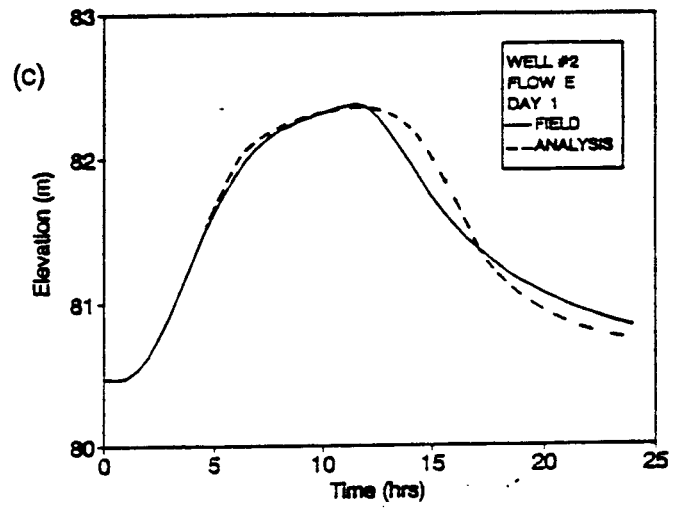
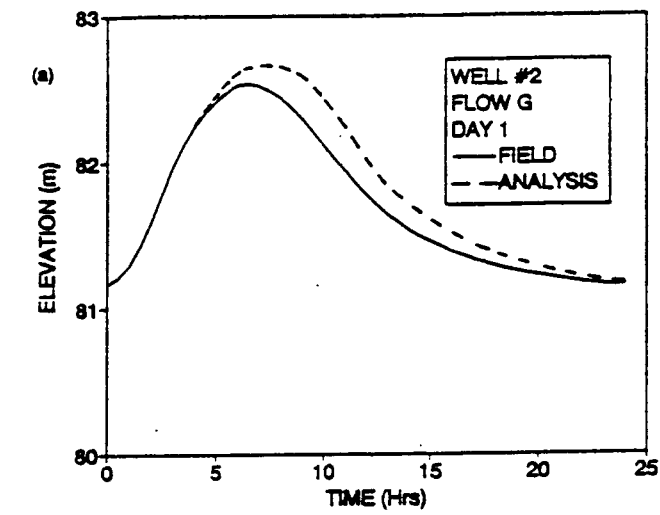
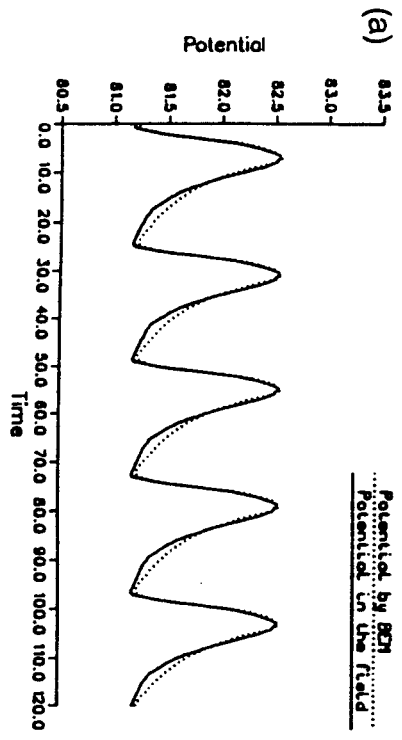
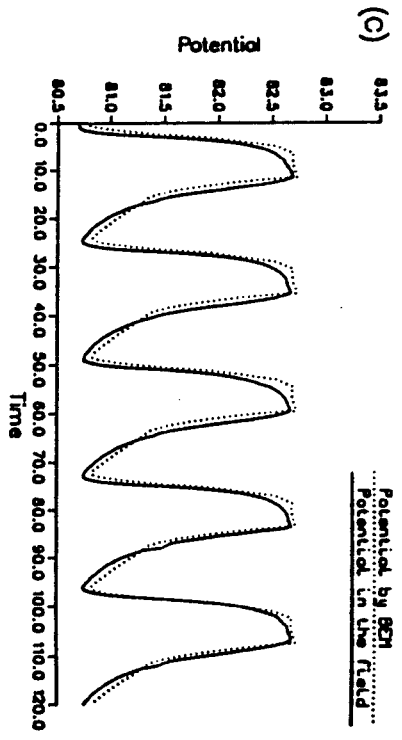


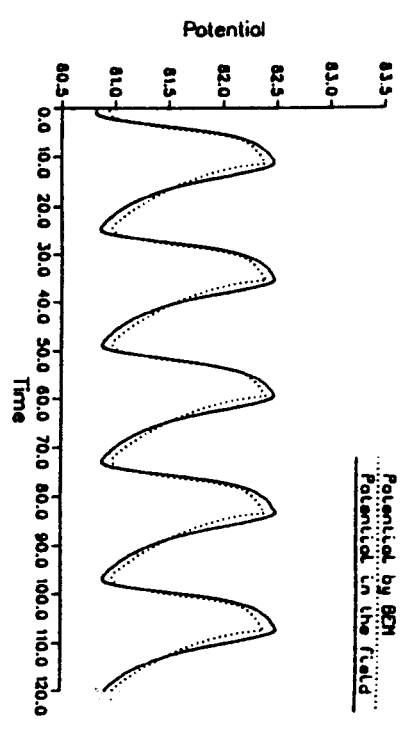
Fig. 15 Comparison of seepage-stress model prediction and field data for well #2 under Flow G (a) day 1 and (b) day 5, and Flow E (c) day 1 and (d) day 5.



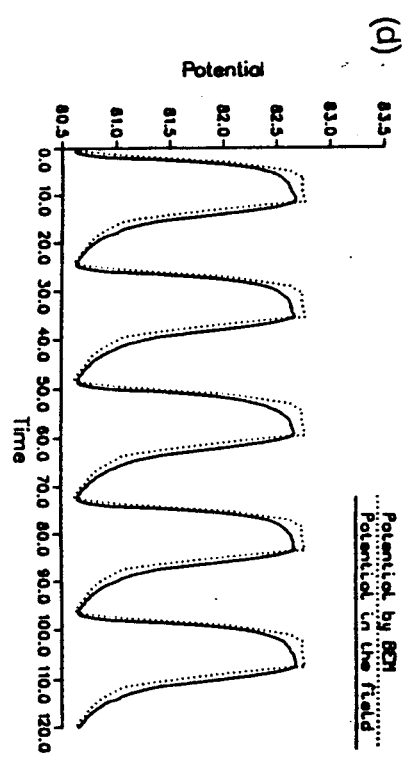
(a) Potential vs. time for well 2 (Flow G)



(a) Potential vs. time for well 3 (Flow E)



(a) Potential vs. time for well 2 (Flow E)



(b) Potential vs. time for well 4 (Flow E)

Fig. 16 Comparison of boundary element method and field data for Flow G (a) well #2 and Flow E (b) well #2 (c) well #3 and (d) well #4.

used to compute the phreatic surfaces at high water level and at low water level for these ramping rates.

For low up ramping rates (Figs.17 and 18), the amount of ground water stored is higher than high up ramping rates as expected. Low down ramping rates allow a larger quantity of the bank stored water to exit the sand bar. Therefore, the lower the up ramping rate, the lower the down ramping rate required to reduce seepage. If a high up ramping rate is followed by a period of constant peak discharge, the volume of water stored in the sand bar increases (Fig. 19). The drainage path for high up ramping rates is much shorter than low up ramping rates at the top portion of the sand bar. Thus, the time required for drainage of the transient stored ground water is shorter for high up ramping rates.

PREDICTION OF SEEPAGE DRIVEN EROSION

As a preliminary test, a hypothetical sand bar was used to check whether the model is making predictions consistent with field observations. A sand bar with a 1:5 slope was discretized into 200 elements and subjected to river stage diurnal variations of $580 \text{ m}^3/\text{s}$ maximum flow and $141.5 \text{ m}^3/\text{s}$ minimum flow. The preliminary results for the hypothetical sand bar using soil properties for sand bar -6.5R (Appendix III) is shown in Fig. 20. The model predicts seepage driven erosion during the down ramping river stage for the first and second river stage fluctuations. After the first fluctuation, the elements of soil for which the effective mean stress becomes zero were removed. The second river stage fluctuation is then imposed and if any further elements show fluidization, these were removed before the next application of river stage fluctuations. The consequence of the removal of these elements is that the slope within the region of the river stage fluctuation becomes steepened. During the third fluctuation, a circular slip plane developed. The area bounded by the slip plane and the sand bar slope extends above the region of the river stage fluctuations. The mass of material enclosed by this area either slips into the river during the down ramping river stage or do so during the next rising river stage. The predictions of the model for this hypothetical sand bar are consistent with the field observations (Cluer, 1992: this report Chapter 5).

PREDICTION OF SEEPAGE DRIVEN EROSION FOR ALTERNATIVE DAM DISCHARGE REGIMES.

Seepage driven erosion appears, based on field data and the model developed here, to be a major contributor to the destruction of sand bars in the Colorado River downstream of the Glen Canyon Dam. A question that arises: Is it possible to tailor a dam discharge regime that will reduce the current rate of seepage driven erosion? This question is explored using the model developed here. Five discharge regimes, shown in Table 1, were arbitrarily selected.

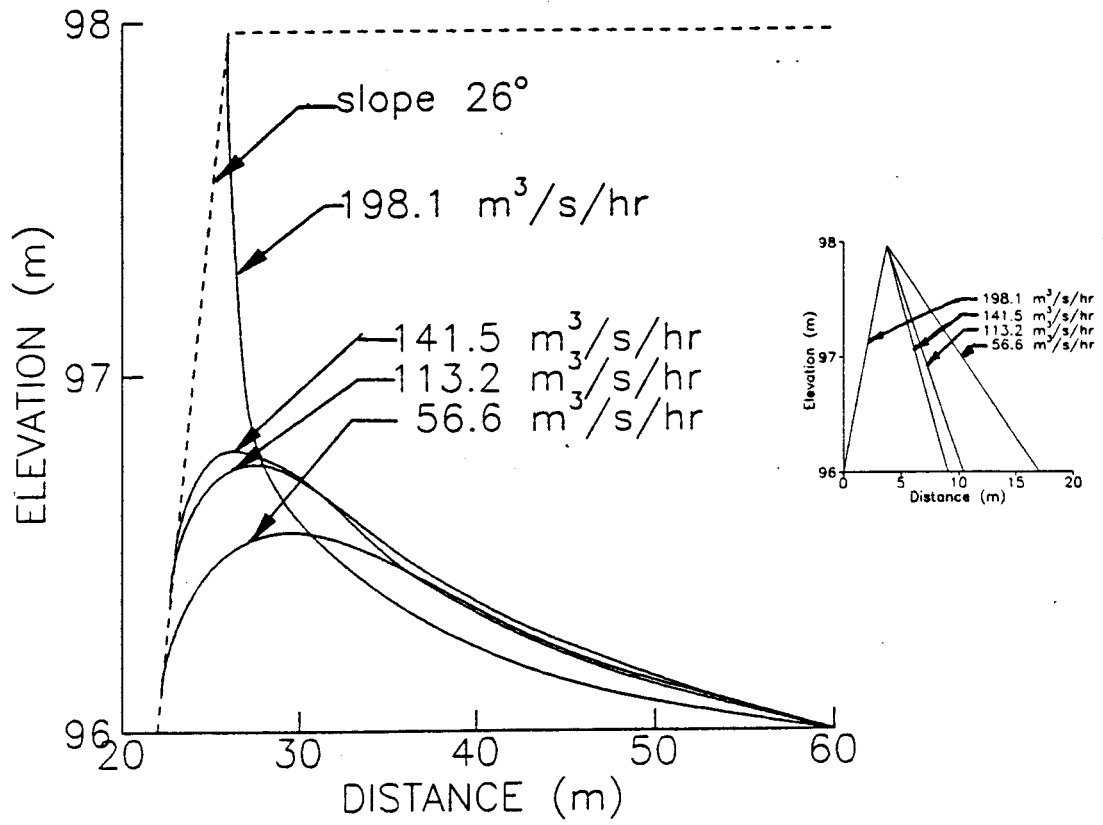


Fig. 17 Effects of down ramping rates on bank stored water.

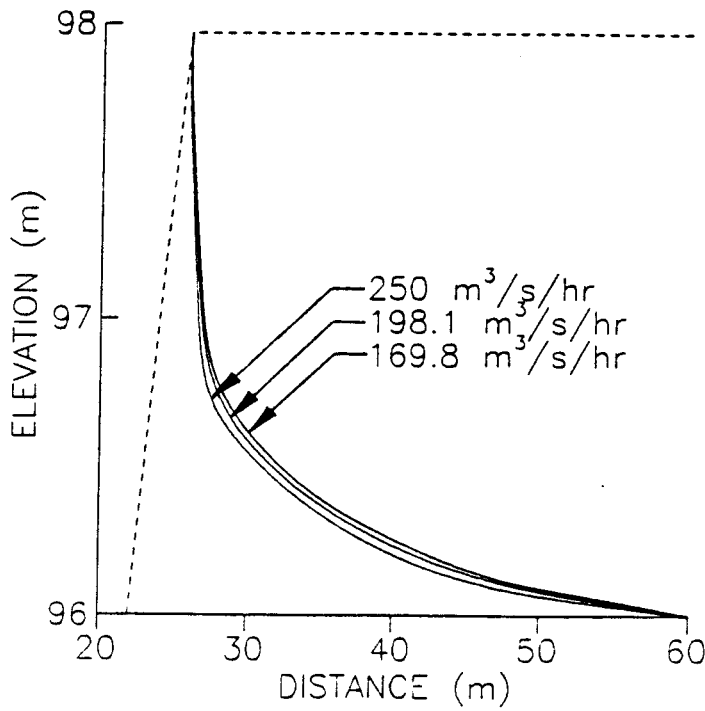


Fig. 18 Effects of up ramping rates on bank stored water.

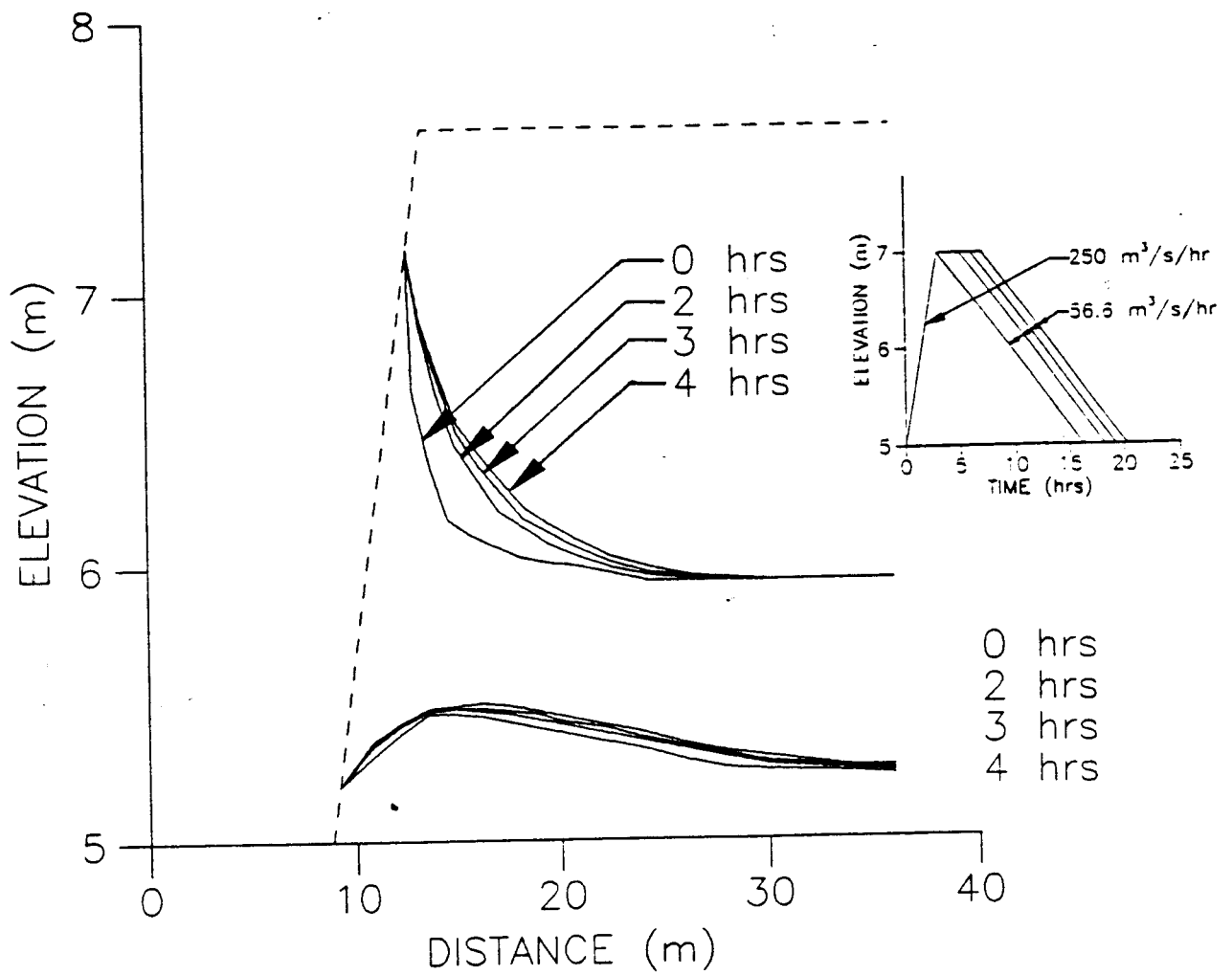


Fig. 19 Effects of a high up ramping rate followed by a period of constant peak discharge on bank stored water.

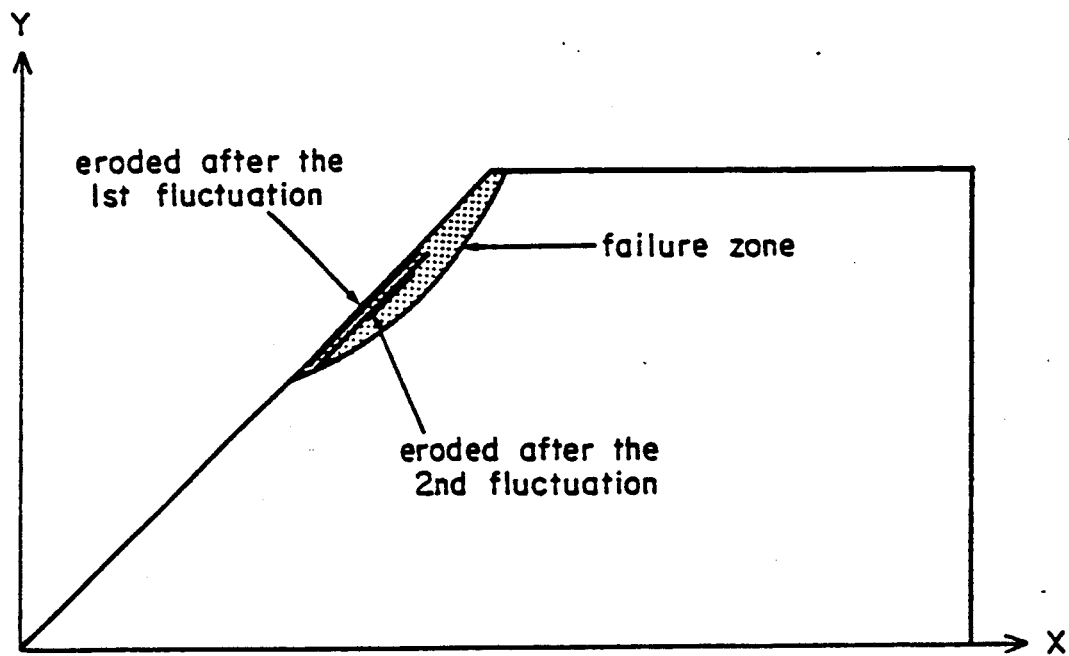


Fig. 20 Model prediction of seepage driven erosion.

TABLE 1: FLOW RATES TO PREDICT EROSION

CASE NUMBER	Up ramping RATE m ³ /s/hr	Down ramping RATE m ³ /s/hr	COMMENTS
1	48.1	48.1	
2	29.0	145	
3	25.5	386.9	
4	116.0	30.4	
5	9.6, 103	77.3	
6	70.8	34	*GCESEIS 3
7	113.2	70.8	*GCESEIS 4
8	141.5	113.2	*GCESEIS 5

*Glen Canyon Dam EIS Alternatives provided for comparison with model up ramping rates

The flow rates were dictated by the finite element mesh we used to discretize the hypothetical sand bar. Any flow regime can be accommodated by building suitable meshes. However, for this exercise, we used a single mesh. Three of GCESEIS up ramping and down ramping flow rate alternatives are also shown for comparisons. A sand bar slope of 1:5 with a homogenous deposit consisting of the sand found in sand bar -6.5R was investigated. It is assumed that for every 70.8m³/s discharge, the river stage rises by about 0.3m. The minimum flow selected is 141.5 m³/s and the maximum increase in flow is 580 m³/s. These selected minimum and maximum flows are different from the GCESEIS alternatives.

The predicted erosion for the selected flow regimes are shown in Fig. 21. The volume of erosion for the minimum up ramping and the minimum down ramping discharge rate (case 1) was used to normalize the results of the model predictions. The results indicate that a high up ramping rate with a slow down ramping rate appear to produce the smallest seepage driven erosion as established by case 4. The closest GCESEIS alternative (for moderate flow) is a up ramping rate of 113.2 m³/s/hr but, the down ramping rate of 70.8 m³/s/hr appears to be excessive.

As up ramping rates increase, the amount of bank stored water decreases as shown earlier in this report. The corollary is the lower the up ramping rates, the higher the amount of bank stored water. As a consequence, a high up ramping rate followed by a down ramping rate lower than the up ramping rate would be a desirable dam management practice to reduce seepage driven erosion. However, it is postulated here that high up ramping rates may lead to higher tractive erosion. More research is, therefore, needed to optimize the up ramping and down ramping rates so that the net

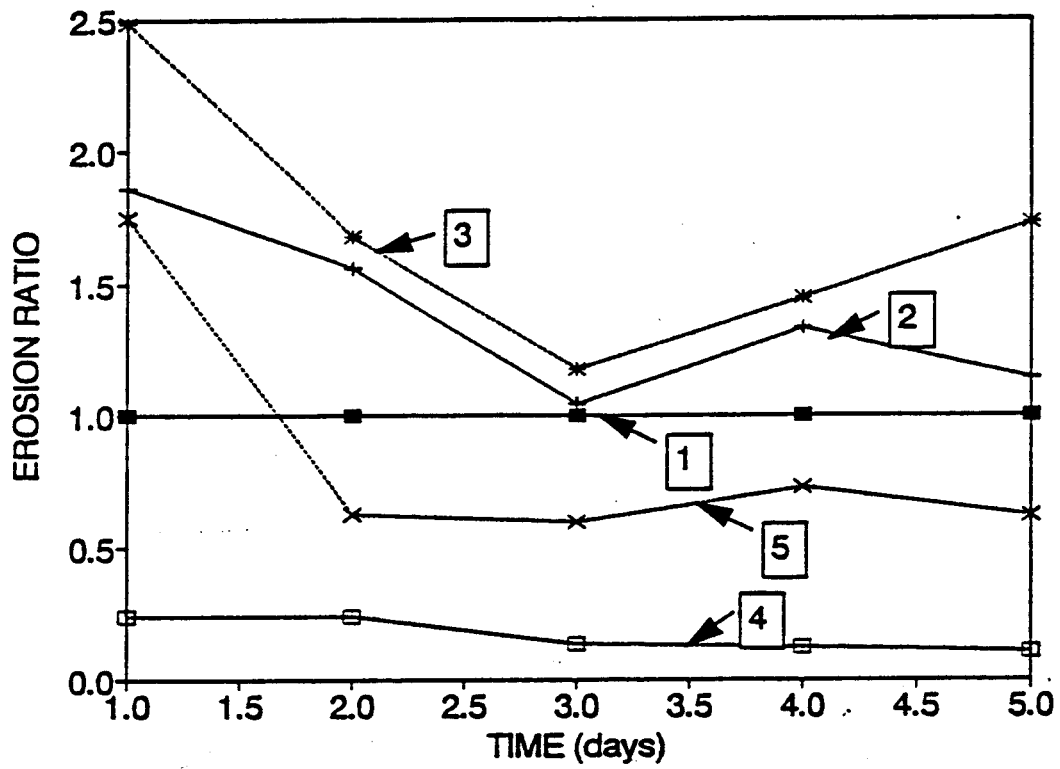


Fig. 21 Model prediction of erosion for various discharge regimes.

erosion will be substantially reduced. A conceptual model summarising the above ramping rate effects along with the erosion mechanisms in relation to discharge and time is shown in Fig. 22.

INTERPRETATION OF FIELD DATA USING THE EROSION MODEL.

Two analyses have been presented here to predict slope failures (mass wasting, bank cuts) due to seepage driven erosion. One, a finite element algorithm, is a coupled seepage-stress model which encompasses seepage and the constitutive relationships for the soils. This model integrates the applied hydrostatic stresses, the soil stresses and deformation, transient flow and seepage stresses into a coherent numerical scheme. The other is a simple analytical model in which flow is assumed to be parallel to the slope. This assumption is reasonable for the lower portion of the seepage face in a slope. It is not expected that this simple analysis will provide results to describe in detail the observed seepage driven erosion. However, it provides a first approximation and give insights into the patterns of expected erosion. We will use this simple model to interpret the observed erosion patterns at the three test sites (-6.5R, 43 and 172L) and then use the more elaborate finite element model to make predictions of seepage driven erosion to (a) compare with field data and (b) to study the effects of the GCESEIS alternatives. We will concentrate on sand bar 172L since this is the most active test site.

(a) Description of mass wasting events at sand bar 172L in 1991

Cluer (1992: this report Chapter 5) observed, during the period January 28, 1991 to November 10, 1991, five slope failures (mass wasting) at sand bar 172L. A summary of these events is shown in Table II. More details on these events can be found in Cluer (1992: this report Chapter 5). After each failure, the sand bar was rebuilt to approximately the same profile prior to failure. We will examine the failure event of June 18, 1991 with the aid of (a) the simple analysis and (b) the finite element model.

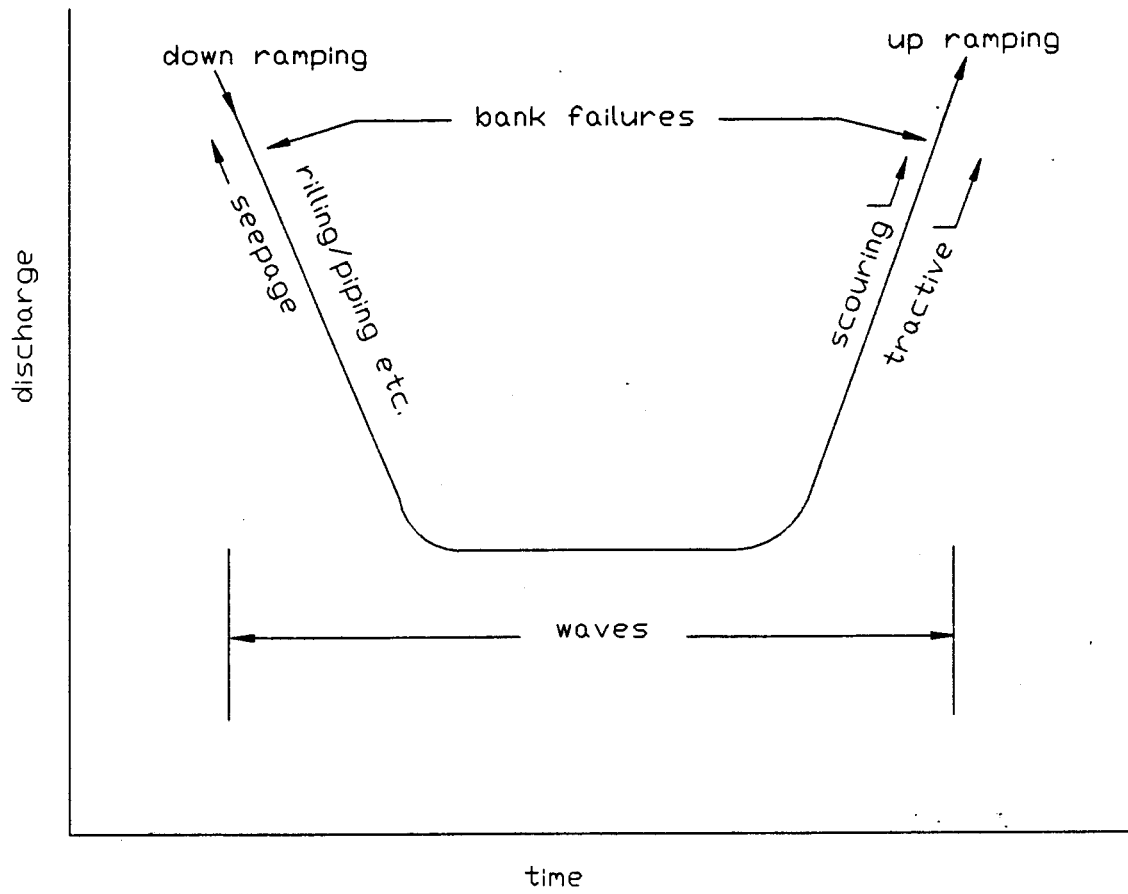


Fig. 22 Conceptual model illustrating erosion as a function of ramping rate.

Table II Chronology of slope failures at sand bar 172L.

Date (Year 1991)	% of sand bar lost	Flow Pattern
April 17	50	Normal Spring Flows
May 8	2	Transition from constant 142 m ³ /s to Flow D
May 13	4	Flow D
June 18	32	Normal Summer Flows
Sept. 1	> 50	Normal Flows

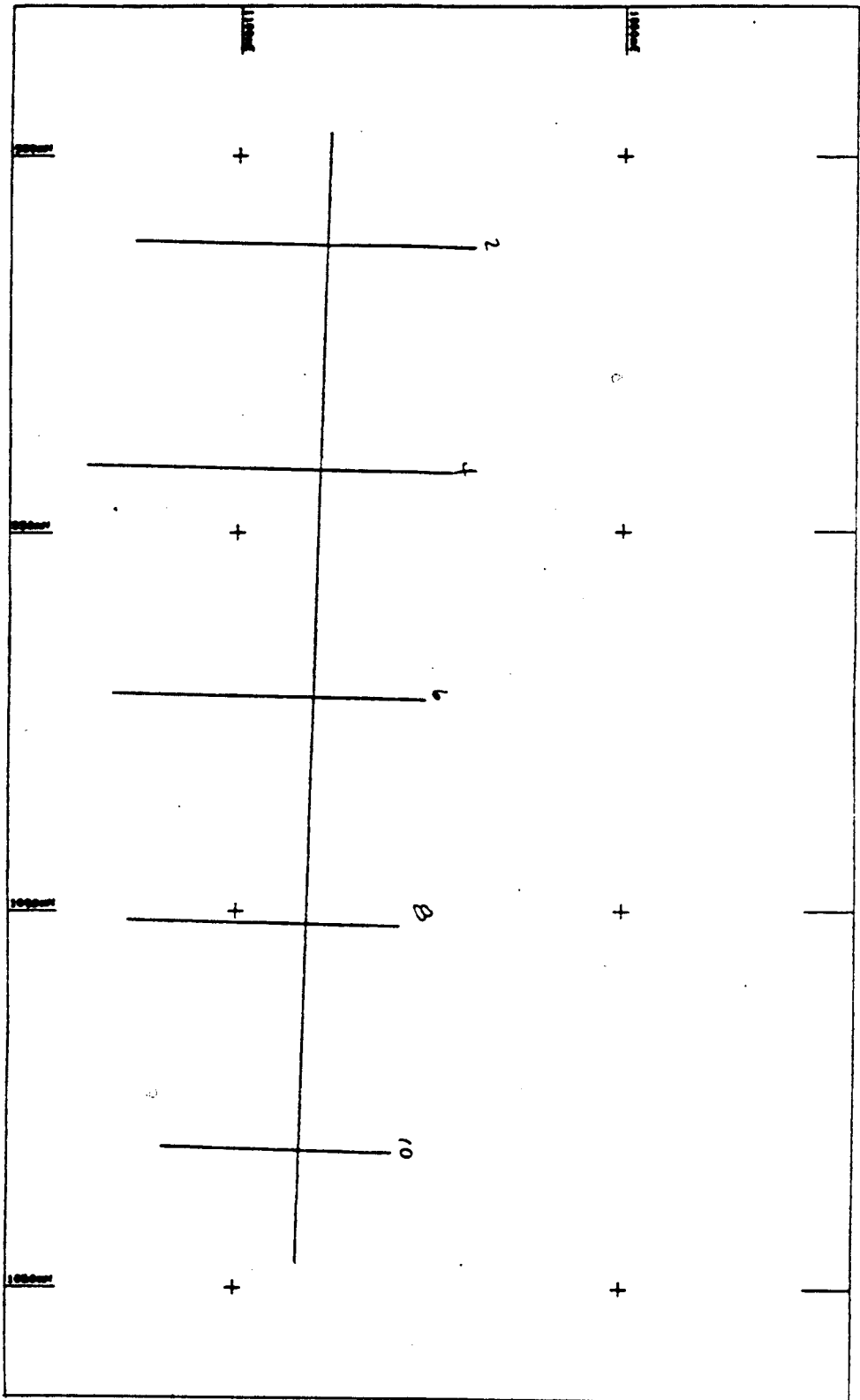
(b) Evaluation of mass wasting events at the test sites

Normal summer fluctuating flows (minimum discharge 85m³/s, maximum discharge 793m³/s) began on June 3, 1991 following a 3 day constant 142m³/s discharge (Cluer, 1992: this report Chapter 5). Five topographic surveys, two prior to June 3, 1991 and three soon afterwards, were conducted on sand bar 172L. The profile along eight cross sections (Fig. 23) were recorded. We arbitrarily select the profile of transect 8 - Profile 8 - for evaluation with the model proposed here.

Laboratory tests (Appendix III), using sand from the test sites, reveal that the maximum slope angle (angle of repose) of the sand under still water is 30°. The maximum slope angle reduces as the flow velocity at which deposition occurs increases (Appendix III). According to the simple theory, the maximum slope angle for a stable slope under seepage parallel to the slope is (equation 1) 13° for $\phi = 30^\circ$ and 11° for $\phi = 26^\circ$. The bulk unit weight of the transient sediment is $\gamma = 16.3 \text{ kN/m}^3$ (Appendix III).

Let us now examine this prediction with respect to the survey data of Profile 8 as reported by Beus et. al. (1992: this report Chapter 6) as shown in Fig. 24. The survey profile of May 18, 1991 shows that the maximum slope AB (Fig. 24) is 26° which indicates that the velocity at which deposition occurred was about 0.0034m/s (see Appendix III). This slope is unstable under seepage conditions. Using equation (1), the maximum slope angle for a stable slope under seepage within the hydraulically active zone is 11° for $\phi = 26^\circ$. That is, if the slope within the river flux zone of sand bar 172L were BC (Fig. 24), mass wasting due to seepage of ground water would be unlikely. On June 2, 1991, the slope AB reduced to 24°. It appears that rilling moved material from the top portions of the slope and deposited it at the toe.

On June 18, 1991 a slope failure was observed by Cluer (1992: this report Chapter 5). The survey of June 29, 1991 showed that a mass wasting event did occur. The failure surface recorded is consistent with a rotational failure mechanism



GCES BEACH SURVEY

27V

x line
172 MILE 7-28-91

1: 500

Fig. 23 Profiles surveyed on sand bar 172L.

172 MILE PROFILE 8

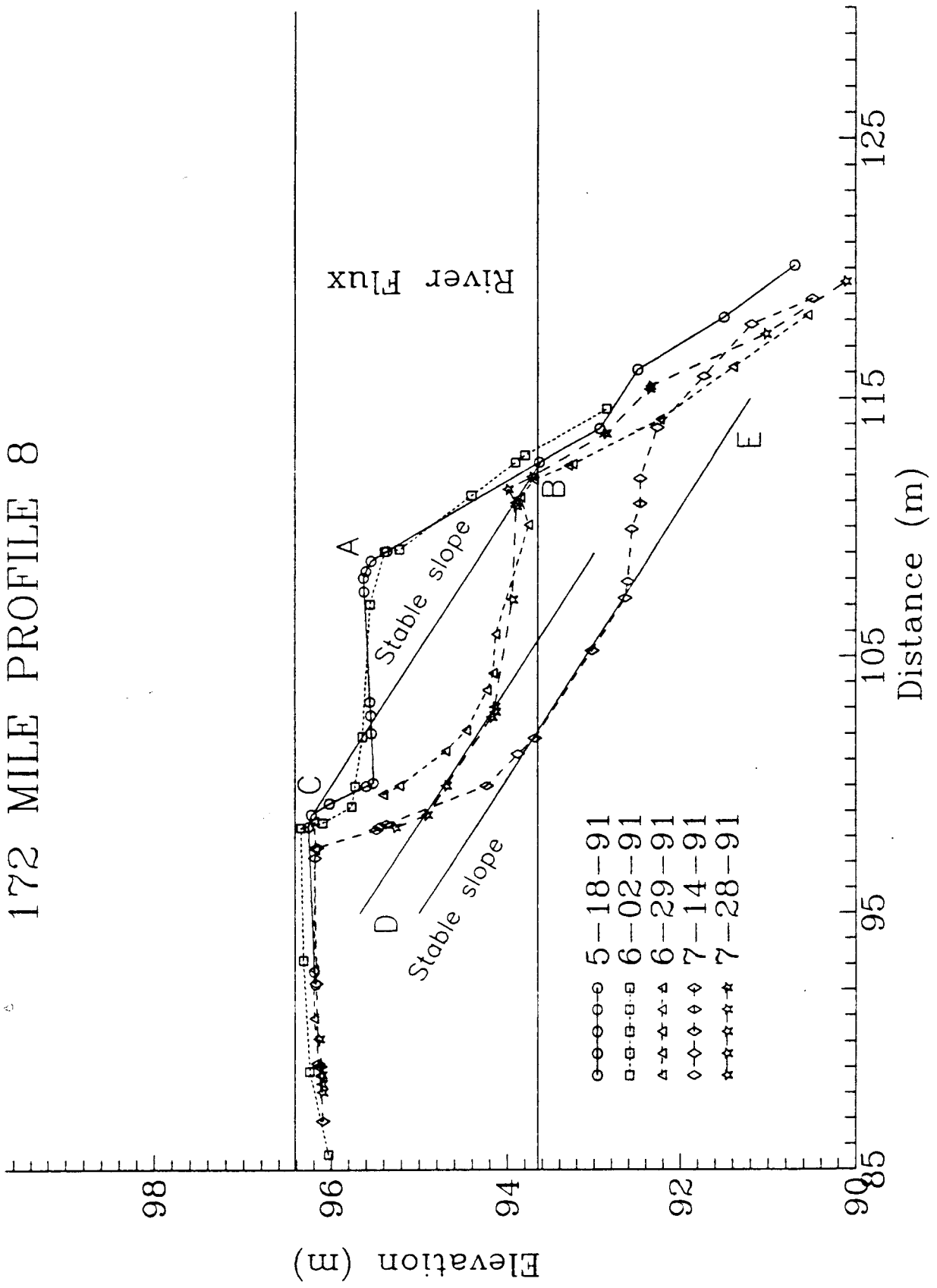


Fig. 24 Topographic Profile 8 and t 72/ and e driu slope

common in slopes. The survey of July 14 revealed a deeper failure surface that appears to be non-circular. A line drawn parallel to the slope BC (the stable slope under seepage conditions predicted by the simple model) lie exactly on the middle slope, DE, of the failure surface measured on July 14.

A similar exercise was conducted for sand bar 43. The maximum slope, DE, for the surveys in 1990 for Profile 3 was 12° (Fig. 25). This slope was built up outwards attaining a slope of 6° about mid-year 1991. Similarly at Profile 5 the surveys at the beginning of 1991 showed a maximum slope DE of 11° (Fig. 26) that later aggregated to a slope of 7° in the latter half of 1991. The slope of sand bar -6.5R during 1990 and 1991 remained constant at 10° (Fig. 27). No mass wasting event was observed at either sand bar 43 or sand bar -6.5R.

We now offer the following interpretation of the observations with the aid of the simple model. The slopes DE are old equilibrium slopes within the then active hydraulic zone. It appears that the minimum water level fluctuation was at about elevation 92.6 for sand bar 172L. Short term accretions occurring within the hydraulically active zone may lead to oversteepened slopes (slopes greater than those required for stability under seepage stresses; for the test sites, these slopes are between 11° and 13°) that are subsequently eroded by mass wasting from seepage and possibly by tractive forces. Other seepage related erosion such as rilling will also participate in the erosion of the sediments above the equilibrium slope in the hydraulically active zone. Thus, any deposition of sediments from floods or high flows or other sources will be reworked by the dynamics of the river system (dam discharge practice) to achieve an equilibrium position. Based on the available data, this equilibrium position under current dam operation is well established. The bulk of the erosion that is evident on the sand bars is of the transient sediments. For the transient sediments to become a stable part of a sand bar within the hydraulically active zone, the slope should be about 11° .

Near the top of many sand bars, slopes greater than the seepage equilibrium slopes exist. These are a result of the vegetation cover, sediments with cohesion and the reduced bank stored water. The latter is accumulated very near to the face of the sand bar and exit rapidly during falling river stage due to the short drainage path (Fig. 18).

(c) Model prediction of mass wasting at sand bar 172L.

Using the finite element seepage model (Appendix I), we imposed on sand bar 172L the measured river stage fluctuations from June 3 to June 29 as reported by Carpenter et. al (1992: this report Chapter 3). Profile 8 as surveyed on May 18, 1991 was used as the sand bar cross section at the commencement of the river stage variations. The mass wasting predicted by the model for June 18 and June 22, 1991 is compared with the field surveys as depicted in Fig. 28. Since no survey was conducted on June 18, 1991, no direct comparison between the model prediction and

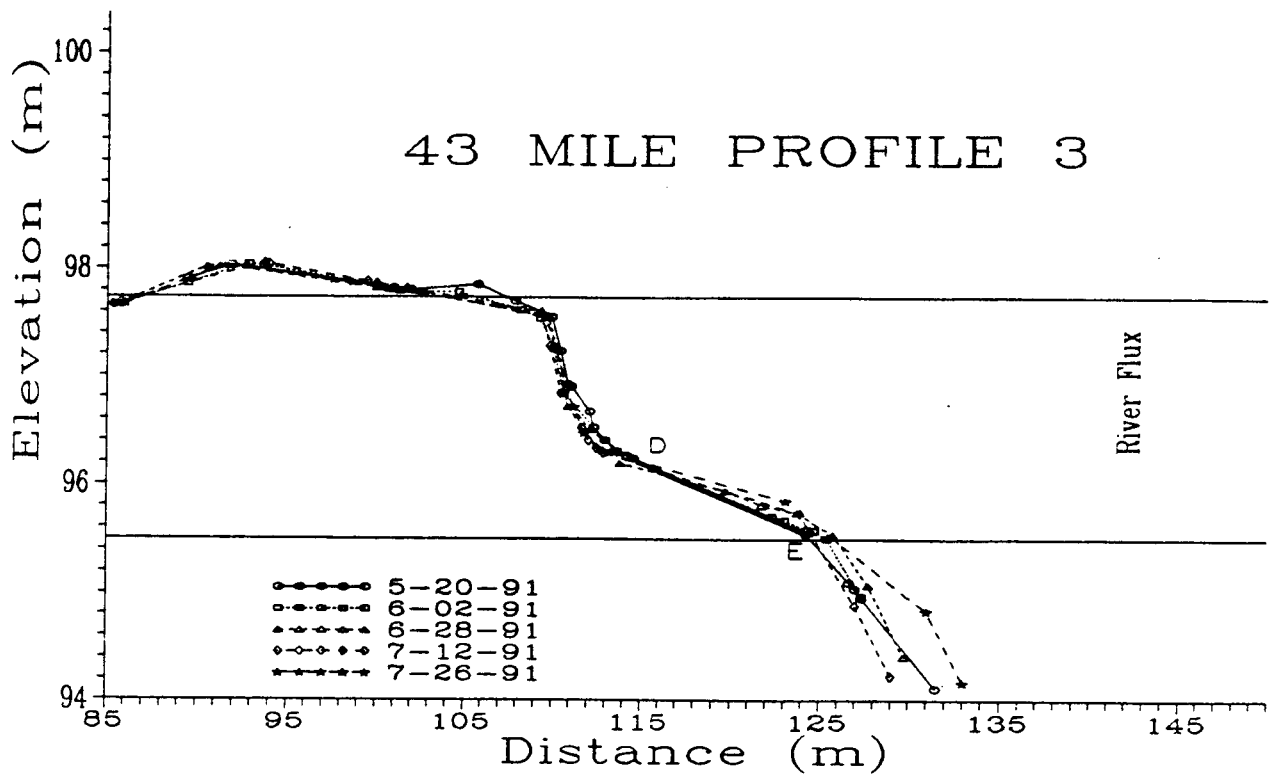


Fig. 25 Topography of Profile 3 - sand bar 43 and equilibrium slopes.

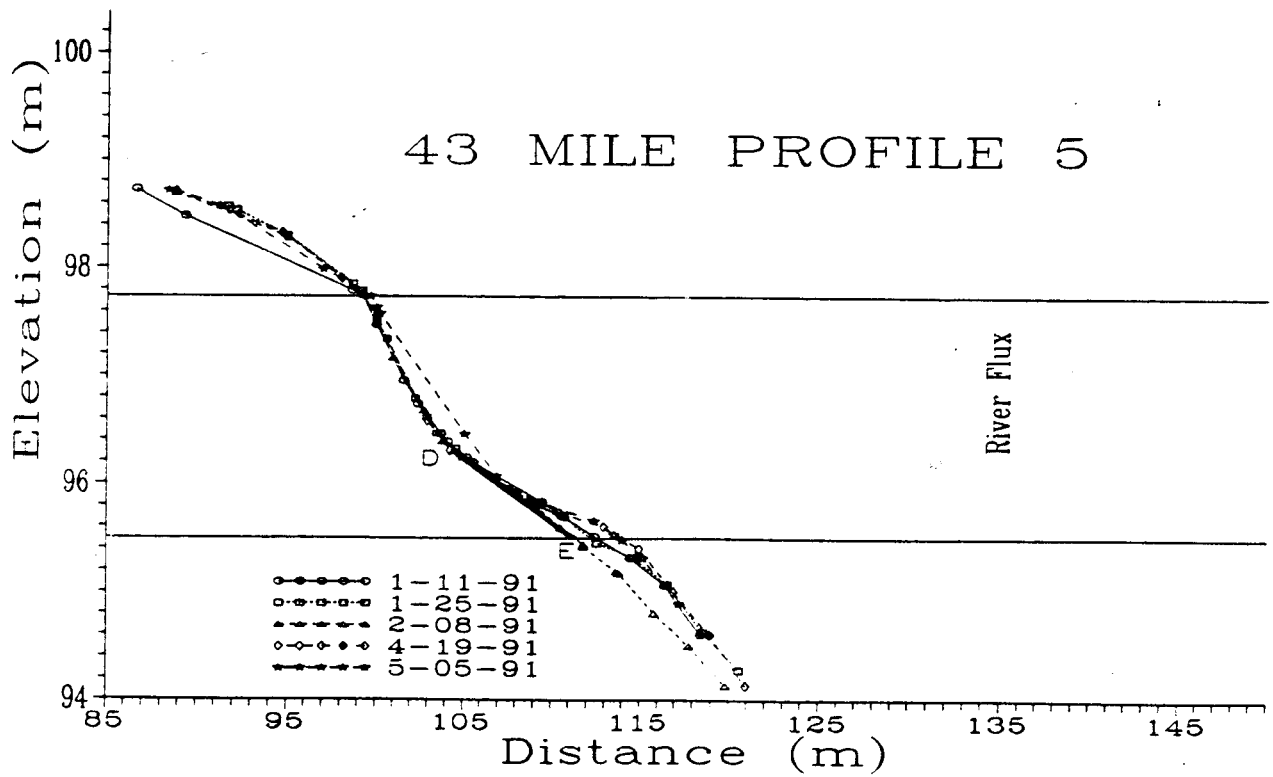


Fig. 26 Topography of Profile 5- sand bar 43 and equilibrium slopes.

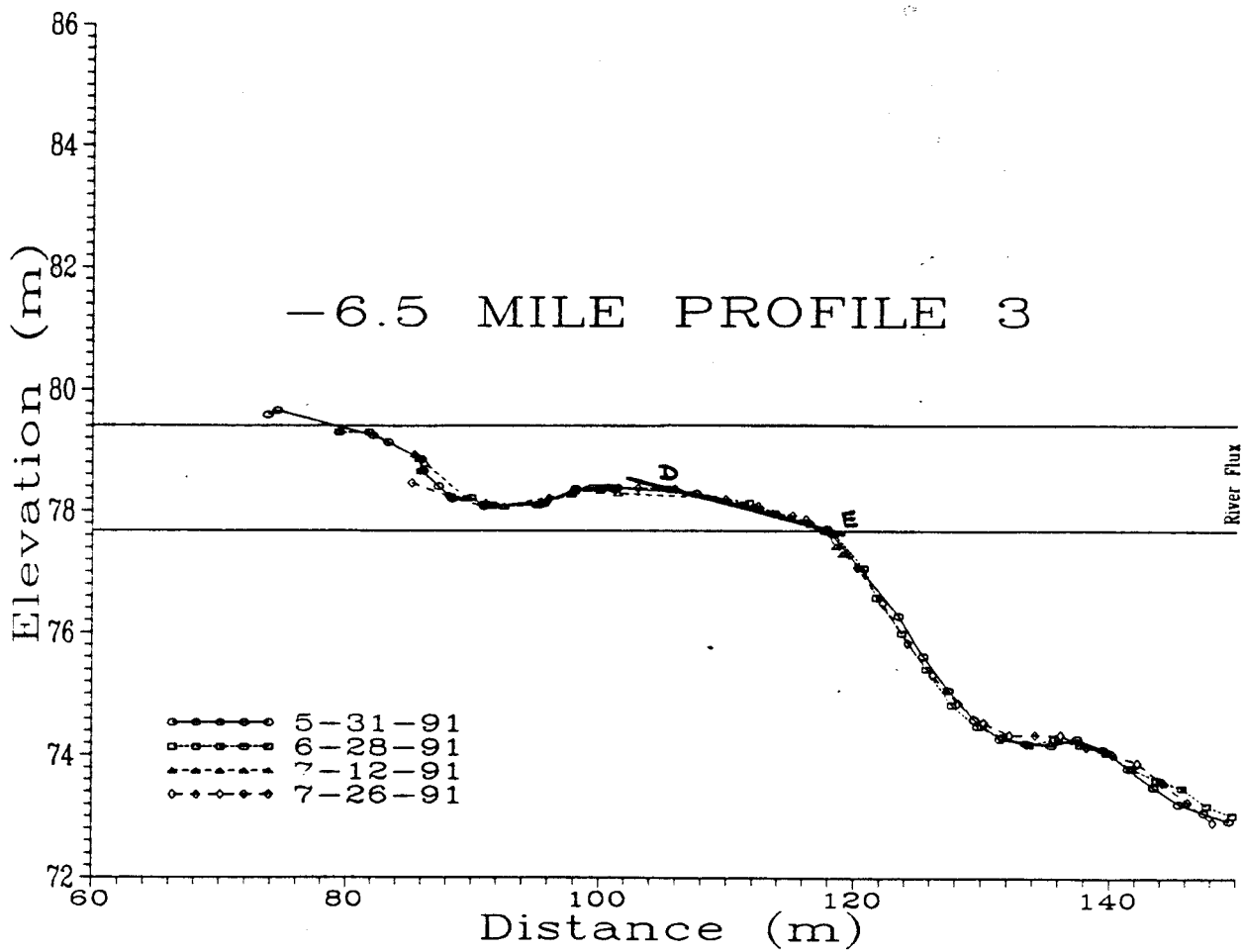


Fig. 27 Topography of Profile 3- sand bar -6.5R and equilibrium slopes.

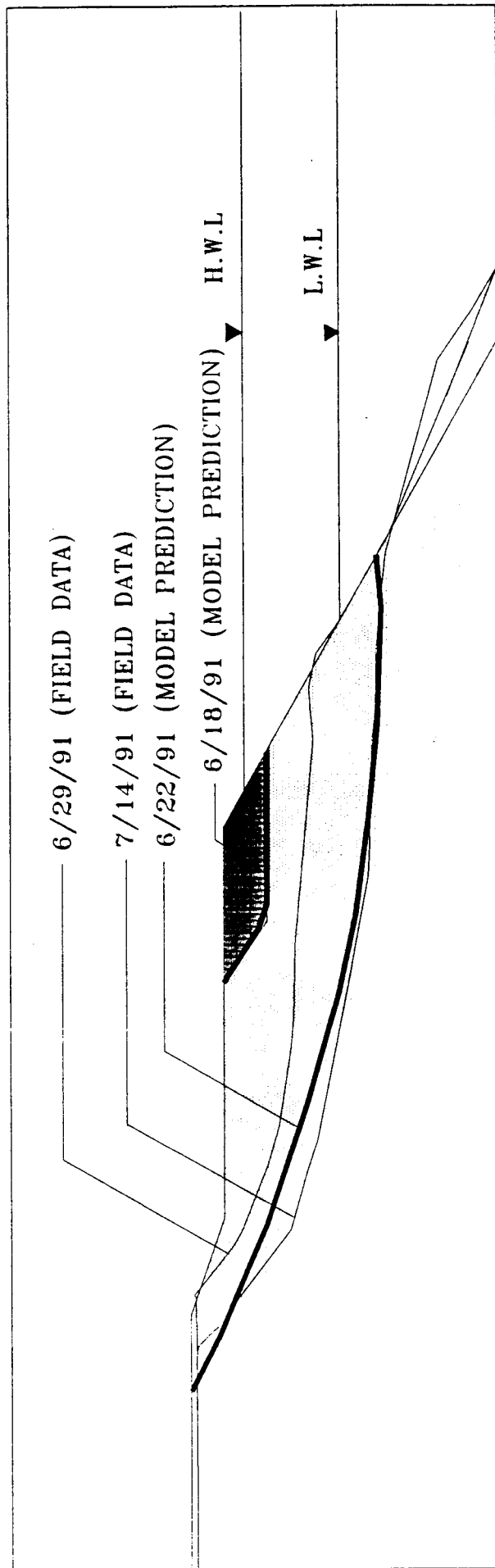


Fig. 28 Seepage-stress model prediction of mass wasting compared to field data for sand bar 172L.

the survey data can be made. However, the mass of material involved in the mass wasting event as predicted by the model is consistent with the photographs taken by Cluer (1992: this report Chapter 5) on June 18, 1991. The mass wasting predicted by the seepage-stress model on June 22, 1991 is much closer to the survey data of July 14 than June 29, 1991. The model did not predict any greater failure zone beyond June 22, 1991. Since no direct observations of events at sand bar 172L were made between June 20 and June 29, 1991, the exact timing of this mass wasting event is difficult to verify. All models, like the one described here, comprise assumptions which are not obeyed in the natural world. Differences between the model predictions and field data are expected. The overall trend and the quantitative predictions of the seepage-stress model developed here are very reasonable, at least, for practical purposes.

We now explore the question, would mass wasting occur under the GCESEIS alternatives assuming the same initial cross section? We found from the measured river stage data at sand bar 172L, a river stage-discharge relationship of 0.3933m per 100m³/s for Profile 8. We introduced river stage variations approximating a 10 day regime each of alternatives 3, 4 and 5 on Profile 8. The model predicted no erosion for alternative 3. The erosion predicted for alternative 4 involves a zone of soil from the top of the slope to just below the high water level (Fig. 29). The model predicted massive mass wasting under alternative 5 as shown in Fig. 30.

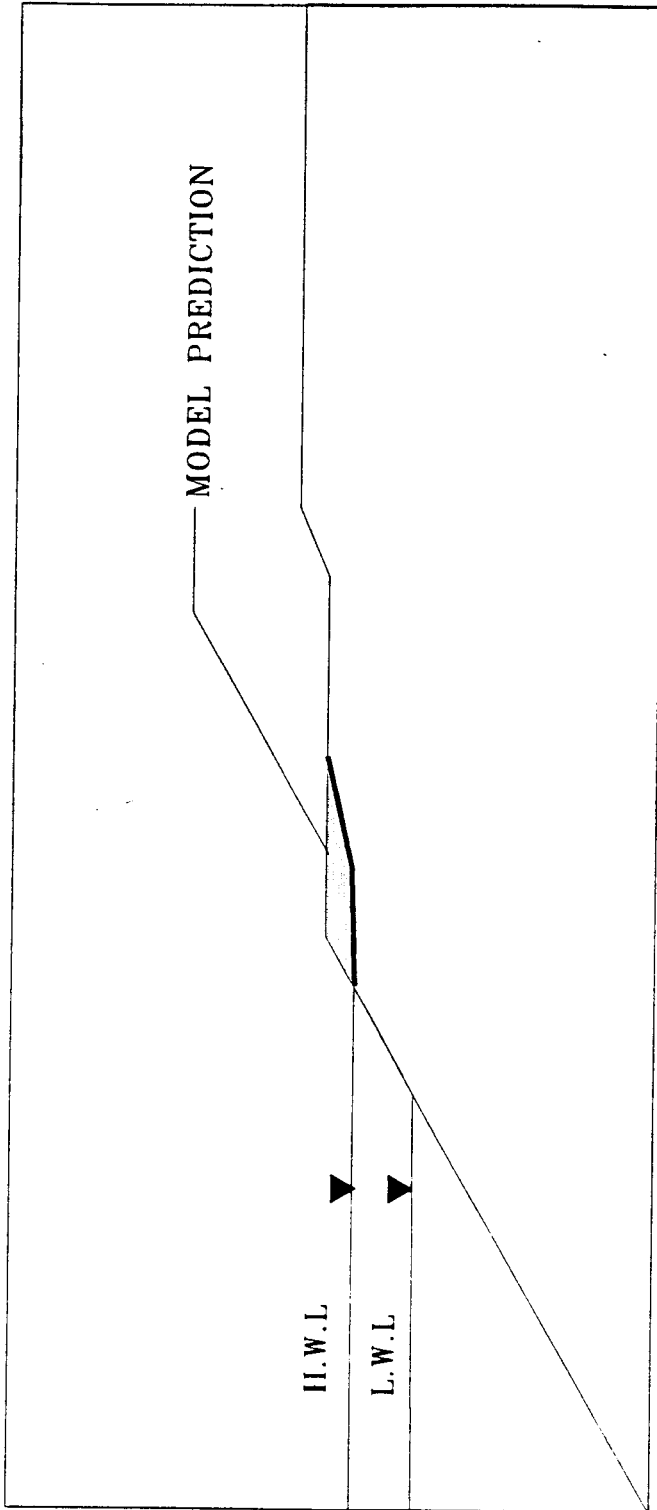


Fig. 29 Seepage-stress model prediction of mass wasting under EAS 4 for sand bar
172L.

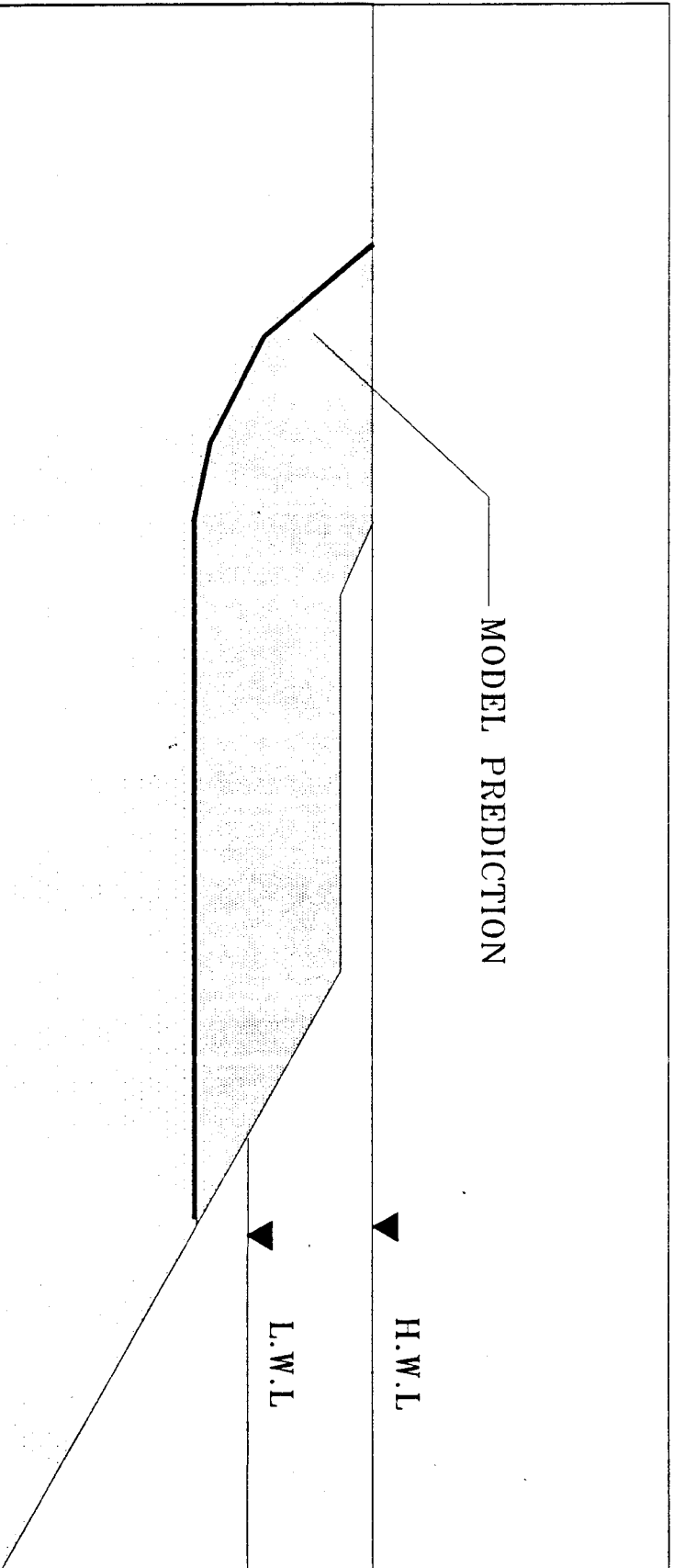


Fig. 30 Seepage-stress model prediction of mass wasting under EAS 5 for sand bar 172L.

CONCLUSIONS

The main conclusions from this part of the research program are as follows.

(1) Three mechanisms - seepage, traction and wave induced - were identified as active participants in the erosion of sand bars in the Colorado River downstream from the Glen Canyon dam.

The following conclusions only pertain to seepage driven events.

(2) For sand bars where seepage driven erosion is predominant, **a dynamic equilibrium slope was established**. Sediments, enclosed by this dynamic equilibrium slope and the maximum slope angle, will undergo **cyclic aggradation and erosion** depending on the dam discharge regimes. For the test site sand bars in the Colorado River downstream of the Glen Canyon Dam, the equilibrium slope, within the lower portion of the hydraulically active zone, is between 11° and 13° . This equilibrium slope is well defined for each sand bar under current dam discharge operation. Sediments from high discharges, floods or other causes accreting above and forming slopes greater than the equilibrium slope will be eroded by seepage and, perhaps, in combination with tractive forces. **The cyclic pattern of erosion and aggradation that is evident on the sand bars involves transient sediments deposited during favorable hydraulic and hydrologic conditions.**

(3) The seepage driven model developed here gave very encouraging results. The model predicts the fluctuations in ground water level in sand bars exceptionally well. The mechanism of seepage driven erosion as predicted by the model is consistent with field observations. The results from the model reveal that mass wasting is minimized more by rapid up ramping rates than slow up ramping rates. The lower the up ramping rate, the larger the amount of bank stored water. Low down ramping rates are more desirable than high down ramping rates.

(4) The lower the river stage level and the larger the river stage fluctuations, the more extensive the seepage driven erosion.

(5) The duration of minimum constant flows following normal flows (especially normal flows where the down ramping rate is large) enhances mass wasting of transient sediments.

(6) The seepage-stress model predicted that of the three GCESEIS alternatives only alternative 3 is likely to reduce mass wasting.

(7) This investigation was concerned only with seepage driven erosion - the ubiquitous erosion mechanism for sand bars down stream of the Glen Canyon Dam. Most of the sand bars seem to be eroded by a combination of seepage, traction and waves. High up ramping rates and low down ramping rates are favored to reduce erosion on sand bars where seepage is the predominant mechanism. However, there is the possibility that high up ramping rates may encourage erosion by tractive forces. Research involving all three mechanisms is needed before any alternative dam operation with regards to up ramping and down ramping rates can be suggested.

(8) At present, the evidences from the model and the field data indicate that any change in dam operation will result in the sand bars acquiring new equilibrium positions. Sediments above and not conforming to the new equilibrium position will be eroded.

(9) A slope of 11° in the hydraulically active zone of the sand bars is likely to be stable for seepage driven mass wasting.

REFERENCES

- Bathe, K.J. and M. R. Khoshgoftaar, Finite element free surface seepage analysis without mesh iteration, *Int. J. Num. Anal. Methods Geomech.*, 3, 13-22, 1979.
- Biot, M. A., Theory of elasticity and three dimensional consolidation, *J. of Applied Physics*, 12, 155-164, 1941.
- Booker, J.R. and J.C. Small, An investigation of the stability of numerical solution of Biot's consolidation, *Int. J. Solids and Structures*, 11, 907-917, 1975.
- Chen, R.T.S. and C. Y. Li, On the solution of transient free-surface flow problems in porous media by the finite element method, *J. of Hydrology*, 20, 49-63, 1973.
- Cividini, A. and G. Gioda, On the variable mesh finite element analysis of unconfined seepage problems, *Géotechnique*, 2, 251-267, 1989.
- Desai, C.S., Finite element residual schemes for unconfined flow, *Int. J. Num. Meth. +Eng.*, 5, 1415-1418, 1976.
- Desai, C.S., Free surface flow through porous media using a residual procedure, *Finite elements in fluids*, 5, Chapter 18, Ed. R.H. Gallagher, J.T. Oden, O.C. Zienkiewicz, T. Kawai and M. Hawahara, 1984.
- Desai, C.S. and G. C. Li, A residual flow procedure and application for free flow in porous media, *Advances in Water Resources*, 6, 27-35, 1983.
- Hagerty, D.J., "Piping/Sapping Erosion: I: Basic Considerations," *Journal of Hydraulic Engineering*, ASCE, Vol. 117, No. 8, 1991a, pp. 991-1008.
- Hagerty, D.J., "Piping/Sapping Erosion: II: Identification - Diagnosis," *Journal of Hydraulic Engineering*, ASCE, Vol. 117, No. 8, 1991b, pp. 1009-1025.
- Hinton, E. and R.J. Owen, *Finite element programming*, Academic Press, New York, 1977.
- Howard, A.D. and McLane III, C.F., "Erosion of Cohesionless Sediment by Groundwater Seepage," *Water Resources Research*, Vol. 24, No. 10, 1988, pp. 1659-1674.
- Lacy, S.J. and J. H. Prevost, *Flow through porous media: a procedure for locating the*

free surface, *Int. J. Num. Anal. Methods Geomech.* 11(6), 585-601, 1987.

Lambe and Whitman, R. *Soil Mechanics*, John Wiley & Sons, Inc., New York, 1969, 553 pp.

Li, G.C. and C. S. Desai, Stress and seepage analysis of earth dams, *J. of Geotechnical Engineering*, 109(7), 946-960, 1983.

Roscoe, K. H. and Burland, J. B. On the generalised stress-strain behaviour of a wet clay, In *Engineering Plasticity*, eds. J. Heyman and F. A. Lechic, Cambridge University Press, Cambridge, 535-609, 1968.

Schofield, A. N. and C. P. Wroth, *Critical state soil mechanics*, McGraw Hill Book Company, London, 1968.

Taylor, R.L., and C. B. Brown, Darcy flow solutions with a free surface, *J. of the Hydraulics Div., ASCE*, 93(2), 25-33, 1967.

U.S.D.I., Glen Canyon Environmental Studies Final Report, 343, 1988.

Wood, D.M. and A. Al-Tabbaa, Some measurements of permeability of kaolin, *Geotechnique*, 37(4), 499-503, 1987.

Zienkiewicz, O.C., P. Mayer and Y. K. Cheung, Solution of anisotropic seepage by finite elements, *J. Eng. Mech.*, 92(1), 111-120, 1966.

APPENDIX 1

COUPLED SEEPAGE-STRESS ANALYSIS FOR TRANSIENT FLOW

I-1 Seepage-Stress-Consolidation Formulation

Biot (1941) presented a coupled theory for consolidation. In the coupled theory, pore water pressures and total stresses are linked by the principle of effective stresses,

$$\sigma_{ij}^t = \sigma_{ij} + \delta_{ij}u \quad (1)$$

where σ_{ij}^t is the total stress, σ_{ij} is the effective stress, δ_{ij} is Kronecker delta and u is the pore water pressure.

From the equations of equilibrium, we obtain

$$\frac{\partial \sigma_{ij}^t}{\partial x_j} + B_i = 0 \quad (2)$$

where B_i is the body force per unit volume. The equation of continuity together with Darcy's law results in

$$\frac{1}{\gamma_w} \left(k_x \frac{\partial^2 u}{\partial x^2} + k_y \frac{\partial^2 u}{\partial y^2} + k_z \frac{\partial^2 u}{\partial z^2} \right) = - \frac{\partial \epsilon_v}{\partial t} \quad (3)$$

where k_x , k_y , k_z are the coefficients of permeability in the x , y and z Cartesian directions and γ_w is the unit weight of water. The volumetric strain ϵ_v is

$$\epsilon_v = \epsilon_x + \epsilon_y + \epsilon_z \quad (4)$$

where ϵ is the principal normal strain in the x, y, z Cartesian directions. The sign convention used is compressive volumetric strain is positive. This equation should be compared with the conventional equation used in ground water modelling, that is,

$$\left(k_x \frac{\partial^2 h}{\partial x^2} + k_y \frac{\partial^2 h}{\partial y^2} + k_z \frac{\partial^2 h}{\partial z^2} \right) = S \frac{\partial h}{\partial t} \quad (5)$$

where S is the storativity and $h (= u/\gamma_w)$ is the head in the aquifer. Thus, we notice that the two equations are identical and

$$-\frac{\partial \epsilon_v}{\partial t} = S \frac{\partial h}{\partial t} \quad (6)$$

The volumetric strain can be found from the constitutive relationship for the porous media. In the case of an elastic porous medium,

$$\epsilon_v = \frac{3(1-2\mu)p}{E} = \frac{p}{K_s} \quad (7)$$

where μ is Poisson's ratio, E is Young's modulus, p is the mean or octahedral effective stress and K_s is the bulk modulus of the soil. Substituting equations (1) and (7) into equation (3), we obtain

$$\left(k_x \frac{\partial^2 u}{\partial x^2} + k_y \frac{\partial^2 u}{\partial y^2} + k_z \frac{\partial^2 u}{\partial z^2} \right) = \frac{1}{K_s} \left(\frac{\partial u}{\partial t} - \frac{\partial p'}{\partial t} \right) \quad (8)$$

or equation (8) can be written as

$$\left(k_x \frac{\partial^2 h}{\partial x^2} + k_y \frac{\partial^2 h}{\partial y^2} + k_z \frac{\partial^2 h}{\partial z^2} \right) = \frac{1}{K_s} \left(\gamma_w \frac{\partial h}{\partial t} - \frac{\partial p'}{\partial t} \right) \quad (9)$$

The superscript t denotes total stress. Thus, through Biot's (1941) theory, the total change in head is equal to the dissipation of the excess head plus the head resulting from the redistribution of total mean stress.

In transient flow, the soil can undergo both elastic and plastic volumetric change. Let us consider the usual void ratio (e) - vertical effective stress consolidation diagram as shown in Fig. I-1a. The curve AM is the loading curve for a normally consolidated soil, MC is the unloading curve and CD is the reloading curve. These curves can be approximated by straight lines in $e - \ln p$ space (Schofield and Wroth, 1968) as shown in Fig. 1b. The hysteric unloading-reloading curves are replaced by a single straight line, MC, of slope κ while the loading curve has a slope of λ . Now consider a soil layer with the ground water level at time, t_0 , at a distance y from the ground surface (Fig. I-2). If the ground water level drops to a new position M, the mean effective stress on a typical element, X, located at a distance z from the surface will increase from say an initial value of p_0 to p_m . The soil consolidates and the total change in void ratio is

$$\delta e = \lambda \ln \frac{p_m}{p_0} \quad (10)$$

and the total volumetric strain is

$$\epsilon_v^t = \frac{\lambda}{1 + e_0} \ln \frac{p_m}{p_0} \quad (11)$$

where e_0 is the initial void ratio. The total volumetric strain can be decomposed into two parts, an elastic part ϵ_v^e and a plastic part ϵ_v^p such that

$$\epsilon_v^t = \epsilon_v^e + \epsilon_v^p \quad (12)$$

If the ground water level were to rise to its original position, the path followed will not be MO but MC (Fig. 1-1b). The soil had previously undergone both elastic and plastic volumetric changes. The elastic volumetric component is obtained from the slope of the line MC whereby

$$\epsilon_v^e = -\frac{\kappa}{1+e_o} \ln \frac{p_m}{p_o} \quad (13)$$

and the plastic component is

$$\epsilon_v^p = \frac{\lambda - \kappa}{1+e_o} \ln \frac{p_m}{p_o} \quad (14)$$

The negative sign in equation (13) indicates expansion or suction (negative head). Suppose that the ground water level now drops at or below the position of the typical soil element. The mean effective stress will now increase to a value p_z which is greater than the maximum past mean effective stress p_m . The total volumetric strain as a result of this loading condition (path CMD) is

$$\epsilon_v^t = \frac{1}{1+e_o} \left\{ \kappa \ln \left(\frac{p_m}{p_o} \right) + \lambda \ln \left(\frac{p_z}{p_m} \right) \right\} \quad (15)$$

If a rise in water level were to subsequently occur up to the original ground water level, the soil will follow path DE. The elasto-plastic volumetric changes resulting from transient conditions can now be easily incorporated into equation (3). For example, if the ground water level fluctuations are within the elastic region, MC, equation (3) becomes

$$\left(k_x \frac{\partial^2 h}{\partial x^2} + k_y \frac{\partial^2 h}{\partial y^2} + k_z \frac{\partial^2 h}{\partial z^2} \right) = \frac{\kappa}{(1+e_o)(p_o' - u)} \frac{\partial}{\partial t} (p_o' - u) \quad (16)$$

and if the past maximum mean effective stress is exceeded, the governing elasto-plastic equation is

$$\left(k_x \frac{\partial^2 h}{\partial x^2} + k_y \frac{\partial^2 h}{\partial y^2} + k_z \frac{\partial^2 h}{\partial z^2} \right) = - \frac{1}{1 + e_o} \left\{ \frac{\lambda}{(p_z^t - u)} \frac{\partial}{\partial t} (p_z^t - u) - \frac{\kappa}{(p_o^t - u)} \frac{\partial}{\partial t} (p_o^t - u) \right\} \quad ..(17)$$

The soil parameters κ and λ can be found by conducting a consolidation test on the soil and finding the slopes of the loading and unloading lines.

The solution for equation (3) over the whole domain is found using standard numerical techniques. For example, for a finite element solution, using Galerkin method with a virtual pore water pressure δu and applying the divergence theorem, equation (3) becomes

$$\begin{aligned} & \frac{1}{\gamma_w} \int_V \left(k_x \frac{\partial \delta u}{\partial x} \frac{\partial u}{\partial x} + k_y \frac{\partial \delta u}{\partial y} \frac{\partial u}{\partial y} + k_z \frac{\partial \delta u}{\partial z} \frac{\partial u}{\partial z} \right) dV^n + \int_V \delta u \frac{\partial \epsilon_v}{\partial t} dV \\ & = \int_A \left(k_x \delta u \frac{\partial u}{\partial x} n_x + k_y \delta u \frac{\partial u}{\partial y} n_y + k_z \delta u \frac{\partial u}{\partial z} n_z \right) dA \end{aligned} \quad (18)$$

where n_x , n_y and n_z are direction cosines of the unit outward normal vector, V is volume and A is the surface area of the domain.

The order to solve this time marching problem, the following approximation is made

$$\int_{t_n}^{t_{n+1}} u(t) dt = \{ (1 - \alpha) u(t_n) + \alpha u(t_{n+1}) \} dt \quad (19)$$

where α is a constant with a magnitude chosen to yield optimum stability. Booker and Small (1975) showed that equation (19) is unconditionally stable provided $\alpha > 0.5$. The virtual work equation, obtained by integrating the equilibrium equations throughout the domain, is

$$\int_V \sigma_{ij}^t \delta \epsilon_{ij} dV = \int_A \sigma_{ij}^t n_j \delta X_i dA + \int_V B_i \delta X_i dV \quad (20)$$

where δ is a small increment, ϵ_{ij} is the strain tensor and X_i is the displacement. The coupled equations (3) and (20) can now be used in a finite element scheme to solve the transient seepage-stress-consolidation problem. The finite element method and programming methodology occur lavishly in the literature (for example, Zienkiewicz et. al., 1966, Hinton and Owen, 1977) and will not be repeated here. In our formulation, we specify a value of $\alpha = 1$.

I-2 Flow in the Unsaturated Zone

Biot's equation is valid for a saturated soil. In order to account for the unsaturated soil domain (soil above the phreatic surface), we selected the invariant mesh procedure (Desai, 1976; Bathe and Khoshgoftaar, 1979, Cividini and Gioda, 1989; Li and Desai, 1983; Lacy and Prevost, 1987). The advantages of using this procedure for transient analysis are presented by Li and Desai (1983). In our analysis, we used the following modifications to effectively use equations (3) and (20).

(1) The real pore water pressures are set to zero for soil domain above the phreatic surface (see Fig. I-3)

(2) Negative pore water pressure distributions (Fig. I-3) are calculated in region A (unsaturated domain). In region B (saturated domain), the pore water pressures are greater than zero.

(3) The permeability of the soil in the unsaturated domain is assumed to be approximately one thousandth of the permeability of the saturated domain (Bathe and Khoshgoftaar, 1979).

(4) The location of the phreatic surface is interpolated between the negative and positive fictitious pore water pressures (Desai, 1984; Li and Desai, 1983).

(5) The permeability in the saturated domain changes as a result of consolidation due to changes in effective stresses from the transient fall and rise of river stage. Based on work done by Wood and Al-Tabba (1987), we adopt an equation of the form

$$k = a e^b \quad (21)$$

where a and b are constants for a particular soil and e is the void ratio. These constants are determined from consolidation tests. The coefficient of permeability will change significantly if the soil is clay or silty clay or very loose sand. For medium dense to dense sand or for clays which have been subjected to many cycles of similar river stage fluctuations, very little change in the coefficient of permeability can be expected unless the loading conditions change.

I-3 Soil Model

We incorporated several constitutive relationships for the soil media in the formulation described earlier. These include isotropic and anisotropic elastic, elastic-rigid plastic and elasto-plastic soil relationships. The elasto-plastic soil model incorporated into the formulation is the modified Cam-clay model (Roscoe and Burland, 1968). The historical river stage records indicate that the sand bars were subjected to river stage fluctuations greater than the current difference in the maximum and minimum river stages. We assumed that the sand in the sand bars can be modelled as an elastic-rigid plastic material obeying the Mohr-Coulomb failure criterion. This criterion is well described in the Soil Mechanics literature. In its simplest form the Mohr-Coulomb failure criterion is given as

$$\tau_f = c + \sigma_f \tan \phi \quad (22)$$

where τ_f is the failure shear strength, c is the cohesion, σ_f is the normal stress at failure and ϕ is the angle of internal friction.

I-4 Procedure for Modelling Seepage Driven Erosion

We instituted the following procedure in the numerical scheme to model seepage driven erosion.

- (a) A check is made at each integration point of every element to find whether the soil at that point has fluidized, i.e. the mean total stress is equal to the pore water pressure. If it is so, then that integration point is flagged as a seepage erosion point. When all the integration points within an element show fluidization, the element is removed from the mesh. Two procedures were adopted. One in which the element was taken out of the mesh and then the mesh was regenerated with the current coordinates. In the other procedure, the element was assigned a low stiffness and a high permeability. There was very little difference in the results from these two procedures. However, the latter procedure was more computationally efficient and was adopted.
- (b) A check is made at each integration point to determine whether failure according to the Mohr-Coulomb occurs. A report is generated identifying all points that reach failure.

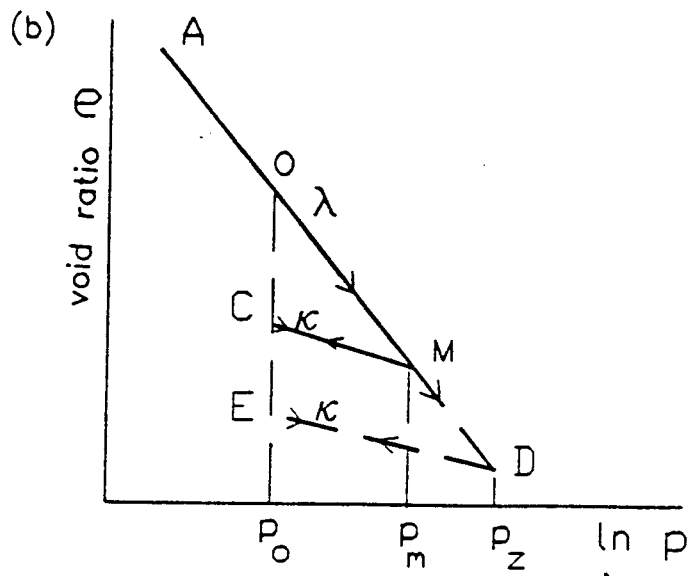
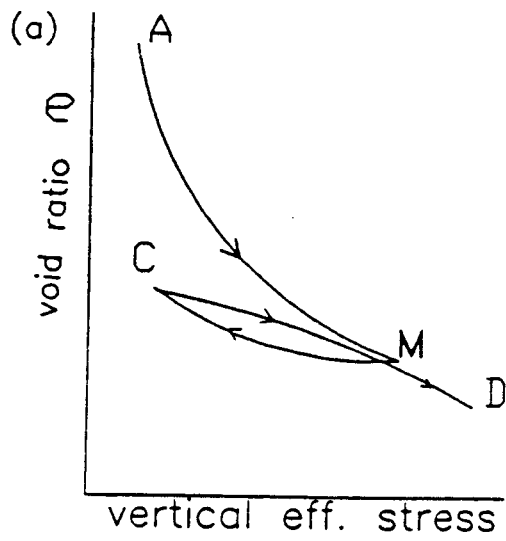


Fig. 1.1 (a) void ratio - vertical effective stress relationship.
 (b) void ratio - mean effective stress relationship.

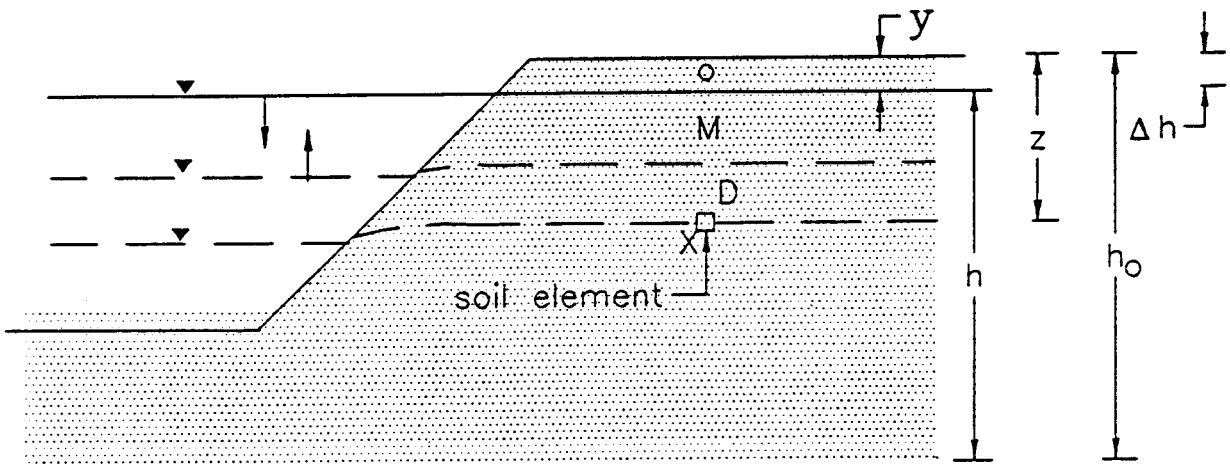


Fig. 1.2 Effects of water level variation on a typical soil element.

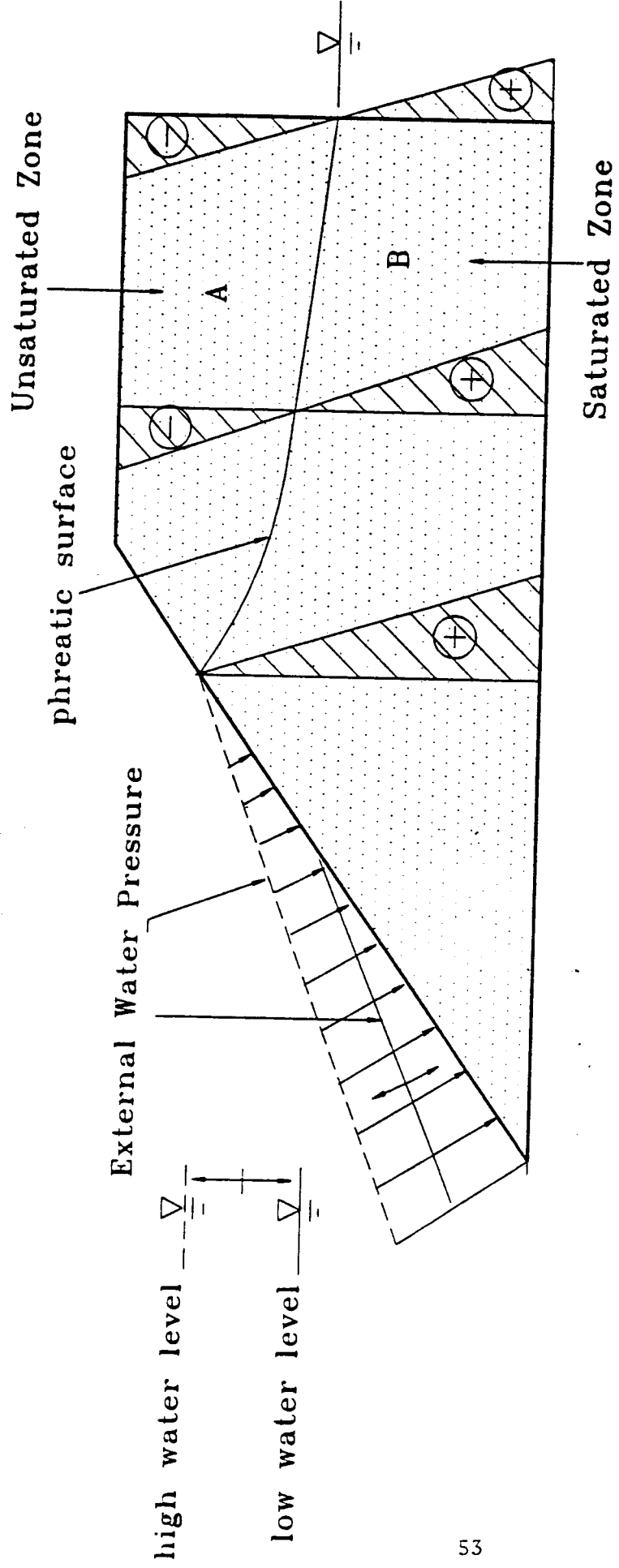


Fig. 1.3 Pore water pressure head variation assumed in the saturated and the unsaturated zones.

APPENDIX II

BOUNDARY ELEMENT METHOD FOR FLOW THROUGH POROUS MEDIA

by

D.N. Contractor and M. Budhu

The boundary element method is one of the several numerical analyses for the solution of flow through porous media, whose governing equation is the classical Laplace equation. This method uses integral transformations and only the boundary needs to be discretized. The values for internal points are then interpolated from the boundary solutions. Since all numerical approximations take place at the boundaries, the dimensionality of the problem (line integration for two-dimensional and surface integration for three-dimensional problem) is reduced by one and a smaller system of equations is obtained in comparison with those determined through differential methods e.g. finite element method. The integral equation for the linear problem represents a relationship between the unknown (potential for fluid flow) and the source density or free space Green's function. The source density is the Newtonian potential for three-dimensional problems or the logarithmic potential for two-dimensional problems and is called the fundamental solution to Laplace's equation. To find the unknowns on the boundary, the boundary is discretized into a series of small segments assuming that the source density remains constant within each element. By using the method of collocation, the discretized equation is applied to a number of particular nodes in each element, and the influence coefficients are computed approximately using Simpson's rule. This results in a system of linear algebraic equations which can be readily solved. The governing boundary integral equations for two-dimensional free surface flow problems are presented in the following.

The expression of continuity in a two-dimensional plane can be written in terms of divergence theorem as:

$$\int_D (\nabla \cdot v) dA = \int_{\Omega} v \cdot n dS \quad \text{II-1}$$

Where ∇ is the vector operator, v is any differentiable vector, D is the domain of integration, Ω is the boundary of D and n is the unit outward normal to D on Ω .

If we take v as $U\nabla u$, where U and W are two functions, twice differentiable in D , such that the equation II-1 can be written as

$$\int_D (U\nabla^2 W - W\nabla^2 U) dA = \int_{\Omega} (U\nabla W - W\nabla U) \cdot n dS \quad \text{II-2}$$

The above equation is *Green's* second identity. Substituting $\nabla W \cdot n = \frac{\partial W}{\partial n}$ and $\nabla U \cdot n = \frac{\partial U}{\partial n}$, the above equation follows

$$\int_D (U \nabla^2 W - W \nabla^2 U) dA = \int_a \left[U \frac{\partial W}{\partial n} - W \frac{\partial U}{\partial n} \right] dS \quad \text{II-3}$$

In Equation II-3, U and W are chosen such that they satisfy Laplace's equation, i.e., $\nabla^2 U = \nabla^2 W = 0$. Then the Equation II-3 becomes (Liggett et al., 1983)

$$\int_a \left[U \frac{\partial W}{\partial n} - W \frac{\partial U}{\partial n} \right] dS = 0 \quad \text{II-4}$$

In the case of potential problem, U is chosen as velocity potential, ϕ , and W is chosen as the 'free space Green's function' which satisfies $\nabla^2 W = 0$ everywhere in D except at the source point P as shown in Fig. II-1a where it becomes infinity. For two-dimensional problems, logarithm potential, i.e. free space green function, W is (Brebbia et al., 1984)

$$W = \ln(r) \quad \text{II-5}$$

where r is the distance between the source point P inside the boundary and the field point Q on the boundary as shown in Fig. II-1. In order to apply equation II-4 to find the potential at P, the point P is excluded by a small circle of radius r to avoid singularity. Thus, the integral equation II-4 becomes

$$\int_r \left[\phi \frac{\partial \ln(r)}{\partial n} - \ln(r) \frac{\partial \phi}{\partial n} \right] ds + \lim_{r \rightarrow 0} \int_a \left[\phi \frac{\partial \ln(r)}{\partial n} - \ln(r) \frac{\partial \phi}{\partial n} \right] ds = 0 \quad \text{II-6}$$

Upon applying limit to the second integral of equation II-6, it follows

$$\lim_{r \rightarrow 0} \int_a \left[-\phi \frac{\partial \ln(r_o)}{\partial n} - \ln(r_o) \frac{\partial \phi}{\partial r} \right] r_o d\theta = 2\pi\phi(P) \quad \text{II-7}$$

Since,

$$\lim_{r \rightarrow 0} \ln(r_o) r_o = 0 \quad \text{II-8a}$$

and

$$\frac{\partial \ln(r)}{\partial n} = \frac{1}{r} \frac{\partial r}{\partial n} = \frac{1}{r} (\nabla r \cdot n) = -\frac{1}{r} \quad \text{II-8b}$$

Equation II-6 can be written as

$$2\pi\phi(P) = \int_r \left[\phi(Q) \frac{\partial \ln(r)}{\partial n} - \ln(r) \frac{\partial \phi(Q)}{\partial n} \right] ds \quad \text{II-9}$$

To find the potential inside the boundary, ϕ and $\frac{\partial \phi}{\partial n}$ must be known everywhere on the boundary. Since, both ϕ and $\frac{\partial \phi}{\partial n}$ are not all known, the point P is moved to the boundary to complete the boundary data as shown in Fig. II. The same consideration holds as before except that the integration as indicated in equation II-9 takes place over an angle which is less than 2π . Therefore, it is necessary to modify equation II-9 as

$$c\phi(P) = \int_r \left[\frac{\phi}{r} \frac{\partial r}{\partial n} - \ln(r) \frac{\partial \phi}{\partial n} \right] ds \quad \text{II-10}$$

In which c is the angle between the boundary segment at P as shown in Fig. II-1b and is equal to 2π for internal point. The boundary data is completed by discretizing the boundary and considering the representative source point as (i) and field points as (j, j+1) (Fig. II-1c).

If N is the total number of elements and nodes for a closed boundary, for each source point i , an equation which relates ϕ and $\frac{\partial \phi}{\partial n}$ over all elements is obtained. In this case equation II-10 can be written as

$$c\phi(i) = \int_r \left[\frac{\phi}{r} \frac{\partial r}{\partial n} - \ln(r) \frac{\partial \phi}{\partial n} \right] d\Gamma = \sum_{j=1}^N \int_{\alpha_j}^{\alpha_{j+1}} \left[\frac{\phi}{r} \frac{\partial r}{\partial n} - \ln(r) \frac{\partial \phi}{\partial n} \right] d\alpha \quad \text{II-11}$$

Assuming a linear variation of potential and its normal derivatives between the nodes in the element such that

$$\phi = \frac{\alpha_{j+1} + l_j - \alpha}{l_j} \phi_j + \frac{\alpha - \alpha_j}{l_j} \phi_{j+1} \quad \text{II-12a}$$

$$\frac{\partial \phi}{\partial n} = \frac{\alpha_{j+1} + l_j - \alpha}{l_j} \left[\frac{\partial \phi}{\partial n} \right]_j + \frac{\alpha - \alpha_j}{l_j} \left[\frac{\partial \phi}{\partial n} \right]_{j+1} \quad \text{II-12b}$$

and from Fig. II-1c

$$\frac{\partial r}{\partial n} = \cos\theta = \frac{\beta_j}{r_{i,\alpha}} \quad \text{II-12c}$$

Equation II-11 becomes

$$\int_{\alpha_v}^{\alpha_v+l_j} \left[\frac{\phi}{r} \frac{\partial r}{\partial n} - \ln(r) \frac{\partial \phi}{\partial n} \right] d\alpha = \int_{\alpha_v}^{\alpha_v+l_j} \frac{\beta_{ij}}{r_{i\alpha}^2} \left[\frac{\alpha_{ij}+l_j-\alpha}{l_j} \phi_j + \frac{\alpha-\alpha_{ij}}{l_j} \phi_{j+1} \right] d\alpha \quad \text{II-13}$$

$$- \int_{\alpha_v}^{\alpha_v+l_j} \ln(r_{i\alpha}) \left[\frac{\alpha_{ij}+l_j-\alpha}{l_j} \left[\frac{\partial \phi}{\partial n} \right]_j + \frac{\alpha-\alpha_{ij}}{l_j} \left[\frac{\partial \phi}{\partial n} \right]_{j+1} \right]$$

or

$$A_{1ij} \phi_j + A_{2ij} \phi_{j+1} + B_{1ij} \left[\frac{\partial \phi}{\partial n} \right]_j - B_{2ij} \left[\frac{\partial \phi}{\partial n} \right]_{j+1} \quad \text{II-14}$$

where, for non singular case ($j \neq i - 1$ or $j \neq i$)

$$A_{1ij} = \frac{\beta_{ij}}{l_j} \left[(\alpha_{ij}+l_j) \int_{\alpha_v}^{\alpha_v+l_j} \frac{1}{\beta_{ij}^2+\alpha^2} d\alpha - \int_{\alpha_{ij}}^{\alpha_v+l_j} \frac{\alpha}{\beta_{ij}^2+\alpha^2} d\alpha \right] \quad \text{II-15a}$$

or

$$A_{1ij} = \frac{\alpha_{ij}+l_j}{l_j} \left[\tan^{-1} \left[\frac{\alpha_{ij}+l_j}{\beta_{ij}} \right] - \tan^{-1} \left[\frac{\alpha_{ij}}{\beta_{ij}} \right] \right] - \frac{\beta_{ij}}{2l_j} \ln \frac{\beta_{ij}^2+\alpha_{ij}+l_j^2}{\beta_{ij}^2+\alpha_{ij}^2} \quad \text{II-15b}$$

$$A_{2ij} = \frac{\beta_{ij}}{l_j} \int_{\alpha_v}^{\alpha_v+l_j} \frac{\alpha}{\beta_{ij}^2+\alpha^2} d\alpha - \frac{\beta_{ij}}{l_j} \cdot \alpha_{ij} \int_{\alpha_v}^{\alpha_v+l_j} \frac{1}{\beta_{ij}^2+\alpha^2} d\alpha \quad \text{II-16a}$$

or

$$A_{2ij} = -\frac{\alpha_{ij}}{l_j} \left[\tan^{-1} \left[\frac{\alpha_{ij}+l_j}{\beta_{ij}} \right] - \tan^{-1} \left[\frac{\alpha_{ij}}{\beta_{ij}} \right] \right] + \frac{\beta_{ij}}{2l_j} \ln \frac{\beta_{ij}^2+\alpha_{ij}+l_j^2}{\beta_{ij}^2+\alpha_{ij}^2} \quad \text{II-16b}$$

$$B_{1ij} = \frac{\alpha_{ij}+l_j}{l_j} \int_{\alpha_v}^{\alpha_v+l_j} \ln(r_{i\alpha}) d\alpha - \frac{1}{l_j} \int_{\alpha_v}^{\alpha_v+l_j} \alpha \ln(r_{i\alpha}) d\alpha \quad \text{II-17a}$$

or

$$B_{1ij} = \frac{\alpha_{ij} + l_j}{l_j} \left[\alpha_{ij} \ln \frac{r_{ij+1}}{r_{ij}} + l_j \{ \ln(r_{ij+1}) - 1 \} + \beta_{ij} \left\{ \tan^{-1} \left[\frac{\alpha_{ij} + l_j}{\beta_{ij}} \right] - \tan^{-1} \left[\frac{\alpha_{ij}}{\beta_{ij}} \right] \right\} \right] - \frac{1}{4l_j} [r_{ij+1}^2 (2 \ln(r_{ij+1}) - 1) - r_{ij}^2 (2 \ln(r_{ij}) - 1) - r_{ij}^2 (2 \ln(r_{ij}) - 1)] \quad \text{II-17b}$$

$$B_{2ij} = \int_{\alpha_{ij}}^{\alpha_{ij} + l_j} \ln(r_{i\alpha}) \frac{\alpha - \alpha_{ij}}{l_j} d\alpha \quad \text{II-18a}$$

or

$$B_{2ij} = -\frac{\alpha_{ij}}{l_j} \left[\alpha_{ij} \ln \frac{r_{ij+1}}{r_{ij}} + l_j \{ \ln(r_{ij+1}) - 1 \} + \beta_{ij} \left\{ \tan^{-1} \left[\frac{\alpha_{ij} + l_j}{\beta_{ij}} \right] - \tan^{-1} \left[\frac{\alpha_{ij}}{\beta_{ij}} \right] \right\} \right] - \frac{1}{4l_j} [r_{ij+1}^2 (2 \ln(r_{ij+1}) - 1) - r_{ij}^2 (2 \ln(r_{ij}) - 1)] \quad \text{II-18b}$$

and for singular case ($j=i$ and $j=i-1$)

$$j=i-1, \quad A_{1ij} = A_{2ij} = 0; \quad B_{1ij} = \frac{l_j}{4} (2 \ln(l_j) - 1); \quad B_{2ij} = \frac{l_j}{4} (2 \ln(l_j) - 3) \quad \text{II-19}$$

$$j=i, \quad A_{1ij} = A_{2ij} = 0; \quad B_{1ij} = \frac{l_j}{4} (2 \ln(l_j) - 3); \quad B_{2ij} = \frac{l_j}{4} (2 \ln(l_j) - 1) \quad \text{II-20}$$

Finally, equation II-11 can be written as,

$$\sum_{j=1}^N L_{ij} \phi_j = \sum_{j=1}^N R_{ij} \left[\frac{\partial \theta}{\partial n} \right]_j \quad \text{II-21}$$

where, $L_{ij} = A_{2ij}$ (previous element) + A_{1ij} (following element) - $\delta_{ij}c_i$ and $R_{ij} = B_{2ij}$ (previous element) + B_{1ij} (following element) in which $\delta_{ij} = 0$ for $i \neq j$ and $\delta_{ij} = 1$ for $i = j$. By moving the source point around the boundary, i.e., $i=1$ to N , the following matrix equation is obtained.

$$[L]\phi = [K] \left\{ \frac{\partial \phi}{\partial n} \right\} \quad \text{II-22}$$

where

$$\{\phi\} = [\phi_1, \phi_2 \dots \phi_N]^T$$

and

$$\left\{ \frac{\partial \phi}{\partial n} \right\} = \left[\left\{ \frac{\partial \phi}{\partial n} \right\}_1, \left\{ \frac{\partial \phi}{\partial n} \right\}_2, \dots, \left\{ \frac{\partial \phi}{\partial n} \right\}_N \right]^T$$

Out of 2N values for ϕ and $\frac{\partial \phi}{\partial n}$, N values will be known from the boundary conditions for a given problem. Equation II-22 can then be solved for the other N values and Equation II-9 can be used to calculate the potential at internal points. The boundary conditions as required for the solution of the N values are as follows.

Along the upstream and downstream surface, potentials are given by

$$\phi = h_1 \quad \text{II-23}$$

$$\phi = h_2 \quad \text{II-24}$$

where h_1 and h_2 are equal to the heights of the water level of the upstream and downstream side respectively (Dirichlet condition). For impervious layer, normal derivative of the potential is zero, i.e.

$$\frac{\partial \phi}{\partial n} = 0 \quad \text{II-25}$$

This means that there is no flow through impervious layer (Neuman condition). Along the seepage surface, potential is equal to the vertical elevation, z, i.e.

$$\phi = z \quad \text{II-26}$$

For unsteady flow, the boundary condition of the free surface is

$$\phi = \eta \quad \text{II-27}$$

where η represents the vertical location of the free surface which is a function of horizontal distance, x and the time, t. For porous media, since the free surface is a material surface, the rate of change of the position of the free surface is equal to vertical velocity on the free surface, i.e.

$$-\frac{\partial \eta}{\partial t} + \frac{q}{n} \cdot \nabla(z-\eta) = 0 \quad \text{II-28}$$

where q is the specific discharge and n is the porosity. If the unit vector is defined as

$$\hat{n} = \frac{\nabla(z-\eta)}{|\nabla(z-\eta)|}$$

the above equation can be written in the following form

$$\frac{\partial \eta}{\partial t} = \frac{q}{n} \cdot \hat{n} |\nabla(z-\eta)| \quad \text{II-29}$$

Substituting

$$|\nabla(z-\eta)| = \left[1 + \left(\frac{\partial \eta}{\partial x} \right)^2 \right]^{\frac{1}{2}}$$

and

$$q = -k \nabla \phi$$

we obtain

$$\frac{\partial n}{\partial t} = -\frac{k}{n} \left[1 + \left(\frac{\partial \eta}{\partial x} \right)^2 \right]^{\frac{1}{2}} \nabla \phi \cdot \hat{n} \quad \text{II-30}$$

or

$$\frac{\partial \eta}{\partial t} = -\frac{k}{n} \left[1 + \left(\frac{\partial \eta}{\partial x} \right)^2 \right]^{\frac{1}{2}} \frac{\partial \phi}{\partial n} \quad \text{II-31}$$

Assuming a dimensionless time, t_D such that

$$t_D = \frac{tk}{nL}$$

where t is the real time, k is the hydraulic conductivity and L is the characteristic length scale, equation II-31 becomes

$$\frac{\partial \eta}{\partial t} = - \left[1 + \left(\frac{\partial \eta}{\partial x} \right)^2 \right]^{\frac{1}{2}} \frac{\partial \phi}{\partial n} \quad \text{II-32}$$

or

$$\left[\frac{\partial \phi}{\partial t} \right]_x = -(1 + \tan^2 \beta)^{\frac{1}{2}} \frac{\partial \phi}{\partial n} \quad \text{II-33}$$

where β is the angle between the free surface profile and the x-axis such that $\frac{\partial \eta}{\partial x} = -\tan \beta$ and $\phi = \eta$. Alternately, equation II-31 can be written as

$$\left[\frac{\partial \phi}{\partial t} \right]_x = \frac{1}{\cos \beta} \frac{\partial \phi}{\partial n} \quad \text{II-34}$$

In finite difference form using weighting factor θ for $t + \Delta t$, we obtain

$$\frac{\phi_{i+\Delta t} - \phi_i}{\Delta t} = \frac{1}{\cos \beta} \left[\theta \left[\frac{\partial \phi}{\partial t} \right]_{i+\Delta t} + (1-\theta) \left[\frac{\partial \phi}{\partial t} \right]_i \right] \quad \text{II-35}$$

or

$$\phi_{i+\Delta t} = \phi_i - \frac{\Delta t}{\cos \beta} \left[\theta \left[\frac{\partial \phi}{\partial n} \right]_{i+\Delta t} + (1-\theta) \left[\frac{\partial \phi}{\partial n} \right]_i \right] \quad \text{II-36}$$

Equation II-36 indicates that, if ϕ and $\frac{\partial \phi}{\partial n}$ can be computed at time t then ϕ and $\frac{\partial \phi}{\partial n}$ can be computed at time $t+\Delta t$ on the free surface.

REFERENCES

1. Liggett, James A. and Liu, Philip L-F., "The Boundary Integral Equation Method for Porous media Flow," George Allen & Unwin (Publishers) Ltd., 1983.
2. Brebbia, C.A., Telles, J.C.F. and Wrobel, L.C., "Boundary Element Techniques," Springer-Verlag (publishers), 1984.

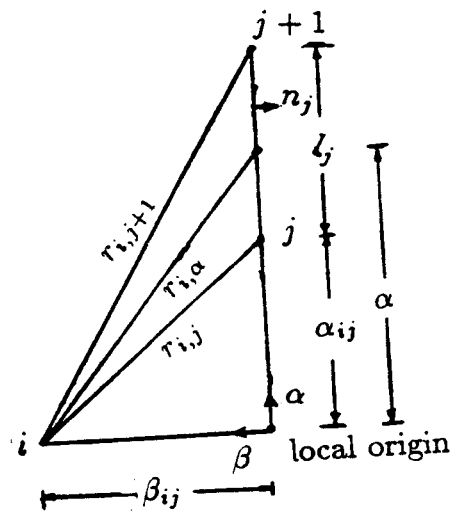
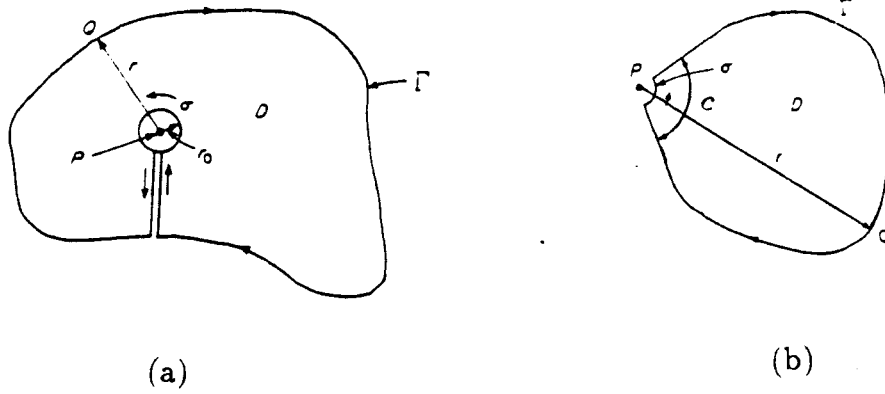


Figure II-1. A typical boundary for 2-D potential problem. (a) Domain D surrounded by the boundary curve Γ and the singular point P is separated from D by the circle σ (b) Point P on the boundary contour forms an angle (c) $\alpha - \beta$ coordinate system.

APPENDIX III

SOIL TEST RESULTS

III-1 INTRODUCTION

The following laboratory tests were performed on sand bars -6.5R, 43 and 172 to determine the relevant soil properties required for the finite element model and the interpretation of the field results.

- (i) Grain size analysis (sieve analysis)
- (ii) Specific gravity
- (iii) Direct shear (shear box)
- (iv) Constant head permeability
- (v) Maximum and minimum void ratio
- (vi) In-situ void ratio and density
- (vii) Compaction test (Standard Proctor)
- (viii) Angle of repose under water

Tests (i) to (vii) were carried out according to the relevant ASTM standards. Tests (viii) is non-standard and will be explained later in this Appendix.

III-2 GRAIN SIZE ANALYSIS

A sieve analysis is performed by shaking the soil sample through a stack of sieves with openings of a known size. The proportion of the soil retained on each sieve is then determined. The grain size of a particle is taken to be that of the sieve on which it is retained. The results of the grain size analysis are shown in Fig. III.1 to Fig III.5

A summary of the results is presented in Table III.1

Table III.1 Summary of grain size analysis (average values)

SAND BAR	D ₁₀	D ₅₀	C _u	C _c
-6.5R	0.05	0.15	6	1
43	0.12	0.24	2	1
172	0.01	0.2	2	1

III-3 SPECIFIC GRAVITY TEST

The specific gravity of a soil is the ratio of the mass of a given volume of the soil at 77° F (25° C) or at 60° F (15.6° C) to the mass of an equal volume of distilled water at the same temperature. The specific gravity of a soil is useful in relating mass

to volume. Thus, if the void ratio ,degree of saturation and specific gravity of a soil are known,the unit weight of a soil can be computed.In this study a knowledge of the unit weight of the soil was essential since it significantly influences the stability characteristics.

The test was carried out on three samples from each sand bar (-6.5R, 43 and 172). The results reveal that the specific gravity of the sand bar material is essentially the same for all three sand bars..

The following results were obtained:
 Average specific gravity = 2.68
 Maximum value obtained = 2.68
 Minimum value obtained = 2.67

III-4 DIRECT SHEAR TEST

The shear strength of a soil can be defined as the maximum shear force that a soil can resist before failing. The shear strength of a soil is not a fundamental property and is related to in-situ conditions such as moisture content and can vary with time. In all soil stability problems, a knowledge of the shear strength of a soil is necessary.

This test was performed using a shear box test following the ASTM test procedure. Disturbed samples were tested. These samples were placed in the mold and immersed in water. The samples were allowed to drain before testing.

The results of this test are shown in the Fig III.6 to Fig. III.8 and summarized in Table III.2

Table III.2 Shear box Test Results

SAND BAR	ANGLE OF FRICTION (°)	COHESION (kN/m ²)
-6.5 R	28	1.00
43	30	0.75
172	32	2.00

III-5 PERMEABILITY

In-situ permeability measurements were made by the USGS. To supplement the in-situ data constant head laboratory permeability tests were conducted. The sand bar material was placed in the permeameter and lightly compacted using a tamper. The sample was then immersed in water and a vacuum applied to achieve fully saturation.

Three different samples were used. The test was repeated five times on each sample over a three minute time span. The following value was obtained as the

average of all the tests:

$$\begin{aligned} \text{Average permeability} &= 4.444 \times 10^{-5} \text{ m/s} \\ \text{Standard deviation} &= 3.775 \times 10^{-6} \text{ m/s} \end{aligned}$$

III-6 COMPACTION TEST

Compaction is a term used to describe the closeness of the packing of the soil particles. Compaction of a soil is achieved by forcing the soil particles closer together thereby reducing the volume of air within the soil mass. Soil strength increases as its degree of compaction increases.

The compaction test performed was the Standard Proctor test. This test is used to determine the maximum dry density and the optimum moisture content of a soil. This test is performed by placing the soil sample in three equal layers at a known water content in a standard mold. Each layer is compacted using a specified compaction effort. The procedure is repeated with different moisture contents.

The following results were obtained (see Fig. III.9)

$$\begin{aligned} \text{Maximum dry density} &= 1750 \text{ kg/m}^3 \\ \text{Optimum moisture content} &= 4.9\% \end{aligned}$$

III-7 MAXIMUM AND MINIMUM VOID RATIO

The maximum void ratio indicates the densest state of compaction which a soil can attain using a standard laboratory procedure which minimizes particle segregation and breakdown. This test for minimum void ratio is performed by placing a measured mass of a soil sample in a mold of known volume. The soil sample is then compacted by placing it on a vibrating table operating at a specified frequency and amplitude for a specified time period. The final volume of the soil is then measured and the maximum void ratio calculated. The minimum void ratio indicates the loosest state of compaction. The results of the maximum and minimum void ratio tests are shown in the Table III.3.

Table III.3 Maximum and Minimum Void Ratio

SAND BAR	MAX. VOID RATIO	MIN. VOID RATIO
-6.5R	1.021	0.569
43	1.012	0.531
172	0.951	0.523

III-9 IN-SITU VOID RATIO AND DENSITY

This test was performed on samples obtained in-situ. These samples were obtained by gently forcing a sampling tube into the sand bar material. The sample were sealed to prevent loss of moisture. The following results were obtained (Table III.4).

Table III.4 In situ Void Ratio and Density

SAND BAR	VOID RATIO	DRY DENSITY (kg/m ³)	BULK DENSITY (kg/m ³)
6.5R	0.759	1520	1741
43	0.722	1537	1783
172	0.847	1426	1627

III-10 ANGLE OF REPOSE UNDER WATER

This test was performed to determine the angle of repose of a soil deposited under water under various flow velocities. The maximum possible slope angle to which a dry cohesionless material will stand unsupported is equal to its angle of repose. There is no established work for the case of a soil deposited under flowing water. Since the sand bar material in the Grand Canyon is deposited under water flowing at various velocities, a laboratory test was devised to simulate the deposition of particles in water under a velocity gradient.

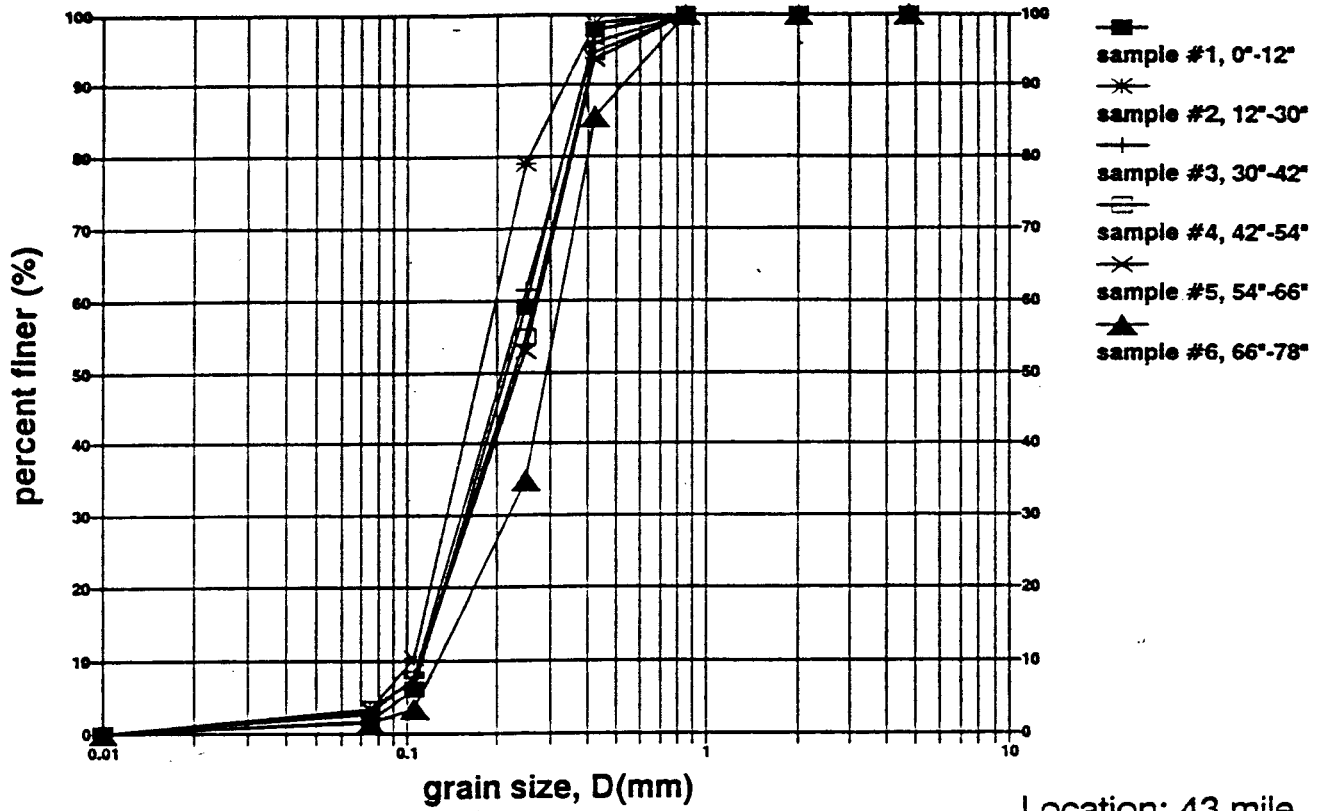
The test was performed using a rectangular tank with an outflow control valve near the bottom through which the rate of flow in the tank could be controlled. This tank was filled with water and the sand was gently poured under the following conditions.

(a) the outflow valve was closed. This simulates deposition under static conditions.

(b) the outflow valve was opened from partial opening to full opening to give a range of flow rates. The results of this test are shown in Fig. III.10

SIEVE ANALYSIS

BORE HOLE #A

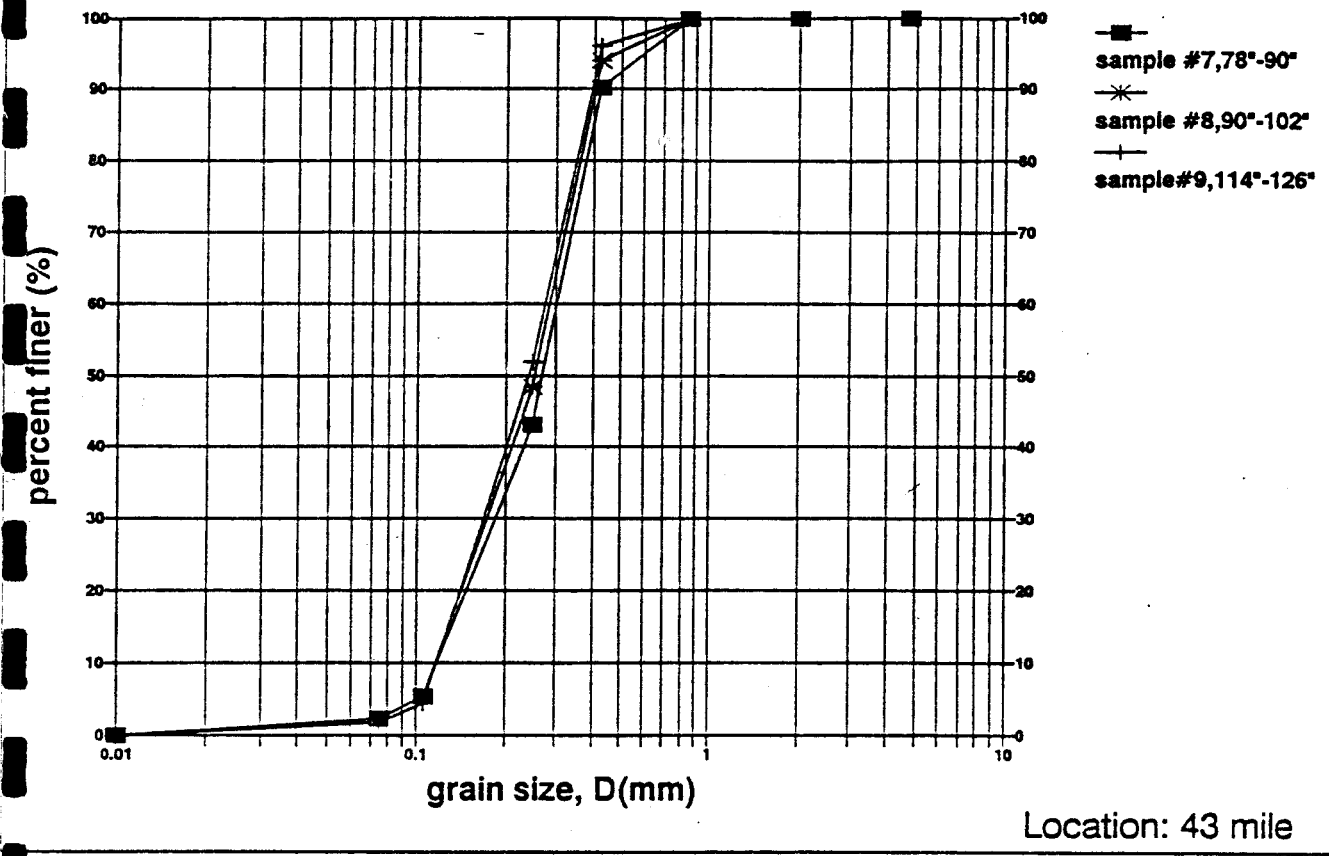


sample no	D10(mm)	D30(mm)	D50(mm)	D60(mm)	Cu	Cc
1	0.12	0.16	0.23	0.26	2.166667	0.820513
2	0.11	0.14	0.18	0.2	1.818182	0.890909
3	0.12	0.16	0.21	0.25	2.083333	0.853333
4	0.12	0.17	0.24	0.28	2.333333	0.860119
5	0.12	0.17	0.24	0.28	2.333333	0.860119
6	0.13	0.23	0.3	0.33	2.538462	1.2331

Fig. III.1 Grain size analysis for sand bar 43

SIEVE ANALYSIS

BORE HOLE #A

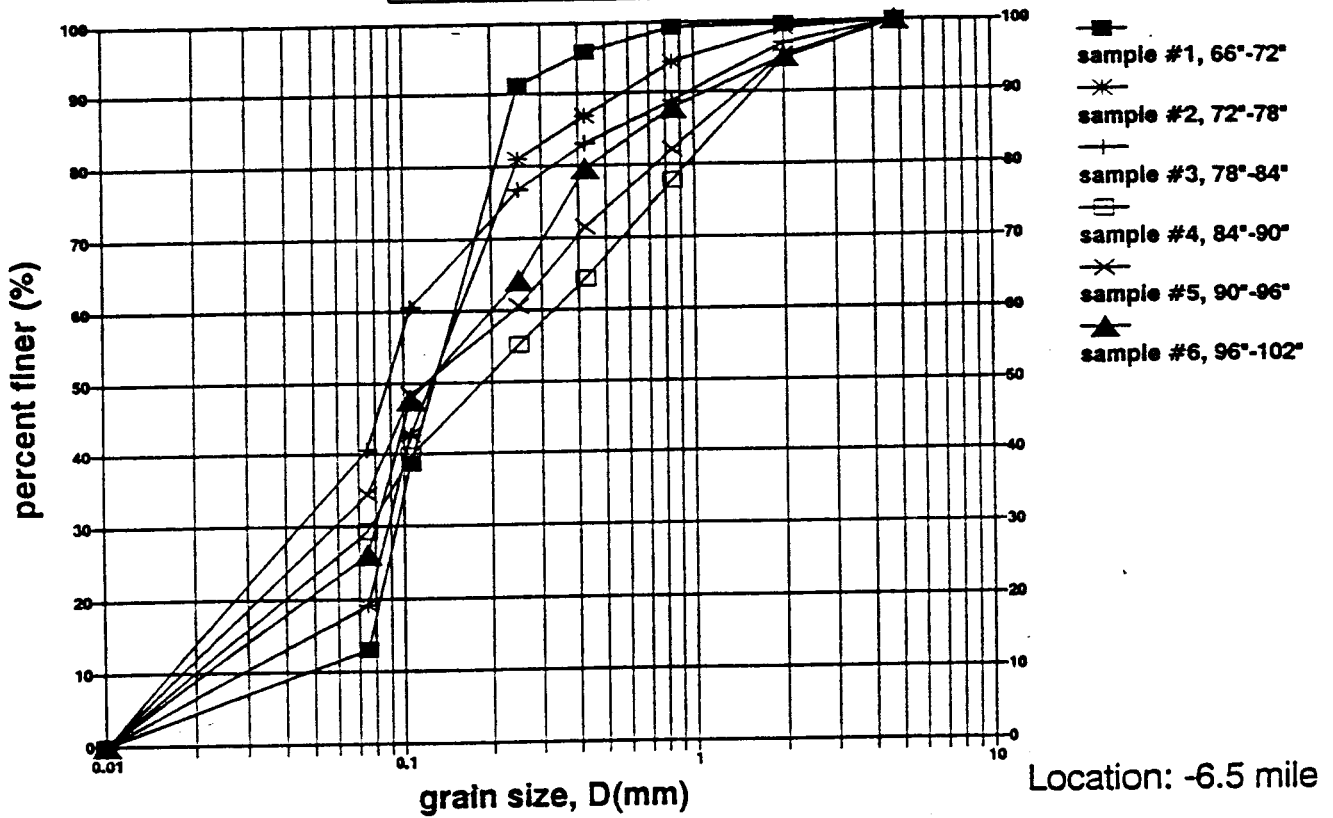


sample no	D10(mm)	D30(mm)	D50(mm)	D60(mm)	Cu	Cc
7	0.13	0.18	0.27	0.3	2.307692	0.830769
8	0.13	0.17	0.26	0.29	2.230769	0.766578
9	0.13	0.17	0.25	0.28	2.153846	0.793956

Fig. III. 2 Grain size analysis for sand bar 43

SIEVE ANALYSIS

BORE HOLE #1

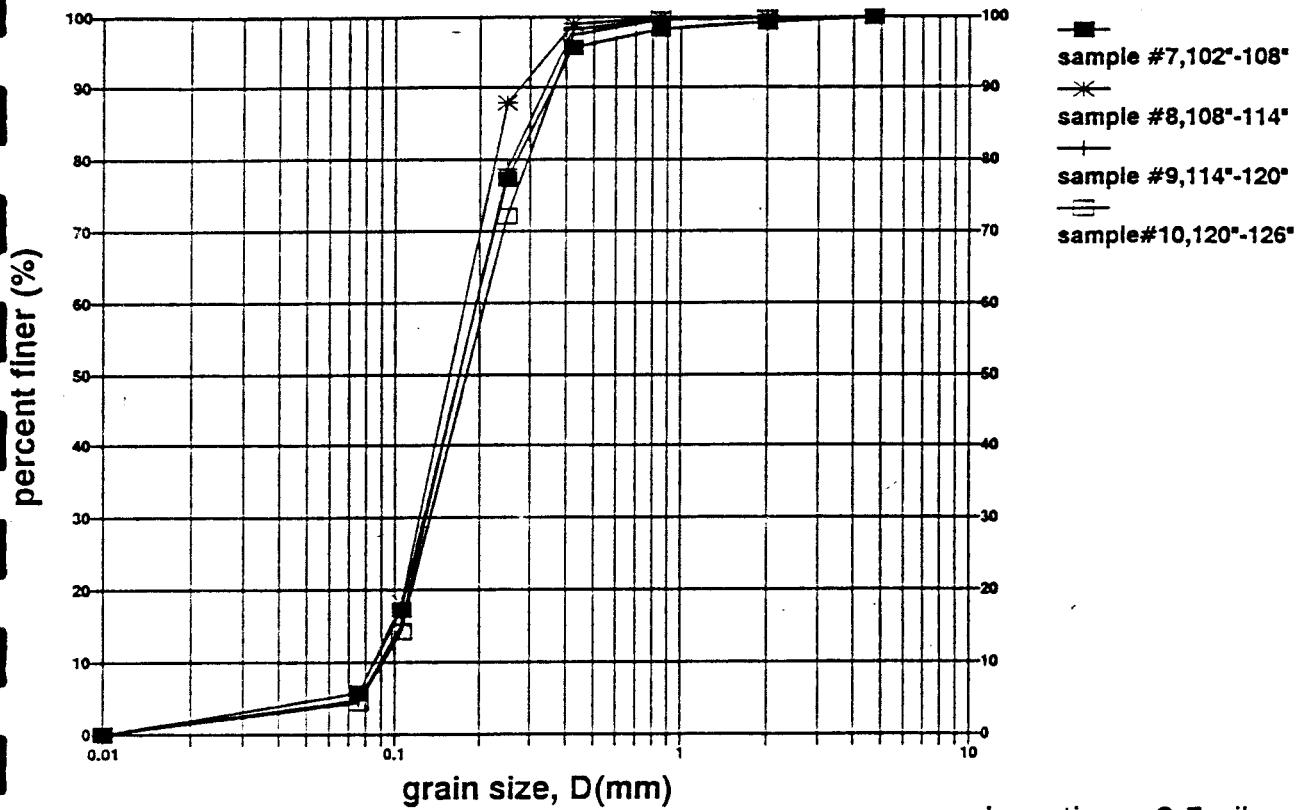


sample no	D10(mm)	D30(mm)	D50(mm)	D60(mm)	Cu	Cc
1	0.037	0.095	0.13	0.15	4.054054	1.626126
2	0.028	0.088	0.128	0.16	5.714286	1.728571
3	0.017	0.044	0.089	0.11	6.470588	1.035294
4	0.02	0.077	0.19	0.34	17	0.871912
5	0.018	0.057	0.115	0.25	13.88889	0.722
6	0.022	0.08	0.116	0.2	9.090909	1.454545

Fig. III. 3 Grain size analysis for sand box 6.57

SIEVE ANALYSIS

BORE HOLE #1

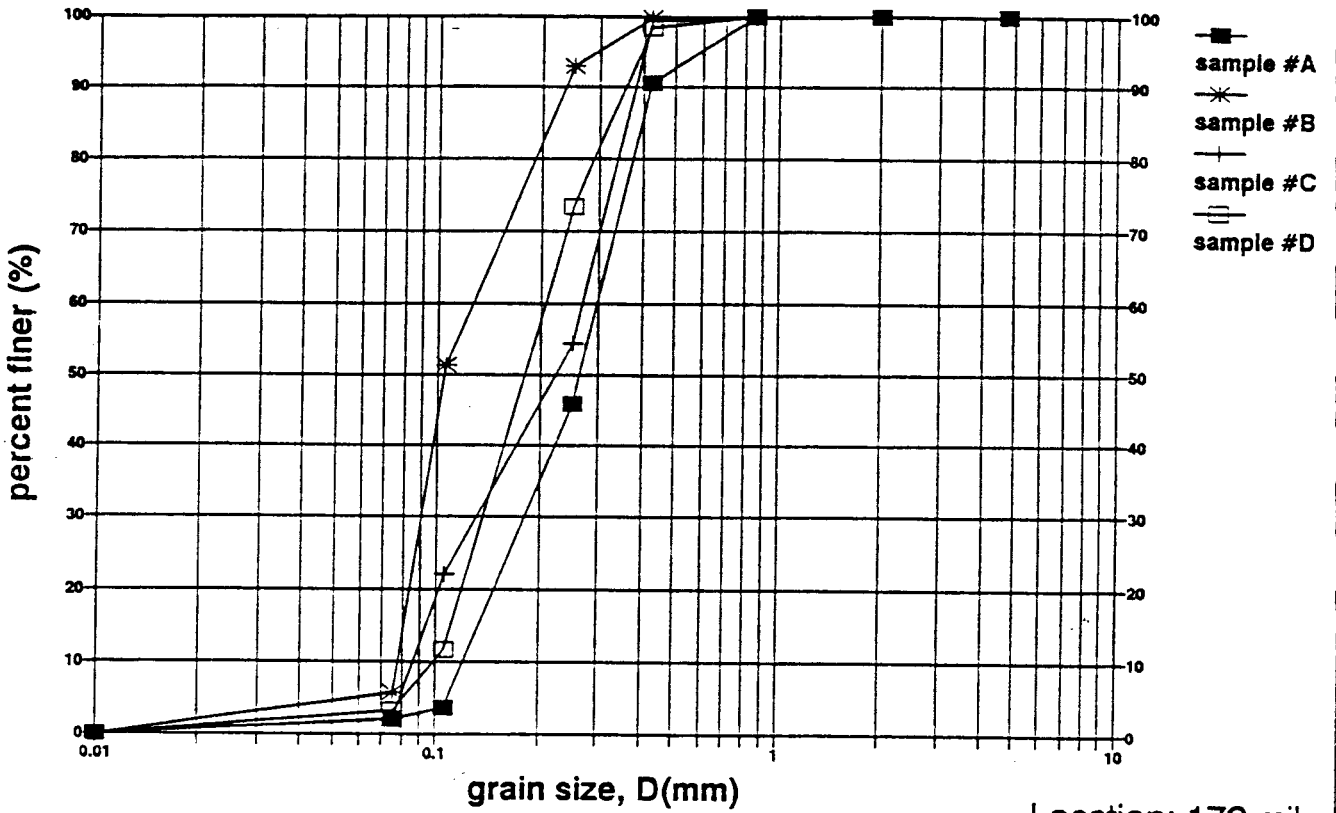


sample no	D10(mm)	D30(mm)	D50(mm)	D60(mm)	Cu	Cc
7	0.085	0.125	0.17	0.19	2.235294	0.967492
8	0.086	0.129	0.16	0.175	2.034884	1.105714
9	0.09	0.13	0.17	0.19	2.111111	0.988304
10	0.092	0.133	0.18	0.22	2.391304	0.873962

Fig. III. 4 Grain size analysis for sand bar -6.5R

SIEVE ANALYSIS

BORE HOLE #6



sample no	D10(mm)	D30(mm)	D50(mm)	D60(mm)	Cu	Cc
1	0.125	0.17	0.26	0.3	2.4	0.770667
2	0.078	0.09	0.11	0.14	1.794872	0.741758
3	0.088	0.14	0.23	0.27	3.068182	0.824916
4	0.1	0.15	0.18	0.22	2.2	1.022727

Fig. III. 5 Grain size analysis for sand bar 172L

BEACH 0.5 MILE
DIRECT SHEAR RESULTS

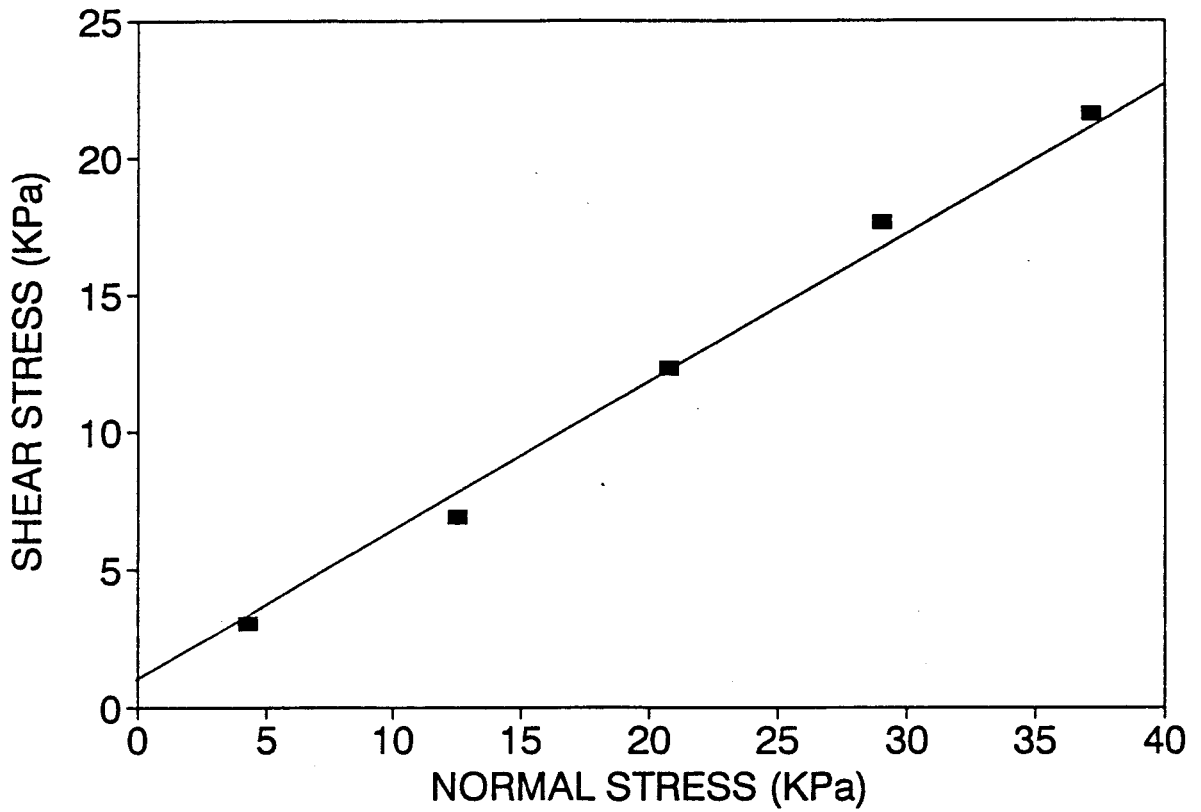


Fig. III. 6 Direct shear tests on sand from sand bar -6.5R.

BEACH 43 MILE
DIRECT SHEAR RESULTS

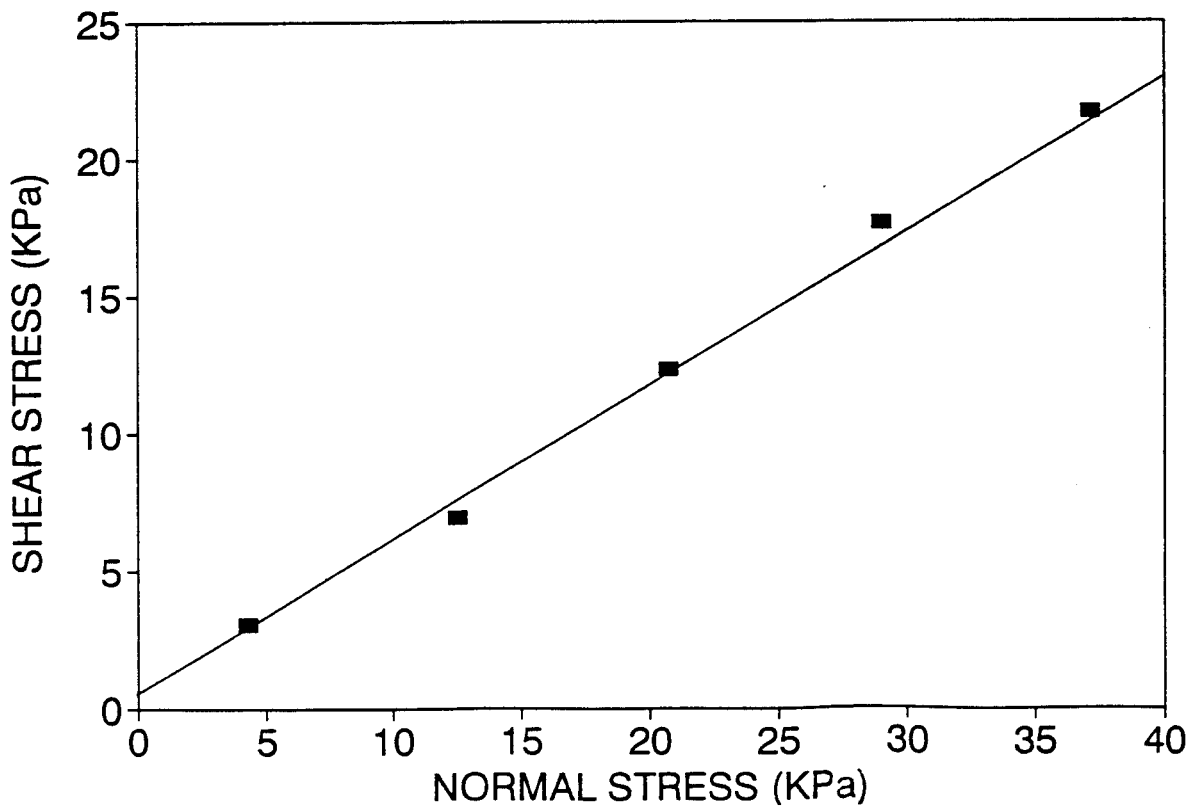


Fig. III. 7 Direct shear tests on sand from sand bar 43.

BEACH 172 MILE DIRECT SHEAR RESULTS

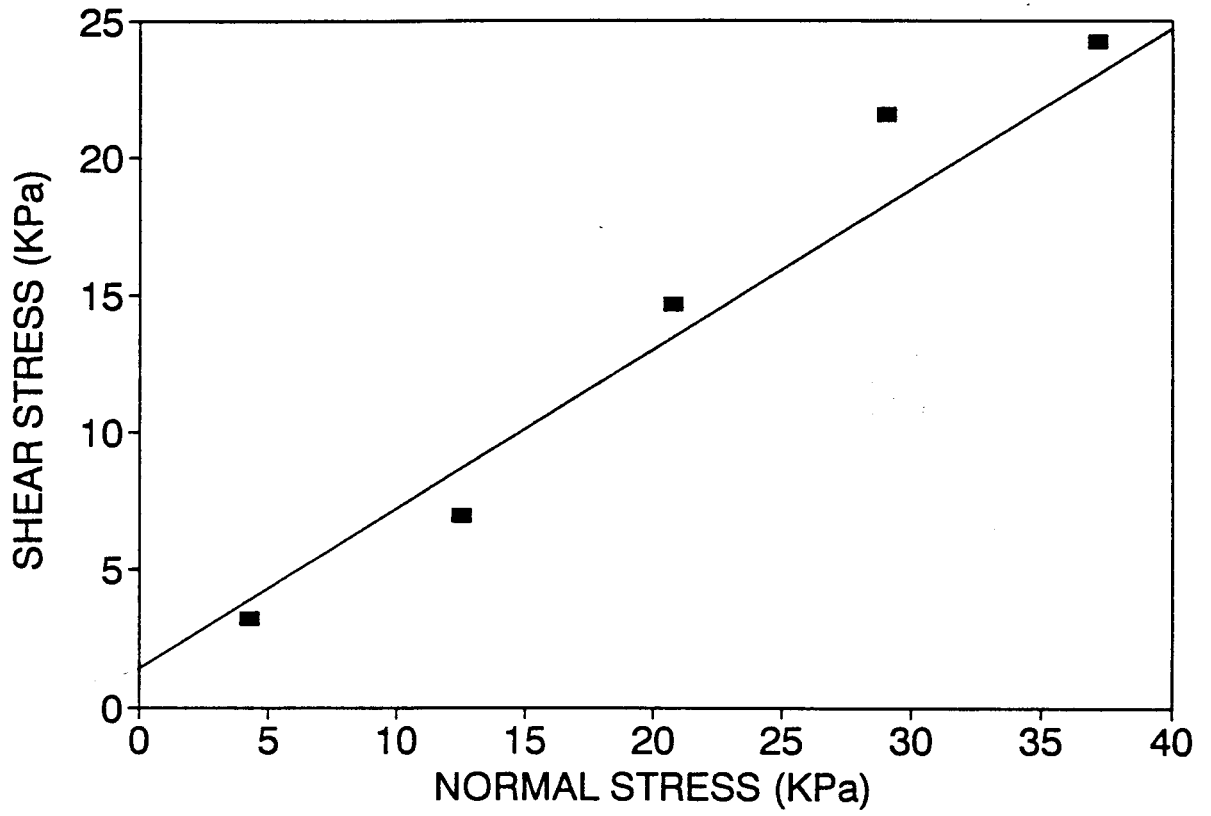


Fig. III. 8 Direct shear tests on sand from sand bar 172L.

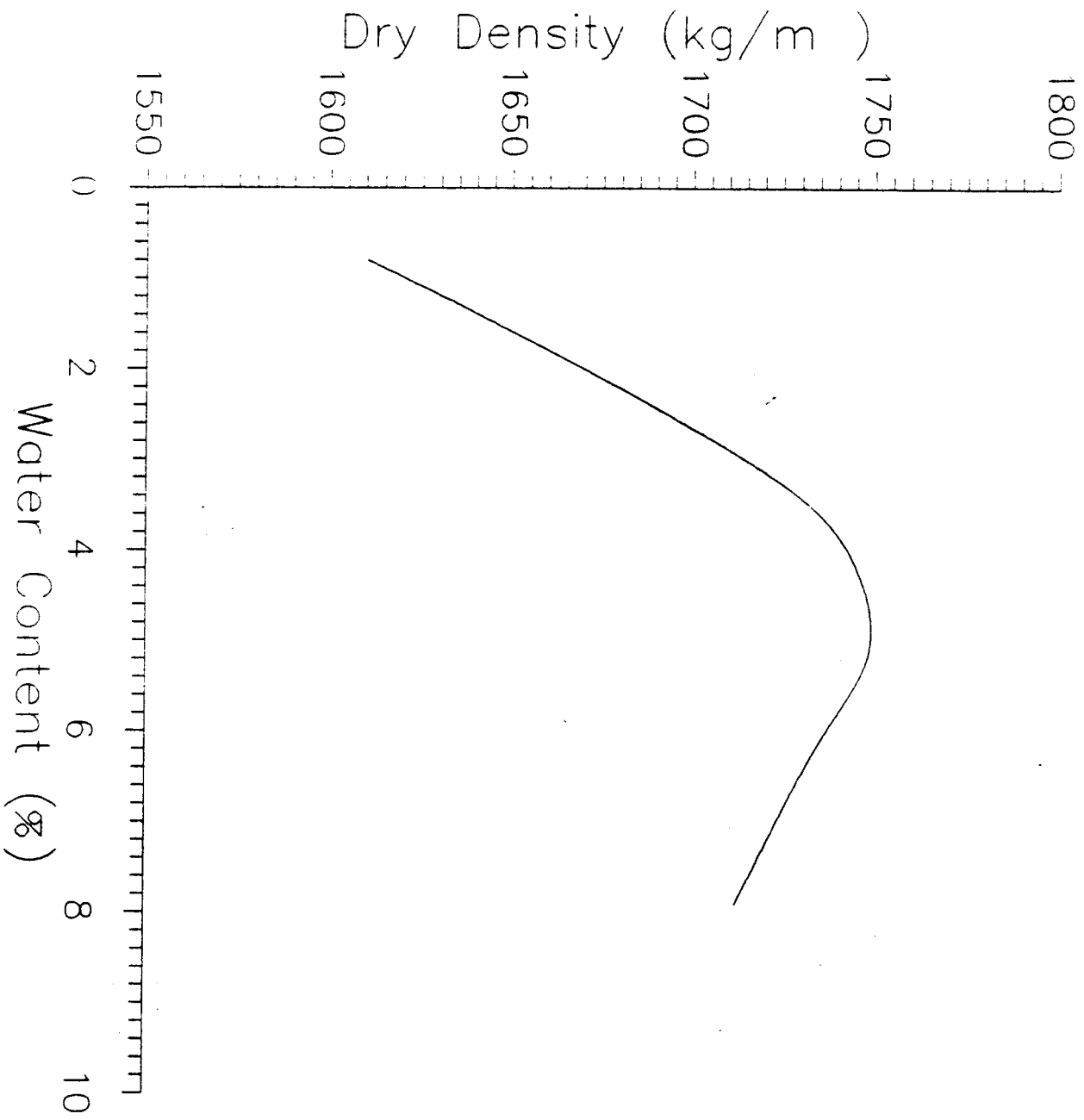


Fig. III. 9 Proctor compaction test results.

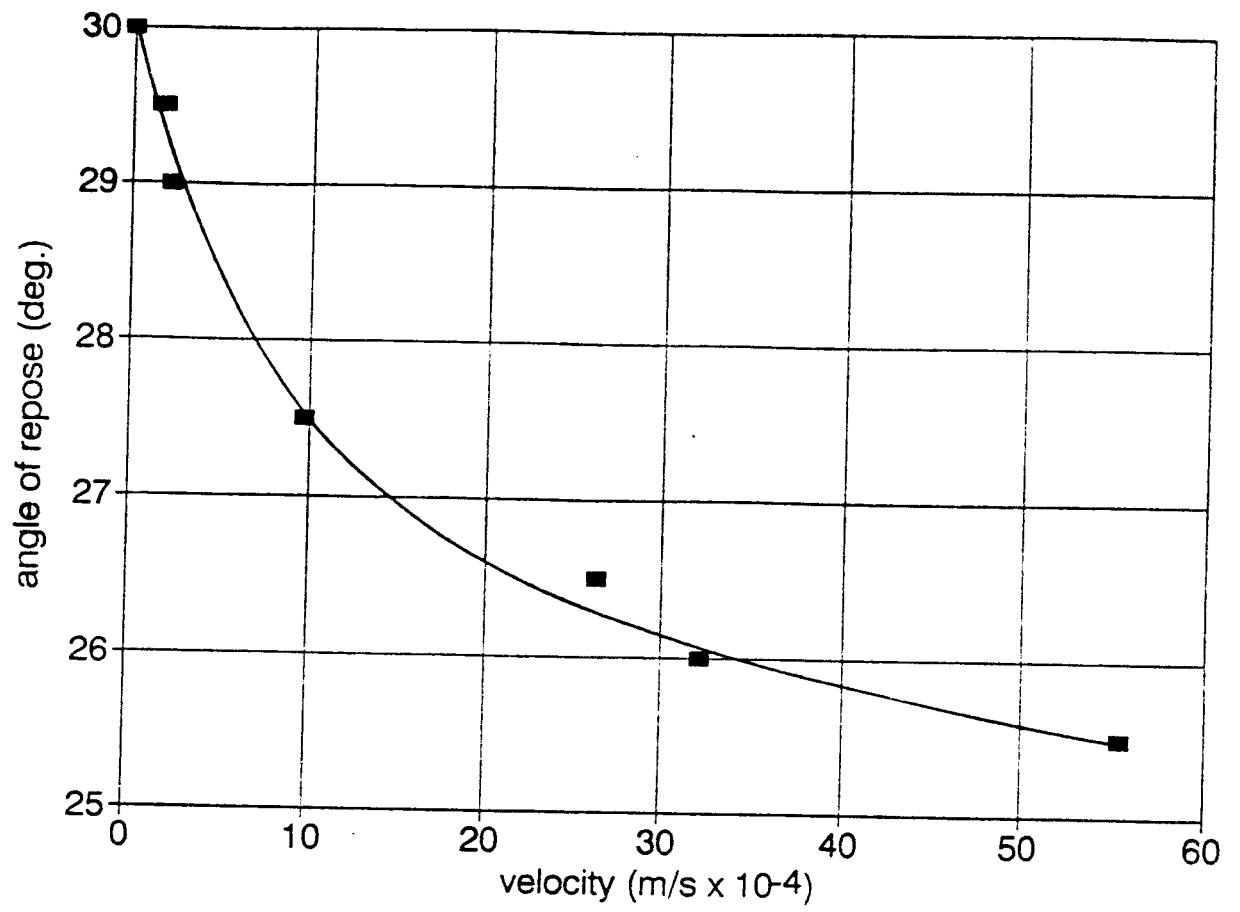


Fig. III. 10 Reduction of angle of repose with increase in velocity.

CHAPTER 3

**HYDROGEOLOGY OF SAND BARS 43.1L AND 172.3L
AND THE IMPLICATIONS ON FLOW ALTERNATIVES
ALONG THE COLORADO RIVER IN THE GRAND CANYON**

M.C. Carpenter, R.L. Carruth, J.B. Fink, J.K. Boling, and B.L. Cluer

**U.S. Geological Survey
Water Resources Division
375 South Euclid
Tucson, AZ 85719**

CONTENTS

	Page
Abstract.....	3
Introduction.....	4
Methods and quality control.....	4
Program status.....	18
Hydrogeology.....	10
Sand bar -6.5R.....	10
Sand bar 43.1L.....	10
Sand bar 172.3L.....	25
Implications for flow alternatives.....	38
Summary and conclusions.....	39
Selected references.....	42

FIGURES

Figure	Page
1. Map showing Colorado River through the Grand Canyon and sand-bar-study areas.....	5
2. Diagram showing geologic section of sand bar -6.5R.....	11
3. Diagram showing geologic section of sand bar 43.1L.....	12
4. Diagram showing modified logarithmic pseudosection of apparent resistivity referenced to land surface at sand bar 43.1L.....	14
5. Graph showing block-averaged, apparent resistivity data from sand bar 43.1L versus theoretical half-space depth of investigation.....	15
6. Graph showing tilt for sensor 18 at sand bar 43.1L, June-July 1991..	17
7. Graph showing river stage at river mile 40, June-July 1991.....	18
8. Graph showing river stage at sand bar 43.1L, June-July 1991.....	19
9. Graph showing water level in well 46 at sand bar 43.1L, June-July 1991	20
10. Graph showing water level in well 40 at sand bar 43.1L, June-July 1991	21
11. Graph showing water level in well 37 at sand bar 43.1L, June-July 1991	22
12. Graph showing water level in well 42 at sand bar 43.1L, June-July 1991	23
13. Diagram showing geologic section of sand bar 172.3L.....	26
14. Diagram showing modified logarithmic pseudosection of apparent resistivity referenced to land surface at sand bar 172.3L.....	27
15. Graph showing tilt for sensor 41 at sand bar 172.3L, June 1991.....	30
16. Graph showing river stage at river mile 170, June 1991.....	31
17. Graph showing river stage at sand bar 172.3L, June 1991.....	32
18. Graph showing water level in well 56 at sand bar 172.3L, June 1991..	33
19. Graph showing tilt for sensor 41 at sand bar 172.3L, September 1991.	34
20. Graph showing river stage at river mile 170, September 1991.....	35
21. Graph showing river stage at sand bar 172.3L, September 1991.....	36
22. Graph showing water level, well 56 at sand bar 172.3L, September 1991	37

CONVERSION FACTORS

<u>Multiply</u>	<u>By</u>	<u>To obtain</u>
millimeter (mm)	0.03937	inch (in.)
meter (m)	3.281	foot (ft)
cubic meter per second (m ³ /s)	35.31	cubic foot per second (ft ³ /s)
kilopascal (kPa)	0.1450	pound per square inch (lb/in ²)
degree Celsius (°C)	°F=(9/5°C)+32	degree Fahrenheit (°F)

HYDROGEOLOGY OF SAND BARS 43.1L AND 172.3L AND THE
IMPLICATIONS ON FLOW ALTERNATIVES ALONG THE
COLORADO RIVER IN THE GRAND CANYON

By

M.C. Carpenter, R.L. Carruth, J.B. Fink,
J.K. Boling, and B.L. Cluer

ABSTRACT

Rill erosion, slumping, and fissuring develop on seepage faces of many sand bars along the Colorado River in the Grand Canyon. These processes, observed at low river stage, are a response to residual head gradients in the sand bars caused by the river stage fluctuation. Three sand bars have been instrumented with sensors for continuous monitoring of stage, pore pressure, ground-water temperature, and tilt to determine the relation between ground-water flow and sand bar deformation. Tilting at sand bar 43.1L occurs on the downward limb of the hydrograph in the absence of scour, indicating slumping or a slump-creep sequence. The deformation is caused by outward-flowing bank storage, oversteepening of the lower part of the slope of the fluctuating zone by rilling, and increased effective stress. At sand bar 172.3L, tilt events are probably all related to scour and occur on the rising limb of a hydrograph. Events occurred on April 17, May 7, May 13, June 18, and September 1, 1991. During the September 1 event, the entire face of sand bar 172.3L was scoured. Rill erosion and slumping accompanied by measured tilts continue in reduced magnitude on sand bar 43.1L during interim flows. Thus, reduction in range of discharge does not eliminate degradation caused by rilling erosion, slumping, and fissuring. The importance of the ground-water processes is that they occur on every sand bar and become increasingly important on all sand bars in the absence of sand-bar-building flows.

INTRODUCTION

Discharge from Glen Canyon Dam on the Colorado River can fluctuate from less than 85 to more than 800 m³/s on a daily basis. Corresponding stage fluctuations on downstream sand bars can exceed 3.4 meters. Rill erosion, slumping, and fissuring on seepage faces of many sand bars, observed at low river stage, are a response to residual head gradients in the sand bars caused by the river stage fluctuation. Seepage faces probably develop on all sand bars in the study area.

The study is designed to document the processes of seepage erosion, slumping, and fissuring and to establish relationships among material properties of sand-bar sediments, threshold of hydraulic gradient for rilling erosion, and effective stresses causing slumping. During the study, three sand bars were instrumented (fig. 1), and results will be modeled using finite-element stress-strain and variably saturated heat and ground-water models. The purpose of this report is to provide preliminary findings of data from the three sand bars. The report describes the stratigraphy of the three sand bars and tilt events on the two downstream sand bars.

Methods and Quality Control

Three sand bars have been instrumented with sensors for continuous monitoring of stage, pore pressure, temperature, and tilt to determine the relation between ground-water flow and sand-bar deformation. Typically, in a sand bar, five vertical clusters of deep, intermediate, and shallow pairs of pore-pressure and temperature sensors are arrayed in a vertical plane orthogonal to the river's edge. The clusters are spaced a few meters apart

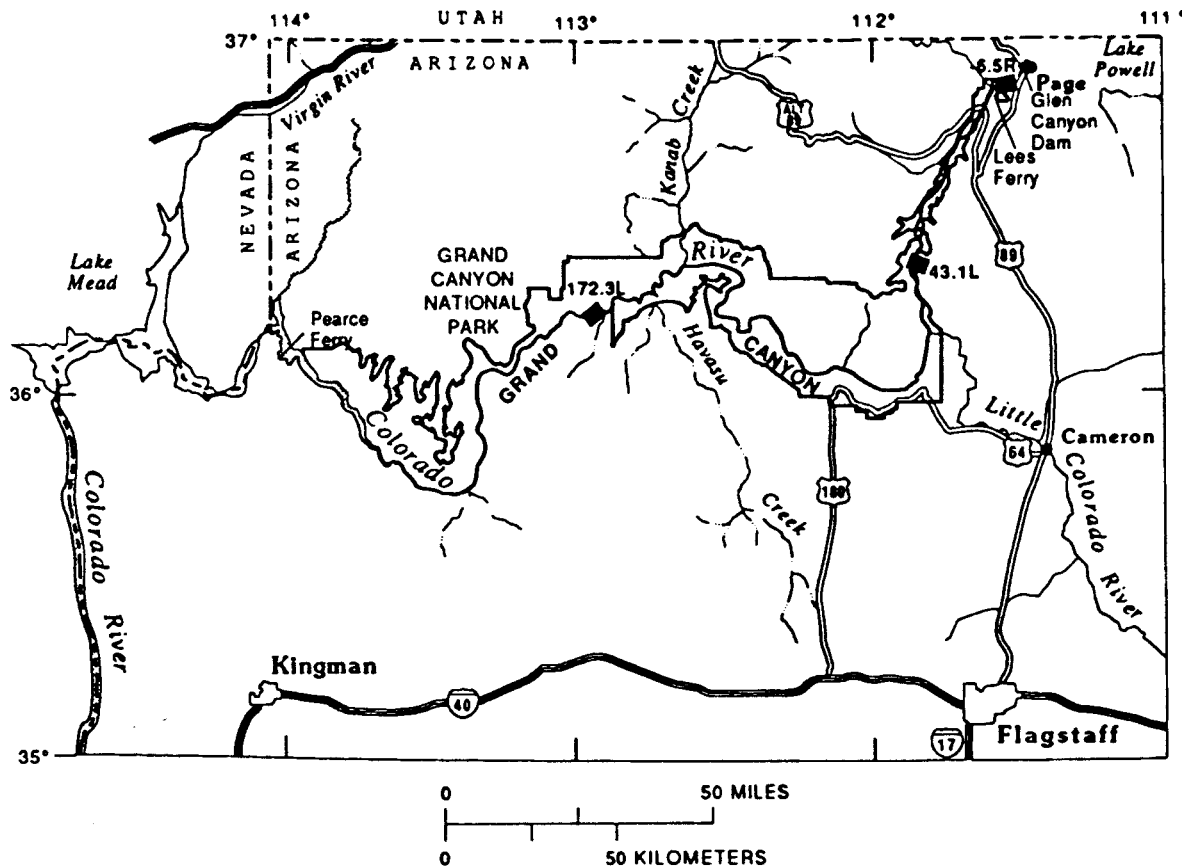


Figure 1.--Location of study sand bars.

in the sand-bar face, above, within, and below the fluctuating zone, to determine the vertical component of ground-water flow in the deforming sand-bar face. The clusters are spaced more than 10 meters apart in the middle and back of the sand bar. Seven tilt sensors are arrayed both parallel with and orthogonal to the river's edge in the deforming sand-bar face. Two vertical clusters of tensiometers at three depths are also in the sand bar. In one sand bar, tensiometers are in vegetated and unvegetated soil. In another sand bar, tensiometers are in a medium sand and a lower bench of silty very fine sand.

Piezometers are placed in the sand bars using a jetting and driving technique. Water is pumped from the river down a 13-mm PVC pipe for jetting inside near the bottom of 50-mm PVC flush-thread pipe. A special section of flush-thread pipe is fitted with a coupling in the middle. A fence-post type driver is used to drive the string of flush-thread pipe with the special section on top. Maximum depth reached was 10 m. The pressure sensor is a Motorola¹ MPX2200AS 0 to 200 kPa absolute device and is attached to the tip of a 13-mm PVC pipe which is fitted with a fine nylon screen about 75 mm long and lowered into the 50-mm casing. The 50-mm casing is then pulled from around the piezometer. In vertical nests of piezometers, each piezometer is set in its own drilled hole. This eliminates the possibility of up-hole pressure contamination. Because the pressure sensors are absolute devices, additional pressure sensors are used as barometers to remove the effect of atmospheric pressure fluctuations. Because of the importance of the correction, each site has three barometers for redundancy. Resolution of the pressure sensors in the data-logging system is 2.5 mm of water-level fluctuation. The temperature sensors are Campbell Scientific 107B

¹ Use of trade names in this report is for identification purposes only and does not constitute endorsement by the U.S. Geological Survey.

thermistors and are inserted to the bottom of the 13-mm PVC pipes to be next to the pressure sensors. Resolution of the temperature sensors is less than 0.01°C , but specified accuracy is $\pm 0.2^{\circ}\text{C}$. Observed performance is $\pm 0.5^{\circ}\text{C}$ before correction for field calibration checks. Data are recorded on Campbell Scientific CR10 data loggers with multiplexers and storage modules. Excitation voltage to pressure sensors is provided by Steinke regulated circuits with a voltage stability of ± 0.01 percent. The electronic equipment is buried in a sealed, desiccated surplus metal box.

The pressure sensors are calibrated at three temperatures and five pressures in a Dewar flask in an isothermal bath. Pressure sensors are calibrated and field checked using a Paroscientific model 760 Portable Pressure Standard with a range of 0-690 kPa absolute and accuracy of ± 0.01 percent. The primary temperature standard is a certified Ever Ready thermometer with an accuracy of $\pm 0.03^{\circ}\text{C}$. The secondary standard for field use is a Doric readout for a YSI 401 thermistor. Accuracy of the secondary standard against the primary standard is $\pm 0.1^{\circ}\text{C}$. The tilt sensors are calibrated using an accurately cut 10° angle for three-point calibration at $+10^{\circ}$, 0° , and -10° from an arbitrary near-horizontal plane. In the field, temperature sensors are placed with all pressure sensors and tilt sensors. Pressure sensors used for water levels are field checked by taping the 13-mm wells for all sensors that are accessible at the time of a site visit. Submerged pressure sensors including stage sensors are checked using surveyed river stage at known times. Accessible temperature sensors are checked by pulling them out of the 13-mm pipes and putting the sensors in a thermos bottle with the secondary standard at two temperatures.

In conjunction with the long term ground-water monitoring efforts, high-resolution, DC resistivity studies were performed at sand bars 43.1L and 172.3L during August 1991. DC resistivity offered the potential for detecting

vertical and lateral differences in the electrical properties of the sand bars. The differences in electrical properties are related to moisture content, porosity, and relative clay content of the sand bars. All of these properties are of interest regarding the hydraulic behavior of the sand bars.

A pole-pole electrode array was used to allow maximum depth of investigation while still allowing small inter-electrode spacings for good lateral resolution. Inter-electrode spacings ranged from 1.5 m to 38 m. Infinite (remote) electrodes were located up- and down-stream from the survey lines at distances greater than ten times the maximum inter-electrode spacing. Time constraints allowed only one line perpendicular to the sand bar from the cliff wall to the river front.

The data are presented in modified pseudosections, referenced to the land surface. The location of the plot points in the modified pseudosections are determined by a logarithmic transformation developed by Fink (1989). Referencing the pseudosection to the land surface lends a more geologic appearance to the data, but does not alter the fact that the plots are still pseudosections.

Program Status

Sand bar -6.5R has water-level, stage, and barometric pressure sensors, temperature sensors, and a screened 50-mm well for aquifer testing or sampling but lacks tilt sensors, tensiometers, and a temperature sensor for the stage record. Record began at that sand bar on October 24, 1990. Downstream sand bars 43.1L and 172.3L have water-level, stage, barometric, and tensiometric pressure sensors; temperature sensors; tilt sensors; and 50-mm screened wells. Record began at 43.1L on April 8, 1991; and at 172.3L on April 18, 1991. Data have been recovered through November 4, 1991, at all

sand bars. The pressure data have been processed through temperature corrections in Quatro Pro, and almost all data have been plotted in rough form up to middle September 1991. Corrections remaining to be done include applying field corrections to temperature records and measured water levels in wells and surveyed river stage to water-level records. Remaining corrections will take several weeks before these data will be ready for insertion into a finite-element stress-strain model or variably saturated flow model. Planned field work includes (1) augmentation and repair or replacement of scour-damaged or failed sensors, (2) recalibration and repair of cavitated tensiometers, (3) aquifer testing, and (4) scaled-down instrumentation of additional sand bars that will include flash photography triggered by data-logger output. On-site studies will include combining rilling-erosion studies (Werrell and others, 1991), monitoring slumps with precise surveying, and 5-minute sampling of water levels and tilts. Modeling plans include incorporating representative water-level, temperature, and tilt data into stress-strain and variably saturated heat and ground-water flow models. Some of the expected specific results of those models are estimation of threshold values of hydraulic gradient and duration of drainage for initiation of rilling erosion and of stress-strain material properties such as cohesion, shear strength, tensile strength, and strain at failure. Report plans include a "Report" in Science planned for submission in late 1992 and an article in Water Resources Research for submission in 1993.

HYDROGEOLOGY

Sand Bar -6.5R

Sand bar -6.5R (fig. 2), upstream from Lees Ferry, consists of a unit of homogeneous fine to medium sand underlain by a confining unit of silty, very fine sand. This unit is 0.14 m thick where it crops out in a gully eroded into the sand bar in fall 1991. The unit dips toward the back of the sand bar where it flattens and attains a depth of about 3.5 m. The confining unit is underlain by another unit of fine to medium sand. The back boundary is sloping talus without a return channel. This sand bar has a gentle slope in the fluctuating zone and exhibits a seepage face with rill erosion but does not exhibit slumping and fissuring. This sand bar is considered to be a control for comparison with the two deforming sand bars. This sand bar presently lacks tilt sensors and is not discussed further in this report.

Sand Bar 43.1L

Sand bar 43L (fig. 3) consists of homogeneous fine to medium sand overlying medium salt-and-pepper sand at a depth of 6 meters. The back boundary is talus with a narrow, deep return channel underlain by a thin, clayey silty sand. A second reddish silty sand with some gravel occurs at a depth of about 4 m in the back of the sand bar. The fluctuating zone is a steeply sloping face that exhibits rill erosion, slumping, and fissuring.

A single line of pole-pole DC resistivity was performed at sand bar 43.1L. The line was 36.5 m long and crossed the sand bar transversely, north to south, beginning at the base of the canyon wall next to outcrop and continuing across the elevated, dry-sand portion of the sand bar, and down

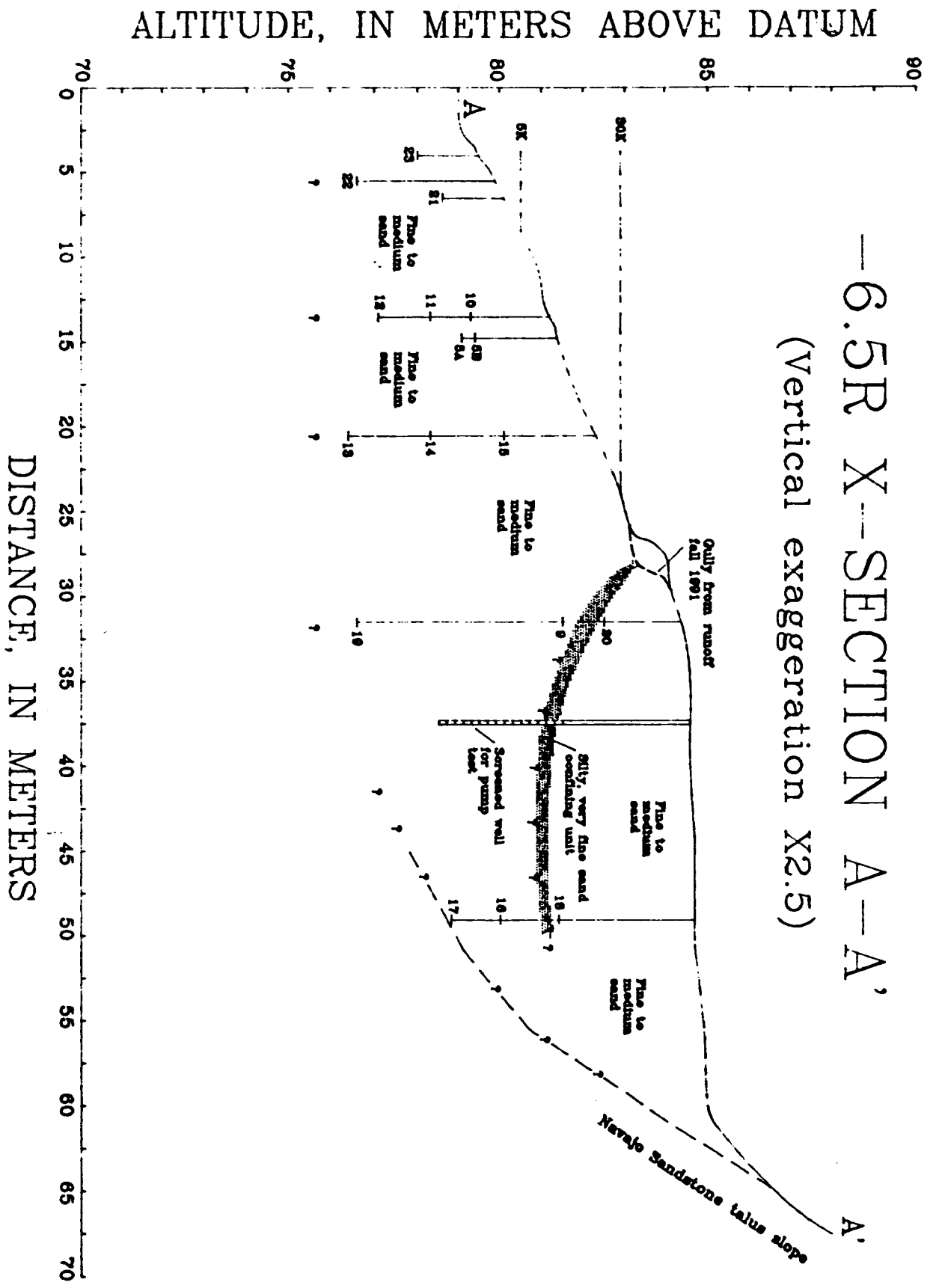
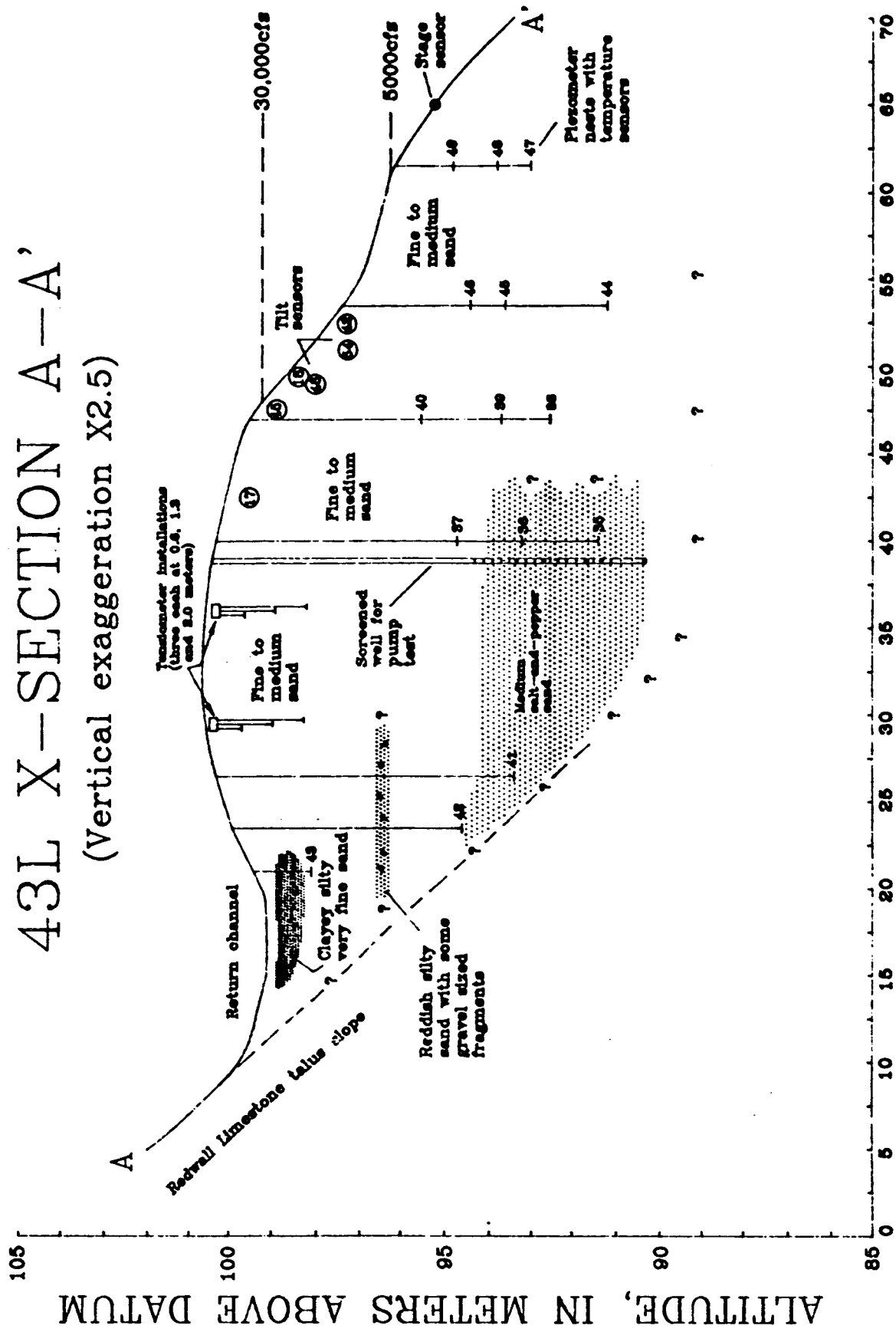


Figure 2.--Geologic section of sand bar -6.5R.

43L X-SECTION A-A'

(Vertical exaggeration X2.5)



DISTANCE, IN METERS

Figure 3.--Geologic section of sand bar 43.1L.

the sand-bar face into the Colorado River approximately 1.5 m (fig. 4). The first 5 m of the line was located in a return channel adjacent to the cliff base.

Apparent resistivities ranged from greater than 2000 ohm-meters (Ω -m) to 50 Ω -m. The high apparent resistivities are related to the dry-sand portion of the sand bar, which underlies approximately 18 m of the line. Data from the central portion of the line were block-averaged and modeled using one-dimensional methods. Modeling results indicated that the dry sand has a nominal true resistivity of 3,800 Ω -m and a probable thickness of 1.65 m (fig. 5, table 1). This thickness correlates very well with the elevation of the dry-sand portion of the sand bar above the average stage of the river during the measurement period.

Table 1. One-dimensional modeling results
of the central portion of sand bar 43.1L.

Layer	Resistivity (Ω -m)	Range (Ω -m)	Thickness (m)	Range (m)
1	3,800	± 400	1.65	$\pm .10$
2	50	± 20	8.5	± 4.0
3	225	± 25	Infinite	

Low apparent resistivities occur on both ends of the line where electrodes are either occasionally submerged in the river or in the return channel. Apparent resistivities in these areas range from 40 to 50 Ω -m, suggesting that the river-water resistivity cannot be any greater than 50 Ω -m. A resistivity of 50 Ω -m is equivalent to a conductivity of 200 μ S/cm. Values of about 40 Ω -m occur in the return channel, which is lower in resistivity than the river water because of the clay content in the sediments

Glen Canyon Environmental Studies Grand Canyon Sand Bars August 1991

Pole-pole DC Apparent Resistivity

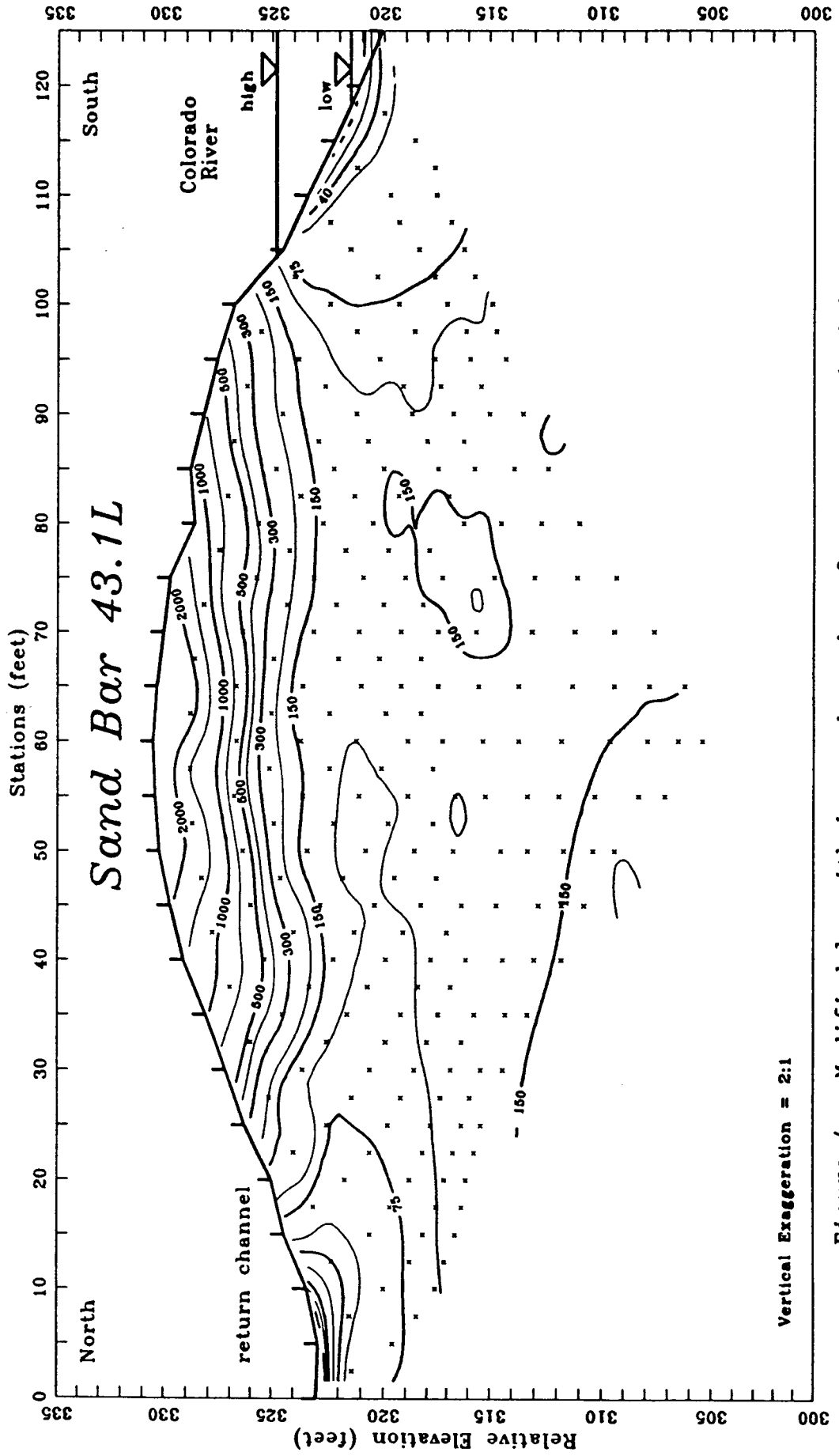


Figure 4.--Modified logarithmic pseudosection of apparent resistivity referred to land surface at sand bar 43.1L.

Glen Canyon Environmental Study
Grand Canyon Sand Bars
DC Resistivity
Aug. 1991

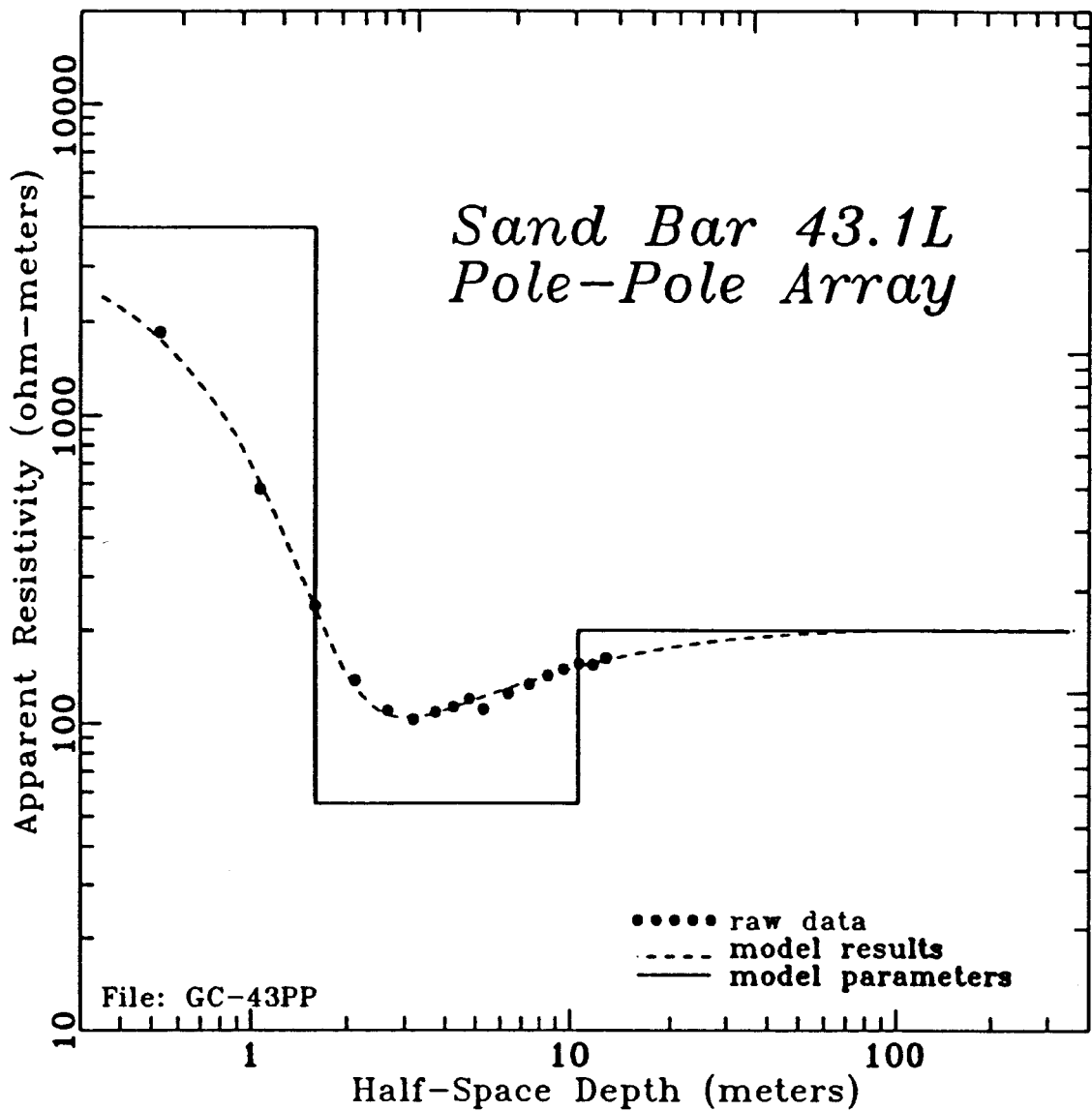


Figure 5.--Block-averaged, apparent resistivity data from sand bar 43.1L versus theoretical half-space depth of investigation.

underlying the return channel or higher TDS of the stagnant return-channel water.

The low apparent near-surface resistivities at the ends of the line are also reflected in the middle layer for which modeling suggests a true resistivity of $50 \pm 20 \Omega\text{-m}$, with a thickness of $8.5 \pm 4.0 \text{ m}$. The middle layer is inferred to represent saturated sand and the overlying capillary zone.

Modeling yielded a higher true resistivity for the third layer that may represent electrical bedrock. The maximum depth penetrated by any of the wells was approximately 10 m, but bedrock was not encountered nor was there any significant change observed in grain size that might indicate penetration of a basal gravel or talus. Based on the resistivity data, bedrock may lie just below the limit of drilling at an estimated depth of 10 to 15 m.

At sand bar 43.1L, a sequence of tilts occurred from July 7, 1991, through July 17, 1991 (fig. 6). The tilts were at least five times greater in the x tilt sensor, which is oriented orthogonal to the river with the convention of increasing inclination being upward tilt toward the river than in the y tilt sensor. The y tilt sensor is oriented parallel to the river with the convention of increasing inclination being upward tilt facing down river. The events were preceded by downward tilt of -0.1° toward the river on the morning of July 2, and upward tilt of 0.1° the evening of July 6. At 7:20 a.m. on July 7, upward tilt of 5.5° occurred in the x sensor. In the morning of July 12, downward tilt of -0.5° occurred; and at 9:20 a.m. on July 17, an additional -3.3° of downward tilt occurred. These major events were followed by continued negative tilt in the x sensor from July 18 to July 26, punctuated with daily downward spikes of about 0.4° that occurred in the morning. With the single exception of the precursor upward tilt on July 6, all of the sudden tilts occurred on downward limbs of the hydrographs (figs. 7-12) when the effective stress (intergranular stress) in the sand-bar face

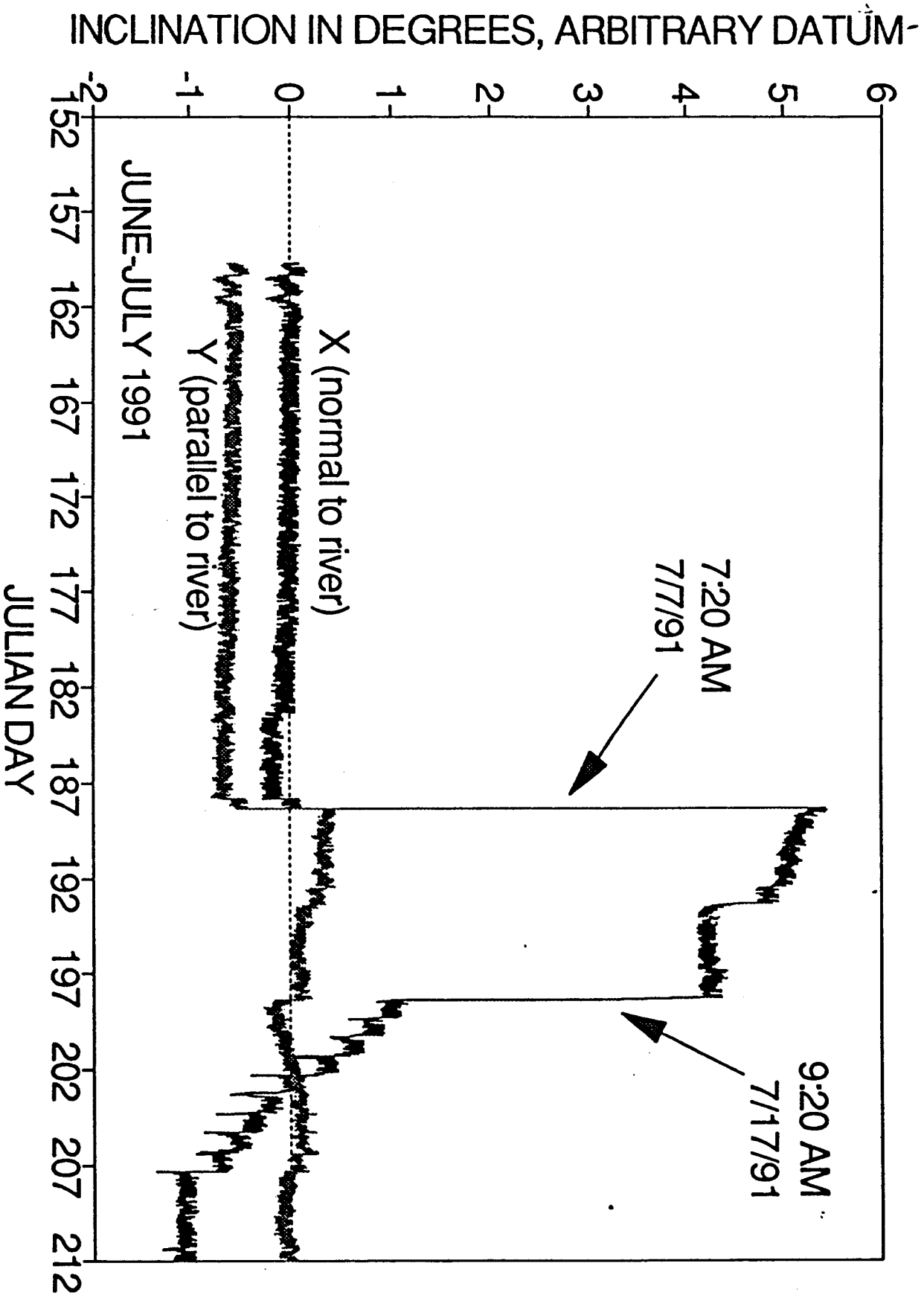


Figure 6.--Tilt for sensor 18 at sand bar 43.1L, June-July 1991.

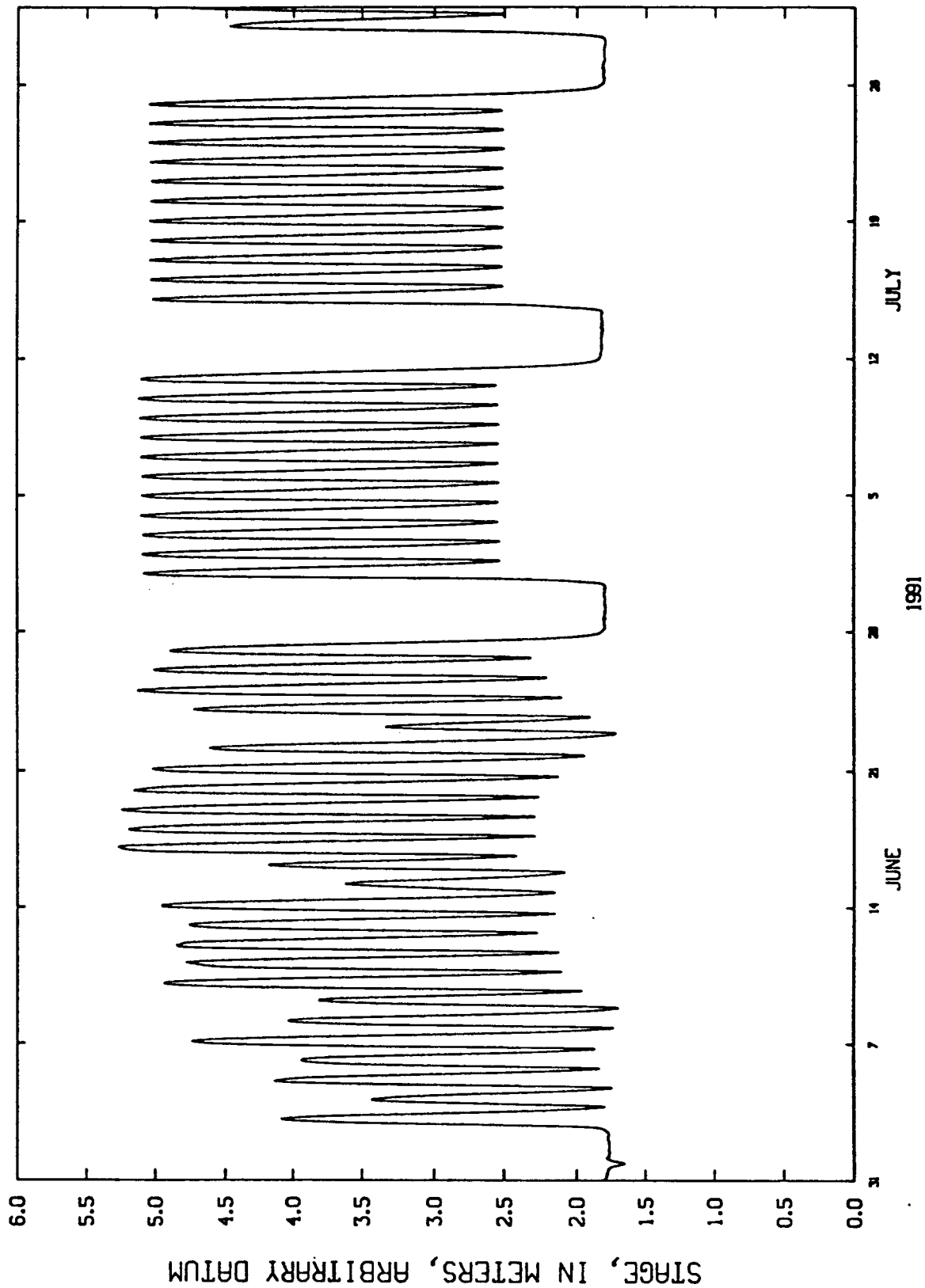


Figure 7.--River stage at river mile 40, June-July 1991.

43L RIVER STAGE

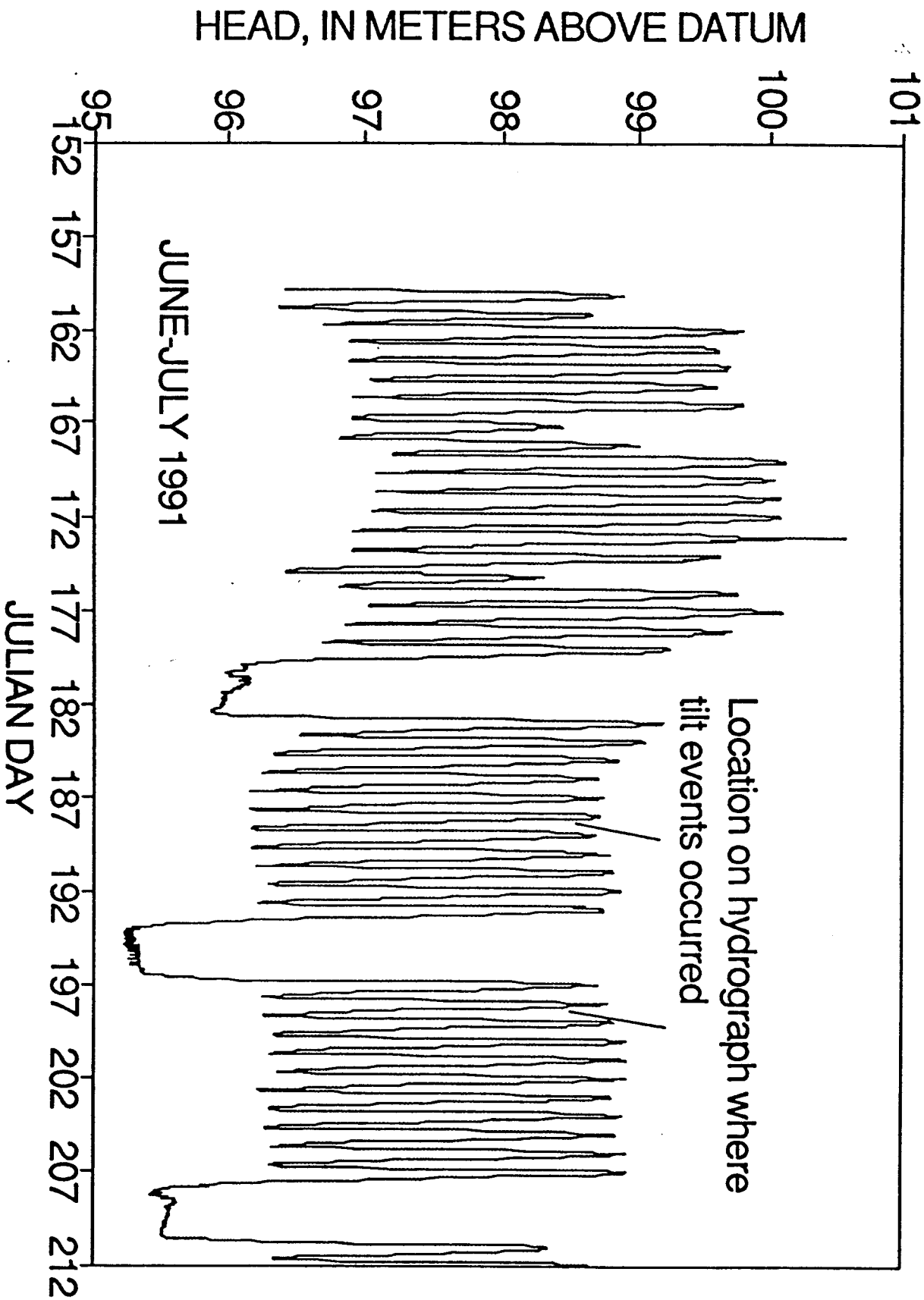


Figure 8.--River stage at sand bar 43.LL, June-July 1991.

PIEZOMETER #46

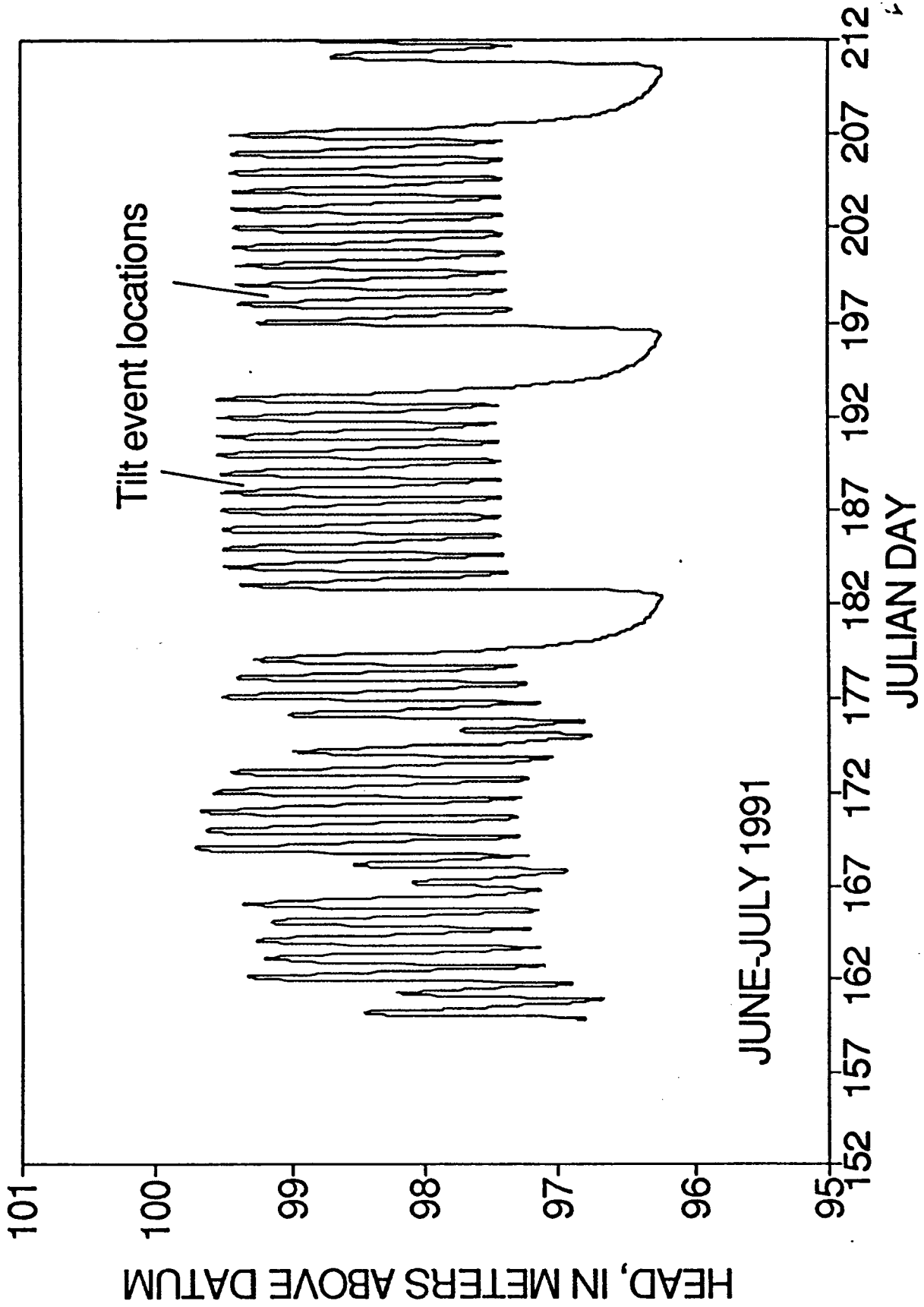


Figure 9. ---Water level in well 46 at sand bar 43.1L, June-July 1991.

PIEZOMETER #40

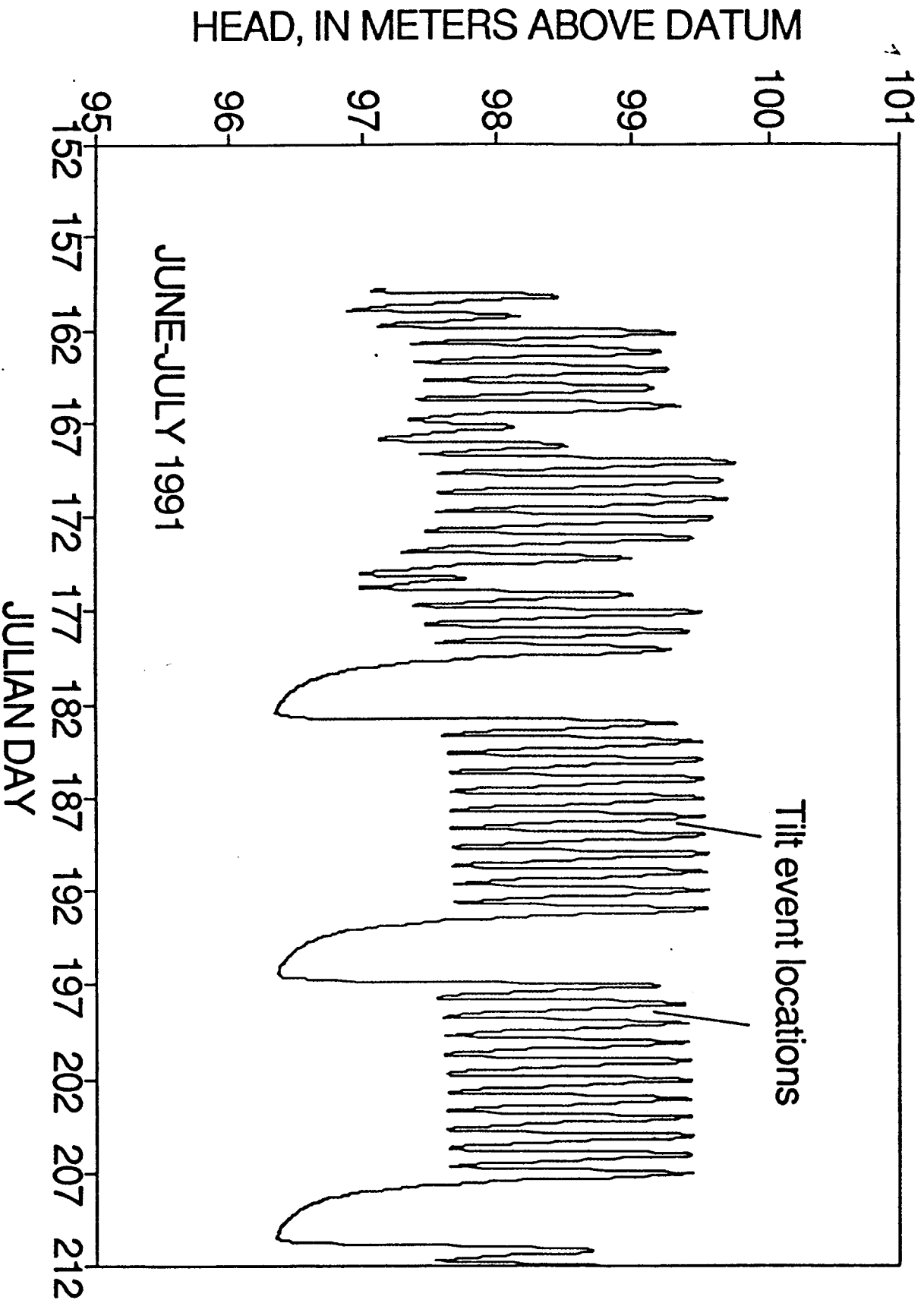


Figure 10.--Water level in well 40 at sand bar 43.1L, June-July 1991.

PIEZOMETER #37

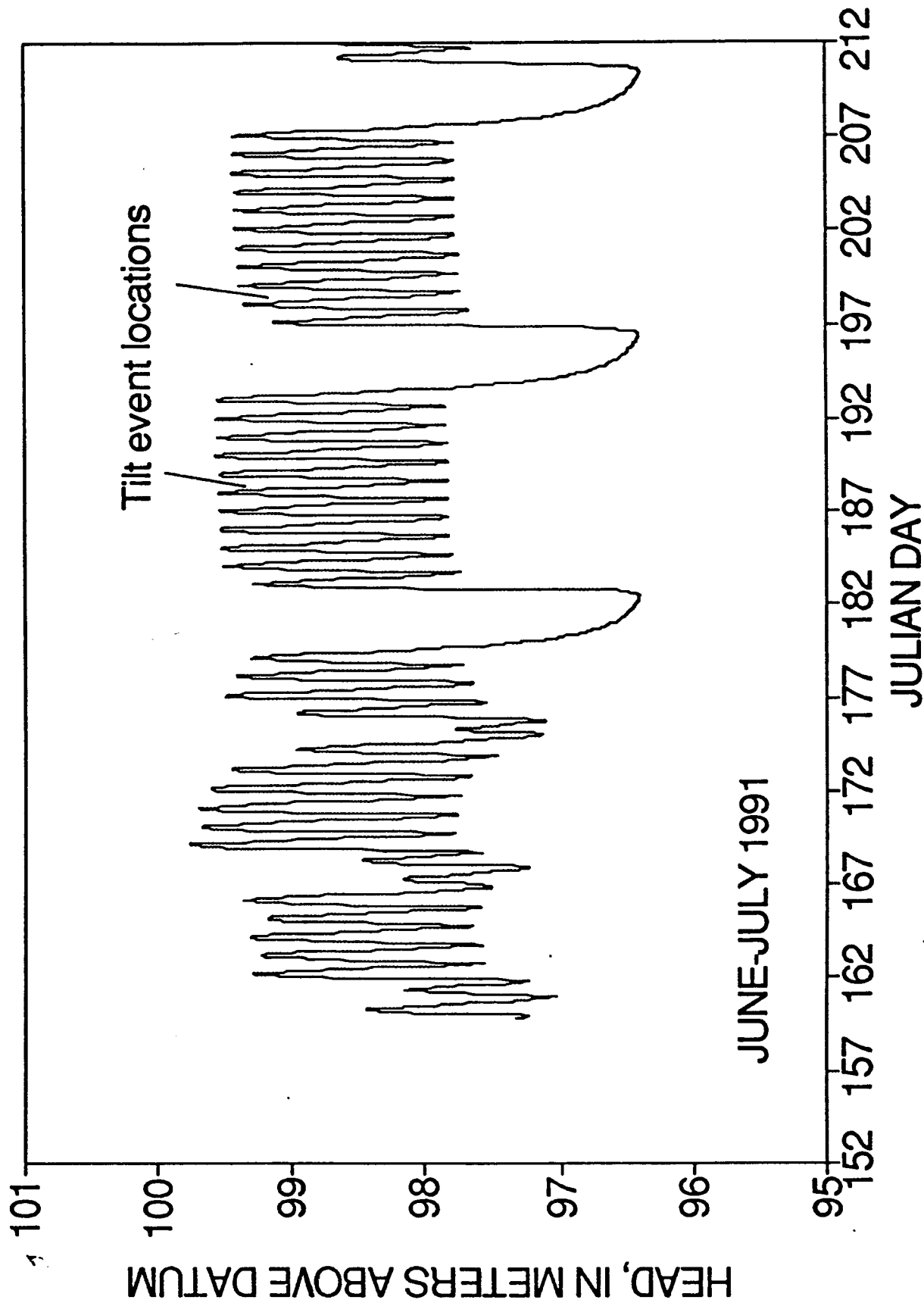


Figure 11.--Water level in well 37 at sand bar 43.1L, June-July 1991.

PIEZOMETER #42

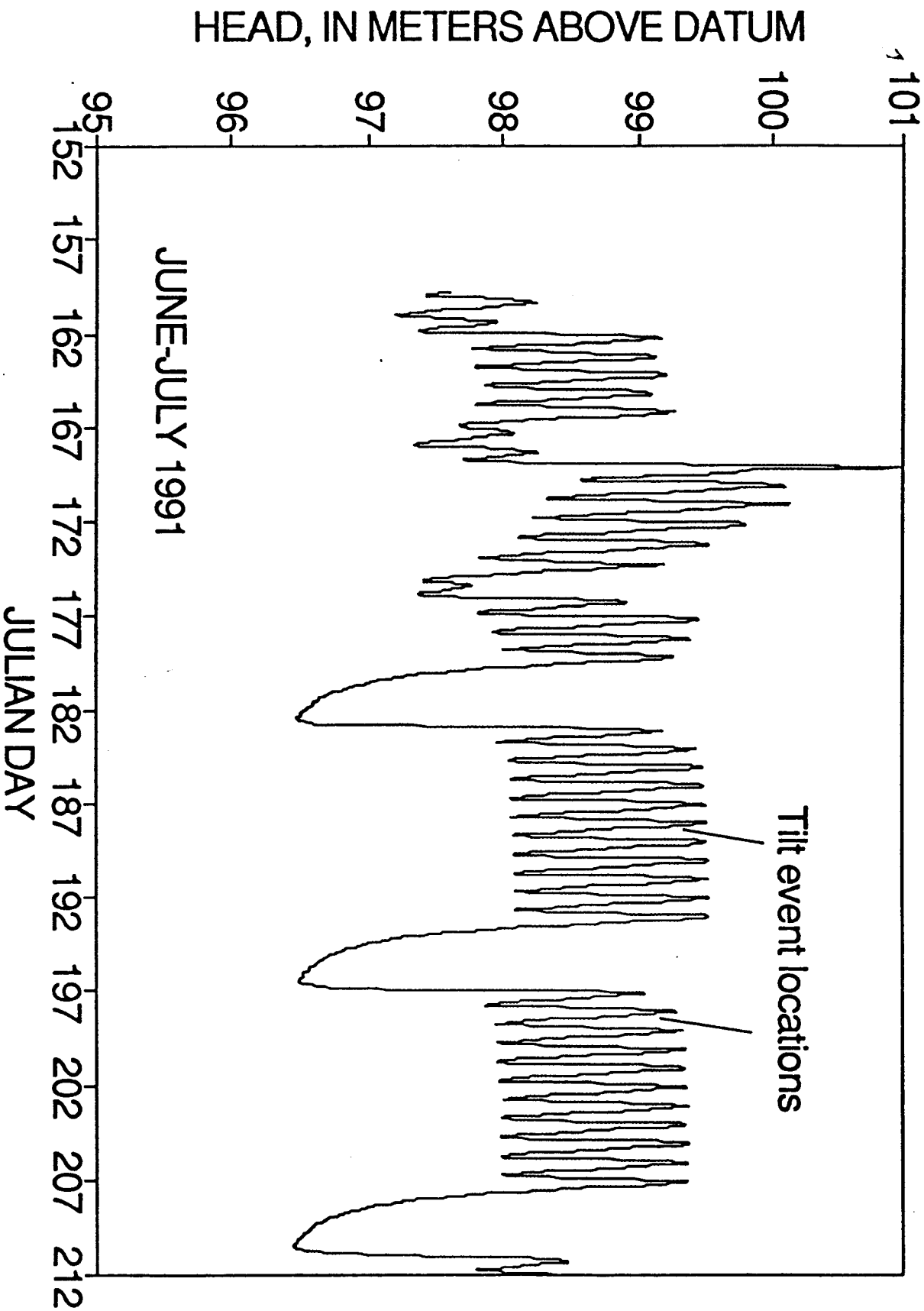


Figure 12.--Water level in well 42 at sand bar 43.1L, June-July 1991.

was increasing. The hypothesis suggested by this sequence of events is slumping or rotational failure in which tilt sensor 18 was within a slump block during the major upward event on July 7 and was outside a block on succeeding events. An alternative hypothesis is a slump-creep sequence of down-slope movement in which tilt alternates from positive to negative. The slope failure is shallow because none of the nearby tilt sensors, 17, 45, 48, or 54 (fig. 3), exhibited any tilt during April to July 1991. Tilt sensor 42 had gone off scale in April 1991. The probable cause of slope failure on this sand bar is oversteepening of the lower part of the slope of the fluctuating zone. This conclusion is supported by evidence of rilling erosion in daily photographs taken automatically from the opposite bank (B.L. Cluer, physical scientist, National Park Service, written commun., 1991; Cluer, 1991). Rilling is enhanced during fluctuating weekend low flows (figs. 7-8). Rilling has been intense after about 1.5 days during research steady low flows.

Attenuation of water-level fluctuation from the front to the back of 43.1L sand bar is evident at piezometers 46, 40, 37, and 42 (figs. 9-12). From piezometer 46 to piezometer 42, the attenuation of fluctuating July flows is 30 percent over a distance of 30 m. The particularly high water level in piezometer 42 beginning on June 17, 1991 (fig. 12), is probably caused by unusually high water level in the return channel with hydraulic connection to the sensor (fig. 3).

Apparent water-level fluctuations at the river-stage sensor at sand bar 43.1L are not stable at constant low flow nor are they constant from one low-flow period to the next (figs. 7-8). This problem also occurs in piezometers 47, 48, and 49. One possible cause of this problem is slumping or creep in the lower part of the sand bar that is always under water. No evidence for river scour exists at this sand bar. Another possible cause is floating or

sinking of the sensors during various stages of liquefaction of the sediments. Although the channel cross section is different, the excellent stage record from river mile 40 (fig. 7) will help in the analysis of the sensors that are always under water and thus inaccessible for measuring water levels. Depending on the usefulness of the temperature records for indicating flow between the river and the sediments, the combined water-level records may yield corrected record of river stage and evidence for geometries of slumping events.

Sand Bar 172.3L

Sand bar 172L (fig. 13) consists of interlayered fine to medium sand and silty very fine sand. The back boundary is talus abutted by a broad shallow return channel underlain with silty fine sand. The fluctuating zone is a steeply sloping face with a bench that is underlain with reddish, silty, very fine sand interlayered with fine to medium sand. This sand bar exhibits rill erosion, slumping, and fissuring.

A single line of pole-pole DC resistivity was performed at sand bar 172.3L. The line was 38 m long and crossed the sand bar transversely, south to north, beginning at the base of the talus slope and continuing across the elevated, dry-sand portion of the sand bar, and down the sand-bar face into the Colorado River approximately 3 m (fig 14). The first 9 m of the line was located in an elevated, dry-sand portion of the sand bar. The central portion of the line crossed a predominantly silty plateau for approximately 17 m before dropping off the the sand-bar face. The north end of the line terminated 3 m into the river. The topography of this survey line is more

172L, X-SECTION A-A'

(Vertical exaggeration X2.5)

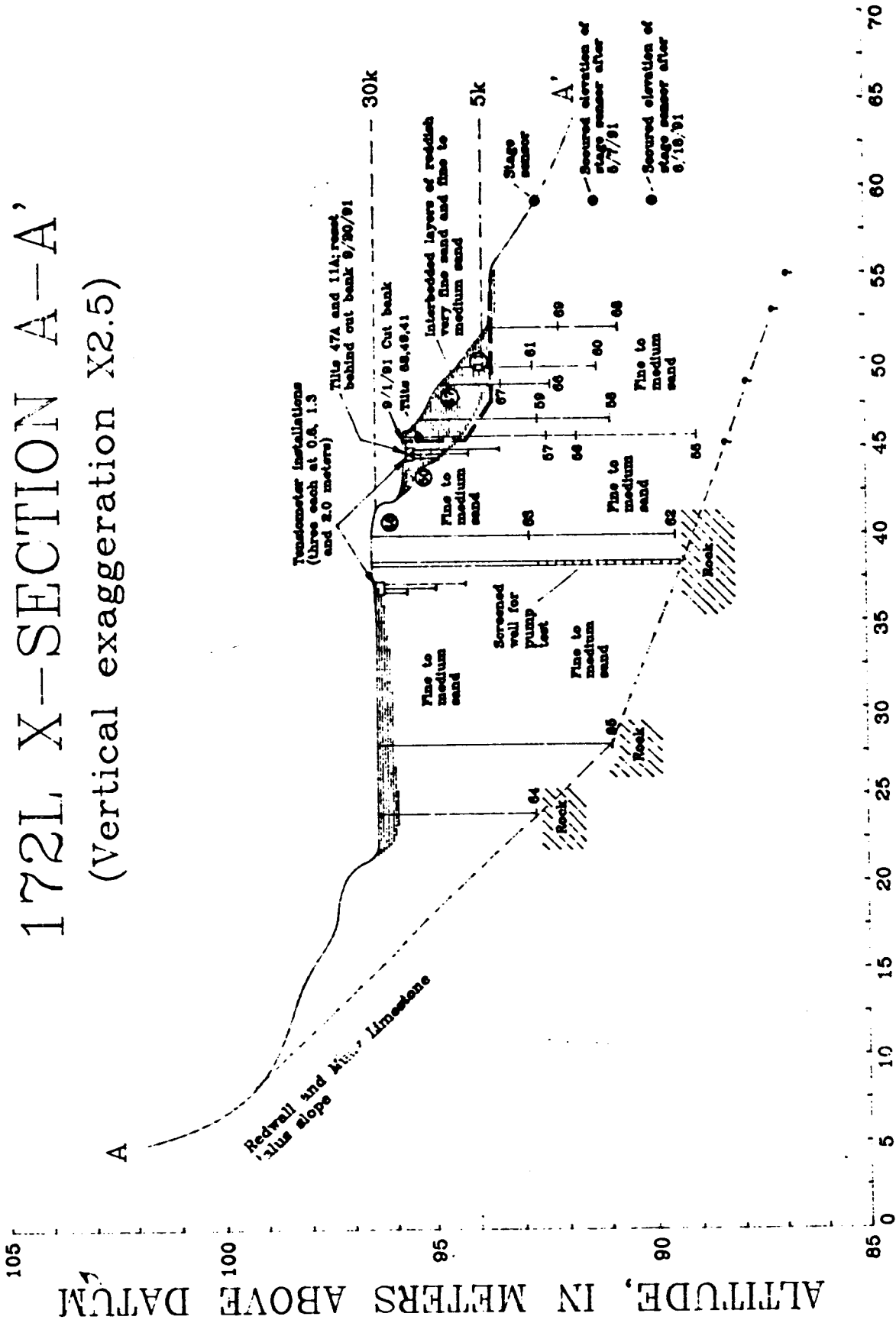


Figure 13.--Geologic section of sand bar 172.3L.

Glen Canyon Environmental Studies
 Grand Canyon Sand Bars
 August 1991

Pole-pole DC Apparent Resistivity

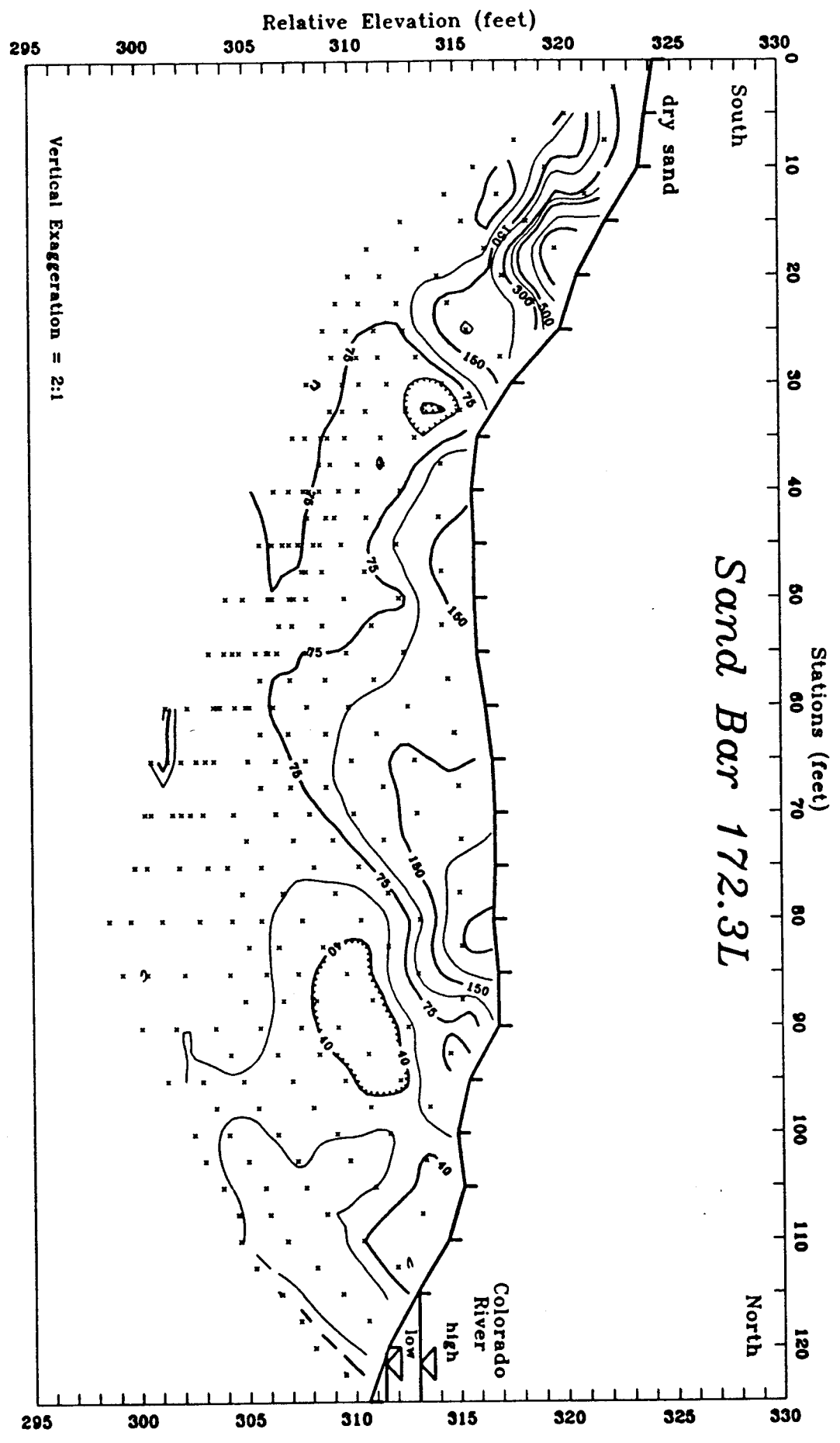


Figure 14--Modified logarithmic pseudosection of apparent resistivity referenced to land surface at sand bar 172.3L.

irregular than the line at sand bar 43.1L and results in greater localized variations in the observed apparent resistivities. Indeed, there are no well defined layered-earth responses evident in the data, and 1-D modeling was not applied.

Apparent resistivities ranged from greater than 1000 Ω -m down to 25 to 30 Ω -m. The highest values are associated with dry sand at the beginning of the line between stations 0 and 30 and near the top of the sand-bar face near station 90.

Although the central portion of the line is well vegetated and has a higher percentage of fines, the associated apparent resistivities were greater than 100 Ω -m. A decrease in apparent resistivity with increasing spacing in the central portion of the line suggests a more conductive lower horizon, but lateral effects caused by surface topography and, perhaps, lateral changes in porosity and-or permeability, mask the deeper effects. Drilling encountered obstacles at depths ranging from 4 to 7 m. If electrical bedrock were present at these shallow depths, a significant increase in apparent resistivity should occur at wider electrode spacings. However, the data show a generally decreasing trend as a function of increasing spacing. This would suggest that electrical bedrock is not being detected and that the obstacles encountered during drilling may be talus blocks rather than in-place bedrock. Depth to electrical bedrock appears to be greater than 20 m.

The two most salient features in the apparent resistivity pseudosection are the two lows associated with sharp changes in topography. The low in the vicinity of stations 30 and 35 is likely restricted to topography. The low in the vicinity of stations 90 to 95 appears to be a combination of topography and subsurface changes. The inferred sub-surface change may be caused by a facies change in the sand bar or an increase in saturation, perhaps due to a zone of increased porosity.

Several tilt events occurred at sand bar 172.3L. At this sand bar, the events documented by tilt sensors occurred on the rising limb of a hydrograph and probably are all related to scour. An event occurred on April 17, 1991, about 11:00 p.m. to April 18, 1:30 a.m. before sensors were installed in the sand bar. In this event, which also occurred on the rising limb of the hydrograph, a large sand peninsula in the upstream end of the eddy was completely eroded. Scour events documented by daily photographs taken automatically by a camera on the opposite bank include May 7, 1991, at about 7:30 p.m., May 13, 1991, June 18, 1991, about 7:30 p.m., and September 1, 1991 (B.L. Cluer, National Park Service, written commun., 1991). Minor downward tilting of -0.3° in the y-axis of tilt sensor 41 occurred in the 2 days following the May 7 event (fig. 13). No other tilt sensors exhibited any tilt during this event.

In the 5 days following the June 18 event, downward tilting of -1.1° in the x-axis and -0.7° in the y-axis of tilt sensor 41 occurred (fig. 15). In this event, tilt sensor 11 went off scale about 7:30 p.m. (figs. 13, 16-18). Sensors 41, 46, and 47 tilted about 8:30 p.m. (fig. 13). Tilt on the x-axis of sensor 46 was -0.6° and on the x-axis of sensor 47 was -0.4° . The succession of tilts from sensors in the river to sensors deeper in the sand bar indicates failure by scour.

On September 1, 1991, the entire face of sand bar 172.3L was scoured (B.L. Cluer, National Park Service, written commun., 1991; fig. 13). At about 7:30 p.m., tilt sensors 11, 41, and 47 went off scale (figs. 13, 19).

Attenuation of water-level fluctuation at piezometer 56 was about 35 percent in June 1991 and about 25 percent in September 1991 (figs. 18, 22). A possible mechanism for the change is scour and removal of the fine-grained

172 TILT DATA

JUNE 1991

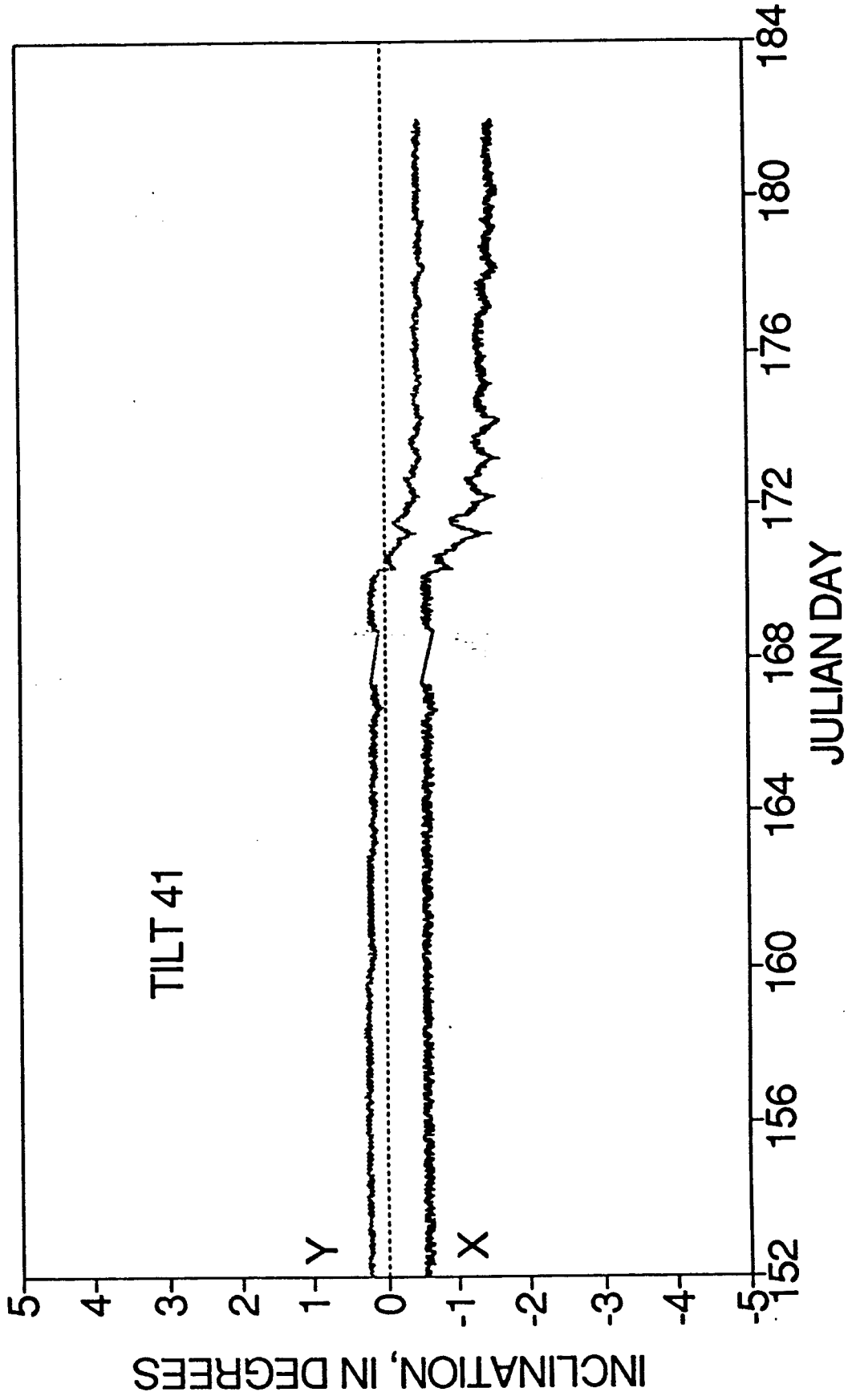


Figure 15. --Tilt for sensor 41 at sand bar 172.3L, June 1991.

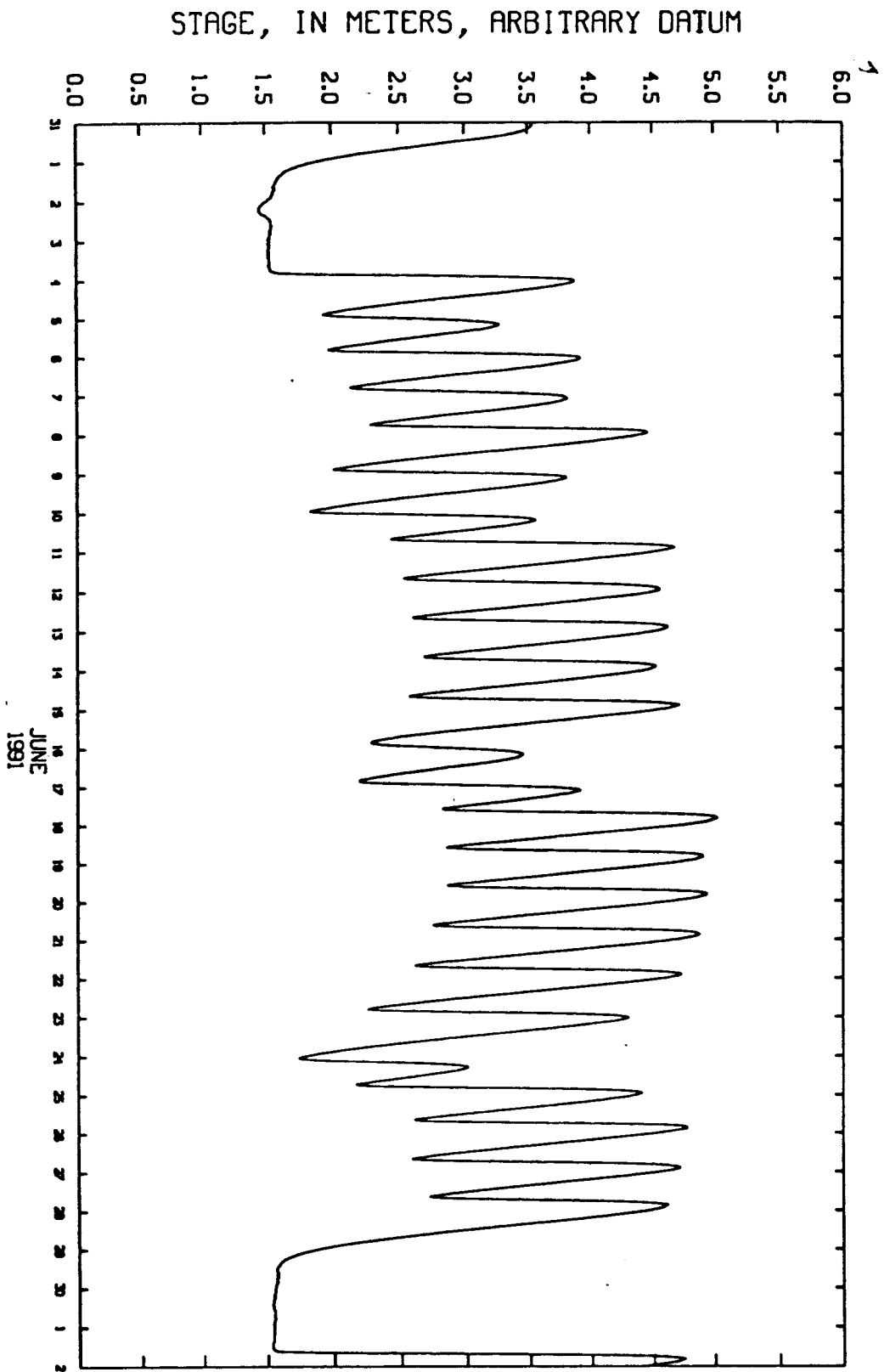


Figure 16.--River stage at river mile 170, June 1991.

172L PRESSURE DATA

JUNE 1991

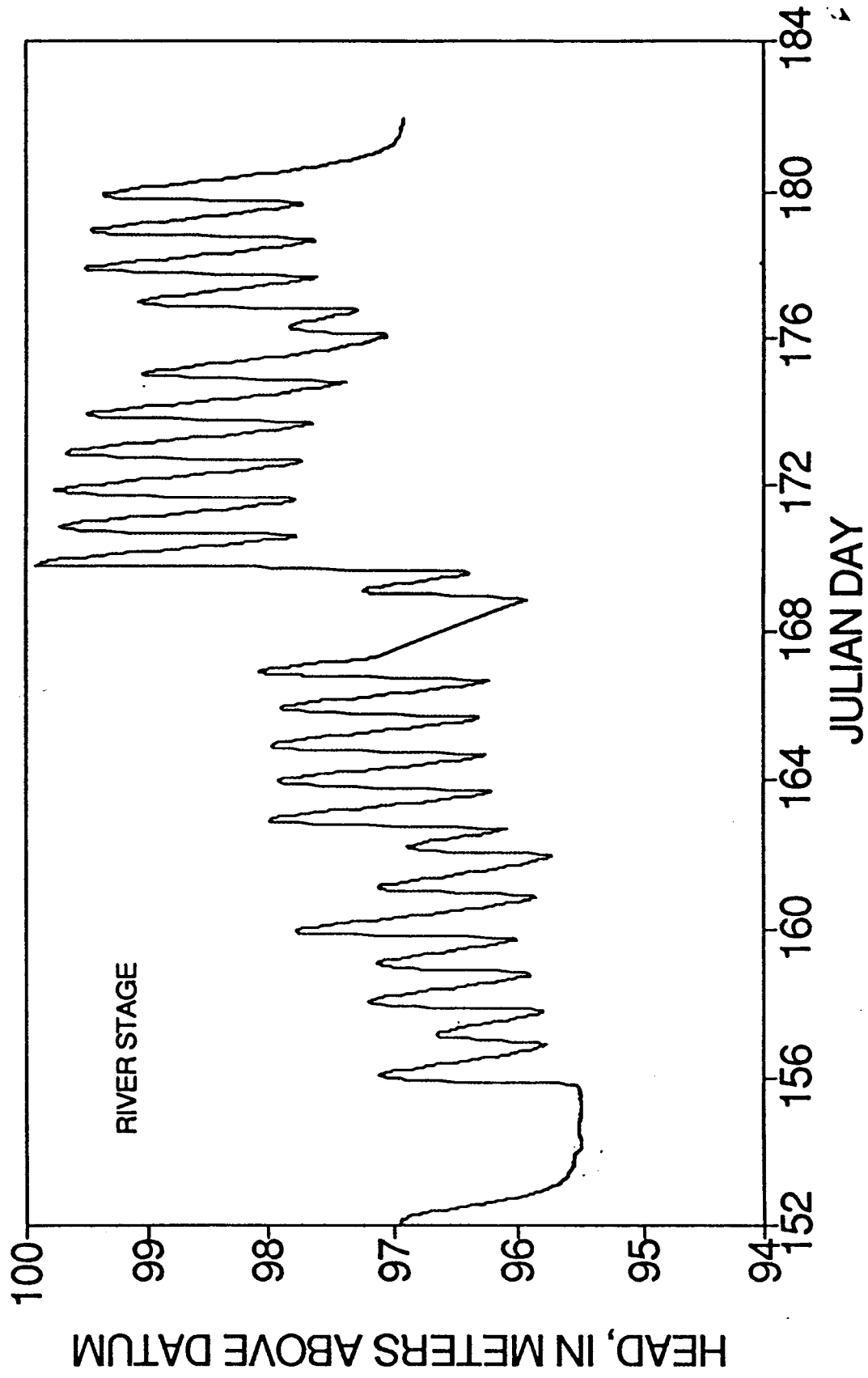


Figure 17. --River stage at sand bar 172.3L, June 1991.

172L PRESSURE DATA

JUNE 1991

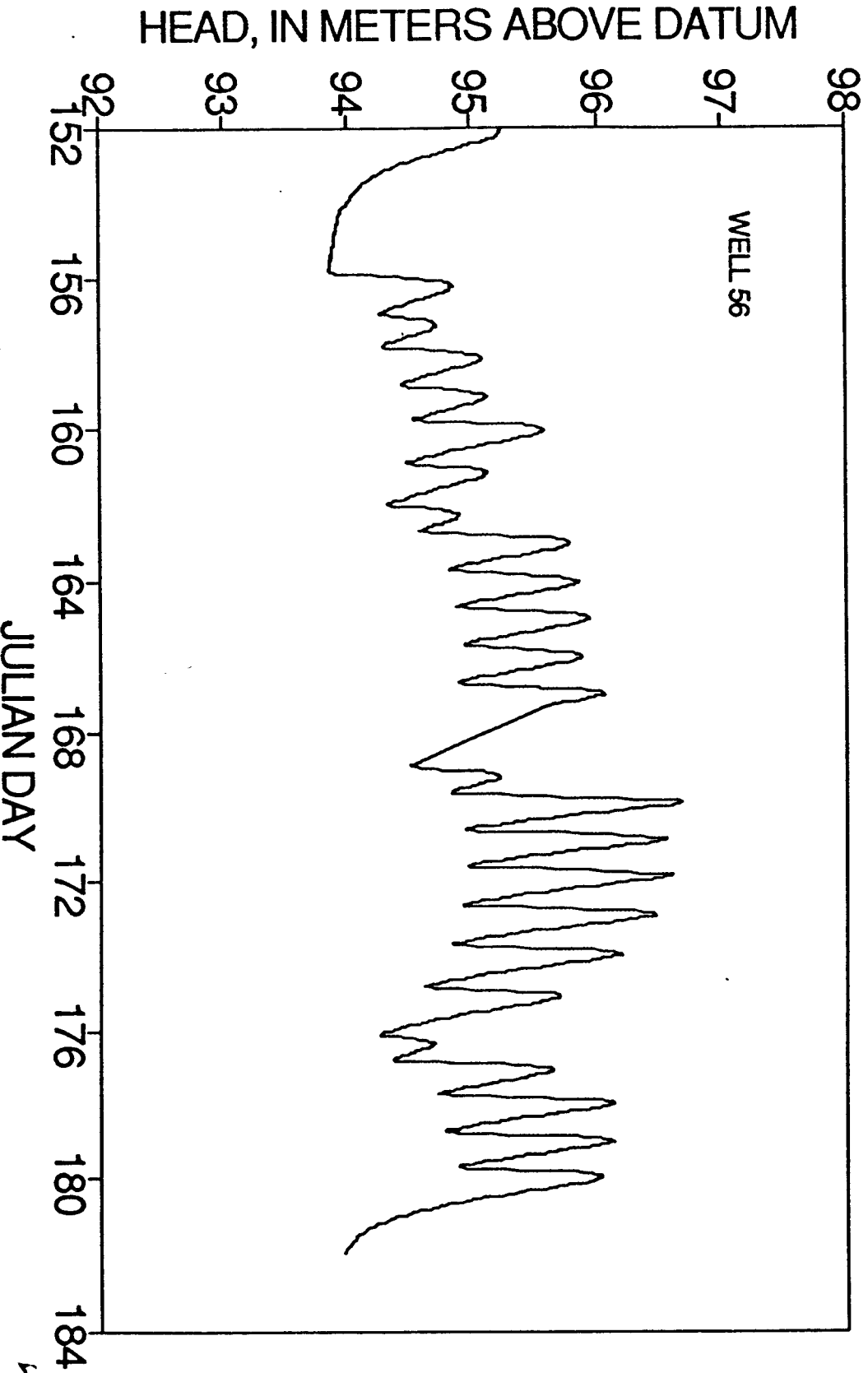


Figure 18. --Water Level in well 56 at sand bar 172.3L, June 1991.

172 TILT DATA

SEPTEMBER 1991

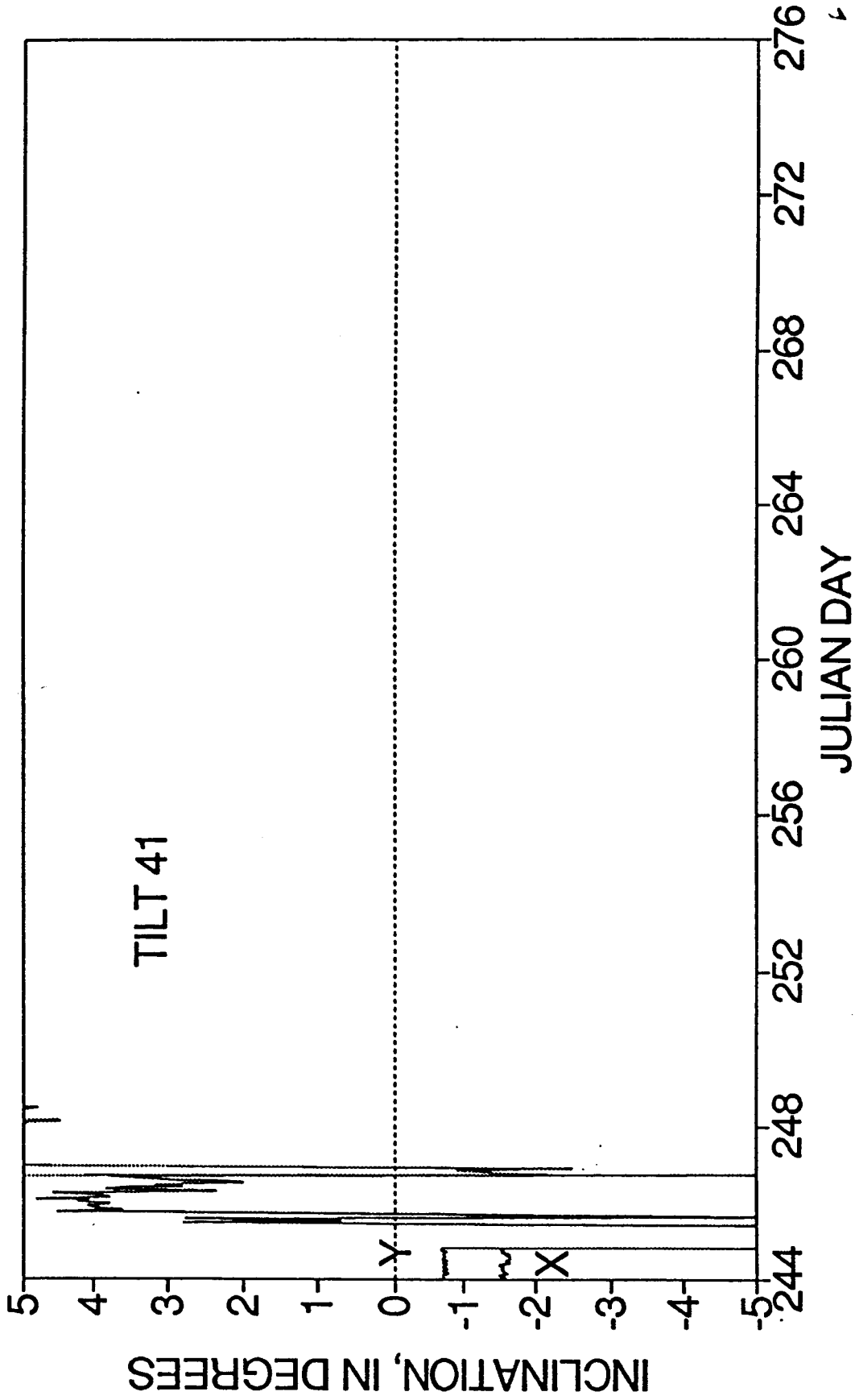


Figure 19.--Tilt for sensor 41 at sand bar 172.3L, September 1991.

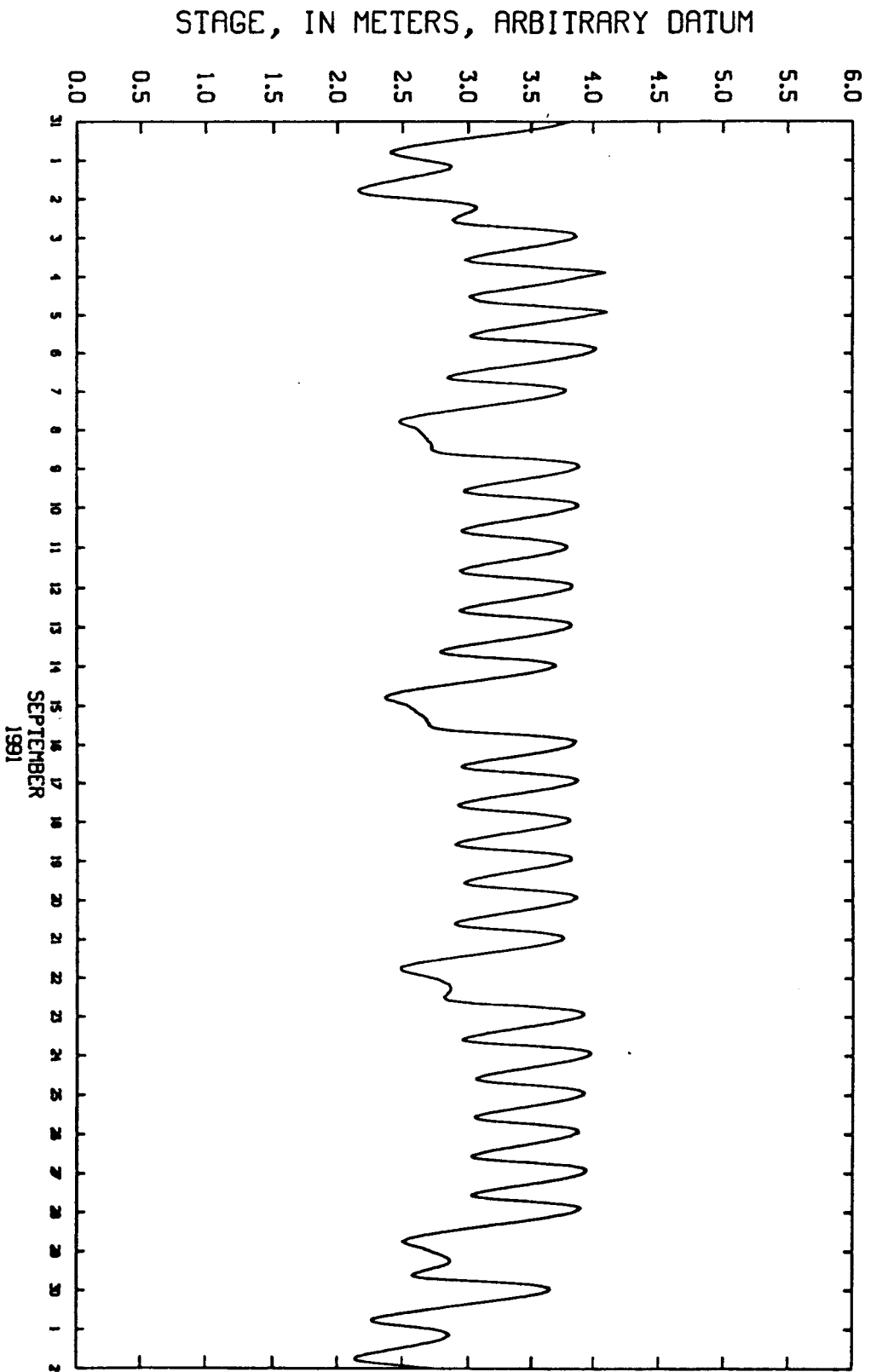


Figure 20.--River stage at river mile 170, September 1991.

172L PRESSURE DATA

SEPTEMBER 1991

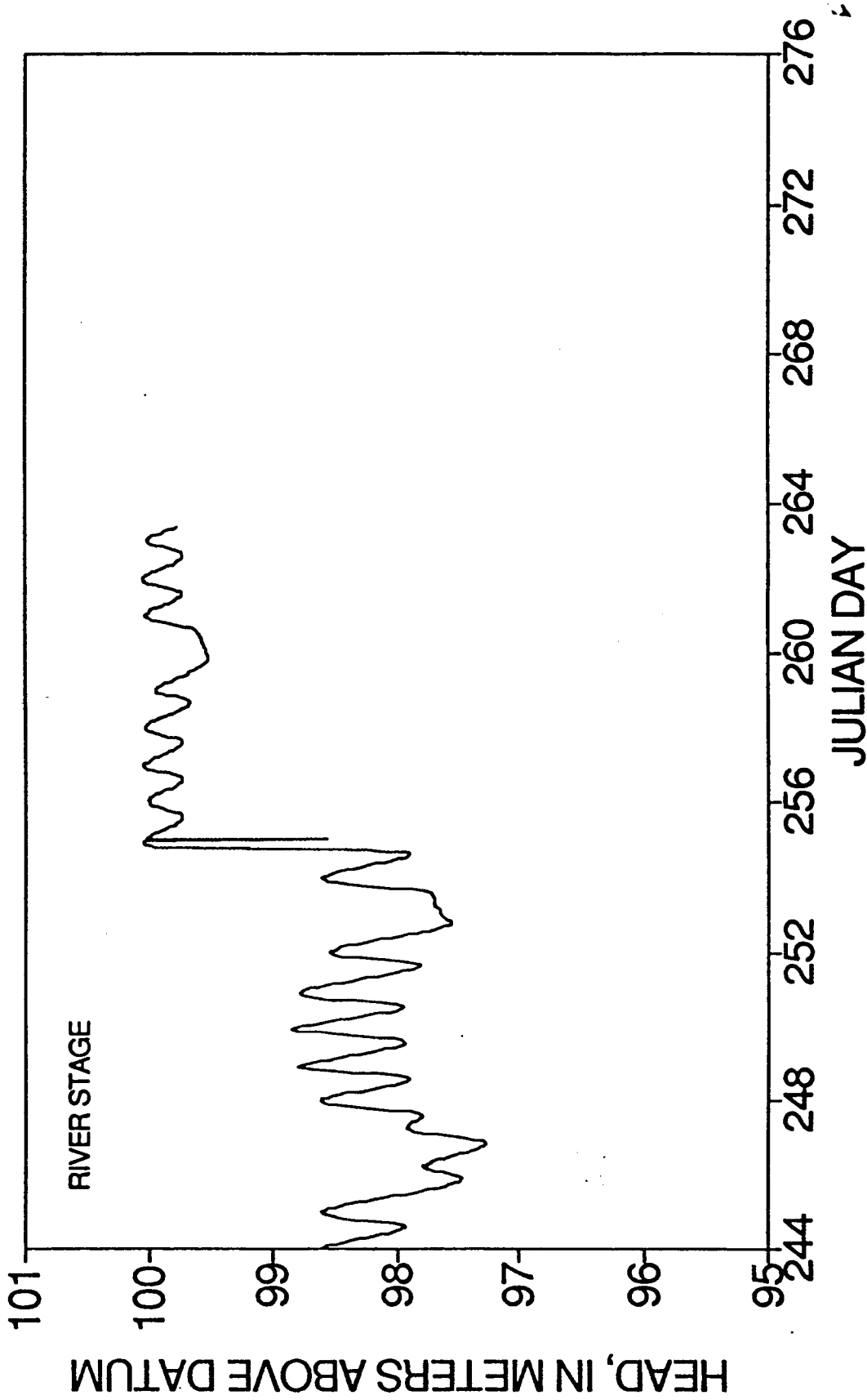


Figure 21. --River stage at sand bar 172.3L, September 1991.

172L PRESSURE DATA SEPTEMBER 1991

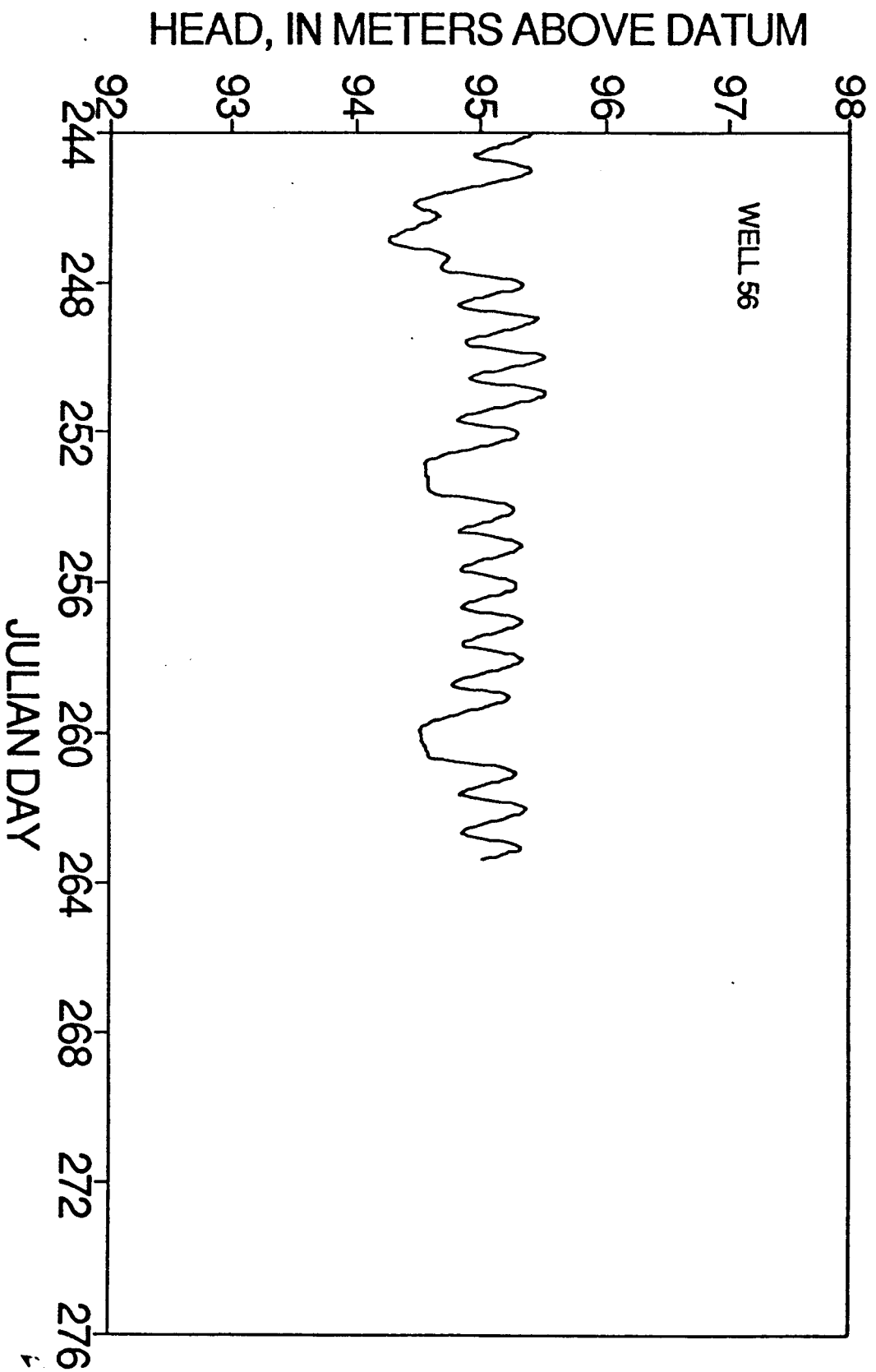


Figure 22.--Water level in well 56 at sand bar 172.3L, September 1991.

barrier to ground-water flow by the event of September 1, 1991. Another possibility is burial of the stage sensor during the scour events. Such burial is indicated by the reduced fluctuations after the September 10 scour (figs. 20-21) and would give the false appearance of change in attenuation.

IMPLICATIONS FOR FLOW ALTERNATIVES

At this stage of analysis, only qualitative remarks can be made regarding bank-storage processes and the flow alternatives. Obviously, because the seepage erosion, slumping, and fissuring mechanisms require head gradient into the river, any steady-flow alternative would be innocuous. The daily photographs opposite sand bar 43.1L during June to July 1991 (B.L. Cluer, National Park Service, written commun., 1991) indicate that duration of drainage is an important factor in rilling erosion. Reduced weekend flows cause enhanced rilling, and constant low flows ($140 \text{ m}^3/\text{s}$) after high flows produce intense rilling until a sand bar is drained. Thus, the unusual suggestion of increasing weekend flows to midweek peaks might alleviate some damage and still allow peak power generation. Otherwise, minimizing the magnitude of downramping would minimize seepage erosion and consequent slumping and fissuring.

Observed rill erosion and slumping accompanied by measured tilts continue in reduced magnitude during interim flows on sand bar 43.1L after reduction of the range of discharge from 85 to $800 \text{ m}^3/\text{s}$ to a range of 340 to $570 \text{ m}^3/\text{s}$. This modification reduced stage fluctuation to less than 2 m. A threshold value of head gradient and thus stage fluctuation necessary for rilling may exist. This threshold has been demonstrated to be less than the interim flow regime. Quantitative estimates of stage fluctuations necessary

for initiation of rilling will result from stress-strain and variably saturated flow modeling.

Ground-water processes occur on every sand bar and become increasingly important if sand-bar-building flows do not occur or are widely spaced in time. Probably no set of prescribed sand-bar-building flows will rebuild all sand bars. Thus, ground-water processes increase in importance on those sand bars that are not rebuilt.

SUMMARY AND CONCLUSIONS

Three sand bars along the Colorado River in Grand Canyon have been instrumented with sensors for continuous monitoring of stage, pore pressure, ground-water temperature, and tilt to determine the relation between ground-water flow and sand-bar deformation. Typically, in a sand bar, five vertical clusters of deep, intermediate, and shallow pairs of pore-pressure and temperature sensors are arrayed in a vertical plane orthogonal to the river's edge.

The stratigraphies of the three sand bars vary considerably. At sand bar -6.5R, a unit of homogeneous fine to medium sand contains an interlayer or confining unit of silty, very fine sand. This unit dips toward the back of the sand bar where it flattens and attains a depth of about 3.5 m. This sand bar has a gentle slope in the fluctuating zone and exhibits a seepage face with rill erosion but does not exhibit slumping and fissuring. At sand bar 43.1L, homogeneous, fine to medium sand overlies medium salt-and-pepper sand at a depth of 6 meters. A lens of red, silty sand with some gravel occurs at a depth of about 4 m in the back of the sand bar. The fluctuating zone is a steeply sloping face that exhibits rill erosion, slumping, and fissuring. At sand bar 172.3L, fine to medium sand is interlayered with

silty, very fine sand. The broad, shallow return channel is underlain with silty fine sand. The fluctuating zone is a steeply sloping face with a bench that is underlain with reddish, silty very fine sand interlayered with fine to medium sand. This sand bar exhibits rill erosion, slumping, and fissuring.

Pole-pole DC resistivity has been shown to produce useful results in a difficult environment. Sand bar 43.1L displays a reasonably well-defined layered-earth response, whereas sand bar 172.3L displays more lateral contrasts and only weakly defined layering. The contrast in geophysical character of the two sand bars may represent a difference in erosional-depositional environments between an upper pool deposit (43.1L) and a reattachment deposit (172.3L).

More resistivity lines parallel to the present lines would be useful in mapping characteristic features such as the clay-rich zone in the return-channel area at sand bar 43.1L and the lateral features seen at sand bar 172.3L. Supplemental measurements might be considered using refraction seismology to determine a more reliable depth to bedrock.

At sand bar 43.1L, tilts occurred from July 7, 1991, through July 17, 1991. At 7:20 a.m. on July 7, upward tilt toward the river of 5.5° occurred; on the morning of July 12, downward tilt of -0.5° occurred; and at 9:20 a.m. on July 17, an additional -3.3° of downward tilt occurred. Continued downward tilt toward the river occurred from July 18 to July 26, punctuated with daily downward spikes of about 0.4° that occurred in the morning. All of the sudden tilts except one upward tilt occurred on downward limbs of the hydrographs when the effective stress in the sand-bar face was increasing. One hypothesis that explains these tilts is slumping or rotational failure with the tilt sensor within a slump block during the major upward event and

outside a block on succeeding events. An alternative hypothesis is a slump-creep sequence of downslope movement in which tilt alternates from upward to downward. The probable cause of slope failure on this sand bar is oversteepening of the lower part of the slope of the fluctuating zone by rilling, which is increased by longer drainage times during fluctuating weekend low flows and steady low flows. Oversteepening of the lower portion of the face of the fluctuating zone accumulates to a critical value. Then, slumping is triggered by a change in effective stress during the falling limb of the hydrograph. Attenuation of water-level fluctuation from the front to the back of 43.1L sand bar is 30 percent over a distance of 30 m.

At sand bar 172.3L, tilt events are probably all related to scour. All events that are documented by tilt sensors occurred on the rising limb of a hydrograph. Events occurred on April 17, May 7, May 13, June 18, and September 1, 1991. Downward tilts toward the river occurred with the May 7 and June 18 events. During the September 1 event, the entire face of sand bar 172.3L was scoured and three tilt sensors went off scale. Attenuation of water-level fluctuation under the fluctuating zone varied from about 35 percent in June 1991 to about 25 percent in September 1991.

Seepage erosion, slumping, and fissuring mechanisms require a head gradient in the sand-bar face toward the river; therefore, any steady-flow alternative would eliminate sand-bar degradation from these processes. Because duration of drainage and height of seepage face are important in these processes, minimizing the magnitude of downramping would minimize seepage erosion and consequent slumping and fissuring. Reduced weekend flows cause enhanced rilling; thus, the unusual suggestion of increasing weekend flows to midweek peaks might alleviate some damage and still allow peak power generation.

Observed rill erosion and slumping accompanied by measured tilts continue in reduced magnitude on sand bar 43.1L during interim flows. Thus, reduction in range of discharge does not eliminate degradation caused by rilling erosion, slumping, and fissuring. If there is a threshold range of stage fluctuation below which rilling does not occur, that range is less than the interim flow regime. The importance of the ground-water processes is that they occur on every sand bar. The processes become increasingly important on all sand bars in the absence of sand-bar-building flows or if sand-bar-building flows are widely spaced in time. It is unlikely that any set of prescribed sand-bar-building flows will rebuild all sand bars. Thus, ground-water processes gain importance on sand bars that are not rebuilt.

SELECTED REFERENCES

- Carpenter, M.C., Carruth, R.L., and Cluer, B.L., 1991, Beach erosion and deformation caused by outward flowing bank storage associated with fluctuating flows along the Colorado River in the Grand Canyon [abs.]: American Geophysical Union Transactions, v. 72, no. 44, p. 222.
- Carruth, R.L., Carpenter, M.C., and Cluer, B.L., 1991, Documentation of beach failure caused by slumping and seepage erosion at two sites on the Colorado River in the Grand Canyon [abs.]: American Geophysical Union Transactions, v. 72, no. 44, p. 223.
- Cluer, B.L., 1991, Catastrophic erosion events and rapid deposition of sandbars on the Colorado River, the Grand Canyon, Arizona [abs.]: American Geophysical Union Transactions, v. 72, no. 44, p. 223.
- Fink, J.B., 1989, Induced polarization: electrochemistry, fractal geometry, and geohydrologic applications, unpublished Ph.D. dissertation, Univ. of Arizona, Tucson, 585 p.
- Howard, A.D., and McLane, C.F. III, 1988, Erosion of cohesionless sediment by groundwater seepage: Water Resources Research, v. 24, no. 10, p. 1659-1674.
- Iverson, R.M., and Major J.J., 1986, Groundwater seepage vectors and the potential for hillslope failure and debris flow mobilization: Water Resources Research, v. 22, no. 11, p. 1543-1548.
- Schmidt, J.C., and Graf, J.B., 1990, Aggradation and degradation of alluvial sand deposits, 1965 to 1986, Colorado River, Grand Canyon National Park, Arizona: U.S. Geological Survey Professional Paper 1493, 74 p.
- Werrell, W.L., Inglis, R.R., and Martin, L.J., 1991, Beach face erosion in the Grand Canyon during falling stage of the Colorado River [abs.]: American Geophysical Union Transactions, v. 72, no. 44, p. 224.

CHAPTER 4

**EROSION OF SAND BAR 43.1 L
ALONG THE COLORADO RIVER IN GRAND CANYON
IN RESPONSE TO GROUND-WATER SEEPAGE
DURING FLUCTUATING FLOW RELEASES
FROM GLEN CANYON DAM**

William Werrell, Richard Inglis Jr., and Larry Martin

**National Park Service
Water Resources Division
301 South Howes Street
Fort Collins, CO 80521**

DRAFT
March, 1992

CONTENTS

ABSTRACT

ACKNOWLEDGEMENTS

INTRODUCTION

PROBLEM STATEMENT

PREVIOUS INVESTIGATIONS

PHYSICAL SETTING

Study Site Selection
Sand Bar 43.1L Characteristics

METHODS

APRIL STUDY PERIOD

Design and Instrumentation
Colorado River Flow Characteristics
Data Analysis
Horizontal Drains
Wind Blown Sand
Video Documentation

AUGUST STUDY PERIOD

Design and Instrumentation
Colorado River Flow Characteristics
Data Analysis

DISCUSSION

FACTORS AFFECTING SAND BAR FACE EROSION

CONCLUSIONS

APPENDICES

Glossary
Design and Operation of the Surface Profile Gage
Interim Flow Releases from Glen Canyon Dam

DRAFT
March, 1992

LIST OF FIGURES

1. Location of study area.
2. Major geomorphic features at Sand Bar 43.1L and location of study sites.
3. Relative locations of monitor wells and transects for the two study periods.
4. Photos of the Soil Profile Gage.
5. Layout of study plots, April 1991.
6. April hydrographs - River stage and monitor wells.
7. Mean elevation of transects in Plot 1, April 1991.
8. Mean elevation of transects in Plot 2, April 1991.
9. Mean elevation of transects in Plot 3, April 1991.
10. Photographs of horizontal drains in the sand bar at River Mile 43.1L, April 7, 1991, about 24 hours after installation of the drains.
11. Layout of study plots, August 1991.
12. August hydrographs - River stage and monitor wells.
13. Mean elevation of Upper Transects, August 1991.
14. Mean elevation of Lower Transects, August 1991.
15. Mean elevation of Perpendicular Transects, August 1991.
16. Effect of river stage fluctuation on the water table in sand bars.

DRAFT
March, 1992

**EROSION OF SAND BAR 43.1L ALONG THE COLORADO RIVER
IN GRAND CANYON IN RESPONSE TO GROUND-WATER SEEPAGE
DURING FLUCTUATING FLOW RELEASES FROM GLEN CANYON DAM**

ABSTRACT

An investigation of sand-bar erosion caused by ground water seepage was conducted by the National Park Service (NPS) in support of the Glen Canyon Environmental Studies (GCES) Program. The GCES Program, funded by the Bureau of Reclamation, is evaluating the effects of daily water release patterns from Glen Canyon Dam on downstream resources in Glen Canyon National Recreation Area and Grand Canyon National Park. This investigation focused on evaluating the effects of shallow ground water seepage on the erosion of sand bars along the Colorado River in this area.

Ground-water movement is the result of recharge and discharge (seepage) from the river banks during daily river stage fluctuations. The study was conducted during two periods under different flow release regimes from the dam. During April 3 - 9, 1991, (7 days) dam releases ranged from about 100 to 425 m³/s resulting in river stage fluctuations of about 1.9 meters. During August 8 - 26, 1991, (19 days) flow releases from the dam ranged from about 280 to 510 m³/s, and river stage fluctuated about 1.2 meters.

River stage and ground water elevations were monitored continuously during each period. Daily measurements of land surface elevations were recorded along transects on the beach face between high and low river levels. Elevation data were collected with a surface profile gage that was designed for this study and built by the authors. The gage provides topographic data at 58 points over a distance of 4.5 meters. In addition, an experiment was conducted with drain pipes set horizontally into the face of the sand bar to enhance ground water drainage from a small area of the sand bar. Photographic and video documentation was acquired during both periods to further demonstrate the role of ground water seepage on sand-bar erosion.

Erosion and deposition processes occur daily in response to changing hydrologic and hydraulic conditions. The net effect of these opposing processes varies with changing river flow characteristics. When the river stage falls below the water table in the sand bar, ground water discharges from the face of the sand bar as a seep or spring line. Seepage erosion occurs as water flowing down the sand bar to the river's edge concentrates and forms rills, scouring loose sand from the sand bar in the process. Sand bar aggradation (or apparent aggradation) could be caused by soil creep, sand deposition by near-shore eddy action, vertical settling of rebar stakes, or surveying errors.

Deposition and erosion processes both occur during daily river stage fluctuations. In April, the net effect of these opposing processes was a decrease in mean elevations of transects. Sand bar erosion of 2 to 12 mm/transect occurred during the April study period of seven days. In August, the net effect was an increase in mean elevations. Sand bar aggradation of 3 to 9 mm/transect occurred during the August study period of nineteen days.

ACKNOWLEDGEMENTS

This study was conducted by a team from the Water Operations Branch, Water Resources Division, National Park Service under the direction of Bill Jackson. Data collection assistance was provided by John Sloat, Beth Glasbrenner and Mike Kearsley as unpaid volunteers. We also wish to thank Brian Cluer (NPS), Larry Stevens (NPS), Mike Carpenter (USGS), and Rob Carruth (USGS) who were also conducting investigations for Glen Canyon Environmental Studies at the study site during our work. Their direct assistance and shared thoughts were invaluable in support of our work.

INTRODUCTION

The Colorado River riparian zone and its associated resources in the Grand Canyon are influenced by the operation of Glen Canyon Dam. The dam was constructed for several reasons, primarily flood control and water storage for Arizona, California and Nevada, as well as hydroelectric generation. The hydroelectric capability is designed to provide peak power generation during daily peak electrical demands. Consequently, release of water from the dam fluctuates with power demand and a daily surge of water continues downstream through the entire length of the Grand Canyon. Water levels in the river have fluctuated in narrow parts of the canyon as much as four meters in one day. A more typical fluctuation is from one to three meters. Interrelated processes occurring between the river and its riparian areas are affected by the fluctuation.

This report describes the relationship of bank stored ground water to sand-bar erosion occurring during fluctuating Colorado River flows. The Colorado River below Glen Canyon Dam is within both Glen Canyon National Recreation Area and Grand Canyon National Park. National Park Service concern for the resources of the parks includes preservation of sand bars along the Colorado River. These sand bars have high natural resources value and are used as camping sites by park visitors floating the river.

The terms; sand bars, alluvial sand deposits, selected alluvial deposits, and sediment deposits, have been used to describe what are colloquially called beaches. In this report, the term sand bar will be used to be consistent with recent reports of other investigators.

The purpose of this report is to evaluate and demonstrate the role of ground water on sand-bar erosion during daily fluctuations of the Colorado River. The objectives are 1) to confirm that ground water is a contributing factor to erosion, 2) to quantify sand-bar erosion rates directly associated with ground water seepage from the sand bar, and 3) present a hypothesis of ground water related processes contributing to sand-bar erosion for review by a general audience.

PROBLEM STATEMENT

Observation of sand bars during the daily Colorado River stage fluctuations

revealed that during times of falling stage, a zone of saturated sand formed on the face of the sand bar adjacent to the water's edge. This zone progressively moved down the face of the sand bar as the stage lowered. As the stage approached minimum, the zone gradually widened to about 2 m wide, remaining adjacent to the river's edge. Rills formed in the saturated zone, moving sand grains down the slope of the sand bar.

The responses of the water table in the sand bar to the fluctuating river stage were thought to be the driving mechanism of seepage erosion processes. During rising river stage, river water infiltrates the sand bar causing the water table to rise in the area adjacent to the face of the sand bar. As the river stage begins to fall, ground water will flow toward the river, exiting from the sand bar as a spring or seep line forming a seepage face. Water flowing down the face of the sand bar to the river's edge concentrates and forms rills, scouring the upper layer of sand in the process. As the river stage begins to rise, the seepage face is submerged, river water begins to recharge the sand bar, and the cycle is completed.

The rate of stage decline, the length of time stage remains at a minimum, and the amplitude of the river stage fluctuation were thought to be important variables in determining the rate of erosion of the sand bar.

The objectives of this investigation are to quantify erosion rates and relate the variation in erosion rates to fluctuations of river stage and the water table in the sand bar. The investigation had four major components:

- 1) Ground elevation transects in the fluctuating zone on the face of the sand bar.
- 2) Continuous monitoring of river stage and the water table in the sand bar.
- 3) Demonstrate the direct relationship of ground-water seepage to rill formation during falling river stage by placing horizontal drains in the beach face to promote faster drainage of ground water during periods of falling river stage.
- 4) Video-tape documentation of the erosion processes related to the river stage, water-table elevation, and the onset of ground-water seepage from the sand bar.

PREVIOUS INVESTIGATIONS

Past and present studies of sand bar morphology and sedimentology of the Colorado River can be divided into three periods. These are works published prior to the Glen Canyon Environmental Studies (GCES), publications from GCES Phase I, and GCES Phase II investigations that are currently under way. A brief discussion of each follows.

The classic description of the geomorphology of the Grand Canyon was written by Leopold (1969). Early work on sand-bar deposits consisted mainly of aerial and ground photography (Laursen and Silverston, 1976; Turner and Karpiscak, 1980) and topographic surveys of deposits begun in 1974 (Howard, 1975; Beus and others, 1985; Ferrari, 1987).

GCES Phase I studies included:

- 1) Collection and analysis of flow and sediment transport data at gaging stations (Graf, 1986; Pemberton and Randle, 1986).

- 2) Analysis of historical sediment data from gaging stations (Burkham, 1986).
- 3) Mapping of channel-bed materials (Wilson, 1986).
- 4) Development and application of a sediment-transport model in the main channel (Orvis and Randle, 1986; Pemberton and Randle, 1986).
- 5) Evaluation of sediment contributions from ungaged tributaries by debris flows (Webb and others, 1987).
- 6) Classification and description of alluvial sand deposits (Schmidt and Graf, 1988).

The results of these studies are also included in the Glen Canyon Environmental Studies Final Report (U.S.D.I., 1988).

Present research related to this investigation are being conducted as part of two of the ten major components of the GCES Phase II studies (U.S.D.I., 1990). The first, Sediment Transport and Beach (sand bar) Studies, has four sub-components:

- 1) Paleoflood Studies.
- 2) Beach Evolution Studies which include sand inventory, depositional history of the sediment deposits, eddy dynamics, slope stability, and debris flow effects.
- 3) Sediment Transport Studies which include flow model development, solute transport models, debris flow models, and eolian inputs.
- 4) Beach and Sediment Deposit Characteristics which include historical data assessment, empirical studies, and modeling studies.

The second major component of the Phase II studies is the Hydrology Study which includes two sub-components:

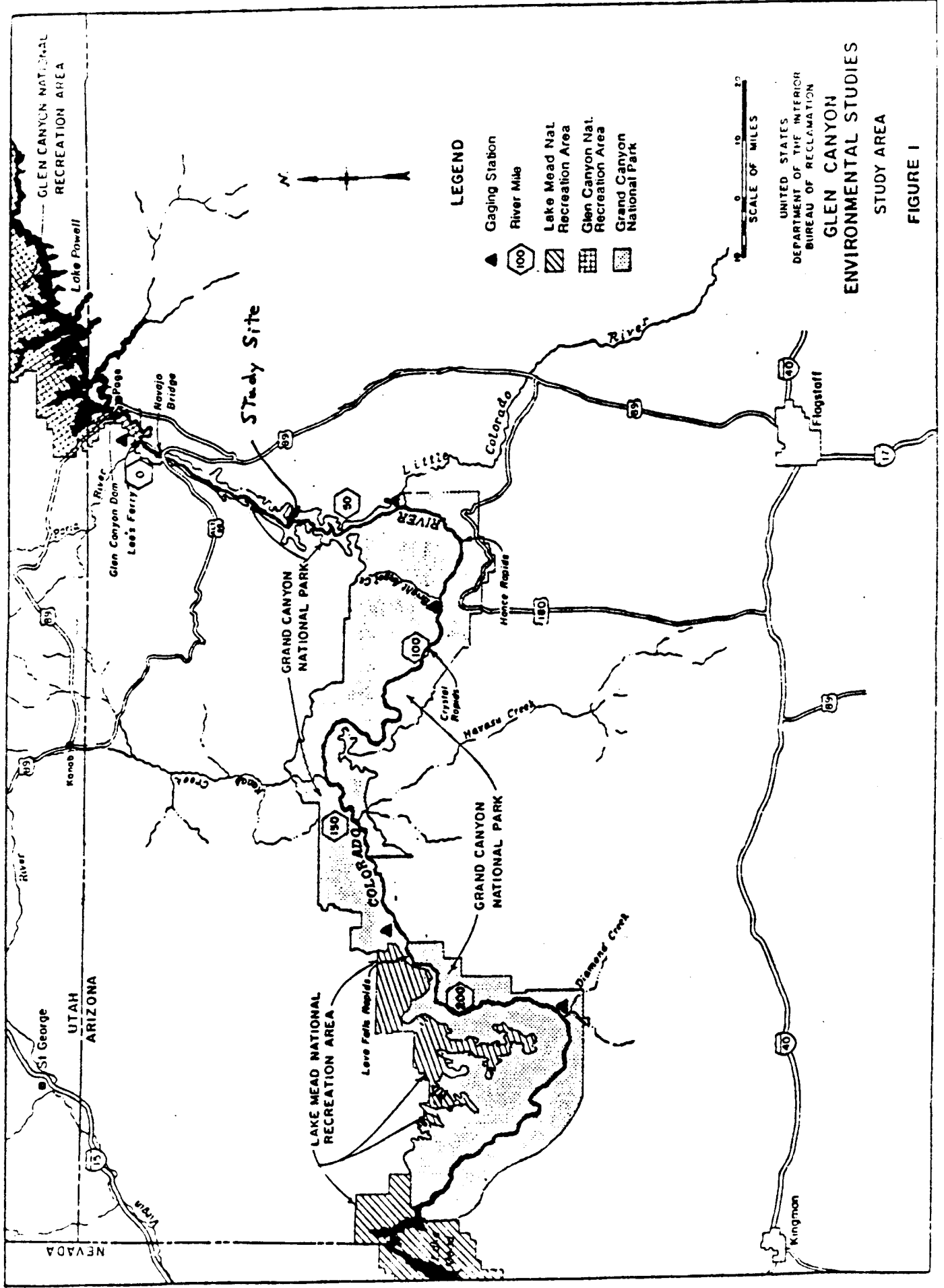
- 1) Gaging of streamflow levels which includes mainstream and tributaries.
- 2) Evaluation of Glen Canyon Dam releases which includes historic review of Glen Canyon Dam releases and review of GCES research flows.

PHYSICAL SETTING

Study Site Selection

The sand bar at River Mile 43.1L was selected as the site for the study. The name 43.1L indicates that the sand bar is 43.1 river miles (69.3 km) downstream from Lees Ferry and on the left bank of the river. Lees Ferry is 24.9 km downstream from Glen Canyon Dam. Thus the study site is 94.2 km below the dam (figure 1). This sand bar was selected for study for the following reasons:

- (1) The sand bar had been selected by other investigators as one of three validation sites (sand bars at River Mile -6.5R, 43.1L, and 172.3L) for GCES research. That selection was based on:
 - (a) Geographic distribution within the reach of the Colorado River between Glen Canyon Dam and Lake Mead.
 - (b) Sufficient sand bar size to sustain erosion and remain as a sand bar for the duration of studies.
 - (c) Not intensively used by park visitors. Expensive scientific equipment could be left unattended at the site without being subject to theft or vandalism.
 - (d) Geomorphic and stratigraphic variation among study sites to allow



investigation of processes at different types of sand bars.

- (2) Other research projects at the site would provide supplementary information, e.g. topographic surveys, stratigraphy, and aerial photography. The other projects included:
 - (a) Long-term vegetative studies.
 - (b) Repeated aerial photography program.
 - (c) Photographic documentation of the sand bar over the last 10 years.
 - (d) Sand bar ground water study (US Geological Survey).
 - (e) Modeling of erosion from the face of the sand bar by ground-water seepage (University of Arizona).
 - (f) Daily photographs of the site to document morphological changes (NPS-GRCA).

- (3) Features of Sand Bar 43.1L favorable to our study were:
 - (a) The steepness of the face of the sand bar was deemed sufficient to study seepage effectively, i.e., very gently sloping sand bars would have large areas of saturated sands exposed at low river stage, making data collection physically difficult and reducing data accuracy.
 - (b) Studies by the USGS indicated that the sand deposits at the site were fairly homogeneous. This would reduce complications in analyzing processes of ground water response to fluctuating river stage.
 - (c) The sand bar at River Mile 43.1L is relatively near Glen Canyon Dam. Effects of river stage fluctuations would be more apparent here than further downstream where natural peak attenuation could reduce the range of fluctuations.
 - (d) Location upstream of the Little Colorado River. The sediment load in this reach is less than downstream of the Little Colorado River. Sediment deposits by eddies at high river stage (i.e. aggradation) will be less of a problem in data analysis. Sand bars in this reach are expected to be more susceptible to depletion than bars further downstream due to the reduced sediment load of water released through Glen Canyon Dam.

Sand Bar 43.1L Characteristics

The study area for this investigation was a sand bar on the left side at River Mile 43.1 of the Colorado River in the Grand Canyon. The sand bar is roughly crescent shaped about 120 m long by about 30 m wide at its widest point (figure 2). It is located just upstream from a moderate-sized rapid of the Colorado River. The rapid is caused by a constriction of the river by a debris fan from a small unnamed tributary on the left bank of the river. The debris fan contains sediments ranging in size from silts to boulders. The sand bar is composed of fairly uniform fine to medium sand and is classified as an upper pool deposit (Schmidt and Graf, 1988). Sand Bar 43.1L was enlarged during the high water period of 1983-84 and is largely covered by reworked sand from that flood.

At the study site, the Colorado River flows from west to east, the sand bar being on the north side of the river. A return channel is present on the sand bar, beginning at the downstream end of the sand bar adjacent to the debris flow some 10 meters from shore and extending in an arc to the west adjacent to the talus/bedrock of the canyon wall for the majority of the sand bar length

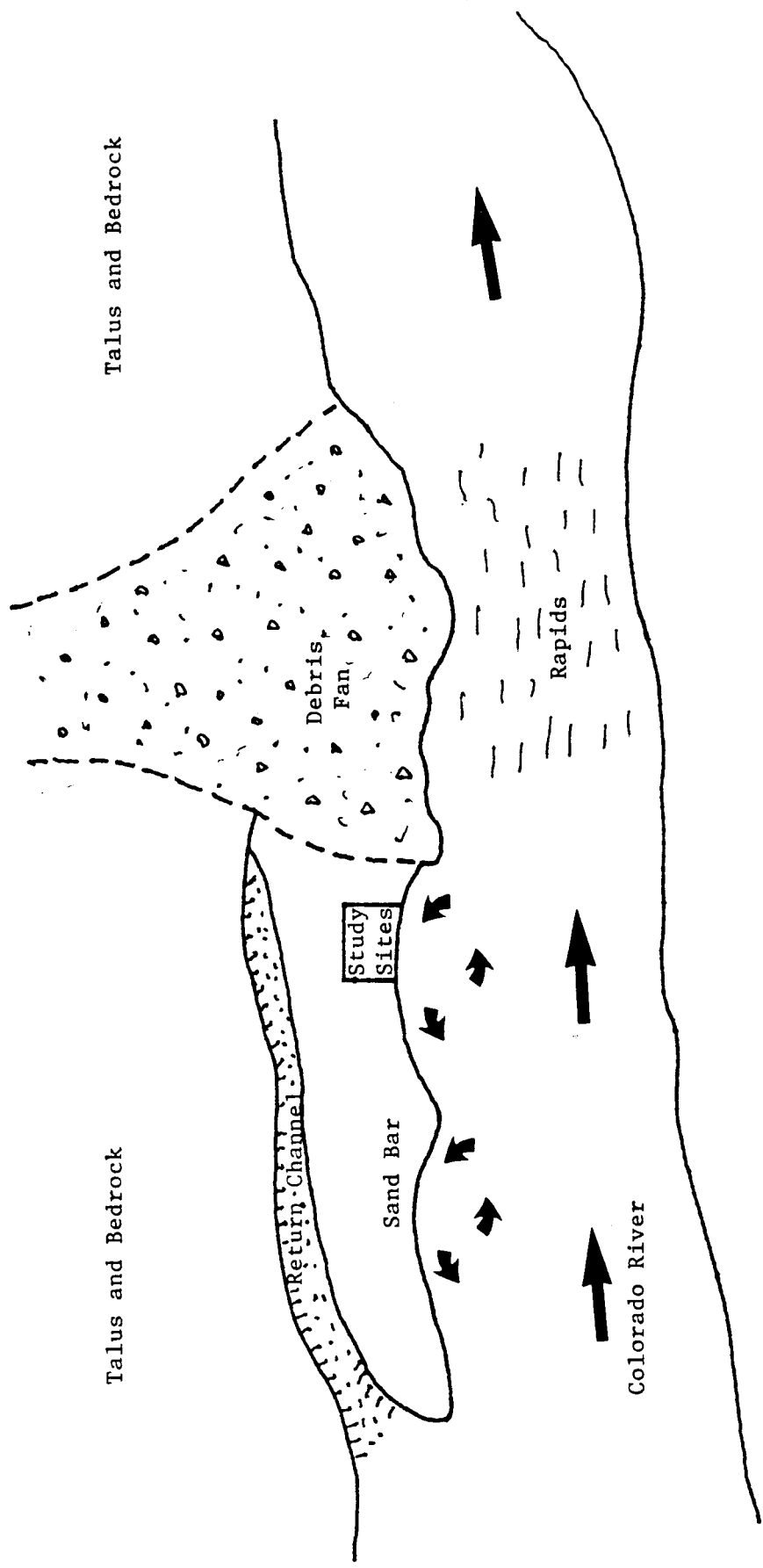


Figure 2. Major geomorphic features at Sand Bar 43.1L and location of study sites.

before joining the Colorado River at the west end of the sand bar. Return channel drainage is east to west. This return channel only operates during flood flows - thus a generic description of a reattachment bar is applicable, however, it is an upper pool deposit with a weak recirculation eddy under normal flow operations.

The main current of the Colorado River as determined by surface flow directions is separated from the sand bar face by two eddies. Each eddy is adjacent to the sand bar and elongated parallel to the shore. One eddy is offshore for approximately the downstream half of the sand bar, and the other eddy is correspondingly present for the upstream half. The eddies were present at all observed river stages, and both have counterclockwise circulation directions. Upstream flow currents adjacent to the shore ranged from near zero to about 0.6 m/s. Eddy circulation extends to about 10 m from shore. At the contact point between the two eddy cells, the sand bar is more gently sloped and projects into the river about 2 - 3 m. In August 1991, the eddy shapes were observed at low and high river stages. There was no longitudinal shift from low to high flow, only lateral compression or expansion of the eddies. There have been two eddies in this location since flows returned to normal. Because they move little, the point in the center of the bar is coincident with the stagnation point between the two eddies. (B. Cluer, personal communication).

METHODS

The investigation was conducted during two study periods, April 3-9 and August 8-26, 1991, to allow investigation during different Glen Canyon Dam flow release regimes. Flow regimes for the two study periods had different ramping rates, ranges, and mean daily discharges. The relative location of monitor wells and transects for the two study periods are shown in figure 3.

A study site was identified in the fluctuating zone on the face of the sand bar during each study period. Study plots, each containing several transects were established. Changes in land surface elevation were measured along the transects on a regular basis, generally daily at low river stage. Transect ends were marked by driving lengths of rebar into the sand (1.5 m lengths in April and 3.3 m lengths in August) with 0.3 m of rebar remaining exposed above the beach surface. While not encountering bedrock, repeated surveys of the rebar elevations did not indicate significant vertical movement. The rebars served as permanent markers for the duration of each of the study periods. The study sites and a buffer area around the sites were marked with flagging to prevent people from accidentally walking through the sites.

Changes in land surface elevation were measured with a surface profile gage which was designed to measure small changes in elevation without disturbing the surface (figure 4). The gage allows accurate measurement of erosion or deposition without trampling or other anthropogenic disturbances. Vertical support stakes (rebar) were installed at each end of a 4.5 meter transect to support the gage. The gage was positioned on the support stakes and the 58 vertical measuring rods, with ping-pong balls attached to the lower end, were allowed to drop to the ground surface. The ping-pong balls prevented the rods from penetrating the sand surface. The measuring rods were clamped in position with the balls resting on the sand surface and the gage was removed to measure and record the extended distance of each rod. Repeated measurements of a transect at different times allowed determination of ground

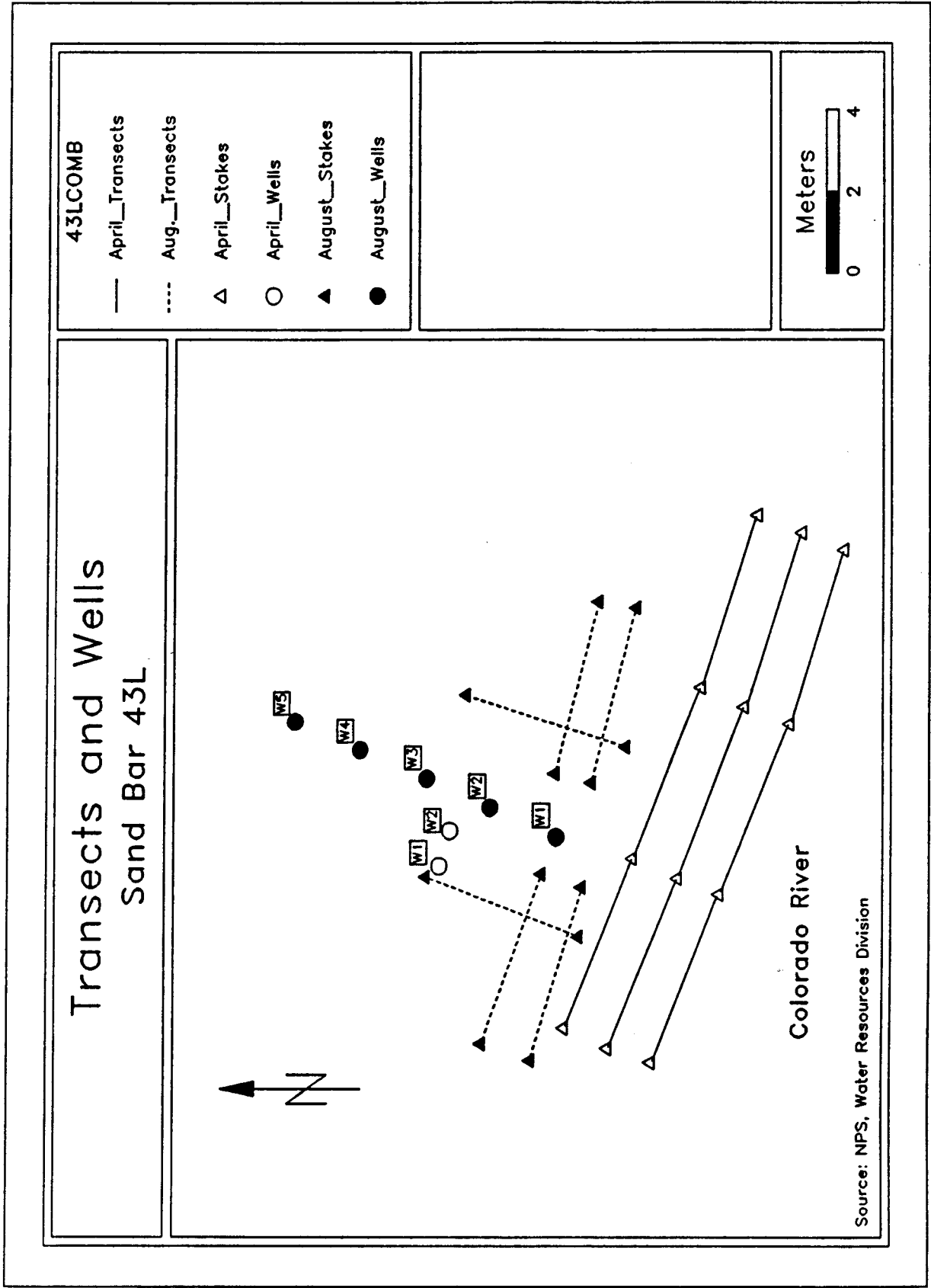


Figure 3. Relative locations of monitor wells and transects for the two study periods.

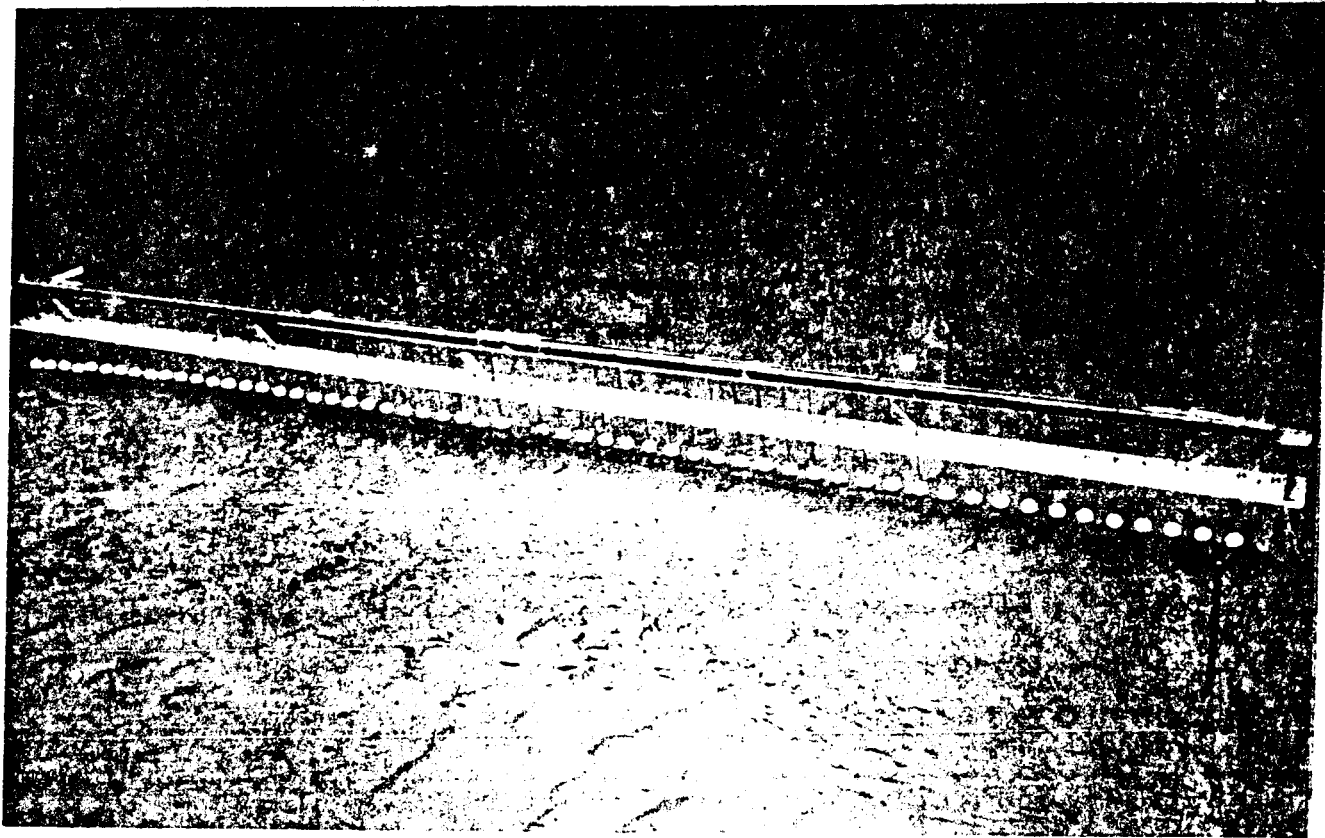


Figure 4. Photos of the Surface Profile Gage.

DRAFT
March, 1992

surface elevation changes. Measurements from the surface profile gage were converted to elevations relative to a local datum on the sand bar. The surface profile gage is further described in Appendix 2.

Transect measurements were made daily following the decline of the river stage. However, measurements were not made on every transect on every day of the study. At times, some transects were still submerged during the lowest river stage, thus preventing access to the ground surface. On other days, river fluctuation did not submerge some transects and no erosion processes (i.e., formation of a seepage face or rilling) were visibly observed. If minor erosion had occurred on days of no measurement, it would be reflected in the measurement of the following day.

Shallow monitor wells were installed in the sand bar in the vicinity of the study plots to monitor water table response to fluctuating river stage. Water levels in each monitor well were monitored with pressure transducers and recorded at ten minute intervals with a digital recorder. River stage was monitored using a pressure transducer attached to a rock and lowered to the bed of the river in the vicinity of the study site.

The elevation of the top of the plot transect stakes (rebar) were surveyed three times during the April study period and five times during the August study period. The surveys were made to determine if any elevation changes (of the stakes) were occurring.

The reference datum for all elevations is a bench mark established by GCES for topographic studies (U.S.D.I., 1990). Survey instruments used were a Lietz SDR 3A Electronic Total Station with an accuracy of 15 seconds of arc and a Topcon AT-F2 Automatic Level with an accuracy of ± 0.3 seconds of vertical arc. Systematic and obvious survey errors were corrected. Elevations of the stakes from each survey were plotted and no upward or downward trends were detected. Relative surveyed elevations of the stakes varied as little as +1.0 mm and as much as +3.0 mm. It is the author's opinion that this variability is a result of measurement errors and limitations of the surveying equipment. The rebar stakes seemed to be stationary after installation and the stakes were presumed to have maintained a stable elevation for the short duration of the field study.

Topographic surveys of the entire sand bar were made by other investigators as part of the GCES studies. Those surveys provided data for mapping contours and geomorphic features.

APRIL STUDY PERIOD

Design and Instrumentation

The April study period consisted of seven days (April 3-9, 1991) during which field studies were conducted. Study plots were located on the face of the sand bar, within the area affected by stage fluctuations of the Colorado River. Three study plots with 3 transects each (for a total of 9 transects) were located in the zone of active erosion as indicated by the presence of rills. The transects were located parallel to the river's edge with a low, middle and high transect spaced about 1.2 m apart (figure 5). The low

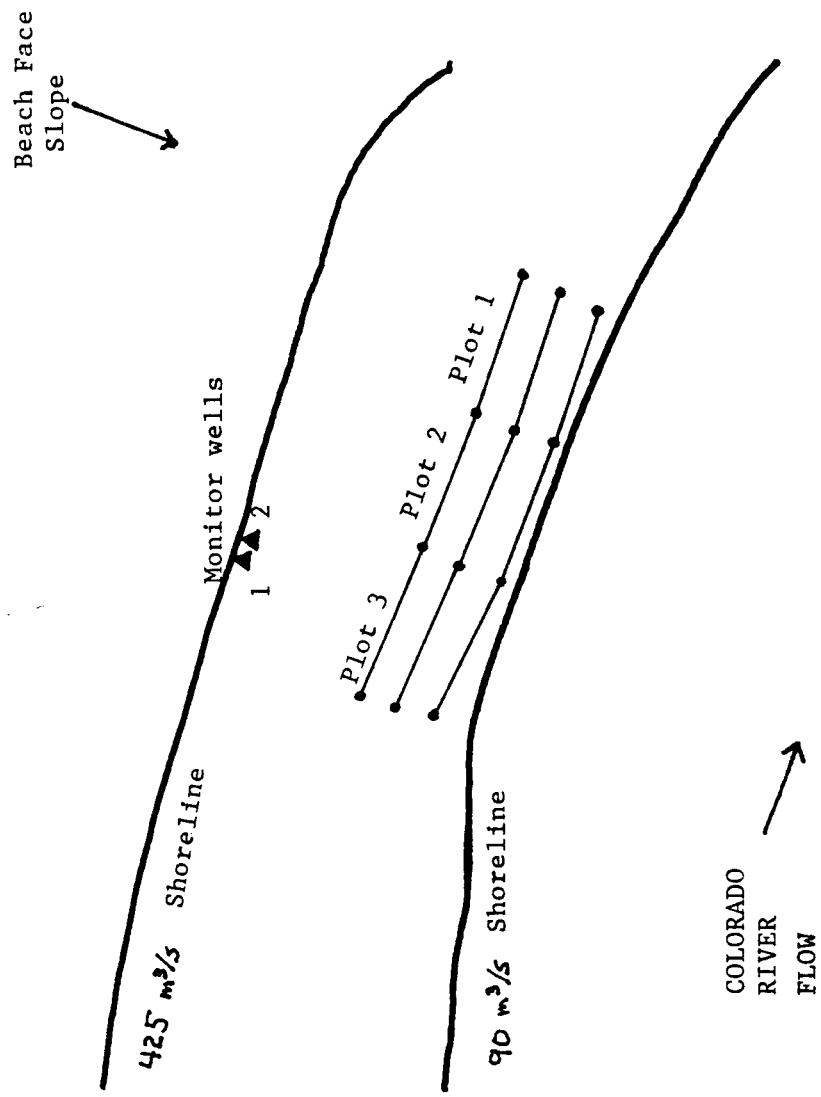


Figure 5. Layout of study plots April 1991.

transects were located about 0.3 m from the river's edge at lowest stage (90 m³/s) and the high transects were approximately midway between the daily high stage (approximately 425 m³/s) and the lowest stage. Plot 1 was in a downstream position and Plot 3 was upstream relative to the other plots. The three study plots were adjacent to one another, the upstream end of Plot 1 coincided with the downstream end of Plot 2 and the upstream end of Plot 2 coincided with the downstream end of Plot 3.

A demonstration to evaluate ground-water flow near the face of the sand bar entailed placing drains in the zone of fluctuations to promote faster drainage of ground water. The demonstration consisted of different treatments on each of three study plots; 1) a control area with no disturbance (Plot 1), 2) horizontal placement of blank (non-perforated) pipe to provide an assessment of disturbance associated with installation (Plot 2), and 3) placement of perforated horizontal drain pipe (Plot 3). The perforated drain treatment was designed to induce faster ground-water drainage near the face of the sand bar and thus prevent erosion.

Two shallow monitor wells were constructed to monitor the water table in the sand bar. The monitor wells were located about 0.3 m above the daily high water mark and up slope from the study plots. The monitor wells were made of PVC pipe. Well 1 was 5 cm (2 inches) in diameter and about 1.5 m long. Well 2 was 2.5 cm (1 inch) in diameter and about 3 m long. Different construction techniques were used for installing the monitor wells: the shallower monitor well was installed by augering to the water table and then driving the casing, the deeper monitor well was jetted. Water level response in the two monitor wells showed that construction techniques did not affect the response of water levels in the monitor wells to water table fluctuations. Water levels in both monitor wells were monitored by means of pressure transducers and digital recorders.

Colorado River Flow Characteristics

During this study period the operation of Glen Canyon Dam and thus the flow release pattern was a continuation of normal dam operations, i.e., operation to generate peak electrical power within the constraints of legal mandates. Dam release discharges ranged from 90 m³/s to 445 m³/s. River stage varied about 1.9 m from low to high stage.

Data Analysis

River stage and water table fluctuations with associated lag times and daily differences of fluctuation for the study period are shown in figure 6. Well 1 was shallow and went dry each day at low river stage. Only data from Well 2 are shown on figure 6. Minimum river stage ranged from about 96.3 to 96.45 meters during the study, corresponding to minimum flow releases from the dam of 90 to 120 m³/s. Maximum river stage varied by more than a meter, from 97.0 to 98.2 meters, in response to differences in the maximum discharge from the dam and the length of time that the maximum discharge was maintained. Large discharges for a short duration are attenuated downstream to produce a maximum stage less than a smaller discharge of greater duration. For example, release of 450 m³/s from the dam for a short duration on April 9th produced a lower

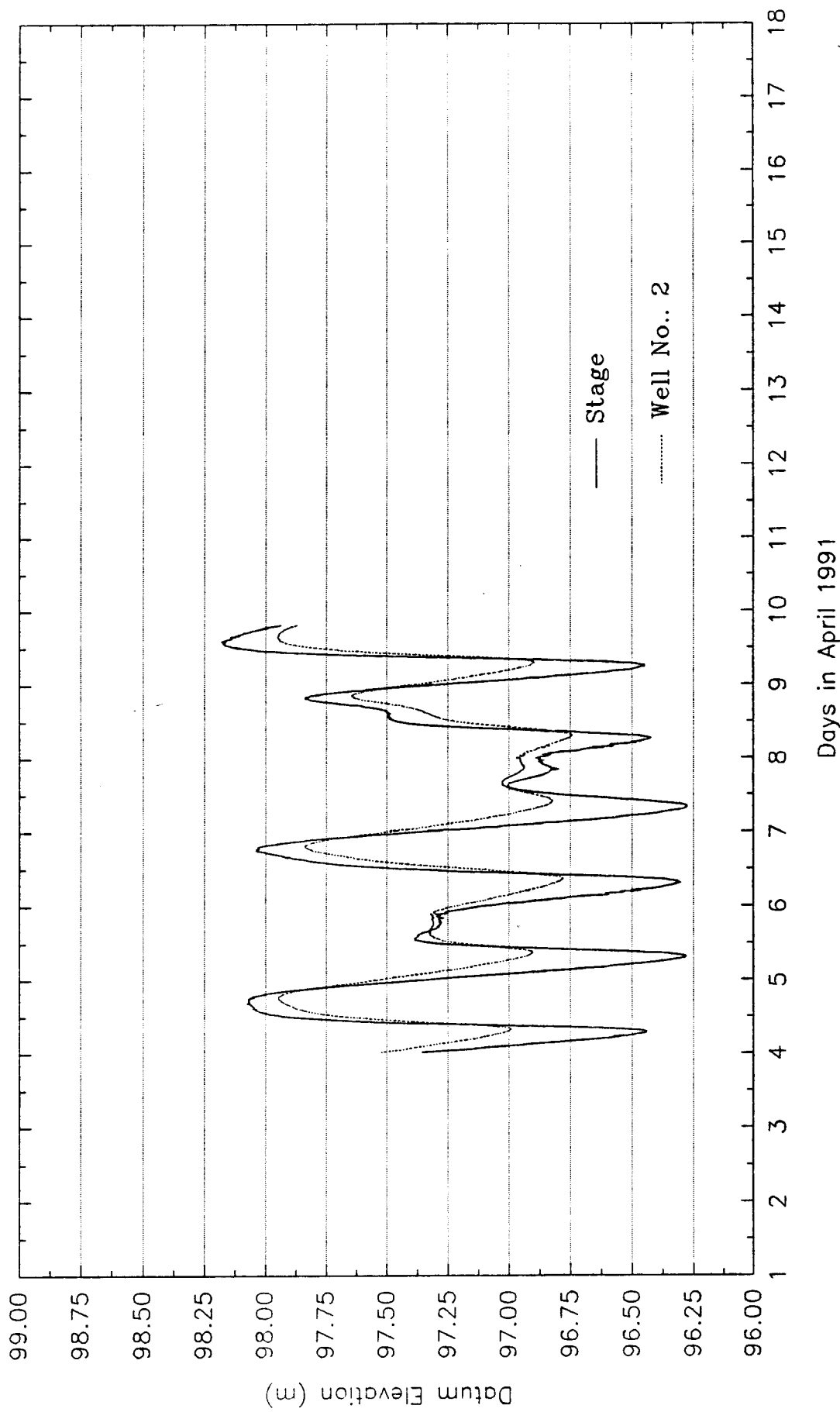


Figure 6. April hydrographs - River Stage and Monitor Well No. 2

(0.2 meter) stage at the study site than did discharge of 430 m³/s for a longer duration on April 5th. The longer peak duration of April 5th caused a water table height closer to peak river stage than short duration peaks of April 7th and 9th. The longer duration of elevated river flows allows increased time for ground-water movement into the sand bar and a corresponding increase in water levels in the wells.

Land surface measurements were made across the transects at each of the plots using the surface profile gage. The length of rod extending from the bottom of the surface profile gage for each of the 58 rods and balls was measured at each of the transects. The mean elevation for each transect was computed to indicate mean values of erosion or deposition over the entire length of the transect. Measurements were made daily, when the river was at its lowest stage. Compaction of the sand due to dewatering in the fluctuating zone was similar for each measurement. The mean elevations for each of the transects during the study period are shown in figures 7, 8, and 9. Mean elevation changes were computed using values for balls 6-54, from the center part of each transect. Balls 1-5 and 55-59 (balls at each end of the gage) were not used in computing means to omit data which might have been subject to some footprint disturbance near the edges of the transects, i.e. to insure that only data from undisturbed areas was used in computing mean elevations.

Figure 7 shows the daily mean elevation changes at Plot 1. Both the high and low transects show very little change (less than 3 mm) during the study period. The mean elevation of the middle transect decreased approximately 12 mm during the study period. The greatest losses occurred following the largest stage fluctuations early in the study period. Lower peak flows on April 6th and 8th allowed drainage of ground water from the sand bar for longer time periods. This resulted in lowering the water table in the sand bar, leading to lesser amounts of erosion for April 9th and 10th, even after larger stage fluctuations resumed.

Mean elevation changes for the transects in Plot 2 are shown in figure 8. The high transect had less than 1 mm elevation change during the study period. The middle transect in Plot 2 showed a gradual decrease in mean elevation of 9 mm from April 3rd to April 6th. The low transect had less than 1 mm elevation change through April 6th. Immediately after the April 6th measurements, blank pvc pipe was buried in the study plot to simulate the disturbance caused by placing horizontal drains in Plot 3 (see next section). Following installation of the blank pipe, the mean elevation of the transect increased slightly due to the disturbance of excavating through the transect. Wave-induced erosion near the end of these blank pipes caused a decrease in the mean elevation of the low transect on April 7th and 9th. The study period did not continue long enough following installation of the blank pvc pipe for measurable elevation changes to occur. Rills were observed to reform in the sand overlying the blank pipe following river stage fluctuations during the remainder of the study period.

Mean elevation changes for the transects in Plot 3 are shown in figure 9. The high transect had less than 1 mm elevation change prior to installation of the horizontal drains on April 6th. Mean elevation of this transect was higher (9 mm) on April 7th and 9th. Nearby foot traffic and/or soil creep may have disturbed this transect during this time period. The middle and low transects showed a gradual elevation decrease of about 6 mm from the start of the study on April 3rd until the horizontal drains were installed on April 6th. Following installation of the drains, the middle transect showed a slight elevation increase on April 7th and 9th due to disturbance from excavation for

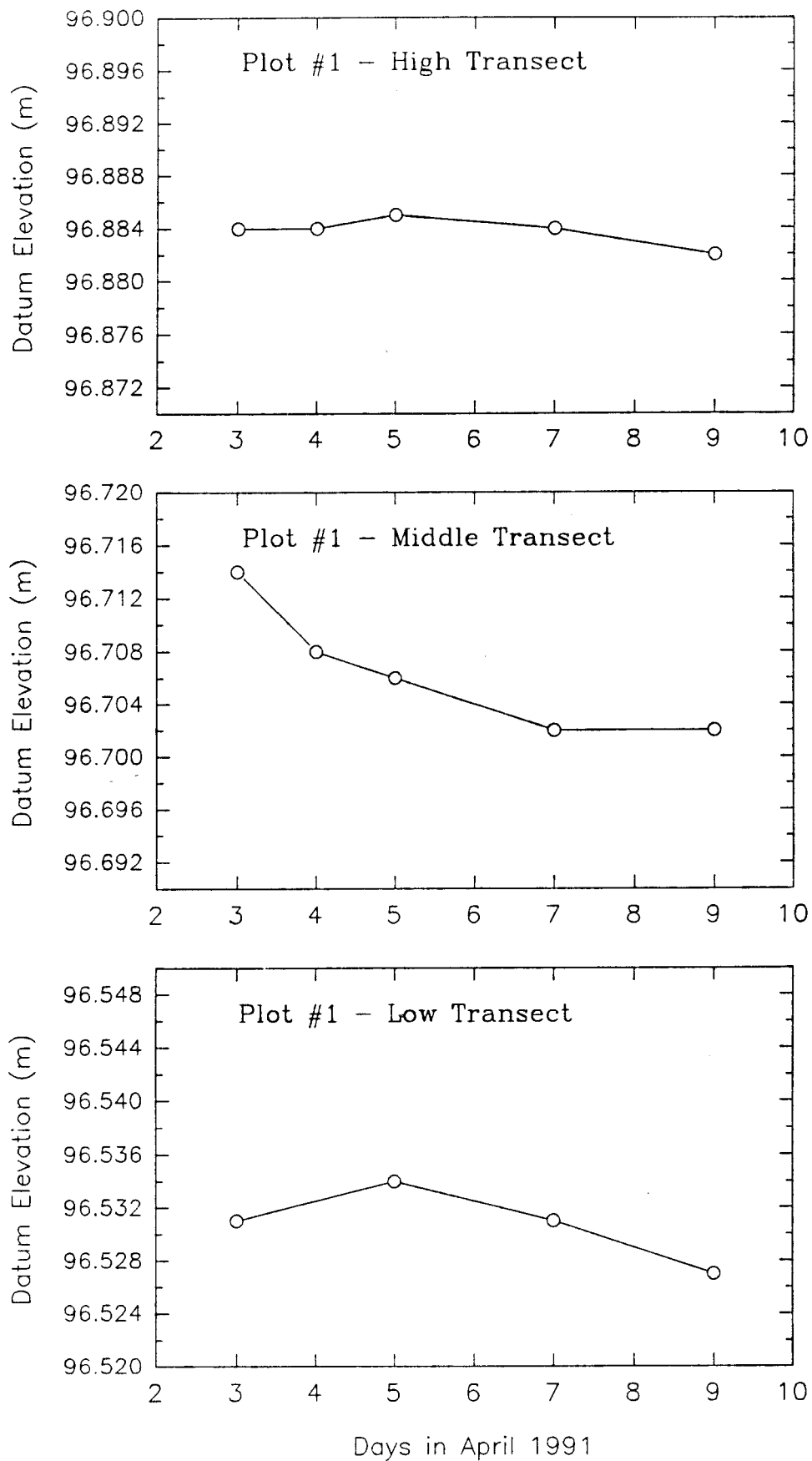


Figure 7. Mean Elevation of Transects in Plot #1, April 1991

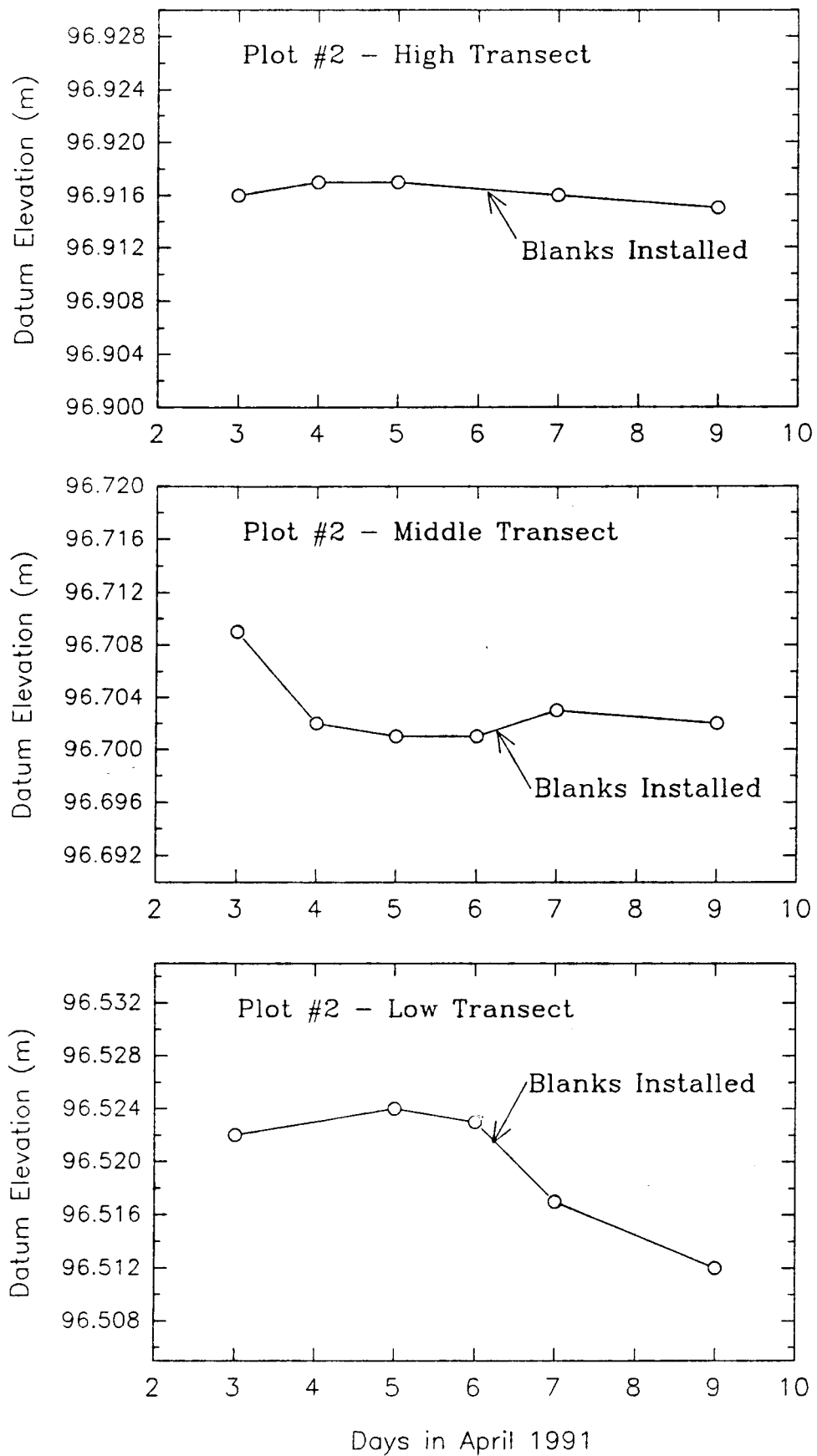


Figure 8. Mean Elevation of Transects in Plot #2, April 1991

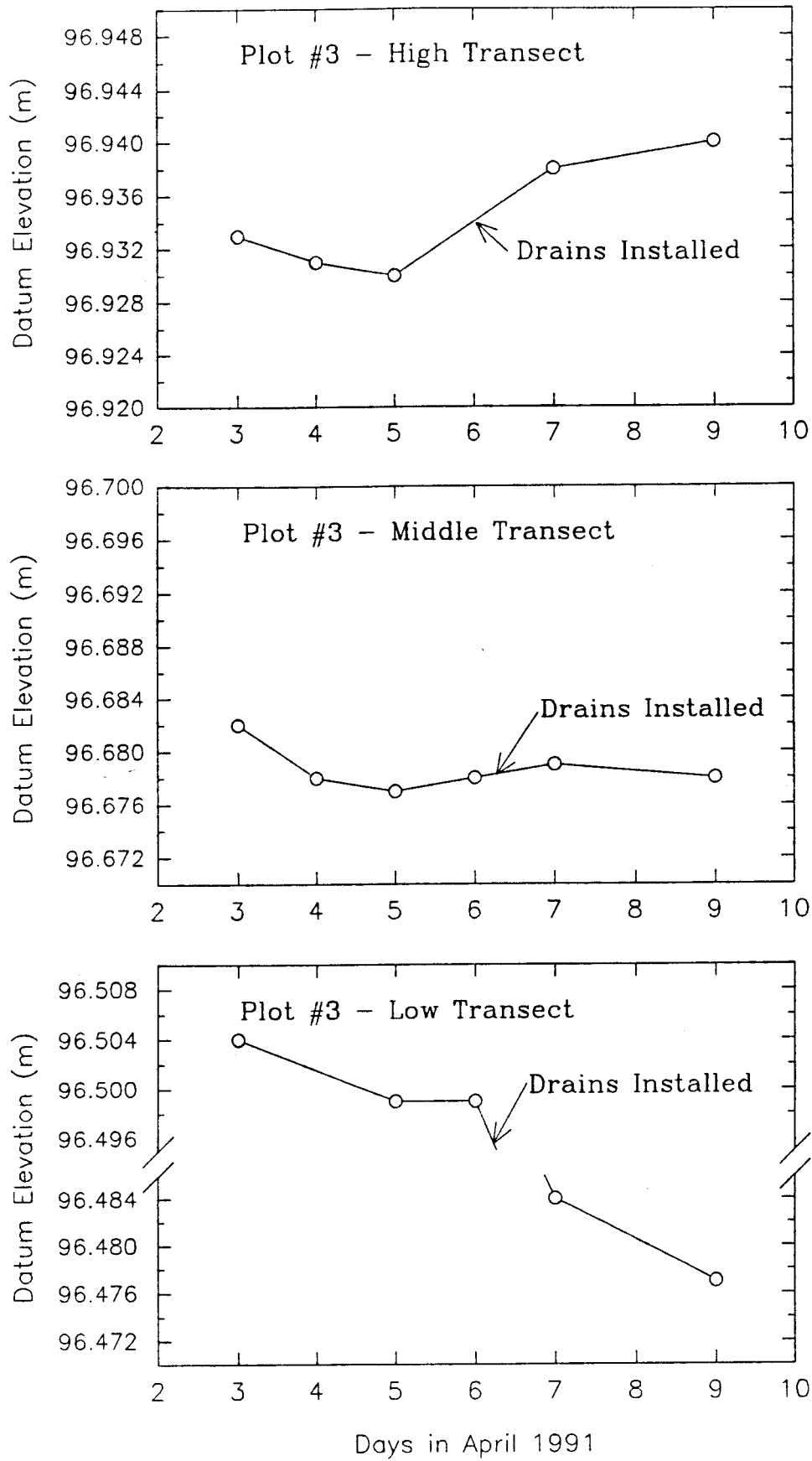


Figure 9. Mean Elevation of Transects in Plot #3, April 1991

drain installation. The mean elevation of the low transect decreased due to erosion caused by water running out the mouth of the horizontal drains. The study period did not continue long enough following installation of the drains to determine if the horizontal drains would prevent erosion from taking place. Rills were not observed to reform over the horizontal drains during the remainder of the study period.

The amount of erosion at each transect was partially determined by the relative position of the transect on the sand bar. For example, those transects that were located higher up on the sand bar were only marginally within the zone of fluctuation for several days during the study and totally above the zone of fluctuation for several other days. Measurable erosion did not occur on these transects on those days having small river stage fluctuations because there was no opportunity for a seepage face to develop. Transects located lowest on the sand bar, near the river's edge at low stage, showed either no change or a slight increase in elevation either from sand grains eroding down the face of the sand bar and being deposited near these transects or from sediment deposition by near-shore eddy action at high river stage. Transects located midway up the face of the sand bar showed the most erosion. These transects were within the zone of fluctuation during each day of the study and were exposed to active rills for longer periods each day than the other transects. Seepage faces developed at these locations every day in response to the rapid fall of the river stage.

Horizontal Drains

Horizontal drains were installed in one of the study plots (Plot 3) late on April 6th. The drains were installed to induce faster ground water drainage from a section of the sand bar during the falling limb of the river fluctuation. Lengths of blank (non-perforated) PVC pipe were placed in an adjacent study plot (Plot 2) as a control to observe the impacts due to the excavation for the placement of the drains. The third study plot (Plot 1) was used as a experimental control to monitor erosion on an undisturbed plot during the seven day (April 3 - 9) study period.

The drains were 5 cm (2-inch) factory slotted (0.020 inch) PVC approximately 2 m long. The drains were buried approximately 0.5 meters deep between (and perpendicular to) the low and middle transects and spaced about 0.6 m apart. The buried end of the drains was capped and the drains were placed at a slight slope toward the river to allow drainage to occur. Installation was by shovel trenching and the pipes were covered with excavated sand.

Blank (not perforated) PVC pipes were installed in Plot 2 in an identical manner to allow evaluation of impacts that may have occurred from installation of the drains and comparison with impacts due to effects of the drains. The blank pipes were 1.5 m long due to available materials at the site and were placed in corresponding locations in the middle group (Plot 2) of transects to serve as a control for effects of drain placement. These pipes were installed in the same manner as the horizontal drains in Plot 3.

Ground elevations along transects in Plots 2 and 3 were measured during the remainder of the study period following installation of the drains and blank pipe. Visual and photographic documentation was made of the observed changes following installation of the drains.

DRAFT
March, 1992

On each subsequent day following installation, the slotted drains in Plot 3 were observed to flow at an estimated rate of 0.25 l/s per drain. These observations were only possible during the brief time of minimum river stage due to the position of the end of the drains. Sand overlying the drains was observed to be distinctly drier than corresponding areas of the other plots as shown in figure 10. Rills did not form, i.e., no running water was seen, on the face of the sand bar overlying the drains. Also, ground elevation measurements indicate no elevation change during the remainder of the study at the middle transect. The low transect was affected by the presence of the drain openings and no conclusions are drawn from these data.

By contrast, Plot 2 which contained the blank PVC pipe exhibited rill formation by flowing water. Analysis of ground elevation data from the middle and low transects indicated subsequent erosion in the low transect. Although data analysis of the middle transect does not indicate subsequent erosion during the remaining 4 days of the study, it is believed that some erosion processes were on-going, due to the observance of rill formation.

Wind Blown Sand

Potential effects due to wind blown sand were investigated by establishing a study site with one transect on the western portion of the sand bar above the area normally affected by river stage fluctuations. This site was selected because:

- 1) It lacked nearby vegetation which might block wind effects.
- 2) It was out of the path of normal foot traffic and thus was not likely to be disturbed.
- 3) Its relatively flat topography would reduce the potential for slumping.

The site also was flagged to maintain its integrity.

The transect was first measured on April 3. The ping-pong balls created a very faint depression in the sand which could be seen by looking at the transect with the sun in the background. This visual observation was made for the next 3 days and appeared unchanged. The following night winds were noted in the early morning hours. A visual check of the transect the following day showed that the ping-pong ball depressions were nearly obliterated. Measurements with the surface profile gage on April 8th showed that elevations across the transect had not changed from the first measurements made on April 3rd.

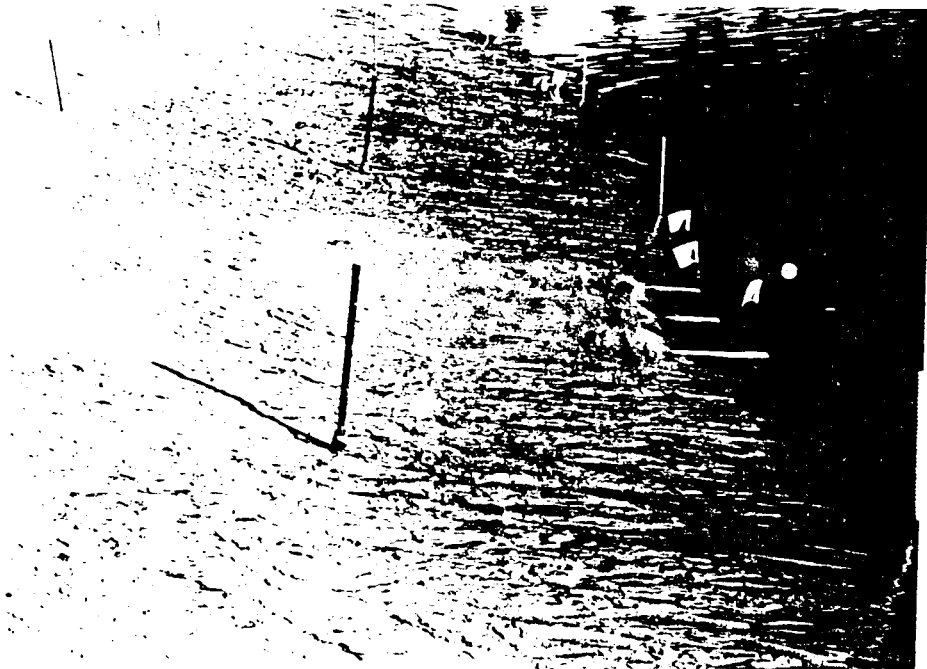
Video Documentation

A video recording camera was used to document physical processes on the face of the sand bar during the falling stage of river fluctuation. The video documents the processes of seepage, rill formation, and movement of sand grains. Record of the date and time of the video recording allowed comparison to river stage and water table elevations for the same time period. Factors affecting the erosion processes were thus identified.

Numerous, small channels on the face of the sand bar were seen to have remained intact from the previous day as the river stage first started to fall. As the river stage continued to fall, these small channels could be



Downstream end of perforated lateral drains showing flow of intercepted groundwater at low stage of Colorado River.



Plot 3 with perforated lateral drains is seen at the center of the photograph. Note relatively dry sand without rivulets overlying the drains. Plot 2 with blank pipe is seen in the center of the photograph. Wet sand and rivulets are seen overlying these pipes.

Figure 10 . Photographs of lateral drains in the sand bar at River Mile 43L, April 7, 1991, about 24 hours after installation of the drains.

seen to extend farther down the face of the sand bar under water. As the river stage fell to expose the channels, rills formed in the channels. As the river stage continued to fall, a seepage face developed and flow could be seen to increase down the face of the sand bar. With substantial river stage decrease, the uppermost portion of the channels became dry. In subsequent days, the small channels were observed daily while still being under water. Their continued presence indicates that river currents were not a major erosion or deposition factor during the study. The elevation of the top of the small channels is believed to approximately coincide with the water table in the sand bar when the river is at low stage.

AUGUST STUDY PERIOD

Design and Instrumentation

The August study period consisted of 19 days (August 8-26, 1991) during which field studies were conducted. Ground elevations were measured daily for 8 days, from August 8 through August 15. The sand bar was unoccupied for 4 days, and measurements were resumed on August 20 and continued through August 26 (7 days). River stage and water table elevations were monitored continuously with digital recorders.

Two study plots, with three transects each, were located on the face of the sand bar, within the area affected by river stage fluctuations. The August study site was in approximately the same location as the April study site. The study plots were located in the zone of active erosion as indicated by the presence of rills. In each study plot, two transects were parallel to the river's edge with a lower and upper transect spaced about 1.2 meters apart (figure 11). The lower transects were located about 0.3 meter from the rivers edge at lowest stage (280 m³/s) and the upper transects were approximately midway between the daily high stage (approximately 510 m³/s) and the lowest stage. The third transect in each study plot was perpendicular to the river. The two study plots were identified as upstream and downstream, according to their position relative to river flow.

Five ground water monitoring wells were installed along a line perpendicular to the river, approximately 1.5 meters apart. In comparison to the April study, the increased number of monitor wells and their positioning at lower elevations were modifications to enhance delineation of the water table in proximity to the transects. The monitor wells were located between the study plots to allow measurement of water table response to fluctuating river stage in the vicinity of transects. The monitor wells were installed by augering to the water table and then driving 5 cm (2 inch) diameter PVC casing to a depth of approximately 1.5 meters below the water table. Slotted casing with a well point on the end provided hydraulic connection with the ground water in each monitor well. Water levels in Wells 1-4 were monitored at 10 minute intervals using pressure transducers in combination with a digital recorder. Data for Well 5 was acquired by manual measurements with a chalked steel tape.

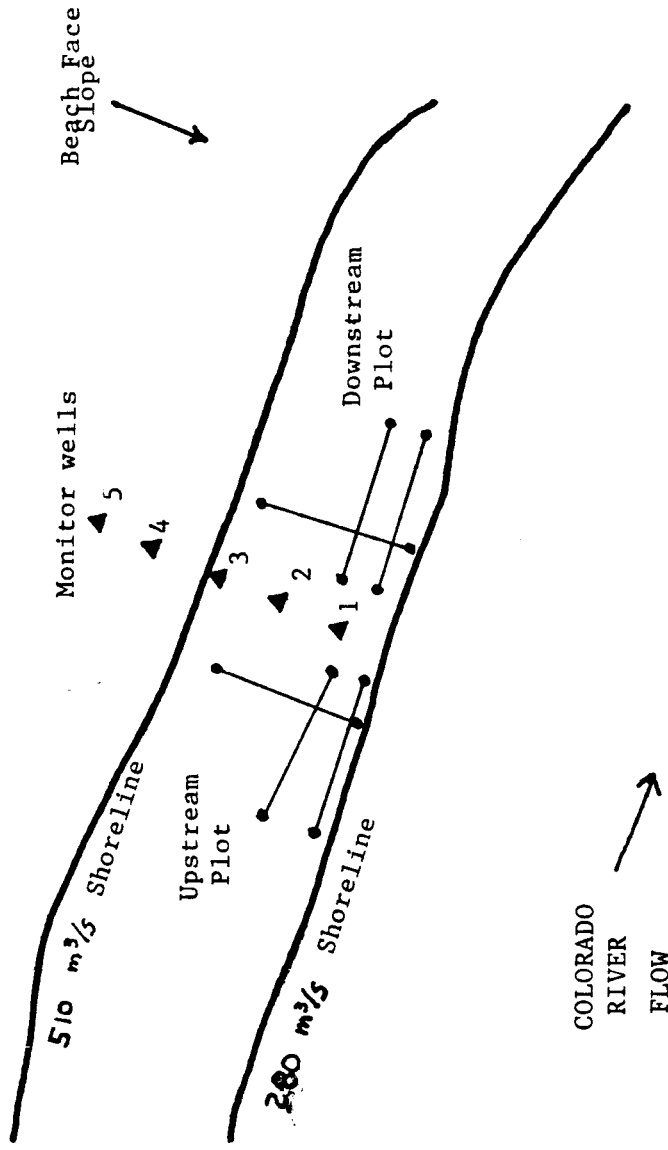


Figure 11. Layout of study plots August 1991

Colorado River Flow Characteristics

During the August study period, the flow of the Colorado River was regulated by Glen Canyon Dam releases in accordance with the Interim Test Flows restrictions, implemented on August 1, 1991 under the direction of the Secretary of Interior. River flow varied from about 280 to about 510 m³/s during this period. Colorado River stage was monitored by a pressure transducer in combination with the same digital recorder used for monitoring water levels in the monitor wells. River stage fluctuated about 1.2 m from low to high stage.

Data Analysis

River stage and water table fluctuations with associated lag times and daily differences in fluctuation for the study period are shown in figure 12. Minimum river stage ranged from about 97.4 to 97.7 m during the study, corresponding to minimum flow releases from the dam of 290 to 305 m³/s. Maximum river stage varied from about 98.6 to 98.9 m, corresponding to dam flow releases of 515 to 545 m³/s. The exception to these ranges occurred during the night of August 18-19 in response to smaller dam flow releases the preceding weekend, maximum stage and discharge were 98.2 m and 415 m³/s respectively. The pressure transducer used to monitor river stage showed some drift during this period, accounting for the apparent increasing trend of the river stage shown on figure 12.

Land surface measurements were made across the transects at each of the plots using the surface profile gage following the daily fall of the river stage using the same methodology that as during the April study period.

Figures 13, 14, and 15 show the mean elevation changes for each of the transects during this study period. All of the transects had a net gain in mean elevation. Mean elevation gain ranged from 4-9 mm/transect. Individual ball elevations varied, with both increases and decreases occurring in response to variations in the amount of erosion and deposition occurring on a daily basis and meandering of rill channels. However, since the net effect was an increase in mean elevation for all of the transects, it can be deduced that the dam flow releases during this period did not result in net erosion of the sand bar.

Analysis of data for the Upper Transects, Figure 13 reveals similar characteristics to the pattern of elevation change during the August study period. The average elevation changes show similar breaks in the trend of aggradation. Mean elevation of the Upper Transects had been increasing for the first 8 days of the study. Measurements were not made for the next 4 days. When measurements resumed, the mean elevation decreased for two days at both transects before resuming an increasing trend. The slightly higher river stage on August 21 may have passed a threshold where seepage erosion became dominant over aggradation processes. Or higher stage may have caused a slight shift in the circulation patterns of the eddy cells. A shift or modification of the eddy vortex and eddy fence in relation to the main river current may locally affect the supply of sand available for accumulation on the study plots.

A similar reversal from aggradation to degradation may be seen in the lower

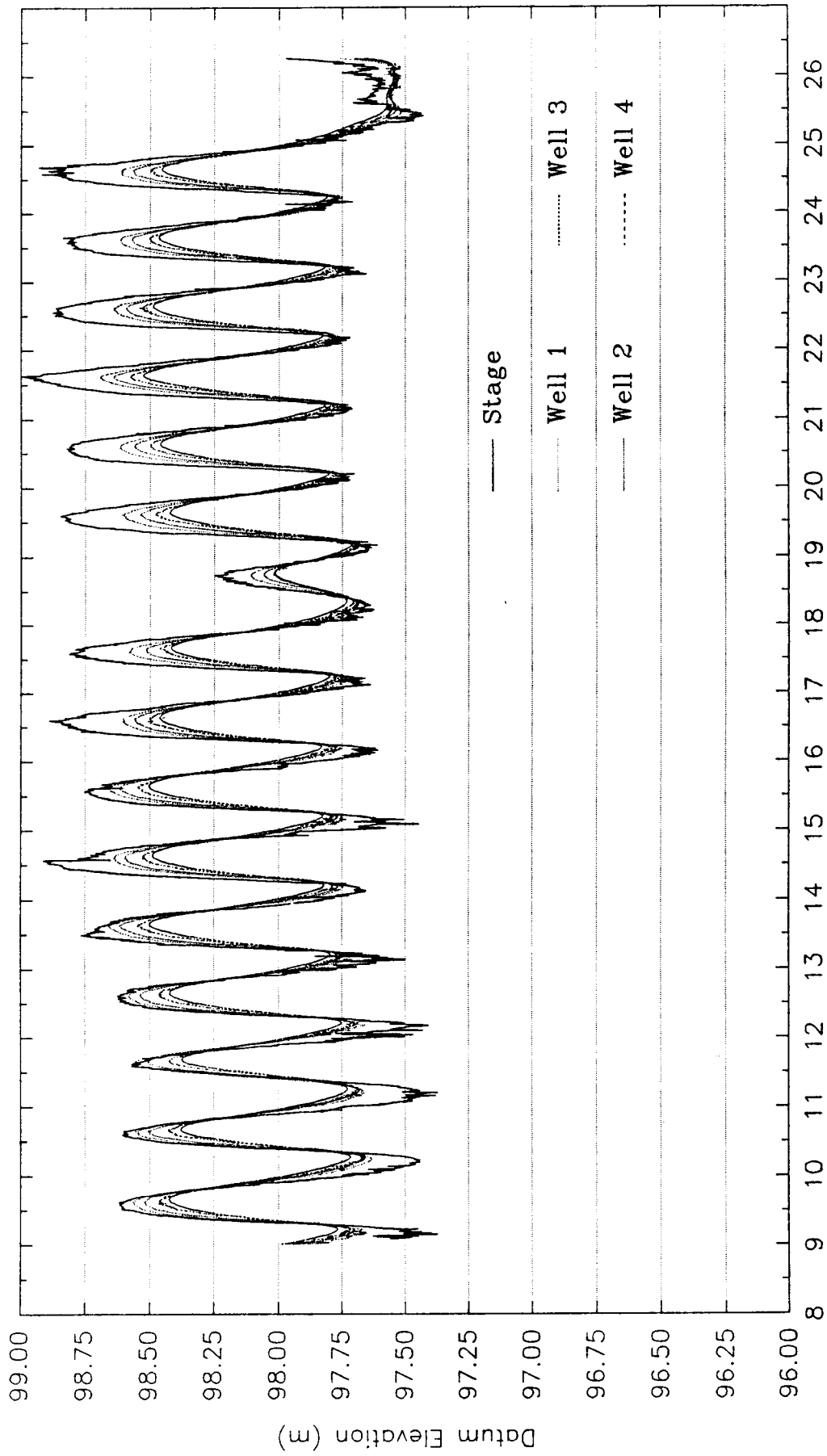


Figure 12. August Hydrographs - River Stage and Monitor Wells

Days in August 1991

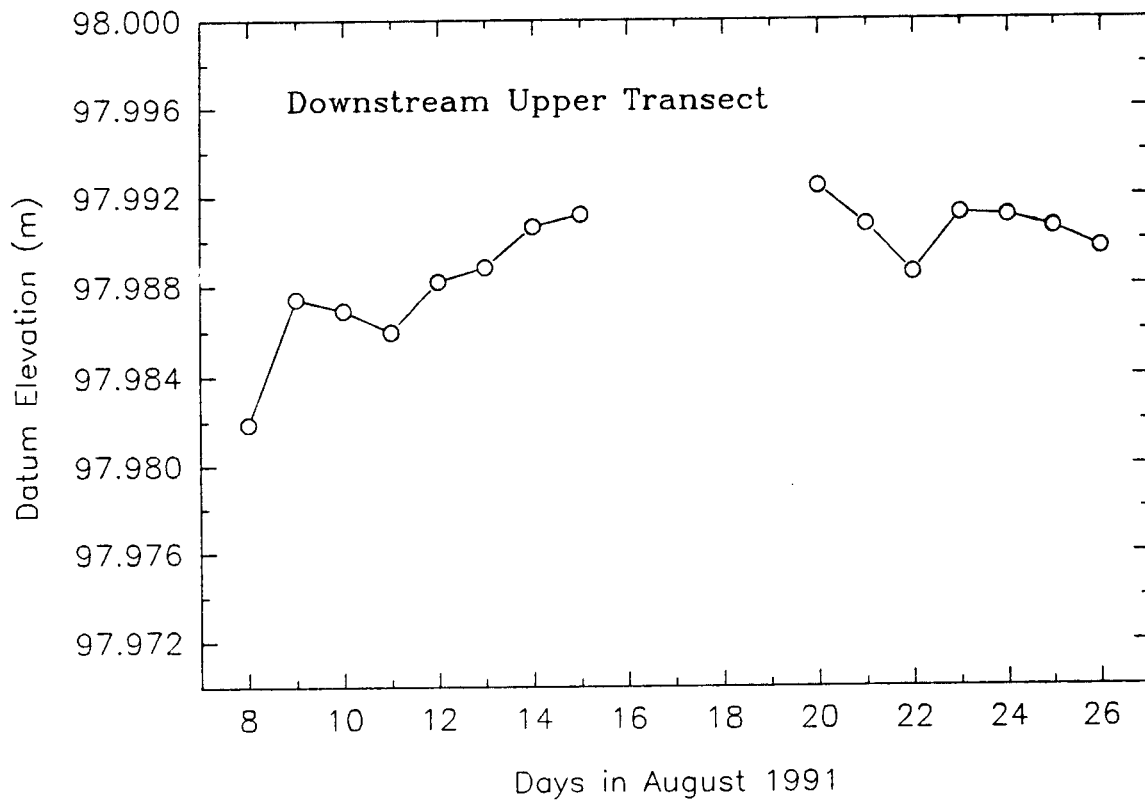
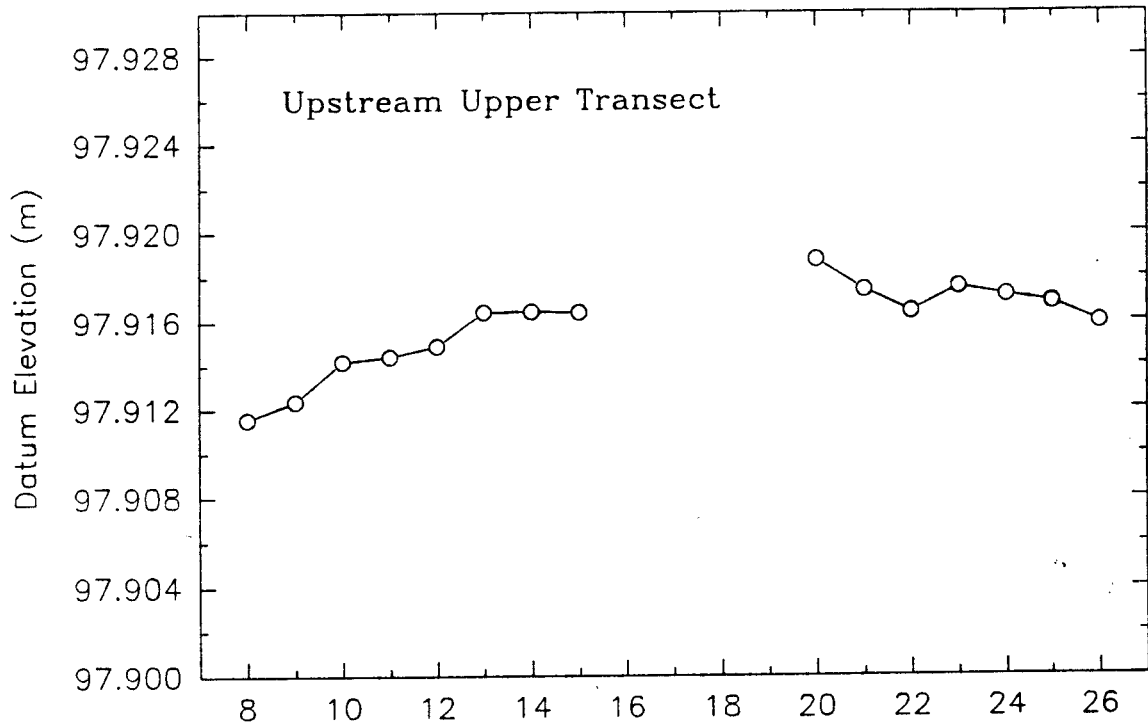


Figure 13. Mean Elevation of Upper Transects, August 1991

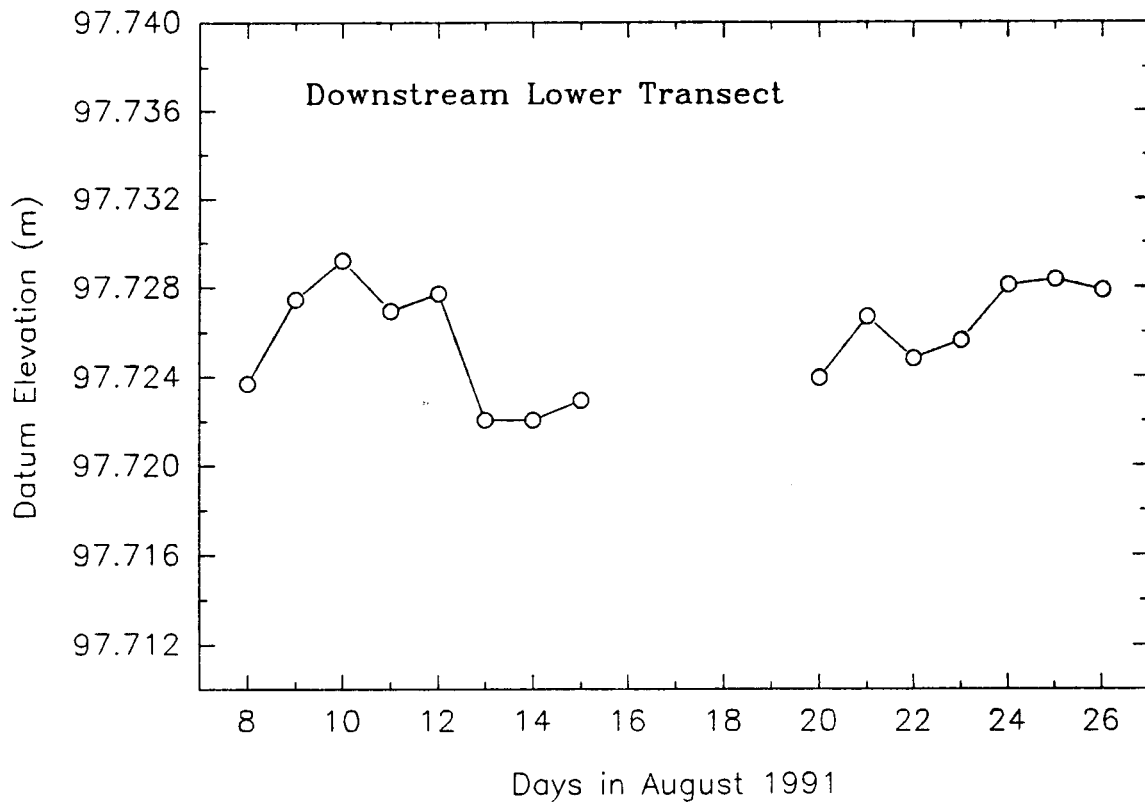
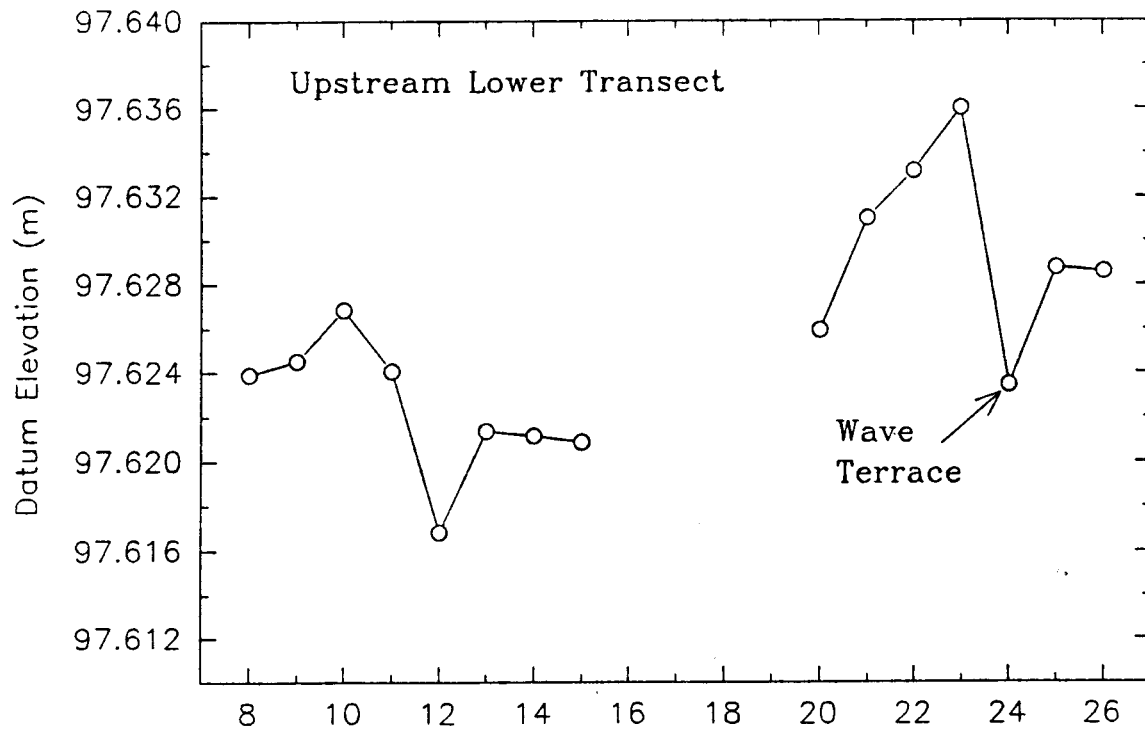


Figure 14. Mean Elevation of Lower Transects, August 1991

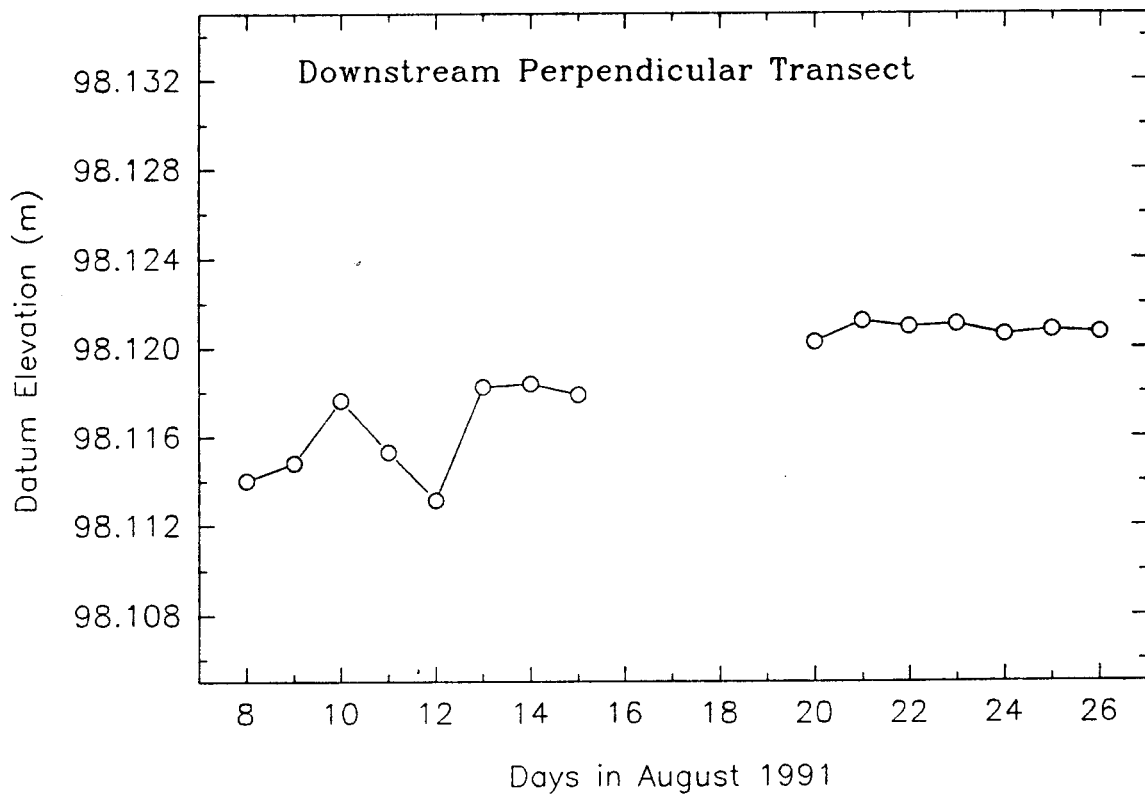
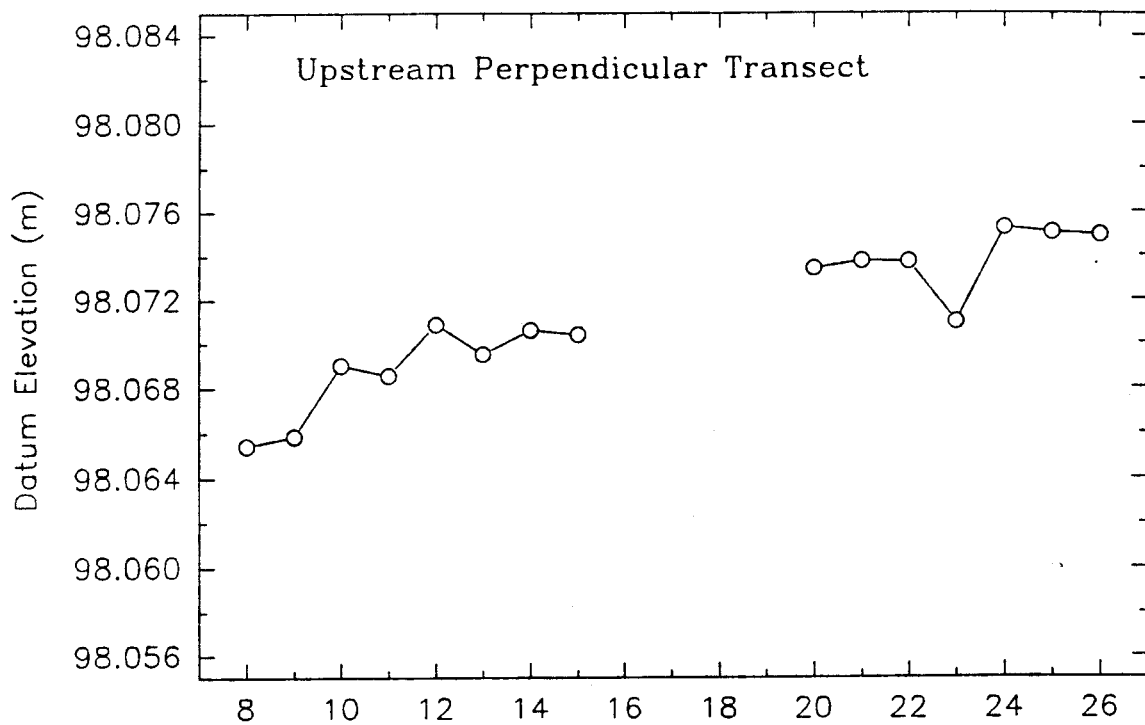


Figure 15. Mean Elevation of Perpendicular Transects, August 1991

DRAFT
March, 1992

transect averages (figure 14) on August 13th. Close examination of river stage and water levels in monitor wells confirm that a higher peak stage occurred on the 13th compared to the previous days. Again, it is believed that erosion processes became dominant or changes in eddy currents resulted from the small difference in stage. Explaining such small changes in aggradation or degradation on the face of the sand bar would require greater sensitivity and quantification of eddy dynamics and sediment transport processes. River stage was coincident with the elevation of the Upstream Lower Transect for some time period on August 23 - 24. During this time, a small wave-cut terrace formed, resulting in a relatively large elevation change at this transect from August 23rd to 24th.

Irregularities in the river stage fluctuation pattern occurred on August 19th in response to lower weekend electrical demand at Glen Canyon Dam. Unfortunately, transect elevations were not measured due to absence of observers from the study site. Subsequent measurements two days after the weekend flow did not reveal significant deviation from the general trend of aggradation.

Perpendicular transects (figure 15) were utilized in the August study period to detect zones of erosion or deposition at different elevations on the face of the sand bar. We hoped to learn if the parallel transects on the lower part of the face of the sand bar truly represented the quantity of aggradation or erosion taking place on the entire face of the sand bar. Generally, aggradation was uniformly distributed throughout the perpendicular transects. However, a narrow region indicated by a finer texture of sand on the surface of the sand bar was detected by the surface profile gage and seen in the photographs. It is believed that this different texture of sand was a recent deposit on the sand bar and was gradually being eroded. A small ledge (estimated height of 10 mm) was slowly retreating up the face of the sand bar. The narrow region of sloughing was not measured by the parallel transects.

Rill formation and movement of sand grains down the face of the sand bar were observed during both the April and August study periods. However, the mean elevation was observed to increase in the August study period, whereas the mean elevation had decreased in April. This apparent contradiction is believed to be the result of two or more, opposing processes. Seepage erosion occurs only during periods of low Colorado River stage. In August, the range of river stage fluctuations was less than in April and therefore, the amount of erosion from the beach face would be expected to be less. Aggradation processes that could have been occurring include sand deposition by near-shore eddies and creep or slumping of sand moving down the face of the beach. Other processes that could have resulted in apparent aggradation include vertical rebar settling or surveying errors in determining the elevation of the top of the rebar. Each of these processes may occur daily, but at different rates depending on flow characteristics of the river for that day.

DISCUSSION

Rills and small channels form on the face of the sand bar in response to ground water seeping from the sand bar at low river stage. Rill channels were also observed below the surface of the Colorado River during the daily recession of river stage, indicating that the channels had remained intact during high river stage (there was no deposition or reworking of the sand-bar

face). Changes in rill and channel form and location were observed at low river stage while water was flowing down the face of the sand bar. Lateral channel shifting and erosion or deposition processes occurred continuously. These small rill and channel changes are reflected in the measurements made with the surface profile gage. Individual ball elevations show large (several millimeters) changes, both increases and decreases, on a daily basis as a result of lateral migration of channels. The daily variance of individual ball elevations makes analysis of individual ball elevations on a daily basis difficult. Thus, the arithmetic mean of ball elevations for an entire transect was used to evaluate elevation changes.

The basic processes observed and conclusions drawn during this investigation were:

- 1) The water table underlying the sand bars in the Grand Canyon fluctuates in response to river stage fluctuations. Water table fluctuation is greatest near the river and dampens with increasing distance from the river.
- 2) When the river stage falls at a rate that is faster than the water table can drain by gravity through the face of the sand bar, a saturated zone (seepage face) forms on the face of the sand bar. The height of this saturated face is dependent on the rate of river stage decline and factors controlling the gravity drainage of water from the sand bar.
- 3) Water seeping from the saturated face of the sand bar forms rills which move sand particles down the face of the sand bar to be deposited in areas with lower gradients or at the river's edge.
- 4) If the water table near the face of the sand bar can be artificially drained to keep up with a falling river stage (i.e., no saturated zone formed), erosion will be prevented or at least lessened.
- 5) When the river stage decline is equal to or less than the rate at which ground water naturally drains from the sand bar, a seepage face will not form.

In a large sand bar, such as the sand bar at River Mile 43.1L, a large volume of ground water is stored in the sediments. The mean water-table elevation in the sand bar is controlled by the elevation of the mean daily river stage, taking into account the pattern of river stage fluctuations. Erosion occurs when the river stage falls significantly below the mean water table in the sand bar and a saturated seepage face forms as ground water flows toward the river in response to the gradient differential. Ground water emits from and flows down the seepage face, forming rills and eroding sand grains down to the river's edge.

The video film produced in this study was compared to river stage and water table fluctuations to determine the sequence of events leading to seepage erosion from daily fluctuations of river stage. The following discussion explains our interpretation of the various phases of the ground water induced seepage erosion process as illustrated in the accompanying figures (16a-16f):

Figure 16a -- Lowest River Stage.

The river is maintained at a low stage for several hours in response to minimal discharges from the dam during times of low demand for electricity. The water table in the sand bar is higher than the river stage due to recharge at high river stage the previous day. The river stage has been at a low level for a long enough time for ground water near the face of the sand bar to drain, lowering the water table. The saturated seepage face is either small or no longer exists, depending on the volume of water draining from the sand bar.

Figure 16b -- Rising River Stage.

As the river stage rises, the area near the face of the sand bar that had been drained is resaturated very rapidly. The river stage continues to rise above the average level of the water table in the sand bar, causing a rise in the water table (recharging the aquifer) with it's high point coincident with the river stage and tapering back to an average height of the water table at some distance from the river.

Figure 16c -- Highest River Stage.

The water table in the sand bar continues to be recharged from the river. The water table near the face of the sand bar is coincident with the river stage. This increase in the water table level will extend some distance into the sand bar depending on the amount of time the river is maintained at high stage and the permeability of the sediments.

Figure 16d -- Falling River Stage, Phase I.

As the river stage begins to fall, gradients are reversed and ground water that was recharged to the sand bar begins to flow back into the river. Initially, this volume of water is small because the top of the recharge ridge does not extend far into the sand bar. The water can drain through the face of the sand bar at a rate such that the water table in the sand bar declines nearly as fast as the river stage. A seepage face normally does not form, and rill erosion does not occur high on the beach face within the zone of fluctuations.

Figure 16e -- Falling River Stage, Phase II.

The river stage has dropped to a level below which the ground water can no longer drain fast enough to keep up with the declining river stage because of the large volume of ground water now influenced. A spring line forms parallel to and above the river's edge, and seepage occurs through the face of the sand bar below the spring line. The water concentrates in rills and flows down the face of the sand bar eroding sand grains in the process.

Figure 16f -- Falling River Stage, Phase III.

The river stage has reached it's lowest level. Ground water continues to drain from the face of the sand bar. The zone of active erosion (flowing rills) is still visible on the face of the sand bar. The seepage face has migrated down the face of the sand bar as the river stage receded. The height of the seepage face will decrease as the volume of stored ground water and the gradient decreases.

FACTORS AFFECTING SEEPAGE EROSION

Based on the preceding discussions, erosion by ground water seepage through the face of a sand bar will primarily be a function of operational factors at the Glen Canyon Dam; range of stage fluctuations, ramping rate, and length of time the river stage is held at high or low stages. Stage range is the change between high and low river stage on a daily basis. Ramping rate is the rate at which stage changes. Whatever the stage range and ramping rates are, the river stage fluctuates cyclically on a daily basis. These operational factors are somewhat interrelated and combine to determine whether the net effect of river fluctuations is erosion or deposition.

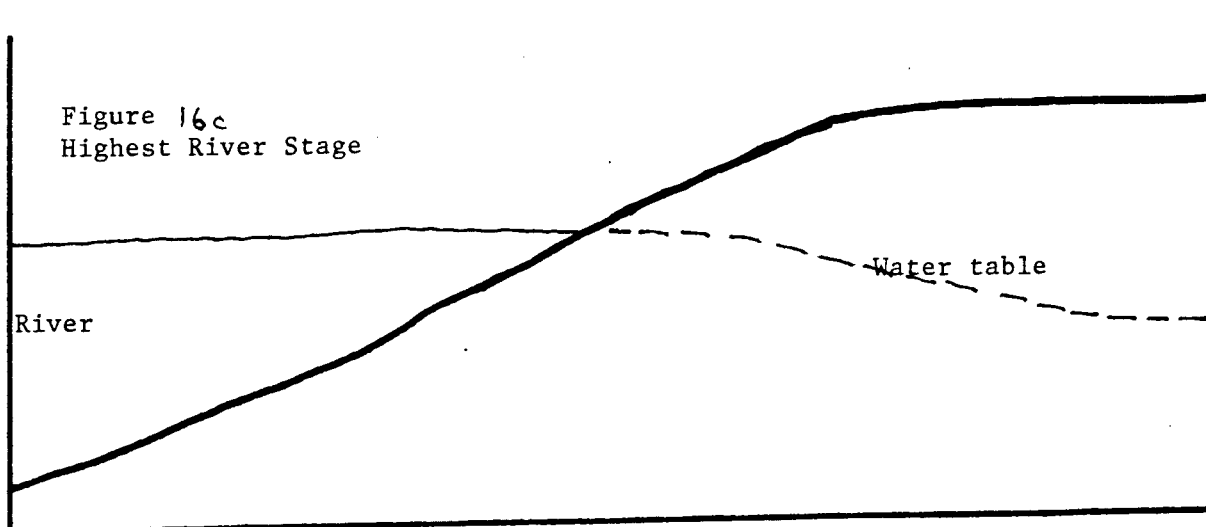
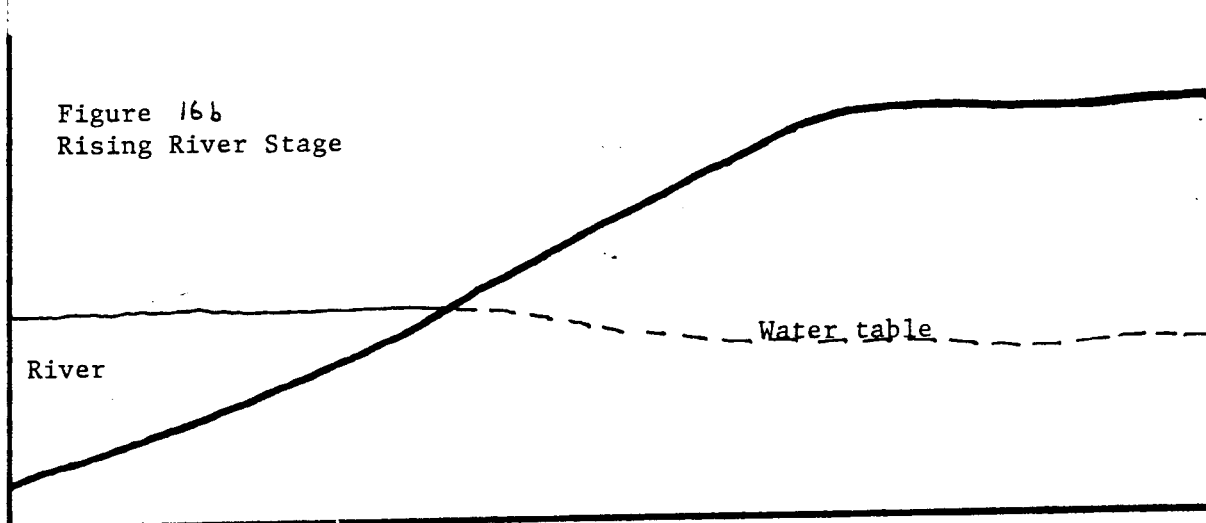
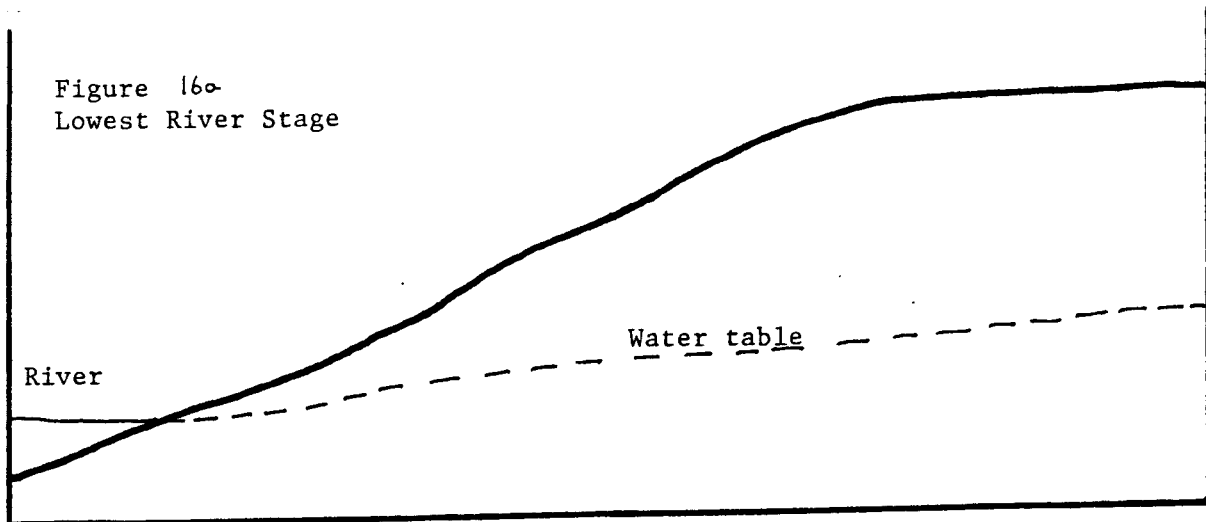


Figure 16. Effect of river stage fluctuation on the water table in beaches.

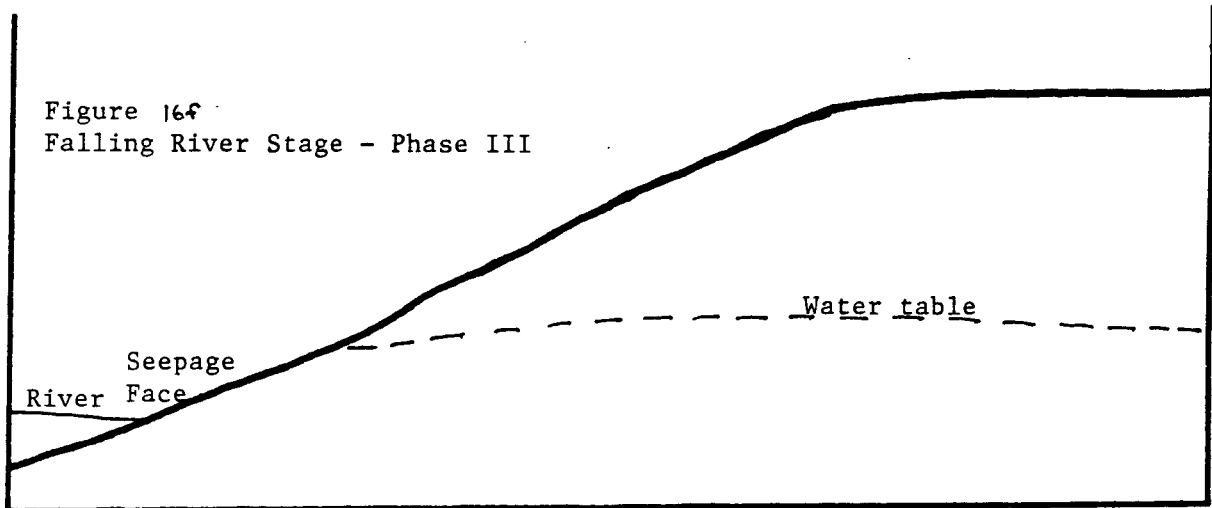
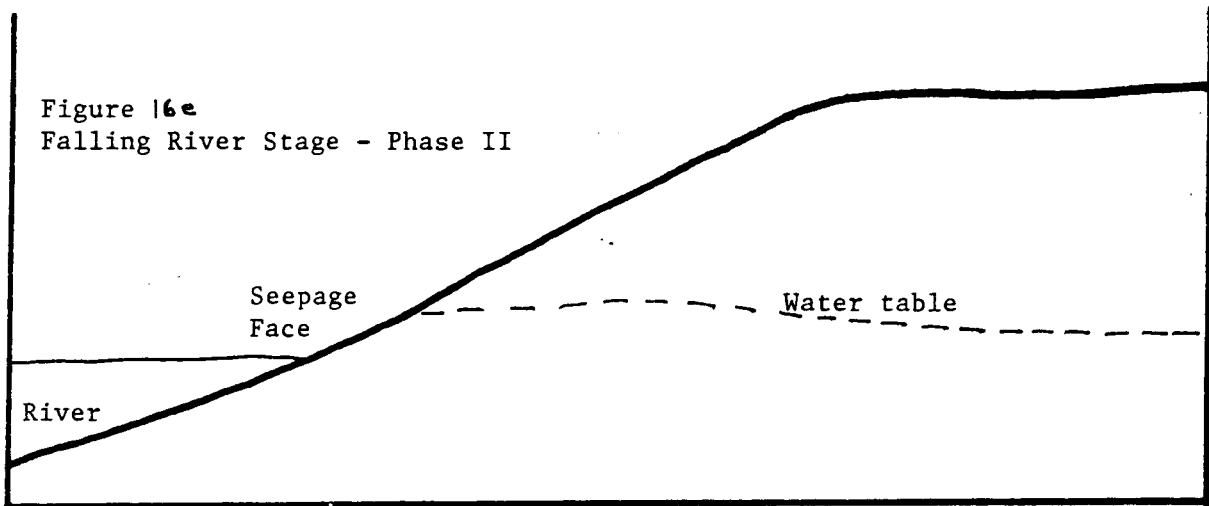
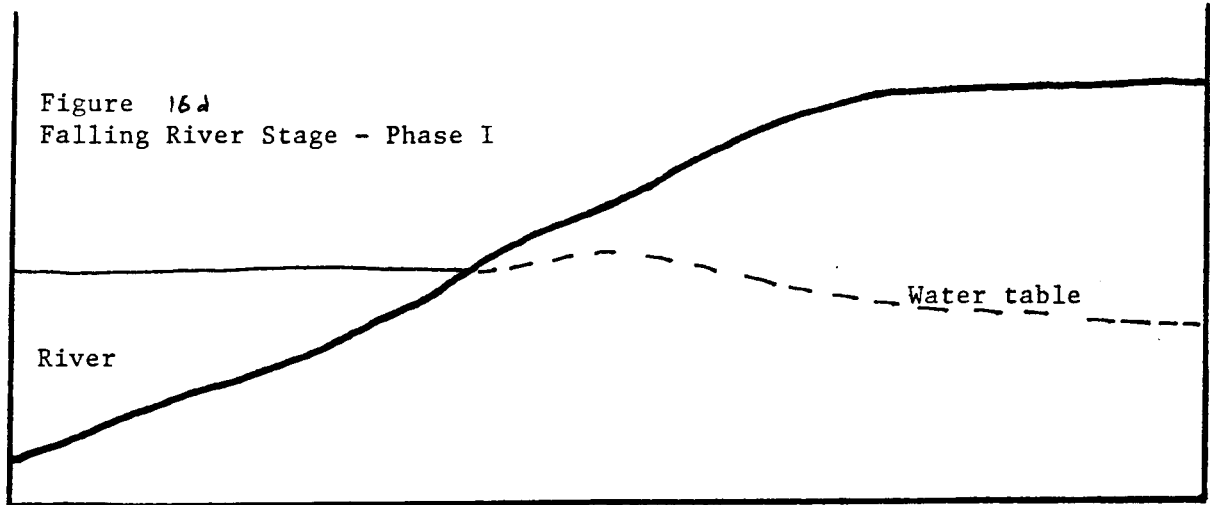


Figure 16. Effect of river stage fluctuation on the water table in beaches.

Stage range is probably the more important of the two factors in affecting ground water seepage and related sand-bar erosion at large sand bars (i.e., sand bars in which ground water storage is large compared to the rate of seepage, and a near "static" water table can be maintained over the period of a daily river stage cycle). If the river stage has a large range, then the river stage will fall further below the average ground water level in the sand bar. (The average ground water level would be approximately the same as the mean daily river stage where it not for the changes in daily fluctuations.) The seepage face that forms will have a greater length (height) and duration and will therefore cause more erosion when the range of river stage fluctuations is large.

Large ramping rates induce the formation of a seepage face when the rate is maintained after the river stage drops below the average level of the water table in the sand bar. However, the seepage face will not form if the ramping rate is reduced after the river stage has dropped to approximately the mean ground water level. Decreasing the ramping rate after the river stage has dropped to approximately the mean ground water level will also reduce the range of fluctuations because there is a limit to how much stage change can occur in a given time with a given rate of change.

Another factor affecting seepage erosion from the face of the sand bar is the volume of water stored in the sand bar, which is directly related to the width of the sand bar. Narrow sand bars will have a smaller volume of ground water in storage. When the river stage falls below the static ground water level, this smaller volume of ground water can drain from the sand bar relatively quickly. Faster drainage time (reduced lag time between river stage and water table decline) reduces the length of time during which erosion from ground-water seepage occurs. In contrast, wide sand bars will have a larger amount of ground water in storage. Seepage through the face of the sand bar will occur, as previously described, when the river stage is lowered below the average ground water level. This seepage will continue for a longer period of time to drain the larger volume of water stored in the sand bar. It is likely that erosion via rill formation will occur for a longer time period.

Other factors affecting the amount of erosion from ground-water seepage on the face of the sand bar include:

- 1) Slope and length of the face of the sand bar.
- 2) Sediment grain size and distribution.
- 3) Sediment cohesion, which is dependent on particle size, particle shape, and to a lesser extent on sediment and water chemistry.
- 4) Geomorphic position above the main river channel.

Horizontal drains installed in one of the study plots verify the role of ground water in seepage erosion. The drains induced more rapid drainage of ground water from near the face of the sand bar, thereby limiting formation of a seepage face. There was a noticeable difference in the appearance of the face of the sand bar in the vicinity of the drains after installation. Ground water near the face of the sand bar drained very quickly through the perforated pipe after the river receded. The area above the drains appeared to dry very quickly. Rills did not reform in the immediate area, indicating that ground water was no longer seeping out the face of the sand bar. Adjacent areas on the sand bar, including the study plots where blank pipes were installed, still appeared saturated and rills reappeared.

CONCLUSIONS

Erosion and deposition processes occur daily in response to changing hydrologic and hydraulic conditions. The net effect of these opposing processes varies with changing river flow characteristics. Sand bar erosion caused by ground water seepage was documented in the April study period, during which the daily range of the Colorado River stage fluctuation was relatively large and the mean stage of the river was low. Net aggradation on the sand bar was documented in the August study period. Several processes could be responsible for the net aggradation. One possibility is that because the daily range of the Colorado River stage fluctuations was less than in April, erosion by ground water seepage was reduced. Also, the mean river stage was higher in August. The higher mean stage may have resulted in slightly different eddy characteristics. Changes in eddy-flow patterns may locally affect the sediment supply available for accumulation on the sand bar. Another possible explanation is creep or other mass wasting. Another is vertical rebar movement. Because several processes have been identified as possibly affecting sand-bar erosion and sediment deposition, future investigations of this type should attempt to isolate effects from each of these processes.

River stage fluctuations occur daily as a result of variable flow releases from the Glen Canyon Dam for power generation. When the river stage is lowered rapidly, the rate at which the sand bar drains will not permit the water table to decline as fast and remain coincident with river stage. The water table in the sand bar is temporarily higher than the river stage. This condition can be described as a difference in potentiometric head between the water table and river stage and will result in ground water movement towards the river. Ground water will drain from the sand bar at a rate limited by the aquifer properties of the sand bar and the head difference between the water table and the river. When sand bar discharge (seepage) is of such quantity that the upper limit of the discharge zone (interface between the water table and the sand bar) is higher than the river stage, water will flow down the face of the sand bar forming rills and transporting sand grains down the slope to the river's edge. This process was documented in the April study period.

The amount of sand-bar seepage (and therefore erosion) decreases when the range of river stage fluctuations is reduced. The reduced range in stage and less prominent formation of rills in the August study period reflected this case.

This study has focused only on the role of ground-water seepage on sand bar erosion. Erosion by ground water seepage is only one of many geomorphic process affecting sand bars in the Grand Canyon. System-wide sediment budget, main channel sediment transport, mass wasting, creep, eddy dynamics and related sediment storage in eddy basins are other aspects being studied that affect sand bar stability. Interaction by research scientists will be necessary to determine dominant components of sand-bar stability affected by river stage fluctuations.

DRAFT
March, 1992

REFERENCES

Beus, S.S., Carothers, S.W., Avery, C.C., 1985, Topographic changes in Fluvial terrace deposits used as campsite beaches along the Colorado River in Grand Canyon: Journal of the Arizona-Nevada Academy of Science, v. 20, p. 111-120.

Burkham, D.E., 1986, Trends in selected hydraulic variables for the Colorado River at Lees Ferry and near Grand Canyon, Arizona, 1922-84: U.S. Bureau of Reclamation, Glen Canyon Environmental Studies Report, 51 p.

Cluer, B.L., 1992, Resource Management and Planning Division, Grand Canyon National Park, personal communication.

Ferrari, Ronald, 1987, Sandy beach area survey along the Colorado River in the Grand Canyon National Park: U.S. Bureau of Reclamation, Glen Canyon Environmental Studies Report, 23 p.

Graf, J.B. 1986, Sediment transport under regulated flow, Colorado River, Grand Canyon National Park, Arizona: EOS, Transactions, American Geophysical Union, v. 67, no. 44, p. 950.

Howard, A.D., 1975, Establishment of benchmark study sites along the Colorado River in Grand Canyon National Park for monitoring of beach erosion caused by natural forces and human impact: University of Virginia Grand Canyon Study, Technical Report No. 1, 182 p.

Laursen, E.M., and Silverston, E., 1976, Camera stations along the Colorado River through the Grand Canyon--Supplement to the final report on the hydrology and sedimentology of the Colorado River: Division of Resource Management, Grand Canyon National Park, 150 p. [Unpublished report to the National Park Service.]

Leopold, L.B., 1969, The rapids and the pools--Grand Canyon, in The Colorado River Region and John Wesley Powell: U.S. Geologic Survey Professional Paper 669, p. 131-145.

Orvis, C.J., and Randle, T.J., 1986, Sediment transport and river simulation model: Fourth Federal Interagency Sedimentation Conference, v. 2, Las Vegas, Nevada, March 24-27, 1986, Proceedings, p. 6-65 to 6-64.

Pemberton, E.L., and Randle, T.J., 1986, Colorado River sediment transport in Grand Canyon: Fourth Federal Interagency Sedimentation Conference, v. 2, Las Vegas, Nevada, March 24-27, 1986, Proceedings, p. 4-123 to 4-130.

Schmidt, J.C., and Graf, J.B., 1988, Aggradation and degradation of alluvial sand deposits, 1965 to 1986, Colorado River, Grand Canyon National Park, Arizona: U.S. Geological Survey Open-File Report 87-555, 120 p.

Turner, R.M., and Karpiscak, M.M., 1980, Recent vegetation changes along the Colorado River between Glen Canyon Dam and Lake Mead, Arizona: U.S. Geological Survey Professional Paper 1132, 125 p.

U.S.D.I., 1988, Glen Canyon Environmental Studies Final Report. 343 pp.

U.S.D.I., 1990, Glen Canyon Environmental Studies Phase II Draft Integrated Research Plan Volume 1. No pagination.

DRAFT
March, 1992

Webb, R.H., Pringle, P.T., and Rink, G.R., 1987, Debris flows in tributaries of the Colorado River, Grand Canyon National Park, Arizona: U.S. Geological Survey Open-File Report 87-118, 64 p.

Wilson, R.P., 1986, Sonar patterns of Colorado riverbed, Grand Canyon: Fourth Federal Interagency Sedimentation Conference, v. 2, Las Vegas, Nevada, March 24-27, 1986, Proceedings, p. 5-133 to 5-142.

APPENDIX 1

GLOSSARY

- Aggradation¹ - The building-up of the Earth's surface by sediment deposition. A synonym of accretion, as in development of a sand bar.
- Drains - Perforated pipe buried in the face of the sand bar and used to intercept and convey ground water to an outlet.
- Eddy¹ - A circular movement of water that is generally in a different direction from that of the main current. It is a temporary current, usually formed at a point where the main current passes some obstruction, or between two adjacent currents flowing in opposite directions, or at the edge of a permanent current.
- Erosion¹ - The general process or the group of processes whereby the materials of the Earth's crust are loosened, dissolved, or worn away, and simultaneously moved from one place to another, by natural processes, which include weathering, solution, corrosion, and transportation, but usually exclude mass wasting. The mechanical destruction of the land and the removal of material (such as soil) by running water (including rainfall), waves and currents, moving ice, or wind.
- Fluctuating Zone - A zone on the face of a sand bar that is influenced by the fluctuation of river stage. The area of a sand bar between the range of high and low water levels.
- Range - The difference between high and low flow releases from Glen Canyon Dam as measured on a daily basis.
- Ramping Rate - The rate of change of flow releases from Glen Canyon Dam.
- Return Channel - A feature of sand bars formed by a large eddy or recirculation zone usually found on the upstream portion of the sand bar where a counter current formed a depression in the deposit by means of scour. The remnant land form is categorized as a return channel by Schmidt and Graf (1989).
- Rill Erosion¹ - The development of numerous, small, closely-spaced channels resulting from the uneven removal of surface soil by running water that is concentrated in rivulets of sufficient discharge and velocity to generate cutting power.
- Sand Bar¹ - A ridge-like accumulation of sand, gravel, or other alluvial material formed in the channel, along the banks, or at the mouth, of a stream where a decrease in velocity induces deposition.
- Sand-Bar Face - The surface of a sediment deposit (sand bar) adjacent to and sloping toward the river. Synonym beach face.
- Seepage Line¹ - The uppermost level at which flowing water emerges along a seepage face; an outcrop of the water table.
- Seepage Face¹ - A belt along a slope, such as the bank of a stream along which water emerges at atmospheric pressure and flows down the slope.

DRAFT
March, 1992

Stage - The elevation of a river water surface relative to a datum.

Surface Profile Gage - A device to determine accurate elevation of 58 points along a transect without disturbing the ground surface, i.e. erosion bridge.

Transects - A line or profile of scientific interest on the ground surface that is delineated by the position of stakes 15 feet apart. Measurements made along the transect are used to document vertical changes in topography. A transect and surrounding area is identified by flagging and protected from trampling by human footprints or other intrusive activities.

Transect Stake - A five or ten foot length of metal rod (1/2-inch reinforcement bar) driven into the sand bar to support the surface profile gage and delineate the end point of a transect.

Zone of Active Erosion - A section of the sand bar susceptible to seepage from bank stored ground water usually indicated by the presence of rilling.

¹Source: Glossary of Geology, 1980 Second Edition, edited by Robert Bates and Julia Jackson, American Geological Institute, Falls Church, VA.

APPENDIX 2

DESIGN AND OPERATION OF THE SURFACE PROFILE GAGE

An instrument to quantify erosion and deposition on the sand bars in the Grand Canyon needed to be portable, accurate and adapted to specific conditions encountered at remote sites. In general, measuring the topography of land surfaces utilizes bench marks, optical leveling devices, rods that serve as measuring sticks and a surveyors notebook. Likewise, measuring the profile of surfaces requires a reference datum, distance indicators and documentation.

Design

The surface profile gage was designed and constructed by Water Operations Branch staff. This instrument measures the elevation of a ground profile at 3-inch intervals over a distance of 15 feet without individuals having to traverse the area to be measured. A total of 58 data points are acquired over the profile.

Preliminary tests were conducted to determine the least penetration of pliable surfaces by falling rods. Several materials including brass and plastic tubes, aluminum arrow shafts, and fiberglass rods were examined for weight, stiffness and length. One-eighth-inch wooden dowels had the best combination of material strength and least weight. Various designs were tested to reduce the sharpness of the end of the dowel. Styrofoam cubes, plastic disks, and ping pong balls were tested on a loose surface of fine sand collected from a sand bar along the Colorado River. Measurements were compared from each assembly to determine the least deformation of the sand surface. Spheres have the advantage of lack of sharp edges found on flat disks or cubes, which tended to cut into sloping surfaces. Ping pong balls were chosen due to good performance in the tests and lack of porous surfaces which could absorb moisture and the ease of removing wet soil that may adhere at the contact surface.

The surface profile gage was developed to collect accurate data on erosion and deposition of soft ground surfaces. The length of the gage allows measurements of undisturbed plots without trampling or other human induced soil deformation. Measurements of vertical distances from a supported beam can be repeated accurately at periodic time intervals. Vertical support stakes delineate 15 foot transects across study plots. The gage is positioned on these stakes and the vertical rods are allowed to drop to the ground surface. Each rod has a ping pong ball attached to the lower end to prevent the rods from penetrating the soil surface. The rods are clamped in position while touching the ground and the gage is removed for measurements. The extended distance of each rod is recorded.

The surface profile gage was designed with specialized features that allow:

1. Measurements without disturbance to the study plot by human foot prints.
2. Long enough span that the vertical support stakes do not affect the study plot.
3. Measurement rods that do not penetrate in soft, pliable ground surfaces.
4. A clamping system that holds the rods in position when the gage is removed from the vertical support stakes.

5. Precise measurements to determine very small differences in ground elevations.
6. Light weight to insure easy operation by two people.
7. Portability to the study site by disassembly for shipping, rafting, and/or backpacking.
8. Durability during field travel.

Construction

The surface profile gage was constructed with an aluminum frame 15 feet long (4.6 m) which positions 58 ping-pong balls, each attached to a 2-foot length of 1/8-inch diameter wooden dowel. The frame is made from two beams which are vertically separated 8 inches by short diagonal braces to form a truss (hence the common term of erosion bridge). Each beam is spliced from two 7-1/2-foot lengths of 2-inch aluminum angle. Small guide holes of 3/16-inch are drilled at a 3-inch spacing, 3/8-inch from the edge of the beams to the center of each hole.

The gage can release the dowels (allowing free movement) or clamp the dowels in place. A clamping bar was constructed from 1-inch aluminum angle and foam weather stripping. The clamping bar rests on the upper beam and may be pressed against the row of dowels to hold them in place or moved away to allow the dowels to slide freely in their guide holes. A mark on each dowel was made to indicate a specific distance from the bottom of the ball. A marking jig was constructed to improve consistency in locating the mark on the dowel. Each ball and guide hole are numbered to insure the balls and dowels could be replaced to their original holes if the dowels were removed. The distance measurement of each dowel is taken from the top beam of the gage.

Two larger holes were drilled at the ends of the surface profile gage where the top of the vertical support stakes fit into place for positive positioning the gage. A thick piece of metal with a hole was attached to the bottom of the upper beam to guide the vertical support stake to rest in the same position for every measurement. Slots were filed in the lower beam to eliminate problems encountered with aligning the holes at the end of the gage with the vertical support stakes. This reduced problems encountered from not driving the vertical support stakes in a true, perpendicular position.

Operation

Transects were established by placement of stakes to support the surface profile gage. In the first study period, stakes were 5-foot long, 1/2-inch diameter rebar. During a second study period, 10-foot long rebar was used. The method of setting the stakes consisted of wading in the river from outside the study plot to the selected point and approaching it directly from the water. The stakes were driven into the ground until about one foot remained exposed. One end of the gage is placed on the first stake while the other end is supported and used to locate the position of the second stake. After setting the second stake the gage is used to check that the distance is equal to the support holes in the gage.

Use of the surface profile gage consisted of positioning the balls close to the lower beam of the bridge by inverting the gage and releasing the dowels and reclamping. After approaching the transect from the water's edge, the gage was carefully placed over the vertical support stakes. The gage support

DRAFT
March, 1992

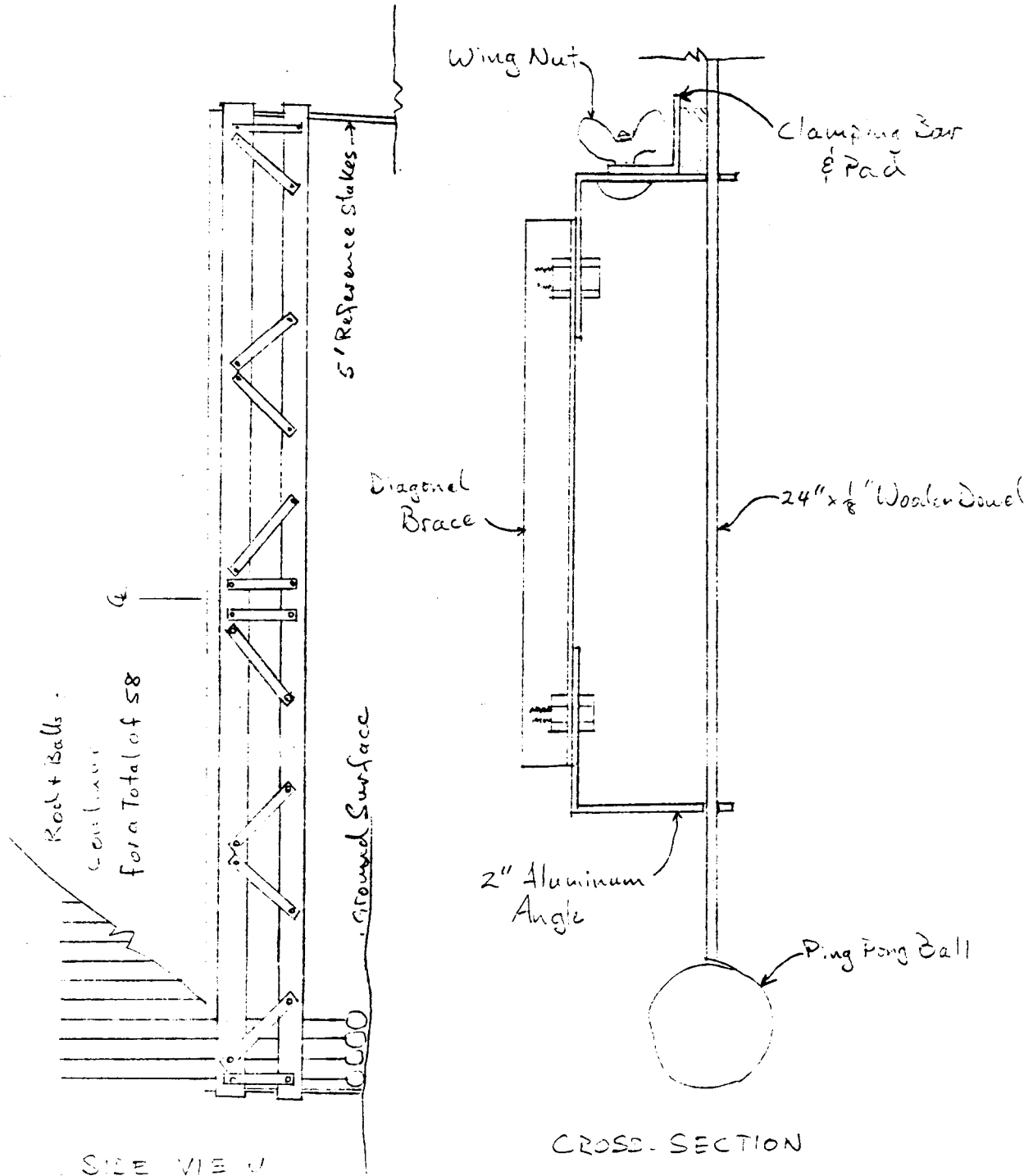
holes are positioned firmly onto the two vertical support stakes. This forces the gage in an upright, rigid position. With the gage in position, the clamping bar is released and the balls fall by gravity to the ground surface. Due to the short distance between the surface profile gage and the ground, the measuring rods drop lightly to the ground surface. The clamp is reset, holding the measuring rods in place while touching the ground surface. The gage is lifted off the support stakes and carried to a staging area for measurement of each rod in the clamped position. The distance from the upper beam of the gage to the mark on the dowel is measured and recorded.

The elevation of the top of the vertical support stakes was surveyed to established bench marks several times during the study to determine if any elevation changes (of the vertical support stakes) were occurring. The surface profile gage was checked for sag or warping by stretching a string line over the length of the upper beam and measuring the distance to the string at the center of the beam. Repeated measurements of a control, fixed transect indicates the reliability of the gage and the recording methodology.

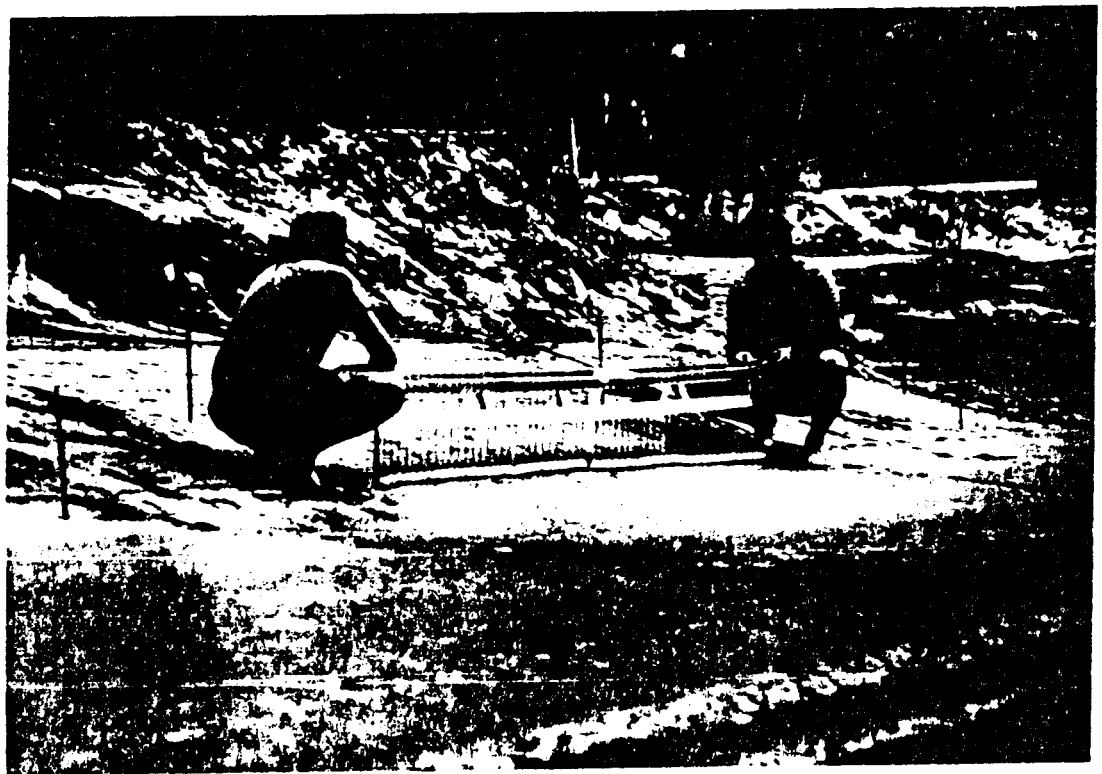
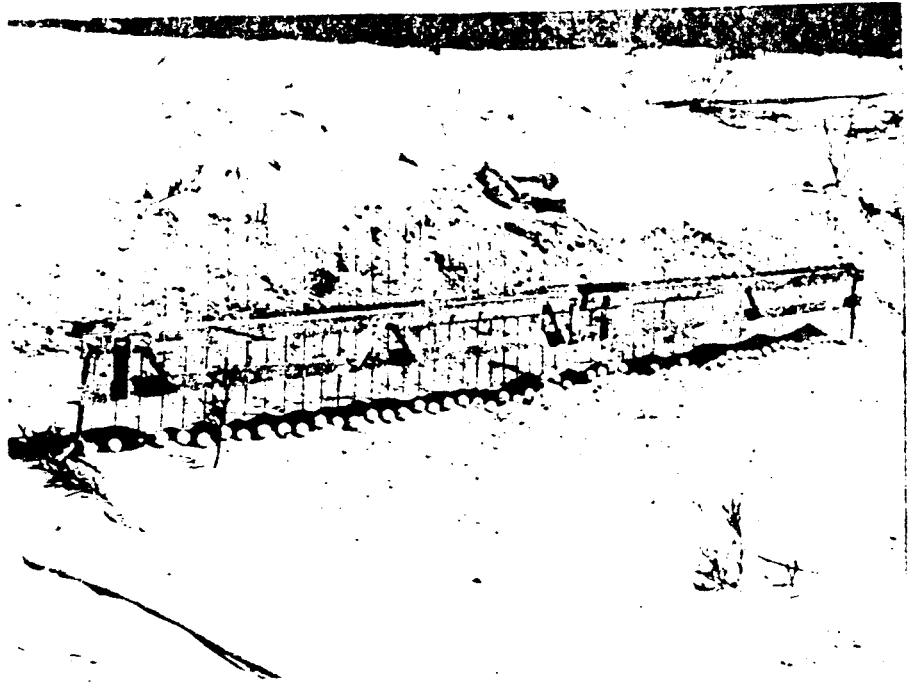
Fifty-eight data points are acquired for each surface profile measurement. The information is recorded on data forms along with transect identification, date, time, and observers names. All balls must drop correctly and the data must be properly recorded. Data points which plot beyond reasonable limits on graphs are discarded from analysis and are probably caused by error in recording or the initial measurement of the individual rods. Elimination of stick measurements near the vertical support stakes from analyses assured that the remaining data points reflected an undisturbed conditions along the transect.

Park <i>Grand Canyon NP</i>	NATIONAL PARK SERVICE		Sheet
Area			of
Project <i>Reach Emission</i>	By <i>R Inglis</i>	Checked	Pkg.
Feature <i>Sketch of GEDG</i>	Date <i>7-23-91</i>	Date	Account

GROUND ELEVATION DIFFERENTIAL GAGE



No Scale



APPENDIX 3
INTERIM OPERATING CRITERIA FOR FLOW RELEASES
FROM GLEN CANYON DAM

On November 1, 1991, the Secretary of the Interior implemented the following criteria for Interim Flows for the Colorado River downstream from Glen Canyon Dam. These criteria are to remain in place through the completion of the Record of Decision for the Glen Canyon Dam - Environmental Impact Statement, currently scheduled for December, 1993. The purpose of the Interim Flows is to minimize the loss of the natural resources in the Grand and Glen Canyons until a longer term solution is defined through the Glen Canyon Dam - Environmental Impact Statement program.

<u>Parameter</u>	<u>Flow in Cubic Feet per Second (cfs)</u>
Maximum Flow	20,000 cfs ¹
Minimum Flow	5,000 cfs - nighttime 8,000 cfs - 7 a.m. to 7 p.m. ²
Ramp Rates	
Ascending	8,000 cfs/ 4 hours not to exceed 2,500 cfs/hour
Descending	1,500 cfs/hour

Daily Fluctuations

5,000, 6,000, or 8,000 cfs³

¹To be evaluated and potentially increased as necessary for years when delivery to the Lower Basin exceeds 8.32 maf.

²The 8,000 cfs minimum flow requirement from 7 a.m. to 7 p.m. will be shifted to 8 a.m. and 8 p.m. respectively beginning the last Sunday in October and ending the first Sunday in April, Arizona local standard time.

³Daily fluctuation limit of 5,000 cfs in months with release volumes less than 600,000 acre-feet, 6,000 cfs for monthly release volumes between 600,000 and 800,000 acre-feet, and 8,000 cfs for monthly volumes over 800,000 acre-feet.

CHAPTER 5

**Daily Responses of Colorado River Sand Bars
to Releases from Glen Canyon Dam, 1990-1991:
Instantaneous Erosion and Dependent Deposition.**

June 30, 1992

Brian L Cluer
Division of Resource Management
Grand Canyon National Park
Grand Canyon, Arizona

TABLE OF CONTENTS	i
List of Figures	ii
List of Tables	ii
ABSTRACT	1
INTRODUCTION	2
METHODS	10
RESULTS	12
DISCUSSION	37
CONCLUSIONS	46
ACKNOWLEDGEMENTS	47
REFERENCES CITED	47

LIST OF FIGURES

Figure 1	3
Figure 2	3
Figure 3	4
Figure 4	5
Figure 5	6
Figure 6	7
Figure 7	8
Figure 8	9
Figure 9	10
Figure 10	11
Figure 11a	12
Figure 11b-c	13
Figure 12a-b	14
Figure 12c-d	15
Figure 13	17
Figure 14	18
Figure 15	19
Figure 16	20
Figure 17	21
Figure 18	22
Figure 19	23
Figure 20	24
Figure 21	26
Figure 22	27
Figure 23	28
Figure 24	29
Figure 25	30
Figure 26	33
Figure 27	34
Figure 28	35
Figure 29	36
Figure 30	37
Figure 31	40
Figure 32	41
Figure 33	44

LIST OF TABLES

Table 1	39
---------	----

ABSTRACT

Six automatic time-lapse cameras were installed overlooking river-bank deposits along the Colorado River in Grand Canyon during a series of test releases from Glen Canyon Dam. Photographs were taken daily, at or near low river stage, from August 1990 to November 1991. Measurements of deposit area were made from photographs taken during regularly scheduled constant low discharge periods. Deposit areas were estimated between measured photographs by visually inspecting daily images. The method was effective in monitoring sand bar responses to test flows.

It was found that sand bars responded daily to changes in flow regime. The most obvious responses were erosional. Day to day photographs documented rapid and large-scale erosion events (bank failures) occurring repeatedly at five out of six sites. Most deposits rebuilt to nearly the same area, or greater, in as little as one week when the dam released daily high fluctuation flows. There were exceptions to this however, where one deposit that eroded rapidly in December, 1990, was still greatly reduced in size at the end of the study. When low fluctuation releases followed erosion events, little deposition occurred. This was observed during "interim" flows, when bank failures were not rebuilt.

External processes were documented on one occasion when a deposit eroded 50% in 4-5 hours. However, out of 23 bank failure events documented, half were temporally associated with dam operations that produced 2-3 day low flow periods following high fluctuations, and followed by high fluctuations. Slumping of high-angle deposits and seepage of bank-stored water explain some of these events. Other events were physically observed where high current velocities from rising river stage were directed toward very low-angle deposits, and scouring occurred. It is probable that seepage and scour are mutual forces in bank failure events. Both types of bank failure are driven by operations of Glen Canyon Dam.

"Weekend" low flows, a component of "normal" fluctuating flows, are responsible for the majority of bank failures. It was also found that "normal" flows eroded two-times more river-bank sediment and deposited one-third as much as did test flows that fluctuated regularly. Since bank failures are caused by dam operations, they are an important new element of river-bank dynamics that needs to be treated in managing the sediment resources along the Colorado River corridor in Grand Canyon.

INTRODUCTION

Background

In 1989, the U.S. Bureau of Reclamation decided to conduct a series of designed releases from Glen Canyon Dam to help evaluate alternative flow scenarios that might reduce impacts to downstream resources from normal daily fluctuations that provide peak hydroelectric power. The designed releases have become known as test flows, each having different hydraulic characteristics in mean discharge, daily range in discharge, up and down ramping rates, and duration. The test flows were designed to imitate seasonal flow patterns during normal operations for hydro-power production, for evaluation of potential alternative flow regimes, and each test flow was separated by a short period of low constant flow so that measurements could be made on otherwise inundated river-bank deposits.

Objective

During a short reconnaissance survey in 1989, during a pre-test flow evaluation, and in the early surveys during the test flows in 1990, it became apparent that Colorado River-bank deposits might erode dramatically over very short periods of time. The driving processes were unknown. Time-lapse photography was selected as a method to study rapid changes in river-bank morphology. The objectives of this investigation were to document daily changes in sand bar morphology and determine if operations of Glen Canyon Dam were responsible for those changes.

Setting

The Colorado River flows through the highly incised Grand Canyon bedrock gorge for 250 miles between impoundments at Glen Canyon Dam and Lake Mead backwaters (Fig. 1). Over most of its length, short, steep, ephemeral tributaries have deposited fans of coarse debris along their confluences resulting in constrictions of the main channel. Where main stem flow is upset by channel constrictions, flow recirculation zones and stagnation points develop, creating depositional environments for sediments transported by the Colorado River. Four types of fluvial deposits have been classified; separation deposits, reattachment deposits, upper pool deposits, and channel margin deposits (Fig. 2) (Schmidt and Graf, 1988). The impoundment of the Colorado River behind Glen Canyon Dam in 1965 efficiently removed the historically high sediment load. Modern fluvial sediment sources are restricted to tributary loads between impoundments, with the Paria and Little Colorado Rivers providing the majority of annual sediment supply. Unexpected high releases from Glen Canyon Dam in the spring of 1983, and the following three years, resulted in reworking the existing river-bank fluvial deposits. There is considerable debate still over the effects of those high releases on fluvial sediments held in storage in both the channel and river-bank settings. Most interest has been paid the river-bank deposits, as they provide substratum for the entire riverine ecology and are more readily observed.

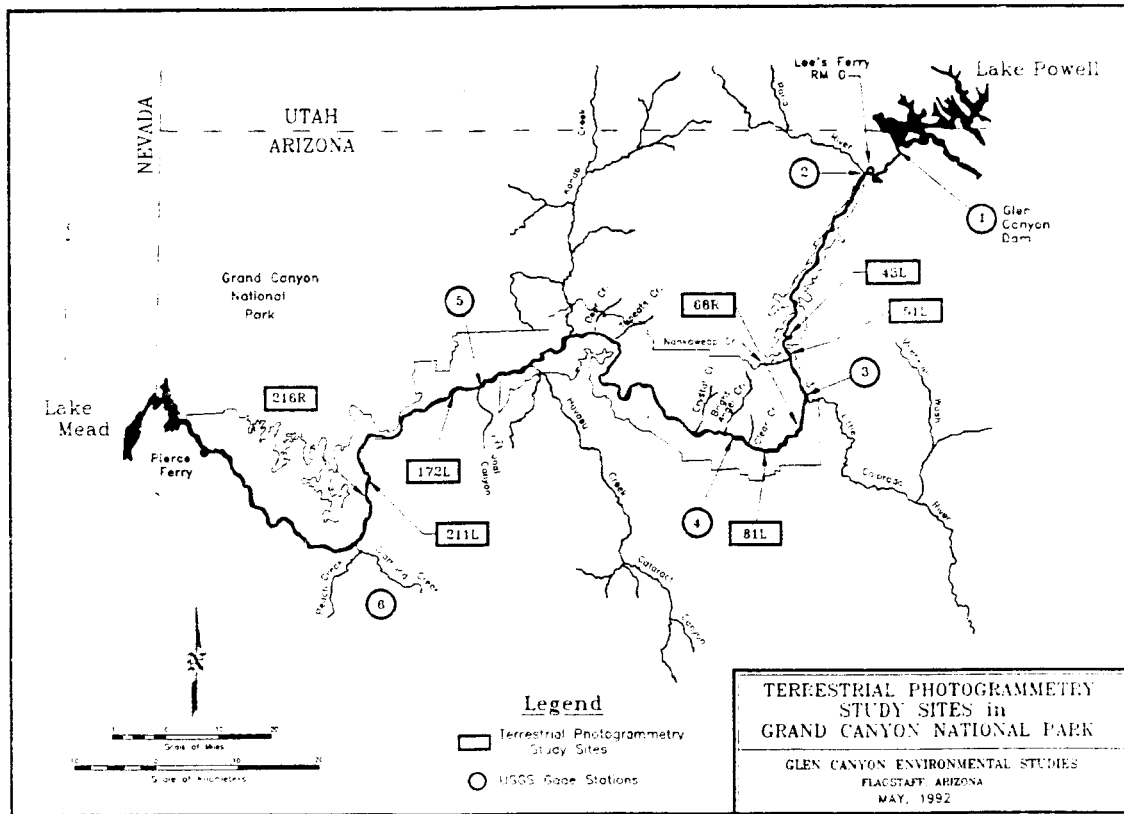


Figure 1. Location map of Grand Canyon and surrounding region, and study sites in this investigation.

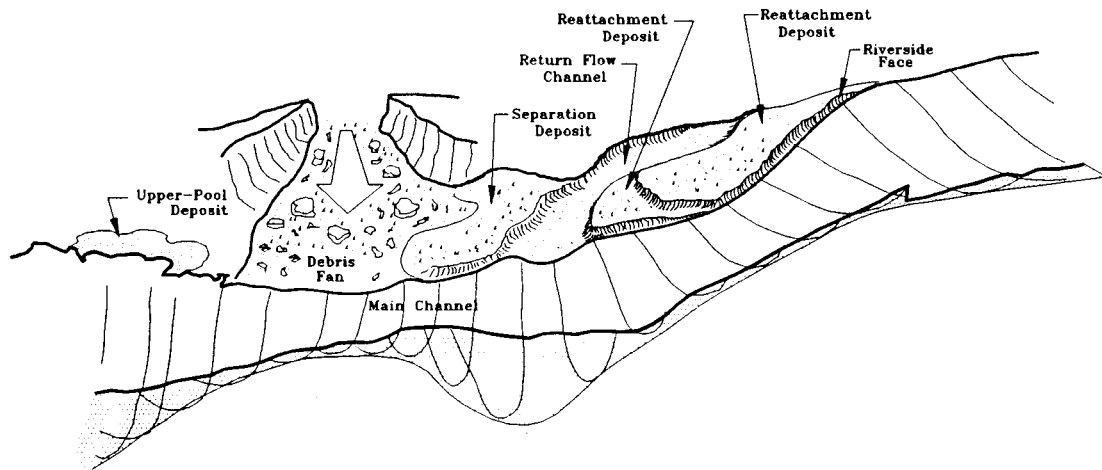


Figure 2. Schematic depiction of fluvial depositional environments along the Colorado River banks in Grand Canyon (after Schmidt and Graf, 1988).

Site Selection and Description

The sites selected for this study were: 1) Colorado River mile 43 left (CR 43 L); 2) CR 51 L; 3) CR 68 R; 4) CR 172 L; 5) CR 211 L; and 6) CR 216 R. (See figure 1). A short period of record was obtained at CR 81 L, however this data is not presented. Site selection criteria included: daylight during low river stage; coincidence with instrumented seepage erosion sites; presumed high activity from prior experience; where high angle slopes suggested vulnerability to fluctuating flows; and where large cut-banks were commonly observed.

CR 43 L The sand deposit at this locale lies immediately upstream of a channel constriction (Fig 3). Consequently, it is classified as an upper pool deposit. There are typically two small recirculating eddies along the face of the deposit that shift and change size in response to changes in river stage. Current velocities at this site are relatively low because of its upper pool environment.



Figure 3. Aerial photograph of study site CR 43 L. River flows from top to bottom of image, note channel constricting debris fan downstream of deposit. Lines indicate location of camera and field of view. Photo taken at 5,000 ft³/s.

CR 51 L This deposit lies downstream of a channel constriction, in a flow recirculation zone, and is classified as a reattachment deposit. The deposit is broad, flat, and low in topographic relief. The heavily vegetated portion is inundated during high daily releases.

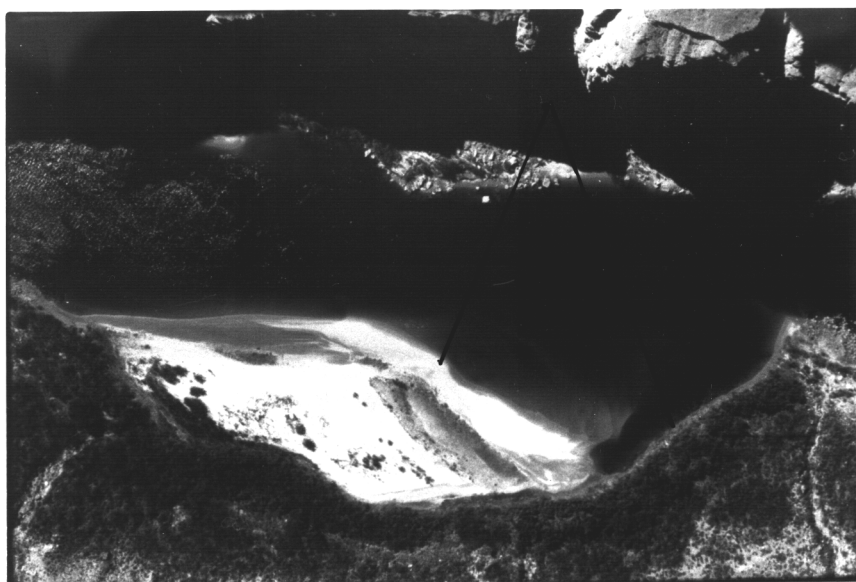


Figure 4. *Aerial photograph of study site CR 51 L. River flows from right to left in the photo. Note small separation deposit at the downstream side of the channel constriction (right center), return flow channel (lower right), and flow reattachment point (center). Photo taken at 5,000 ft³/s.*

CR 68 R This is a complex deposit consisting of separation and reattachment deposits along the inside of a tight river meander. Much of the upstream gravel bar was over-topped by high flows in the 1980's, so the fine grained deposit would have originated in a separation environment. It has since been reworked by lower flows, and discrete separation and reattachment deposits currently exist. This site was the first instrumented with time-lapse cameras in August, 1990.

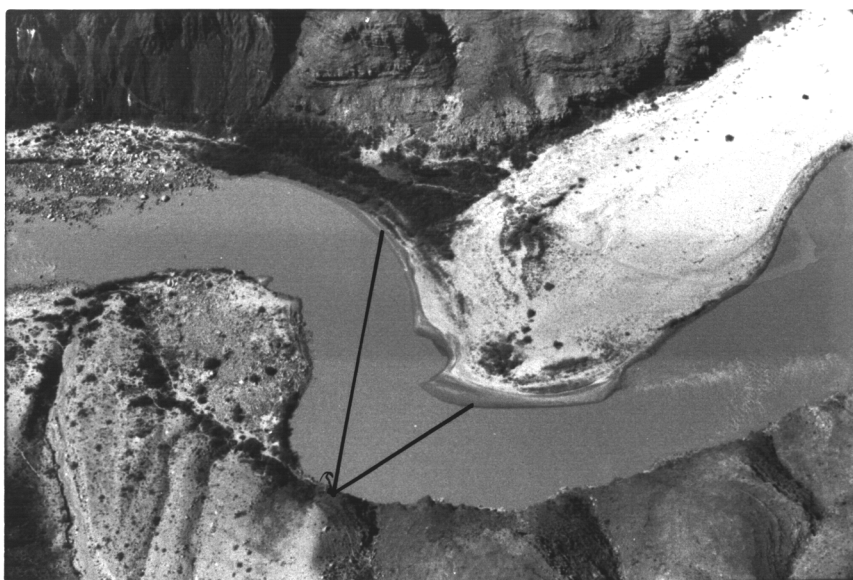


Figure 5. Aerial photograph of study site CR 68 R. River flows from right to left in image around two channel constrictions. Lines indicate camera location and approximate field of view. Note narrow reattachment deposit, elongated separation deposit, and semi-circular return flow channel between the two deposits. Photo taken at 5,000 ft³/s.

CR 172 L About 104 miles downstream is the next study site, 1-mile downstream of Mohawk and Stairway canyons. This deposit is in a relatively narrow portion of the canyon, and consists of a narrow, flat reattachment deposit with a strong recirculating eddy.



Figure 6. Aerial photograph of study site CR 172 L. River flows from left to right in image. Note separation deposit at flow constriction (upper left) and reattachment deposit in channel expansion (upper right and center). Lines indicate camera location and approximate field of view. Photo taken at 5,000 ft³/s.

CR 211 L Next downriver is a reattachment deposit with an uncommonly long and steep slope that extends to river level during all normal fluctuations. Vegetation on this slope was suspected as being disturbed by fluctuating flows.

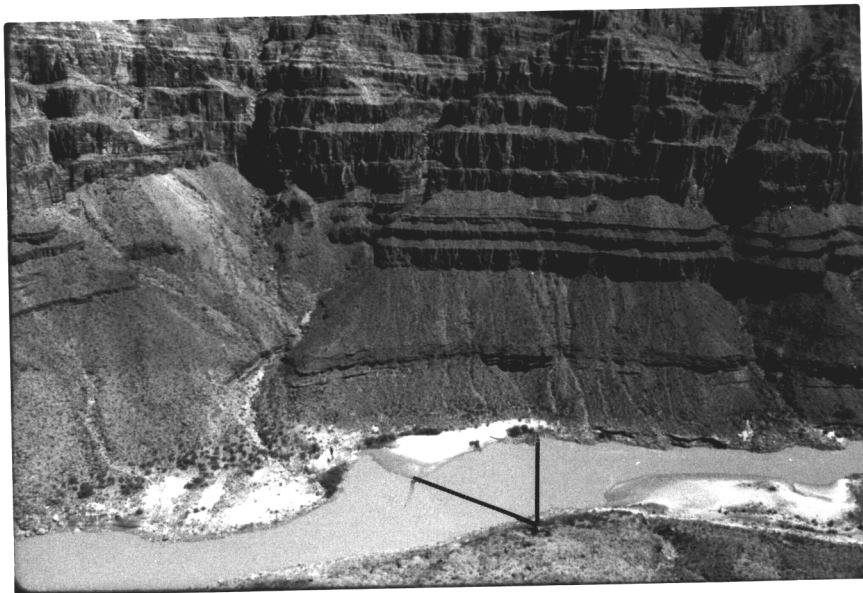


Figure 7. Aerial photograph of study site CR 211 L. River flows from left to right in photo. Study site is a reattachment deposit, downstream of a debris fan channel constriction. Lines indicate camera location and approximate field of view. Photo was taken at 5,000 ft³/s.

CR 216 R The last study site is typical of Grand Canyon reattachment deposits, formed downstream of a channel constriction.



Figure 8. Aerial photograph of study site CR 216 R. River flows from lower right to upper left in image. Channel constriction appears in the lower right portion, associated with the separation deposit. Reattachment deposit at channel expansion is at right center. Lines indicate location of camera and approximate field of view. Photo taken during interim flows at approximately $10,000 \text{ ft}^3/\text{s}$.

METHODS

This project was originally conceived to provide supporting qualitative descriptions to existing land surveying approaches to sand bar investigations (Beus and Avery, 1992). However, it became apparent that consistent and comparable quantitative measurements of sand bar area could be made from photographs taken at known constant river stages.

Cameras and Installation

During the fall of 1990, an elaborate Nikon time-lapse camera system was temporarily installed overlooking the fluvial deposits at Colorado River mile 68 to test the feasibility of time-lapse photography in fluvial deposit studies. The initial results were encouraging, and preparations were made to install six additional cameras during a November-December, 1990 surveying trip. Pentax Camera Corporation had introduced their first inexpensive programmable camera just months prior to the beginning of this project. The camera, model IQ Zoom 105, was the only point and shoot (inexpensive) camera then available with an integral 24-hour intervalometer. This feature was necessary in order to allow daily image capture while providing 30-35 days of film capacity in an off-the-shelf camera. The cameras used for this study also had optional datebacks to imprint each image with the date or time.

A weather proof enclosure was designed to house and protect the cameras in the harsh Grand Canyon environment. Standard military surplus steel ammunition containers were used. They are readily available, inexpensive, water-proof, and easily modified for this application. The containers were modified to include an optically transparent acrylic window, a mounting base for the camera to ensure repeatable camera alignment, and a sun and rain shade for the window (Figure 9). The camera housings were affixed to large and immobile rocks using inert silicone adhesive. The housings were aligned to insure desired photo coverage prior to fixing. This system resulted in remarkable camera performance through wide ambient temperature swings and severe thunderstorms.

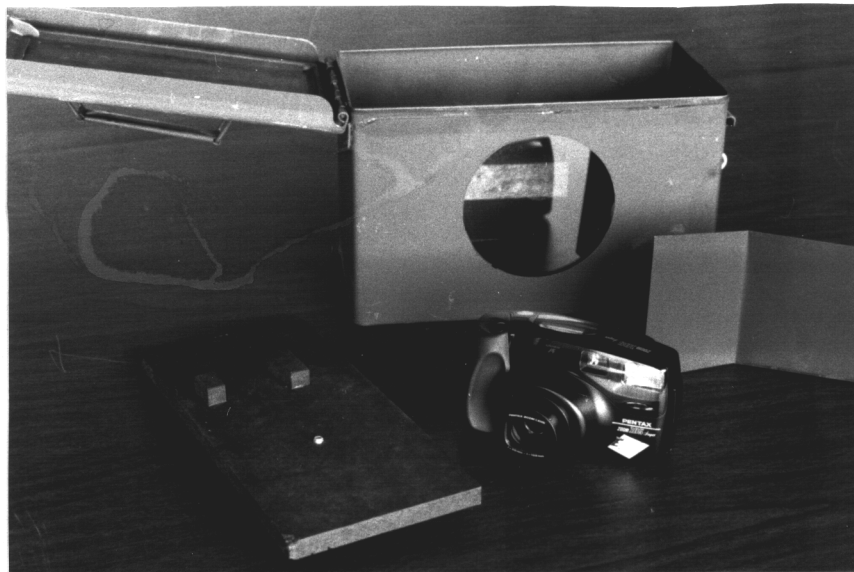


Figure 9. Camera and weather proof housing used in this study.

Data Gathering

Six cameras were installed and collecting daily images by December 10, 1990. During regularly scheduled sand bar surveying river trips (Beus and Avery, 1992) and other pre-scheduled trips, film was replaced in the cameras and batteries were checked. The film used was standardized early in the investigation to ensure color balance from roll to roll. Kodachrome 64 Professional color reversal film was used almost exclusively. Various processing laboratories and mounting systems were experimented with. However, the most consistent and flexible method was Kodalux processing without cutting or mounting the film.

Analysis

All images were reviewed under 4x magnification while still in strips. When low flows occurred (5,000 ft³/s constant for 3 days following each test flow) images were selected from all sites for measurement. Measurements were taken from images using a 10x magnifying loupe with a scaled base lens. The scaled lens was placed directly on the image surface to eliminate distortion, and cross-section lengths were measured. Vertical cross-sections were originated at geographic reference points visible in all photographs, and were chosen to adequately cover the width and various features of the subject (Fig 10). Cross-section lengths were averaged and multiplied by horizontal length to yield area values.

Because the cameras were immobile and consequently in the same position for each photograph, reliable and repeatable measures of sand bar area were readily obtained. Fixed-camera photogrammetry lends itself to repeatable measurement of any visible change or movement in the field of view. A fixed-camera system also makes it possible to make comparable measurements from photo to photo without having ground-control even photographic scale information. The results presented in this report are daily area values expressed as percentages of the original area measured. Daily area values were estimated between measured values by carefully inspecting each daily image for changes in deposit morphology. Many technological refinements of this precursory analytical method are possible and some have been instituted since the beginning of the interim flows period.

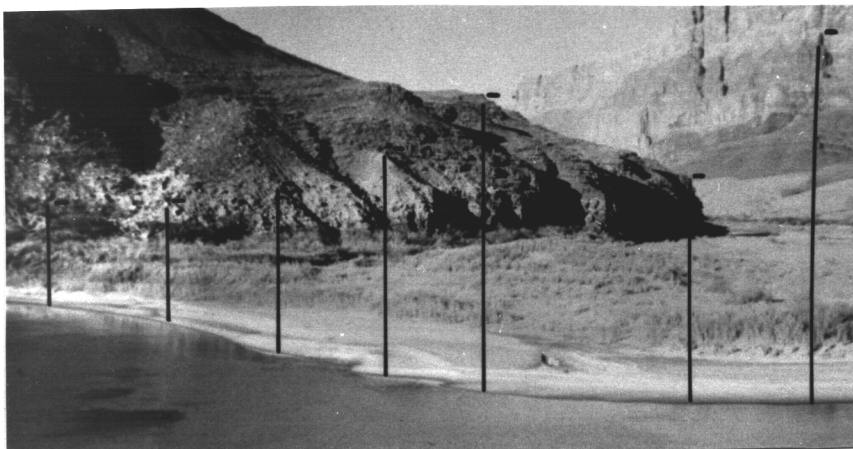


Figure 10. Depiction of photogrammetric measurement scheme used for this analysis. Black lines are cross-sections repeated on each measured photograph, each beginning at prominent geographic reference points. Sample site is CR 68 R.

Oblique terrestrial photography permits perception of sand bar morphology in three dimensions. Horizontal planar measurements can be qualified by observations in the vertical dimension. For example, it is easy to differentiate between low-angle slopes and high-angle slopes. This qualitative information is further refined through field observations of the commonly encountered slope angles. Although not directly measured in this investigation, slope angles will be discussed in the qualitative terms of low and high, or gentle and steep. From field experience, these generally correspond to the theoretical minima and maxima of 11 and 26 degrees for wet and dry materials composing Grand Canyon sand bars (see Budhu, this report).

RESULTS

This investigation resulted in over 1,800 time-lapse photographs, of which about 100 were used for actual sand bar area measurements. All images will eventually be transferred to video format and time-lapse animation products will be available. The sand bar area tables were graphically prepared as daily time-series plots of deposit area and associated river hydraulic parameters (Figs. 11, 13, 14, 16, 17 and 20). Hydraulic descriptions of each test flow were compiled from test flow hydrographs and GCES-II test flow designs (Appendix I, this report). Comparisons of relative sediment transport capacity were made using data presented also in Appendix I and are plotted on the time-series diagrams as relative indexes for comparing the different test flows. Photographs of the more dramatic findings accompany the time-series plots (Figs. 12, 15, 18, 19, 21, 22, 23, 24, 25, and 26).

Normal Flow August 8-September 17, 1990 The first time-lapse camera was installed on August 8, 1990, at CR 68 R. Using a standard roll of film with 36 exposures, and programming the intervalometer for 6 hours between photos, 9 days of record were obtained (Fig. 11a). Film was replaced on September 2, 1990, and the intervalometer was programmed for 1 photo each day at estimated low stage, about 5:30 PM. The photographs of September 5 and 6, 1990 show that approximately 10% area of sediment in the return flow channel was eroded in the previous 24 hours (Fig 12a-b). This occurred on the second day of fluctuation following 2 days of low fluctuating "weekend" flows (see Appendix I, hydrograph of September, 1990). The CR 68 R deposits remained constant in size through the remainder of the **Normal Flow** and deposit areas were measured on September 17, during the 5,000 ft³/s evaluation period.

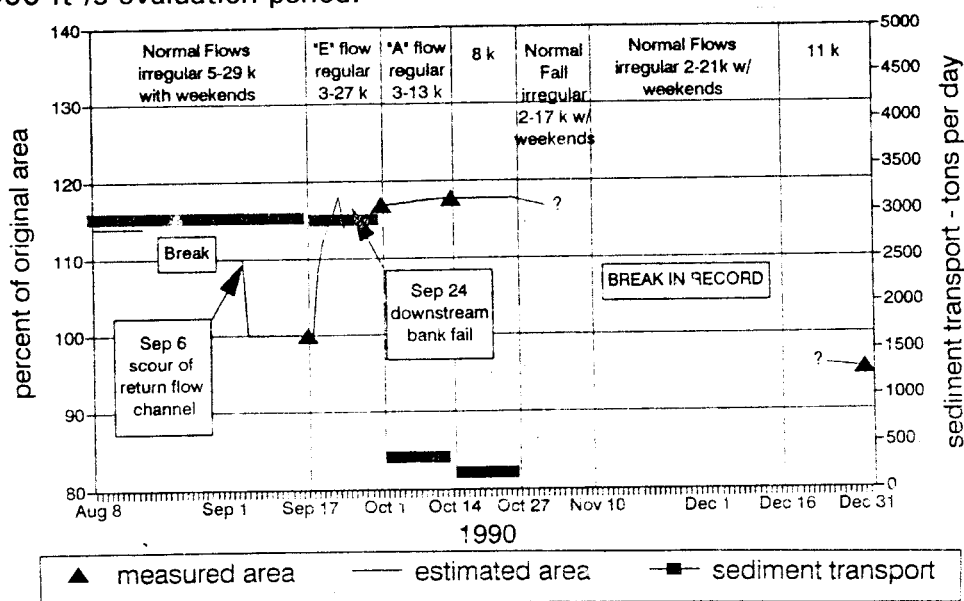
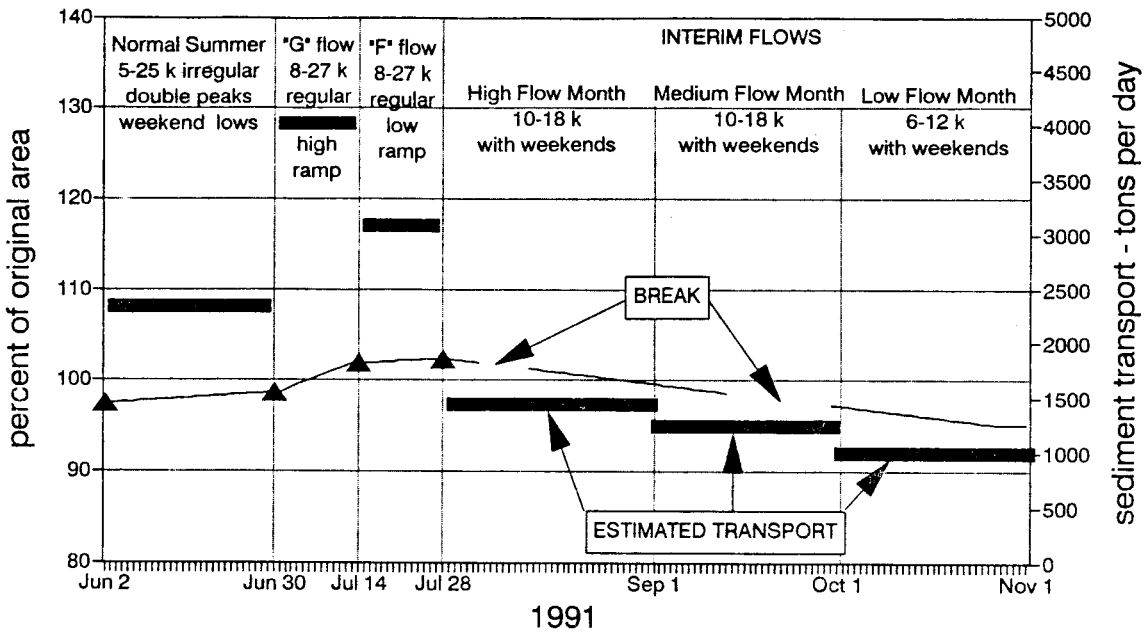
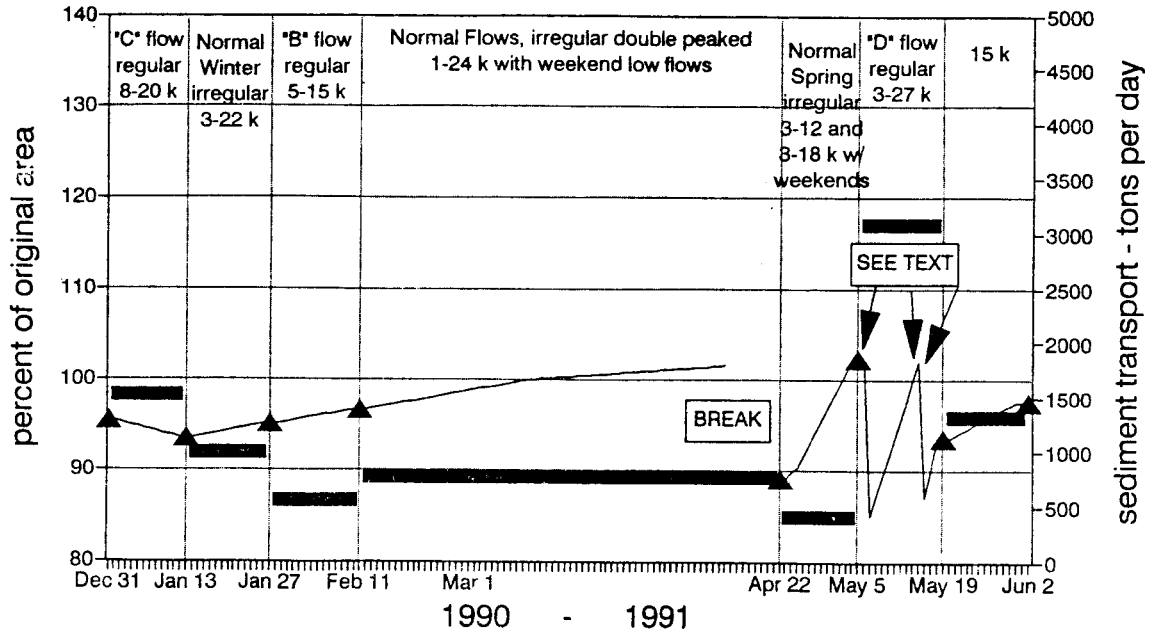


Figure 11a. Time series plot of daily deposit area at CR 68 R. Area is expressed as a percentage of area measured in original photograph. Test flow details are described along the top, and sediment transport capacities are shown as the heavy horizontal lines.

CR 68 RIGHT



▲ measured area — estimated area —■— sediment transport

Figure 11b-c. Time series plots of daily deposit areas at CR 68 R.



Figure 12a-b. Photographs of September 5 (a) and September 6 (b), 1990, at CR 68 R. Note erosion of return flow channel area (right center) in lower photograph.

"E" Flow September 17-October 1, 1990 The **"E" flow** immediately began depositing sediments along the separation deposit, and the area of CR 68 R was increased 10% by September 20 (Fig. 11a). The deposits continued to increase in size until sometime between September 23 and 24, when the return flow area was eroded, reducing area about 4% in the past 24 hours. This erosion event occurred in the middle of the regularly fluctuating test flow (see Appendix I). The downstream portion of the reattachment deposit was also being eroded during this period of test flow (Fig. 12c-d) even though the overall area was increasing.



Figure 12c-d. Photographs taken on September 23 (c) and September 24 (d) at CR 68 R. Note enlarged return flow channel (right center) and cut-bank formation (left center) in lower photograph.

"A" Flow October 1-October 14, 1990 During the "A" flow, CR 68 R stabilized from its prior rapid deposition and erosion, and enlarged in area about 2% (Fig. 11a).

Normal Fall October 27-November 10, 1990 Record was not obtained for this test flow.

Normal Flow November 10-December 16, 1990 Six sites were instrumented with time-lapse cameras between November 28 and December 10, 1990. The **Normal Flow** test was the first test recorded at sites other than CR 68 R. At CR 43 L, no measurable changes were recorded (Fig. 13a). At CR 51 L, the reattachment deposit eroded about 10% (Fig. 14a) between photographs taken on December 12 and 13 (Fig. 15a-b). Area stabilized for the remainder of the test flow at CR 51 L. Records had not been established for the remaining sites.

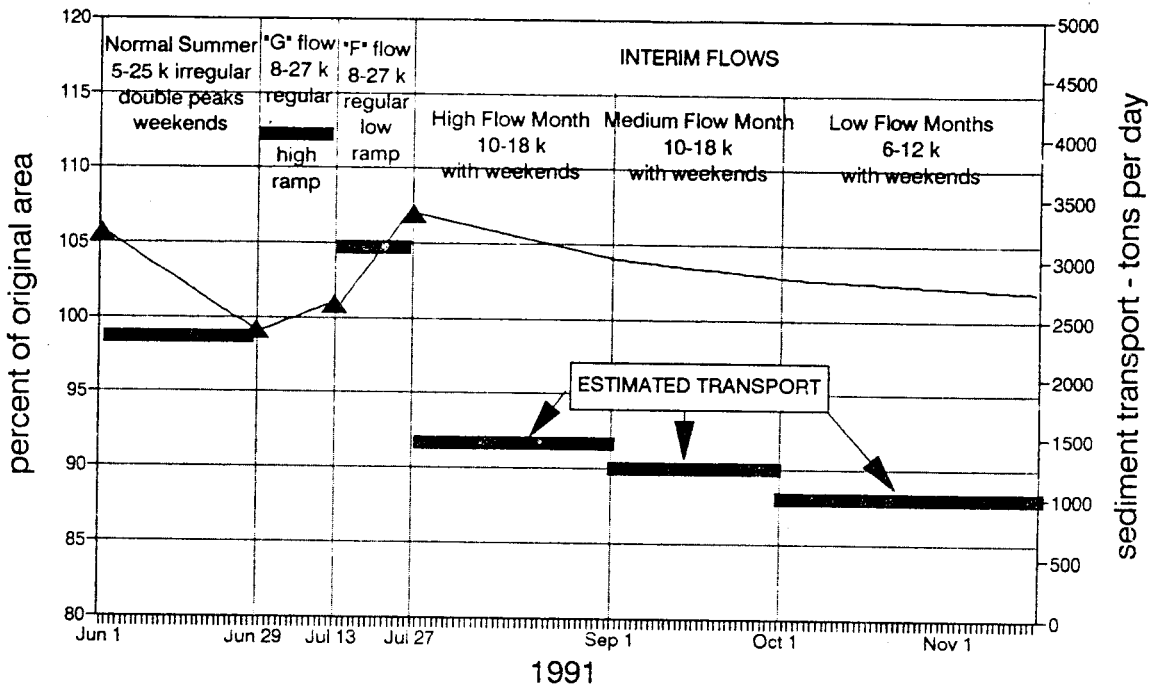
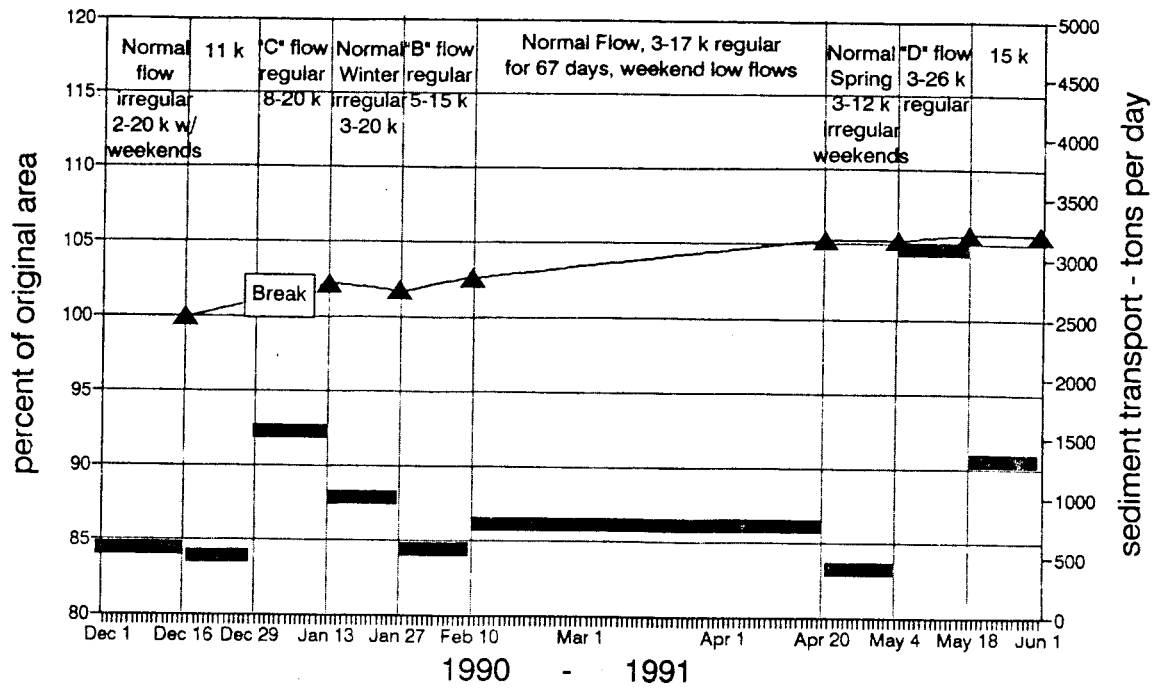
11,000 ft³/s Constant Flow December 16-December 31, 1990 At CR 43 L, the constant flow test resulted in slight area increase (about 1%) (Fig. 13a). Slight area decrease was recorded at CR 51 L (Fig. 14a). The constant flow test was not recorded at CR 68 R and CR 172 L. At CR 211 L, the test reduced deposit area about 1% (Fig. 16a), and at CR 216R, the deposit eroded 5% over the two-week test period (Fig. 17a).

"C" Flow December 29, 1990-January 13, 1991 No record was acquired at CR 43 L. At CR 51 L, deposit area increased about 3% to the pre-**11,000 ft³/s** test area (Fig. 14a). CR 68 R eroded about 2% during the two-week test (Fig. 11b). Camera malfunction at CR 172 L resulted in no record for the "C" test. At CR 211 L, dramatic erosion occurred over the two-week test period (Fig. 18a-b), resulting in about 17% reduced area (Fig. 16a). An increase of about 7% area was recorded at CR 216 R during the same period (Fig. 17a).

Normal Winter Flow January 14-January 28, 1991 Approximately 1% area reduction was recorded at CR 43 L (Fig. 13a). At CR 51 L, erosion of about 16% area was documented (Fig. 14a). About 2% increased area was measured at CR 68 R for this test (Fig. 11b). Camera malfunction still affected CR 172 L. CR 211 L eroded approximately 17% over the two-week test period (Fig. 16a). CR 216 R eroded about 3% during the last day of the prior evaluation flow (Fig. 19 18?), but rebuilt and gained about 1% area over two-weeks (Fig. 17a).

"B" Flow January 27-February 10, 1991 Area increased at CR 43 L about 1% over the two-week test period (Fig. 13a). Area continued to decrease at CR 51 L by about 3% (Fig. 14a). At CR 68 R, area continued to increase at a rate similar to the previous test, resulting in about 2% increase (Fig. 11b). The camera system was operating at CR 172 L during the "B" test, and the deposit area increased about 2% (Fig. 20a). At CR 211 L, the previous erosion was recovered in about 8 days, and the deposit increased about 2% during the test flow (Fig. 16a). CR 216 R responded similarly to the **Normal Winter** and "B" tests through erosion of the exposed high-angle bank, forming a cut-bank, reducing area about 4% in the last day of the evaluation period. However, the area loss was recovered quickly during the ensuing "B" test, and the deposit enlarged about 1% overall (Fig. 17a).

CR 43 LEFT



▲ measured area — estimated area ■ sediment transport

Figure 13a-b. Time-series plots of daily deposit area at CR 43 L.

CR 51 LEFT

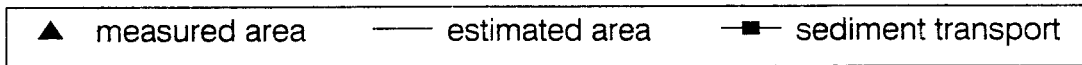
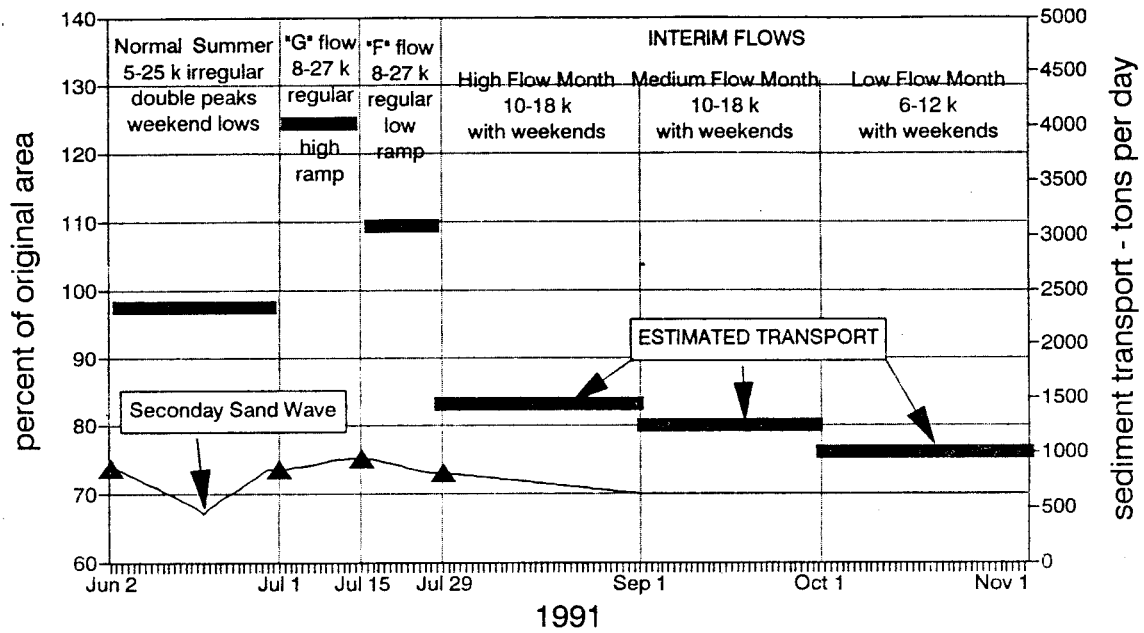
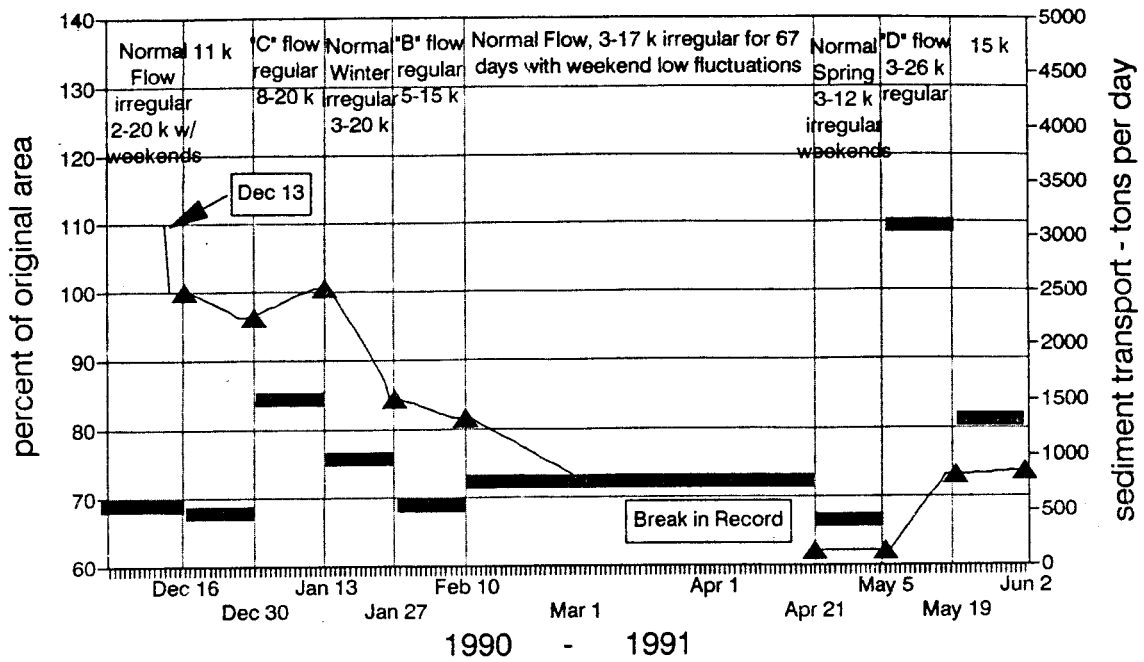


Figure 14a-b. Time-series plots of daily deposit area at CR 51 L.



Figure 15a-b. Photographs taken on December 12(a) and 13(b), 1990, at CR 51 L. Note eroded area at right edge of lower photograph.

CR 211 LEFT

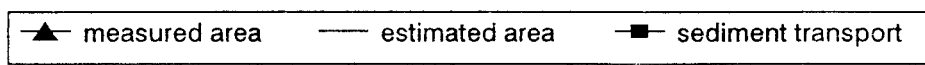
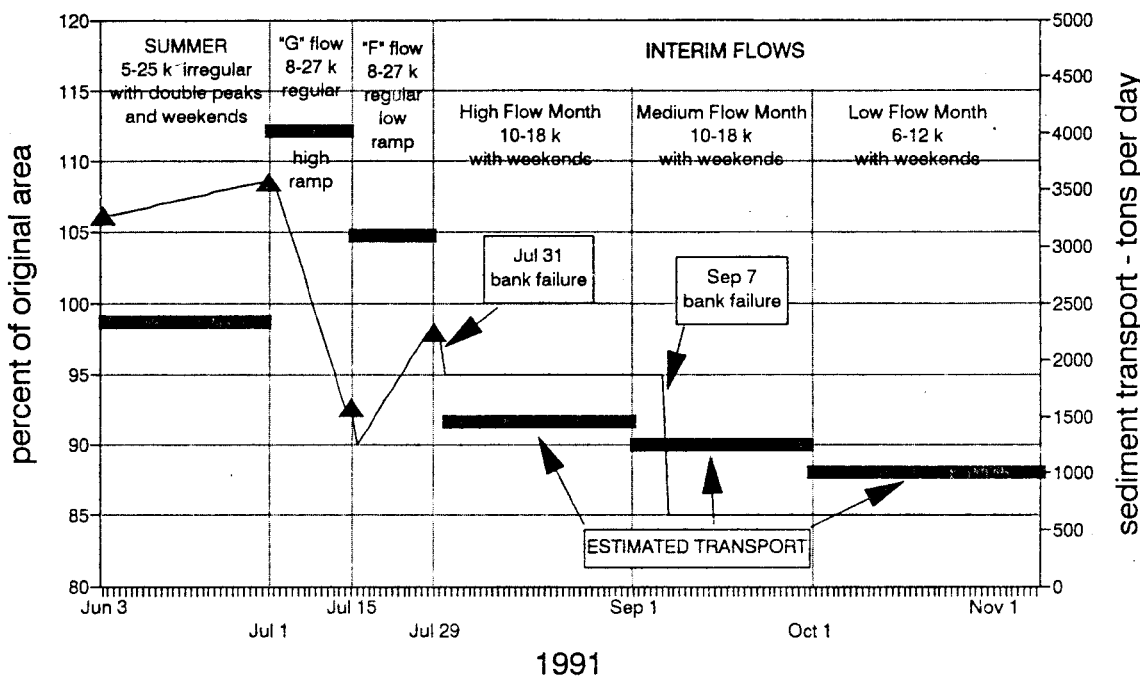
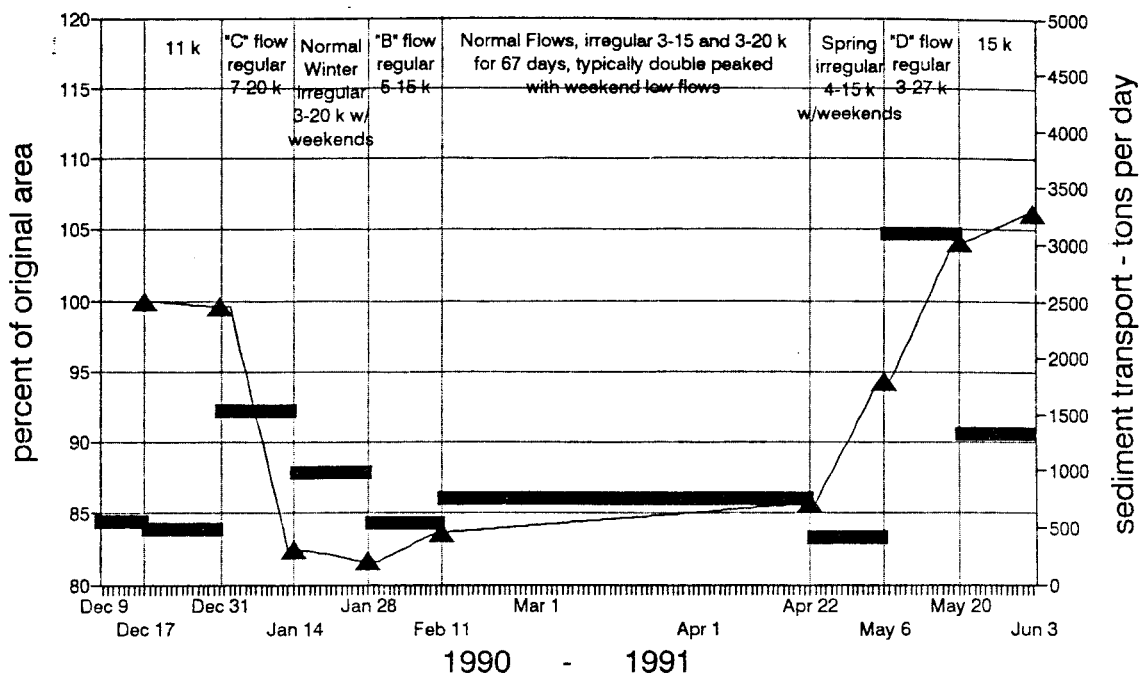
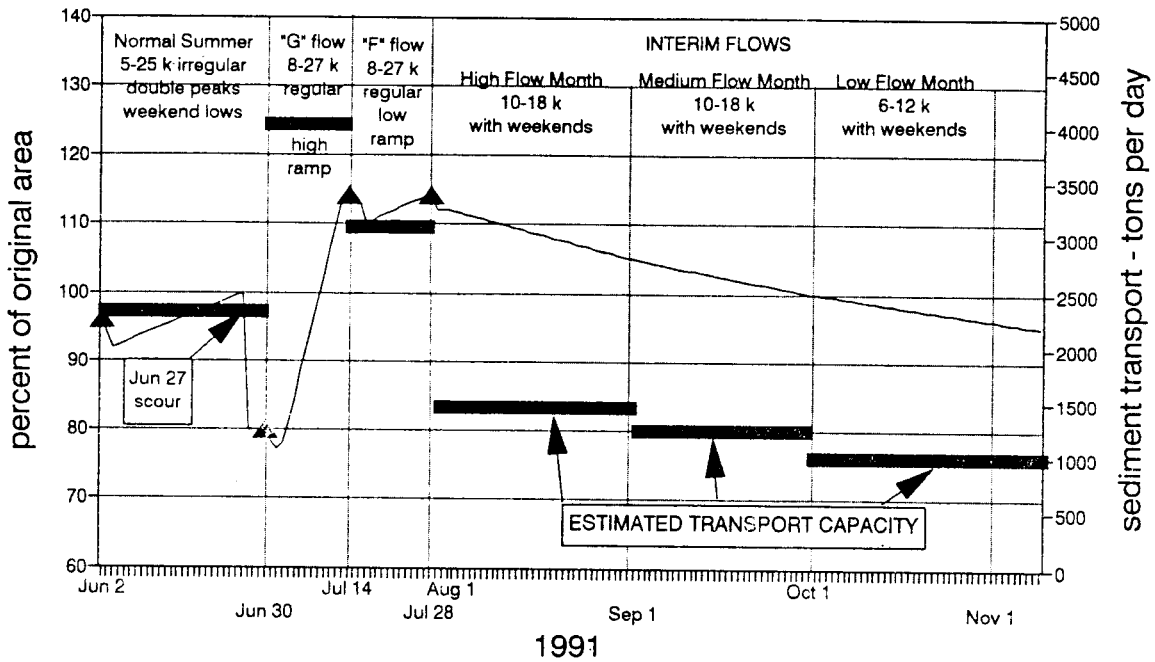
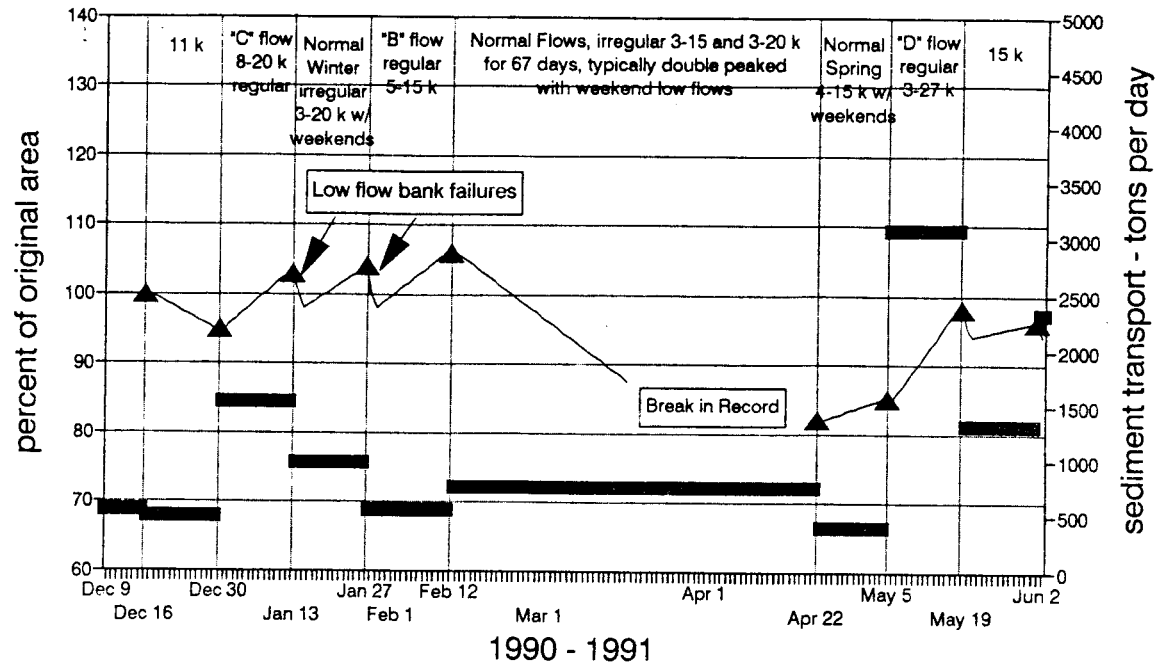


Figure 16a-b. Time-series plots of daily deposit area at CR 211 L.

CR 216 RIGHT



▲ measured area — estimated area ■ sediment transport

Figure 17a-b. Time-series plots of daily deposit area at CR 216 R.



Figure 18a-b. Photographs taken on December 31, 1990(a) and January 14, 1991(b) at CR 211 L. Note erosion of reattachment platform (left center) in lower photograph.



Figure 19. Photograph taken on January 14, 1991, at CR 216 R. Note cut-bank formation along reattachment deposit (right center).

CR 172 LEFT

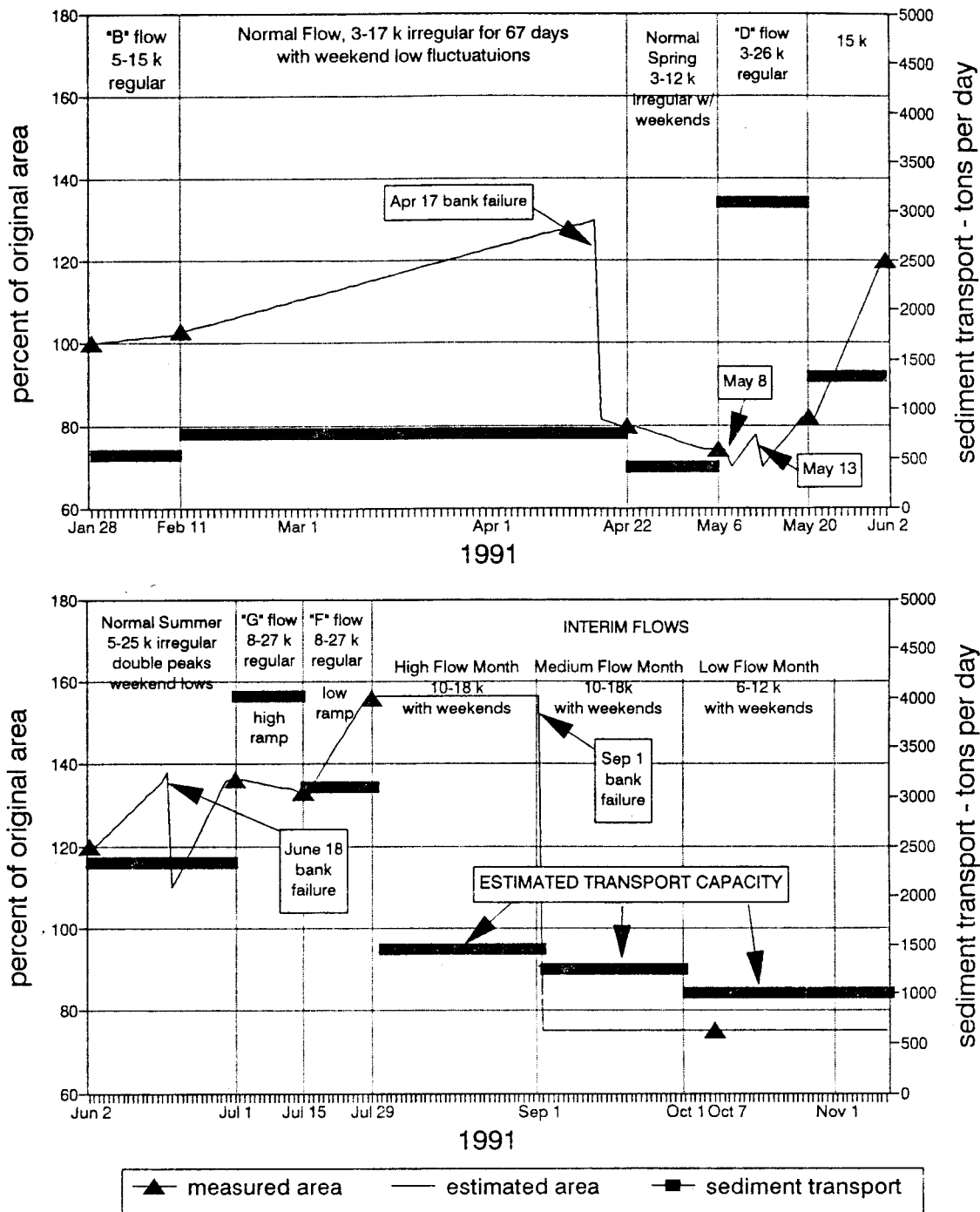


Figure 20a-b. Time-series plots of daily deposit area at CR 172 L.

Normal Flow February 10-April 20, 1991 Gradual deposition occurred at CR 43 L over the lengthy test flow period, resulting in 2% increased area (Fig. 13a). Erosion continued at CR 51 L for the first month of the test period, and record was not obtained for the remainder of the test (Fig. 14a). At CR 68 R, deposition was continuous at rates similar to those of the prior two tests. A break in record between April 13-22 however, apparently missed documenting rapid erosion of about 12% during that period (Fig. 11b). CR 172 L also aggraded during the *Normal Flow* period until on the evening of April 17, during rising river stage, about 30% of the deposit was eroded in 5-6 hours (Fig. 21a-b). This dramatic erosion event was witnessed by the author and others who had been working at the site for 4-days prior. Erosion occurred on the first stage increase following a 3-day low fluctuation "weekend" period (see Appendix I). At CR 211 L, there was a gradual 3% increase in area over the test period (Fig. 16a). CR 216 R was eroding at a high but steady rate for the first half of the test period (Fig. 17a). A break in record occurred during the second half due to battery failure, but the deposit was about 25% smaller at the end of the *Normal* test flow (Fig. 22a-b).

Normal Spring Flow April 20-May 4, 1991 There were no changes in area at CR 43 L (Fig. 13a) or CR 51 L (Fig. 14a) during this test. There was a dramatic increase in size recorded at CR 68 R, approximately 13% increase, bringing the area curve to a point similar to the end of the prior *Normal Flow* response just before rapid erosion occurred (Fig. 11b). CR 172 L eroded gradually during the two-week test period, resulting in about 10% decreased area (Fig. 20a). Rapid deposition occurred at CR 211 L during the same period, with about 10% increased area. CR 216 R increased about 5% over the test period.

"D" Flow May 4-May 18, 1991 CR 43 L increased area slightly during the test, about 1% (Fig. 13a). The "D" test increased the area at CR 51 L about 12%, the first substantial increase since rapid erosion on December 13, 1990 (Fig. 14a). CR 68 R responded wildly to the "D" test, first by erosion of about 17% area between May 6 and 7 (Fig. 23a-b), followed by rapid deposition until May 15. Then between May 15 and 16, about 15% area was eroded within 24-hours (Fig. 24a-b). The first erosion event occurred between the first and second fluctuations of the "D" flow, and the second erosion event occurred during the last fluctuation of the test flow (see Appendix I, May 1991, "D" test flow).

The "D" flow test had similar but less dramatic results at CR 172 L. On May 8, the deposit had eroded about 3% in the past 24-hours. Deposition followed until May 13, when the same area eroded about 7% in the previous 24-hour period. Carpenter et al., this report, documented both erosion events by sudden drops in the stage record of 1.3 meter each during rising river stage. CR 211 L and CR 216 R both responded to the "D" test with high deposition rates (10 and 13% respectively) over the two-week test period (Figs. 16a and 17a).

15,000 ft³/s Constant Flow May 18-June 1, 1991 No area change was measured at CR 43 L during the test period (Fig. 13a), and only minor area increase (1%) was measured at CR 51 L (Fig. 14a). At CR 68 R, the deposits increased area about 5% (Fig. 11b) and at CR 172 L, the deposit increased dramatically (20%, Fig. 20a) in the reattachment platform area (Fig. 25a-b). CR 211 L increased in area steadily by about 2% over the test period (Fig. 16a). CR 216 R also increased in area during the test period, but not enough to overcome the erosion that occurred on the last two days of the prior evaluation period (Fig. 17a).



Figure 21a-b. Photographs taken on April 17(a) and April 20(b), 1991, at CR 172 L. Note erosion of reattachment platform area in lower photograph.

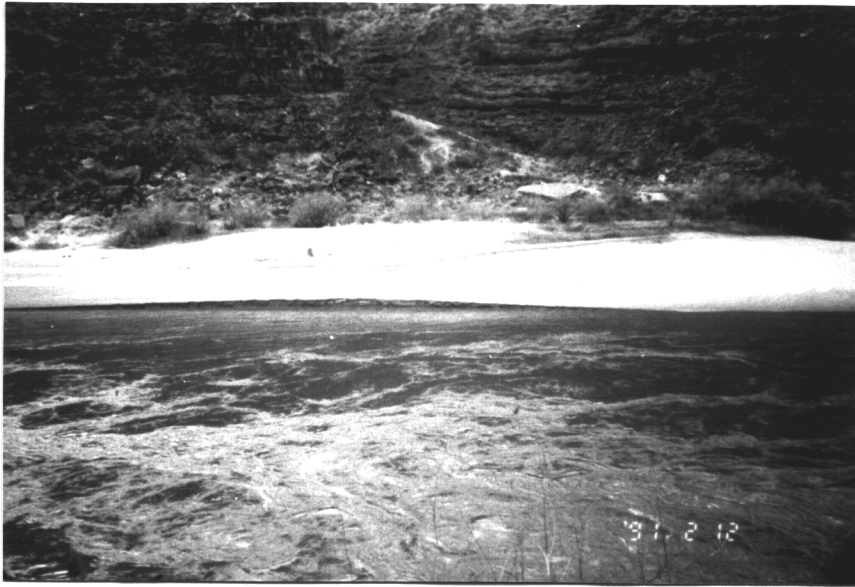


Figure 22a-b. Photographs taken on March 12 and April 22, 1991, at CR 216 R. Note reduction of area along water line in lower photograph.

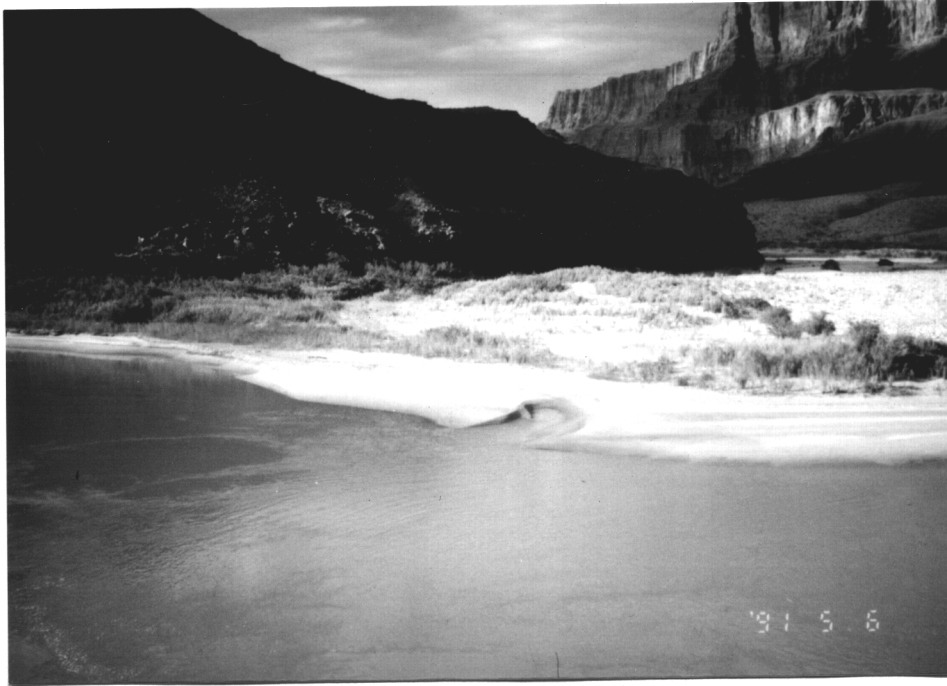


Figure 23a-b. Photographs taken on May 6(a) and 7(b), 1991, at CR 68 R. Note enlargement of return flow area in lower photograph.



Figure 24a-b. Photographs taken on May 15(a) and 16(b), 1991, at CR 68 R. Note enlarged return flow area in lower photograph.

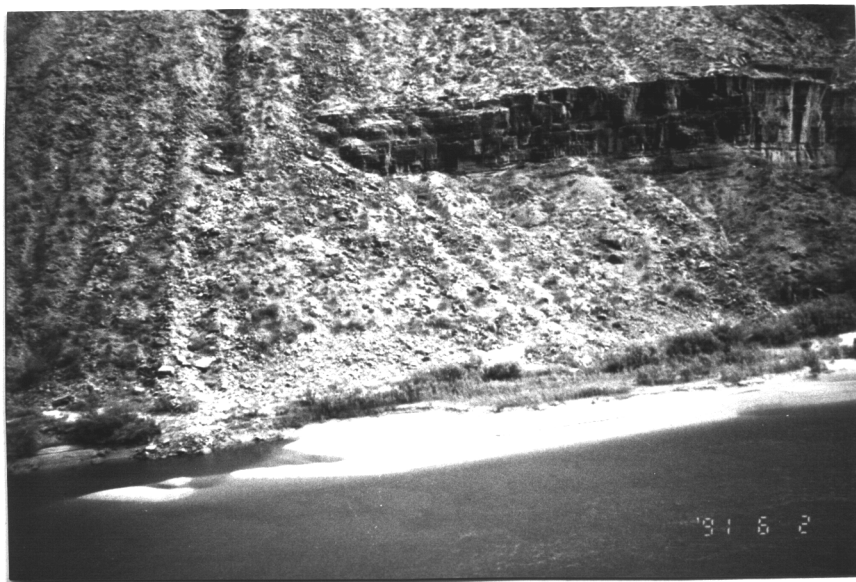


Figure 25a-b. Photographs taken on May 20 and June 2, 1991, at CR 172 L. Note elongated reattachment deposit in lower photograph.

Normal Summer Flow June 1-29, 1991 The *Summer* test flow eroded the deposit at CR 43 L about 7% over the test period (Fig. 13b). This was the highest erosion rate documented at CR 43 L. CR 51 L also eroded at a high rate during the test flow, but a secondary sand wave came into view on June 18, and the deposit increased in area for the remainder of the test as the sand wave migrated further into the recirculation zone (Fig. 14b). Area increased at CR 68 R about 2% (Fig. 11c). The *Summer* test flow produced more dynamic results at the three down river sites. CR 172 L began rapid deposition, about 18% area increase in 16 days, but on June 18, massive erosion reduced the area about 25% (Fig. 26a-b). Rapid deposition resumed at CR 172 L for the remainder of the test flow. At CR 211 L, area increased gradually about 3% over the test period. CR 216 R responded to the test similarly to CR 172 L. Following erosion of the lower deposit toe during the evaluation flow, rapid deposition began. Area increased about 8% in the first 25 days, but between photographs taken on June 26 and 27 (Fig. 27a-b), 20% of the downstream portion of the reattachment deposit had been eroded (Fig. 17b).

"G" Flow June 29-July 13, 1991 Similar small increases in deposit area were measured during the "G" test flow at CR 43 L, CR 51 L, and CR 68 R (Figs. 13b, 14b, and 11c). CR 172 L responded with area reduction of about 5% (Fig. 20b) and CR 211 L eroded at a very high rate of 16% in 11-days (Fig. 16b). The antithetical response was measured at CR 216 R where deposition increased area about 35% (Fig. 17b).

"F" Flow July 13-27, 1991 A mixture of results were measured during the "F" flow test. CR 43 L responded with a rapid area increase of 7% over the 11-day test (Fig. 13b). CR 51 L actually decreased area about 2% (Fig. 14b) and CR 68 R remained constant (Fig. 11c). However, at CR 172 L, deposition increased deposit area by about 20% (Fig. 20b). CR 211 L responded similarly with about 8% area increase, following small cut-bank formation during the preceding 3-day evaluation period (Fig. 16b). CR 216 R experienced cut-bank formation also during the evaluation period, but deposition following resulted in little area change (Fig. 17b).

INTERIM FLOWS

High Flow Month August 1-31, 1991 All sites responded negatively to the first month of reduced-range flows. CR 43 L, CR 51 L, and CR 68 R gradually eroded, at rates of about 3% during the first month (Figs. 13b, 14b, and 11c). Area at CR 172 L remained constant. However, at CR 211 L, about 3% area was eroded between July 30 and 31 (Fig. 16b). Gradual erosion pervaded at CR 216 R, reducing area about 6% during the month-long period.

Medium Flow Month September 1-30, 1991 Gradual erosion continued but at reduced rates at CR 43 L, CR 51 L, and CR 68 R (Figs. 13b, 14b, and 11c). September 1 at CR 172 L was eventful (Fig. 28a-b). Scientists working at that site reported rapid erosion beginning about 5PM, and continuing for about 4 hours. Within 4 hours, the deposit had eroded about 50% (Fig. 20b). The erosion event occurred during a normal daily rise in river stage, but was coincident with local flash flooding of nearby Mohawk Canyon about 1 mile upstream. One scientist reported observing foam suspended on the river surface flowing toward the left bank, impinging upon the deposits, rather than down the center or right of center portion of the channel where main current flow normal exists. Rapid erosion was documented a few days

latter at CR 211 L between photographs taken on September 6 and 7 (Fig. 29a-b). Approximately 10% of the deposit area was eroded within the 24-hour period (Fig. 16b). Gradual erosion continued at CR 216 R (Fig. 17b).

Low Flow Month October 1-31, 1991 Gradual but reduced erosion continued at CR 43 L (Fig. 13b) and CR 51 L became stable (Fig. 14b). CR 68 R continued to respond with gradual erosion (Fig. 11c). The two deposits that experienced rapid erosion events in the prior month appeared stable throughout the **Low Flow Month** (CR 172 L and CR 211 L)(Figs. 20b and 16b). CR 216 R continued to respond with gradual but reduced erosion (Fig. 17b).



Figure 26a-b. Photographs taken on June 18(a) and 19(b), 1991, at CR 172 L. Note erosion of deposit face in lower photograph (right center).



Figure 27a-b. Photographs taken on June 26 and 27, 1991, at CR 216 R. Note erosion of downstream portion of reattachment deposit in lower photograph.

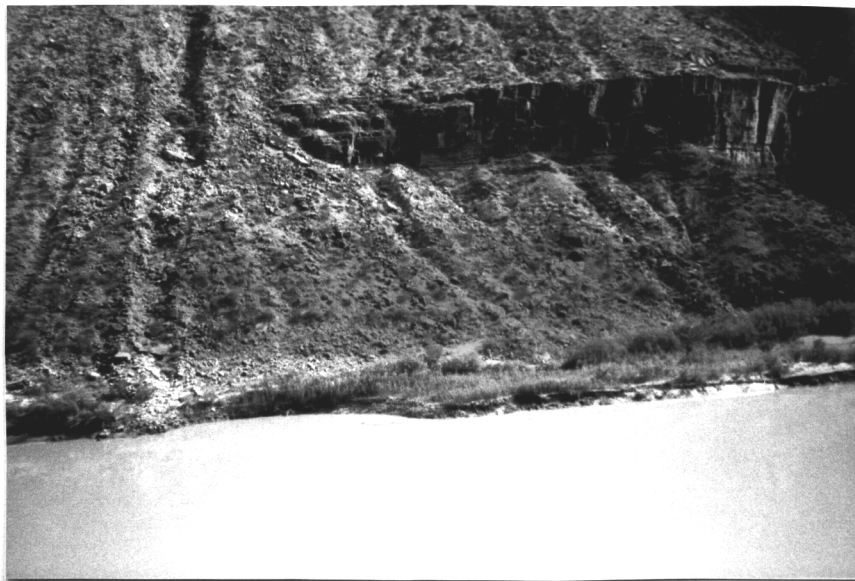


Figure 28a-b. Photographs taken on September 1 and 2, 1991, at CR 172 L. Note erosion of entire reworked portion of deposit in lower photograph.



Figure 29a-b. Photographs taken on September 6 and 7, 1991, at CR 211 L. Note erosion of reattachment deposit platform in lower photograph.

DISCUSSION

It was discovered during the course of this study that sand bars in the Grand Canyon are generally composed of two sections: 1) the static perennial section; and 2) the dynamic ephemeral section along the face of the perennial section (Fig. 30). The ephemeral deposit is a highly reworked zone that absorbs the stresses of daily river stage fluctuations and other changes in flow regime that would otherwise impact the perennial deposit. The ephemeral portion acts as a buffer for the perennial portion. All the dynamic activity documented in this study occurred within the ephemeral section of sand bars. Very rapid erosion and deposition (measurable daily) were documented at most sites. On two occasions, the entire ephemeral deposit at one site was eroded in less than one day, and redeposited in a period of about one week. The ephemeral section varies in size depending on deposit type and environment. At reattachment bars, the whole platform area (Fig. 2) is usually ephemeral. At separation and channel margin deposits, the ephemeral section is usually a narrow band extending the whole length of the deposit. The ephemeral section of deposits is vertically bounded by the high-water line above and extends to some variable and unknown depth toward the main channel.

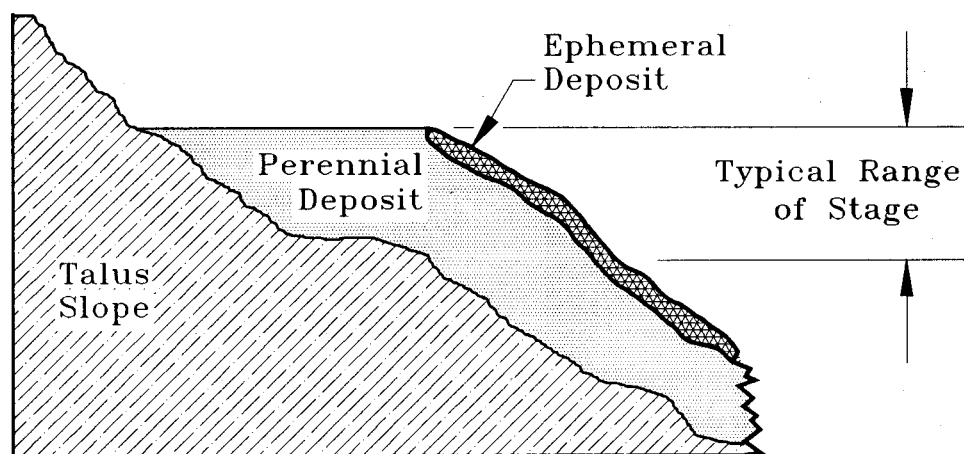


Figure 30. Schematic cross-section of two-part sand bar model. Perennial portion was deposited either before closure of Glen Canyon Dam or during the high releases in the 1980's. It is not usually inundated by flows at power plant capacity. It is often composed of a mixture of sediment sizes, it serves as habitat substrate, recreational area, and stores large volumes of fluvial sediment. The ephemeral portion is highly reworked, with each high flow. It is usually composed of well sorted sand to silt sized material. The ephemeral deposit protects the perennial deposit from erosion processes that occur within the range of power plant capacity. The ephemeral portion extends vertically from the high water line to some unknown depth, and horizontally depending on deposit type and local environment. At reattachment deposits, the whole platform area (Fig. 2) may be ephemeral. At separation and channel margin deposits, the ephemeral deposit is usually a narrow band extending the length of the deposit.

Erosion

Erosion occurred at essentially two rates, gradual and rapid. Gradual erosion rates were observed at all sites under various flow conditions. The predominant erosion events were however, rapid, and often at rates so high that photographs separated by 24-hours showed only the aftermath. These erosion events are called bank failures in this report.

Bank Failures Large-scale erosion occurred on many occasions between photographs that were taken 24 hours apart. The author and others also observed large-scale erosion events on several occasions that affected as much as 1/3 of a sand bar in as little as 3-5 hours. Table 1 summarizes the bank failure events documented in this investigation. Bank failures were observed on slopes with angles ranging from steep to gentle. On steep deposits, bank failures occurred during extended drawdown periods ("weekend" low flows or 3-day evaluation periods), or within 1-2 days following such a period. Bank failures also occurred on steep deposits during regularly fluctuating flows.

On gradually sloped deposits, bank failures were observed that occurred on the rising limb of the river hydrograph. One observation of gentle slope bank failure (from CR 172 L, April 17, 1991) was on a small reattachment platform with about 1 meter relief and slope angle of about 5-10 degrees (see Fig. 21 for before and after photos). During this event, current into the eddy was noticeably stronger than usual, and the direction of flow was directly toward the reattachment platform. The platform was undercut and eroded away within a few hours.

The occurrence of bank failure events on two distinctively different slope angles is explained by a two process model that includes seepage and traction processes (Fig. 31). River stage fluctuation is the driving mechanism for both tractive and seepage processes. In the model, seepage processes occur within the zone of river stage fluctuation, as a result of outward flowing bank water that infiltrated the sand bar during high stage. As river stage recedes, the outward component of flow increases, ultimately resulting in bank failure during descending or lowest river stage (see Carpenter et al., and Budhu, this report).

Traction processes occur over the whole wetted perimeter of the river, predominantly during rising or peak river stage, when the hydraulic gradient is greatest. The model premise is that seemingly minor changes in local river or eddy current velocity or geometry result in redistribution of channel sediments, likely resulting in minor scouring or filling. Any subsequent scouring that occurred at the toe of the fluvial deposit would be translated upslope as subaqueous landslides, and observed at the surface as a bank failure event. Changes depicted here could also develop secondary recirculation vortexes that could reach the surface. Both manifestations of traction could trigger movement along pre-existing seepage induced failure planes, thus obscuring the dominant process in analysis.

Table 1. Chronology of rapid erosion events at sites on the Colorado River. DATE is date of event when timing is known to 2 hours or less, or date of photograph when event appears. TIME QUALITY indicates quality of known timing of event, relevant to corresponding test flow HYDRAULICS. SITE lists Colorado River mile and left or right bank.

DATE	TIME QUALITY	SITE	HYDRAULICS
9/6/90	24 hrs	68 R	Second fluctuation following two days of low flow
9/20/90	24 hrs	68 R	Middle of test flow period, "E"
12/13/90	24 hrs	51 L	Last fluctuation before 3 days of low flow
1/14/91	24 hrs	216 R	Middle of 3 day 5,000 ft ³ /s constant flow
1/28/91	24 hrs	216 R	Middle of 3 day 5,000 ft ³ /s constant flow
4/15/91	24 hrs	68 R	First fluctuation flow 3 days of low flow
4/17/91	¹ 2 hrs	172 L	Rising stage, 1st fluctuation after 3 days of low flow
5/7/91	24 hrs	68 R	Second fluctuation after 3 day low, highest in 90 days, "D"
5/8/91	² 20 min	172 L	ditto
5/13/91	20 min	172 L	Rising stage, middle of "D" flow
5/16/91	24 hrs	68 R	Last fluctuation of high fluctuation "D" flow
5/20/91	24 hrs	216 R	Middle of 3 day 5,000 ft ³ /s constant flow
6/3/91	24 hrs	216 R	Middle of 3 day 5,000 ft ³ /s constant flow
6/18/91	20 min	172 L	First fluctuation following 2 days of low flow
6/27/91	24 hrs	216 R	Middle of high fluctuating flow
7/16/91	24 hrs	211 L	Middle of 3 day 5,000 ft ³ /s constant flow
7/16/91	24 hrs	216 R	Middle of 3 day 5,000 ft ³ /s constant flow
7/17/91	³ 2 hrs	225 R	Rising stage following 3 day 5,000 ft ³ /s low, beginning of "F"
7/29/91	24 hrs	211 L	Middle of 3 day 5,000 ft ³ /s constant flow
7/30/91	24 hrs	216 R	Middle of 3 day 5,000 ft ³ /s constant flow
9/1/91	24 hrs	⁴ 81 L	Last fluctuation in high release interim flow period
9/1/91	20 min	172 L	Rising stage in middle of regular fluctuations
9/7/91	24 hrs	211 L	Second fluctuation following 2 days of low fluctuation flows

¹ All 24 hour data is from author's photographic records.

² 20 minute data is from Carpenter et al., this report.

³ 2 hour data is from anecdotal information related by other observers of events.

⁴ Event at CR 81 L was captured photographically by recently installed time-lapse camera.

Examples of both types of bank failure were documented during this study. The first traction induced bank failure was observed on April 17, 1991, at CR 172 L (Fig. 21). The author and a team of NPS and USGS scientists were instrumenting the site for seepage monitoring when the failure occurred. During the rising stage, about 10 PM on April 17, loud splashing noises were heard coming from upstream. Inspection of the reattachment bar platform area revealed that the deposit was eroding at an alarming rate. Swift current was transporting the eroded material away from the bar as rapidly as the bank collapsed. The current velocity affecting the collapsing bank was estimated to be in excess of 1 meter per second, and was the primary recirculating flow pattern. However, the pattern was directed at a high angle to the deposit, unlike the pattern observed during the prior 4 days. Progressive erosion of the later stages of this bank failure was documented using time-lapse photography (Fig. 32). The event lasted about 4 hours, and approximately 30% of the sand bar was eroded.

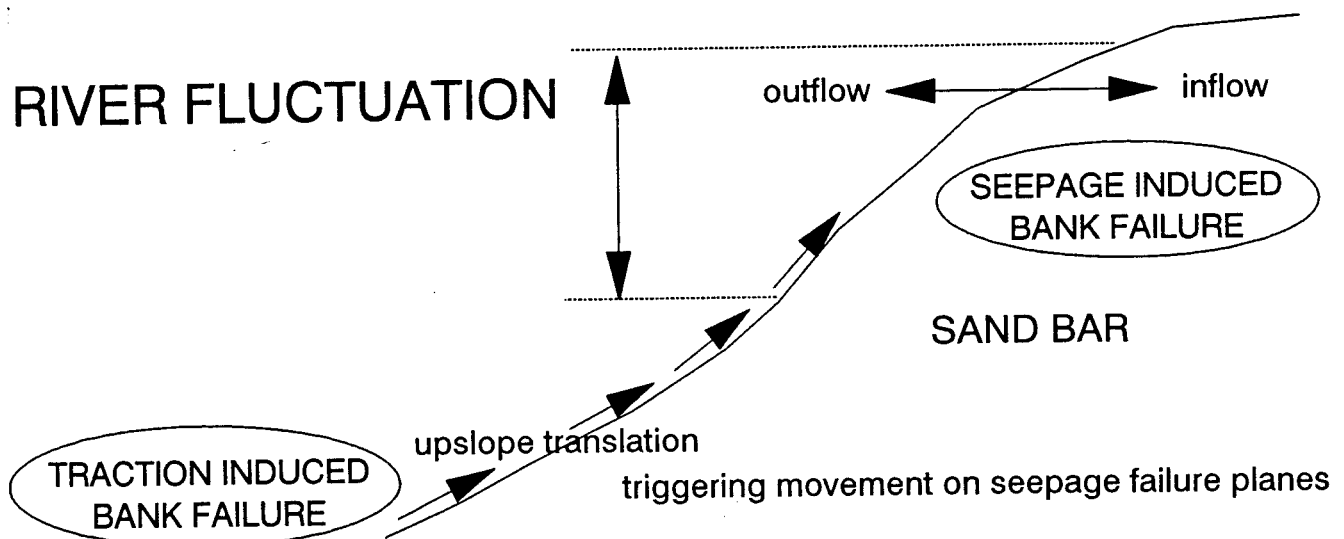


Figure 31. Model of two-process bank failure system. River stage fluctuations drive bank failure processes that result from rising stage and from descending stage. Rising and peak river stages are associated with the greatest hydraulic gradient in the typical daily river fluctuation, resulting in increased turbulence and current velocity. Dynamic activity of channel and eddy-stored sediments would be expected during rising and peak river stage. This is when traction induced bank failure would occur, and translate upslope. As river stage recedes and bottoms out, bank water outflow increases, sometimes resulting in bank failure or development of incipient failure planes (Budhu, this report).



Figure 32. *Time-lapse images of April 17, 1991, bank failure event at the reattachment platform on CR 172 L. First image was taken at 23:59, on April 17, and the second image was taken at 0:29, on April 18.*

Other bank failures occurred at CR 172 L that were documented with land tilt sensors and water column height sensors recording at 20-minute intervals (Carpenter et al., this report), and recorded by daily photography. The most spectacular bank failure event documented in this study occurred at CR 172 L on September 1, 1991. Fortunately, riparian scientists and interested boatmen were camped at the site when erosion began, and they documented their observations. At about 5 PM on September 1, the automatic time-lapse camera took its daily photograph (Fig. 28a). Shortly thereafter, as the river stage began typical rising, the river became very turbid. Local thunderstorm activity had caused Mohawk Canyon (1 mile upstream) to flash flood. The boatmen reported that main channel current was observed across the entire width of the channel, and that their boats were covered with floating foam that was traveling along the left bank, where recirculating eddy current normally exists. Within the next few minutes, massive erosion of the sand bar began, as large blocks of consolidated sediment calved into the current. About 4 hours later, 50-60% of the sand bar had been eroded away (Fig. 28b). Colorado River stage records were checked at the USGS temporary stage recorders above Mohawk Canyon and below, and no measurable evidence of tributary input from Mohawk Canyon can be seen on a 2-week record. This is evidence that the event was caused by a sudden increase in sediment supply (particularly bedload) rather than a sudden increase in river stage. It suggests that main channel and recirculating stream currents can shift rapidly, causing rapid large-scale erosion of river-bank deposits. Although this bank failure event was caused by external processes, this scenario may operate at a smaller scale during daily river stage fluctuations, explaining many of the smaller-scale bank failure events documented. Further investigation is necessary to determine if this process occurs regularly as river stage fluctuates on a daily basis.

Formation of temporary secondary recirculation vortexes may have been documented on several occasions at various sites. For example, the bank failure on December 13, 1990, at CR 51 L appears in aerial photography to be a semi-circular feature (Chapter 7, this report, Fig. A6h). Similar examples were documented with fixed-camera photography at CR 68 R on May 7, 1991, (Fig. 23) May 16, 1991 (Fig. 24) and at CR 216 R on June 27, 1991 (Fig. 27). The contoured, semi-circular shapes suggest that bank failures of this type are caused by newly formed recirculation vortexes that reached the surface and eroded the adjacent sand bar in a characteristic semi-circular pattern. However, it is not known exactly when during the daily fluctuating river stage these features developed. Further information on timing and river conditions are needed to fully understand this process.

Seepage-induced bank failures are most likely to occur on steep deposits during periods of extended low river stage (Budhu, this report). Periods like these occurred often during the study, as 3-day evaluation periods between regular test flows and as "weekend" flows during the "normal" and seasonal test flows. Several bank failure events were documented during this period of time. In fact, half of the 23 events documented in this study (Table 1) were temporally associated with "weekend" or 3-day evaluation flows. Other seepage processes were also documented during these periods, such as seepage rill and tunnel scour development (Howard and McLain, 1988) on steep, newly deposited slopes. An example of seepage-induced bank failure is from CR 172 L, on June 18, 1991 (Fig. 26). Between photographs taken on June 18, and 19, about 25% of the sand bar was eroded. This occurred during the first river stage fluctuation following a 2-day "weekend" low flow, during moderately high river stage fluctuations. The steep, downstream portion of the deposit was eroded, leaving the gentle-angle reattachment platform untouched. This event has been very

closely modeled by a seepage-induced failure model (see Budhu, this report). However, the local river stage sensor record indicates that it dropped about 1.3 meters in 20 minutes during rising river stage about 1-hour after the photograph was taken on June 18, (Carpenter et al., this report). This is probably an example of traction-induced processes triggering seepage-induced incipient failure planes, resulting in bank failure observation during rising river stage.

Deposition

Six out of seven sand bars that sustained rapid erosion events during highly fluctuating flows were subsequently rebuilt to pre-event areas within a few days or weeks. This was documented at CR 68 R in September, 1990 during the "E" test flow. Also at CR 68 R during the "D" test flow in May, 1991, 2 events eroded the bar about 15% each. The first eroded area was rebuilt in 8-days, the second failure occurred 3-days before the "15,000" constant flow test began, and did not recover to pre-event area until the end of the high fluctuation "G" test flow in July, 1991, 60-days later. Similarly, at CR 172 L, two events occurred during the May, 1991, "D" test flow, and both times the bar was rebuilt within 3-days. During the high fluctuation "normal" Summer test flow, the sand bar at CR 216 R eroded about 20% on June 27, 1991. Twelve days later, during the high fluctuation "G" test flow, the area had been completely rebuilt, and 4-days later at the end of "G", the area was 13% larger than before the bank failure event. Following bank failure events, very rapid deposition usually occurred, but only if flow regimes with high river stage followed. During the time between failure and redeposition of the ephemeral deposit, the perennial deposit is exposed to the various erosion processes. Consequently, maintenance of the ephemeral deposits protects the higher, older, vegetated, and recreationally important perennial deposit. This observation indicates that the bank failures documented during the first 3-months of interim flows (August-October, 1991) have exposed the perennial segments of deposits at CR 81 L, CR 172 L, and CR 211 L to erosion forces. It also indicates that those deposits will remain exposed until the river stage raises to normal peak level where the ephemeral segment can be re-deposited.

General

Rapid deposition often lead to instantaneous erosion, or bank failure, indicating over-steepening of newly deposited slopes. Bank failure was usually followed by rapid deposition, provided high river stage followed. This is evidence that sediments may be stored in the local eddy during bank failure. Contrary to this observation is the observation at CR 51 L, where the area of bank failure on December 13, 1990, was not redeposited during subsequent high fluctuation flows (Figs. 14 and 15). This is evidence that sediment from bank failure may not be stored in the local eddy at some sites or under certain conditions. Unless the eddy at CR 51 L behaves uniquely, this suggests that there is greater sediment supply and storage in eddies downstream of the major tributary, the Little Colorado River. Supporting evidence is the much higher dynamic activity observed in the deposits downstream of the Little Colorado River [this report, land surveying (Beus et al., Chapter 6 this report), and aerial photogrammetry (Cluer, Chapter 7 this report)]. Consequently, bank failures in sediment-poor reaches are more critical than in sediment-rich reaches. Further studies should address this observation.

The responses of sand bars to the "normal" flows and the imitation "seasonal" flows (i.e., Normal Summer) were distinctive. For example, there was a marked divergence between the amount of active sand bar area and the net or resulting area during the "normal" flows. Conversely, there was a demonstrated convergence of active area and net area during the regularly fluctuating test flows (Fig. 33). Plots of discharge time-series for each of the GCES-II test releases reveal the basic hydraulic differences between "normal" and regular test flows (Appendix I, this report). The most basic difference is the "weekend" 2-3 day low fluctuation period that was an integral element of each of the "normal" test flows. Figure 33 shows that the number of bank failures increased during periods of "normal" flow and that the active and net area curves diverge simultaneously. This indicates that bank failures were most often observed during "normal" flow periods, in fact "normal" flows resulted in 72% of the bank failures that involved more than 5% area. Regular test flows resulted in 28% of the bank failures that eroded more than 5% area. During the 17 test flows studied, 7 were "normal" and 10 fluctuated regularly. The "normal" flows accounted for 69% of the total erosion and 27% of the total deposition. The regularly fluctuating test flows resulted in 31% of the total erosion and 73% of the total deposition (Fig. 34). During the course of the study, the overall area of the six sand bars increased about 7%.

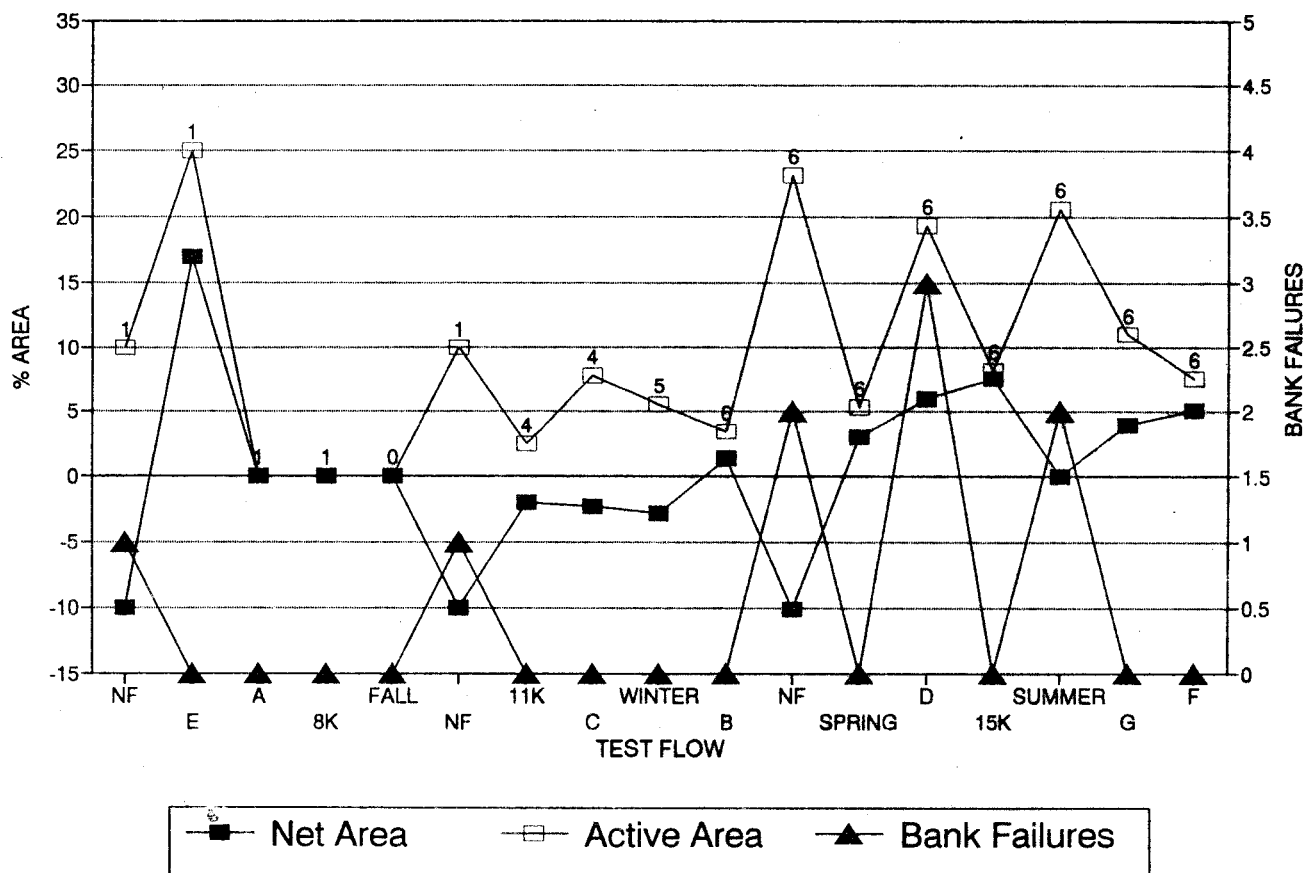


Figure 33. Test flow-series plot of three variables; net area, active area, and number of bank failures. Net area is average resulting area at the end of each test flow. Active area is the average sum of eroded and deposited area during each test flow. Number of bank failures is the average number per test flow.

RANGE OF AREA CHANGE AND NET RESULT

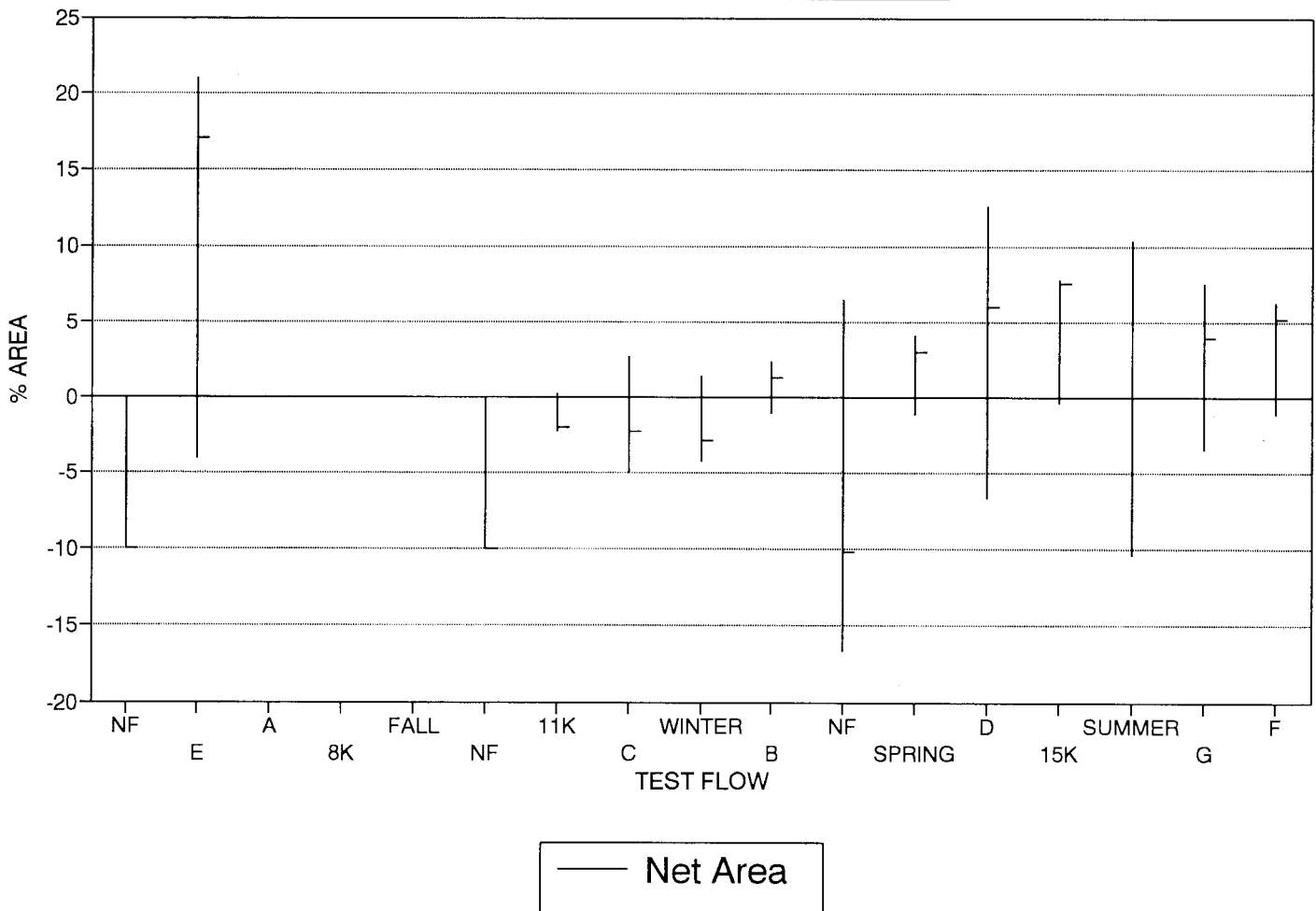


Figure 34. Test flow-series plot of average final (net) area at the end of each test flow and the range of erosion and deposition during the test.

CONCLUSIONS

- 1) Fixed-camera terrestrial photogrammetry was an effective method for monitoring sand bar responses to the test flows from Glen Canyon Dam.
- 2) Sand bars respond daily to changes in flow regime, and the sand bars upstream of the Little Colorado River were less responsive than those downstream.
- 3) There are two parts to Colorado River sand bars, the perennial and ephemeral components. The ephemeral component serves as a protective buffer around the perennial component.
- 4) Bank failures were documented during rising and declining river stages. Declining stage failures are explained by seepage of bank-stored water. Rising stage failures may be caused by deposit scour resulting from increased hydraulic gradient during rising river stage. Future studies should consider this possibility.
- 5) Bank failure is the most erosive process affecting Colorado River sand bars.
- 6) "Weekend" type low flows, a component of "normal" flows, are responsible for the majority of bank failures.
- 7) "Normal" flows, fluctuating irregularly, eroded two-times more river-bank sediment and deposited one-third as much as regularly fluctuating test flows did.

ACKNOWLEDGEMENTS

Many dedicated persons assisted in the development and operation of this project. Film was changed in the fixed-cameras by Mike Kearsley, Teresa Yates, Steve White, Joe Hazel, Chris Dunn, Ken Walters, and others. Other who documented bank failures were Don Bills, USGS-Flagstaff, and Lars Neimi, OARS. Those sharing observations in the field and providing discussions on bank failure processes include Mike Carpenter and Rob Carruth, both USGS-Tuscon, and Rich Inglis and Larry Martin, both NPS-Fort Collins. Jerry Mitchell, Grand Canyon National Park Resources Management, allowed the creative freedom to pursue the project. Earlier manuscripts were thoroughly reviewed by Bill Jackson and Larry Stevens, and their valuable comments have been incorporated in this draft. Finally, special thanks go to the many competent OARS employees who went the extra mile during already long days in the field to ensure that quality results were the rule, not the exception. The contents of this paper the entirely the responsibility of the author.

REFERENCED CITED

- Budhu, M., 1991. A model to predict seepage driven erosion due to transient flow. in Beus, S.S. and Avery, C.C., eds., The influence of variable discharge regimes on Colorado River sand bars below Glen Canyon Dam: 1992 Quarterly Report.
- Carpenter, M.C., et al., 1992. Hydrogeology of beaches 43.1L and 172.3L and the implications on flow alternatives along the Colorado River in the Grand Canyon. in Beus, S.S., and Avery, C.C., 1992. The influence of variable discharge regimes on Colorado River sand bars below Glen Canyon Dam: 1992 Quarterly Report.
- Howard, A.D., and McLain, C.F., III, 1988. Erosion of cohesionless sediment by groundwater seepage. *Water Resources Research*, v.24, n.10, p.1659-1674.
- Schmidt, J.C., and Graf, J.B., 1988. Aggradation and degradation of alluvial sand deposits 1965 to 1986, Colorado River, Grand Canyon National Park, Arizona. U.S. Geological Survey, Open-File Report 87-555.

CHAPTER 6

**THE INFLUENCE OF VARIABLE DISCHARGE REGIMES ON
COLORADO RIVER SAND BARS BELOW GLEN CANYON DAM:
FINAL REPORT**

PRINCIPAL INVESTIGATORS:

STANLEY S. BEUS AND CHARLES C. AVERY

NORTHERN ARIZONA UNIVERSITY

WITH CONTRIBUTIONS FROM:

L. STEVENS AND B. CLUER

(NPS-RMD, GRAND CANYON, ARIZONA)

AND

**M. KAPLINSKI, P. ANDERSON, J. BENNETT, C. BROD, J. HAZEL, M. GONZALES, H. MAYES,
F. PROTIVA AND J. COURSON**

(NORTHERN ARIZONA UNIVERSITY GEOLOGY DEPARTMENT, FLAGSTAFF, AZ)

TABLE OF CONTENTS

LIST OF TABLES	i
LIST OF FIGURES	ii
ABSTRACT	iii
INTRODUCTION	1
Problem Statement	1
Objectives	1
METHODS AND SCOPE	2
Study Sites	2
Field Data Collection	4
Response Variables	4
Survey Precision and Accuracy	8
RESULTS AND DISCUSSION	11
Variability Between Sand Bars	11
Effects of Test Flows on Sand Bars	49
Factors Responsible for Sand Bar Change	53
Multiple Stepwise Regression Analysis	55
Future Monitoring	57
SUMMARY OF OBSERVATIONS	58
CONCLUSIONS	59
ACKNOWLEDGEMENTS	60
LITERATURE CITED	61

LIST OF TABLES

Table 1. Sand bar study sites on which topographic survey, net volume change and other data were collected.

Table 2. Summary of survey precision and accuracy results at Mile 45L.

Table 3. Compilation of sand bar survey data and volume plots for 29 sand bars.

Table 4. Summary of Table 3. The values in each column represent the percent HAZ volume change rate/d for each study site. Estimated sediment contributions (mt/d) from the Paria and Little Colorado Rivers are provided at the end of the table.

Table 5. An evaluation of the relative stability of 29 sand bars during the test flow period.

LIST OF FIGURES

- Figure 1. Map showing study locations, Colorado River corridor, Arizona.
- Figure 2. Sample topographic map of the 43L mile site.
- Figure 3. Selected beach profiles of the 43L mile site.
- Figure 4. Examples of sand bars having different volume to area relationships.
- Figure 5. Daily repeated surveys of the Mile 45 reattachment sand bar during May, 1991.
- Figure 6. Net HAZ volume change occurring from Oct. 26, 1990 to July 30, 1991 in relation to distance downstream from Lees Ferry, AZ.
- Figure 7. Average percent HAZ volume change/day for 29 Colorado River study sites as a function of distance downstream from Lees Ferry, Arizona.
- Figure 8. Average percent HAZ volume change/day for 29 Colorado River study sites, and average daily tributary sediment input rate (mt/d) from the Paria and Little Colorado Rivers from September, 1990 through July, 1991 (Julian Day 250 = Sept. 7, 1990; Julian Day 577 = July 31, 1991).
- Figure 9. Average percent HAZ volume change/day above the Little Colorado River, and average daily tributary sediment input rate (mt/d) from the Paria River, from September, 1990 through July, 1991 (Julian Day 250 = Sept. 7, 1990; Julian Day 577 = July 31, 1991).
- Figure 10. Average percent HAZ volume change/day for 17 study sites below the Little Colorado River confluence (Mile 61), and mean total sediment input rate (mt/d) from the Paria and Little Colorado rivers, from September, 1990 through July, 1991.
- Figure 11. Average percent HAZ volume change/day and estimated sediment transport capacity from September, 1990 through July, 1991.
- Figure 12. Relationship between HAZ percent volume change rate/d (%VCR), lagged %VCR and estimated sediment transport capacity for 29 sand bars from September, 1990 through July, 1991.

ABSTRACT

This study involved evaluation of the effects of 16 experimental discharge test from Glen Canyon Dam on sand bars along the Colorado River in Glen and Grand canyons, Arizona. This series of test flows was designed by the Bureau of Reclamation's Glen Canyon Environmental Studies Phase II (GCES-II) program to bracket the range of discharge parameters that comprise normal dam operations. We collected and analyzed ground-based topographic and bathymetric survey data from 33 sand bars during test flows from September, 1990 through July, 1991. These results may be useful for the GCES-II/ EIS process and for the testing of sediment transport models under development in long-term studies by the U.S. Geological Survey.

Fluctuating discharges from Glen Canyon Dam affected the geomorphology and stability of downstream sediment deposits in Glen and Grand Canyons during the GCES-II test flows. Changes in topography, volume and area occurred on sand bar faces in what we termed the "hydrologically active zone" (HAZ), lying between 142 and 900 m³/sec stage elevations. HAZ volume change rate (%VCR) and HAZ areal change rates varied on a bi-weekly basis between the 29 study sites for which sufficient data were available and between the 16 test flows. From late summer, 1990 through July, 1991, three bars (10.3%) sustained significant net losses of HAZ sand, eleven bars (37.9%) remained relatively unchanged, and 15 bars (51.7%) gained sand. The 29 sand bars under study sustained a mean aggradation of 2.9% by volume (s.e. = 2.6%) between 27 October, 1990 (the first run for which survey coverage was virtually complete) and 31 July, 1991. During that period the total 87,435 m³ of HAZ sand under study decreased by 1,034 m³ (1.2%) because several large losses occurred at a few sites, in contrast with the general condition of near-equilibrium observed on most sites.

Factors influencing sand bar stability included geomorphic setting, distance downstream, season, recreational use intensity and flow regime parameters. Although mean %VCR was approximately equal between reattachment and separation bars (mean %VCR = 0.040 and 0.037 percent/d, respectively), the standard deviation on 13 reattachment bars was 0.072 percent/d, one third greater than that of separation bars (0.054 percent/d). This finding supports the assertion that reattachment bars are less stable than separation bars. Bar instability increased with distance downstream from Glen Canyon Dam, perhaps attributable to sediment supply. Fall and winter flows in 1990-1991 were generally erosive, whereas some spring and summer flows were aggradational; however, this seasonality effect may also reflect sediment contribution by tributaries. Recreational use intensity was not significantly correlated with sand bar erosion or aggradation.

Constant and controlled low-fluctuation test flows resulted in little change or in degradation. Three of five regular, high-fluctuation flows of short duration resulted in system-wide aggradation of HAZ sand volume, while two such flows resulted in system-wide degradation. Each of the three constant flow tests resulted in stable or slight net erosion of HAZ sand volume.

Aggradational events were correlated with regular, highly fluctuating flows coupled with significant tributary sediment input. High stage levels (larger fluctuations) were required to deliver sand to higher elevations. Aggradation was observed following three of the five high-fluctuation flows ("E", "D" and normal summer in June, 1991), whereas one of the high fluctuation flows ("G" in 1991) was strongly degradational and the other ("F" in 1991) resulted in little net change. Two of the three aggradational flows were associated with significant sediment input from tributaries; however, the normal summer, 1991 flow was not associated with sediment input. In addition, two minor aggradational flows ("Normal Fall" in 1990, and "C" in 1991) were associated with minor pulses of sediment input.

Antecedent conditions exerted an important influence over subsequent %VCR under daily fluctuating flow regimes. A significant pattern of cyclic aggradation and degradation characterized these sand bars. Periods of aggradation tended to be followed by periods of degradation, particularly when large-fluctuation flows were followed by low-fluctuation or constant flows.

INTRODUCTION

Problem Statement

Regulated flow from Glen Canyon Dam influences the stability and dynamics of fine-grained alluvial deposits in Glen and Grand canyons (Howard and Dolan 1981; Beus et al. 1985; Webb et al. 1987; Rubin et al. 1990; Schmidt and Graf 1990; Water Science Technology Board 1991). Fine-grained sediments tend to accumulate in areas of reduced velocity in the Colorado River corridor below Glen Canyon Dam, particularly in recirculation zones associated with channel constrictions (Schmidt and Graf 1990). Recent public concern stimulated the Bureau of Reclamation to conduct an environmental assessment and, most recently, an Environmental Impact Statement analysis, to determine whether and how dam operations influence sand bar dynamics.

The purpose of this study was to determine how the Bureau of Reclamation's Glen Canyon Environmental Studies Phase II (GCES-II) test flows affected sand bars along the Colorado River downstream from Glen Canyon Dam. Present knowledge of fluvial sand bar dynamics (aggradation, degradation, and rates of change) and stability (morphologic continuity) in the Colorado River downstream from Glen Canyon Dam is based on sporadic profile surveys of 30 sand bars since 1973, and occasional aerial photography since 1965 (Howard 1975; Howard and Dolan 1981; Beus et al. 1984 et subsequent; Zink 1989; Schmidt and Graf 1990; Schmidt 1989 and this report). These previous studies documented slight to significant erosion of sand bars under the post-dam fluctuating flow regimes. Aggradation was reported for some deposits and degradation of others under the high flows of 1983-1986, with both prior and subsequent erosion. Erosional patterns are obscured by variability in reach characteristics, local channel geometry, poorly developed stage/discharge relationships, unknown antecedent conditions, and unknown survey accuracy. Additionally, the historic study sites are heavily used campsites by river runners and therefore may not be representative of system-wide sand bar conditions. Schmidt and Graf (1990) suggested that sand bars typically used as campsites were an unusually stable subset of the entire population of sand bars.

Under the auspices of the Bureau of Reclamation's Glen Canyon Environmental Studies program and the Glen Canyon Dam Environmental Impact Statement, the National Park Service, Northern Arizona University and the U.S. Geological Survey have undertaken a study of short-term sand bar dynamics in the Grand Canyon. The Bureau of Reclamation conducted a series of 11-day test flows in 1990-1991 to determine the impacts of specific dam operations on downstream resources (Appendix I, this report). These test flows provided an ideal opportunity to collect data and test hypotheses relating sand bar responses to flow regimes. The present study was designed to document volumetric and areal changes on representative sand bars through the test flow series from September, 1990 through July, 1991, and evaluate survey data and several possible mechanisms influencing sand bar dynamics. This report summarizes the large-scale patterns found during this period of study. This study was designed to serve in short-term management decision making until completion of long-term sediment transport models by the U.S. Geological Survey.

Objectives

The research objectives of this project were to statistically evaluate the effects of GCES-II experimental flow test regimes on sand bar stability in the Colorado River corridor downstream from Glen Canyon Dam. Specifically we investigated:

1. The effect of discharge parameters (magnitude, range of daily fluctuation, and ramping rate) on sand bar volume and area changes.
2. The effect of estimated sediment transport potential of test flows on sand bar dynamics.

3. The effects of normal dam operations on sand bars.
4. The effects of constant flows on sand bars.
5. The effects of various other flow regimes on sand bars.
6. The relationship between sand bar dynamics and distance downstream from Glen Canyon Dam.
7. The relationship between sand bar dynamics and seasonality.
8. The surveying and data analysis protocol suitable for long-range monitoring.

Study Assumptions

The GCES-II test flow program was designed to distinguish the optimal flow criteria for sand bar maintenance from a wide array of alternative discharge regimes. Several initial assumptions were made regarding these test flows:

- 1) A 14-day test flow duration could generate a measureable topographic change in sand bar volume. Survey precision studies suggested that surveys were capable of detecting changes greater than approximately 0.2 percent/day for the HAZ. Changes of this magnitude were encountered regularly, thus a 14-day test flow duration was capable of generating measureable change.
- 2) Measureable changes in HAZ sand bar volumes were attributable to test flow parameters and not the intervening, three day "constant 141 m³/sec" evaluation flows or other factors. This assumption was tested during the daily repeated surveys at Mile 45 (below). A bank failure event on the reattachment bar was associated with a "constant 141.5 m³/sec" evaluation period, while aggradation may have occurred during the following "D"(high-fluctuations) test flow period.
- 3) Hydrologic characteristics of test flows from Glen Canyon Dam were consistent relative to each other through the Grand Canyon. We clearly recognize that discharge parameters change over distance downstream from Glen Canyon Dam. We obtained hydrographic information on the GCES-II test flows from the Bureau of Reclamation and the U.S. Geological Survey and these are compiled in Appendix I (this report). Relative differences between test flows were detected at different gaging stations downstream for most parameters, although up-ramping rate may be an exception. The translation of flow parameters over distance are being described by the U.S. Geological Survey, and we anticipate incorporating these flow translation analyses to the patterns observed in this study.

METHODS AND SCOPE

Study sites

Thirty-three fine-grained alluvial deposits (sand bars) were selected for repeated surveys of bar topography through the GCES-II test flow series (Figure 1). This set of sand bars comprises approximately 15% of the 219 major sand bars between Glen Canyon Dam and Diamond Creek (Kearsley and Warren 1992) and is believed to be representative of the kinds of sand bar found throughout the river corridor. Twenty-nine of the 33 sand bars were surveyed with sufficient consistency to provide useful comparative information on GCES test flow effects. Survey data are available from the four sites omitted here, but are not included in this analysis. Sand bars were selected on the basis of: (1) distribution throughout the geomorphic reaches identified by Schmidt and Graf (1990); (2) sufficient size to guarantee persistence through the period of study; (3) geomorphic diversity within and between

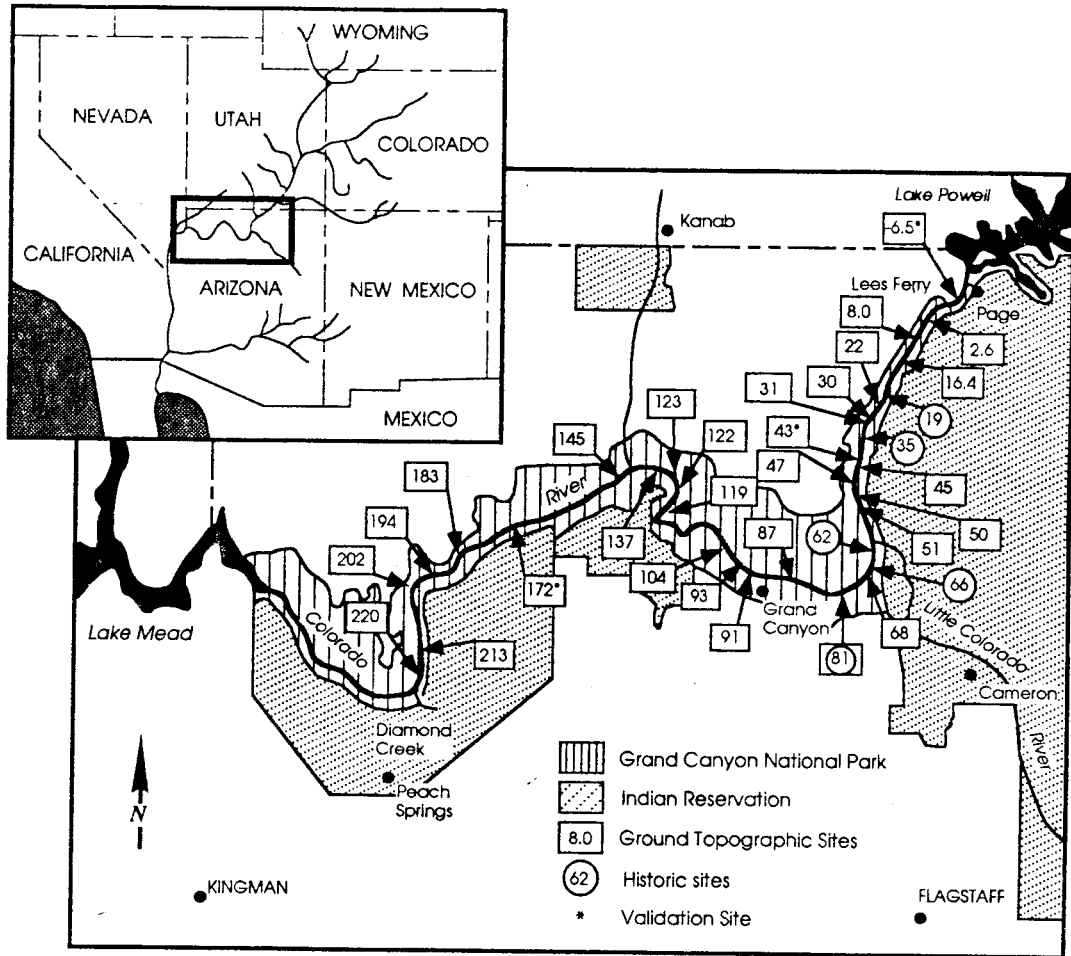


Figure 1. Map showing study locations, Colorado River corridor, Arizona.

sites (separation and reattachment bars, with or without return current channels); (4) availability of historical topographic data; (5) variation in recreational use intensity and vegetation cover (Howard and Dolan 1981; Beus et al. 1984 and subsequently; Schmidt and Graf 1990). Site selection, baseline surveys, and protocol development were accomplished during June and August, 1990. Study sites (sand bars) were named on the basis of river mile from Lees Ferry, Arizona. General descriptions of study sites, metric conversions of site names (river mile to river kilometer), are provided in Table 1. One of the 29 sand bars (Mile-6) was located above Lees Ferry. Eleven of the 29 sand bars were situated between the Paria and Little Colorado River confluences, a reach supplied with largely from the Paria River. Seventeen sand bars were located between the Little Colorado River and Diamond Creek, and receive sediment from the Paria, Little Colorado River and other tributaries. Survey runs were designated "A" through "V" and corresponded to test flows "A" through "G", with "N" denoting normal dam operations periods. Unconstrained releases were called normal flows. These study sites appear to be representative of the kinds of sand bars downstream from Glen Canyon Dam and can, as a group, be used to characterize system-wide responses of sand bars to flow regimes.

Field Data Collection

Following each 11-day GCES test flow, discharge was reduced to a constant $141.5 \text{ m}^3/\text{s}$ (5,000 cfs) for three days to allow evaluation of test flow effects. During these 17 evaluation periods, four motorized craft, each with a six-person survey crew, were positioned throughout the canyon at river miles -10, 43, 91, and 145. Individual survey crews consisted of a foreman, a surveyor/instrument operator, a data entry assistant, a rodman, a depthfinder operator and a boat alignment assistant. Using Lietz SET and SET 4C electronic total stations, data collectors and printers, the six-person crews surveyed subaerial topography on two to three sand bars per day, for a total of approximately eight sand bars per crew during the three days of low water.

In addition to ground surveying, bathymetric surveys of the subaqueous zone (water's edge to the shear zone (eddy/current interface) were conducted using a Lowrance X-16 depthfinder mounted on the raft. Sonar profiles were located by attaching one end of a metered cable to the transducer mount on the boat and locating a survey assistant with a cable/reel system on the beach at a surveyed point along the longitudinal beach profile. Two points along the beach were marked and used to guide the boat along the proper azimuth. Distances from the cable operators location to the boat were recorded every two meters and corresponded to fiducial marks on the analog sonar recording. Coordinates of individual depth and distance were obtained by calculating offsets along the azimuth of the profile based on the surveyed location of the cable reel operator. Elevations of the bathymetry points were calculated by subtracting the sonar depths from surveyed water's edge elevations. The sonar equipment was calibrated daily to control for changes in the suspended sediment load.

Surveying protocol was developed and documented according to standard practices for ground surveying. Benchmark and backsight relationships were verified on all sites during mid-March, 1991. Upon completion of a survey run, field data were transferred to micro-computers and edited. Preliminary maps were made that combined ground and bathymetric surveys to detect anomalous survey points using SOKKIA/LIETZ mapping software. Survey and bathymetric data were modeled using triangular irregular networks to produce topographic contour maps for each sand bar (e.g. Figures 2, 3). Site photographs were repeated at each site from camera stations established during the baseline surveys. Beginning in September, 1990, as many as 33 sand bars were surveyed during each of the three-day evaluation-flows, for a total of 561 surveys.

Response Variables

For each sand bar a specific area was defined as the "hydrologically active zone" (HAZ), a zone directly affected by fluctuating dam releases (Figure 2), and lying above the permanently wetted "bathymetric

Table 1: Sandbar study sites on which historic, topographic volumetric data surveys, and/or fixed camera data were collected. Distance downstream from Lees Ferry, Arizona, after Stevens (1983). Deposit types after Schmidt and Graf (1990): R - reattachment deposit, S - separation deposit, UP - upper pool deposit. Relative recreational use intensity data from interviews with 36 commercial river guides: 1 (no use) to 5 (high use). Weighting values applied to recreational use indices: 1 for winter, 2 for spring and fall, and 3 for summer. Reach (0-11) and channel width (W - wide, N - narrow) after Schmidt and Graf (1990).

RIVER MILE/SIDE (RIVERKM)	SITE NAME	DEPOSIT TYPE	REACH/ RELATIVE WIDTH	RELATIVE RECREATIONAL USE INTENSITY	TOTAL VOLUMETRIC CHANGE (m ³) (10/90 -7/92)
-10.5R (-16.8)	---	R	0 W	Moderate	NA
v** -6.5R (-10.5)	Hidden Sloughs	R	0 W	Moderate	-20
vh* 2.6L (4.2)	---	R	1 W	2.4	+403
vh 8.0L (12.9)	Lower Jackass Cyn.	S	1 W	4.2	-50
v 16.4L (26.4)	Lower Hot Nana	S	2 N	3.5	-116
h 19.0L (30.6)	Opposite 19-Mile Cyn.	R	2 N	Moderate	NA
v* 22.0R (35.1)	---	R	2 N	1.6	+157
v 30.0R (48.3)	---	R	3 N	3.3	+52
vh 31.2R (50.2)	Lower South Canyon	R	3 N	4.5	+46
33.0L (53.2)	Redwall	R	3 N	High	NA
h 34.7L (55.8)	Nautiloid Canyon	S	3 N	High	NA
vh**43.0L (69.3)	Anasazi Bridge	R/UP	4 W	2.7	-38
vh* 45.0L (71.6)	Eminence Break	S	4 W	3.6	+349
vh* 47.0R (75.8)	Lower Saddle Cyn.	R	4 W	4.6	-530
v 50.0R (80.5)	Dino	S	4 W	3.2	+65
vh* 51.0L (82.9)	---	R	4 W	1.9	-1853
h 61.7R (99.3)	Lower LCR Confl.	S	5 W	Moderate	NA
h 65.5L (105.4)	Tanner Mine	S	5 W	Moderate	NA
v* 68.0R (109.6)	Upper Tanner	R/UP	5 W	3.0	-104
vh* 81.1L (130.5)	Upper Grapevine	R/S	6 N	4.5	+168
v 87.5L (140.8)	Upper Cremation	R/UP	6 N	4.7	-2
v 91.1R (146.6)	Upper Trinity	S	6 N	3.2	+59
vh 93.0L (149.6)	Upper Granite	R/UP	6 N	4.7	-74
98.0R (157.7)	Middle Crystal	R/UP	6 N	4.3	NA
v 103.9R (167.2)	Upper 104 Mile	R/UP	6 N	3.1	+32
v 119.0R (191.5)	---	R	7 N	3.6	+825
vh 122.1R (196.5)	---	R	7 N	3.3	+7
vh 122.8L (197.6)	Upper Forester	R/UP	7 N	3.1	-114
v 137.0L (220.4)	Middle Ponchos	R	8 N	4.6	+268
139.0R (223.7)	Upper Fishtail	R/UP	8 N	2.8	NA
v 145.0L (223.3)	---	R	9 N	2.5	+125
vh*172.0L (276.9)	---	R/UP	10 W	2.0	-109
v 183.5R (295.3)	---	R/UP	10 W	3.4	+81
vh 194.1L (312.3)	---	R/UP	10 W	3.1	+14
vh 202.0R (325.0)	202 Mile	S	10 W	3.4	+182
vh 213.0L (342.7)	Pumpkin Spring	R/UP	10 W	4.0	-929
vh 219.9R (353.8)	Middle 220-Mile	S/UP	11 N	4.5	+72
225.3R (362.5)	---	R/UP	11 N	1.6	NA

* Sites for which QA/QC data have been compiled and analyzed

** Bankstored groundwater/seepage erosion model validation sites

h Sites used in historic analyses of sandbar changes

v Sites for which volumetric measurements were analyzed

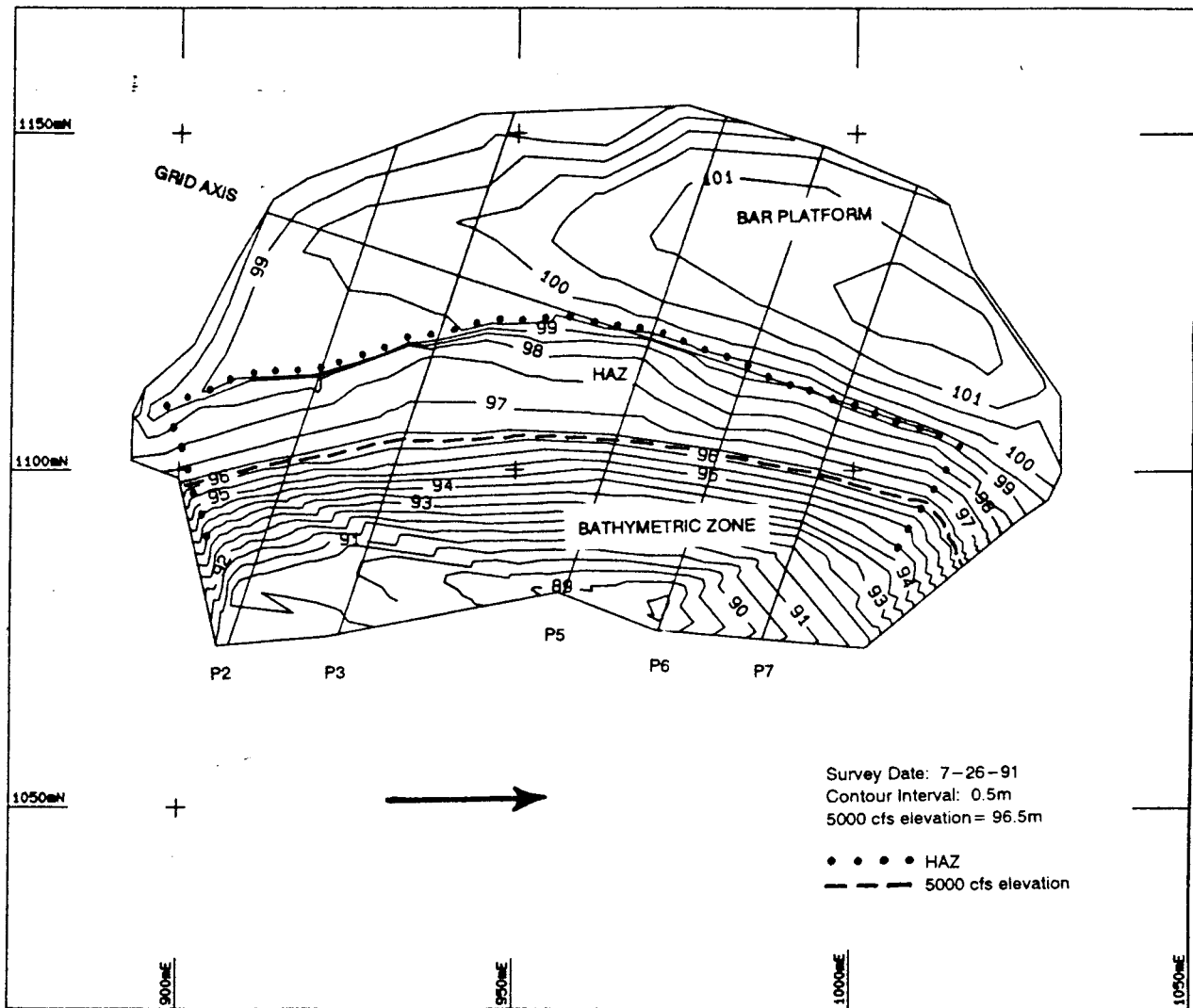


Figure 2. Sample topographic map of the 43L mile site.

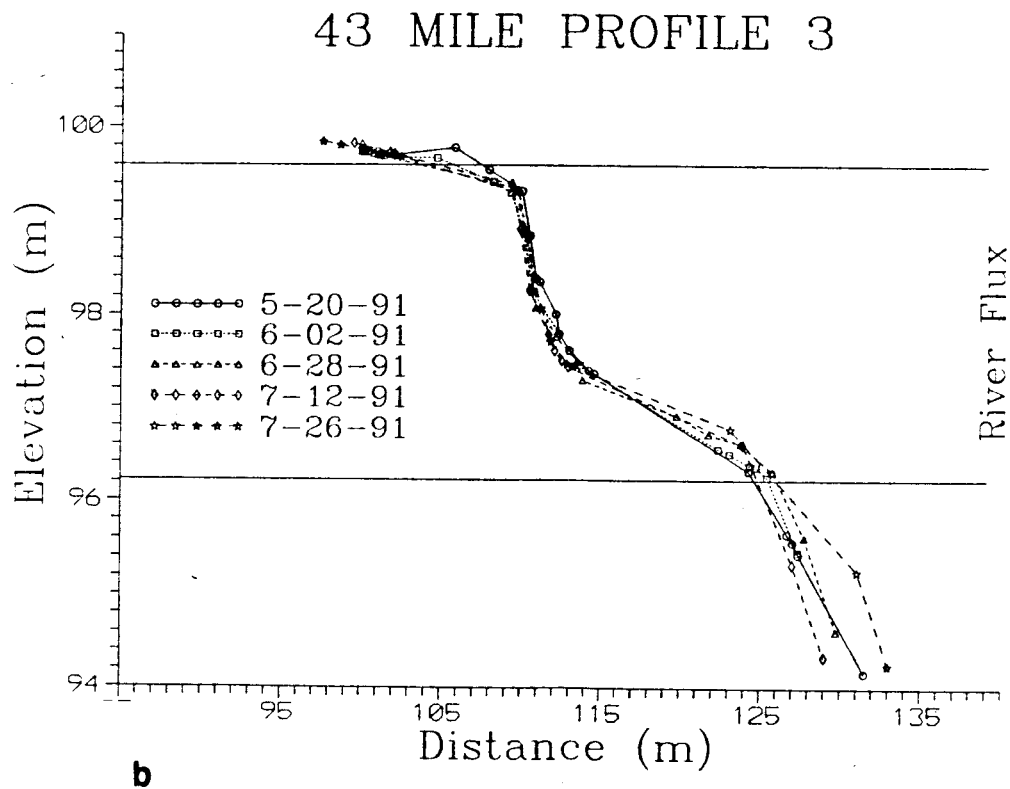
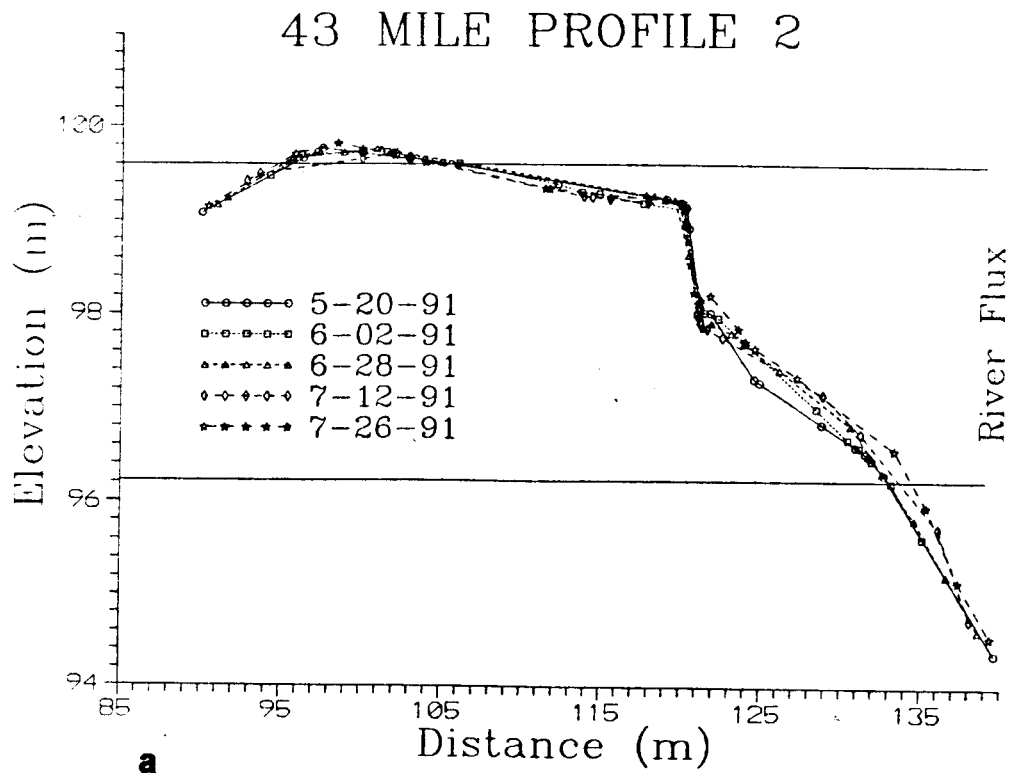


Figure 3. Selected beach profiles at a) P2 and b) P3 from 43L mile site (Figure 2) from runs R-V, spring and summer, 1991. River flux is the hydrologically active zone (HAZ) from the 5,000 cfs flow level to about 28,000 cfs flow level. Profile data below the river flux zone obtained by integrated bathymetric analysis.

zone." The HAZ lay within the area of survey coverage and between the discharge range of normal dam operations (141.5 m³/sec and 900 m³/sec stage elevations), and was therefore the zone most likely to change in response to dam operations. An examination of six sand bars showed that the HAZ occupied 15 to 50 percent of the total area of the sand bar. Sand volume and area were calculated within the HAZ. The percent volume change rate per day (%VCR) was calculated between each survey run by dividing the volume difference between successive runs with the volume of the previous survey:

$$\%VCR_i = \{-100 * [(V_{Tx} - V_{Tx+1}) / V_{Tx}]\} / D$$

where %VCR is the percent volume change rate per day for sand bar *i*, V_{Tx} is the HAZ volume of sand bar *i* at time *x*, V_{Tx+1} is the volume of sand bar *i* at time *x+1*, and *D* is the number of days between time *x* and time *x+1*. One longitudinal and five normal cross sections that corresponded to profiles staked during the field survey were generated from the modeled surface. Field and analysis procedures were approved by Charles W. Dryden, PE, RLS (Arizona Engineering, Inc., Flagstaff, AZ).

The area of sand bars is of considerable importance to managers concerned with campsite availability and riparian habitat; however, we considered HAZ volume (m³) to be a better primary response variable for evaluating sand bar change. Although planimetric area (m²) is commonly employed as a response variable, we reasoned that areal measurement may become less reliable for estimating change on sand bars with steeply sloping faces. The correlation between HAZ volume and corresponding HAZ area for all study sites and test flows was:

$$V = 1.149A + 382.770$$

where *V* = HAZ volume (m³) and *A* = area (m²). This correlation was highly significant but was somewhat variable ($R^2 = 0.843$; $F = 2334.896$, $p < 0.0001$, $df = 1,434$). Because the HAZ represented 15 to 50 percent of the sand bars under study here, this correlation typically represents a substantial portion of HAZ area. The variation in correlation between volume and area was attributable to irregularities in sand bar morphology. For example, Mile 43L sand bar was flat with a steep face, whereas the Mile 51L bar was broad with a gently sloping face (Figure 4).

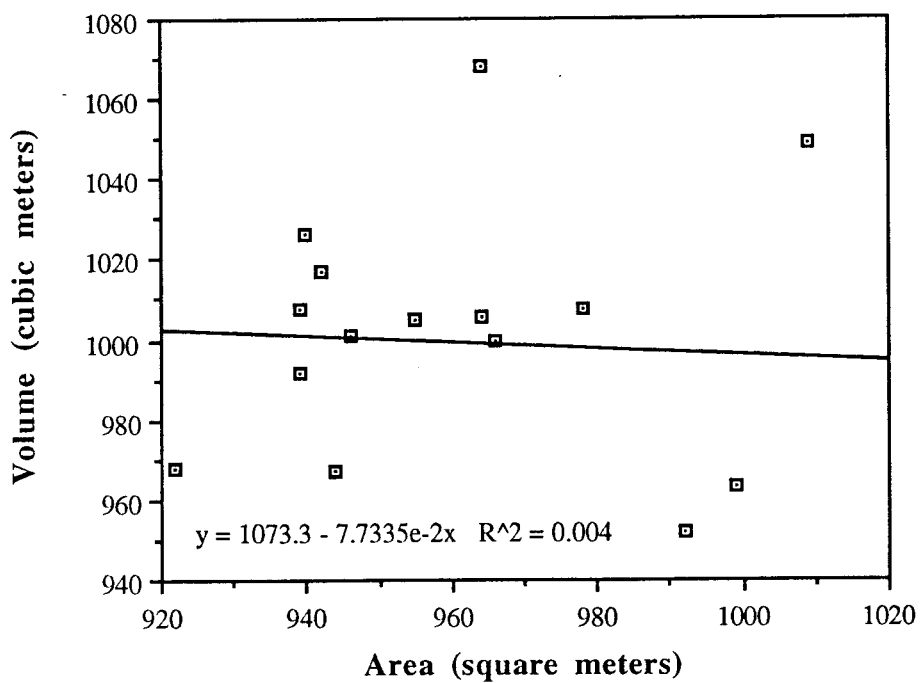
Survey Precision and Accuracy

Survey accuracy and precision were evaluated by conducting repeated daily surveys on two sand bars and comparing backsight controls and HAZ volumes. Repeated daily surveys were conducted on the separation (upper) and reattachment (lower) bars at Mile 45 from 6 May, 1991 through 31 May, 1991 (Table 2). One total station location was established for both sand bars during the "D" and "Constant 15,000 cfs" test flows and used each day for all surveying. Surveys crews were switched in mid-May between flow tests.

Survey accuracy was evaluated using repeated surveys of backsight control points. Mean difference from the grand mean on Backsite 1 elevation was 0.008 m (1 sd = 0.007 m, $n = 16$) and 0.027 m for Backsite 2 elevation (1 sd = 0.031 m, $n = 16$). Multiple analysis of variance (MANOVA) was employed for assessment of these survey data because several response variables were measured from the single station location. These differences were not significantly different in the MANOVA test (Wilk's lambda = 0.602; approximate $F = 1.322$; $p = 330$, $df = 5,10$; $p_{BS1} = 0.973$, $p_{BS2} = 0.117$ with $df = 1,14$ for each). Horizontal deviation from the grand mean value was 0.027 m (1 sd = 0.027 m, $n = 17$) and did not differ significantly between crews (same MANOVA statistics, $p = 0.350$, $df = 1,14$).

The same MANOVA test was employed to evaluate survey precision for the HAZ zone between the 425 m³/sec and 900 m³/sec stages in the HAZ. This zone was selected because it was continuously exposed, at least during low water, during the period of repeated surveys. The mean deviation from the grand mean on the separation bar was -0.44 percent (1 sd = 2.621, $n = 18$) and -0.48 percent (1 sd =

Sand Bar at Mile 43



Sand Bar at Mile 51

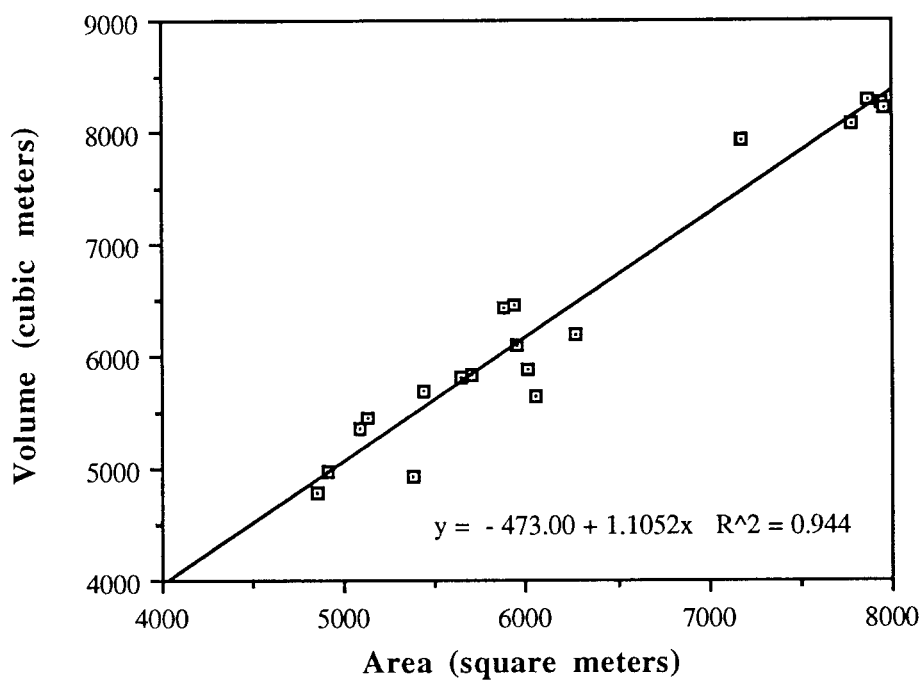


Figure 4: Examples of sand bars having greatly different volume to area relationships.

Table 2: Daily repeated topographic surveys of the 45 Mile separation and reattachment bars (5-06-91 to 5-31-91). Volume refers to the HAZ volume above the 425 m³ stage elevation.

DATE	TEST FLOW	SURVEY CREW	SEPARATION BAR HAZ VOLUME ABOVE 425 m ³	REATTACHMENT BAR HAZ VOLUME ABOVE 425 m ³
5-06-91	141 m ³ constant	1	1098.08	2298.88
5-07-91	D flow	1	1102.64	2031.32
5-12-91	D flow	1	1117.04	2032.17
5-13-91	D flow	1	1087.21	2045.63
5-14-91	D flow	1	1068.80	2103.42
5-15-91	D flow	1	1060.74	2151.00
5-16-91	D flow	1	1140.12	2083.21
5-17-91	141 m ³ constant	1	1064.16	1061.69
5-21-91	141 m ³ constant	2	1129.69	2131.02
5-22-91	425 m ³ constant	2	1069.80	2176.13
5-23-91	425 m ³ constant	2	1065.38	2187.60
5-25-91	425 m ³ constant	2	1086.80	2188.57
5-26-91	425 m ³ constant	2	1084.84	2183.71
5-27-91	425 m ³ constant	2	1084.36	2136.35
5-28-91	425 m ³ constant	2	1060.70	2181.80
5-29-91	425 m ³ constant	2	1045.89	2171.70
5-30-91	425 m ³ constant	2	1053.30	2154.28
5-31-91	141 m ³ constant	2	1134.92	2181.82

3.238, $n = 18$) for the reattachment bar. The MANOVA test using arcsine, squareroot-transformed percent change from the grand mean at these two sites showed no difference in survey precision between crews on the separation bar (same MANOVA statistics, $p = 0.487$, $df = 1,14$). Although the overall MANOVA showed no significant difference between survey crews, the lower bar HAZ did change significantly in response to a bank failure event observed on the second day of the surveying effort. These results indicate that survey error was less than plus or minus three percent on the separation bar, a relatively stable sand bar during this survey period. We generalized this estimate of three percent as our estimated survey precision for all surveys.

The daily repeated surveys of the Mile 45 reattachment bar documented a bank failure event (Figure 5). The upstream portion of the sand bar failed on the night of May 6, 1991 on the second day of a constant $141 \text{ m}^3/\text{sec}$ evaluation flow. Gradual bar rebuilding was recorded on this site during subsequent weeks. The bank failure at this site resulted in a detectable 10.9% decrease in volume during the "D" test flow.

RESULTS AND DISCUSSION

Variability Between Sand Bars

The percent volume change rates (%VCR) and areal change of sand bar hydrologically active zone (HAZ) varied considerably between the 29 study sites for which sufficient data were available and between the 16 flow tests evaluated (Tables 3, 4). Sand bars that demonstrated %VCR less than ± 0.3 percent/d were categorized as being "stable" during a given test flow, while bars having greater than 0.3 percent HAZ %VCR were classified as "gains" and those with less than -0.3% HAZ %VCR were "losses" (Table 5). From late summer, 1990 through July, 1991, three bars sustained significant net losses of HAZ sand, eleven remained relatively unchanged, and 15 sand bars gained sand (Table 5). From 27 October, 1990 (the first run for which survey coverage was virtually complete) to 30 July, 1991, the 29 sand bars under study sustained mean aggradation of 2.9% by volume (s.e. = 2.6%); however, the total $87,435 \text{ m}^3$ of sand under study in the HAZ was reduced by $1,034 \text{ m}^3$, a volume loss of 1.2% because several large losses occurred at a few sites in contrast with the general condition of near-equilibrium observed on most sites (Figure 6).

Stability varied considerably between sand bars, as demonstrated in the mean %VCR of sand bars to all discharge tests (Tables 4, 5; Figure 6). The Mile -6.5 site in Glen Canyon showed the least change, with about 6% gain or loss in December, 1990, while the Mile 172 site was the least stable. Differences in stability between sand bars may be, in part, attributable to changes in sediment supply with distance downstream. Study sites below the Little Colorado River (Mile 61) demonstrated far more variability than those upstream from that confluence (Figure 7).

Sand bar stability also varied between depositional environments. Although the differences in mean %VCR on separation (mean %VCR = 0.040) versus reattachment bars (mean = 0.037 percent/d) were not significantly different ($t = -0.031$, $p = 0.976$), the %VCR standard deviation for 13 reattachment bars was 0.072, much greater than that of eight separation bars (0.054). These results generally support the conclusion of Schmidt and Graf (1990) that reattachment bars are inherently less stable than separation bars.

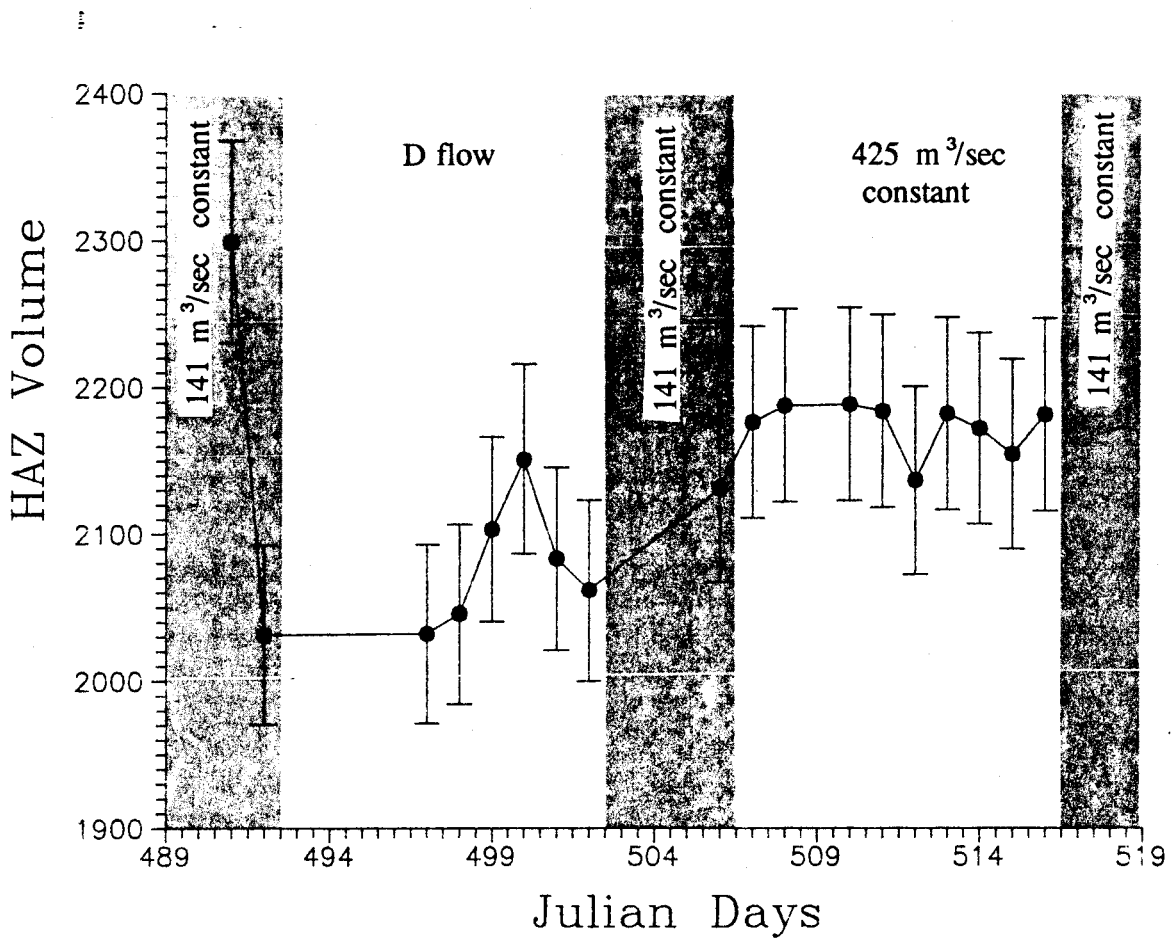


Figure 5. Daily repeated surveys of the Mile 45 reattachment sand bar during May, 1991 (adjusted Julian day 489 = May4). Note the bank failure event during the initial "constant 5,000 cfs" (141.5 m³/sec) test flow.

Table 3. Compilation of sand bar survey data and volume plots for 29 sand bars.

MILE: -6.5		KILOMETER: -10.5											
BEACH #: 2		DEPOSIT TYPE:		REATTACHMENT									
RUN ID	SURVEY DATE	TEST FLOW EVALUATED	JULIAN DAYS	HAZ AREA	HAZ VOL.	AREA CH.	VOL. CH.	AREA CH./DAY	% AREA CH.	% AREA CH./DAY	VOL CH./DAY	% VOL CH.	% VOL CH./DAY
A		NORM											
B		NORM											
C	900712	G	188	3441	3655								
D	900727	F	208	3417	3491	-24	-164	-1.200	-0.697	-0.035	-8.200	-4.487	-0.224
E		NORM											
F	900914	NORM	257	3383	3455	-34	-36	-0.694	-0.995	-0.020	-0.735	-1.031	-0.021
G	900928	E	271	3440	3456	57	1	4.071	1.685	0.120	0.071	0.029	0.002
H	901012	A	285	3407	3438	-33	-18	-2.357	-0.959	-0.069	-1.286	-0.521	-0.037
I	901026	8000 CFS	299	3419	3408	12	-30	0.857	0.352	0.025	-2.143	-0.873	-0.062
J	901109	NORM	313	3426	3584	7	176	0.500	0.205	0.015	12.571	5.164	0.369
K	901214	NORM	348	3399	3397	-27	-187	-0.771	-0.788	-0.023	-5.343	-5.218	-0.149
L	901228	11000 CFS	362	3425	3623	26	226	1.857	0.765	0.055	16.143	6.653	0.475
M	910111	C	376	3429	3536	4	-87	0.286	0.117	0.008	-6.214	-2.401	-0.172
N	910125	NORM	390	3412	3429	-17	-107	-1.214	-0.496	-0.035	-7.643	-3.026	-0.216
O	910208	B	404	3441	3532	29	103	2.071	0.850	0.061	7.357	3.004	0.215
P	910419	NORM	474	3446	3499	5	-33	0.071	0.145	0.002	-0.471	-0.994	-0.013
Q		NORM											
R	910517	D	502	3474	3608	28	109	1.000	0.813	0.029	3.893	3.115	0.111
S	910531	15000 CFS	516	3540	3586	66	-22	4.714	1.900	0.136	-1.571	-0.610	-0.044
T	910628	NORM	544	3543	3362	3	-224	0.107	0.085	0.003	-8.000	-6.247	-0.223
U	910712	G	558	3537	3347	-6	-15	-0.429	-0.169	-0.012	-1.071	-0.446	-0.032
V	910726	F	572	3523	3388	-14	41	-1.000	-0.396	-0.028	2.929	1.210	0.087

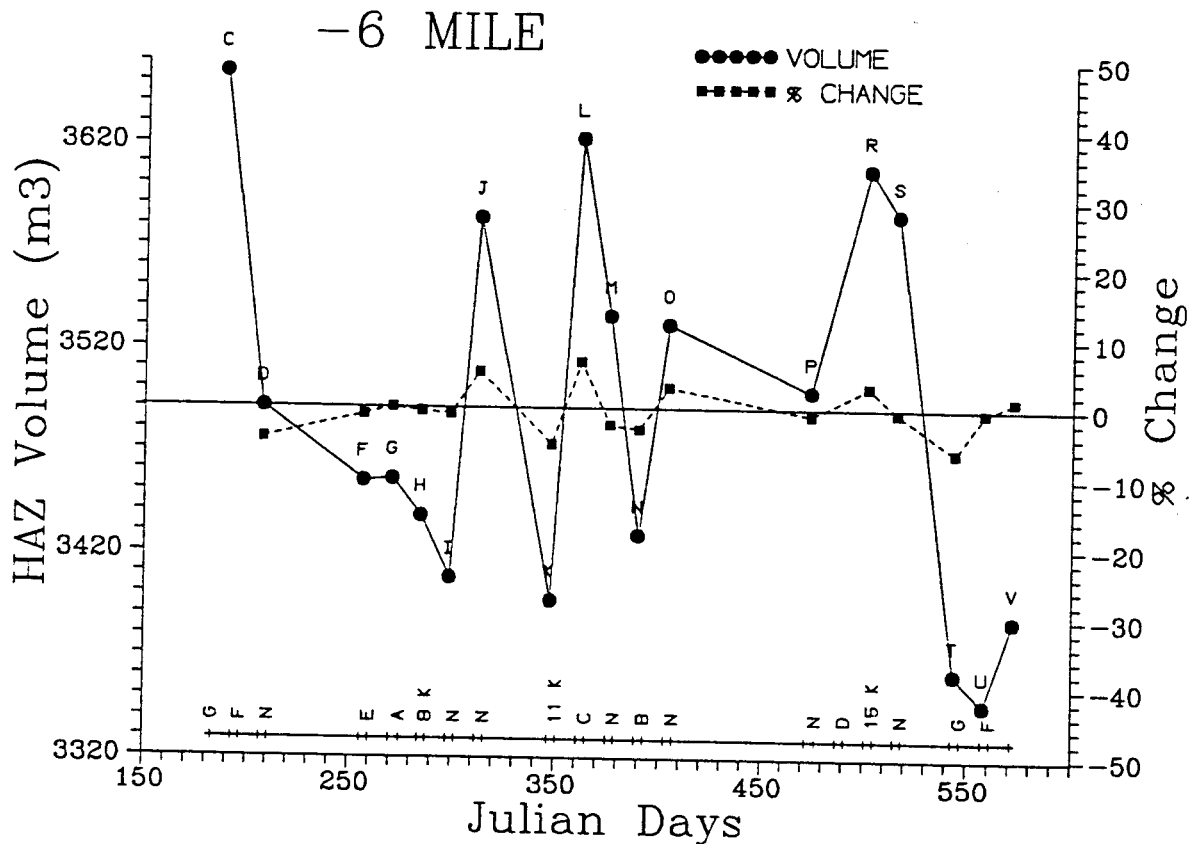


Table 3. (continued)

		MILE:	2.6	KILOMETER:	4.2								
		BEACH #:	3	DEPOSIT TYPE:	REATTACHMENT								
RUN ID	SURVEY DATE	TEST FLOW EVALUATED	JULIAN DAYS	HAZ AREA	HAZ VOL	AREA CH.	VOL. CH.	AREA CH./DAY	% AREA CH.	% AREA CH./DAY	VOL. CH./DAY	% VOL. CH.	% VOL. CH./DAY
A		NORM											
B		NORM											
C		G											
D		F											
E		NORM											
F	900914	NORM	257	2487	2793								
G	900928	E	271	2723	3109	236	316	16.857	9.489	0.678	22.571	11.314	0.808
H	901012	A	285	2670	3155	-53	46	-3.786	-1.946	-0.139	3.286	1.480	0.106
I	901026	8000 CFS	299	2722	3161	52	6	3.714	1.948	0.139	0.429	0.190	0.014
J	901109	NORM	313	2754	3122	32	-39	2.286	1.176	0.084	-2.786	-1.234	-0.088
K		NORM											
L	901228	11000 CFS	362	2897	3219	143	97	2.918	5.192	0.106	1.980	3.107	0.063
M	910111	C	376	2989	3444	92	225	6.571	3.176	0.227	16.071	6.990	0.499
N	910125	NORM	390	2861	3250	-128	-194	-9.143	-4.282	-0.306	-13.857	-5.633	-0.402
O	910208	B	404	2866	3200	5	-50	0.357	0.175	0.012	-3.571	-1.538	-0.110
P	910419	NORM	474	2769	3230	-97	30	-1.386	-3.385	-0.048	0.429	0.938	0.013
Q	910503	NORM	488	2826	3195	57	-35	4.071	2.059	0.147	-2.500	-1.084	-0.077
R	910517	D	502	2874	3542	48	347	3.429	1.699	0.121	24.786	10.861	0.776
S	910531	15000 CFS	516	2835	3578	-39	36	-2.786	-1.357	-0.097	2.571	1.016	0.073
T	910628	NORMS	544	2726	3591	-109	13	-3.893	-3.845	-0.137	0.464	0.363	0.013
U	910712	G	558	2950	3606	224	15	16.000	8.217	0.587	1.071	0.418	0.030
V	910726	F	572	3016	3564	66	-42	4.714	2.237	0.160	-3.000	-1.178	-0.083

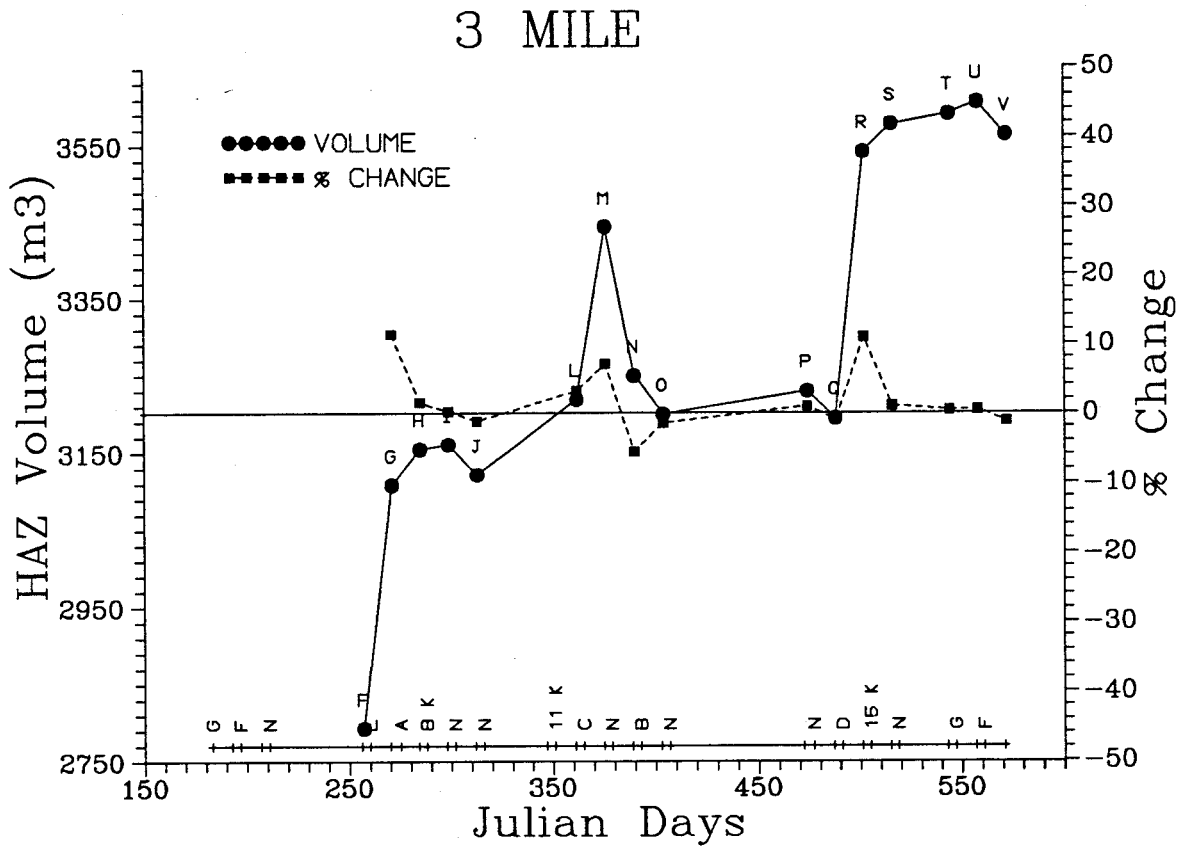


Table 3. (continued)

MILE: 8 KILOMETER: 12.9
 BEACH #: 4 DEPOSIT TYPE: SEPARATION/REATTACHMENT

RUN ID	SURVEY DATE	TEST FLOW EVALUATED	JULIAN DAYS	HAZ AREA	HAZ VOL	AREA CH.	VOL CH.	AREA CH./DAY	% AREA CH.	% AREA CH./DAY	VOL CH./DAY	% VOL CH.	% VOL CH./DAY
A		NORM											
B		NORM											
C		G											
D	900725	F	206	1630	1416								
E		NORM											
F	900915	NORM	258	1559	1432	-71	16	-1.365	-4.356	-0.064	0.308	1.130	0.022
G	900929	E	272	1573	1468	14	36	1.000	0.898	0.064	2.571	2.514	0.180
H	901013	A	286	1558	1360	-15	-108	-1.071	-0.954	-0.068	-7.714	-7.357	-0.525
I	901027	8000 CPS	300	1605	1401	47	41	3.357	3.017	0.215	2.929	3.015	0.215
J	901110	NORM	314	1585	1348	-20	-53	-1.429	-1.246	-0.089	-3.786	-3.783	-0.270
K	901215	NORM	349	1587	1342	2	-6	0.057	0.126	0.004	-0.171	-0.445	-0.013
L	901229	11000 CPS	363	1574	1430	-13	88	-0.929	-0.819	-0.059	6.286	6.557	0.468
M	910112	C	377	1611	1464	37	34	2.643	2.351	0.168	2.429	2.378	0.170
N	910126	NORM	391	1591	1381	-20	-83	-1.429	-1.241	-0.089	-5.929	-5.669	-0.405
O	910209	B	405	1511	1370	-80	-11	-5.714	-5.028	-0.359	-0.786	-0.797	-0.057
P	910419	NORM	474	1502	1337	-9	-33	-0.130	-0.596	-0.009	-0.478	-2.409	-0.035
Q	910503	NORM	488	1506	1343	4	6	0.286	0.266	0.019	0.429	0.449	0.032
R	910518	D	503	1643	1411	137	68	9.133	9.097	0.606	4.533	5.063	0.338
S	910601	15000 CPS	517	1571	1360	-72	-51	-5.143	-4.382	-0.313	-3.643	-3.614	-0.258
T	910629	NORM	545	1534	1365	-37	5	-1.321	-2.355	-0.084	0.179	0.368	0.013
U	910713	G	559	1496	1387	-38	22	-2.714	-2.477	-0.177	1.571	1.612	0.115
V	910727	F	573	1482	1351	-14	-36	-1.000	-0.936	-0.067	-2.571	-2.665	-0.185

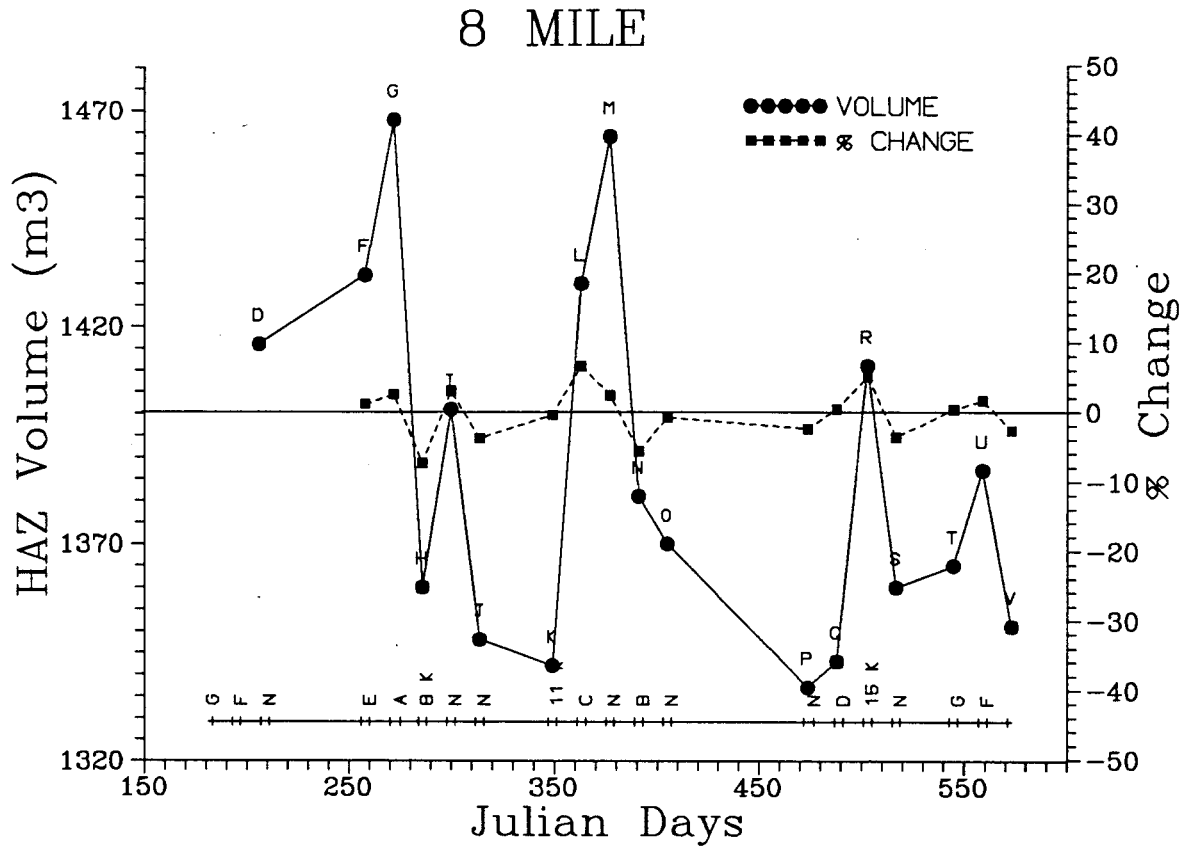


Table 3. (continued)

		MILE:	16	KILOMETER:	26.4								
		BEACH #:	5	DEPOSIT TYPE:	SEPARATION								
RUN#	SURVEY	TEST	JULIAN	HAZ	HAZ	AREA	VOL.	AREA	%	% AREA	VOL.	%	% VOL.
ID	DATE	FLOW EVALUATED	DAYS	AREA	VOL	CH.	CH.	CH./DAY	AREA CH.	CH./DAY	CH./DAY	VOL CH.	CH./DAY
A		NORM											
B		NORM											
C	900714	G	195	1047	1478								
D	900728	F	209	1115	1555	68	77	4.857	6.495	0.464	5.500	5.210	0.372
E		NORM											
F	900915	NORM	258	1207	1761	92	206	1.878	8.251	0.168	4.204	13.248	0.270
G	900929	E	272	1294	1880	87	119	6.214	7.208	0.515	8.500	6.758	0.483
H	901013	A	286	1288	1794	-6	-86	-0.429	-0.464	-0.033	-6.143	-4.574	-0.327
I	901027	8000 CFS	300	1298	1838	10	44	0.714	0.776	0.055	3.143	2.453	0.175
J	901110	NORM	314	1292	1758	-6	-80	-0.429	-0.462	-0.033	-5.714	-4.353	-0.311
K	901215	NORM	349	1328	1827	36	69	1.029	2.786	0.080	1.971	3.925	0.112
L	911229	11000 CFS	363	1338	1848	10	21	0.714	0.753	0.054	1.500	1.149	0.082
M	910112	C	377	1368	1948	30	100	2.143	2.242	0.160	7.143	5.411	0.387
N	910126	NORM	391	1343	1832	-25	-116	-1.786	-1.827	-0.131	-8.286	-5.955	-0.425
O	910209	B	405	1346	1820	3	-12	0.214	0.223	0.016	-0.857	-0.655	-0.047
P	910420	NORM	475	1379	1835	33	15	0.471	2.452	0.035	0.214	0.824	0.012
Q	910504	NORM	489	1362	1753	-17	-82	-1.214	-1.233	-0.088	-5.857	-4.469	-0.319
R	910518	D	503	1083	1584	-279	-169	-19.929	-20.485	-1.463	-12.071	-9.641	-0.689
S	910601	15000 CFS	517	1110	1564	27	-20	1.929	2.493	0.178	-1.429	-1.263	-0.090
T	910629	NORM	545	1207	1631	97	67	3.464	8.739	0.312	2.393	4.284	0.153
U	910713	G	559	1248	1663	41	32	2.929	3.397	0.243	2.286	1.962	0.140
V	910727	F	573	1280	1722	32	59	2.286	2.564	0.183	4.214	3.548	0.253

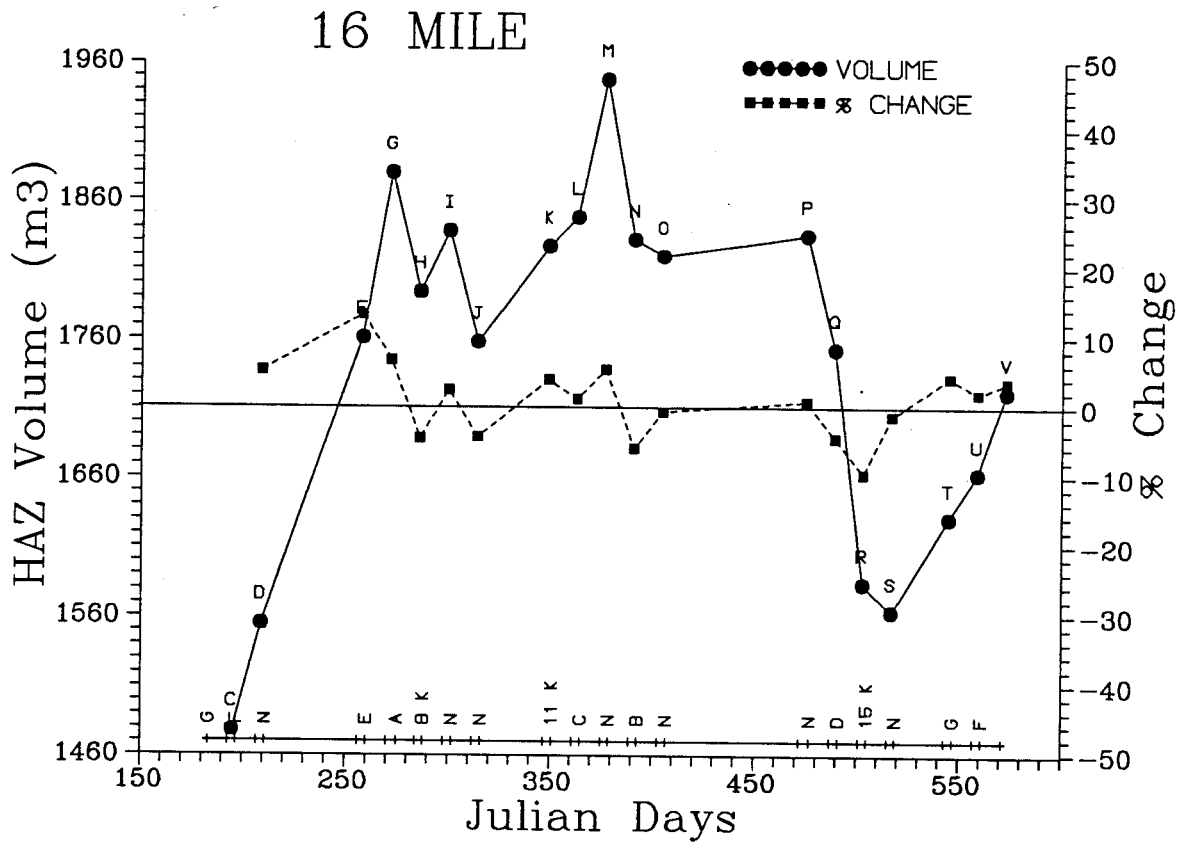


Table 3. (continued)

		MILE:	22	KILOMETER:	35.1								
		BEACH #:	6	DEPOSIT TYPE:	REATTACHMENT								
RUN IC	SURVEY DATE	TEST FLOW EVALUATED	JULIAN DAYS	HAZ AREA	HAZ VOL.	AREA VOL.	VOL. CH.	AREA CH./DAY	% AREA CH.	% AREA CH./DAY	VOL. CH./DAY	% VOL. CH.	% VOL. CH./DAY
A		NORM											
B		NORM											
C		G											
D		F											
E		NORM											
F		NORM											
G	900930	E	273	1703	3534								
H		A											
I	901028	8000 CFS	301	1660	3421	-43	-113	59.286	-2.525	-0.090	-4.036	-3.198	-0.114
J	901111	NORM	315	1694	3430	34	9	121.000	2.048	0.146	0.643	0.263	0.019
K	901216	NORM	350	1658	3363	-36	-67	47.371	-2.125	-0.061	-1.914	-1.953	-0.056
L	901230	11000 CFS	364	1625	3438	-33	75	116.071	-1.990	-0.142	5.357	2.230	0.159
M	910113	C	378	1685	3494	60	56	120.357	3.692	0.264	4.000	1.629	0.116
N	910127	NORM	392	1636	3409	-49	-85	116.857	-2.908	-0.208	-6.071	-2.433	-0.174
O	910209	B	405	1624	3379	-12	-30	124.923	-0.733	-0.056	-2.308	-0.880	-0.068
P	910420	NORM	475	1633	3451	9	72	23.329	0.554	0.008	1.029	2.131	0.030
Q	910504	NORM	489	1550	3306	-83	-145	110.714	-5.083	-0.363	-10.357	-4.202	-0.300
R	910519	D	504	1908	3731	358	425	127.200	23.097	1.540	28.333	12.855	0.857
S	910601	15000 CFS	517	1787	3586	-121	-145	137.462	-6.342	-0.488	-11.154	-3.886	-0.299
T	910629	NORM	545	1866	3731	79	145	66.643	4.421	0.158	5.179	4.044	0.144
U	910713	G	559	1777	3680	-89	-51	126.929	-4.770	-0.341	-3.643	-1.367	-0.098
V	910727	F	573	1727	3578	-50	-102	123.357	-2.814	-0.201	-7.286	-2.851	-0.198

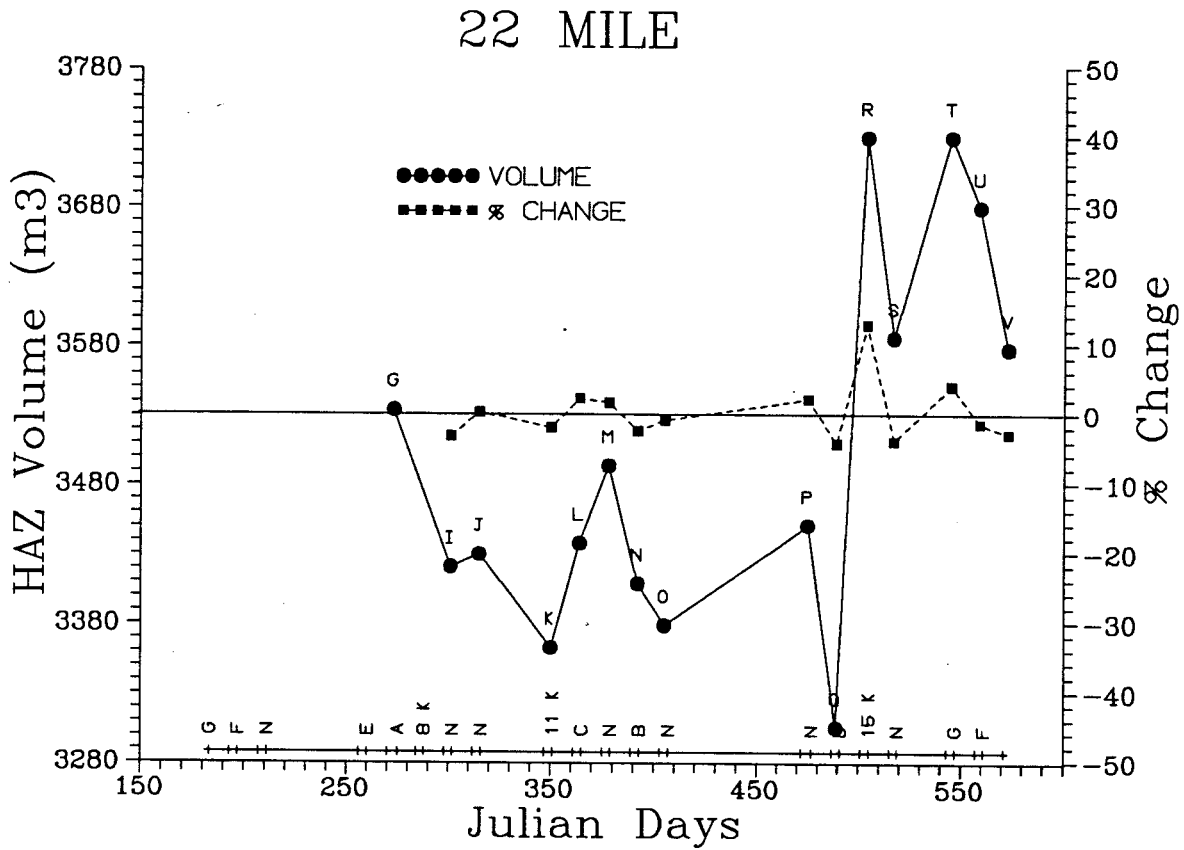


Table 3. (continued)

		MILE:	30	KILOMETER:		48.3							
		BEACH #:	7	DEPOSIT TYPE:		REATTACHMENT							
RUN ID	SURVEY DATE	TEST FLOW EVALUATED	JULIAN DAYS	HAZ AREA	HAZ VOL.	AREA CH.	VOL. CH.	AREA CH./DAY	% AREA CH.	% AREA CH./DAY	VOL CH./DAY	% VOL CH.	% VOL CH./DAY
A		NORM											
B		NORM											
C		G											
D		F											
E		NORM											
F		NORM											
G		E											
H	901014	A	287	3732	7336								
I	901028	8000 CFS	301	3672	7314	-60	-22	-4.286	-1.608	-0.115	-1.571	-0.300	-0.021
J	901111	NORM	315	3655	7216	-17	-98	-1.214	-0.463	-0.033	-7.000	-1.340	-0.096
K	901216	NORM	350	3705	6889	50	-327	1.429	1.368	0.039	-9.343	-4.532	-0.129
L	901230	11000 CFS	364	3686	7061	-19	172	-1.357	-0.513	-0.037	12.286	2.497	0.178
M	910113	C	378	3813	7140	127	79	9.071	3.445	0.246	5.643	1.119	0.080
N	910125	NORM	390	3812	6953	-1	-187	-0.083	-0.026	-0.002	-15.583	-2.619	-0.218
O	910210	B	406	3762	6673	-50	-280	-3.125	-1.312	-0.082	-17.500	-4.027	-0.252
P	910420	NORM	475	3741	6631	-21	-42	-0.304	-0.558	-0.008	-6.609	-0.629	-0.009
Q	900506	NORM	491	3752	6525	11	-106	0.688	0.294	0.018	-6.625	-1.599	-0.100
R	910519	D	504	3794	7352	42	827	3.231	1.119	0.086	63.615	12.674	0.975
S	910602	15000 CFS	518	3765	7076	-29	-276	-2.071	-0.764	-0.055	-19.714	-3.754	-0.268
T	910630	NORM	546	3444	7299	-321	223	-11.464	-8.526	-0.304	7.964	3.151	0.113
U	910714	G	560	3569	7254	125	-45	8.929	3.630	0.259	-3.214	-0.617	-0.044
V	910728	F	574	3656	7366	87	112	6.214	2.438	0.174	8.000	1.520	0.110

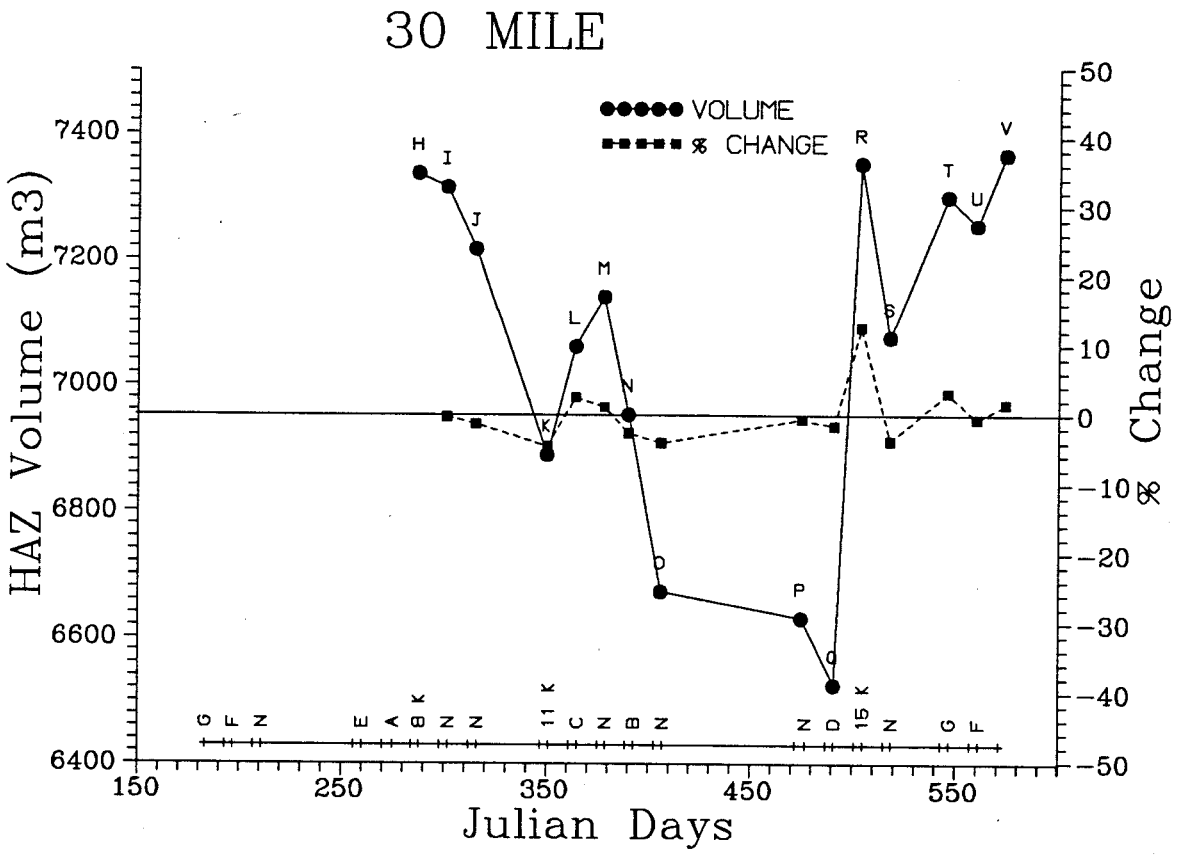


Table 3. (continued)

		MILE:	31	KILOMETER:		50.2								
		BEACH #:	8	DEPOSIT TYPE:		REATTACHMENT								
RUN ID	SURVEY DATE	TEST		JULIAN DAYS	HAZ AREA	HAZ VOL.	AREA CH.	VOL. CH.	AREA CH./DAY	% AREA CH.	% AREA CH./DAY	VOL. CH./DAY	% VOL. CH.	% VOL. CH./DAY
		FLOW EVALUATED												
A		NORM												
B		NORM												
C		G												
D		F												
E	900829	NORM		241	2066	1987								
F	900916	NORM		259	1972	1933	-94	-54	-5.222	-4.550	-0.253	-3.000	-2.718	-0.151
G	900930	E		273	1997	2039	25	106	1.786	1.268	0.091	7.571	5.484	0.392
H	901015	A		288	2032	1919	35	-120	2.333	1.753	0.117	-8.000	-5.885	-0.392
I	901029	8000 CFS		302	2053	2009	21	90	1.500	1.033	0.074	6.429	4.690	0.335
J	901112	NORM		316	2048	1997	-5	-12	-0.357	-0.244	-0.017	-0.857	-0.597	-0.043
K	901217	NORM		351	2066	2072	18	75	0.514	0.879	0.025	2.143	3.756	0.107
L	901231	11000 CFS		365	2054	2032	-12	-40	-0.857	-0.581	-0.041	-2.857	-1.931	-0.138
M	910114	C		379	2111	1989	57	-43	4.071	2.775	0.198	-3.071	-2.116	-0.151
N	910128	NORM		393	2048	1920	-63	-69	-4.500	-2.984	-0.213	-4.929	-3.469	-0.248
O	910210	B		406	2035	1818	-13	-102	-1.000	-0.635	-0.049	-7.846	-5.313	-0.409
P	910421	NORM		476	2084	1878	49	60	0.700	2.408	0.034	0.857	3.300	0.047
Q	910505	NORM		490	2071	1909	-13	31	-0.929	-0.624	-0.045	2.214	1.651	0.118
R	910519	D		504	2173	1960	102	51	7.286	4.925	0.352	3.643	2.672	0.191
S	910602	15000 CFS		518	2185	1905	12	-55	0.857	0.552	0.039	-3.929	-2.806	-0.200
T	910630	NORM		546	2289	2020	104	115	3.714	4.760	0.170	4.107	6.037	0.216
U	910714	G		560	2343	2026	54	6	3.857	2.359	0.169	0.429	0.297	0.021
V	910728	F		574	2407	2055	64	29	4.571	2.732	0.195	2.071	1.431	0.102

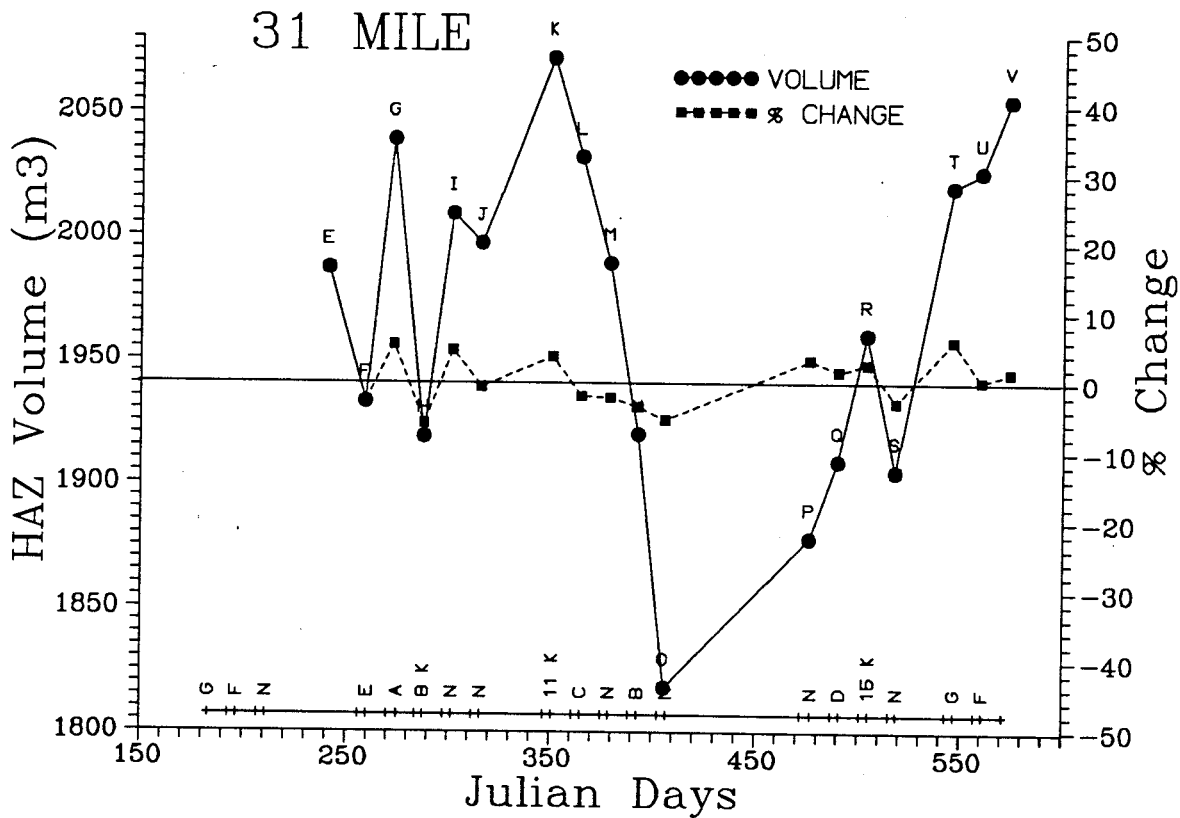


Table 3. (continued)

MILE: 43		KILOMETER: 69.3											
BEACH #: 10		DEPOSIT TYPE: REATTACH/UPPER POOL											
RUN ID	SURVEY DATE	TEST FLOW EVALUATED	JULIAN DAYS	HAZ AREA	HAZ VOL	AREA CH.	VOL CH.	AREA CH./DAY	% AREA CH.	% AREA CH./DAY	VOL CH./DAY	% VOL CH.	% VOL CH./DAY
A		NORM											
B		NORM											
C		G											
D		F											
E		NORM											
F	900914	NORM	257	978	1008								
G	900928	E	271	1009	1049	31	41	2.214	3.170	0.226	2.929	4.067	0.291
H	901012	A	285	964	1068	-45	19	-3.214	-4.460	-0.319	1.357	1.811	0.129
I	901026	8000 CFS	299	946	1001	-18	-67	-1.286	-1.867	-0.133	-4.786	-6.273	-0.448
J	901109	NORM	313	955	1005	9	4	0.643	0.951	0.068	0.286	0.400	0.029
K	901214	NORM	348	939	992	-16	-13	-0.457	-1.675	-0.048	-0.371	-1.294	-0.037
L		11000 CFS											
M	910111	C	376	922	968	-17	-24	-0.607	-1.810	-0.065	-0.857	-2.419	-0.086
N	910125	NORM	390	940	1026	18	58	1.286	1.952	0.139	4.143	5.992	0.428
O	910208	B	404	939	1008	-1	-18	-0.071	-0.106	-0.008	-1.286	-1.754	-0.125
P	910419	NORM	474	942	1017	3	9	0.043	0.319	0.005	0.129	0.893	0.013
Q	910505	NORM	490	966	1000	24	-17	1.500	2.548	0.159	-1.063	-1.672	-0.104
R	910520	D	505	964	1006	-2	6	-0.133	-0.207	-0.014	0.400	0.600	0.040
S	910602	15000 CFS	518	944	967	-20	-39	-1.538	-2.075	-0.160	-3.000	-3.877	-0.298
T	910628	NORM	544	992	952	48	-15	1.846	5.085	0.196	-0.577	-1.551	-0.060
U	910712	G	558	992	952	0	0	0.000	0.000	0.000	0.000	0.000	0.000
V	910726	F	572	999	963	7	11	0.500	0.706	0.050	0.786	1.142	0.083

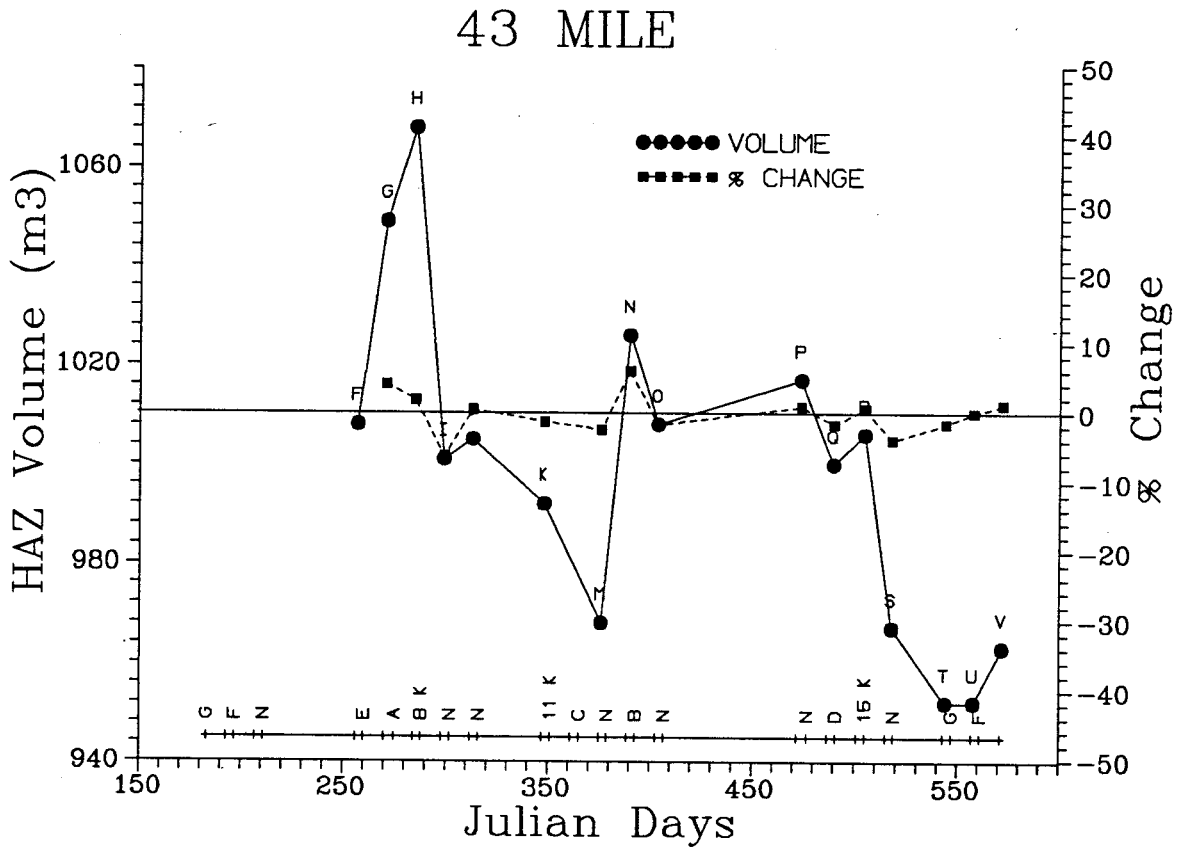


Table 3. (continued)

		MILE:	45	KILOMETER:		71.6								
		BEACH #:	11	DEPOSIT TYPE:		SEPARATION								
RUN ID	SURVEY DATE	TEST FLOW		JULIAN DAYS	HAZ AREA	HAZ VOL.	AREA CH.	VOL. CH.	AREA CH./DAY	% AREA CH.	% AREA CH./DAY	VOL CH./DAY	% VOL CH.	% VOL CH./DAY
		EVALUATED												
A		NORM												
B		NORM												
C		G												
D		F												
E		NORM												
F		NORM												
G		E												
H	901012	A	285	2578	3801									
I	901026	8000 CFS	299	2417	3107	-161	-694	-11.500	-6.245	-0.446	-49.571	-18.258	-1.304	
J	901109	NORM	313	2551	3618	134	511	9.571	5.544	0.396	36.500	16.447	1.175	
K	901214	NORM	348	2611	3802	60	184	1.714	2.352	0.067	5.257	5.086	0.145	
L	901228	11000 CFS	362	2722	3663	111	-139	7.929	4.251	0.304	-9.929	-3.656	-0.261	
M	910111	C	376	2688	3642	-34	-21	-2.429	-1.249	-0.089	-1.500	-0.573	-0.041	
N	910125	NORM	390	2577	3502	-111	-140	-7.929	-4.129	-0.295	-10.000	-3.844	-0.275	
O	910208	B	404	2604	3663	27	161	1.929	1.048	0.075	11.500	4.597	0.328	
P	910419	NORM	474	2623	3478	19	-185	0.271	0.730	0.010	-2.643	-5.051	-0.072	
Q	910502	NORM	487	2633	3776	10	298	0.769	0.381	0.029	22.923	8.568	0.659	
R	910517	D	502	2632	3481	-1	-295	-0.067	-0.038	-0.003	-19.667	-7.813	-0.521	
S	910603	15000 CFS	519	2674	3536	42	55	2.471	1.596	0.094	3.235	1.580	0.093	
T	910628	NORM	544	2646	3552	-28	16	-1.120	-1.047	-0.042	0.640	0.452	0.018	
U	910712	G	558	2675	3586	29	34	2.071	1.096	0.078	2.429	0.957	0.068	
V	900726	F	572	2585	3456	-90	-130	-6.429	-3.364	-0.240	-9.286	-3.625	-0.259	

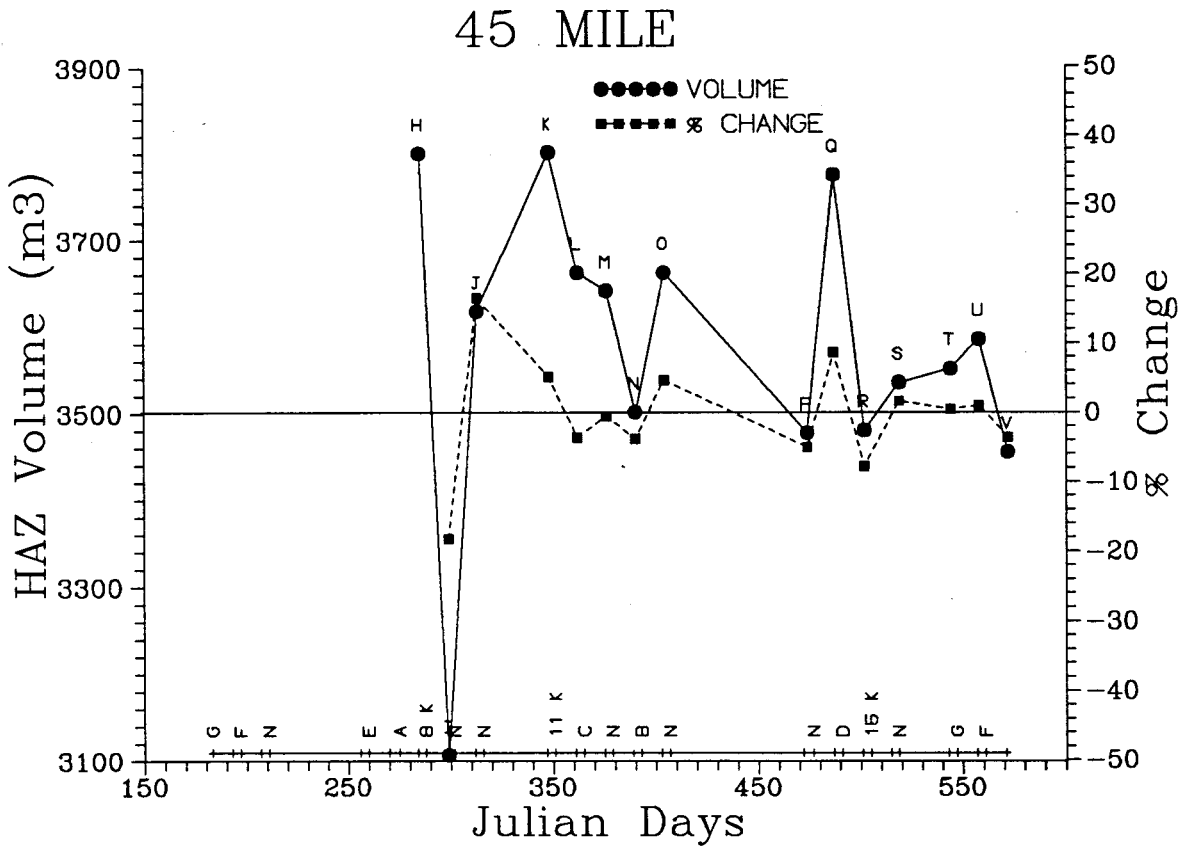


Table 3. (continued)

MILE: 47 KILOMETER: 75.8
 BEACH #: 12 DEPOSIT TYPE: REATTACHMENT

RUN ID	SURVEY DATE	TEST FLOW EVALUATED	JULIAN DAYS	HAZ AREA	HAZ VOL	AREA CH.	VOL CH.	AREA CH./DAY	% AREA CH.	% AREA CH./DAY	VOL CH./DAY	% VOL CH.	% VOL CH./DAY
A		NORM											
B		NORM											
C	907014	G	195	6620	6752								
D	900728	F	209	6967	7035	347	283	24.786	5.242	0.374	20.214	4.191	0.299
E		NORM											
F	900915	NORM	258	7626	8202	659	1167	13.449	9.459	0.193	23.816	16.588	0.339
G	900929	E	272	7900	9146	274	944	19.571	3.593	0.257	67.429	11.509	0.822
H	901013	A	286	7762	8135	-138	-1011	-9.857	-1.747	-0.125	-72.214	-11.054	-0.790
I	901027	8000 CFS	300	7794	8226	32	91	2.286	0.412	0.029	6.500	1.119	0.080
J	901110	NORM	314	7681	8479	-113	253	-8.071	-1.450	-0.104	18.071	3.076	0.220
K	901215	NORM	349	7696	8565	15	86	0.429	0.195	0.006	2.457	1.014	0.029
L		11000 CFS											
M	910112	C	377	7360	8256	-336	-309	-12.000	-4.366	-0.156	-11.036	-3.608	-0.129
N	910126	NORM	391	7272	8200	-88	-56	-6.286	-1.196	-0.085	-4.000	-0.678	-0.048
O	910209	B	405	7134	7966	-138	-234	-9.857	-1.898	-0.136	-16.714	-2.854	-0.204
P	910420	NORM	475	6836	7434	-298	-532	-4.257	-4.177	-0.060	-7.600	-6.678	-0.095
Q	910503	NORM	488										
R	910518	D	503	6838	7456	2	22	0.071	0.029	0.001	0.786	0.296	0.011
S	900601	15000 CFS	517	6685	7471	-153	15	-10.929	-2.237	-0.160	1.071	0.201	0.014
T	910629	NORM	545	7001	7715	316	244	11.286	4.727	0.169	8.714	3.266	0.117
U	910713	G	559	7152	7826	151	111	10.786	2.157	0.154	7.929	1.439	0.103
V	910727	F	573	7233	7696	81	-130	5.786	1.133	0.081	-9.286	-1.661	-0.119

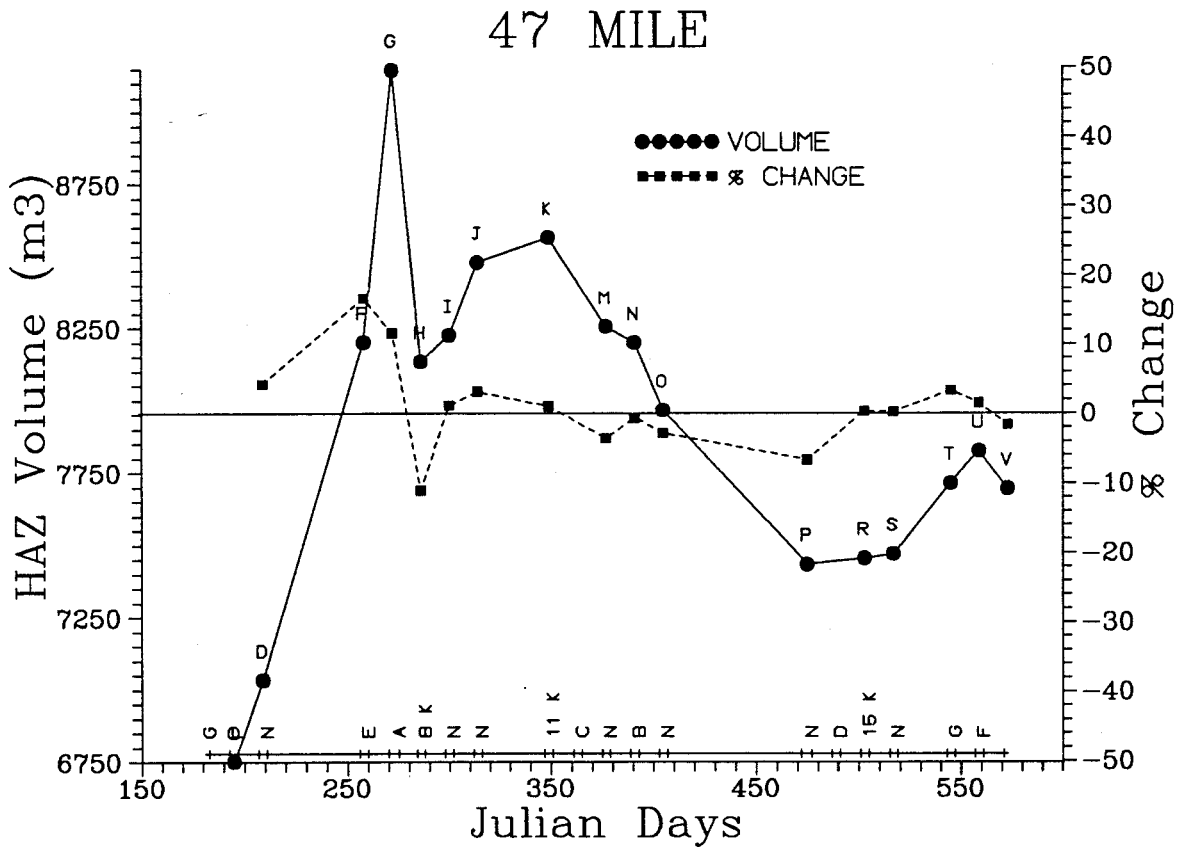


Table 3. (continued)

		MILE:	50	KILOMETER:	80.5								
		BEACH #:	13	DEPOSIT TYPE:	SEPARATION								
RUN ID	SURVEY DATE	TEST FLOW EVALUATED	JULIAN DAYS	HAZ AREA	HAZ VOL.	AREA CH.	VOL. CH.	AREA CH./DAY	% AREA CH.	% AREA CH./DAY	VOL CH./DAY	% VOL CH.	% VOL CH./DAY
A		NORM											
B		NORM											
C		G											
D		F											
E		NORM											
F	900915	NORM	258	2760	4269								
G		E											
H	901013	A	286	2750	4178	-10	-91	-0.357	-0.362	-0.013	-3.250	-2.132	-0.076
I	901029	8000 CFS	302	2714	4169	-36	-9	-2.250	-1.309	-0.082	-0.563	-0.215	-0.013
J	901110	NORM	314	2705	4195	-9	26	-0.750	-0.332	-0.028	2.167	0.624	0.052
K	901215	NORM	349	2652	4097	-53	-98	-1.514	-1.989	-0.056	-2.800	-2.336	-0.067
L	901229	11000 CFS	363	2741	4178	89	81	6.357	3.356	0.240	5.786	1.977	0.141
M	910113	C	378	2732	4074	-9	-104	-0.600	-0.328	-0.022	-6.933	-2.489	-0.166
N	910127	NORM	392	2636	3936	-96	-138	-6.857	-3.514	-0.251	-9.857	-3.387	-0.242
O	910209	B	405	2662	4008	26	72	2.000	0.986	0.076	5.538	1.829	0.141
P	910420	NORM	475	2645	3753	-17	-255	-0.243	-0.639	-0.009	-3.643	-6.362	-0.091
Q	910504	NORM	489	2707	3766	62	13	4.429	2.344	0.167	0.929	0.346	0.025
R	910518	D	503	2759	3903	52	137	3.714	1.921	0.137	9.786	3.638	0.260
S	910601	15000 CFS	517	2678	3817	-81	-86	-5.786	-2.936	-0.210	-6.143	-2.203	-0.157
T	910629	NORM	545	2807	4282	129	465	4.607	4.817	0.172	16.607	12.182	0.435
U	910713	G	559	2854	4387	47	105	3.357	1.674	0.120	7.500	2.452	0.175
V	910730	F	576	2813	4234	-41	-153	-2.412	-1.437	-0.085	-9.000	-3.614	-0.205

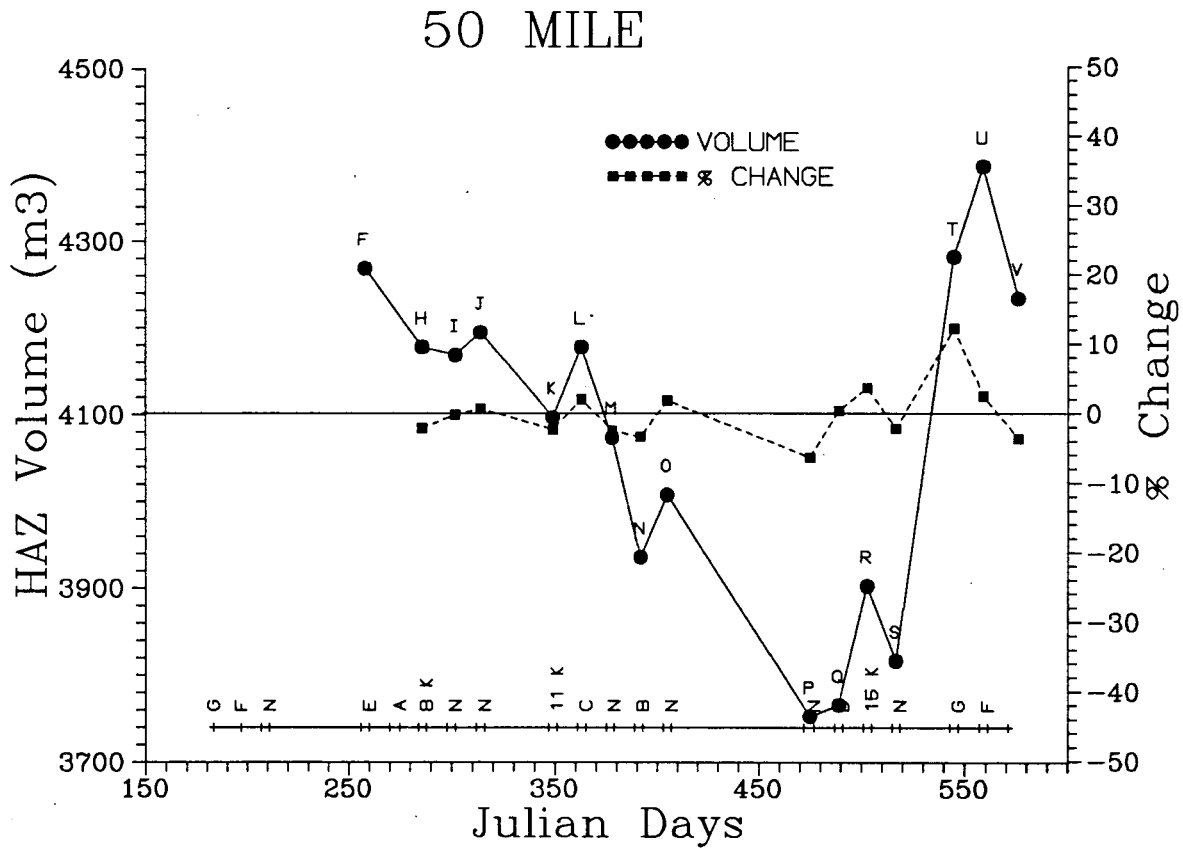


Table 3. (continued)

MILE: 51 KILOMETER: 82.9
 BEACH #: 14 DEPOSIT TYPE: REATTACHMENT

RUN ID	SURVEY DATE	TEST FLOW EVALUATED	JULIAN DAYS	HAZ AREA	HAZ VOL	AREA CH.	VOL CH.	AREA CH./DAY	% AREA CH.	% AREA CH./DAY	VOL CH./DAY	% VOL CH.	% VOL CH./DAY
A	900611	NORM	162	5370	4930								
B		NORM											
C	900715	G	196	6058	5634	688	704	20.235	12.812	0.377	20.706	14.280	0.420
D	900729	F	210	6272	6184	214	350	15.286	3.533	0.252	39.286	9.762	0.697
E		NORM											
F	900916	NORM	259	7177	7938	905	1754	18.469	14.429	0.294	35.796	28.364	0.579
G	900930	E	273	7944	8257	767	319	54.786	10.687	0.763	22.786	4.019	0.287
H	901014	A	287	7781	8068	-163	-189	-11.643	-2.052	-0.147	-13.500	-2.289	-0.163
I	901028	8000 CFS	301	7869	8294	88	226	6.286	1.131	0.081	16.143	2.801	0.200
J	901111	NORM	315	7955	8211	86	-83	6.143	1.093	0.078	-5.929	-1.001	-0.071
K	901216	NORM	350	5955	6095	-2000	-2116	-57.143	-25.141	-0.718	-60.457	-25.770	-0.736
L		11000 CFS											
M	910113	C	378	6009	5883	54	-212	1.929	0.907	0.032	-7.571	-3.478	-0.124
N	910127	NORM	392	5693	5831	-316	-52	-22.571	-5.259	-0.376	-3.714	-0.884	-0.063
O	910210	B	406	5436	5687	-257	-144	-18.357	-4.514	-0.322	-10.286	-2.470	-0.176
P	910420	NORM	475	5085	5355	-351	-332	-5.087	-6.457	-0.094	-4.812	-5.838	-0.085
Q	910504	NORM	489	5126	5443	41	88	2.929	0.806	0.058	6.286	1.643	0.117
R	910518	D	503	4904	4968	-222	-475	-15.857	-4.331	-0.309	-33.929	-8.727	-0.623
S	910602	15000 CFS	518	4852	4795	-52	-173	-3.467	-1.060	-0.071	-11.533	-3.482	-0.232
T	910630	NORM	546	5645	5819	793	1024	28.321	16.344	0.584	36.571	21.356	0.763
U	910713	G	559	5869	6421	224	602	17.231	3.968	0.305	46.308	10.345	0.796
V	910728	F	574	5939	6441	70	20	4.667	1.193	0.080	1.333	0.311	0.021

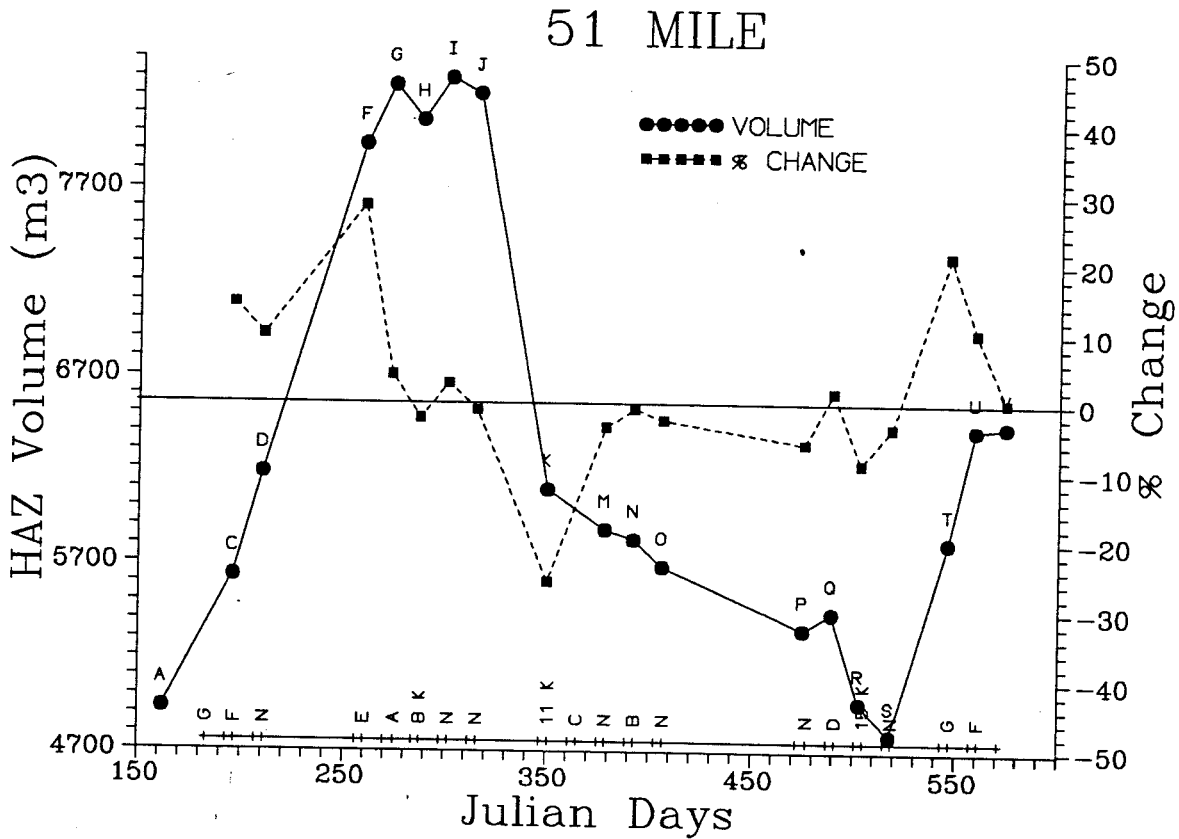


Table 3. (continued)

MILE: 68		KILOMETER: 109.6		DEPOSIT TYPE: REATTACH/SEPAR.									
BEACH #:	15												
TEST													
RUN ID	SURVEY DATE	FLOW EVALUATED	JULIAN DAYS	HAZ AREA	HAZ VOL.	AREA CH.	VOL. CH.	AREA CH./DAY	% AREA CH.	% AREA CH./DAY	VOL. CH./DAY	% VOL. CH.	% VOL. CH./DAY
A		NORM											
B		NORM											
C	900715	G	196	2990	3348								
D	900729	F	210	2649	2894	-341	-454	-24.357	-11.405	-0.815	-32.429	-13.560	-0.969
E		NORM											
F	900916	NORM	259	2764	3174	115	280	2.347	4.341	0.089	5.714	9.675	0.197
G		E											
H	901014	A	287	3163	3940	399	766	14.250	14.436	0.516	27.357	24.134	0.862
I	901028	8000 CFS	301	3155	3827	-8	-113	-0.571	-0.253	-0.018	-8.071	-2.868	-0.205
J	901112	NORM	316	3116	3490	-39	-337	-2.600	-1.236	-0.082	-22.467	-8.806	-0.587
K	901216	NORM	350	2943	3536	-173	46	-5.088	-5.552	-0.163	1.353	1.318	0.039
L	901230	11000 CFS	364	2940	3511	-3	-25	-0.214	-0.102	-0.007	-1.786	-0.707	-0.051
M	910114	C	379	2971	3579	31	68	2.067	1.054	0.070	4.533	1.937	0.129
N	910128	NORM	393	2963	3469	-8	-110	-0.571	-0.269	-0.019	-7.857	-3.073	-0.220
O	910210	B	406	3063	3478	100	9	7.692	3.375	0.260	0.692	0.259	0.020
P	910421	NORM	476	2954	3269	-109	-209	-1.557	-3.559	-0.051	-2.986	-6.009	-0.086
Q	910505	NORM	490	3288	3459	334	190	23.857	11.307	0.808	13.571	5.812	0.415
R	910519	D	504	2808	3020	-480	-439	-34.286	-14.599	-1.043	-31.357	-12.692	-0.907
S	910602	15000 CFS	518	3019	3256	211	236	15.071	7.514	0.537	16.857	7.815	0.558
T	910701	NORM	547	2998	3409	-21	153	-0.724	-0.696	-0.024	5.276	4.699	0.162
U	910714	G	560	3162	3919	164	510	12.615	5.470	0.421	39.231	14.960	1.151
V	910729	F	575	3077	3723	-85	-196	-5.667	-2.688	-0.179	-13.067	-5.001	-0.333

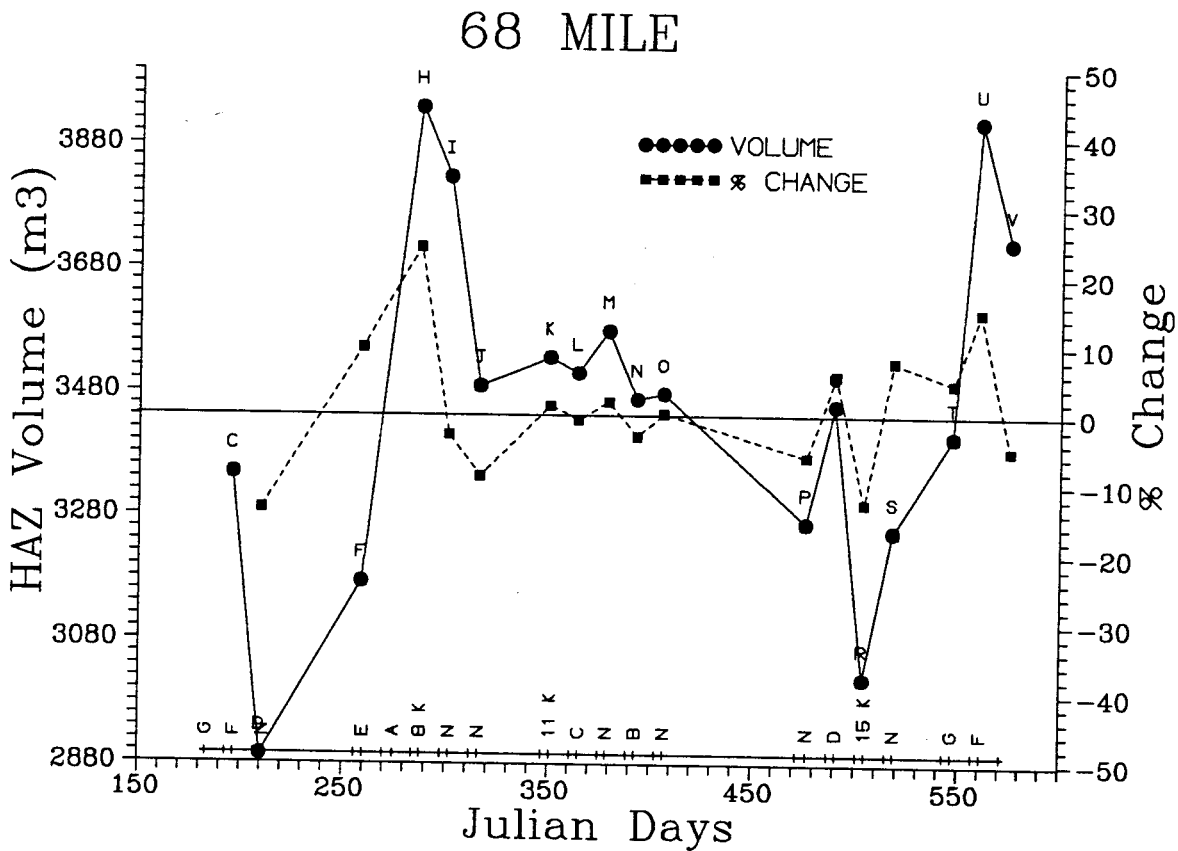


Table 3. (continued)

MILE: 81 KILOMETER: 130.5
 BEACH #: 16 DEPOSIT TYPE: SEPARATION

RUN ID	SURVEY DATE	TEST FLOW EVALUATED	JULIAN DAYS	HAZ		AREA		VOL		% AREA		% VOL	
				AREA	VOL	CH.	CH.	CH./DAY	CH./DAY	CH.	CH./DAY	CH.	CH./DAY
A		NORM											
B		NORM											
C	900716	G	197	426	393								
D	900730	F	211	372	399	-54	6	-3.857	-12.676	-0.905	0.429	1.527	0.109
E		NORM											
F	900917	NORM	260	390	442	18	43	0.367	4.839	0.099	0.878	10.777	0.220
G	901001	E	274	401	458	11	16	0.786	2.821	0.201	1.143	3.620	0.259
H	901016	A	289	346	383	-55	-75	-3.667	-13.716	-0.914	-5.000	-16.376	-1.092
I	901029	8000 CFS	302	312	369	-34	-14	-2.615	-9.827	-0.756	-1.077	-3.635	-0.281
J	901112	NORM	316	310	364	-2	-5	-0.143	-0.641	-0.046	-0.357	-1.355	-0.097
K	901217	NORM	351	303	323	-7	-41	-0.200	-2.258	-0.065	-1.171	-11.264	-0.322
L	901227	11000 CFS	361	284	291	-19	-32	-1.900	-6.271	-0.627	-3.200	-9.907	-0.991
M	910114	C	379	375	365	91	74	5.056	32.042	1.780	4.111	25.430	1.413
N	910128	NORM	393	310	294	-65	-71	-4.643	-17.333	-1.238	-5.071	-19.452	-1.389
O	910211	B	407	291	274	-19	-20	-1.357	-6.129	-0.438	-1.429	-6.803	-0.486
P	910422	NORM	477	298	270	7	-4	0.100	2.405	0.034	-0.057	-1.460	-0.021
Q	910506	NORM	491	294	278	-4	8	-0.286	-1.342	-0.096	0.571	2.963	0.212
R	910520	D	505	407	496	113	218	8.071	38.435	2.745	15.571	78.417	5.601
S	910603	15000 CFS	519	319	362	-88	-134	-6.286	-21.622	-1.544	-9.571	-27.016	-1.930
T	910701	NORM	547	414	549	95	187	3.393	29.781	1.064	6.679	51.637	1.845
U		G											
V	910729	F	575	405	537	-9	-12	-0.321	-2.174	-0.078	-0.429	-2.186	-0.078

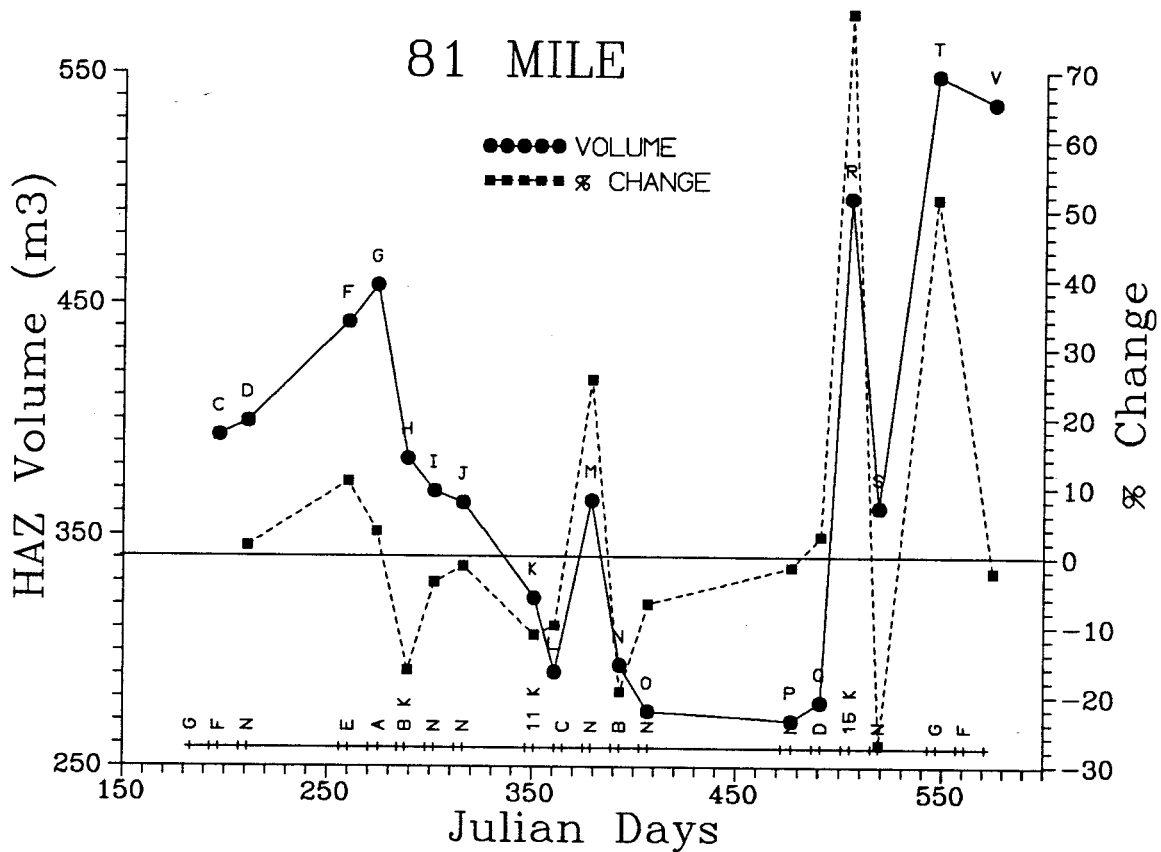


Table 3. (continued)

MILE:		87	KILOMETER:		1403		SEPARATION/REATTACHMENT					
BEACH #:		17	DEPOSIT TYPE:									
RUN ID	SURVEY DATE	TEST FLOW EVALUATED	JULIAN DAYS	HAZ AREA	HAZ VOL.	AREA CH.	VOL. CH.	AREA CH./DAY	% AREA CH.	% AREA CH./DAY	VOL. CH./DAY	% VOL. CH./DAY
A		NORM										
B		NORM										
C		G										
D		F										
E	900903	NORM	246	307	505							
F		NORM										
G		E										
H		A										
I	901029	8000 CFS	302	305	495	-2	-10	-0.036	-0.651	-0.012	-0.179	-1.980
J	901112	NORM	316	315	473	10	-22	0.714	3.279	0.234	-1.571	-4.444
K	901217	NORM	351	334	524	19	51	0.543	6.032	0.172	1.457	10.782
L	901231	11000 CFS	365	310	433	-24	-91	-1.714	-7.186	-0.513	-6.500	-17.366
M	910114	C	379	347	525	37	92	2.643	11.935	0.853	6.571	21.247
N	910128	NORM	393	340	522	-7	-3	-0.500	-2.017	-0.144	-0.214	-0.571
O	910211	B	407	351	519	11	-3	0.786	3.235	0.231	-0.214	-0.575
P	910422	NORM	477	387	571	36	52	0.514	10.256	0.147	0.743	10.019
Q	910506	NORM	491	404	585	17	14	1.214	4.393	0.314	1.000	2.452
R	910520	D	505	340	565	-64	-20	-4.571	-15.842	-1.132	-1.429	-3.419
S	910603	15000 CFS	519	351	585	11	20	0.786	3.235	0.231	1.429	3.540
T	910701	NORM	547	321	533	-30	-52	-1.071	-8.547	-0.305	-1.857	-8.889
U		G										
V	910729	F	575	317	493	-4	-40	-0.143	-1.246	-0.045	-1.429	-7.505

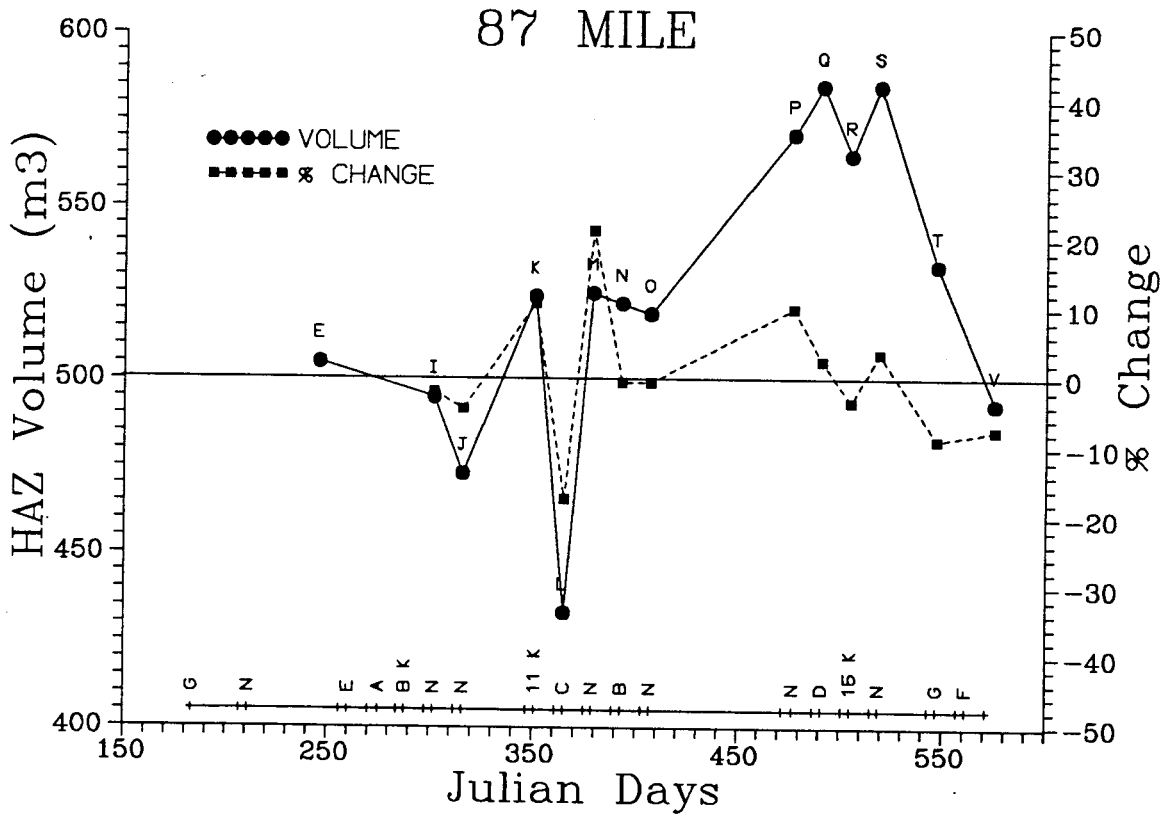


Table 3. (continued)

MILE:		91	KILOMETER:		1466		SEPARATION						
BEACH #:		18	DEPOSIT TYPE:										
RUN ID	SURVEY DATE	TEST FLOW EVALUATED	JULIAN DAYS	HAZ AREA	HAZ VOL	AREA CH.	VOL CH.	AREA CH./DAY	% AREA CH.	% AREA CH./DAY	VOL CH./DAY	% VOL CH.	% VOL CH./DAY
A		NORM											
B		NORM											
C	900714	G	195	215	207								
D		F											
E		NORM											
F		NORM											
G	900928	E	271	177	183	-38	-24	-0.50	-17.67	-0.23	-0.32	-11.59	-0.15
H	901012	A	285	176	183	-1	0	-0.07	-1.56	-0.04	0.00	0.00	0.00
I	901026	8000 CFS	299	178	182	2	-1	0.14	1.14	0.08	-0.07	-0.55	-0.04
J	901109	NORM	313	172	176	-6	-6	-0.43	-3.37	-0.24	-0.43	-3.30	-0.24
K	901214	NORM	348	174	182	2	6	0.06	1.16	0.03	0.17	3.41	0.10
L	911228	11000 CFS	362	177	196	3	14	0.21	1.72	0.12	1.00	7.69	0.55
M	910112	C	377	223	215	46	19	3.07	25.99	1.73	1.27	9.69	0.65
N	910126	NORM	391	238	224	15	9	1.07	6.73	0.48	0.64	4.19	0.30
O	910209	B	405	235	208	-3	-16	-0.21	-1.26	-0.09	-1.14	-7.14	-0.51
P	910420	NORM	475	182	186	-53	-22	-0.76	-22.55	-0.32	-0.31	-10.58	-0.15
Q	910504	NORM	489	189	180	7	-6	0.50	3.85	0.27	-0.43	-3.23	-0.23
R	910518	D	503	225	232	36	52	2.57	19.05	1.36	3.71	28.89	2.06
S	910601	15000 CFS	517	142	176	-83	-56	-5.91	-36.89	-2.63	-4.00	-24.14	-1.72
T	910702	NORM	545	217	265	75	89	2.68	52.82	1.89	3.18	50.57	1.81
U	910712	G	558	198	212	-19	-53	-1.46	-8.76	-0.67	-4.08	-20.00	-1.54
V	910727	F	573	223	241	25	29	1.67	12.63	0.84	1.93	12.03	0.91

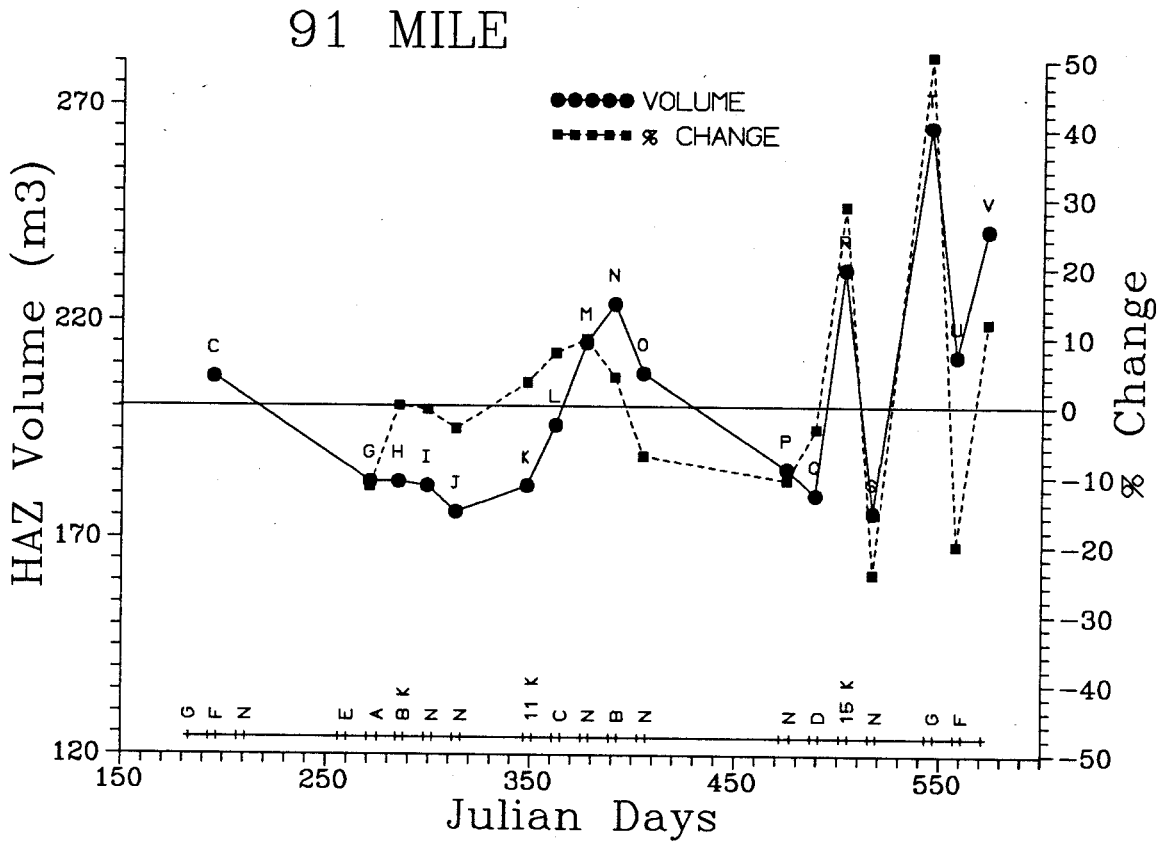


Table 3. (continued)

MILE: 93 KILOMETER: 149.6
 BEACH #: 19 DEPOSIT TYPE: UPPER POOL

RUN ID	SURVEY DATE	TEST FLOW EVALUATED	JULIAN DAYS	HAZ AREA	HAZ VOL	AREA CH.	VOL CH.	AREA CH./DAY	% AREA CH.	% AREA CH./DAY	VOL CH./DAY	% VOL CH.	% VOL CH./DAY
A		NORM											
B		NORM											
C		G											
D		F											
E		NORM											
F		NORM											
G		E											
H	901013	A	286	1394	1688								
I	901027	8000 CFS	300	1390	1708	-4	20	-0.29	-0.29	-0.02	1.43	1.18	0.08
J	901110	NORM	314	1397	1735	7	27	0.50	0.50	0.04	1.93	1.58	0.11
K	901215	NORM	349	1433	1727	36	-8	1.03	2.58	0.07	-0.23	-0.46	-0.01
L	901229	11000 CFS	363	1417	1719	-16	-8	-1.14	-1.12	-0.08	-0.57	-0.46	-0.03
M	910112	C	376	1631	1904	214	185	16.46	15.10	1.16	14.23	10.76	0.83
N	910126	NORM	391	1598	1915	-33	11	-2.20	-2.02	-0.13	0.73	0.58	0.04
O	910209	B	405	1601	1897	3	-18	0.21	0.19	0.01	-1.29	-0.94	-0.07
P	910420	NORM	475	1574	2010	-27	113	-0.39	-1.69	-0.02	1.61	5.96	0.09
Q	910504	NORM	489	1637	1949	63	-61	4.50	4.00	0.29	-4.36	-3.03	-0.22
R	910518	D	503	1380	1826	-257	-123	-18.36	-15.70	-1.12	-8.79	-6.31	-0.45
S	910601	15000 CFS	517	1418	1805	38	-21	2.71	2.75	0.20	-1.50	-1.15	-0.08
T	910629	NORM	545	1001	1302	-417	-503	-14.89	-29.41	-1.05	-17.96	-27.87	-1.00
U	910713	G	559	1231	1485	230	183	16.43	22.98	1.64	13.07	14.06	1.00
V	910727	F	573	1401	1634	170	149	12.14	13.81	0.99	10.64	10.03	0.72

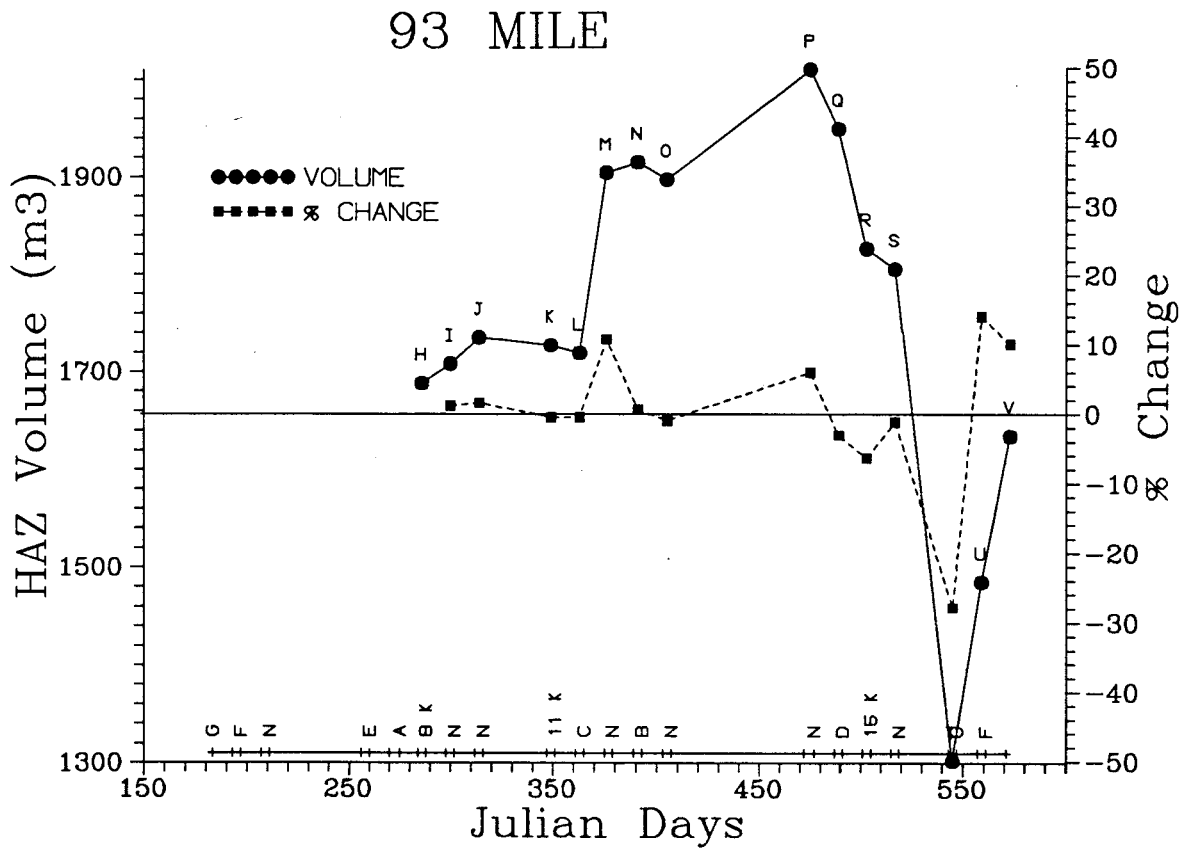


Table 3. (continued)

		MILE:	104	KILOMETER:	1672										
		BEACH #:	20	DEPOSIT TYPE:	UPPER POOL										
RUN ID	SURVEY DATE	TEST FLOW EVALUATED	JULIAN DAYS	HAZ AREA	HAZ VOL	AREA CH.	VOL CH.	AREA CH./DAY	% AREA CH.	% AREA CH./DAY	VOL CH./DAY	% VOL CH.	% VOL CH./DAY		
A		NORM													
B		NORM													
C		G													
D		F													
E		NORM													
F		NORM													
G	900929	E	272	348	594										
H	901013	A	286	350	583	2	-11	0.14	0.57	0.04	-0.79	-1.85	-0.13		
I	901027	8000 CFS	300	350	569	0	-14	0.00	0.00	0.00	-1.00	-2.40	-0.17		
J	901110	NORM	314	354	579	4	10	0.29	1.14	0.08	0.71	1.76	0.13		
K	901215	NORM	349	365	616	11	37	0.31	3.11	0.09	1.06	6.39	0.18		
L	901229	11000 CFS	363	379	621	14	5	1.00	3.84	0.27	0.36	0.81	0.06		
M	910113	C	378	331	546	-48	-75	-3.20	-12.66	-0.84	-5.00	-12.08	-0.81		
N	910126	NORM	391	354	559	23	13	1.77	6.95	0.53	1.00	2.38	0.18		
O	910209	B	405	361	559	7	0	0.50	1.98	0.14	0.00	0.00	0.00		
P	910420	NORM	475	342	561	-19	2	-0.27	-5.26	-0.06	0.03	0.36	0.01		
Q	910504	NORM	489	333	568	-9	7	-0.64	-2.63	-0.19	0.50	1.25	0.09		
R	910518	D	503	307	514	-26	-54	-1.86	-7.81	-0.56	-3.86	-9.51	-0.68		
S	910601	15000 CFS	517	333	535	26	21	1.86	8.47	0.60	1.50	4.09	0.29		
T	910629	NORM	545	380	649	47	114	1.68	14.11	0.50	4.07	21.31	0.76		
U	910713	G	559	305	479	-75	-170	-5.36	-19.74	-1.41	-12.14	-26.19	-1.87		
V	910727	F	573	391	601	86	122	6.14	28.20	2.01	8.71	20.30	1.82		

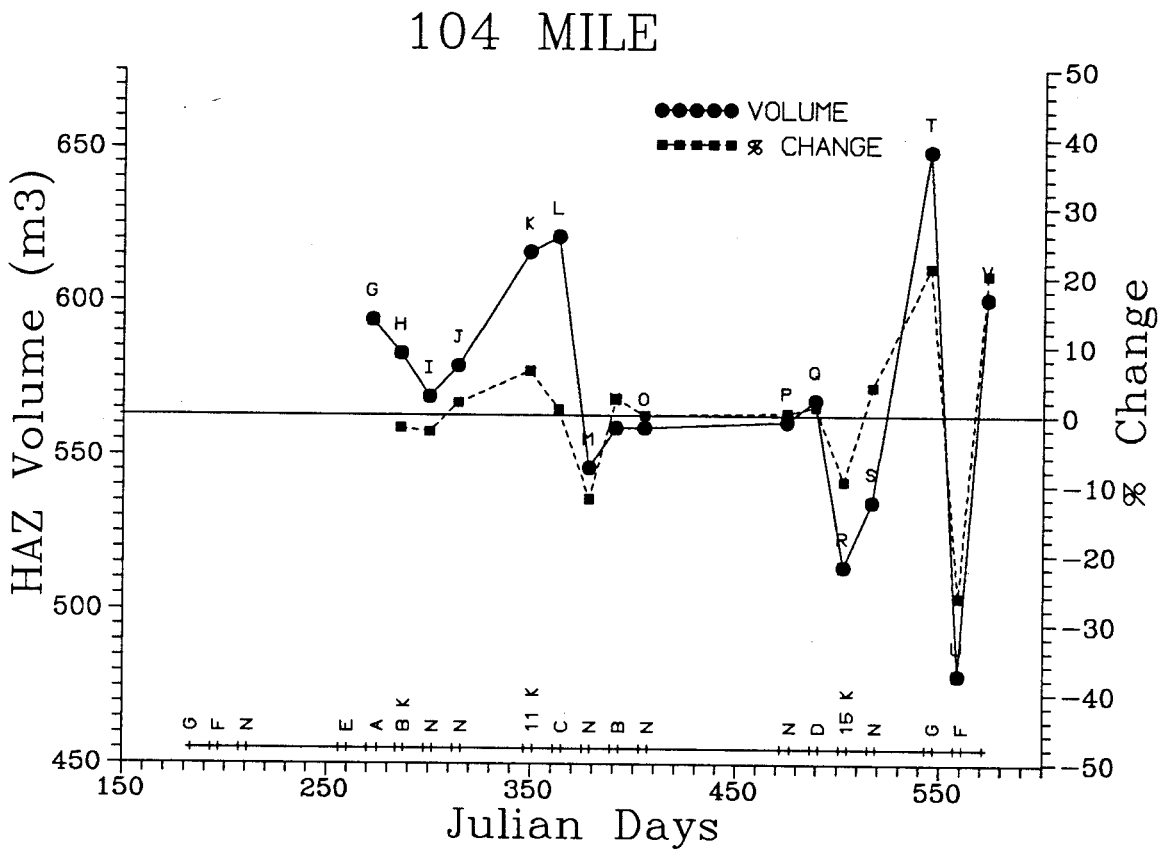


Table 3. (continued)

MILE: 119		KILOMETER: 1915											
BEACH #: 21		DEPOSIT TYPE: REATTACHMENT											
TEST													
RUN ID	SURVEY DATE	FLOW EVALUATED	JULIAN DAYS	HAZ AREA	HAZ VOL	AREA CH.	VOL. CH.	AREA CH./DAY	% AREA CH.	% AREA CH./DAY	% VOL CH./DAY	% VOL CH./DAY	% VOL CH./DAY
A		NORM											
B		NORM											
C		G											
D	900729	F											
E		NORM											
F	900916	NORM	259	2586	3809								
G	900930	E	273	2725	4273	139	464	9.93	5.38	0.38	33.14	12.18	0.87
H	901014	A	287	2556	4116	-169	-157	-12.07	-6.20	-0.44	-11.21	-3.67	-0.26
I	901028	8000 CFS	301	2454	4000	-102	-116	-7.29	-3.99	-0.29	-8.29	-2.82	-0.20
J	901111	NORM	315	2352	4005	-102	5	-7.29	-4.16	-0.30	0.36	0.13	0.01
K	901216	NORM	350	2260	3757	-92	-248	-2.63	-3.91	-0.11	-7.09	-6.19	-0.18
L		11000 CFS											
M	910113	C	378	2326	3780	66	23	2.36	2.92	0.10	0.82	0.61	0.02
N	910127	NORM	392	2252	3677	-74	-103	-5.29	-3.18	-0.23	-7.36	-2.72	-0.19
O	910210	B	406	2205	3619	-47	-58	-3.36	-2.09	-0.15	-4.14	-1.58	-0.11
P	910421	NORM	476	2093	3219	-112	-400	-1.60	-5.08	-0.07	-5.71	-11.05	-0.16
Q	910505	NORM	490	2036	3180	-57	-39	-4.07	-2.72	-0.19	-2.79	-1.21	-0.09
R	910519	D	504	2465	3807	429	627	30.64	21.07	1.51	44.79	19.72	1.41
S	910602	15000 CFS	518	2312	3655	-153	-152	-10.93	-6.21	-0.44	-10.86	-3.99	-0.29
T	910630	NORM	546	2709	4459	397	804	14.18	17.17	0.61	28.71	22.00	0.79
U	910714	G	560	2814	4822	105	363	7.50	3.88	0.28	25.93	8.14	0.58
V	910728	F	574	2792	4825	-22	3	-1.57	-0.78	-0.06	0.21	0.06	0.00

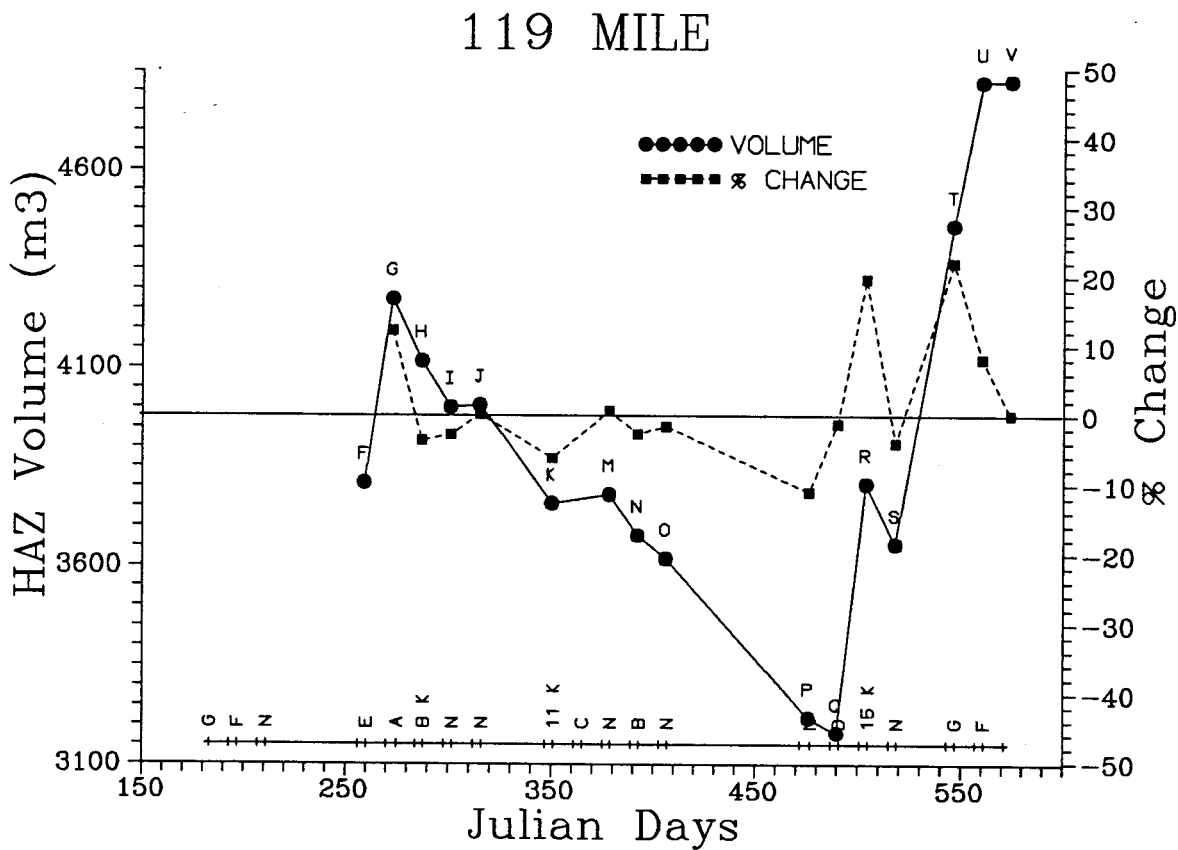


Table 3. (continued)

MILE: 122		KILOMETER: 196.5											
BEACH #: 22		DEPOSIT TYPE: REATTACHMENT											
RUN ID	SURVEY DATE	TEST FLOW EVALUATED	JULIAN DAYS	HAZ AREA	HAZ VOL	AREA CH.	VOL CH.	AREA CH./DAY	% AREA CH.	% AREA CH./DAY	VOL CH./DAY	% VOL CH.	% VOL CH./DAY
A		NORM											
B		NORM											
C		G											
D	900729	F	210	3642	4778								
E		NORM											
F	900917	NORM	260	3785	4988	143	210	2.86	3.93	0.08	4.20	4.40	0.09
G	901001	E	274	3779	5011	-6	23	-0.43	-0.16	-0.01	1.64	0.46	0.03
H	901014	A	287	3428	4987	-351	-24	-27.00	-9.29	-0.71	-1.85	-0.48	-0.04
I	901029	8000 CFS	302	3293	4921	-135	-66	-9.00	-3.94	-0.26	-4.40	-1.32	-0.09
J	901111	NORM	315	3215	4694	-78	-227	-6.00	-2.37	-0.18	-17.46	-4.61	-0.35
K	901216	NORM	350	3183	4480	-32	-214	-0.91	-1.00	-0.03	-6.11	-4.56	-0.13
L	901230	11000 CFS	364	3126	4327	-57	-153	-4.07	-1.79	-0.13	-10.93	-3.42	-0.24
M	910113	C	378	3332	4391	206	64	14.71	6.59	0.47	4.57	1.48	0.11
N	910127	NORM	392	3518	4420	186	29	13.29	5.58	0.40	2.07	0.66	0.05
O	910210	B	406	3491	4370	-27	-50	-1.93	-0.77	-0.05	-3.57	-1.13	-0.08
P	910421	NORM	476	3522	4472	31	102	0.44	0.89	0.01	1.46	2.33	0.03
Q	910505	NORM	490	3524	4431	2	-41	0.14	0.06	0.00	-2.93	-0.92	-0.07
R	910519	D	504	3645	4500	121	69	8.64	3.43	0.25	4.93	1.56	0.11
S	910602	15000 CFS	518	3895	4695	250	195	17.86	6.86	0.49	13.93	4.33	0.31
T	910630	NORM	546	3585	4870	-310	175	-11.07	-7.96	-0.28	6.25	3.73	0.13
U	910714	G	560	3498	5028	-87	158	-6.21	-2.43	-0.17	11.29	3.24	0.23
V	910728	F	574	3622	4928	124	-100	8.86	3.54	0.25	-7.14	-1.99	-0.14

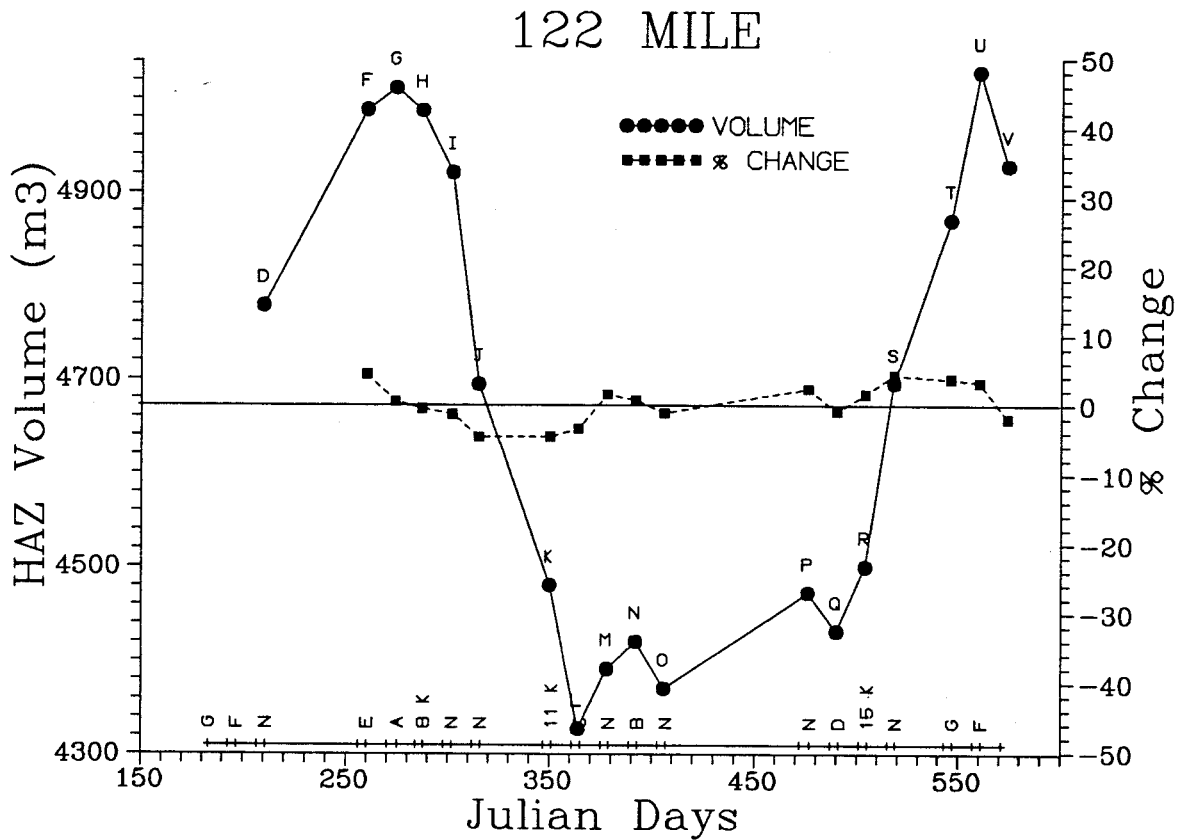


Table 3. (continued)

		MILE:	123	KILOMETER:	197.6									
		BEACH #:	23	DEPOSIT TYPE:	REATTACHMENT/UPPER POOL									
RUN ID	SURVEY DATE	TEST		JULIAN DAYS	HAZ AREA	HAZ VOL.	AREA CH.	VOL. CH.	AREA CH./DAY	% AREA CH.	% AREA CH./DAY	VOL. CH./DAY	% VOL. CH.	% VOL. CH./DAY
		FLOW EVALUATED												
A		NORM												
B		NORM												
C		G												
D		F												
E		NORM												
F	900917	NORM	260											
G	901001	E	274	1453	1469									
H	901015	A	288	1423	1424	-30	-45	-2.14	-2.06	-0.15	-3.21	-3.06	-0.22	
I		8000 CFS												
J	901112	NORM	316	1383	1369	-40	-55	-1.43	-2.81	-0.10	-1.96	-3.86	-0.14	
K	901217	NORM	351	1300	1231	-83	-138	-2.37	-6.00	-0.17	-3.94	-10.08	-0.29	
L	901231	11000 CFS	365	1322	1222	22	-9	1.57	1.69	0.12	-0.64	-0.73	-0.05	
M	910114	C	379	1481	1304	159	82	11.36	12.03	0.86	5.86	6.71	0.48	
N	910128	NORM	393	1477	1397	-4	93	-0.29	-0.27	-0.02	6.64	7.13	0.51	
O	910211	B	407	1450	1336	-27	-61	-1.93	-1.83	-0.13	-4.36	-4.37	-0.31	
P	910422	NORM	477	1495	1480	45	144	0.64	3.10	0.04	2.06	10.78	0.15	
Q	910506	NORM	491	1475	1449	-20	-31	-1.43	-1.34	-0.10	-2.21	-2.09	-0.15	
R	910520	D	505	1097	1073	-378	-376	-27.00	-25.63	-1.83	-26.86	-25.95	-1.85	
S	910603	15000 CFS	519	1084	1051	-13	-22	-0.93	-1.19	-0.08	-1.57	-2.05	-0.15	
T	910701	NORM	547	1501	1469	417	418	14.89	38.47	1.37	14.93	39.77	1.42	
U	910715	G	561	1181	1198	-320	-271	-22.86	-21.32	-1.52	-19.36	-18.45	-1.32	
V	910728	F	574	1280	1310	99	112	7.62	8.38	0.64	8.62	9.35	0.72	

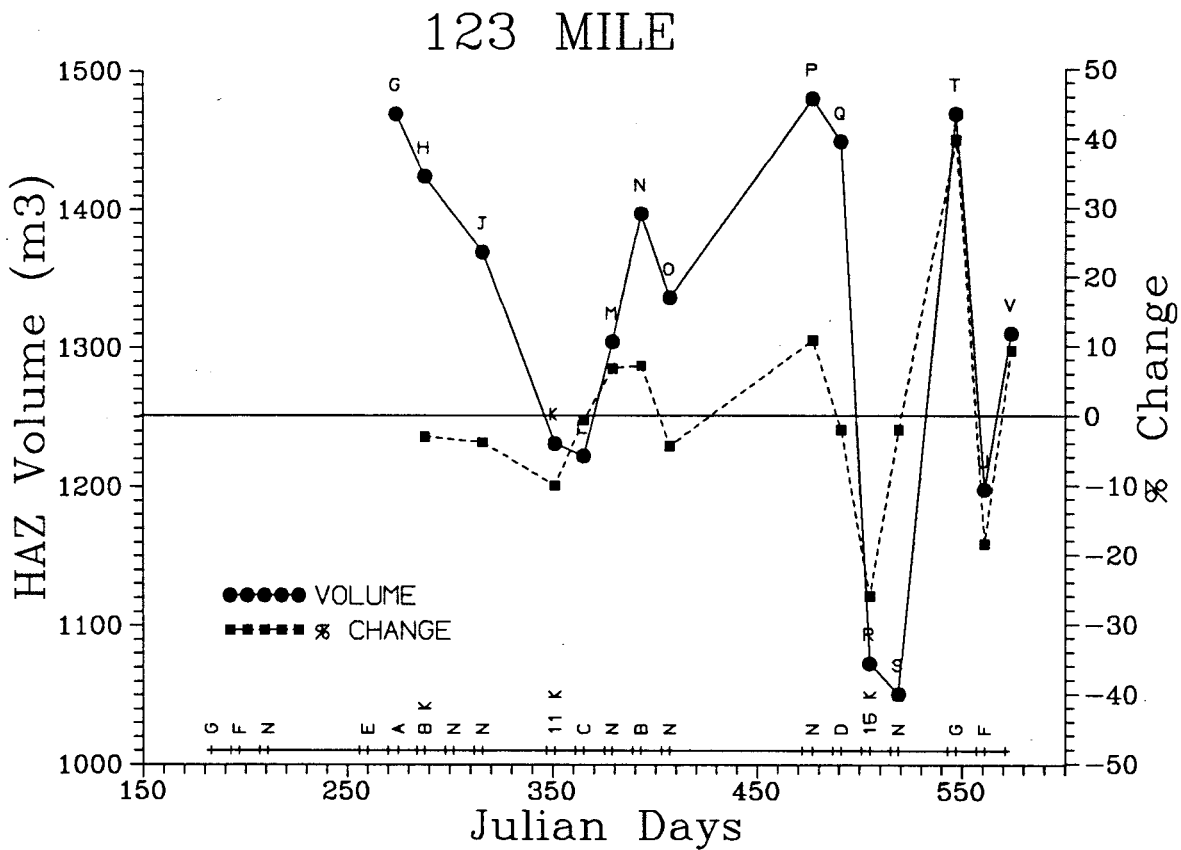


Table 3. (continued)

MILE: 137 KILOMETER: 220.4
 BEACH #: 24 DEPOSIT TYPE: REATTACHMENT

RUN ID	SURVEY DATE	TEST FLOW EVALUATED	JULIAN DAYS	HAZ AREA	HAZ VOL.	AREA CH.	VOL. CH.	AREA CH./DAY	% AREA CH.	% AREA CH./DAY	VOL CH./DAY	% VOL CH.	% VOL CH./DAY
A	900617	NORM	168	3025	4222								
B		NORM											
C	900716	G	197	2953	4537	-72	315	-2.48	-2.38	-0.08	10.86	7.46	0.26
D	900729	F	210	2957	4727	4	190	0.31	0.14	0.01	14.62	4.19	0.32
E		NORM											
F	900918	NORM	261	2976	4762	19	35	0.37	0.64	0.01	0.69	0.74	0.01
G	901002	E	275	2943	4827	-33	65	-2.36	-1.11	-0.08	4.64	1.36	0.10
H	901016	A	289	2923	4769	-20	-58	-1.43	-0.68	-0.05	-4.14	-1.20	-0.09
I	901029	8000 CFS	302	2905	4721	-18	-48	-1.38	-0.62	-0.05	-3.69	-1.01	-0.08
J	901113	NORM	317	2933	4914	28	193	1.87	0.96	0.06	12.87	4.09	0.27
K	901217	NORM	351	3012	4599	79	-315	2.32	2.69	0.08	-9.26	-6.41	-0.19
L	910101	11000 CFS	366	2989	4568	-23	-31	-1.53	-0.76	-0.05	-2.07	-0.67	-0.04
M	910114	C	379	3009	4422	20	-146	1.54	0.67	0.05	-11.23	-3.20	-0.25
N	910128	NORM	393	3016	4374	7	-48	0.50	0.23	0.02	-3.43	-1.09	-0.08
O	910211	B	407	3018	4371	2	-3	0.14	0.07	0.00	-0.21	-0.07	-0.00
P	910422	NORM	477	2943	4067	-75	-304	-1.07	-2.49	-0.04	-4.34	-6.95	-0.10
Q	910506	NORM	491	2953	4014	10	-53	0.71	0.34	0.02	-3.79	-1.30	-0.09
R	910520	D	505	2854	4661	-99	647	-7.07	-9.35	-0.24	46.21	16.12	1.15
S	910603	15000 CFS	519	2946	4379	92	-282	6.57	3.22	0.23	-20.14	-6.05	-0.43
T	910701	NORM	547	2831	4679	-115	300	-4.11	-3.90	-0.14	10.71	6.85	0.24
U	910715	G	561	2864	4917	33	238	2.36	1.17	0.08	17.00	5.09	0.36
V	910729	F	575	2924	4989	60	72	4.29	2.09	0.15	5.14	1.46	0.10

137 MILE

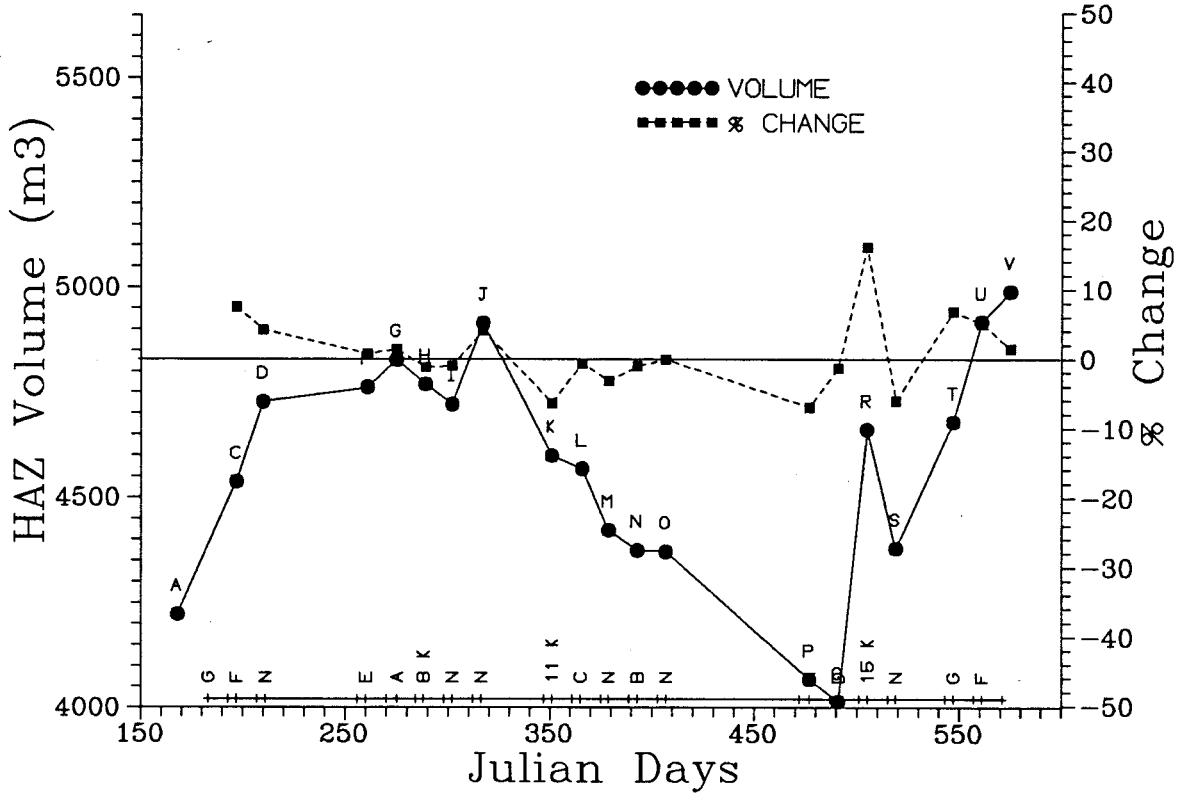


Table 3. (continued)

		MILE: 145		KILOMETER: 233										
		BEACH #: 26		DEPOSIT TYPE: REATTACHMENT										
RUN ID	SURVEY DATE	TEST		JULIAN DAYS	HAZ AREA	HAZ VOL.	AREA CH.	VOL. CH.	AREA CH./DAY	% AREA CH.	% AREA CH./DAY	VOL. CH./DAY	% VOL. CH.	% VOL. CH./DAY
		FLOW EVALUATED												
A		NORM												
B		NORM												
C	900716	G		197	531	781								
D	900730	F		212	536	846	5	65	0.33	0.94	0.06	4.33	8.32	0.55
E		NORM												
F	900915	NORM		258	540	820	4	-26	0.09	0.75	0.02	-0.57	-3.07	-0.07
G	900928	E		271	544	803	4	-17	0.31	0.74	0.06	-1.31	-2.07	-0.16
H	901013	A		286	520	787	-24	-16	-1.60	-4.41	-0.29	-1.07	-1.99	-0.13
I	901027	8000 CFS		300	515	803	-5	16	-0.36	-0.96	-0.07	1.14	2.03	0.15
J	901110	NORM		314	482	766	-33	-37	-2.36	-6.41	-0.46	-2.64	-4.61	-0.33
K	901215	NORM		349	491	725	9	-41	0.26	1.87	0.05	-1.17	-5.35	-0.15
L	901229	11000 CFS		363	482	735	-9	10	-0.64	-1.83	-0.13	0.71	1.38	0.10
M		C												
N	910125	NORM		390	528	745	46	10	1.70	9.54	0.35	0.37	1.36	0.05
O	910208	B		404	505	718	-23	-27	-1.64	-4.36	-0.31	-1.93	-3.62	-0.26
P	910420	NORM		475	535	793	30	75	0.42	5.94	0.08	1.06	10.45	0.15
Q	910504	NORM		489	481	658	-54	-135	-3.86	-10.09	-0.72	-9.64	-17.02	-1.22
R	910518	D		503	545	804	64	146	4.57	13.31	0.95	10.43	22.19	1.58
S	910601	15000 CFS		517	549	788	4	-16	0.29	0.73	0.05	-1.14	-1.99	-0.14
T	910629	NORM		545	566	913	17	125	0.61	3.10	0.11	4.46	15.86	0.57
U	910713	G		559	576	946	10	33	0.71	1.77	0.13	2.36	3.61	0.26
V	910727	F		573	581	928	5	-18	0.36	0.87	0.06	-1.29	-1.94	-0.14

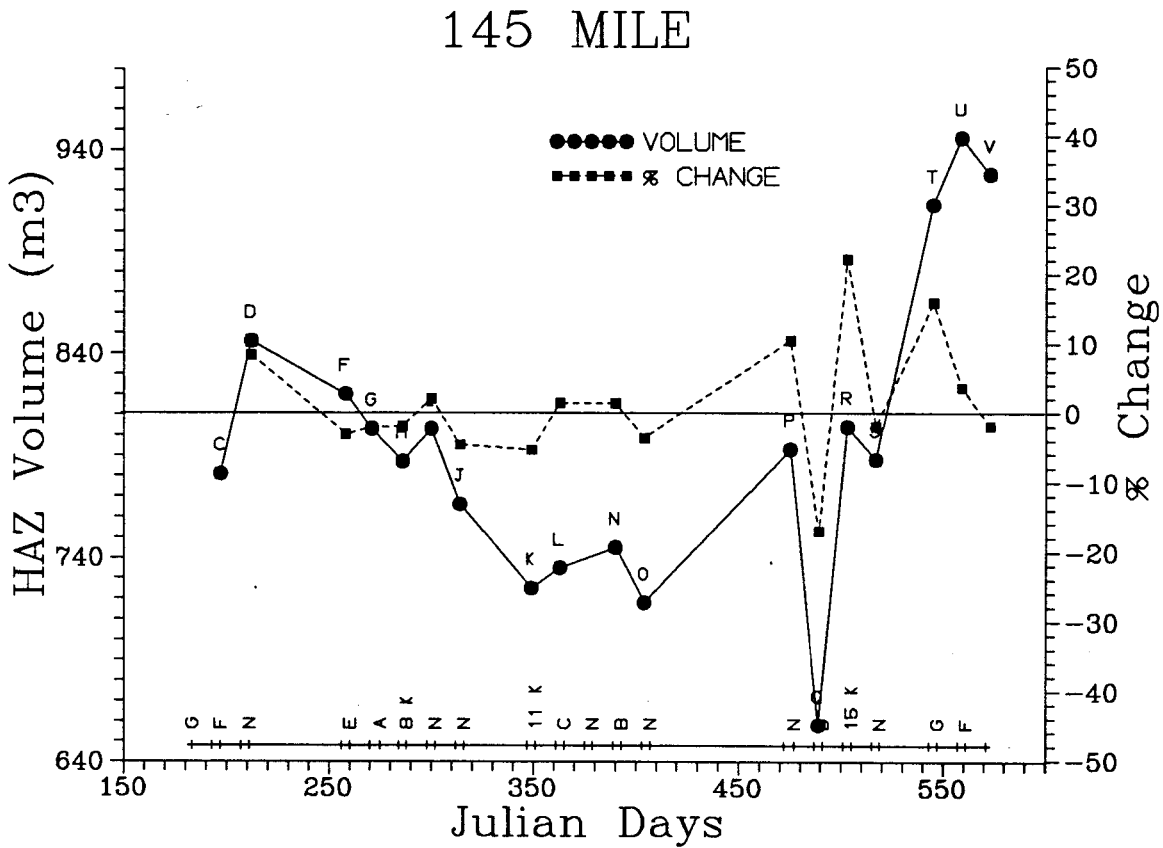


Table 3. (continued)

		MILE:	172	KILOMETER:	276.9								
		BEACH #:	27	DEPOSIT TYPE:	REATTACH/UPPER POOL								
RUN ID	SURVEY DATE	TEST FLOW EVALUATED	JULIAN DAYS	HAZ AREA	HAZ VOL.	AREA CH.	VOL. CH.	AREA CH./DAY	% AREA CH.	% AREA CH./DAY	VOL CH./DAY	% VOL CH.	% VOL CH./DAY
A	900618	NORM	169	2370	2583								
B		NORM											
C	900717	G	198	2451	2912	81	329	2.79	3.42	0.12	11.34	12.74	0.44
D	900731	F	212	2379	2963	-72	51	-5.14	-2.94	-0.21	3.64	1.75	0.13
E	900908	NORM	251	2380	2970	1	7	0.03	0.04	0.00	0.18	0.24	0.01
F	900916	NORM	259	1363	1248	-1017	-1722	-127.13	-42.73	-5.34	-215.25	-57.98	-7.25
G		E											
H	901014	A	287	1798	1807	435	559	15.54	31.91	1.14	19.96	44.79	1.60
I	901028	8000 CFS	301	1799	1757	1	-50	0.07	0.06	0.00	-3.57	-2.77	-0.20
J	901111	NORM	315	1822	1779	23	22	1.64	1.28	0.09	1.57	1.25	0.09
K	901216	NORM	350	1885	1893	63	114	1.80	3.46	0.10	3.26	6.41	0.18
L	901230	11000 CFS	364	1850	1775	-35	-118	-2.50	-1.86	-0.13	-8.43	-6.23	-0.45
M	910112	C	377	1169	1219	-681	-556	-52.38	-36.81	-2.83	-42.77	-31.32	-2.41
N	910126	NORM	391	1252	1254	83	35	5.93	7.10	0.51	2.50	2.87	0.21
O	910209	B	405	1240	1256	-12	2	-0.86	-0.96	-0.07	0.14	0.16	0.01
P	910420	NORM	475	1556	1430	316	174	4.51	25.48	0.36	2.49	13.85	0.20
Q	910504	NORM	489	1669	1586	113	156	8.07	7.26	0.52	11.14	10.91	0.78
R	910518	D	503	1653	1881	-16	295	-1.14	-0.96	-0.07	21.07	18.60	1.33
S	910602	15000 CFS	518	1776	2036	123	155	8.20	7.44	0.50	10.33	8.24	0.55
T	910629	NORM	545	1754	1834	-22	-202	-0.81	-1.24	-0.05	-7.48	-9.92	-0.37
U	910714	G	560	1461	1419	-293	-415	-19.53	-16.70	-1.11	-27.67	-22.63	-1.51
V	910728	F	574	1803	1648	342	229	24.43	23.41	1.67	16.36	16.14	1.15

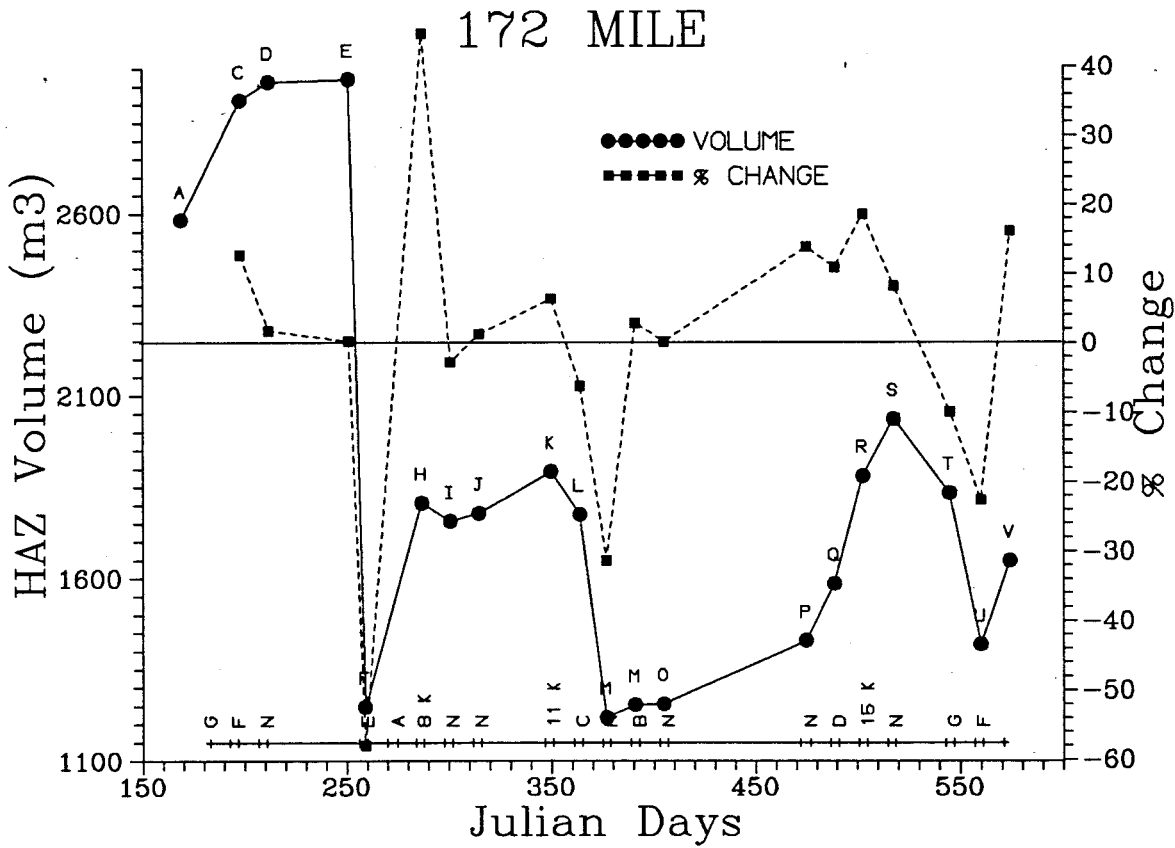


Table 3. (continued)

MILE: 183 KILOMETER: 295.3
 BEACH #: 28 DEPOSIT TYPE: REATTACH/UPPER POOL

RUN ID	SURVEY DATE	TEST FLOW EVALUATED	JULIAN DAYS	HAZ AREA	HAZ VOL	AREA CH.	VOL. CH.	AREA CH./DAY	% AREA CH./DAY	% AREA CH./DAY	VOL CH./DAY	% VOL CH./DAY
A		NORM										
B		NORM										
C		G										
D		F										
E		NORM										
F		NORM										
G		E										
H	901014	A	287	2067	2880							
I	901028	8000 CPS	301	1856	2620	-211	-260	-15.07	-10.21	-0.73	-18.57	-9.03
J	901111	NORM	315	1820	2615	-36	-5	-2.57	-1.94	-0.14	-0.36	-0.19
K	901216	NORM	350	1893	2426	73	-189	2.09	4.01	0.11	-5.40	-7.23
L	901230	11000 CPS	364	1948	2554	55	128	3.93	2.91	0.21	9.14	5.28
M	910112	C	377	2102	2780	154	226	11.85	7.91	0.61	17.38	8.85
N	910128	NORM	393	2073	2736	-29	-44	-1.81	-1.38	-0.09	-2.75	-1.58
O	910210	B	406	2054	2637	-19	-99	-1.46	-0.92	-0.07	-7.62	-3.62
P	910421	NORM	476	2145	2703	91	66	1.30	4.43	0.06	0.94	2.50
Q	910506	NORM	491	2123	2680	-22	-23	-1.47	-1.03	-0.07	-1.53	-0.85
R	910519	D	504	2242	3364	119	684	9.15	5.61	0.43	52.62	25.52
S	910602	15000 CPS	518	2245	3098	3	-266	0.21	0.13	0.01	-19.00	-7.91
T	910630	NORM	546	2172	3195	-73	97	-2.61	-3.25	-0.12	3.46	3.13
U	910714	G	560	2108	2948	-64	-247	-4.57	-2.95	-0.21	-17.64	-7.73
V	910728	F	574	2106	2701	-2	-247	-0.14	-0.09	-0.01	-17.64	-8.38

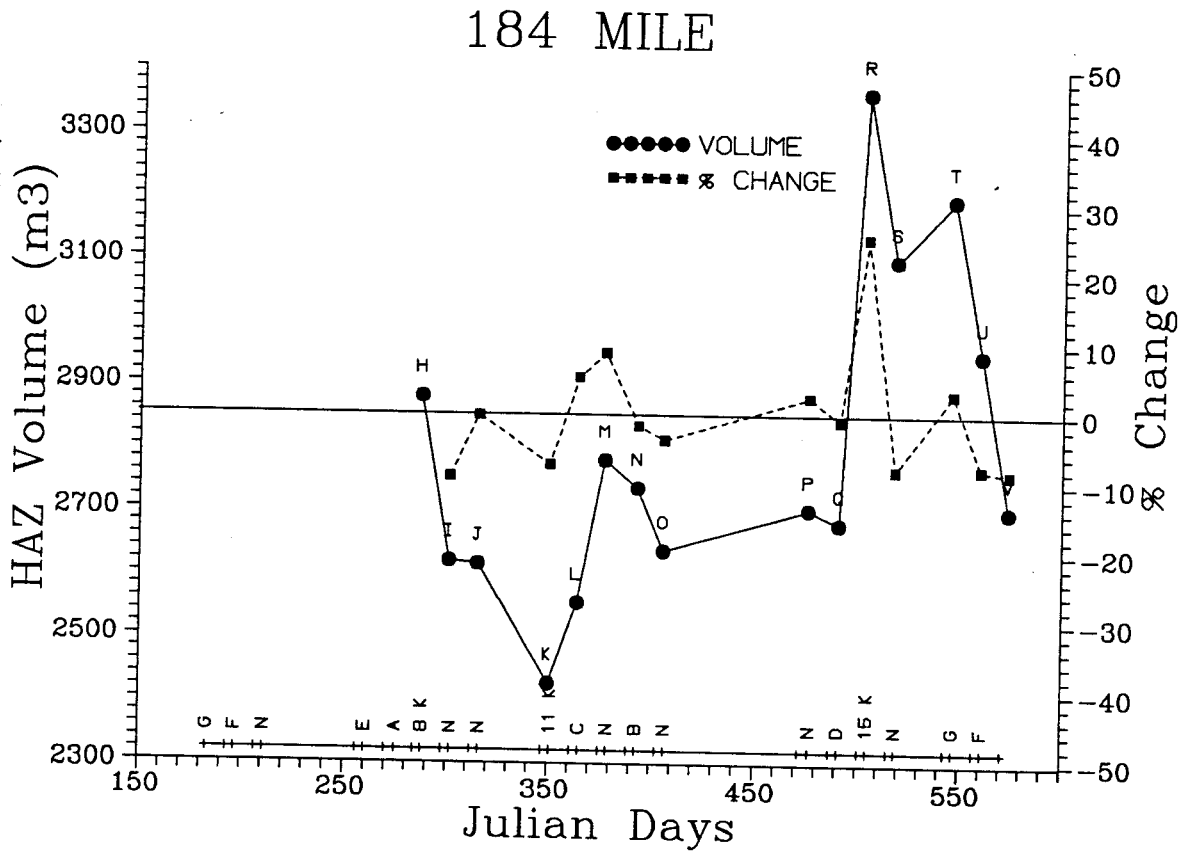


Table 3. (continued)

MILE:		194		KILOMETER:		312							
BEACH #:		29		DEPOSIT TYPE:		REATTACHMENT							
RUN ID	SURVEY DATE	TEST FLOW EVALUATED	JULIAN DAYS	HAZ	HAZ	AREA	VOL.	AREA	%	% AREA	VOL	%	% VOL
				AREA	VOL.	CH.	CH.	CH./DAY	AREA CH.	CH./DAY	CH./DAY	VOL CH.	CH./DAY
A		NORM											
B		NORM											
C	900717	G	198	3025	3524								
D	900731	F	212	3049	3704	24	180	1.71	0.79	0.06	12.86	5.11	0.36
E		NORM											
F	900917	NORM	260	3245	4102	196	398	4.08	6.43	0.13	8.29	10.75	0.22
G	901002	E	275	3384	4235	139	133	9.27	4.28	0.29	8.87	3.24	0.22
H	901015	A	288	3392	4163	8	-72	0.62	0.24	0.02	-5.54	-1.70	-0.13
I	901029	8000 CFS	302	3379	4343	-13	180	-0.93	-0.38	-0.03	12.86	4.32	0.31
J	901112	NORM	316	3303	4231	-76	-112	-5.43	-2.25	-0.16	-8.00	-2.58	-0.18
K	901217	NORM	351	3154	4171	-149	-60	-4.26	-4.51	-0.13	-1.71	-1.42	-0.04
L	901231	11000 CFS	365	3075	4163	-79	-8	-5.64	-2.50	-0.18	-0.57	-0.19	-0.01
M	910113	C	378	3245	4209	170	46	13.08	5.53	0.43	3.54	1.10	0.08
N	910127	NORM	392	3228	4136	-17	-73	-1.21	-0.52	-0.04	-5.21	-1.73	-0.12
O	910210	B	406	3156	3938	-72	-198	-5.14	-2.23	-0.16	-14.14	-4.79	-0.34
P	910421	NORM	476	3122	4007	-34	69	-0.49	-1.08	-0.02	0.99	1.75	0.03
Q	910506	NORM	491	3120	4061	-2	54	-0.13	-0.06	-0.00	3.60	1.35	0.09
R	910520	D	505	3221	4291	101	230	7.21	3.24	0.23	16.43	5.66	0.40
S	910603	15000 CFS	519	3353	4336	132	45	9.43	4.10	0.29	3.21	1.05	0.07
T	910630	NORM	546	3344	4456	-9	120	-0.33	-0.27	-0.01	4.44	2.77	0.10
U	910715	G	561	3210	4301	-134	-155	-8.93	-4.01	-0.27	-10.33	-3.48	-0.23
V	910729	F	575	3284	4357	74	56	5.29	2.31	0.16	4.00	1.29	0.09

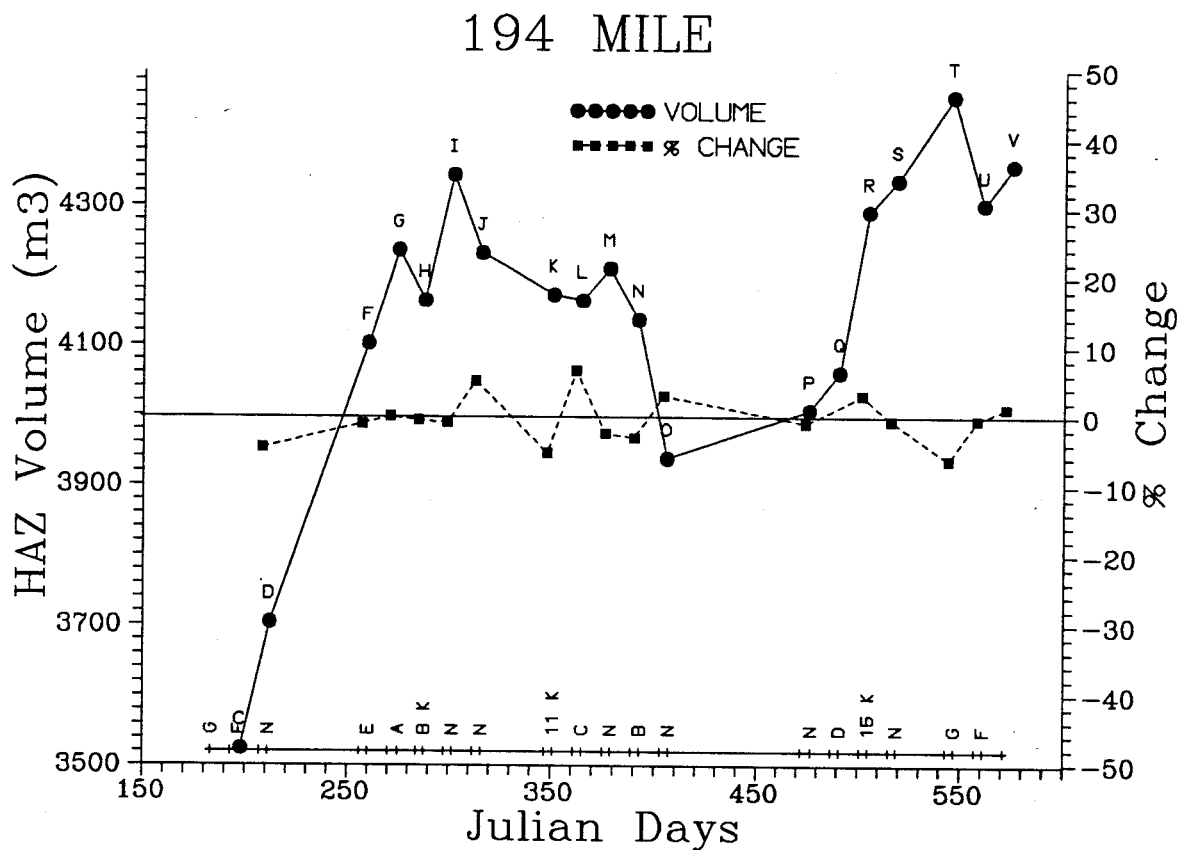


Table 3. (continued)

MILE: 203		KILOMETER: 325											
BEACH #: 30		DEPOSIT TYPE:		SEPARATION									
RUN ID	SURVEY DATE	TEST FLOW EVALUATED	JULIAN DAYS	HAZ AREA	HAZ VOL.	AREA CH.	VOL. CH.	AREA CH./DAY	% AREA CH.	% AREA CH./DAY	VOL. CH./DAY	% VOL. CH.	% VOL. CH./DAY
A		NORM											
B		NORM											
C		G											
D		F											
E		NORM											
F		NORM											
G		E											
H	901016	A	289	2089	3570								
I	901030	8000 CFS	303	2060	3528	-29	-42	-2.07	-1.39	-0.10	-2.07	-1.18	-0.08
J	901113	NORM	317	2131	3588	71	60	5.07	3.45	0.25	5.07	1.70	0.12
K	901218	NORM	352	2142	3527	11	-61	0.31	0.52	0.01	0.31	-1.70	-0.05
L	910101	11000 CFS	366	2158	3458	16	-69	1.14	0.75	0.05	1.14	-1.96	-0.14
M	910114	C	379	2213	3596	55	138	4.23	2.55	0.20	4.23	3.99	0.31
N	910128	NORM	393	2246	3573	33	-23	2.36	1.49	0.11	2.36	-0.64	-0.05
O	910211	B	407	2263	3619	17	46	1.21	0.76	0.05	1.21	1.29	0.09
P	910422	NORM	477	2328	3591	65	-28	0.93	2.87	0.04	0.93	-0.77	-0.01
Q	910506	NORM	491	2328	3653	0	62	0.00	0.00	0.00	0.00	1.73	0.12
R	910520	D	505	2445	3899	117	246	8.36	5.03	0.36	8.36	6.73	0.48
S	910603	15000 CFS	519	2410	3861	-35	-38	-2.50	-1.43	-0.10	-2.50	-0.97	-0.07
T	910701	NORM	547	2132	3605	-278	-256	-9.93	-11.54	-0.41	-9.93	-6.63	-0.24
U	910715	G	561	2224	3726	92	121	6.57	4.32	0.31	6.57	3.36	0.24
V	910729	F	575	2230	3710	6	-16	0.43	0.27	0.02	0.43	-0.43	-0.03

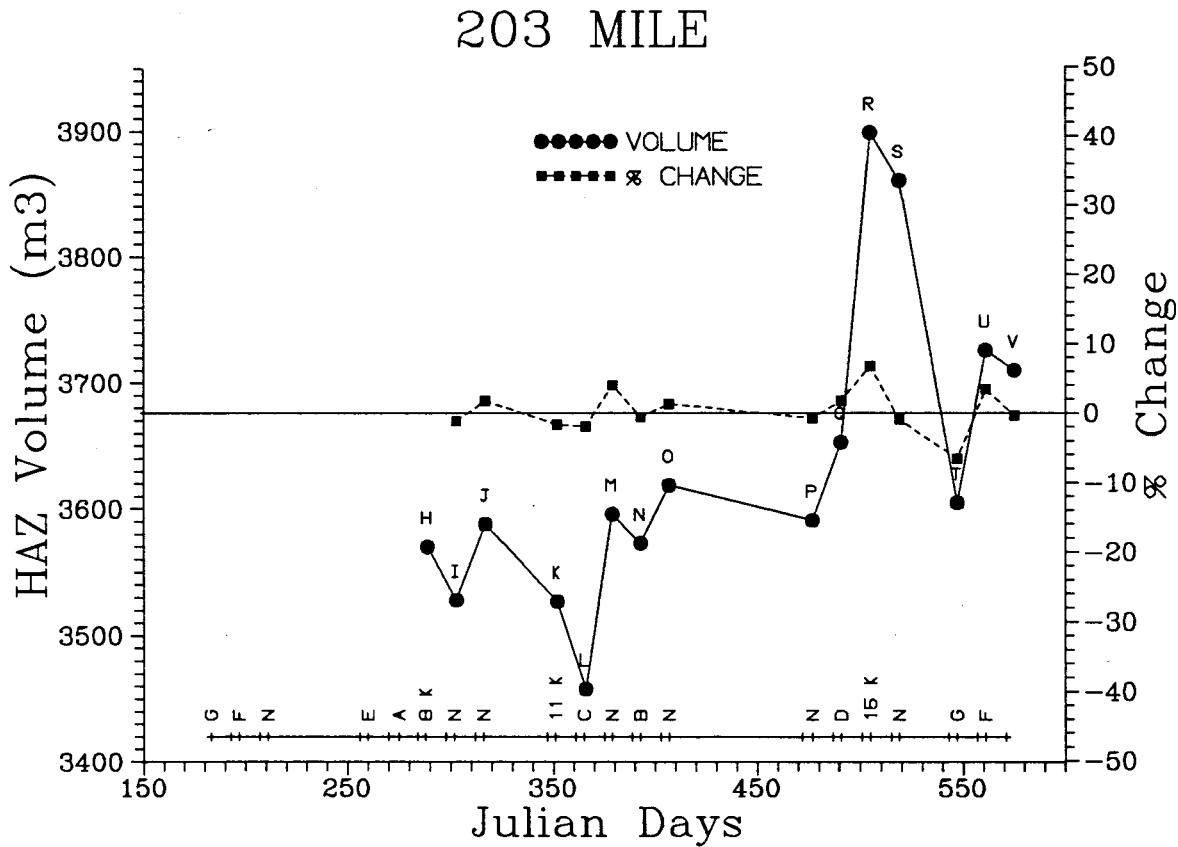


Table 3. (continued)

MILE: 213		KILOMETER: 342.7											
BEACH #: 31		DEPOSIT TYPE: REATTACHMENT/UPPER POOL											
RUN ID	SURVEY DATE	TEST FLOW EVALUATED	JULIAN DAYS	HAZ AREA	HAZ VOL.	AREA CH.	VOL. CH.	AREA CH./DAY	% AREA CH.	% AREA CH./DAY	VOL CH./DAY	% VOL CH.	% VOL CH./DAY
A		NORM											
B		NORM											
C		G											
D		F											
E		NORM											
F	900918	NORM	261	1600	3587								
G		E											
H	901017	A	290	1859	3775	259	188	8.93	16.19	0.56	6.48	5.24	0.18
I	901031	8000 CFS	304	1736	3701	-123	-74	-8.79	-6.62	-0.47	-5.29	-1.96	-0.14
J	901113	NORM	317	1789	3903	53	202	4.08	3.05	0.23	15.54	5.46	0.42
K	901218	NORM	352	1820	3810	31	-93	0.89	1.73	0.05	-2.66	-2.38	-0.07
L	910101	11000 CFS	366	1823	3840	3	30	0.21	0.16	0.01	2.14	0.79	0.06
M	910114	C	379	1887	4166	64	326	4.92	3.51	0.27	25.08	8.49	0.65
N	910128	NORM	393	1904	4179	17	13	1.21	0.90	0.06	0.93	0.31	0.02
O	910211	B	409	1911	4137	7	-42	0.44	0.37	0.02	-2.63	-1.01	-0.06
P	910422	NORM	477	1588	3627	-323	-510	-4.75	-16.90	-0.25	-7.50	-12.33	-0.18
Q	910507	NORM	492	1622	3585	34	-42	2.27	2.14	0.14	-2.80	-1.16	-0.08
R	910521	D	506	1774	4080	152	495	10.86	9.37	0.67	35.36	13.81	0.99
S	910604	15000 CFS	520	1805	4138	31	58	2.21	1.75	0.12	4.14	1.42	0.10
T	910701	NORM	547	1842	4504	37	366	1.37	2.05	0.08	13.56	8.84	0.33
U	910716	G	562	1987	5077	145	573	9.67	7.87	0.52	38.20	12.72	0.85
V	910729	F	575	1334	2772	-653	-2305	-50.23	-32.86	-2.53	-177.31	-45.40	-3.49

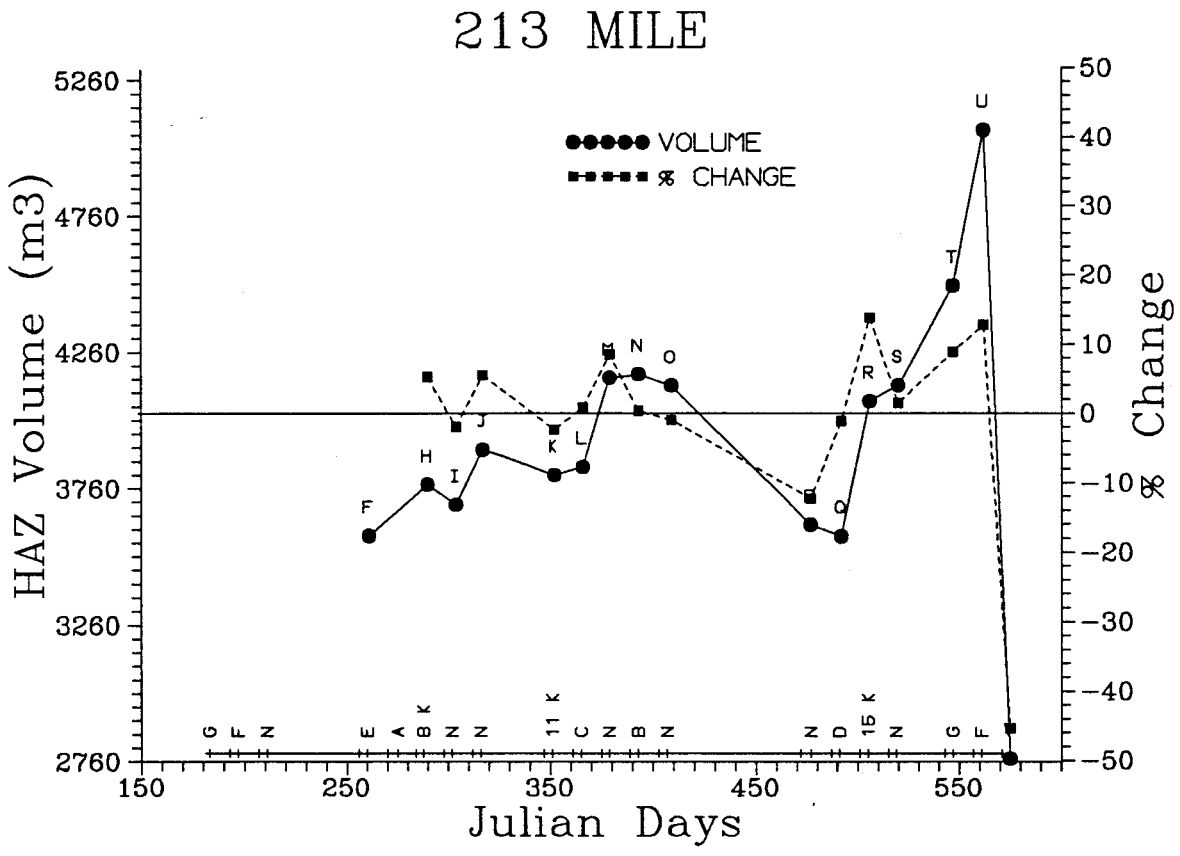


Table 3. (continued)

MILE: 220		KILOMETER: 353.8											
BEACH #: 32		DEPOSIT TYPE: SEPARATION/UPPER POOL											
RUN ID	SURVEY DATE	TEST FLOW EVALUATED	JULIAN DAYS	HAZ AREA	HAZ VOL.	AREA CH.	VOL. CH.	AREA CH./DAY	% AREA CH.	% AREA CH./DAY	VOL. CH./DAY	% VOL. CH.	% VOL. CH./DAY
A		NORM											
B		NORM											
C	900718	G	199	726	1080								
D		F											
E		NORM											
F	900918	NORM	261	696	1078	-30	-2	-0.48	-4.13	-0.07	-0.03	-0.19	-0.00
G	901003	E	276	715	1143	19	65	1.27	2.73	0.18	4.33	6.03	0.40
H	901017	A	290	711	1135	-4	-8	-0.29	-0.56	-0.04	-0.57	-0.70	-0.05
I	901031	8000 CFS	304	726	1118	15	-17	1.07	2.11	0.15	-1.21	-1.50	-0.11
J	901114	NORM	318	715	1120	-11	2	-0.79	-1.52	-0.11	0.14	0.18	0.01
K	901219	NORM	353	741	1094	26	-26	0.74	3.64	0.10	-0.74	-2.32	-0.07
L	910102	11000 CFS	367	776	1153	35	59	2.50	4.72	0.34	4.21	5.39	0.39
M	910115	C	380	721	1064	-55	-89	-4.23	-7.09	-0.55	-6.85	-7.72	-0.59
N	910129	NORM	394	737	1063	16	-1	1.14	2.22	0.16	-0.07	-0.09	-0.01
O	910212	B	408	749	1038	12	-25	0.86	1.63	0.12	-1.79	-2.35	-0.17
P	910423	NORM	478	732	1086	-17	48	-0.24	-2.27	-0.03	0.69	4.62	0.07
Q	910507	NORM	492	666	913	-66	-173	-4.71	-9.02	-0.64	-12.36	-15.93	-1.14
R	910521	D	506	714	1036	48	123	3.43	7.21	0.51	8.79	13.47	0.96
S	910604	15000 CFS	520	735	1053	21	17	1.50	2.94	0.21	1.21	1.64	0.12
T	910702	NORM	548	721	1153	-14	100	-0.50	-1.90	-0.07	3.57	9.50	0.34
U	910716	G	562	706	1137	-15	-16	-1.07	-2.08	-0.15	-1.14	-1.39	-0.10
V	910730	F	576	718	1190	12	53	0.86	1.70	0.12	3.79	4.45	0.33

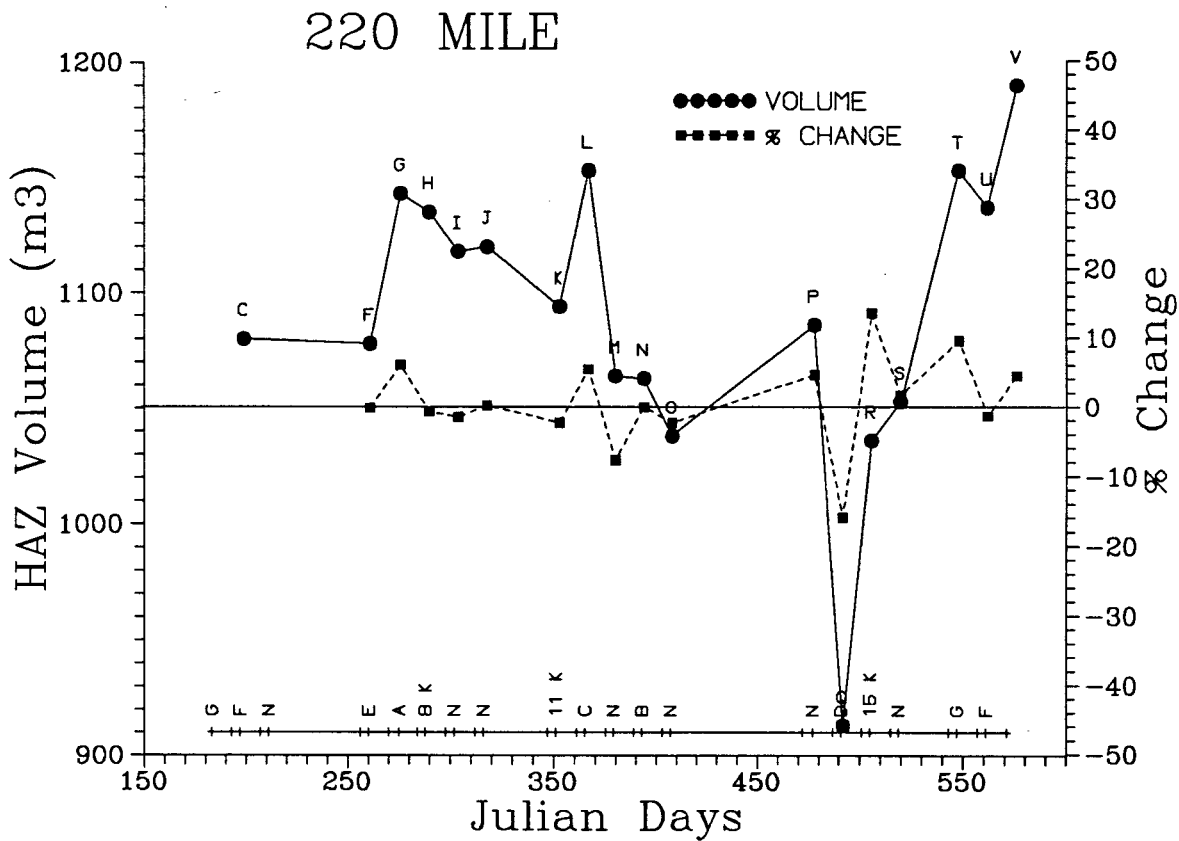


Table 4. (continued)

STUDY SITES (%VCR)

TEST FLOW EVALUATED	JULIAN DAY	109.6	130.5	140.8	146.6	149.6	167.2	191.5	196.5	197.6	220.4	223	276.9
		68	81	87	91	93	104	119	122	123	137	145	172
G	196										1.153		0.439
F	210	-0.969	0.109								-1.238	0.555	0.125
NORM	251												0.006
NORM	259												-7.247
E	273								0.088				
A	287	3.858	0.259		-0.153			0.870	0.033		0.097	-0.159	
8000	301	0.862	-1.092		0.000		-0.132	-0.257	-0.037	-0.219	-0.086	-0.133	
FALL	315	-0.205	-0.281	-0.035	-0.039	0.085	-0.172	-0.206	-0.088		-0.077	0.145	
NORM	350	-0.587	-0.097	-0.317	-0.236	0.113	0.126	0.009	-0.355		0.273	-0.329	0.089
11000	362	0.039	-0.322	0.308	0.166	-0.013	0.183	-0.177	-0.130	-0.288	-0.189	-0.153	0.183
C	378	-0.051	-0.991	-1.240	0.549	-0.033	0.058		-0.244	-0.052	-0.045	0.099	-0.445
WINTER	392	0.129	1.413	1.518	0.646	0.828	-0.805		0.106	0.479	-0.246		-2.410
B	406	-0.220	-1.389	-0.041	0.299	0.183	0.183	-0.195	0.047	0.509	-0.078		0.205
NORM	475	0.020	-0.486	-0.041	-0.510	-0.067	0.000	-0.113	-0.081	-0.312	-0.005	0.147	0.011
SPRING	489	-0.086	-0.021	0.143	-0.151	0.085	0.005	-0.158	0.033	0.154	-0.093	-1.216	0.198
D	503	0.415	0.212	0.175	-0.230	-0.217	0.089	-0.087	-0.065	-0.150	-0.093	-1.216	0.779
15000	518	-0.907	5.601	-0.244	2.063	-0.451	-0.679	1.408	0.111	-1.853	1.151	1.585	1.329
SUMMER	546	0.558	-1.930	0.253	-1.724	-0.082	0.292	-0.285	0.310	-0.146	-0.432	-0.142	0.549
G	559	0.162	1.845	-0.317	1.806	-0.995	0.761	0.786	0.133	1.420	0.245	0.567	-0.367
F	574	1.151			-1.538	1.004	-1.879	0.581	0.232	-1.318	0.363	0.258	-1.509
avg		-0.333			0.912	0.717	1.819	0.004	-0.142	0.719	0.105	-0.136	1.153
std		0.226	0.189	0.013	0.116	0.072	-0.010	0.156	-0.003	-0.081	0.044	0.072	-0.384
se		1.055	1.725	0.600	0.959	0.494	0.764	0.511	0.162	0.804	0.514	0.570	1.865
		0.256	0.445	0.173	0.240	0.132	0.197	0.137	0.039	0.223	0.121	0.147	0.440
Vol (Oct., 1990)		3827	369	495	182	1708	569	4000	4921	1424 *	4721	803	1757
Vol (July, 1991)		3723	537	493	241	1634	601	4825	4928	1310	4989	928	1648
Vol. Change (m3)		-104	168	-2	59	-74	32	825	7	-114	4989	125	-109

* 'A' flow data

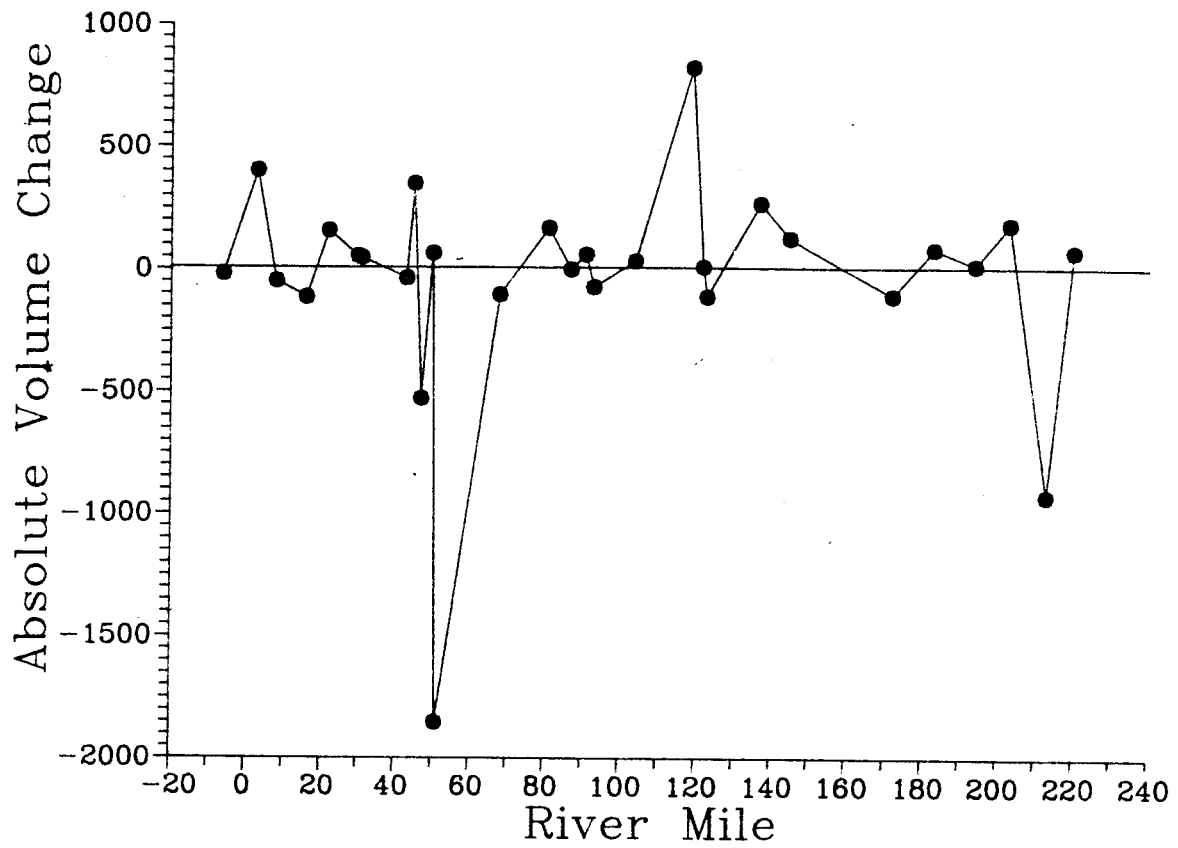


Figure 6. Net HAZ volume change occurring from Oct.26, 1990 to July 30, 1991 in relation to distance downstream from Lees Ferry, AZ.

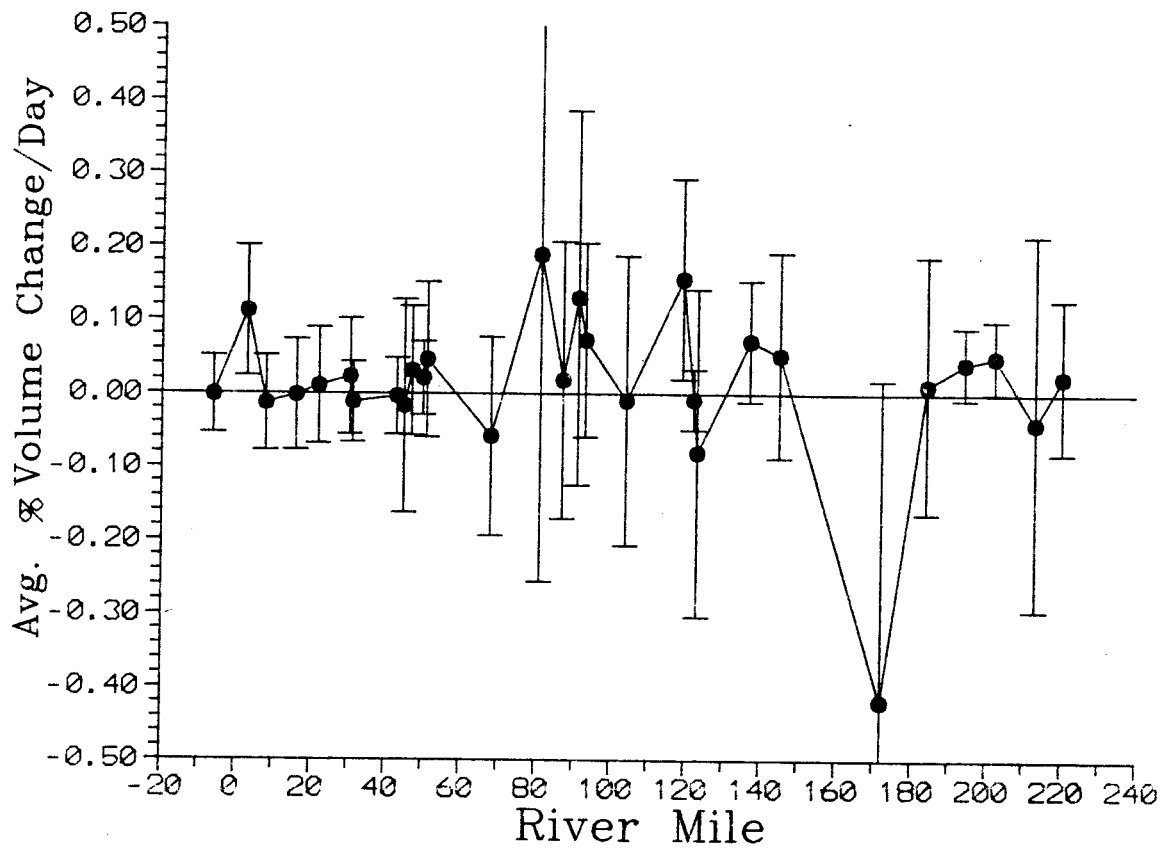


Figure 7. Average percent HAZ volume change/day for 29 Colorado River study sites as a function of distance downstream from Lees Ferry, Arizona.

Effects of Test Flows on Sand Bars

Mean %VCR varied significantly between test flows among this group of 29 sand bars (Figures 8-10; (Friedman $t = 53.254$, $p < 0.001$, $df = 15$). An *a posteriori* multiple comparison test (Conover 1980:300) demonstrated that several large-fluctuation test flows ("E", "Normal Summer" and "F2") exerted significantly different impacts on the 29 study sites, as compared to several low fluctuation or constant test flows ("B", normal spring, "Normal Spring" and "Constant 15,000 cfs" flows). These high fluctuation flows resulted in net aggradation, whereas the low fluctuation or constant test flows resulted in neutral or slight net degradation among the study sites. The other flow tests resulted in little net change of %VCR among the sand bars. Figure 8 displays the mean %VCR (open circles) and one standard error of the mean for all sand bars surveyed during each test flow, with each data point representing %VCR for the previous flow. For example, the mean %VCR during flow "E" was 0.34, as measured just prior to the beginning of the "A" flow.

We compared test flow effects on pooled sand bar responses ($n = 12$) in the upper canyon reach above the Little Colorado River (a reach with a limited sediment supply) with responses of downstream sand bars ($n = 17$) to determine whether sediment availability influenced patterns of sand bar dynamics (Figures 9 and 10). Both reaches revealed similar patterns to those obtained using grand mean data; however, the upper reach was far less dynamic in relation to the test flows than was the lower reach. This observation suggests that increased sediment availability interacts with the discharge regime to create the dynamics of recirculation zone sediment distribution.

Limited aggradation occurred during late summer and early fall months in 1990, slight degradation took place during test flows in the winter of 1990-1991, and both aggradation and degradation occurred during spring and summer in 1991. Although more than half of the sand bars showed neutral or net gain in sand between September, 1990 and July, 1991, more than 10 percent of those sand bars studied continued to degrade. A significant proportion of sand bars remaining in this system may be lost under fluctuating flow regimes with limited sediment availability.

Effects of test flows on sand bars was not uniformly predictable, as demonstrated by the Friedman analysis. Aggradation was observed following three of the five high fluctuation flows (E, D, and normal summer, 1991), whereas one of the high fluctuation flows ("G" in 1991) was strongly degradational and the other ("F" in 1991) resulted in little net change. A major loss of sand at Mile 172L, involving the loss of more than 50% of the HAZ sand volume, occurred during normal flows in September, 1990 (Cluer, this report), while other sand bars in that reach showed aggradation or no net change during the same period.

Each of the three prolonged constant flows resulted in net erosion of HAZ sand volume (Table 4, Figure 6). Field observers during these flow tests reported cutbanks on bar faces throughout the river corridor, suggesting that oversteepened bars were subject to undercutting and subsequent sloughing. The effects of the three levels of constant discharge were approximately equivalent, suggesting no increase in erosion across a low to moderate range of constant discharges. By 31 July, 1991, many of the sand bars of the Colorado River corridor had degraded after several repeated high-fluctuation flow tests.

We documented rapid bank failure during a $141 \text{ m}^3/\text{sec}$ constant evaluation test flow on the 45 Mile reattachment bar (Figure 5). The upstream portion of the sand bar failed on the night of May 6, 1991 during the "constant 5,000 cfs" evaluation flow. Gradual bar rebuilding was observed during the high fluctuations of the subsequent 11-day "D" flow on this site, although the rebuilding was within the range of survey error established during that period. This failure event conformed to the seepage-driven bank failure phenomenon predicted by Budhu (this report) and documented by Carpenter et al. (this report) and Cluer (this report).

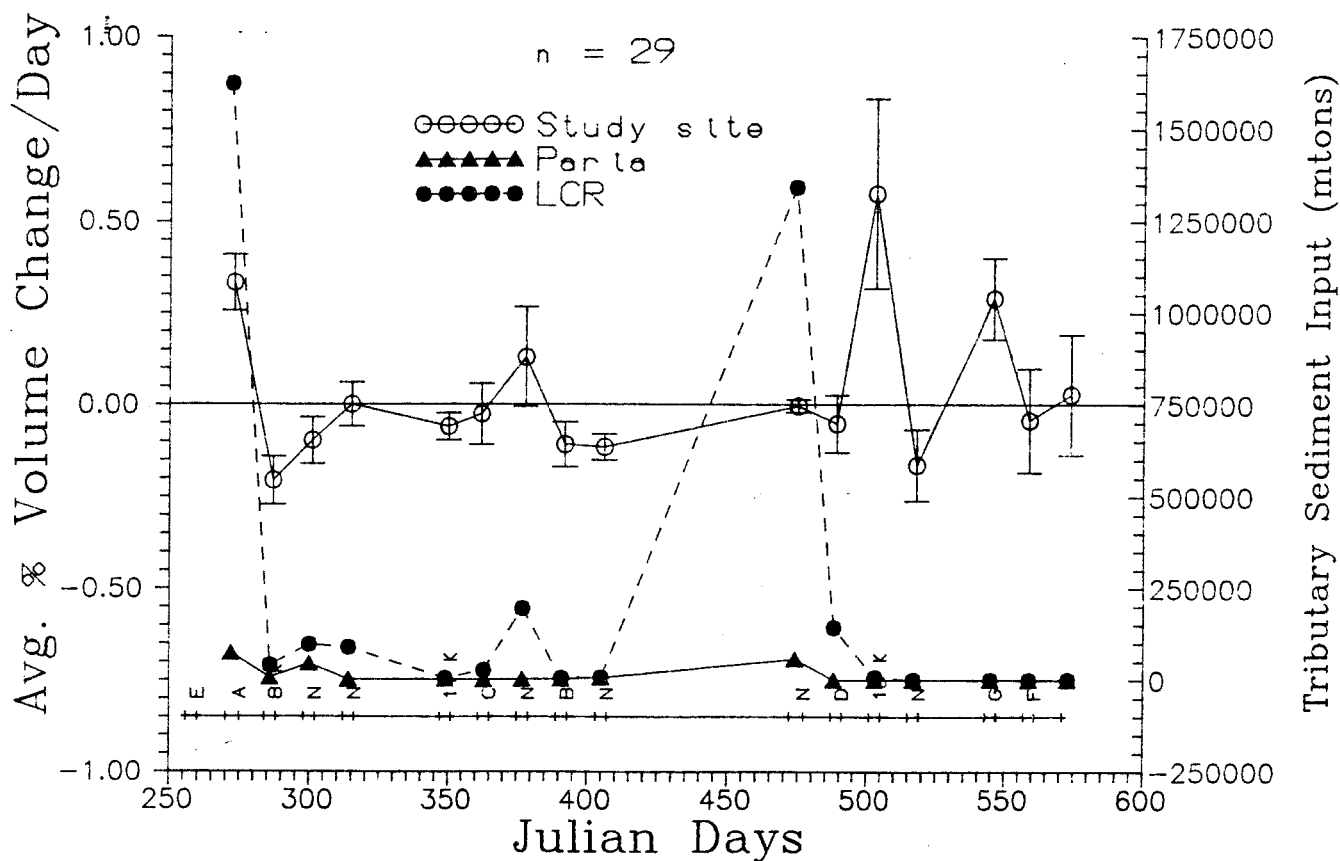


Figure 8. Average percent HAZ volume change/day for 29 Colorado River study sites, and average daily tributary sediment input (mt/d) from the Paria and Little Colorado Rivers from September, 1990 through July, 1991 (Julian Day 250 = Sept. 7, 1990; Julian Day 577 = July 31, 1991). The mean %VCR (open circles) and one standard error are presented for all sand bars surveyed during each test flow, and represents %VCR for the previous flow. For example, the mean %VCR during flow "E" was 0.34, as measured just prior to the beginning of the "A" flow.

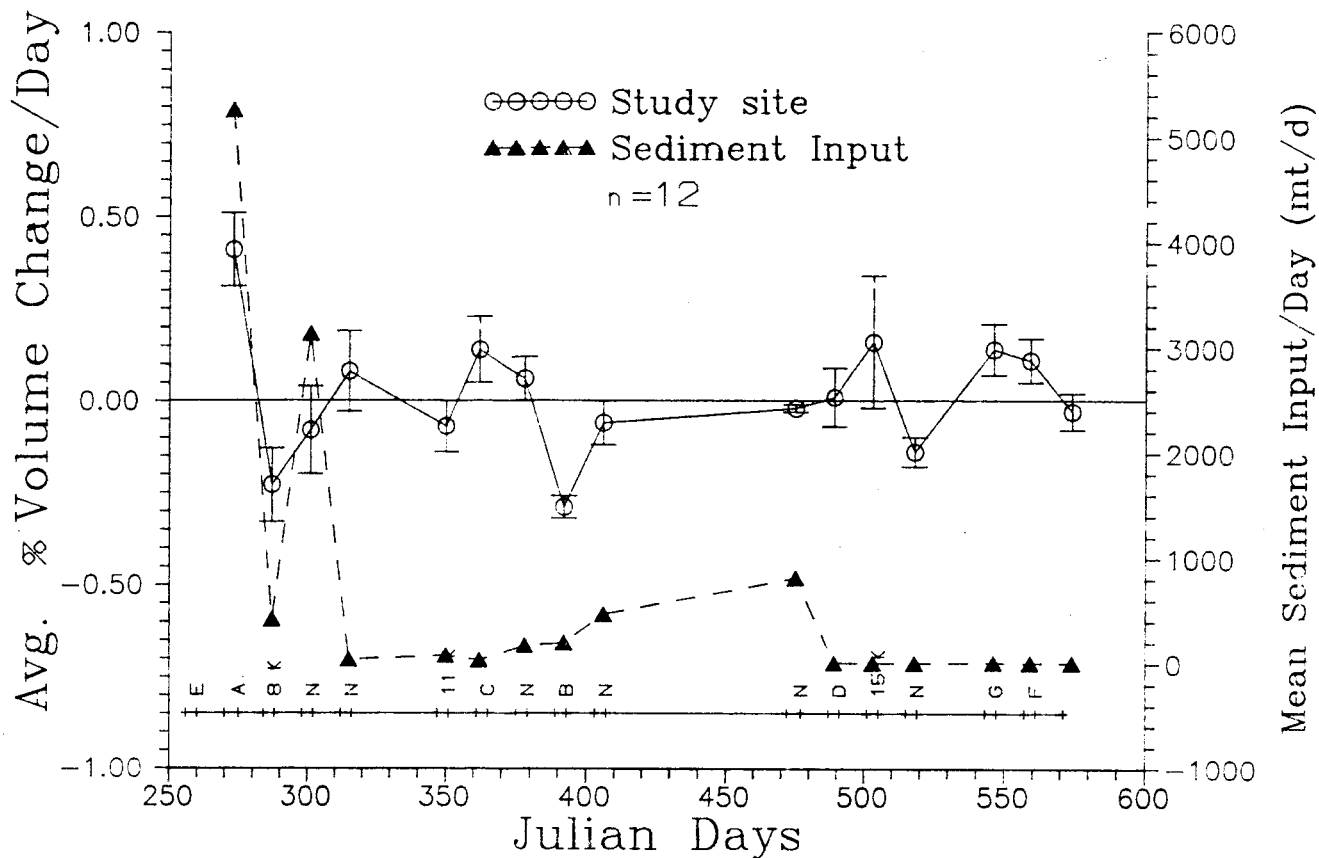


Figure 9. Average percent HAZ volume change/day (%VCR) for 12 study sites above the Little Colorado River, and average daily tributary sediment input (mt/d) from the Paria River from September, 1990 through July, 1991 (Julian Day 250 = Sept. 7, 1990; Julian Day 577 = July 31, 1991). The mean %VCR (open circles) and one standard error are presented for all sand bars surveyed during each test flow, and represents %VCR for the previous flow. For example, the mean %VCR during flow "E" was 0.42, as measured just prior to the beginning of the "A" flow.

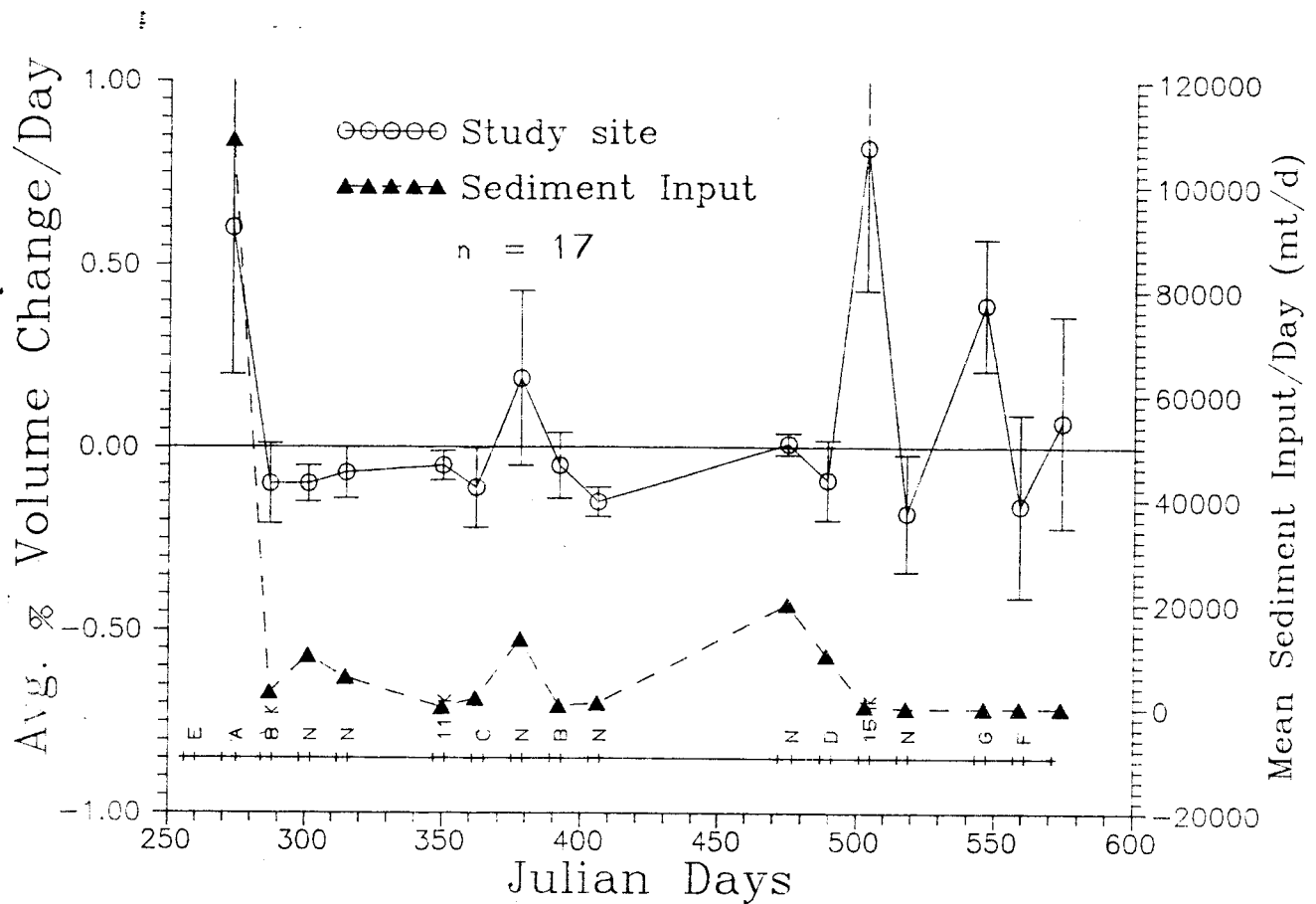


Figure 10. Average percent HAZ volume change/day (%VCR) for 17 study sites below the Little Colorado River, and average daily tributary sediment input (mt/d) from the Paria and Little Colorado Rivers from September, 1990 through July, 1991 (Julian Day 250 = Sept. 7, 1990; Julian Day 577 = July 31, 1991). The mean %VCR (open circles) and one standard error are presented for all sand bars surveyed during each test flow, and represents %VCR for the previous flow. For example, the mean %VCR during flow "E" was 0.62, as measured just prior to the beginning of the "A" flow.

Factors Influencing Sand Bar Change

In the following section we discuss the factors influencing changes in sand bar topography as indicated by these data. We evaluated combined effects of estimated sediment inflow from tributaries, estimated sediment transport capacity, antecedent sand bar morphology, recreational use intensity, and distance from Glen Canyon Dam.

Sediment Transport During Test Flows: The Paria (RM 0.5) and Little Colorado Rivers (RM 61) are the two primary sources of sediment for the Colorado River between Lees Ferry and Lake Mead. We obtained discharge information from the U.S. Geological Survey stream gages for the Paria River near its confluence with the Colorado River, and on the Little Colorado River near Cameron, Arizona. Using the temporally adjusted sediment-to-discharge data of Randle and Pemberton (1987), we calculated the total estimated sediment input into the Colorado River for each test flow period, normalized by duration of the flow (Table 4, Figures 8-10). Estimated daily sediment input rate was then compared with topographic data for the sand bars in the reaches influenced by those tributaries.

Estimated tributary sediment input showed a typical, strongly seasonal pattern during the GCES-II test flow period (Table 4, Figure 8). Sediment input from the Paria River was high in September, with a maximum of 3,140 mt/d during the "Constant 8,000 cfs" flow in late October, 1990, dropping in November, increasing in the mid- and late winter, and low (> 8 mt/d) from April through July, 1991 (Figure 9). Sediment input from the Little Colorado River typically followed a similar pattern, but with much greater sediment contributions. High sediment loads from the Little Colorado River occurred during the "E", "C", normal spring (late February to mid-April, 1991) and "Normal Spring (late April, 1991) flows, with a maximum estimated input of 103,492 mt/d during the September, 1990 "E" flow period (Figure 10). Few tributaries in the lower Grand Canyon have adequate stream flow and sediment data but many contribute sediment on an irregular basis. Floods exceeding a 50-year return interval occurred in Havasu Creek and probably in Kanab Creek in September, 1990. A large bank failure event occurred at the Mile 172 site and was documented by Cluer (Chapter 5, this report) and was possibly associated with these lower canyon tributary floods.

Four of the five test flows that resulted in net aggradation were either directly associated with significant tributary input (the "E", normal fall in 1990, and "C" flows), or followed shortly thereafter (flows "D"). Only the normal summer flow in June, 1991 resulted in system-wide aggradation without significant tributary input.

Sand bar instability generally increased with distance downstream from Glen Canyon Dam, as demonstrated by the increasing variance around the mean %VCR with distance (Figure 7). The Little Colorado River confluence lies at Mile 61.4 (river kilometer 99) and is the primary sediment source for the post-dam Colorado River. Downstream from the Little Colorado River the magnitude of sand bar %VCR increased (Figure 7). Mean %VCR values for each sand bar indicated that study sites above the Little Colorado River confluence were less dynamic as compared to some sites downstream from the Little Colorado River (Figures 9, 10). Seven of 12 (58%) sand bars above the Little Colorado River confluence were essentially stable, while only three of 17 (18%) sand bars below the LCR confluence were stable (Figures 9, 10; Table 5).

Estimated Sediment Transport Capacity of Test Flows: Aggradation was positively correlated with estimated sediment transport capacity of test flows (Fig 11). Using the model of Smillie et al. (this report), we estimated sediment transport capacity during each of the test flows. These data were compared with calculated %VCR for pooled sand bar survey data. This comparison showed that constant and low-fluctuation flows were erosive or resulted in little volumetric change. In contrast, the effects of high-fluctuation flows were less predictable. Three of the five high-fluctuation flows ("E", "D" and normal summer in June 1991) were aggradational, while two high fluctuation flows ("G" and "F")

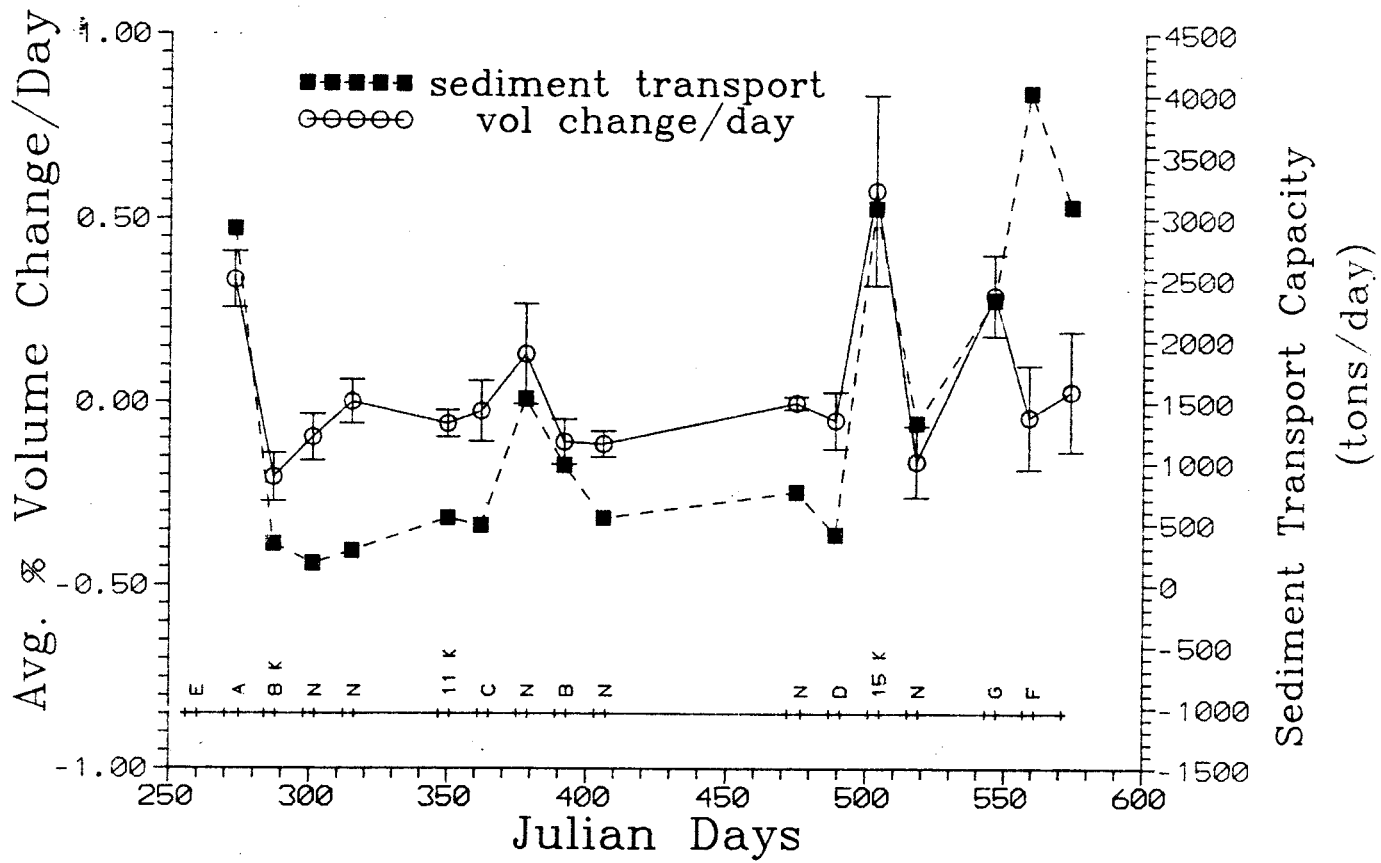


Figure 11. Average percent HAZ volume change/day and sediment transport capacity during the GCES test flow period.

were erosive or resulted in little change, respectively. The high-fluctuation normal flows differed from the test flows by having irregular (week-end) low flows (Appendix I, this report).

Antecedent Conditions: Antecedent conditions of sand bars exerted a significant influence on the subsequent direction and magnitude of topographic changes (Figure 12). A cyclic pattern of aggradation and degradation was commonly observed from one test flow to the next. This cyclic pattern is illustrated for the normal spring through the "F" flow in July, 1991 (Figure 10). High-fluctuation flows that resulted in aggradation (e.g. flow "D") apparently leave sand bars in an oversteepened condition, making them susceptible to subsequent degradation during the next flow interval (e.g. the "Constant 15,000 cfs" flow). Degradation rates tended to be large when the subsequent flow was a low-fluctuation or constant discharge test (e.g. Flow "E" to flow "A" and flow "D" to "Constant 15,000 cfs" flow, Figures 9 and 10, respectively).

Recreational Use Intensity: The sand bars under study here had a wide range of recreational use intensity and use intensity varies seasonally. Relative recreational use intensity was estimated by interviewing 37 licensed Colorado River whitewater guides. Guides were requested to rank recreational use intensity on each sand bar on a 1 (no) to 5 (high) scale. The data were compiled and the mean value was used as an index of relative recreational use intensity (Table 1). Recreational use intensity was weighted for seasonal variation in visitation: winter (December-February) received a weighting of 1; spring and fall months (April-May, October-November) received a weighting of 2; and summer periods (June-September) received a weighting of 3. Recreational use was not significantly correlated with %VCR in the stepwise multiple regression (below). From this analysis it appears that recreational use intensity was not an important factor influencing sand bar topographic change in relation to other factors studied.

Multiple Stepwise Regression Analysis

A stepwise multiple regression analysis was performed on individual sand bars and on the pooled topographic data set (all test flows, all sand bars). Percent VCR was used as a response variable against several predictor variables: 1) estimated sediment transport capacity (ESTC) for each test flow (calculated from the model of Smillie et al., Chapter 9); 2) sediment input/day for the Paria and Little Colorado Rivers; 3) previous sediment input rate during the previous test flow period; 4) prior volume of each sand bar; 5) prior %VCR of each sand bar; 6) seasonally weighted recreational use intensity; and 7) Julian day (Tables 1, 4, 5). Separate analyses showed that %VCR values from 20 of 29 sand bars were significantly negatively correlated with the sand bar conditions (either lagged volume or lagged %VCR) during the previous survey run. Exclusion of an outlier (Grapevine camp) rendered a Kolmogorov-Smirnov Lilliefors test of the normality of distribution of the slopes associated with both ESTC and lagged %VCR as non-significant ($p > 0.05$).

The multiple stepwise regression analysis was conducted on the pooled data set, excluding the exceptional Grapevine camp %VCR during the "D" flow in 1991 ($n = 386$ cases). Percent VCR was significantly influenced by two of the seven response variables ($R^2 = 0.14$; $F = 32.69$, $p < 0.001$, $df = 2$, 383). Percent VCR was significantly negatively correlated with lagged %VCR (coefficient = -0.369 , $p < 0.001$). This pattern suggests that the cyclic aggradation/degradation cycle is a predictable response of sand bars subjected to fluctuating flows. ESTC was the second significant factor in this analysis, and was positively correlated with %VCR ($p < 0.001$). Thus sand bars tend to aggrade under conditions of high sediment transport.

Sediment input variables did not contribute to the predictability of %VCR because aggradation was unpredictable (Figures 8-10). As mentioned above, aggradation was observed following three of the five high-fluctuation flows ("E", "D" and normal summer in June, 1991), whereas one of the high-fluctuation

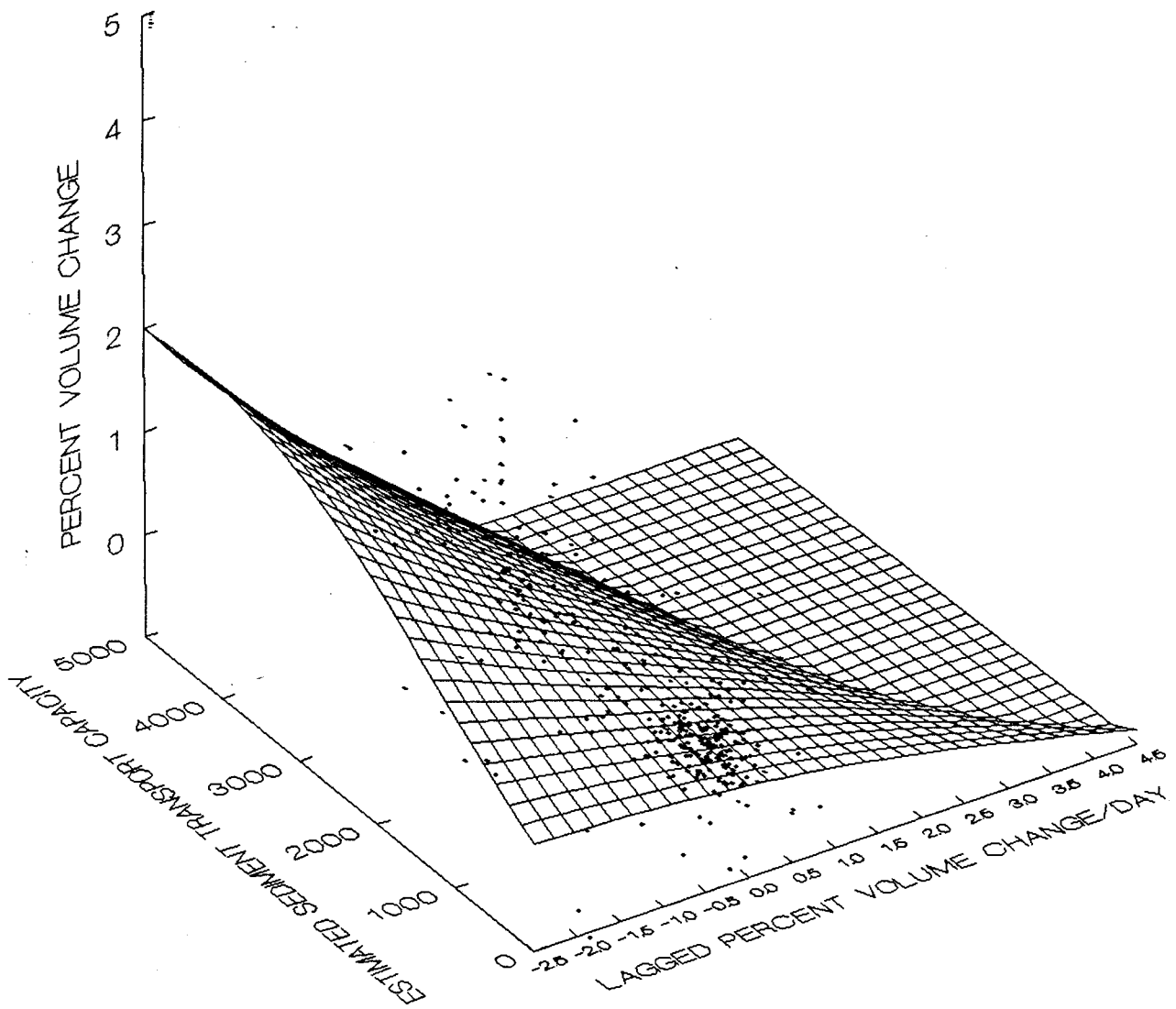


Figure 12. Relationship between HAZ percent volume change rate/d (%VCR), lagged %VCR and estimated sediment transport capacity for 29 sand bars from September, 1990 through July, 1991.

flows ("G" in 1991) was strongly degradational and the other ("F" in 1991) resulted in little net change. Four of five aggradational flows took place during or just after substantial sediment input; however, the normal summer, 1991 flow was not associated with substantial sediment inflow. Two of these aggradational events were relatively minor ("Normal Fall" in 1990, and "C" in 1991) but were associated with small pulses of sediment input. High stage elevations during larger fluctuations were required to deliver sand to higher elevations.

In summary, two patterns emerge from these analyses. 1) Cyclic aggradation and degradation characterized sand bars subjected to fluctuating discharges; and 2) aggradation occurred under large fluctuations associated with significant sediment input, but high fluctuation flows produced unpredictable results when sediment influx was low.

Future Monitoring

We recommend monitoring these and several additional study sites during the Interim Flows period six times per year. The interim flows prescriptions involve low, medium and high volume flow months. Surveys, at least of a subset of the sand bars should take place monthly to capture the effects of these three kinds of flows, and seasonally to capture low inflow periods (spring) versus high inflow periods (summer and fall). Alternatively, remote sensing of sand bars may serve to supply short term change data, with annual surveys; however, the direct application remote sensing data to the kinds of volumetric and areal data collected through surveying is incomplete. Because the changes observed in sand bars result from interactions between sediment inflow and dam operations, we recommend paying close attention to changes in flow regimes between months or due to flow exceptions.

SUMMARY OF OBSERVATIONS

1. Sand bar stability varied significantly between the 29 study sites and between test flows. From late summer, 1990 through July, 1991, three bars (10.3%) sustained significant net losses of HAZ sand, eleven bars (37.9%) remained relatively unchanged, and 15 bars (51.7%) gained sand. The 29 sand bars under study sustained a mean aggradation of 2.9% by volume (s.e. = 2.6%) between 27 October, 1990 (the first run for which survey coverage was virtually complete) and 31 July, 1991. During this time the total 87,435 m³ of HAZ sand under study decreased by 1,034 m³ (1.2%) because several large losses occurred at a few sites in contrast with the general condition of near-equilibrium observed on most sites.
2. Bar instability (both loss and gain of sand) increased with distance downstream from Glen Canyon Dam, particularly below the Little Colorado River drainage.
3. A degradation event documented during this study occurred relatively rapidly (< 1 day) during a 3-day "5,000 cfs constant" low flow. Subsequent aggradation appeared to have taken place gradually during subsequent high-fluctuation flows, but the volume change recorded lay within the error margin of survey accuracy (3%).
4. In this series of test flows, constant and low fluctuation flows at three test flow levels resulted in net erosion or negligible change in the HAZ volume during the 14-day flow test periods.
5. Relatively low discharge and corresponding low estimated sediment transport capacity (e.g. the A, B, normal fall flows) were associated with degradation or little net change in sand bar volume, particularly during the winter of 1990-1991.
6. Flows characterized by large daily fluctuations in this test flow series resulted in aggradation if associated with sediment contribution from tributaries. Aggradation was observed following three of the five high-fluctuation flows, whereas the others resulted in degradation or little net change in volume. Four of five aggradational flows were associated with significant sediment input from tributaries, and one was not.
7. Reattachment bars were less stable than separation bars. Although mean %VCR were almost identical between two deposit types, mean reattachment bar %VCR standard variation was 0.072 (n = 13), whereas that for separation deposits was 0.054 (n = 8).
8. Periods of aggradation tended to be followed by periods of degradation, particularly when large fluctuation flows were followed by low-fluctuation or constant flows. Thus, antecedent conditions exerted an important cyclic influence over subsequent HAZ changes under daily fluctuating flow regimes.

CONCLUSIONS

1. Except for unusual events, such as possible flows above $800 \text{ m}^3/\text{sec}$ (29,000 cfs) and not described in this report, changes in sand bar volume and area are generally restricted to an observed hydrologically active zone (HAZ). This zone occupied from 15 to 50 percent of the total sand bar area of six sand bars examined.
2. No single type of test flow affected all sand bars in the same manner.
3. In this series of test flows, degradation took place under low, low-fluctuation and constant flows. Aggradation of sand bars was unpredictable but took place most often during high-fluctuation flows associated with significant sediment input from tributaries.

ACKNOWLEDGEMENTS

This project was funded by the Bureau of Reclamation's Glen Canyon Environmental Studies Program. We thank Mr. David Wegner and his staff at the GGES for their logistical and office support of this study. We received significant assistance from the National Park Service staffs at the Cooperative Parks Study Unit in Flagstaff, Grand Canyon National Park and Glen Canyon National Recreation Area. In particular, we wish to thank Dr. Peter Rowlands, Dr. Charles Van Riper, Mr. Jerry Mitchell, Mr. Vick Brown and Mr. Tom Workman for their enthusiastic assistance with this project. Dr. William Jackson (NPS Water Resources Division, Ft. Collins, CO) and his staff provided support throughout this project. Mr. Carl Cawood (NAU Engineering Department) and Mr. Frederick Angell (NPS Western Region Survey Project Supervisor) provided significant assistance in the early stages of the field efforts. Mr. Chuck Dryden provided invaluable surveying critique. The boatmen, cooks and management of O.A.R.S., Inc. devoted innumerable hours and much energy to this project and we thank them for their care and enthusiasm.

We wish to express our deepest appreciation to the surveyors and survey assistants, without whose expertise, devotion and good humor this project could not have succeeded: Jeffe Aronson, Jon Hirsch, Brian Bates, Gary Baumhoffer, Peggy Benenati, Jeff Bennett, Hans Bodenhamer, Christopher Brod, James Courson, Steven White, Chris Dunn, F. Mark Gonzales, Stacey Griffith, Scott Groene, Joseph Hazel, Matthew Kaplinski, Michael Kearsley, Hilary Mayes, Kwansue Jung, Theodore Melis, Alan Peterson, Frank Protiva, Dennis Silva, Jeanette Smith, Katherine Thompson, and Debra Von Gonten. In addition to the regular staff, we wish to thank the more than 100 NPS volunteers who assisted in this project, particularly Rick Miller, Peter Mui and Greg Sponenberg. Cindy Mapston and Ken Walters provided indispensable accounting and managerial support.

LITERATURE CITED

- Beus, S.S., S.W. Carothers and F.B. Lojko. 1984 et. subsequ. Colorado River investigations. Grand Canyon National Park Repts., Grand Canyon. Unpublished.
- Cluer, B.L., 1991a, Summary of Scheduled Research Discharges, and Research Discharge Hydrographs, June 1990 through July 1991: Instantaneous Discharges. This report.
- Cluer, B.L., 1991b, Catastrophic erosion events and rapid deposition of sand bars on the Colorado River, the Grand Canyon, Arizona. EOS. v. 72. no. 44. p. 223.
- Howard, A.D. 1975. Establishment of benchmark study sites along the Colorado River in Grand Canyon National Park for monitoring of beach erosion caused by natural forces and human impact. Univ. Virginia Grand Canyon Study Tech. Rept. No. 1. Grand Canyon National Park. 182 pp.
- Howard, A.D. and R. Dolan. 1981. Geomorphology of the Colorado River in the Grand Canyon, J. Geol. 89: 269-298
- Patten, D.T. 1990. Glen Canyon Environmental Studies Phase II draft integrated research plan, Vol. 1. Bureau of Reclamation Glen Canyon Environmental Studies Office, Flagstaff.
- Randle, T.J. and E.L. Pemberton. 1987. Results and analysis of STARS modeling efforts of the Colorado River in Grand Canyon. Bureau of Reclamation Glen Canyon Environmental Studies Report, Salt Lake City. NTIS PB88-183421.
- Rubin, D.M., J.C. Schmidt, and J.N. Moore. 1990. Origin, structure, and evolution of a reattachment bar, Colorado River, Grand Canyon, Arizona. J. Sed. Petrol. 60: 982-991.
- Schmidt, J.C. 1989. Colorado River bank erosion monitoring report. Grand Canyon National Park, Grand Canyon. Unpublished.
- Schmidt, J.C. and J.B. Graf. 1990. Aggradation and degradation of alluvial sand deposits, Colorado River, Grand Canyon National Park. U.S. Geol. Surv. Prof. Pap. 1493, 74p.
- Stevens, L.E., J.C. Schmidt, T.J. Ayers and B.T. Brown. In preparation. Geomorphic control of fluvial marsh development in the Grand Canyon.
- Water Science and Technology Board, 1991, Colorado River Ecology and Dam Management. Proceedings of a Symposium May 24-25, Santa Fe, New Mexico. National Academy Press, Washington D.C. 276 p.
- Webb, R.H., P.T. Pringle and G.R. Rink. 1987. Debris flows in tributaries of the Colorado River, Grand Canyon National Park, Arizona. U.S. Geol. Survey Open File Rept. 87-118. 64 pp.
- Zink, L.L. 1989. Effects of Glen Canyon Dam on sand bars of the Colorado River in Grand Canyon. Unpublished Middlebury College senior thesis. 53 pp.

CHAPTER 7

**ANALYSIS OF SAND BAR RESPONSE
ALONG THE COLORADO RIVER IN GLEN AND GRAND CANYONS
TO TEST FLOWS FROM GLEN CANYON DAM,
USING AERIAL PHOTOGRAPHY**

**Brian L Cluer
Resource Management Division
Grand Canyon National Park
July 1, 1992**

ANALYSIS OF SAND BAR RESPONSE ALONG THE COLORADO RIVER IN GLEN AND GRAND CANYONS TO TEST FLOWS FROM GLEN CANYON DAM, USING AERIAL PHOTOGRAPHY

ABSTRACT

This investigation presents the first analysis of aerial photography captured during the GCES Phase II test flow program. Seventy four sites were photographed 17 times from September 30, 1990 to July 27, 1991. Sixteen test flows were bracketed with before and after photography. The ten sites presented in this report were analyzed using a new technique developed to obtain two-dimensional measures from images that were designed with stereo overlap and intended for three-dimensional analysis. True scale area measurements and comparison plots resulted in measures of; whole deposit area, area of aggradation; and area of degradation for each photo epoch. The combination of aggraded and degraded area yields a measure of the minimum area that was reworked during bracketed test flows.

Sediment transport capacity calculations for each of the test flows provided an index of relative hydraulic energy for the individual flows. This index correlates well with the reworked area measurements. The net area results were however not strongly correlated, indicating the natural variability in the fluvial system, and a combination of immediate and delayed responses to changes in flow regimes. Overall, flows with reduced energy following high energy flows resulted in increased area. Consequent return to a higher energy flow resulted in decreased deposit area. This generality held until the last two test flows where aggradation during the high energy "G" test flow was followed by degradation during the subsequent "F" test flow (with slightly lower energy). However, further sediment transport capacity modeling may show that there was little difference between the "G" and "F" test flows at some distance downstream.

Several hydrogeomorphic features were captured during this investigation. At two sites, secondary recirculation eddies formed during a normal flow period in November and December, 1990. The secondary eddy features persisted and ultimately eroded large percentages of the two deposits. Seepage of ground water during highly fluctuating flows produced rills and larger tunnel scours. At one site, the large tunnel scour features were associated with an aggradational period. Consequently, it appears that there is a well developed linkage between erosional and depositional processes affecting sand bars along the Colorado River in Grand Canyon. The two polarized processes operate together at all sites, but certain hydraulic perturbations allow one process to temporarily overpower the other. Understanding these linkages and the responses to hydraulic changes will require full development of sand bar monitoring techniques (and existing databases) that will provide the highest temporal and spatial resolutions possible.

INTRODUCTION

It was recognized early in the NPS/GCES beach erosion project that a large sample size was desirable in order to adequately constrain sand bar responses to multiple variables related to test flow hydraulics, a wide variety of sedimentologic and geomorphic environments, sediment inputs from tributaries, and distance from Glen Canyon Dam. Aerial photogrammetry offered a method that could capture a large number of subjects during the short three day evaluation periods between test flows.

From August 1990, to July 1991, aerial photographs were taken of 75 sand bars in Glen and Grand Canyon dispersed between 5 miles below Glen Canyon Dam and 240 miles down river at Diamond Creek. Seventeen photo epochs were completed which bracket 16 different test flows. The photographs captured a variety of sand bars all exposed at a low and constant river level at 5,000 cfs.

The original intent was for the photography to be analyzed three-dimensionally and produce topographic maps of the subject sand bars. Problems with photo geometry and image motion rendered a high percentage of the photographs incapable of producing reasonable accuracy, especially in elevation. A small contract for QA/QC work with the Planetary Mapping Division-USGS in Flagstaff, Arizona, allowed for experimental development of two-dimensional analysis from overlapping stereo imagery.

Objective The original objective of this study was to develop topographic maps of a large number of sand deposits along the Colorado River that could be used to analyze the affects of test flows from Glen Canyon Dam. Multiple technical and bureaucratic problems prevented the project from achieving this initial objective.

Purpose An alternative method of photo analysis was devised that overcame most of the technical problems, resulting in planimetric analyses of the photography. This paper presents the results of analysis of 10 sites through the test flow period from September 1990 to July 1991. It includes 17 planimetric analyses for each site, bracketing 16 unique test flows.

METHODS

Site Selection

Sites were selected for the original investigation to provide longevity through the test period, wide dispersion from the Dam to Diamond Creek, and adequate variety of geomorphic and sedimentologic typology. The sites were at river miles: -10, -6.5, -2.8, 1, 2.6, 4, 8, 16.4, 20, 20.5, 21.8, 29.1, 29.2, 30.4, 31.6, 33, 35.1, 37.5, 40, 43.1, 44.6, 47, 50, 51, 55, 56, 64, 66, 68, 75.6, 75.8, 76, 81, 83, 87, 91, 93, 98, 104, 108, 119, 120, 122.2, 122.7, 132, 134, 137, 139, 145, 153, 157, 168, 172, 182.2, 182.4, 183.9, 194, 202, 211, 213, 220, and 225.

For this paper, a sub-sample of 10 sites was selected that provided greatest concentration upstream of the Little Colorado River, variety in geomorphic type, and overlap with land surveying efforts (see Beus et al, this report). The sites were at river miles: -6.5, 8, 43, 45, 47, 51, 66, 68, 81, and 172 (Fig. 1). Schmidt and Graf (1988) categorized depositional environments and deposit types in Grand Canyon. Their nomenclature is used in this report (Fig. 2).

Site Description

The -6.5 right site is located in Glen Canyon, in the Ferry Swale area. The sand bar is upstream of a minor channel constriction in a very quiet reach. Recirculation in the local eddy often switches direction rapidly, however, recirculating current is usually very slow. This site is perhaps most impacted by motor boat wakes.

The 8 left site is located at Badger rapid, immediately downstream of the Jackass side canyon. The sand bar is within a recirculation zone, but waves from the nearby rapid probably mask other fluvial processes on this deposit.

The next site down river is the Anasazi Bridge site, at 43 left. This sand bar is immediately upstream of a channel constriction, thus it is an upper pool deposit. It has two persistent recirculation eddies, but they are generally slow velocity and the deposit is probably dominated by seepage processes.

The next site is 45 left, at the Eminence Break trail. A major channel constriction from river left and the sweeping right turn of the canyon around Hansborough Point have developed a large separation and reattachment bar environment at this site. Recirculating currents are swift in this eddy, and high river stages impinge on the separation deposit.

Next down river is 47 left, where Saddle Canyon enters from the right. Here only the reattachment deposit was consistently captured. This eddy has high recirculating currents that often form sand waves on the platform deposit.

Next down stream is 51 left. This site is another reattachment bar formed down stream of a minor channel constriction in a relatively calm reach. Surprisingly strong recirculation currents exist in this eddy during high river stages.

Next is a site near the Hopi Salt Mines, at 66 left. This sand bar is located immediately upstream of a large mid-channel gravel bar where high flows split and flow around both sides of the island. At the upstream end of the sand bar there is a minor channel constriction from a side stream on the left. This combination of local channel conditions creates a very energetic recirculating eddy. A combination of separation and reattachment deposits was captured here.

Next down stream is a large sand bar at 68 right, across from the Tanner trail. This site is located on the inside of a large right bend in the river, downstream of a long shallow riffle, and upstream of Tanner rapid. Both separation and reattachment deposits were captured consistently.

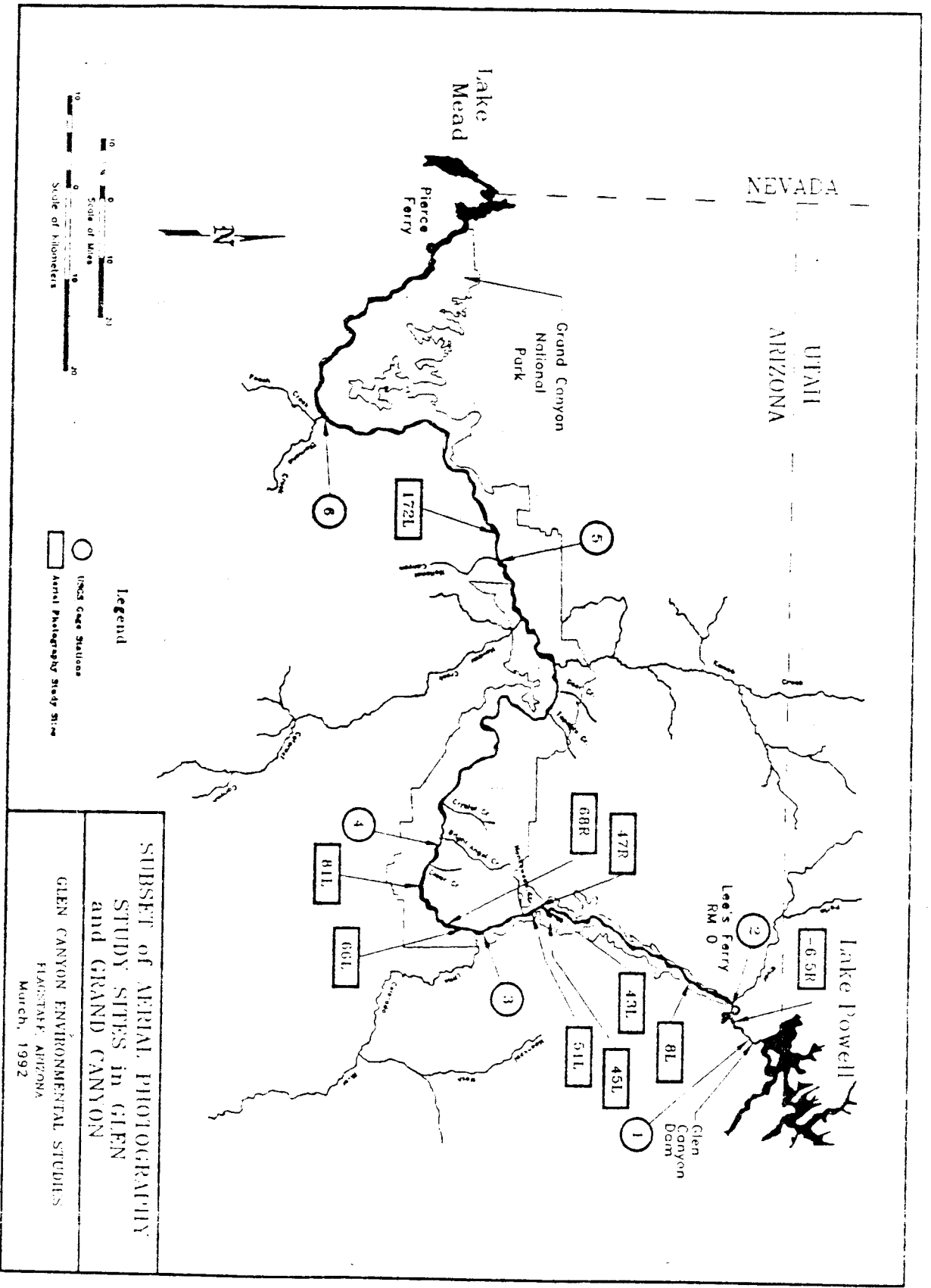


Figure 1. Location map of study sites along the Colorado River in Glen and Grand Canyons, Arizona.

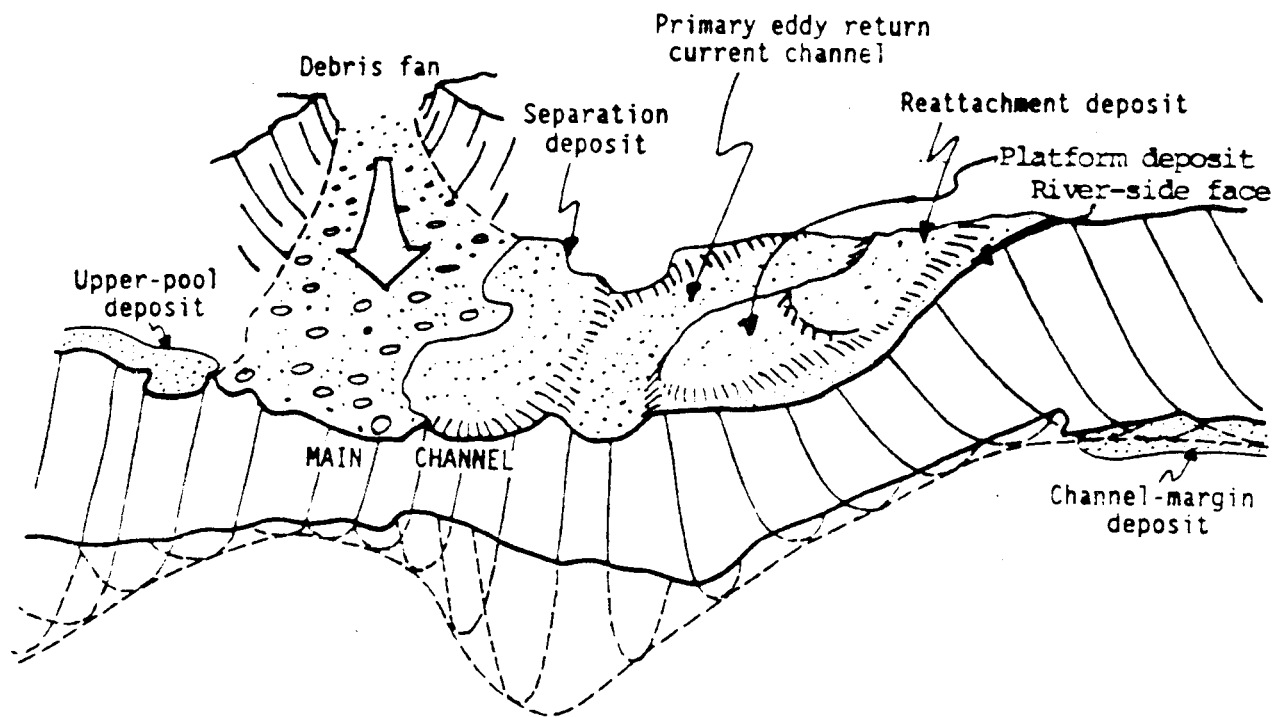
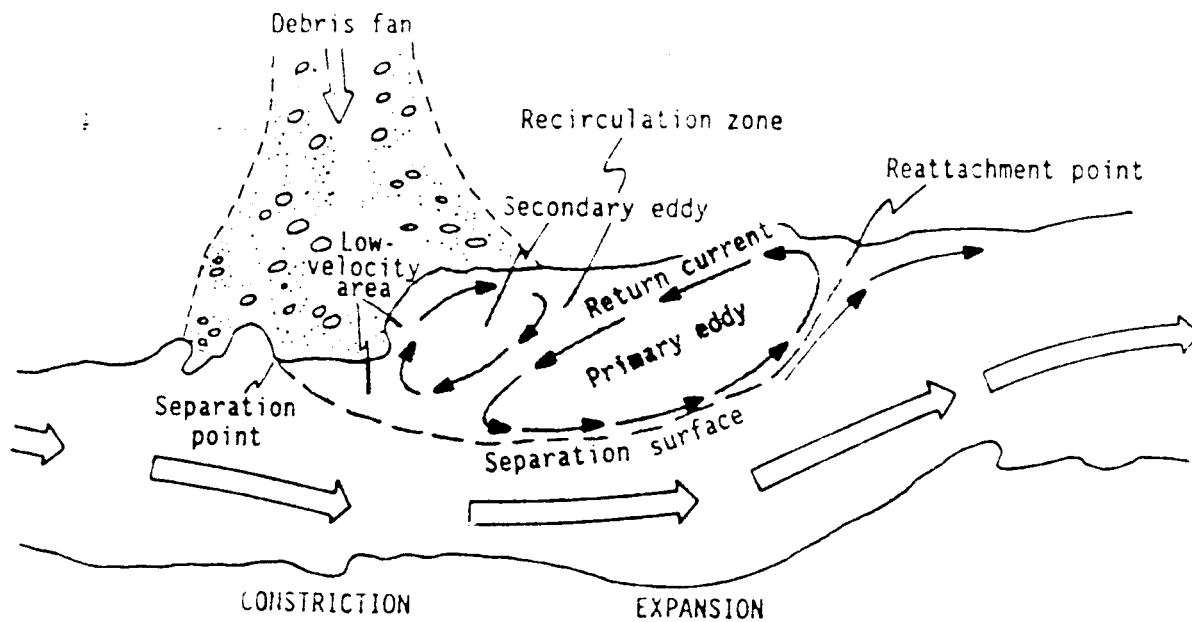


Figure 2. Diagram of deposit types and sedimentary environments in the Grand Canyon, with nomenclature used in this report. Modified from Schmidt and Graf, 1988 (Fig. 3).

The next site is 81 left, Grapevine camp. This sand bar is located between two small side channel constrictions in the narrow and swift Inner Gorge reach. At high river stages, main channel flow affects the face of the deposit. At lower river stages, small recirculation eddies form along the bar face.

The last sand bar in this study is 172 left, below Mohawk rapid. This site is located immediately down stream of a secondary channel constriction below Mohawk and Gateway canyons. Strong recirculation currents exist in this eddy under a wide range of river stages. Both separation and reattachment deposits were consistently captured at this site.

Site Preparation

During November and December, 1990, survey crews placed aerial photo panels on the sites selected for this investigation. All panels were surveyed to local datum and benchmark references using state-of-the-art equipment and techniques. Photographs taken during the ensuing evaluation period in mid-December, 1990, captured the photo panels and provided photo scale and orientation for all photography.

Two-dimensional analysis development

The overlapping original black and white negatives were mechanically fitted under magnification to carefully align water edge at the front of the sand bar and immobile rocks at the back and edges of the sand bar. The aligned overlapping images were fixed onto a stable transparency base to create a composite full coverage image for each photo epoch. The composite images were then digitized, surrounded along the water edge and between repeatable rocks outside the fluctuating zone to enclose a perimeter that defined an area. A technique was developed to process the digital perimeter on a video monitor, and a computer program counted the number of pixels filling the perimeter and applied scaling factors to calculate the area within the perimeter in meters².

To compare photo epochs and develop ubiquitous photo scales, additional corrections were made to rectify angular variations between photographs taken at different epochs. By choosing one composite image as the base, all other photo epochs were manually adjusted on the color video monitor to align at common rock points. With common immobile points aligned, the differences in area between epochs were visually obvious, and attributable to hydraulic processes operating during the subsequent test flows. By assigning individual layers unique colors, further comparison on the color video monitor resulted in distinguishing areas of aggradation from areas of degradation between photo epochs.

Quality Control

The quality of the digitally derived area values was checked by carefully examining each photo epoch to verify areas of aggradation and degradation between test flows and water level for each epoch. Photo epochs that captured subjects at water levels visually differing from the

normal 5,000 cfs stage were removed from the data base. This process also resulted in description of fluvial geomorphic processes that left evidence on the surface of sand bars.

RESULTS

The results from two-dimensional analysis of the aerial photography are: perimeter plots of each epoch; area calculations of each epoch; comparison plots of contiguous epochs, with differently shaded areas of aggradation and degradation; calculations of area of aggradation and degradation; and descriptions of fluvial evidence preserved on the surface of deposits.

Table 1. Summary of photography captured for each site and each test flow.

<i>SITE/ FLOW</i>	<i>DATE</i>	<i>- 6.5 right</i>	<i>8 left</i>	<i>43 left</i>	<i>45 left</i>	<i>47 right</i>	<i>51 left</i>	<i>66 left</i>	<i>68 right</i>	<i>81 left</i>	<i>172 left</i>
"E"	9/30/90	x	x	x	x	x	x	x			x
"A"	10/14/90	x	x	x			x	x		x	
8,000	10/30/90	x	x	x					x	x	x
Fall	11/11/90		x	x	x	x	x	x			x
Normal	12/17/90	x	x	x	x		x	x		x	x
11,000	12/30/90	x	x	x	x	x	x	x	x	x	x
"C"	1/12/91	x	x	x	x	x		x	x	x	x
Winter	1/26/91	x	x	x	x	x	x	x	x	x	x
"B"	2/9/91	x	x	x	x	x	x	x	x	x	x
Normal	4/20/91	x	x	x	x	x	x	x	x	x	x
Spring	5/5/91	x	x	x	x	x	x	x		x	x
"D"	5/19/91	x	x	x	x	x	x	x	x	x	x
15,000	6/2/91	x	x	x	x	x	x	x	x	x	x
Summer	6/30/91	x	x	x	x	x	x	x	x	x	x
"G"	7/14/91	x	x			x	x				x
"F"	7/27/91	x	x	x	x	x	x	x	x	x	x

MAP PRODUCTS

Planimetric Plots Each photo epoch resulted in complete photographic coverage of selected sand deposits exposed at a constant low river level of 5,000 cfs. Subsequent planimetric

plots were overlaid with the prior plot to discern the areas that changed during the test flow. These areas were digitally compared also, resulting in calculated areas of erosion and deposition associated with each test flow. The results of this process are included in Appendix A, this report.

Calculated Areas Once digitized and corrected for angular variation between photo epochs, the area of each sand bar was calculated for each epoch using a computer program that counted the number of pixels within the perimeter. Areas of aggradation and degradation were also calculated between photo epochs. These results are presented in table 2.

SEDIMENT TRANSPORT CAPACITY

A method of providing unique measures of the hydraulic effects of individual test flows was desired in order to compare the field results against the potential sediment transport of each test flow. Sediment transport capacity of each test flow was calculated in order to compare potential sediment movement in the main channel with measures of sediment stored in channel margin environments. A simple computer program was used that calculates sediment discharge using water discharge treated with sediment transport functions (Smilie et al, 1992). The equation used was:

$$Q_s = aQ_w^b \quad (1)$$

where Q_s is sediment discharge, Q_w is water discharge, a is $0.46047(10)^{-10}$, and b is 3.2228. The transport functions a and b were derived from measured values at the USGS gaging stations (Fig. 1) at Grand Canyon above the Little Colorado River, Grand Canyon Gage at Phantom Ranch, and Grand Canyon Gage at Diamond Creek. Inputs for Q_w were taken from mean daily values at the Lees Ferry Gage, for each test flow.

The resulting sediment transport capacity values range from a low of about 2,000 tons for the 11 day 8,000 cfs constant flow during the period October 15-25, 1990, to a high of over 135,000 tons for the 46 day "Normal Flow" test that lasted February 11-April 17, 1991. Daily sediment transport values range from a low 174 tons per day for the 8,000 cfs constant flow to a high of 4021 tons per day for the "G" flow in July 1991. The results of sediment transport modeling are presented in Figure 3. This exercise was intended to provide an indication of the stream energy associated with each of the test flows, for comparative purposes only. It is not intended that the calculations of sediment transport capacity represent transport through the system.

SITE	6.5 RIGHT - FERRY SWALE			8 LEFT - JACKASS CAMP			43 LEFT - ANASAZI BRIDGE			45 LEFT - EMINENCE BREAK			47 RIGHT - SADDLE CANYON				
	TEST FLOW	EPOCH	AREA m2	+ AREA	- AREA	AREA m2	+ AREA	- AREA	AREA m2	+ AREA	- AREA	AREA m2	+ AREA	- AREA	AREA m2	+ AREA	- AREA
"E"	09/30/90					4884.21			19029.88			17084.44					
"A"	10/15/90					4920.53	43.38	-6.05									
9,000	10/30/90				1513.18	2.33	-42.23	214.19	-0.50								
Fall	11/11/90				1517.58	4.92	-8.03	4784.85	0.00	-328.52	19131.37	487.18	-342.00	17129.80	818.16	-842.89	
Normal	12/17/90		4243.47	370.75	0.00	1589.08	49.22	0.00	4856.14	78.18	-33.86	19289.84	207.54	-877.35			
11,000	12/30/90		4023.37	0.00	-130.70	1545.30	0.26	-18.91	4837.83	45.56	-19.84	18724.80	509.08	-155.18	16885.13	860.03	-1058.72
"C"	01/12/91		4141.21	0.00	-64.93	1571.98	9.84	-2.33	5188.88	199.73	0.00	19242.70	478.63	-159.73	16544.47	755.80	-1118.86
Winter	01/26/91		4080.99	119.07	0.21	1578.39	11.86	-8.03	5288.81	125.09	-0.17	18460.52	220.09	-789.54	18000.22	219.16	-748.06
"B"	02/09/91		4141.87	8.88	-10.36	1551.78	1.55	-11.40	5159.81	0.50	-133.88	19851.32	1071.26	-60.00	15888.87	412.31	-515.80
Normal	04/20/91		4100.13	4.65	-15.23	1506.70	5.70	-33.84	5153.38	23.03	-13.82	19082.18	272.45	-881.53	18118.92	604.90	-385.83
Spring	05/05/91		4282.26	33.83	0.00	1530.27	5.70	-0.78	5034.89	0.00	-80.87	19059.20	183.18	-177.00	15825.09	221.56	-448.82
"D"	05/19/91		4261.45	183.28	-7.19	1558.25	77.88	-59.07	5130.02	110.96	-3.03	18564.06	550.08	-836.28	15354.77	274.32	-738.09
15,000	06/02/91		4123.50	0.21	-142.76	1756.44	187.35	0.00	5207.52	15.47	-6.88	21339.73	2834.14	-287.00	15515.92	326.89	-148.66
Summer	06/30/91		3946.02	42.30	-15.65	1807.73	0.00	-116.58	5035.36	6.73	-124.75	19614.82	228.81	-1784.25	13430.54	0.00	-1978.34
"G"	07/14/91		4223.26	44.63	-2.86	1598.89	8.22	-5.70							14850.29	1491.87	-53.31
"F"	07/27/91		4127.48	16.07	-8.46	1414.73	0.00	-157.25	4878.17	0.34	-121.72	20480.45	841.08	-235.91	15405.12	572.43	-186.21

Table 2a. Data from two-dimensional analysis of aerial photography from sites -6.5 right, 8 left, 43 left, 45 left, and 47 right. All values reported in meters².

SITE	EPOCH	51 LEFT			66 LEFT - HIGH SALT MINE			68 RIGHT - TANNER			81 LEFT - GRAPEVINE			172 LEFT - BELOW MOHAWK		
		AREA m2	+ AREA	- AREA	AREA m2	+ AREA	- AREA	AREA m2	+ AREA	- AREA	AREA m2	+ AREA	- AREA			
TEST FLOW																
E-	08/30/90	28862.79			8313.27									6319.58		
A-	10/15/90	29021.41	101.88	-2512.41	6334.48	176.40	-139.08				1588.67					
6,000	10/30/90							4378.51			1595.29	4.97	-0.26	6242.89	14.67	
Fill	11/1/90	27115.29	1080.99	-115.41	7883.47	28.09	-446.48						0.00		0.00	
Normal	12/1/90	25129.42	105.60	-1980.12	7307.33	136.52	-680.61				1584.58	1.05	-2.35	6013.80	72.33	
11,000	12/30/90	24785.83	58.67	-314.48	7323.83	68.36	-91.54	4196.42	222.31	-392.48	1559.75	2.87	-14.63	6023.91	117.12	
C-	01/12/91				7370.19	295.52	-212.54	4218.43	292.13	285.97	1655.39	65.59	0.00	5463.47	118.51	
Winter	01/26/91	25422.97	890.82	-419.13	7780.56	376.76	-11.79	4397.61	223.32	-100.24	1631.35	0.00	-18.55	5178.69	106.62	
B-	02/09/91	24571.63	184.33	-820.96	7711.79	68.40	-152.24	4596.18	197.45	-16.17	1577.52	0.00	-15.42	4971.60	80.66	
Normal	04/20/91	25019.97	673.08	-353.48	7651.29	685.75	-744.88	4186.32	58.00	-462.20	1623.51	18.55	-0.26	5544.13	694.01	
Spring	05/05/91	23447.65	0.47	-1397.32	8629.53	868.42	-65.41				1596.07	2.35	-10.45	5541.75	53.51	
0-	05/19/91	24589.80	1304.33	-274.51	8259.45	561.02	-846.63	4115.78	188.56	-174.21	1624.03	23.52	4.44		0.00	
15,000	06/02/91	24093.77	289.46	-694.34	7967.94	417.42	-730.54	4443.19	493.13	-220.69	1621.68	3.40	-13.07	6171.74	514.66	
Summer	06/30/91	25410.46	1494.97	-231.28	8110.35	785.95	-634.68	4279.08	157.84	-337.71	1652.78	23.26	-2.35	5256.75	133.57	
G-	07/14/91	23722.24	80.60	-1689.82									0.00	6183.63	1189.05	
F-	07/27/91	24871.82	1219.29	-111.44	8109.76	264.79	-238.08	4499.37	370.25	-149.35	1649.12	6.01	-3.40	5637.30	326.39	

Table 2b. Data from two-dimensional analysis of aerial photography from sites 51 left, 66 left, 68 right, 81 left, and 172 left. All values reported in meters².

SEDIMENT TRANSPORT CAPACITY

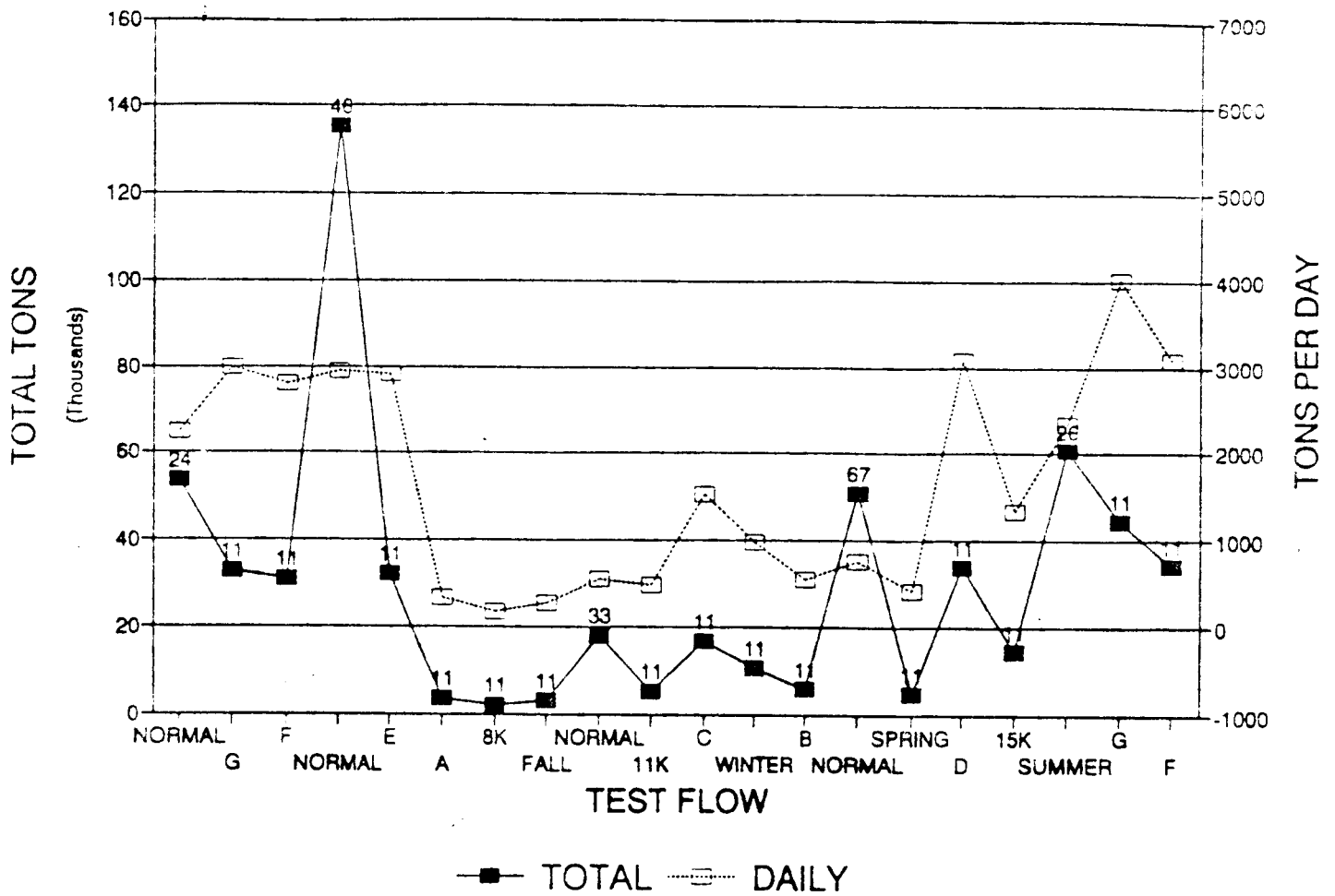


Figure 3. Graph of sediment transport capacity results for each test flow and daily values for each test flow. The numbers over the solid blocks indicate the duration in days of each test flow.

DISCUSSION

Comparison of Field Measurements and Sediment Transport Capacity

Reworked sediment area was derived from adding area of sediment increase to area of sediment decrease, or cut plus fill. A strong correlation was found between the area of reworked sediment and sediment transport capacity (Fig 4). This relationship is particularly well represented at site 66 left (Fig. A7), where the trends between reworked area and sediment transport capacity follow closely. The relationship is also evident at sites 45 left, 47 right, 51 left, 68 right, and 172 left (Figs. A4, A5, A6, A8, and A10 respectively). Overall, the composite of reworked area follows the sediment transport trends remarkably well (Fig. 5) where increased sediment transport results in increased reworked sand bar area.

The important metric to the fluvial sediment resource is the amount of reworked sediment that remains stored in the eddy following a particular test flow. The comparison of reworked area and net area is less clear (Fig. 6). Photography captured most of the sites during the September 28-30, 1990 evaluation period. Sand bar area at that time was used as the baseline value to compare subsequent changes to. The consistency of photo capture increased steadily as the study progressed (Table 1). Eight out of ten sites were captured on September 30, 1990 prior to the "A" test period. Discussion of sand bar area and changes relating to ground water and stream hydraulics begins with this flow.

GEOMORPHIC DESCRIPTIONS

A principal use of aerial photography is for describing surficial hydraulic features and general geomorphology. During the course of this study several interesting hydrogeomorphic features developed and disappeared. Others developed and persisted. The photographs reveal some very interesting process and product relationships. This paper presents the most interesting of the geomorphic observations and each observation is related to a particular test flow. Consequently the reader is advised to referred to Appendix I of this document for details about each test flow throughout the following discussion.

Flow Pattern Changes and Geomorphic Results

In some of the photography it was obvious that main channel flow or eddy flow patterns had changed during the previous test flow. Notable occurrences were at sites 45 left, 51 left, 66 left, 68 right, and 172 left. Most sites were captured by photography taken on September 30, 1990, prior to the "A" test flow. Discussion of flow pattern change from geomorphic evidence begins with the "A" test flow.

"A" test flow The "A" test flow fluctuated daily from 3,000-13,000 cfs for 11 days in early October 1990. On the 5 sand bars sampled, about 5% of the total area was reworked and there was a slight net gain in area of about 0.5% (Fig. 6). The 51 left site underwent a remarkable change during the "A" test flow (Fig. A6b). The sand bar retained all of its prior geomorphic features, including a small pond along the down stream end, but rather significant

TRANSPORT AND REWORKED AREA

N = 10

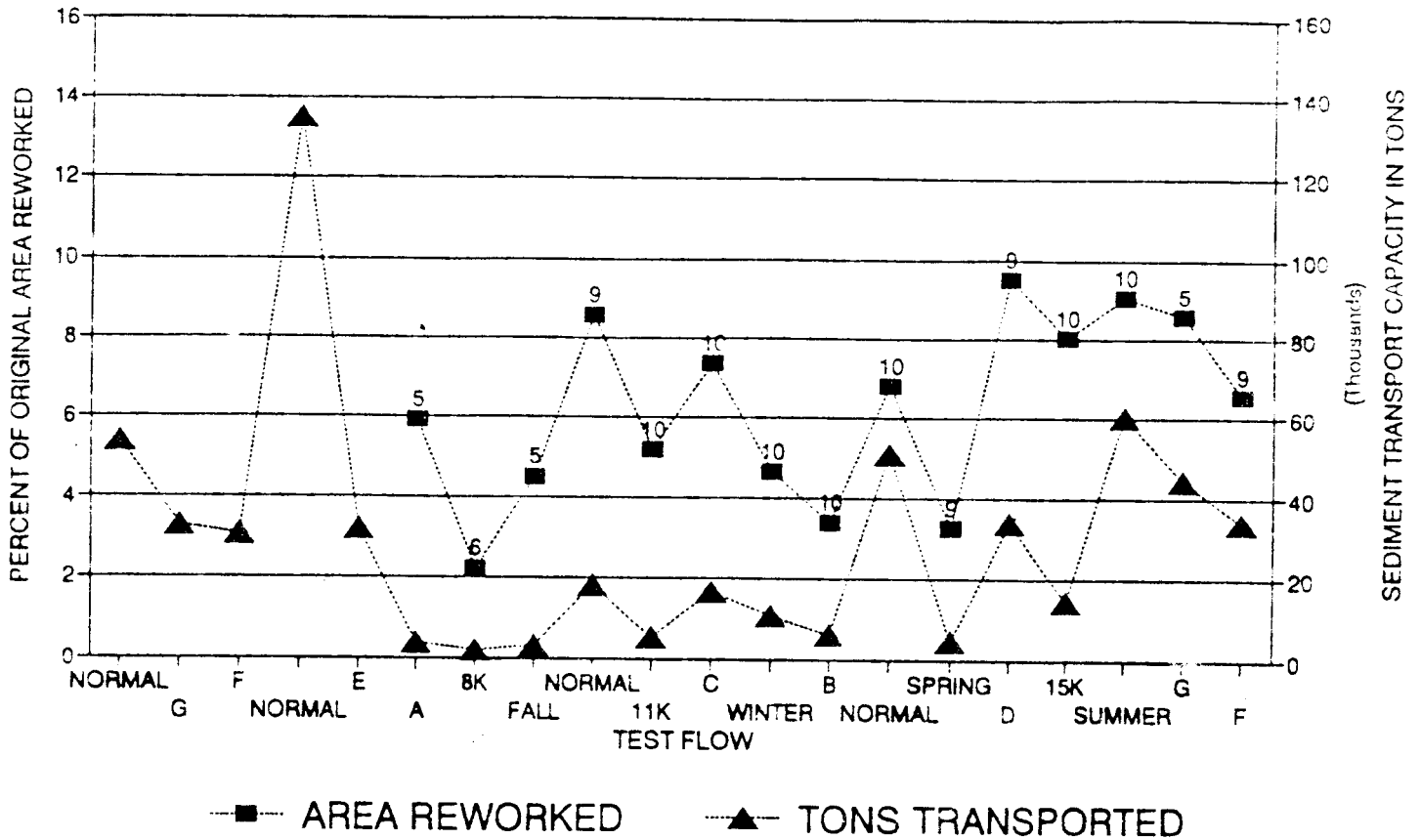


Figure 4. Graph of sediment transport capacity and reworked area for the study period. Numbers above solid blocks indicate sample size out of 10 sites chosen for this report.

REWORKED AREA VS TRANSPORT

N = 10

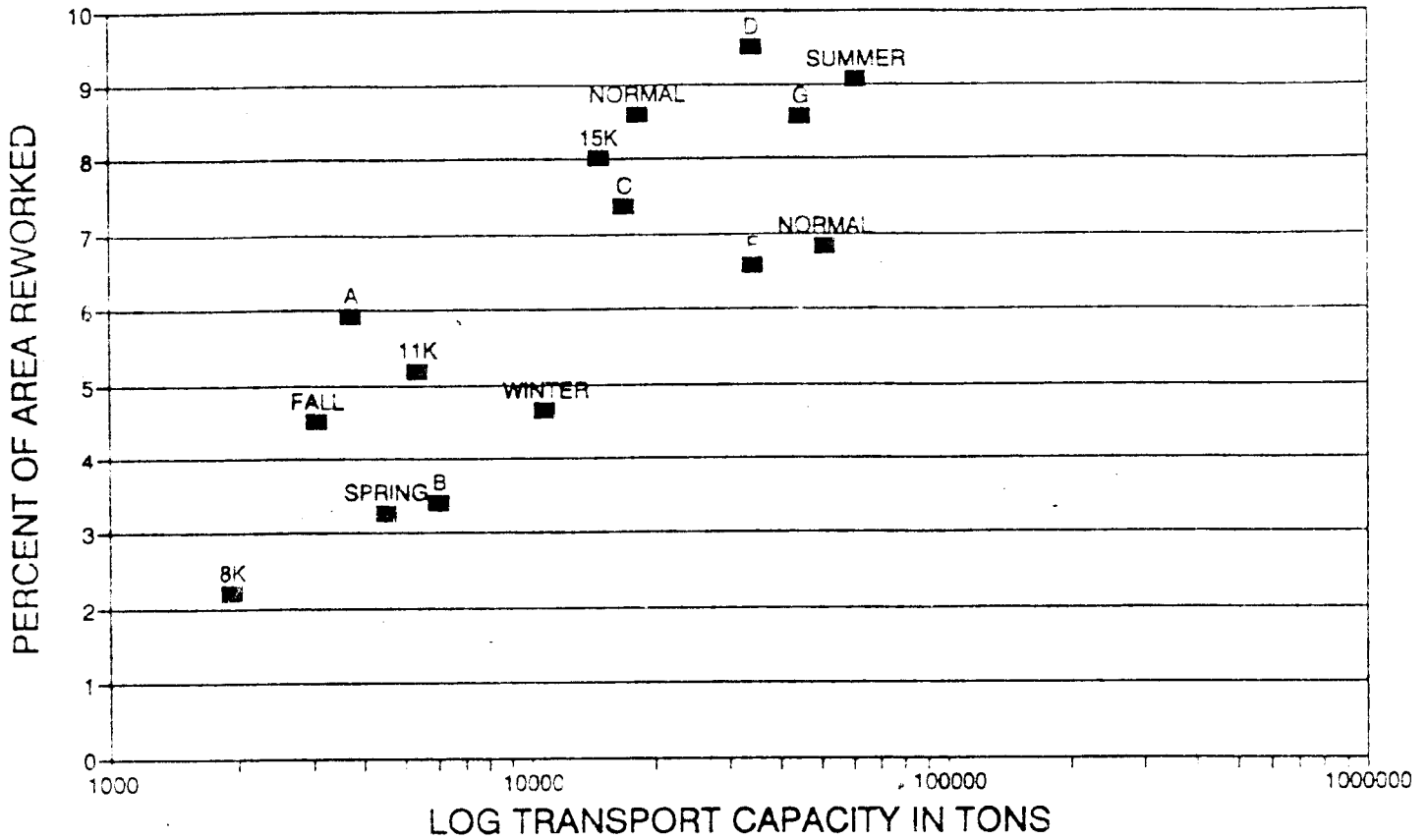


Figure 5. Graph of log transport capacity and percent of area reworked for the test flows included in this report.

REWORKED AND NET AREA

N = 10

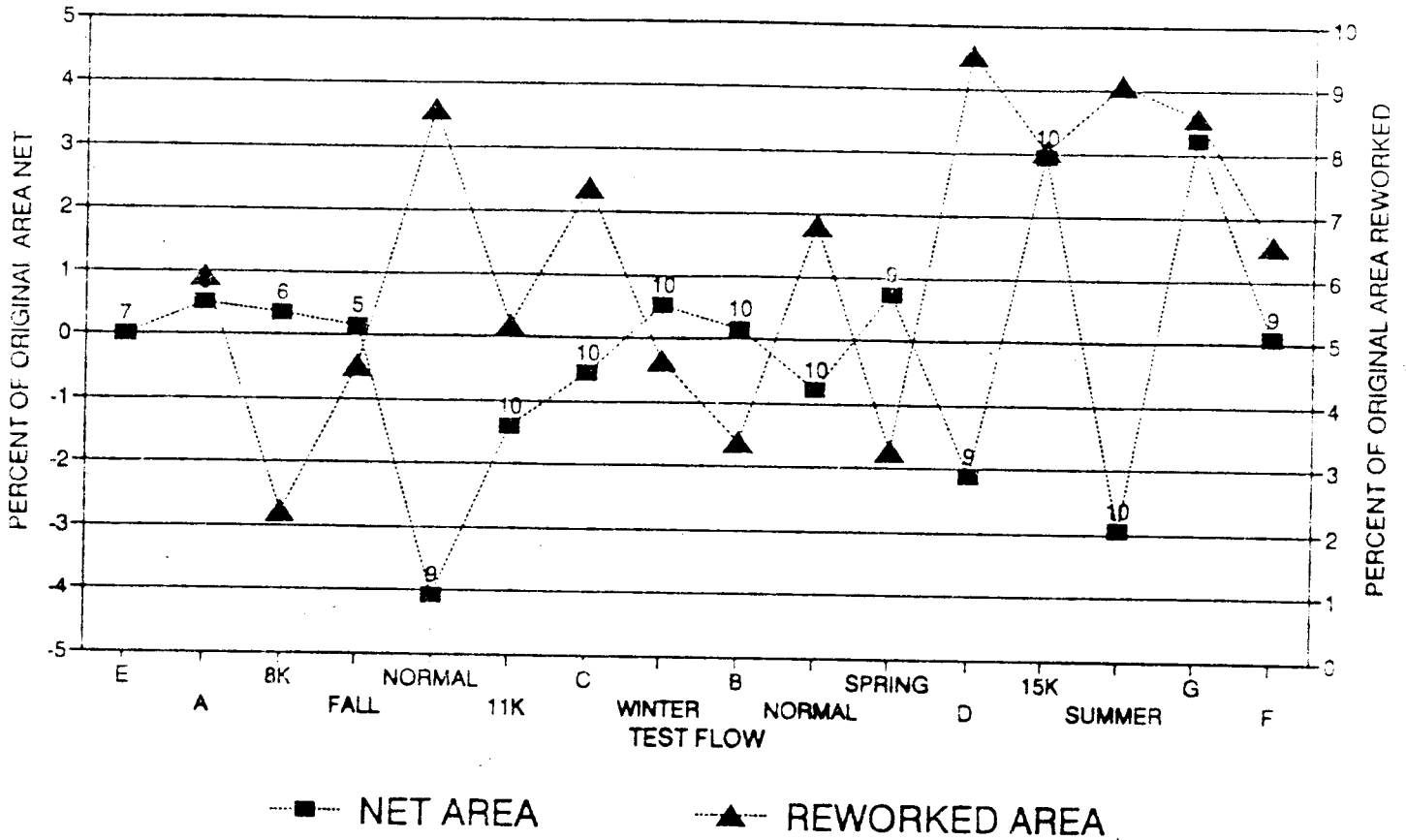


Figure 6. Graph of reworked and total areas for each of the test flows studied in this report. The numbers over the solid blocks indicate the number of sites measured, out of ten possible.

erosion occurred along the whole river side of the deposit involving 2,440 meters², 10%. This change would probably be unnoticed by any casual observer. The 66 left site also underwent erosion localized at the down stream end, accompanied by deposition within preexisting erosion features (Fig. A7b). The net result was enlarged area of about 30 meters². There were no other photos captured that allow analysis of sand bars for the "A" test flow.

This pattern of change, although from only two sites, indicates that the "A" test flow concentrated its energy on the lower portions of the deposits, and although it fluctuated from 3,000-13,000 cfs, it eroded materials that were probably deposited or stable during the previous "E" test flow that fluctuated from 3,000-26,000 cfs.

"8,000" cfs constant test flow This test was the least energetic of any of the test flows (Fig. 3) and reworked about 2% of total sand bar area for the 6 sites sampled. Overall, it resulted in about 1% decreased area (Fig. 6). This constant flow created minor cut banks at most sites. However, the low constant flow test resulted in significant sand bar change at only one site. At 43 left 215 meters² (0.5%) were aggraded during the 11-day test period (Fig. A3d).

The "8,000" cfs constant flow created minor cut banks along the bars either from direct stream scouring or simply from surface waves that were concentrated at the constant river stage. The slight area loss associated with cut bank formation is probably due to the prior steepness of slopes created during the highly energetic "E" (Fig. 3) test flow in September 1990.

"Normal Fall" test flow The "Normal Fall" test flow fluctuated irregularly from about 2,000-14,000 cfs on average for 11 days. Overall the "Fall" test reworked about 4.5% of the sand bar area and slightly decreased net area by about 0.25% (Fig. 6). The notable results were erosion of about 330 meters² at 43 left (0.8%) (Fig. A3e). This involved material that was deposited during the previous 8,000 cfs constant flow.

Although the fluctuations were small, the "Fall" test reversed the trend of deposition that occurred locally at 43 left. This may be due to renewed rill formation and seepage erosion (Table 3).

"Normal Flow" test The "Normal Flow" period lasted for 33 days, and fluctuated daily from about 2,000-15,000 cfs on average. There were discharge spikes to over 20,000 cfs and weekend low flows during this test flow. There was also twice daily discharge peaking. The overall effects of this test were increased reworking (about 8.5%) and decreased net area (about 4%) (Fig. 6). The results of this flow were discretely measured at sites 51 left and 66 left. At 51 left a large semi-circular area (about 1,800 meters²) was eroded from the bar near the reattachment point (Fig. A6d). This was probably due to development of a secondary recirculating eddy. At 66 left a similar semi-circular area was eroded, also near the reattachment point, that involved about 660 meters² (Fig. A7d). This event was also probably due to development of a secondary eddy.

The overall net area loss associated with the "Normal Flow" test is probably a response to increased energy and daily fluctuation range acting upon materials that were shifted to lower positions during the prior low energy "A", "8,000", and "Fall" test flows (Fig. 3). Development of secondary recirculating eddies indicates that the change to higher flow regime scoured some deposits through main channel processes that are not understood.

"11,000 cfs constant" test flow This 11-day constant flow test produced cut banks at all deposits and rearranged sediment on most. The overall results were reworking of about 5% of the sand bar area and an increase in net area of about 2.5% from the previous test flow (Fig. 6). The greatest changes were at -6.5 right, 45 left, 47 right, and 51 left. At -6.5 right about 130 meters² of material eroded from the low elevation portion of the bar (Fig. A1e). At 45 left an apron of sediment was deposited around the entire eddy, indicating a general lowering and reduction of slope of the previous deposits (Fig. A5c). At the 51 left site the secondary eddy that formed during the previous flow test continued to erode material from that part of the bar (Fig. A6e).

The mixed results from the "11,000" cfs test were a combination of cut bank development and deposition of cut bank derived materials at lower positions, thus increasing sand bar area exposed at 5,000 cfs. The previous test flow, being higher in peak discharge than the previous 3 tests, probably formed over-steepened deposits at many locations. These deposits would have responded rapidly to the fairly energetic "11,000" cfs constant flow (Fig. 3), and any surface waves would have concentrated at that unique river stage.

"C" test flow The "C" test flow was for 11 days and involved regular fluctuations from 8,000-20,000 cfs daily. Overall the "C" test reworked about 7.5% of the original area and increased net bar area by about 1% over the previous area (Fig. 6). Specifically, 43 left increased in area overall, especially at the upstream end where often sediment is scoured from the base of the large rock there (Fig. A3g). At 47 right the reattachment platform was eroded, but the downstream end of the reattachment bar was widened (Fig. A5g). The remaining platform deposit at 51 left was further eroded, but deposition occurred over most other area along the bar face (Fig. A6f). The semi-circular secondary eddy feature at 66 left eroded deeper into the deposit and impinged on the vegetated portion (Fig. A7f). At 68 right erosion in the return flow channel enlarged this scour feature, but the separation bar experienced deposition (Fig. A8c). Deposition also occurred at 81 left along most of the upstream end (Fig. A9e). At 172 left, the reattachment bar eroded significantly (675 meters², 11%) while minor aggradation occurred along the bank within the eddy zone and along the separation deposit (Fig. A10e).

In general, this test flow deposited material on separation bars and eroded material from reattachment bars. This indicates that the stagnation areas at separation bars and reattachment bars were generally enlarged, and perhaps materials were deposited at higher positions during the "C" test that were shifted to lower positions during the prior "11,000" cfs test flow.

"Normal Winter" test flow The 11-day "Normal Winter" test flow fluctuated daily from about 2,500-18,000 cfs in an irregular fashion with daily double peaks. It produced a small amount of deposit reworking (about 4.5%) and resulted in a slight (1%) increase of net sand bar area (Fig. 6). Individually, at -6.5 right deposition covered the area that had eroded during the 11,000 constant and "C" flows (Fig. A1g). At 45 left erosion occurred over the whole perimeter except for the slip face of the reattachment platform (Fig. A4f). The river side face of the reattachment bar 47 right lost the material previously deposited (Fig. A5e). At 51 left more of the platform deposit eroded, but the river side face was widened, and the small pond was retained in a new position (Fig. A6f). The entire perimeter of 66 left received a narrow band of newly deposited material (Fig. A7g). At 68 right the return flow channel eroded, but the river side face of the reattachment and separation bars built up (Fig. A8d). The entire perimeter of 172 left eroded during this test with deposition of an island in the eddy zone (Fig. A10f).

The pattern of area changes during the "Winter" test flow was similar to the patterns during the preceding "C" test flow. This indicates that most sand bars responded positively to decreased energy (Fig. 3), although the daily double peak may have actually increased the peak flow duration from the prior "C" test flow. At some distance downstream of the Dam, there may have been little difference between the "C" and "Winter" tests.

"B" test flow The "B" test flow fluctuated daily from 5,000-15,000 cfs on a regular schedule for 11 days. Overall it resulted in reworking about 3.5% of all sand bar area, and the net result was negligible area change (-0.25%) (Fig. 6). Locally, the "B" test flow eroded the face of 43 left (Fig. A3i) about 134 meters², deposited material around the perimeter of 45 left (Fig. A4g), continued to erode the platform deposit at 51 left (Fig. A6g), and eroded most the perimeter of 172 left except for minor deposition on the reattachment platform (Fig. A11g).

The comparatively small fluctuations of the "B" test, following the much greater fluctuations of the preceding "C" and "Winter" tests apparently had little overall effect on the sand bars.

"Normal Flows" period The 67-day "Normal Flow" period fluctuated irregularly daily from average lows of about 3,000 cfs to average highs of about 17,000 cfs, with weekend low flows that fluctuated much less. Each daily fluctuation was usually double peaked. The overall result was a high reworked area (about 7%) and a net decrease (1%) in total area (Fig. 6). Specifically, at 8 left the upstream portion eroded about 35 meters² (Fig. A2i). At 45 left the perimeter of the reattachment deposit eroded about 860 meters², but the separation deposit aggraded about 250 meters (Fig. A5g). Erosion removed the remaining platform deposit at 51 left (Fig. A6h). The eddy at 66 left underwent major rearrangement with erosion along the main deposit body and deposition of a large island in the eddy zone (Fig. A7i). At 68 right the whole reattachment deposit face eroded about 460 meters² and the separation bar changed little (Fig. A8f). At 172 left the reattachment deposit aggraded considerably (about 550 meters²) as did the banks within the eddy zone (Fig. A10h). However, the platform deposit and eddy island were eroded about 250 meters². The separation bar aggraded slightly.

This pattern of sand bar change is highly random, and reflects the randomness of pattern in the "Normal Flow". The pattern also suggests that individual sand bars may be subjected to different flow dynamics from the same release patterns depending on local channel geometry or flow routing characteristics as flows migrate downstream.

"Normal Spring" test flow The "Normal Spring" test ran for 11 days and fluctuated on average from about 3,000 cfs to 12,000 cfs with a weekend period of fluctuations from 3,000-8,000 cfs. The overall result of this test flow was a very small reworked area (about 3.5%) and a slight increase in net area (about 1%) (Fig. 6). The 51 left site eroded during this test period by about 1,400 meters² along the whole perimeter (Fig. A6i). The 66 left site aggraded about 900 meters² during the same period mostly within the eddy zone (Fig. A7j). Reworking with little net area change was the norm at all other sites.

The "Spring" test flow was not much different in range or daily energy from the preceding "Normal" test flow (Fig. 3). Consequently, sand bar responses were similarly random.

"D" test flow The "D" test flow fluctuated daily and regularly from 3,000-26,000 cfs for 11 days. This was a highly energetic test flow (Fig. 3) and resulted in the highest amount of reworked area during the study period (about 9.5%). The net result was a slight decrease (2.5%) in sand bar area (Fig. 6). Aggradation resulted on the -6.5 right, 8 left, and 43 left sites (Figs. A1k, A2k, and A3l). Mixed erosion and deposition occurred on the other sites. At 45 left erosion occurred everywhere except on the platform deposit which lengthened (Fig. A4j). At 47 right erosion occurred on the platform deposit and a thin deposit was laid down along the river side face (Fig. A5i). At 51 left the platform enlarged as did the downstream river side face, but another secondary eddy formed that eroded a semi-circular area along the middle of the bar (Fig. A6j). At 66 left the return flow channel aggraded but the upstream face eroded (Fig. A7k). 81 left also increased in size through deposition of about 20 meters² (Fig. A9j). Photography was missed at 68 right and 172 left for this epoch.

This pattern of area change resulting from the "D" test flow indicates that in general flow separation points moved downstream and recirculation zones were larger and probably of greater velocity than during the preceding "Normal" and "Spring" fluctuating flows. The resulting sand bar morphologies reflect the general response to enlargement of recirculation zones from a high fluctuation test flow.

"15,000" cfs constant test flow The "15,000" cfs constant flow lasted 11 days. Overall it reworked about 8% of the total sand bar area and resulted in a dramatic increase in net area (5%) (Fig. 6). -6.5 right responded with degradation of about 140 meters² (Fig. A1l) while 8 left aggraded by about 170 meters² (Fig. A2l). 45 left responded to the "15,000" constant flow with aggradation over most of the perimeter by about 2,800 meters² (Fig. A4k). The platform deposit shortened slightly. The platform deposit at 51 left eroded as did the extreme downstream end of the river side face (Fig. A6k). At 66 left the eddy zone eroded while the upstream portion aggraded (Fig. A7l). Reversal of the previous behavior occurred at 68 right, with erosion of the return flow channel and deposition on the separation bar (Fig. A8h). 81

left remained much as it was before the test flow (Fig. A9k). Sometime during the "D" or 15,000 cfs tests the 172 left site aggraded by deposition on the platform deposit of about 500 meters² of sediment.

The pattern of sand bar changes resulting from the "15,000" cfs constant flow indicates that at sites with low separation bars (ie, 68 right), the 15,000 cfs constant flow provided sufficient current of sufficient duration to scour sediment. This material was however probably redeposited in the reattachment environment. Generally, the "15,000" cfs flow following the high fluctuation "D" test flow redistributed sediments that were reworked during "D", and deposited them at lower positions along the toes of reattachment bars to increase area exposed at 5,000 cfs.

"Normal Summer" test flow The "Normal Summer" test was for 26 days in June 1991, and fluctuated daily from about 5,000 cfs to about 25,000 cfs on average. Each daily fluctuation was unique, often with double peaks, and three weekend low fluctuations occurred that ranged from 5,000 to about 16,000 cfs. This was an energetic flow test (Fig. 3) that reworked about 9% of the sand bar area on average and decreased overall net area by about 6% (Fig. 6). The upstream end of 43 left eroded about 125 meters² around the large rocks (Fig. A3n). At 45 left significant erosion occurred around the reattachment deposit (about 1,800 meters², 0.8%) (Fig. A4n). The whole perimeter of 47 right eroded, involving about 1,900 meters² of sediment (Fig. A5k). 51 left however aggraded by about 1,200 meters² (Fig. A6l). The 66 left site showed mixed aggradation and degradation, largely reversing the prior events during the "15,000" flow. Photography was not captured at 68 right. Aggradation occurred at 81 left even though tunnel scour features were present (Fig. A9l) (see next section). At 172 left nearly the whole perimeter degraded (about 890 meters²) but the platform deposit lengthened.

This pattern of sand bar morphology change indicates that the "Summer" test flow disrupted the deposits that were enlarged during the preceding "15,000" cfs constant flow test. This may be a response to the duration of the test, the range of fluctuations, or the weekend low fluctuation periods. Carpenter and Carruth (1992) showed that bank failure events often occurred following weekend draw-down periods at 172 left. Cluer (1992) documented bank failures at four other sites that occurred immediately after weekend low flow periods.

"G" test flow The "G" test flow involved 11 days of regular fluctuations from 8,000 cfs to 27,000 cfs daily. Overall, "G" reworked about 8.5% of the sand bar area and resulted in a dramatic net increase of area by about 6% (Fig. 6). Many of the sites are not represented by photographs for this test flow. However, the prior trends of aggradation and degradation were largely reversed at sites 47 right, 51 left, and 172 left. At 47 right the whole perimeter aggraded by about 1,925 meters² (Fig. A5l). 51 left eroded over its whole perimeter, about 1,690 meters² (Fig. A6m). Deposition occurred at 172 left along the river side face, around the eddy zone, and on the separation deposit. Some erosion on the platform area created an island of the platform deposit (Fig. A10l).

The mixed results of the "G" test flow may in part be due to the smaller than normal sample size. The pattern of changes indicates that the highly energetic flow test (Fig. 3) resulted in highly erratic responses. Because of the smaller than normal sample size, the aggradation measured at 47 left dominates the analysis.

"F" test flow The "F" test flow had the same daily fluctuation range as "G", 8,000-27,000 cfs, but with a lower ramping rate. This resulted in shorter duration at peak discharge and consequently was a less energetic flow (Fig. 3). It reworked about 6.5% of the sand bar area and resulted in a decrease in net area by about 3% overall (Fig. 6). "F" degraded the whole perimeters of 8 left and 43 left (Figs. A2o and A3o). 47 left was slightly enlarged by deposition along the downstream river face and in the eddy zone (Fig. A5m). Aggradation also increased the size of 51 left along most of its perimeter (Fig. A6n). Minor reworking occurred at 66 left with little net change in area (Fig. A7n). The prior trends at 172 left were reversed during the "F" flow. Erosion occurred along the downstream river side face, within the eddy zone, on the platform deposit, and on the separation bar.

The pattern of change associated with the switch from "G" to "F" test flows indicates that a flow with the same range but shorter duration at peak results in net loss of sand bar area. This suggests that duration at peak discharge is an important variable in sand bar response. This is illustrated in the sediment transport model comparing test flows "G" and "F" (Fig. 3). Conversely, the comparison may also indicate that the "G" and "F" flows were not all that different, especially at some distance downstream, just that there was insufficient sediment stored for aggradation to continue during the "F" test flow as it had during the "G" test flow. Further sediment transport modeling should clarify this issue as would a larger sample size for analysis.

Seepage Related Features

Seepage of residual bank-stored water following river stage lowering causes a spring line to develop at the contact point of sand bar surface and ground water surface (Werrell et al, 1992). Below this line erosion features often developed when residual head was great enough. The most common features were rills and rill networks, and occasionally larger scale tunnel scour (Howard and McLain, 1988) features developed. Residual head increases where daily stage fluctuation is high and where sand bar slope is great. Sites where these features commonly developed along the river side face were 43 left and 81 left. At other sites rills commonly developed along the steep slip faces of return flow channels (Fig. 2). Werrell et al (1992) showed that deposition and seepage erosion operate simultaneously on Grand Canyon sand bars, but that either process may dominate given certain flow conditions.

The test flows that resulted in seepage processes were generally those with high stage fluctuations. However, every fluctuating flow resulted in rills at sites 43 left, 45 left, and 81 left. These observations are summarized in table 3.

Table 3. Summary of seepage features and associated test flows.

SITE/FLOW	-6.5 L	8 L	43 L	45 L	47 R	51 L	66 L	68 R	81 L	172 L
"A"			r	r				r	r	
8,000 c										
Fall			r	r					r	
11,000 c										
"C"			r	r		r	r		r	
Winter			r	r			r	r	r	
"B"			r	r					ts	
Normal			r	r					ts	
Spring			r	r					r	r
"D"			r	r					r	r
15,000 c										
Summer			r	r					r	r
"G"			r	r					ts	r
"F"			r	r					ts	r

Key: r = rills, ts = tunnel scour

It is notable that the formation of seepage features often accompanied deposition of new sediment along the face of sand bars. Site 81 left was unique in the size of tunnel scour features that developed (Figs. 7 and A9I). The "B", "Normal", "G", and "F" test flows all resulted in tunnel scour at 81 left, and were all highly reworking flows. The "C" and "Normal Winter" test flows resulted in rill development at five out of ten sites. The "A", "Normal Spring", and "D" test flows produced rills at four out of ten sites.

Figure 7. Aerial photographs of site 81 left taken on June 2 and June 29, 1991. Note tunnel scour formation coincident with aggradation during the "Normal Summer" test flow.

CONCLUSIONS

The strong correlation between calculated sediment transport capacity and actual reworked area for the test flows during the study period indicates that this method of comparison may result in an accurate tool for predicting overall sand bar responses to alternative flow regimes. This would require completing development of the aerial photography database. Currently, the sample size is too small to allow confident prediction.

The changes documented at 51 left suggest that major sediment erosion or deposition can occur while leaving almost imperceptible change in overall geomorphology. Even subtle features such as the small pond on the river side face were retained during large changes in area. This suggests that sand bars may appear stable when in fact they are dynamic. 47 right and 51 left responded to the test flows most often by degradation, and ultimately were 11% and 13% smaller, respectively, than in the beginning. Final results at the other sites were: -3% at -6.5 right; -2% at 8 left; no change at 43 left; +7% at 45 left; -2% at 66 left; +3% at 68 right; +4% at 81 left; and -6% at 172 left. The large losses at 47 right and 51 left are unique for the test flow period, and may indicate a lack of sediment storage in the main channel, resulting in reductions of storage from eddy deposits.

In general, during the test flow program, reductions in stream energy and range of daily fluctuations following flows with higher energy and fluctuation ranges resulted in greater area. This was due to reworking of over-steepened deposits created during highly fluctuating flows. Conversely, flows with increased energy and fluctuation ranges following low energy low fluctuation range flows resulted in decreased area. This is due to reworking of sediments that were previously shifted to lower positions and deposition at higher positions. The long term effects of this type of deposit increase are not clear, and should be studied further.

The "15,000" cfs constant flow following the high energy "D" test flow produced the largest net gain in area. This was due to reworking sediments that were deposited in higher positions and at steep slope angles by the "D" flow. This observation has implications for the benefits of bar building test flows.

Overall, this investigation concludes that regularly fluctuating flows were less damaging than the irregularly fluctuating "Normal" flows that included weekend low fluctuation periods. The flows that most positively increased sand area were the "15,000" cfs constant and the "G" test. The flows that most obviously resulted in net erosion were the "Normal" flow in November and December 1990, and the "Summer" flow test.

RECOMMENDATIONS

The potential offered by completing development of the aerial photography database is significant. Clearly, a large sample size is necessary to understand the range of effects particular flow regimes have on the wide variety of fluvial deposits along the Colorado River. This report includes 10 out of 74 sites photographed during the test flow program. Full reduction and development of this database is strongly recommended. With this database as background, the ensuing interim flow period should be evaluated by similar methods, provided that equivalent periods of 5,000 cfs constant discharge are possible for photo capture.

The equilibration rates of the particularly rapid erosive and gaining test flows needs to be understood. Similarly, the long-term effects of the clearly aggradational or degradational test flows need to be understood before the full range of flow alternatives can be evaluated. There is a strong need for daily evaluation of a large sample of sand bars to determine short-term temporal and spatial responses, so that prediction of responses at longer temporal scales may become possible.

Further modeling of the test flow dynamics is suggested. Questions raised in this investigation about downstream migration of some of the variables that made test flows unique can be answered by comparing transport capacities for individual flows calculated at the string of USGS Gages from Lees Ferry to Diamond Creek.

REFERENCES CITED

- Carpenter, M.C., and Carruth, R.L., 1992. Hydrogeology of beaches 43.1L and 172.3L and the implications on flow alternatives along the Colorado River in the Grand Canyon. *in* Beus, S.S., and Avery, C.C., 1992. The influence of variable discharge regimes on Colorado River sand bars below Glen Canyon Dam: 1991 Annual Report.
- Cluer, B.L., 1992. Daily responses of Colorado River sand bars to Glen Canyon Dam test flows, Grand Canyon, Arizona. *in* Beus, S.S., and Avery, C.C., 1992. The influence of variable discharge regimes on Colorado River sand bars below Glen Canyon Dam: 1991 Annual Report.
- Howard, A.D., and McLain, C.F., III, 1988. Erosion of cohesionless sediment by groundwater seepage. *Water Resources Research*, v.24, n.10, p.1659-1674.
- Schmidt, J.C., and Graf, J.B., 1988. Aggradation and degradation of alluvial sand deposits 1965 to 1986, Colorado River, Grand Canyon National Park, Arizona. U.S. Geological Survey, Open-File Report 87-555.
- Smillie, G., Jackson, W.L., and Tucker, D., 1992. Colorado River sand budget: Lees Ferry to Little Colorado River including Marble Canyon. *in* Beus, S.S., and Avery, C.C., 1992. The influence of variable discharge regimes on Colorado River sand bars below Glen Canyon Dam: 1991 Annual Report.
- Werrell, W., Inglis, R., Jr., and Martin, L., 1992. Beach face erosion in Grand Canyon National Park. *in* Beus, S.S., and Avery, C.C., 1992. The influence of variable discharge regimes on Colorado River sand bars below Glen Canyon Dam: 1991 Annual Report.

ACKNOWLEDGMENTS

Bill Jackson and Gary Smillie of the National Park Service Water Resources Branch provided valuable direction and support in modeling the test flows to determine sediment transport capacity. Tim Randle of the Bureau of Reclamation in Denver provided updated transport functions and necessary discussion prior to modeling. John Rote and Don Bills at the Flagstaff Field Office USGS provided the basic hydrographic information that was input to the sediment transport model. Certainly not least, Sherman Wu and his staff at the USGS Planetary Mapping Division in Flagstaff provided unending creativity and persistence in utilizing the flawed images, and made the aerial photography analysis possible.

APPENDIX A

**RESPONSE CURVES OF INDIVIDUAL SITES AND
PLANIMETRIC OUTLINES ARRANGED BY TEST FLOW**

Original planimetric outlines and subsequent comparisons of bracketing outlines. Dark shaded areas were eroded. Light shaded areas were aggraded.

SITE -6.5 RIGHT

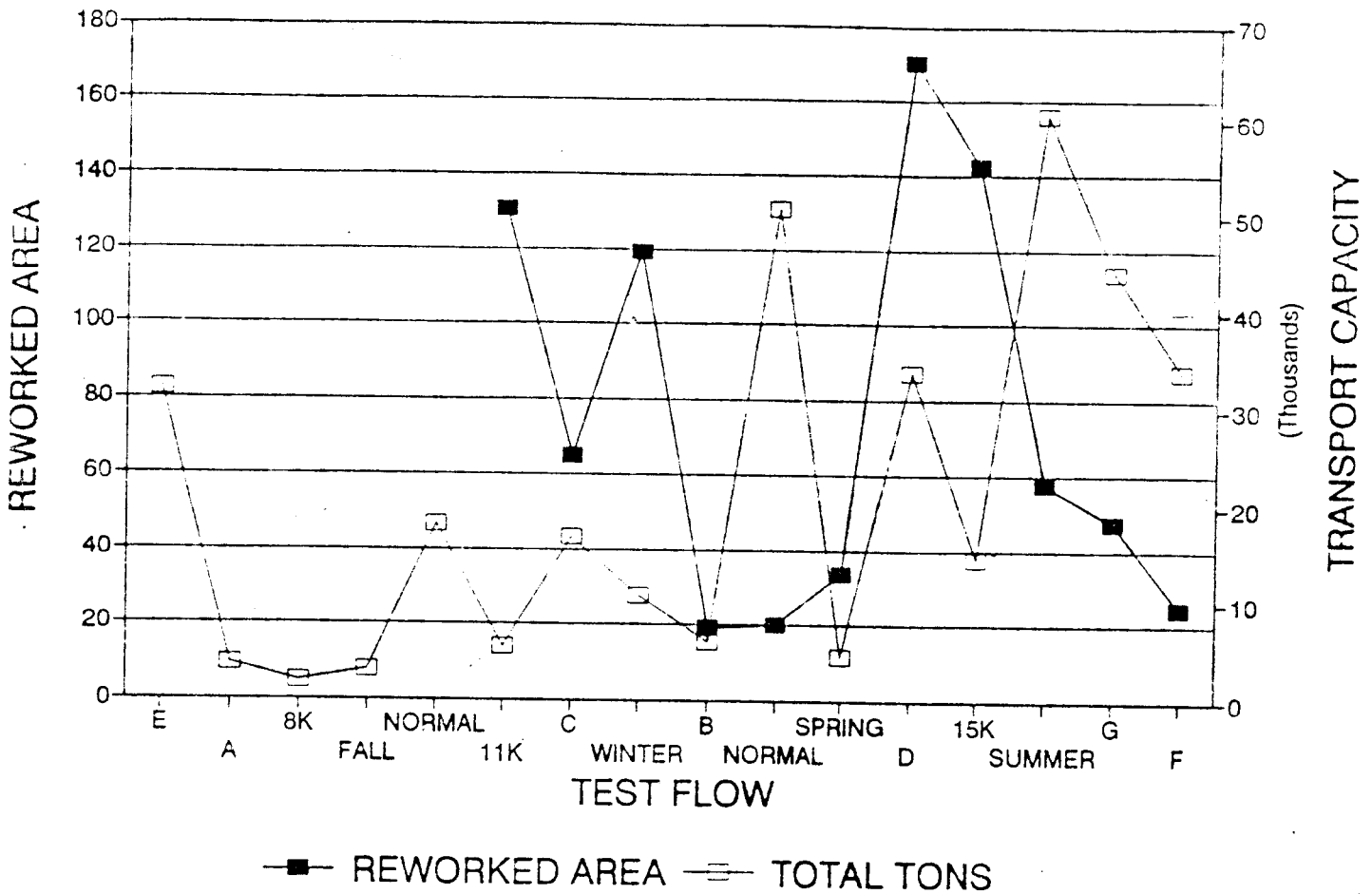


Figure A1. Time-series plot of reworked area and sediment transport capacity for site CR -6.5 R.

Figures A1a-A1l. Original planimetric outlines and subsequent comparisons of bracketing outlines. Dark shaded areas were eroded. Light shaded areas were aggraded.

A1a



12/17/90

A1b



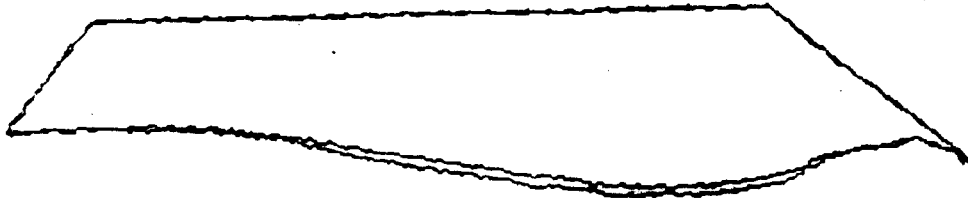
12/17/90 12/30/90 11,000 cf

A1c



12/30/90 01/12/91 "C"

A1d



01/12/91 01/26/91 WINTER

A1e



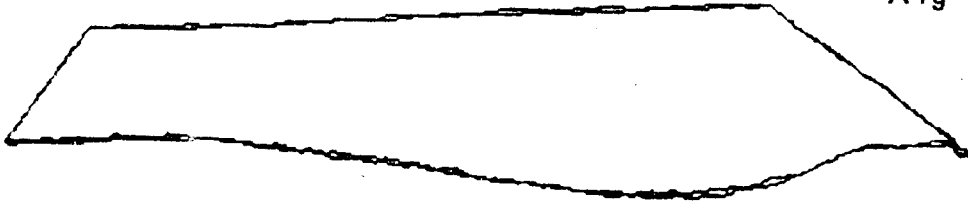
01/26/91 02/09/91 "B"

A1f



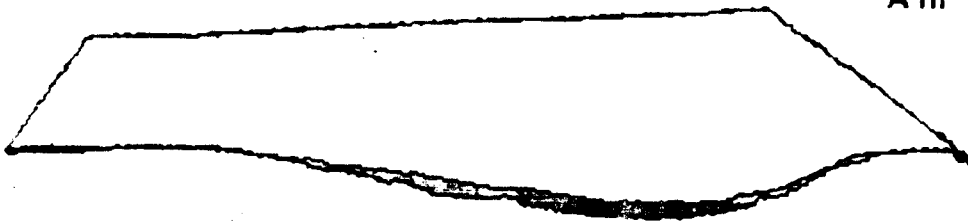
02/09/91 04/20/91 NORMAL

A1g



04/20/91 05/05/91 SPRING

A1h



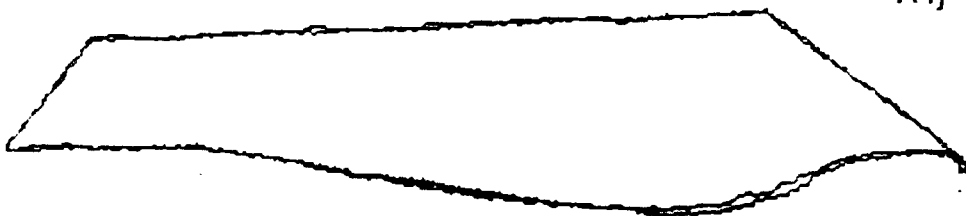
05/05/91 05/19/91 "D"

A1i



05/19/91 06/02/91 15,000 cf

A1j



06/02/91 06/30/91 SUMMER



A1k



06/30/91 07/14/91 "G"

A1l



07/14/91 07/27/91 "F"

SITE 8 LEFT

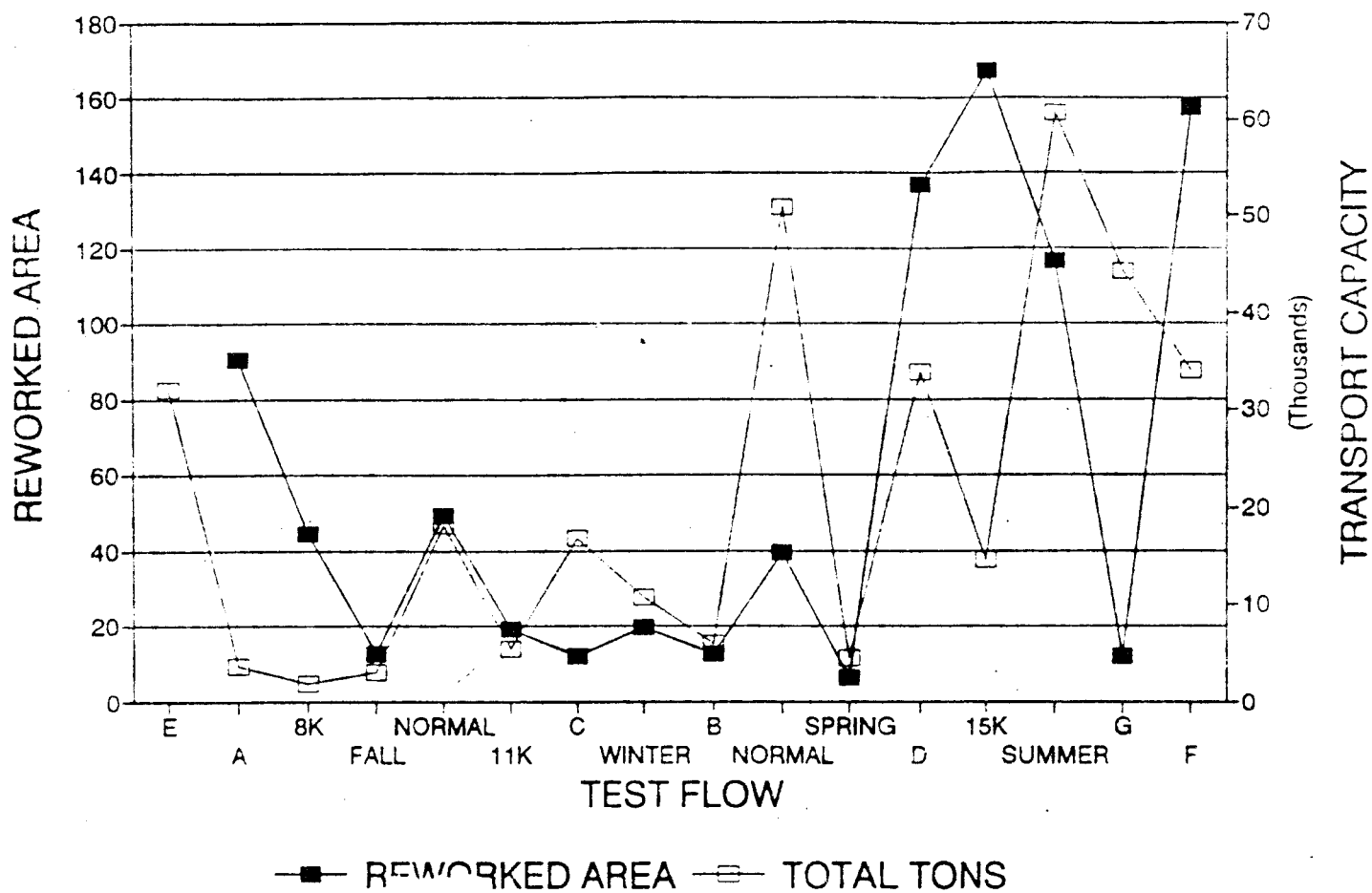
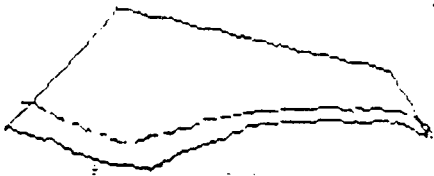


Figure A2. Time-series plot of reworked area and sediment transport capacity for site CR 8 L.

Figures A2a-A2n. Original planimetric outlines and subsequent comparisons of bracketing outlines. Dark shaded areas were eroded. Light shaded areas were aggraded.

A2a



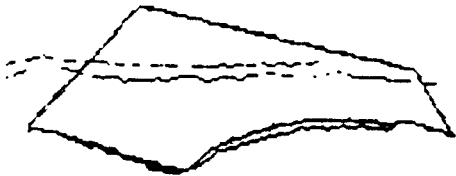
10/30/90

A2b



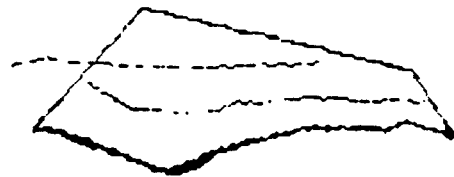
10/30/90 11/11/90 FALL

A2c



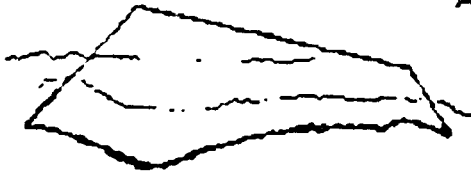
11/11/90 12/17/90 NORMAL

A2d



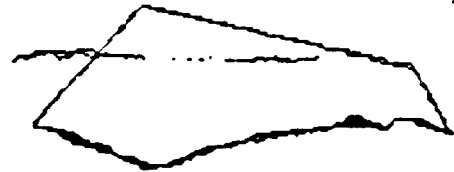
12/17/90 12/30/90 11,000 cfs

A2e



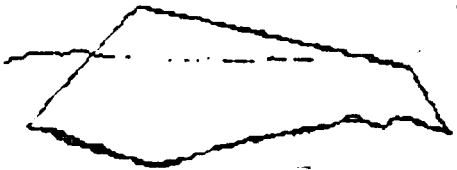
12/30/90 01/12/91 "C"

A2f



01/12/91 01/26/91 WINTER

A2g



01/26/91 02/09/91 "B"

A2h



02/09/91 04/20/91 NORMAL

A2i



04/20/91 05/05/91 SPRING

A2j



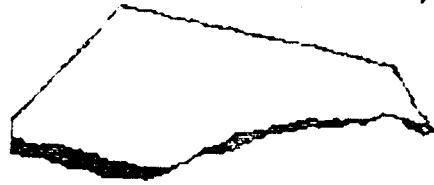
05/05/91 05/19/91 "D"

A2k



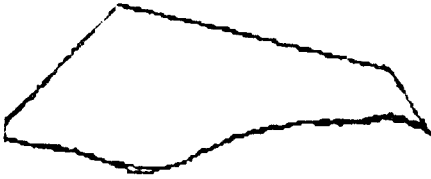
05/19/91 06/02/91 15,000 cfs

A2i



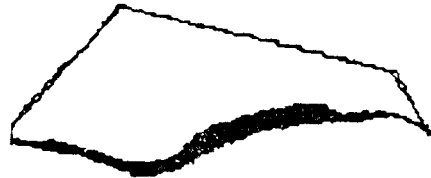
06/02/91 06/30/91 SUMMER

A2m



06/30/91 07/14/91 "G"

A2n



07/14/91 07/27/91 "F"

SITE 43 LEFT

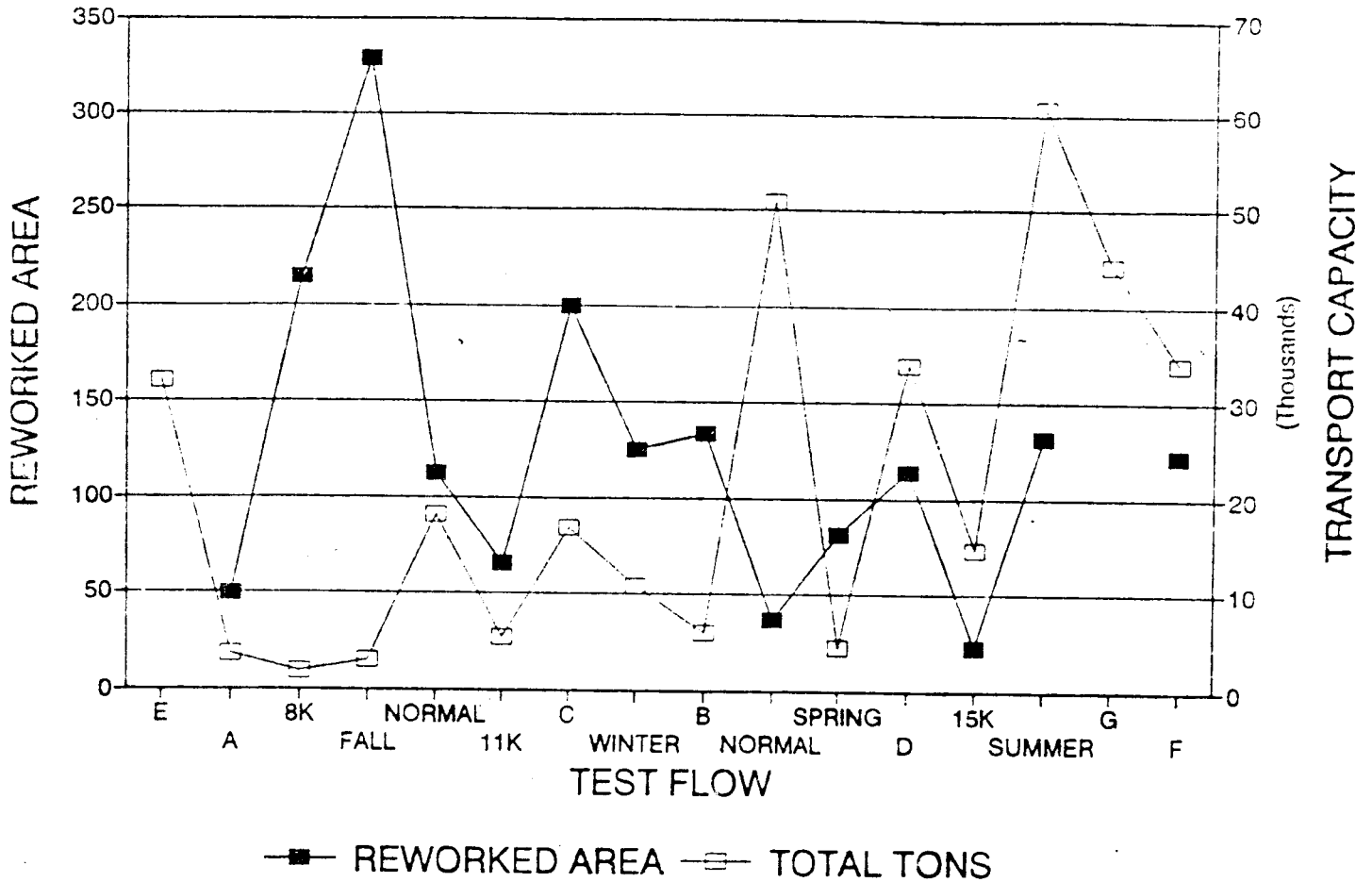
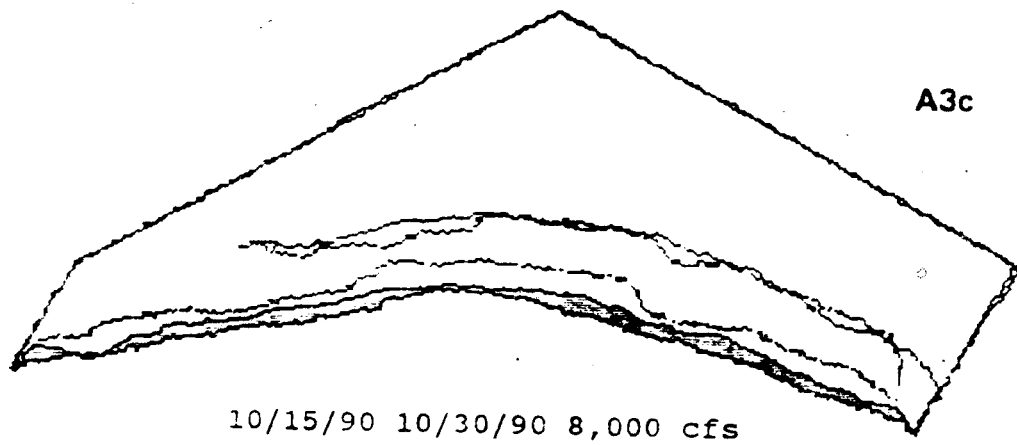
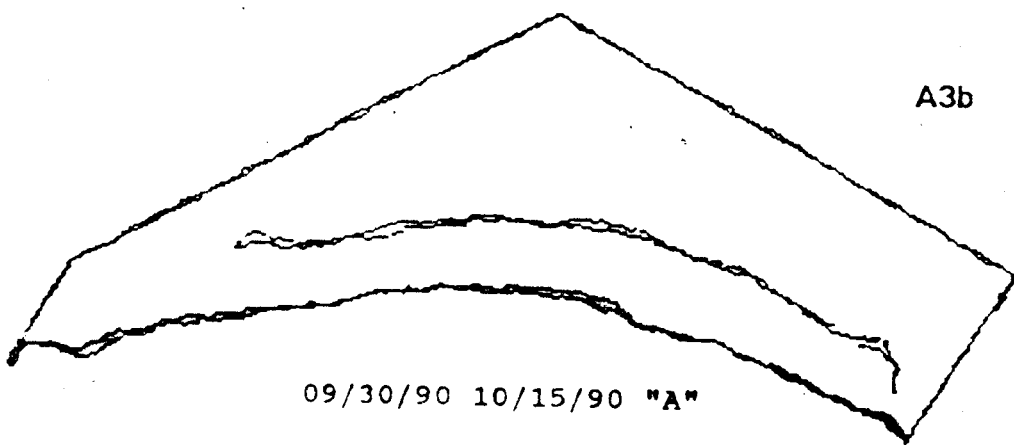
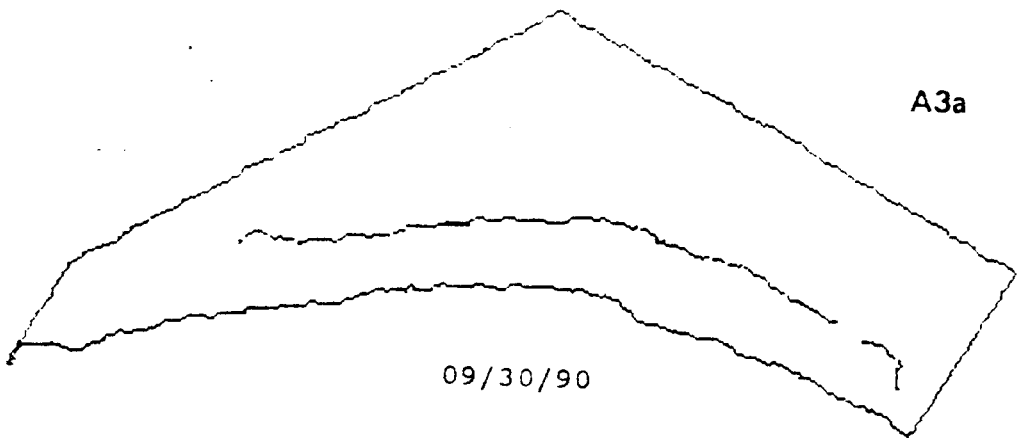
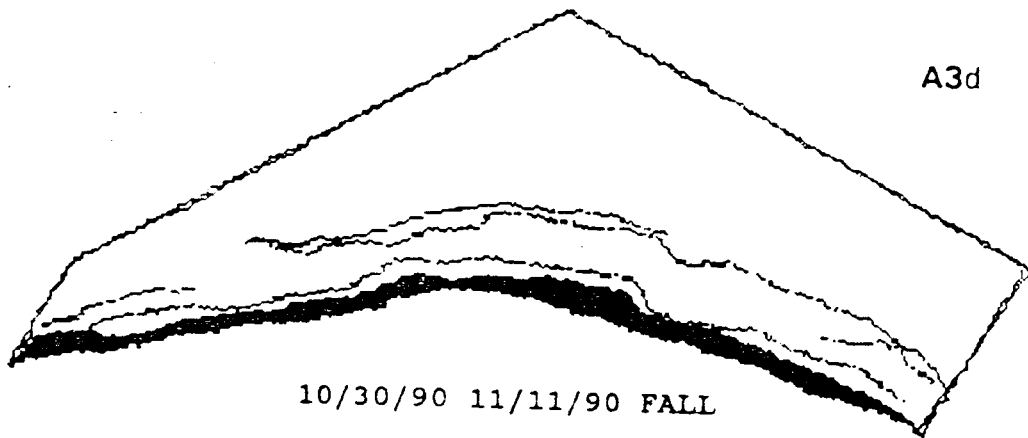


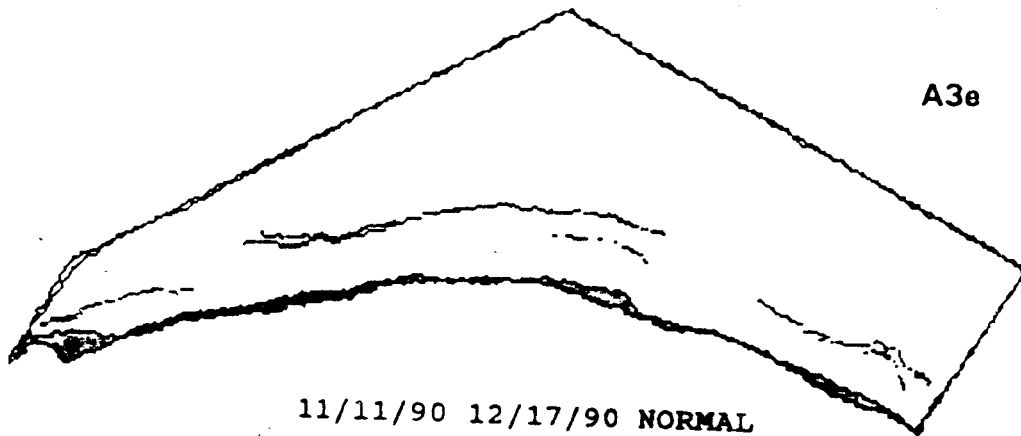
Figure A3. Time-series plot of reworked area and sediment transport capacity for site CR 43.

Figures A3a-A3o. Original planimetric outlines and subsequent comparisons of bracketing outlines. Dark shaded areas were eroded. Light shaded areas were aggraded.

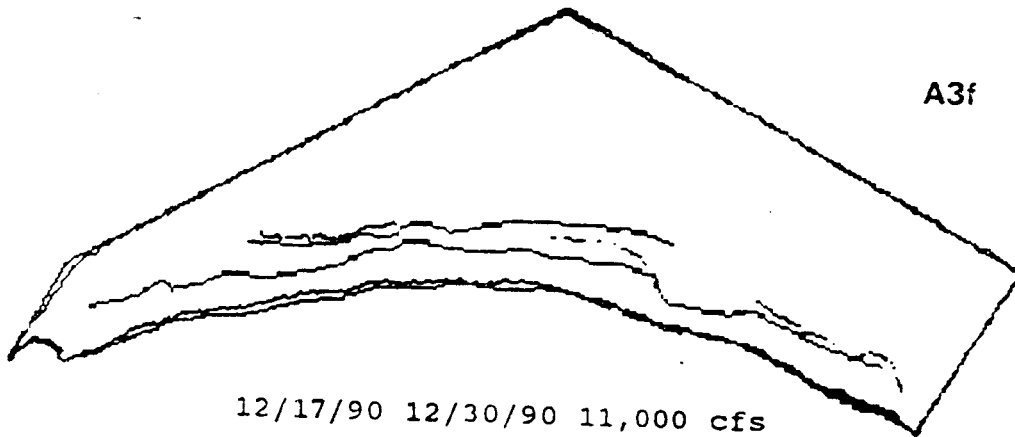




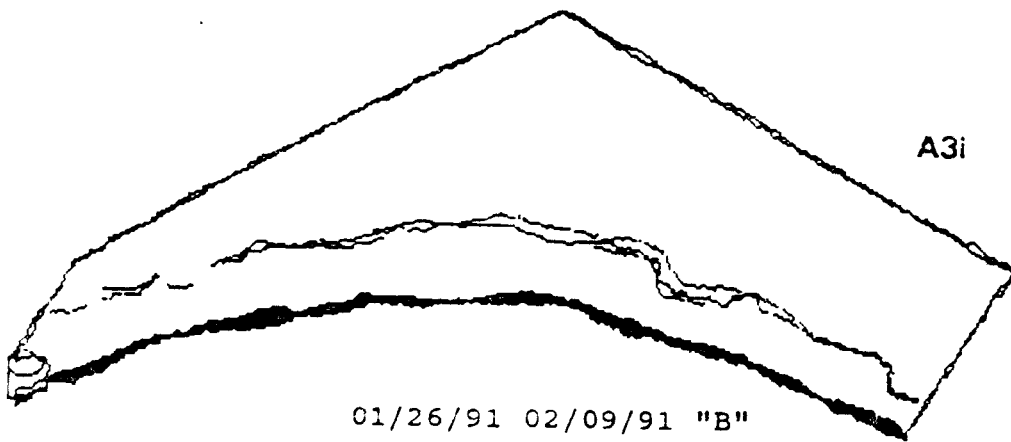
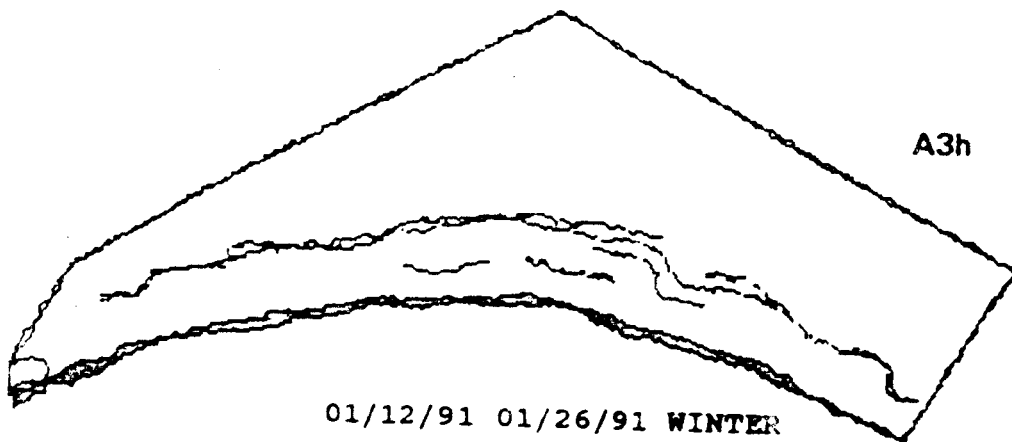
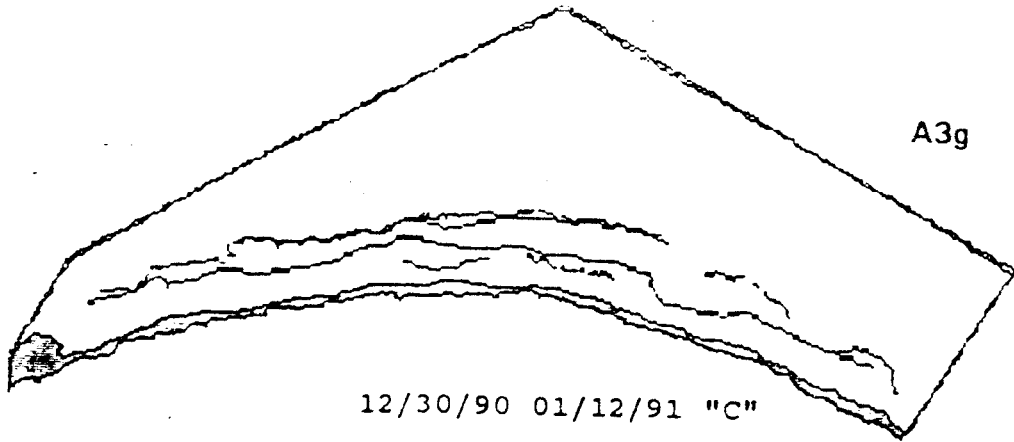
10/30/90 11/11/90 FALL

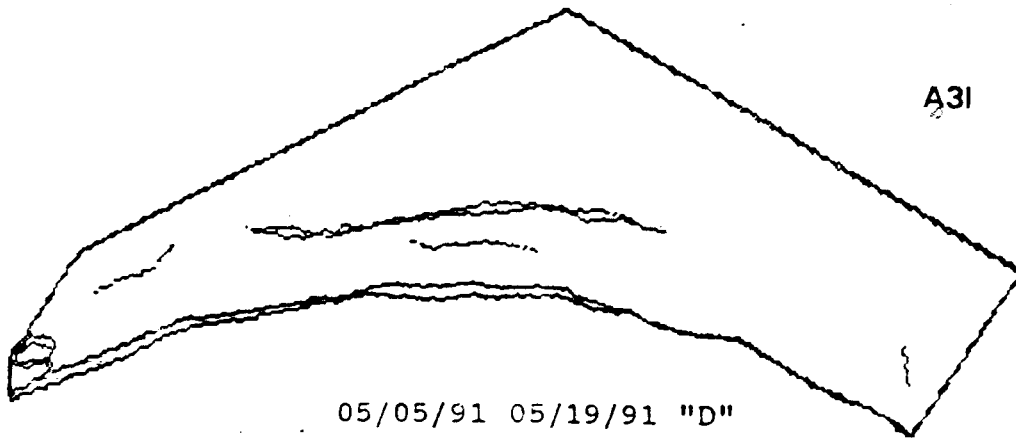
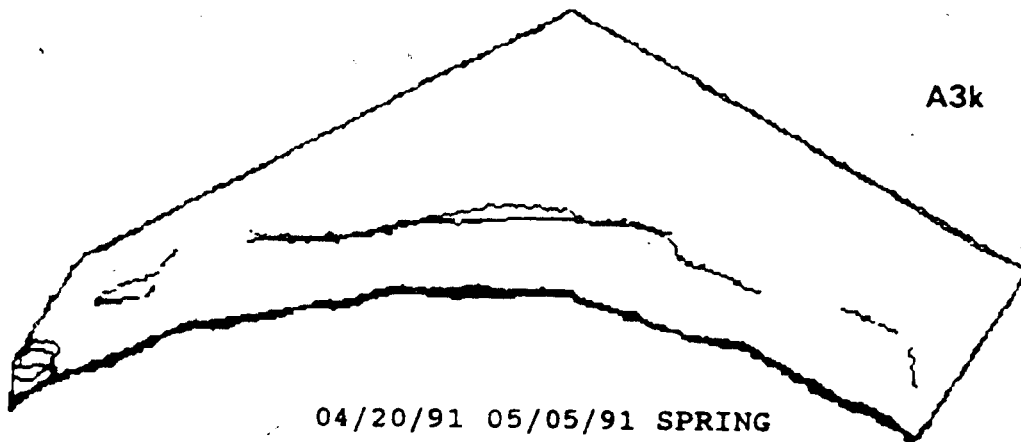
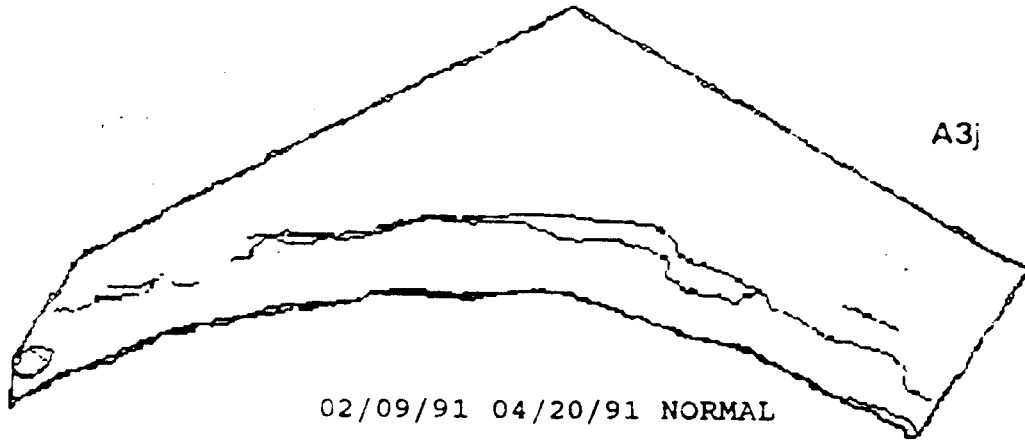


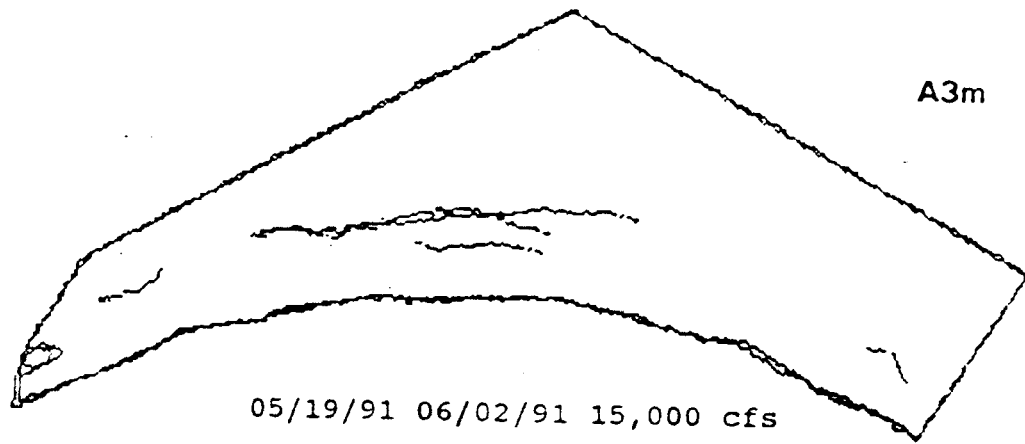
11/11/90 12/17/90 NORMAL



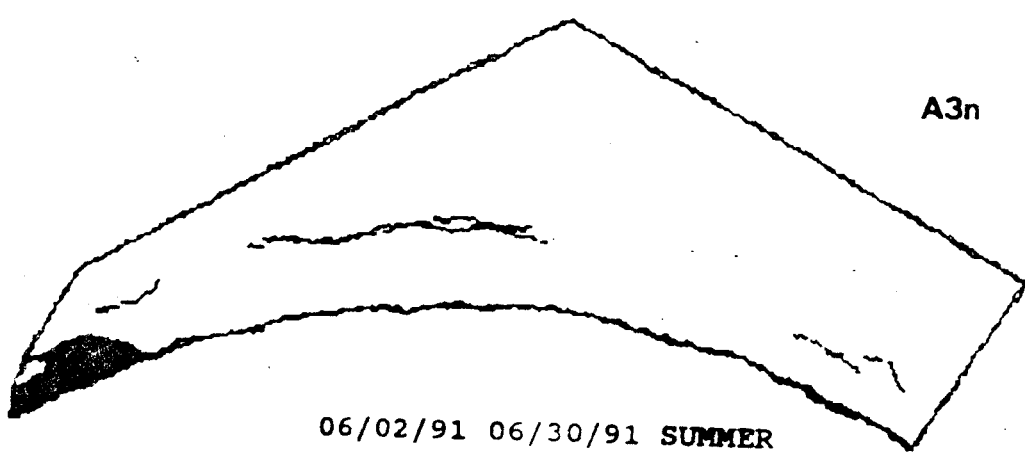
12/17/90 12/30/90 11,000 cfs



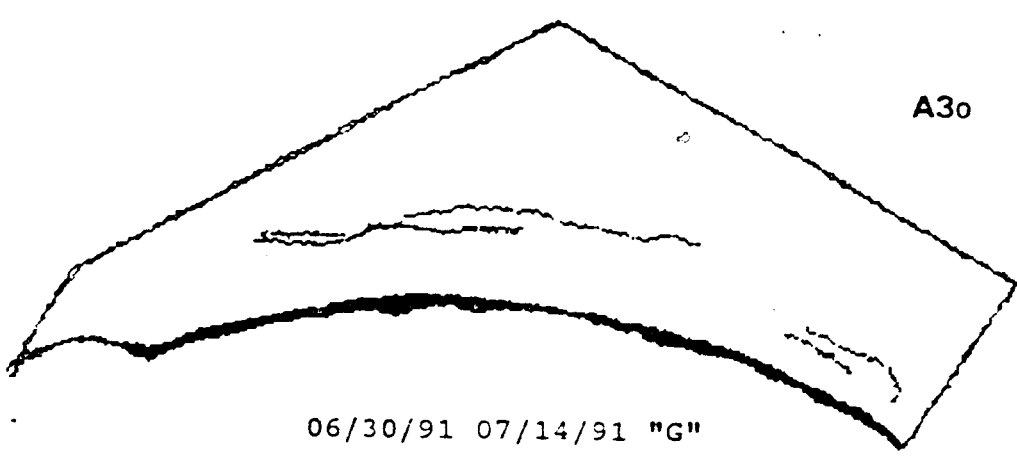




05/19/91 06/02/91 15,000 cfs



06/02/91 06/30/91 SUMMER



06/30/91 07/14/91 "G"

07/14/91 07/27/91 "F"

SITE 45 LEFT

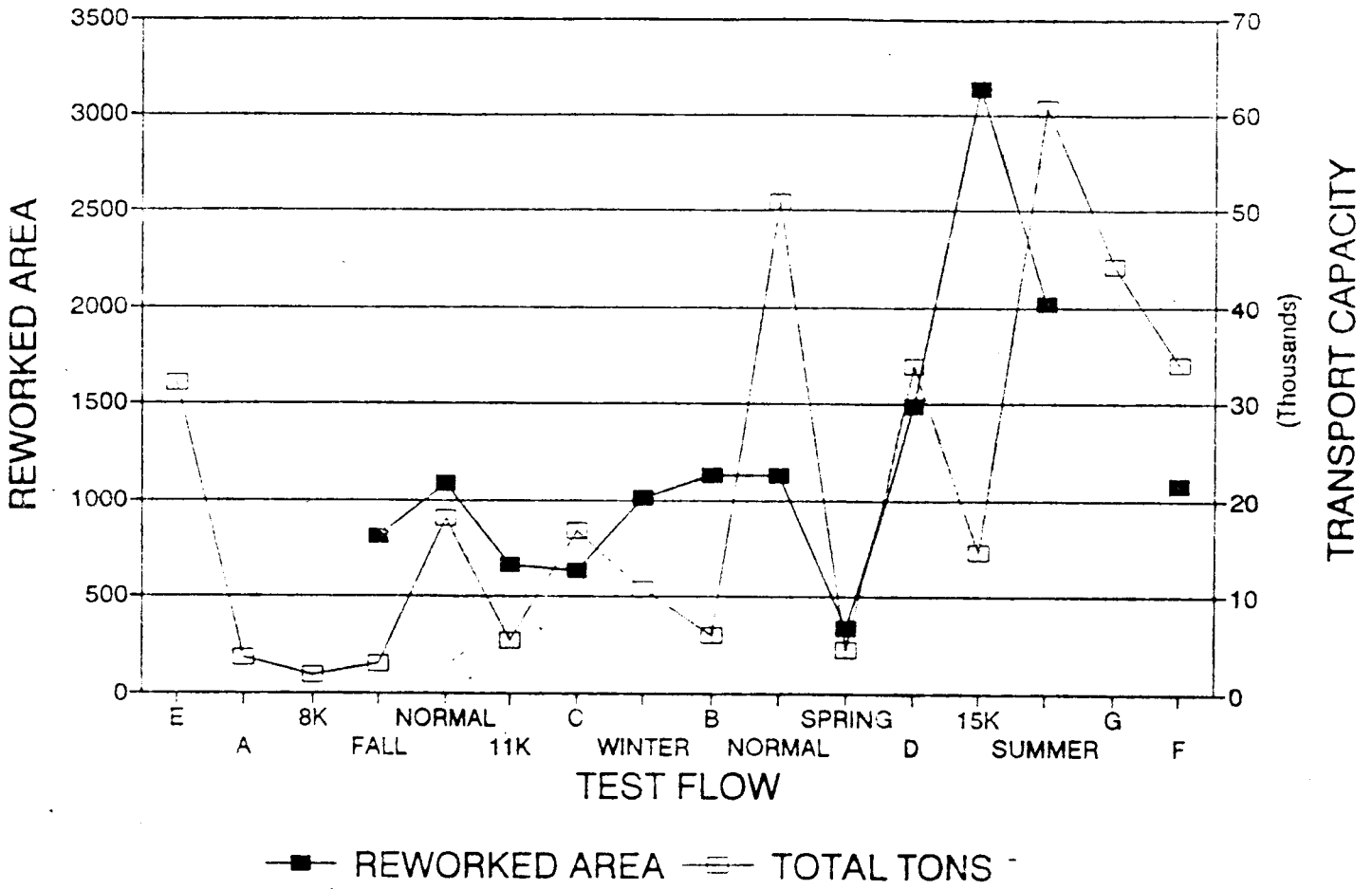
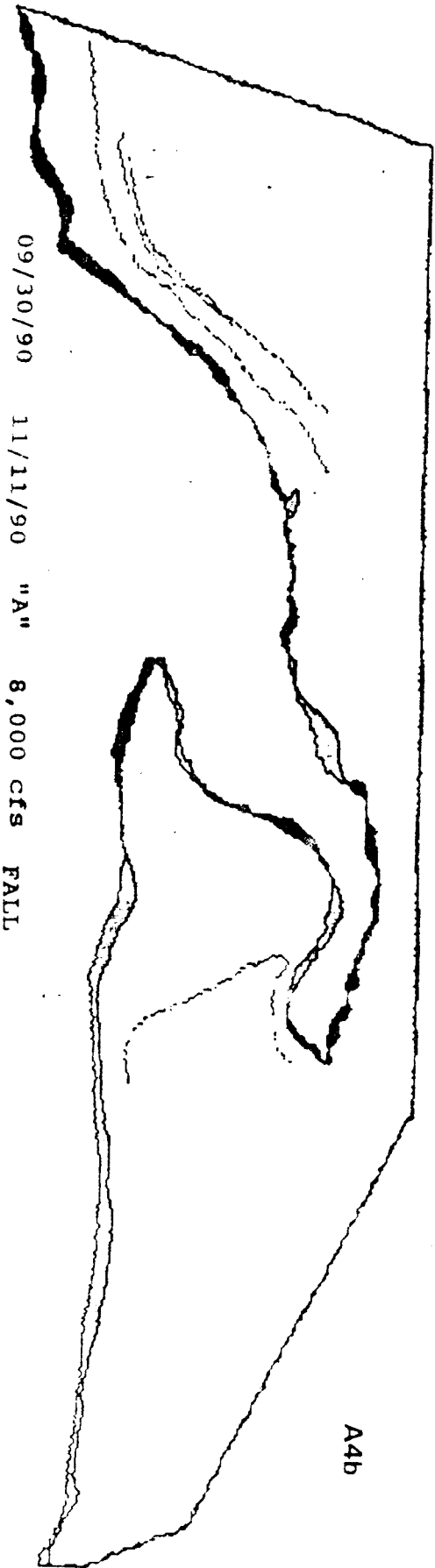
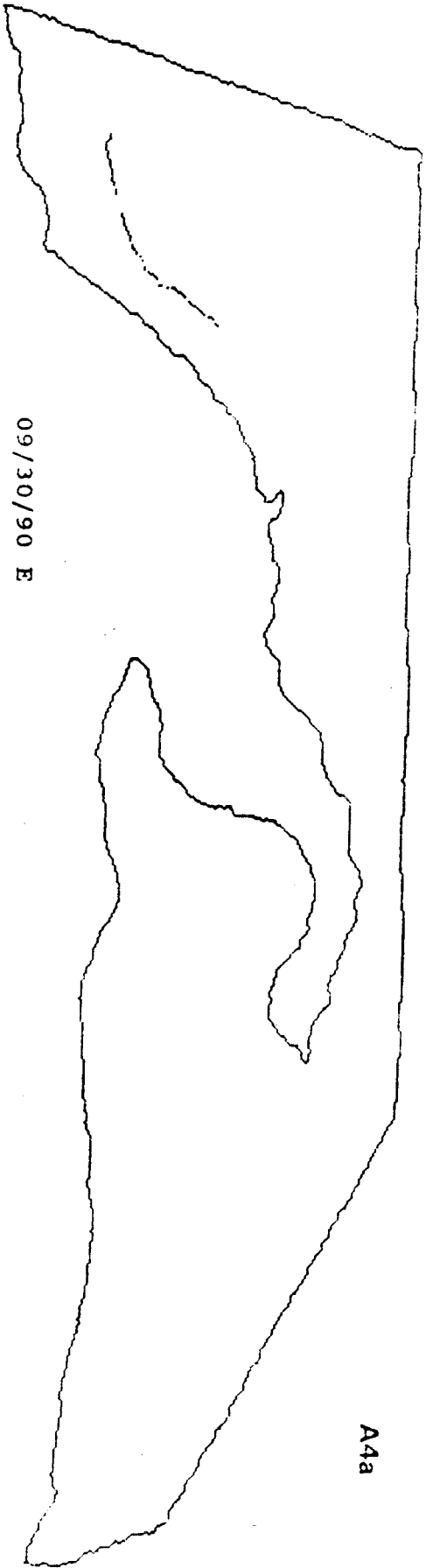
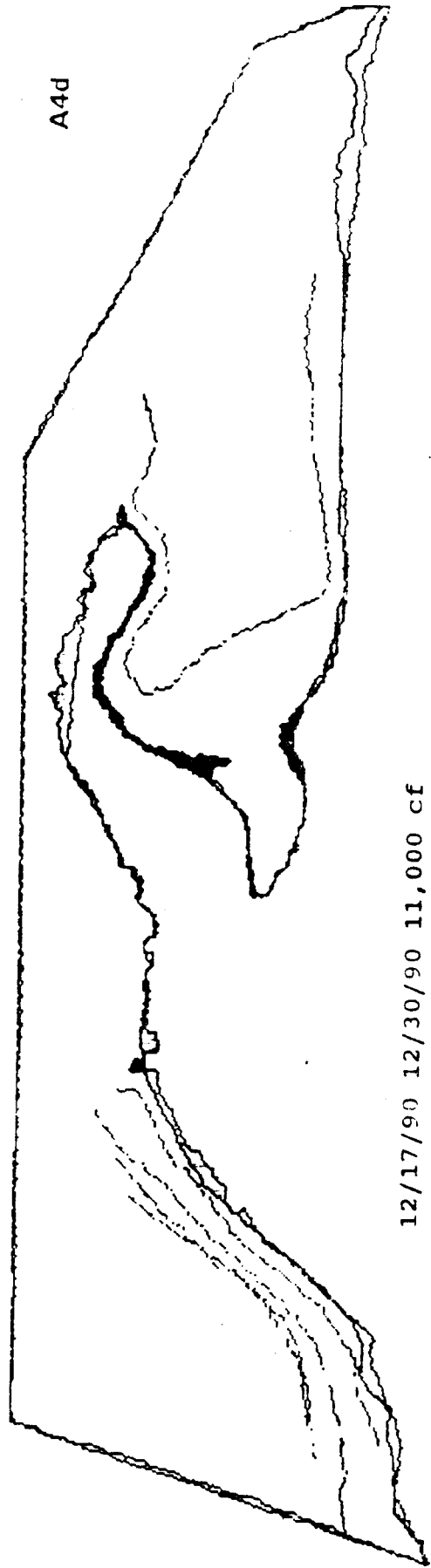
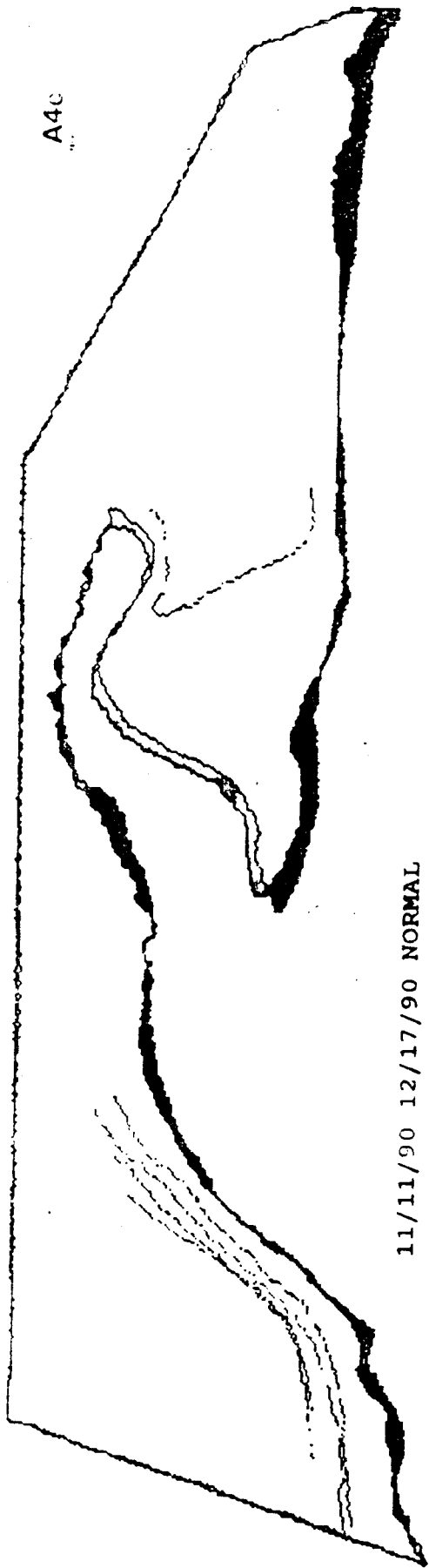
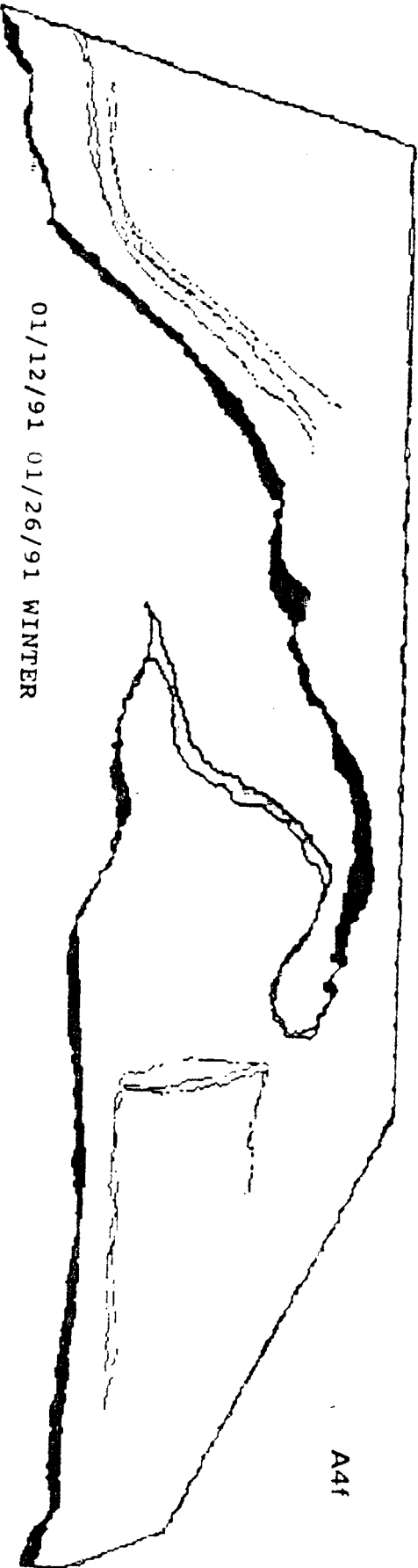
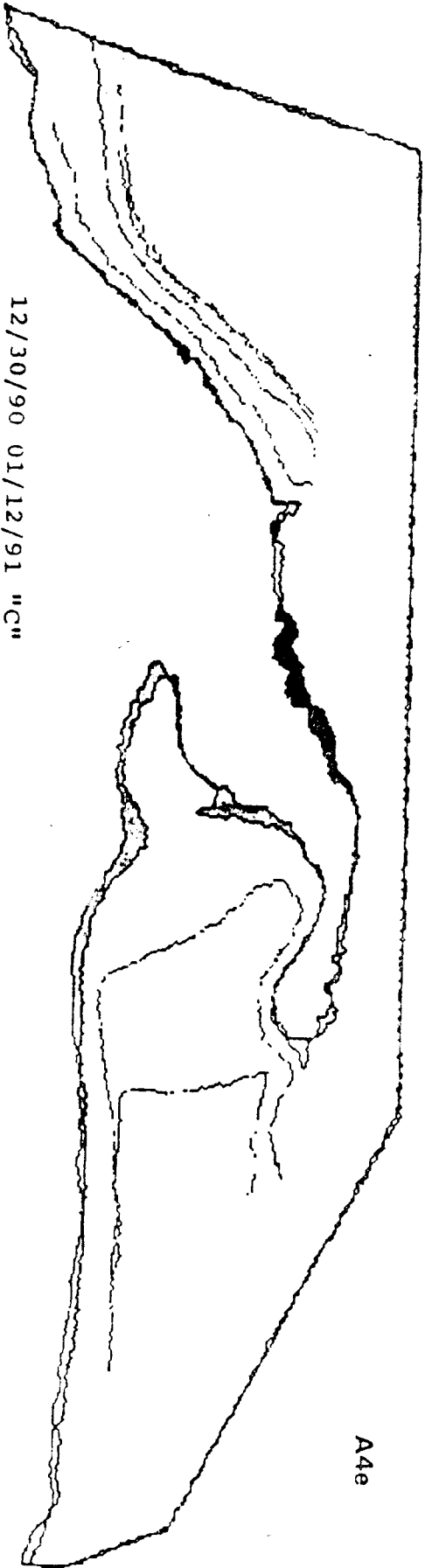


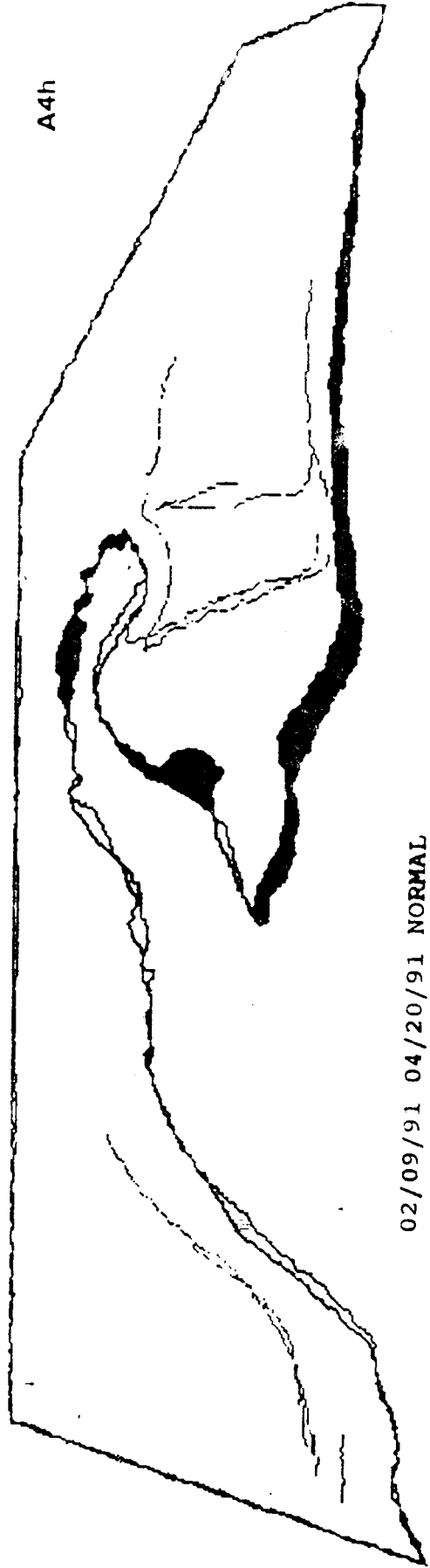
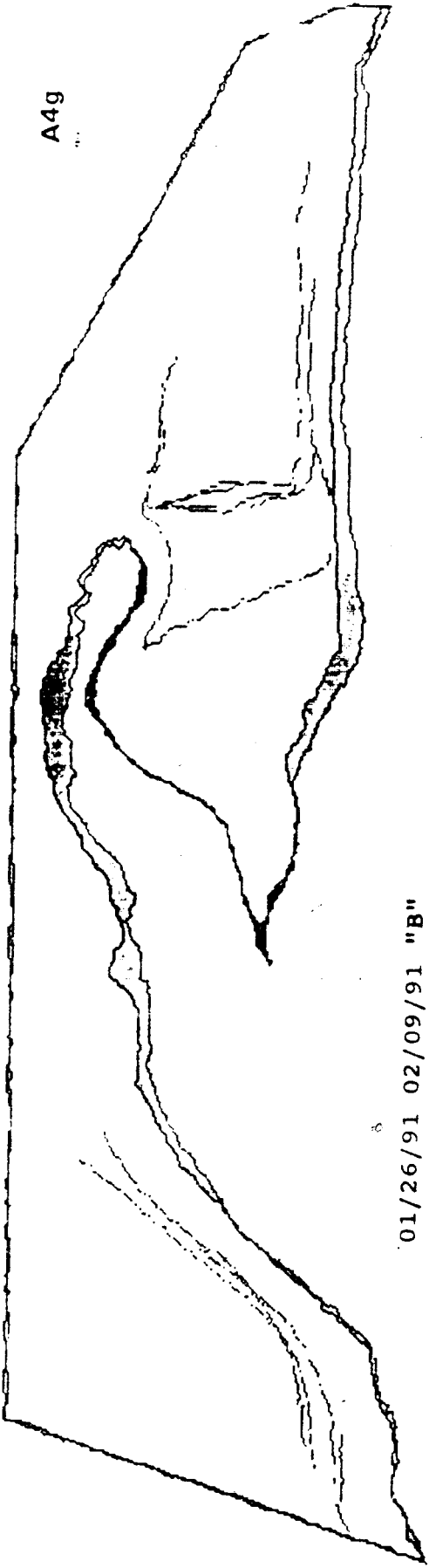
Figure A4. Time-series plot of reworked area and sediment transport capacity for site CR 45 L.

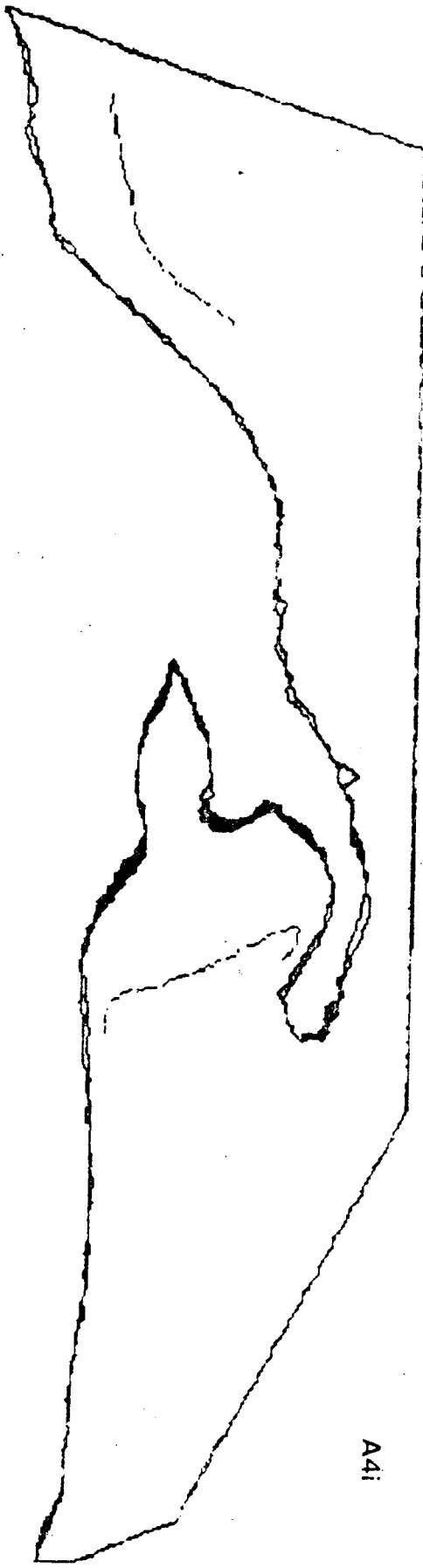
Figures A4a-A4m. Original planimetric outlines and subsequent comparisons of bracketing outlines. Dark shaded areas were eroded. Light shaded areas were aggraded.











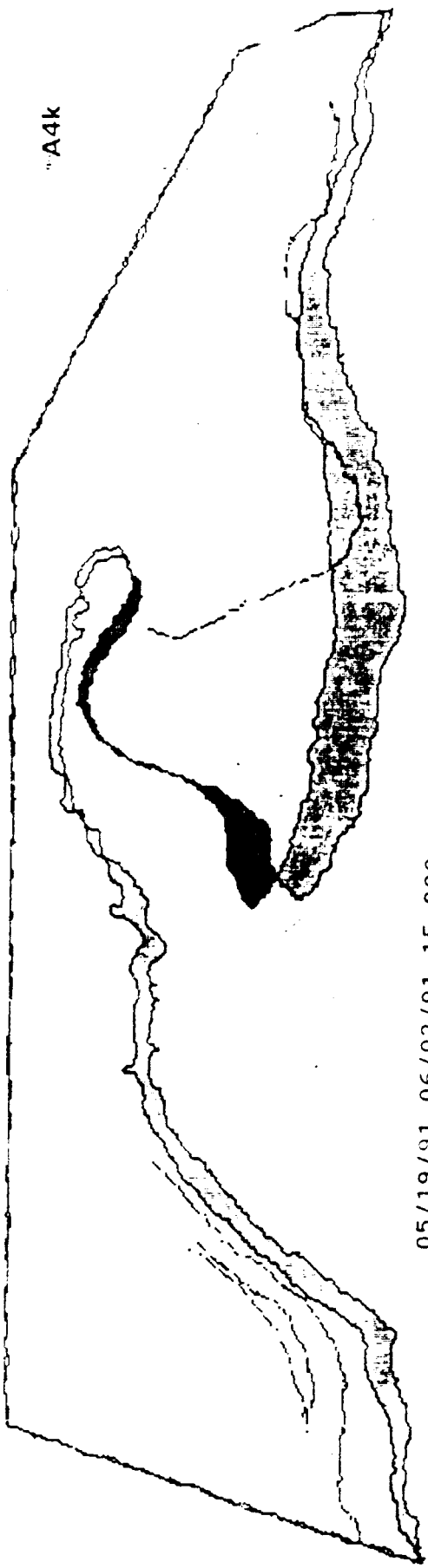
04/20/91 05/05/91 SPRING

A4i



05/05/91 05/19/91 "D"

A4j

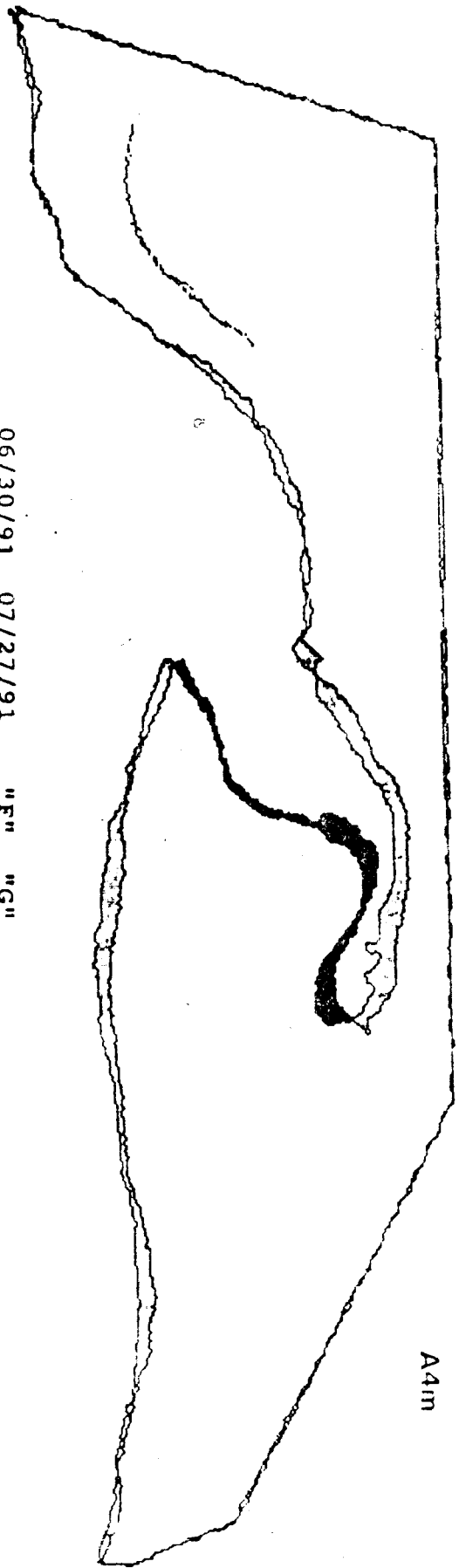


05/19/91 06/02/91 15,000



06/02/91 06/30/91 SUMMER





06/30/91 07/27/91 "F" "G"

A4m

SITE 47 LEFT

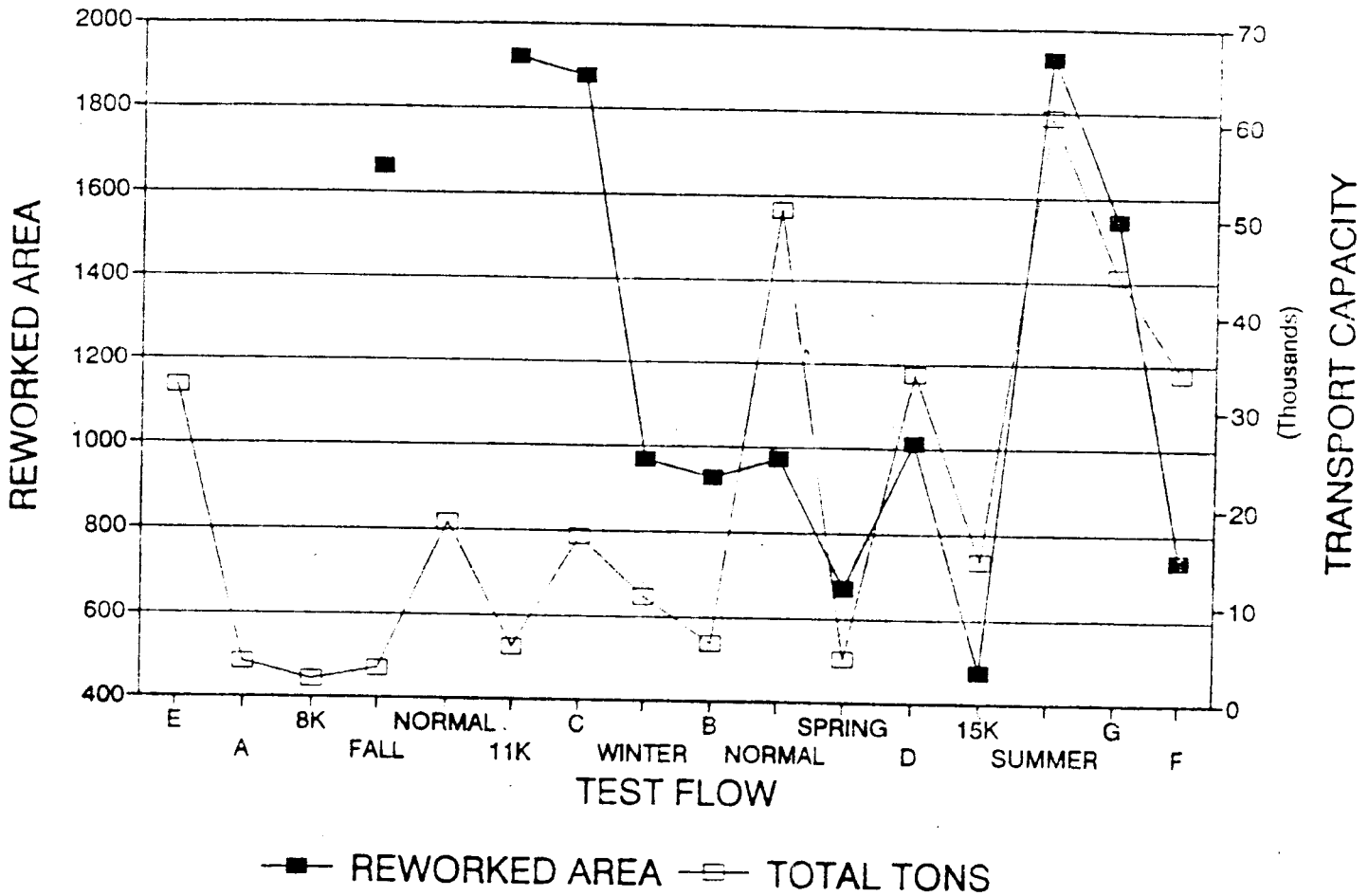
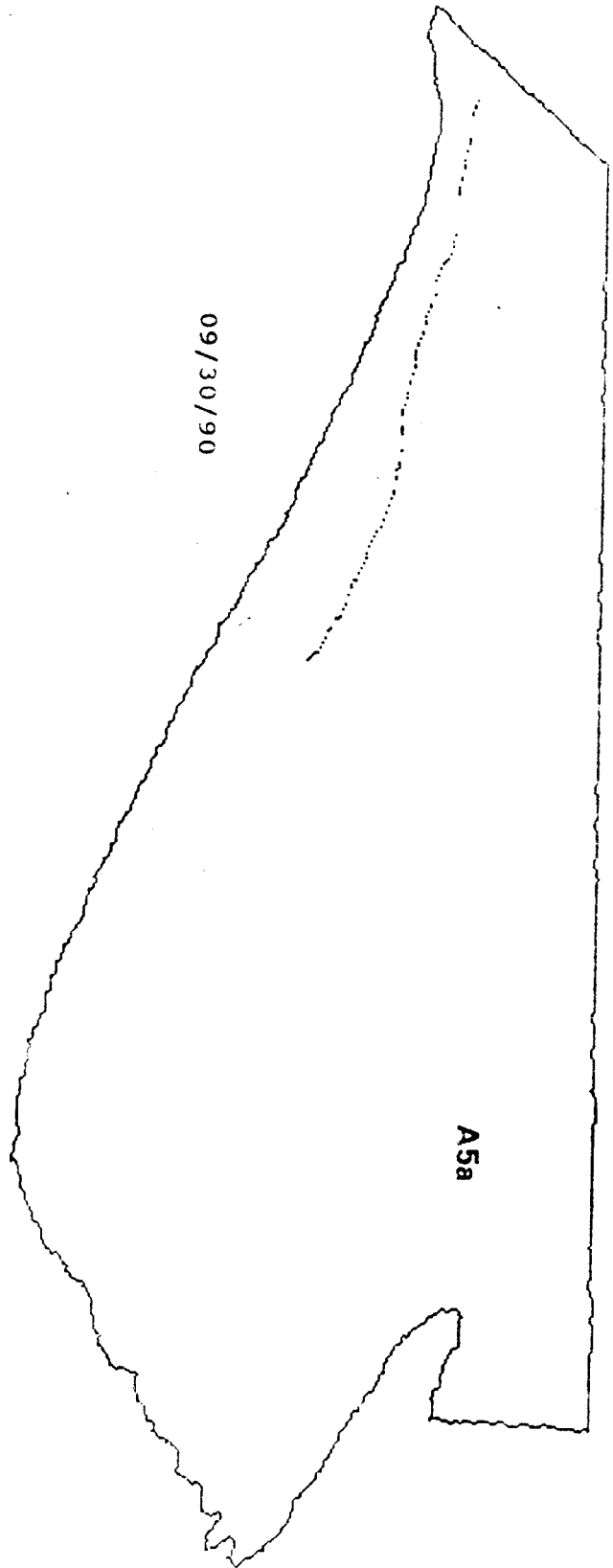
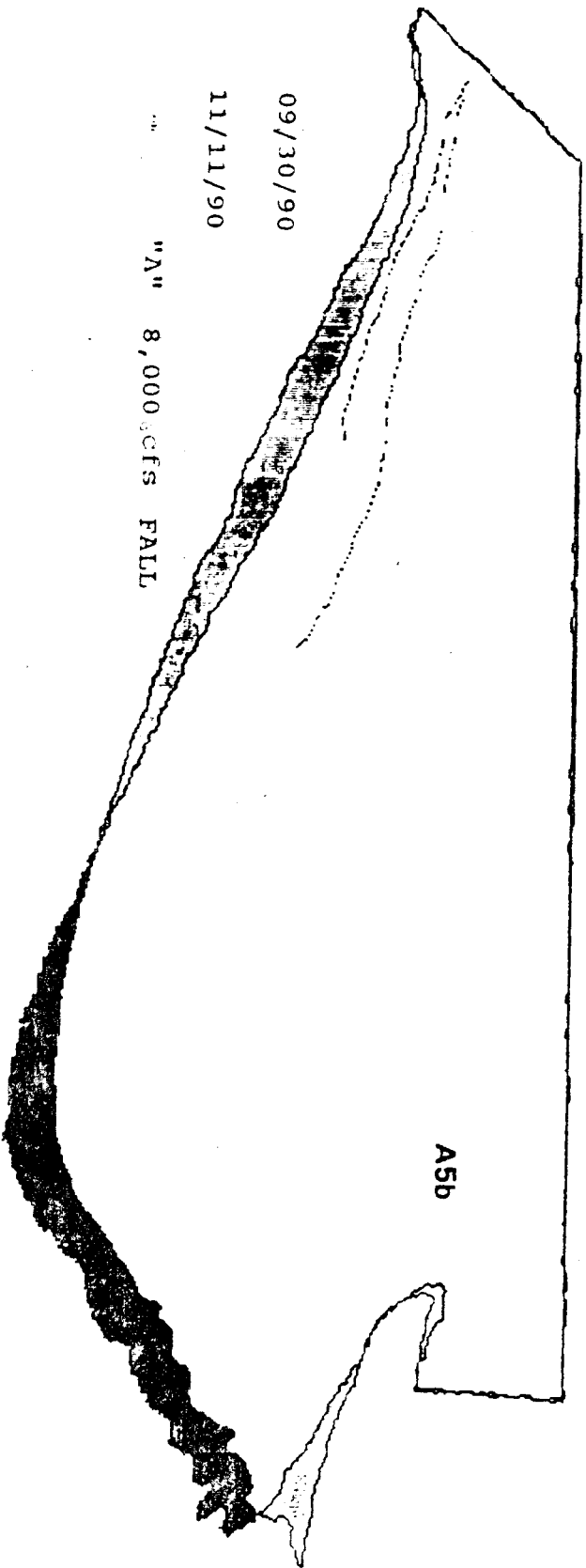
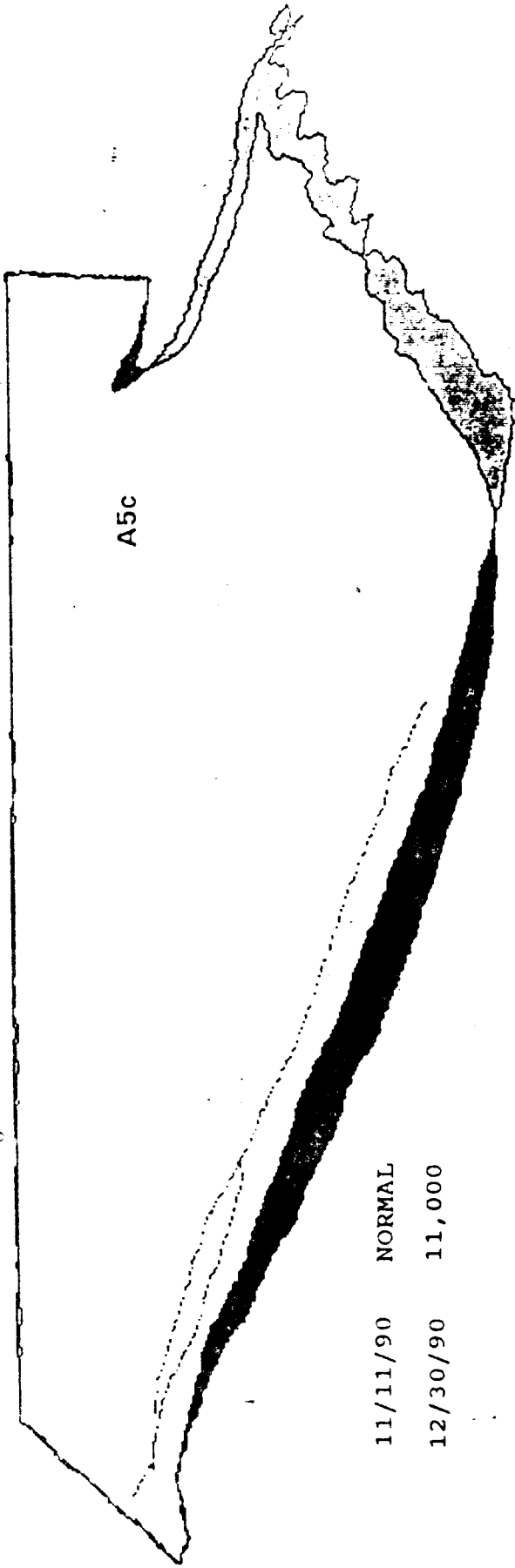


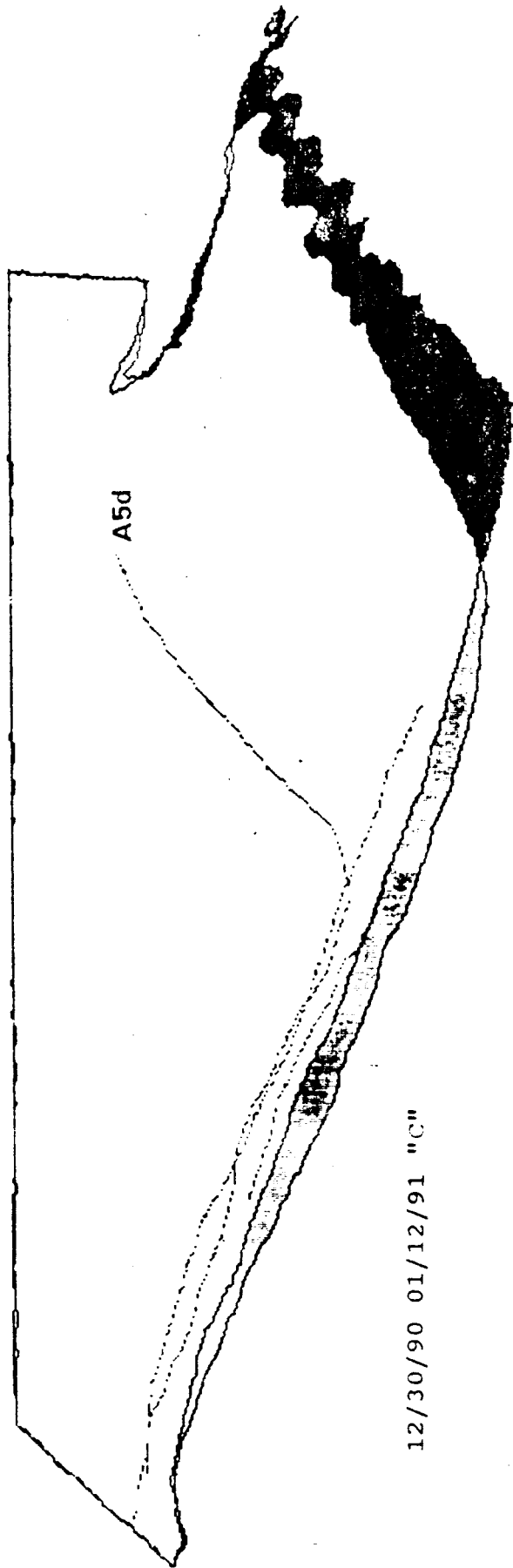
Figure A5. Time-series plot of reworked area and sediment transport capacity for site CR 47 R.

Figures A5a-A5m. Original planimetric outlines and subsequent comparisons of bracketing outlines. Dark shaded areas were eroded. Light shaded areas were aggraded.

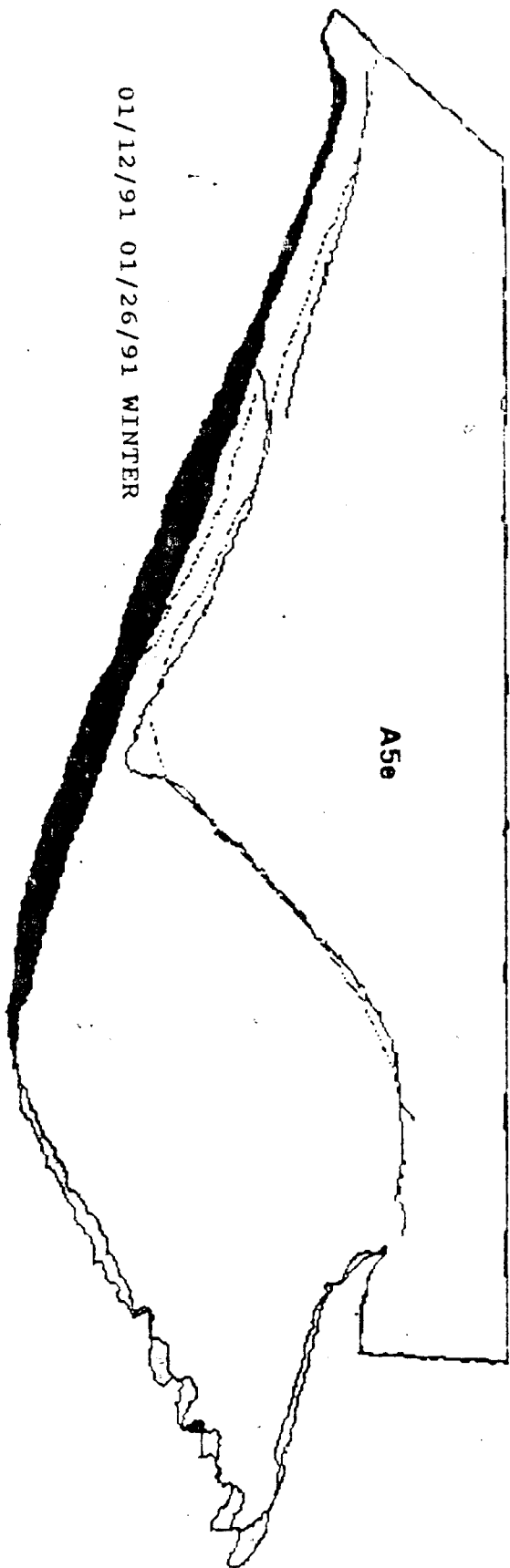
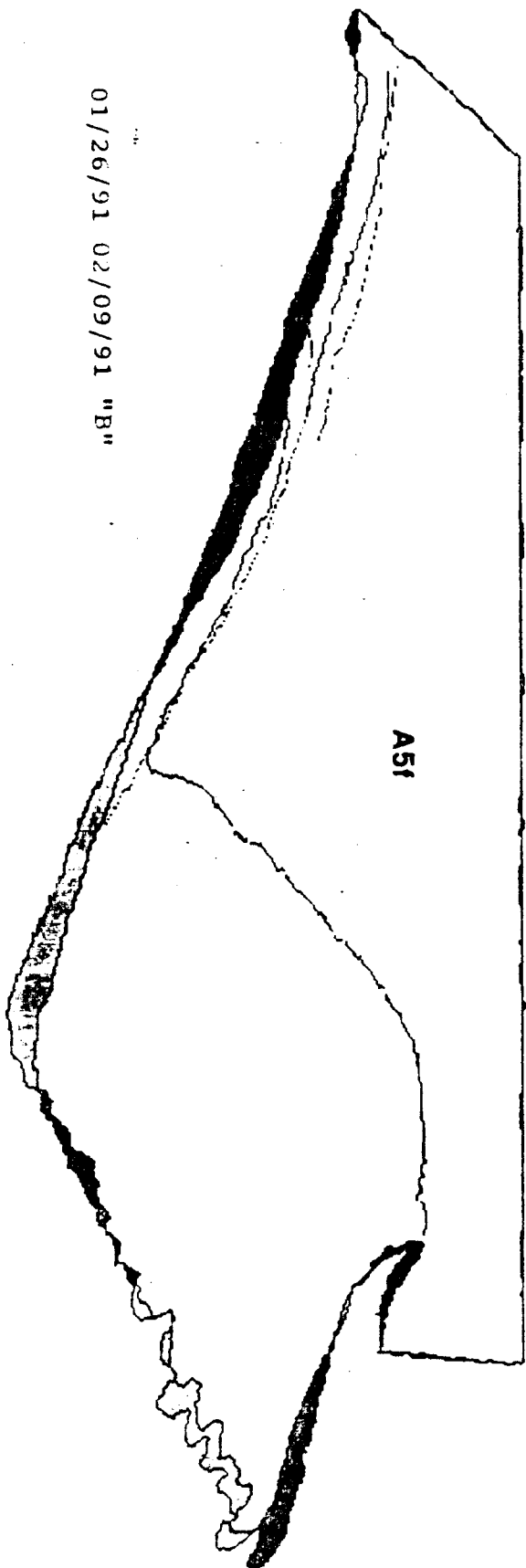


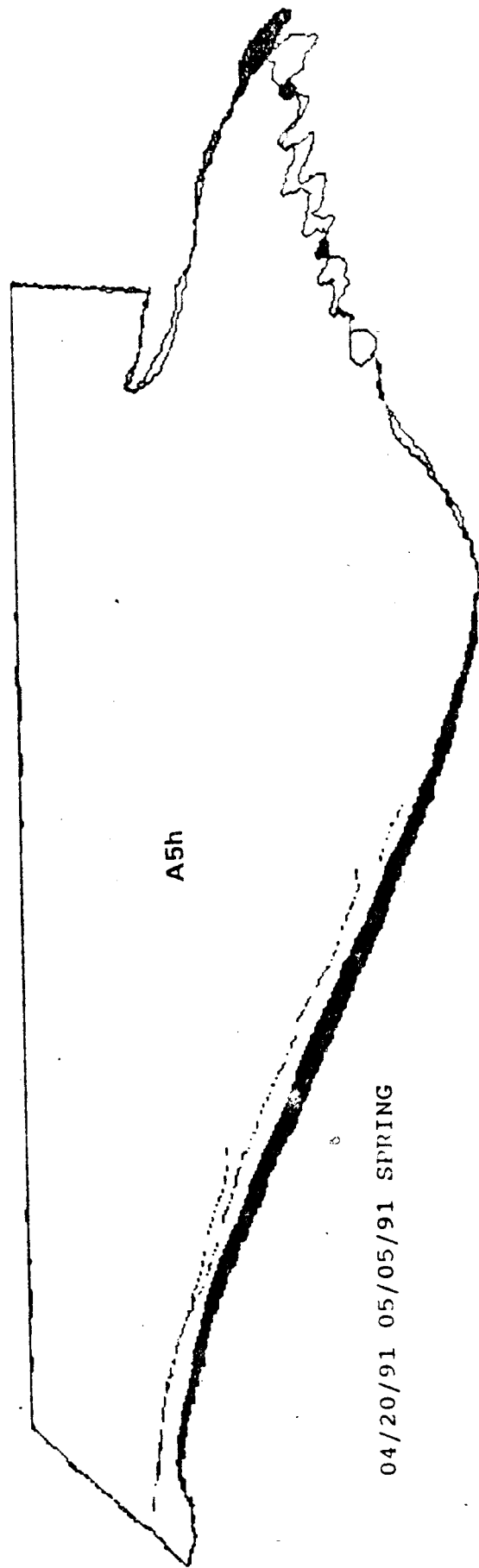
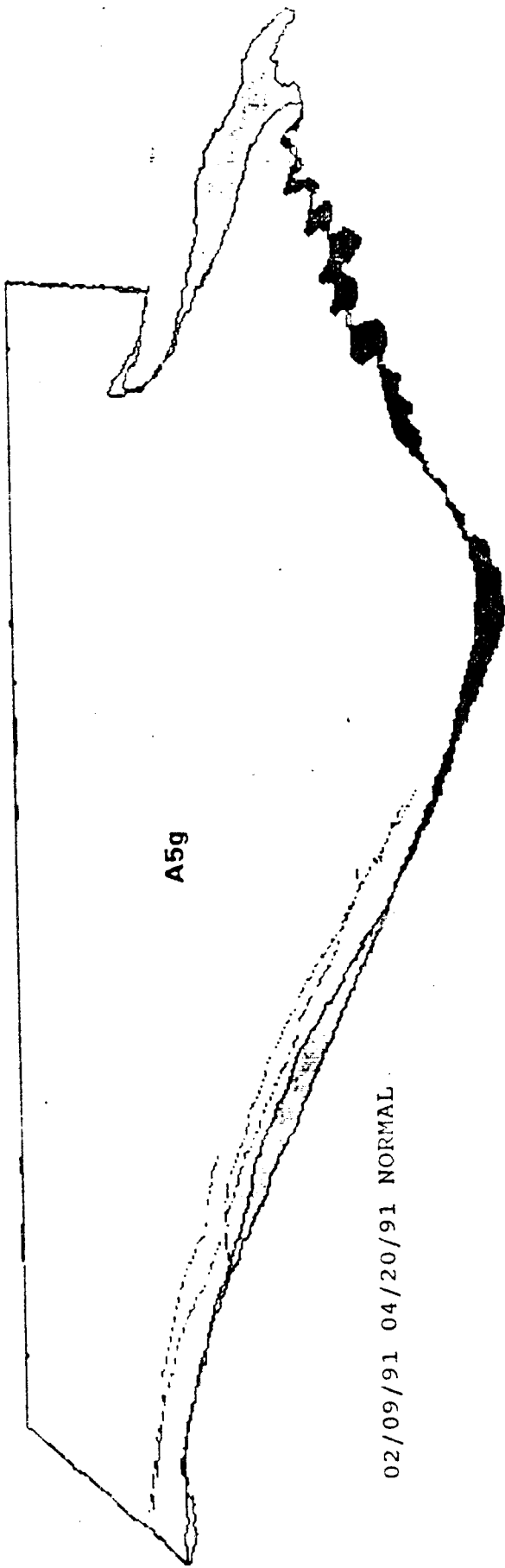


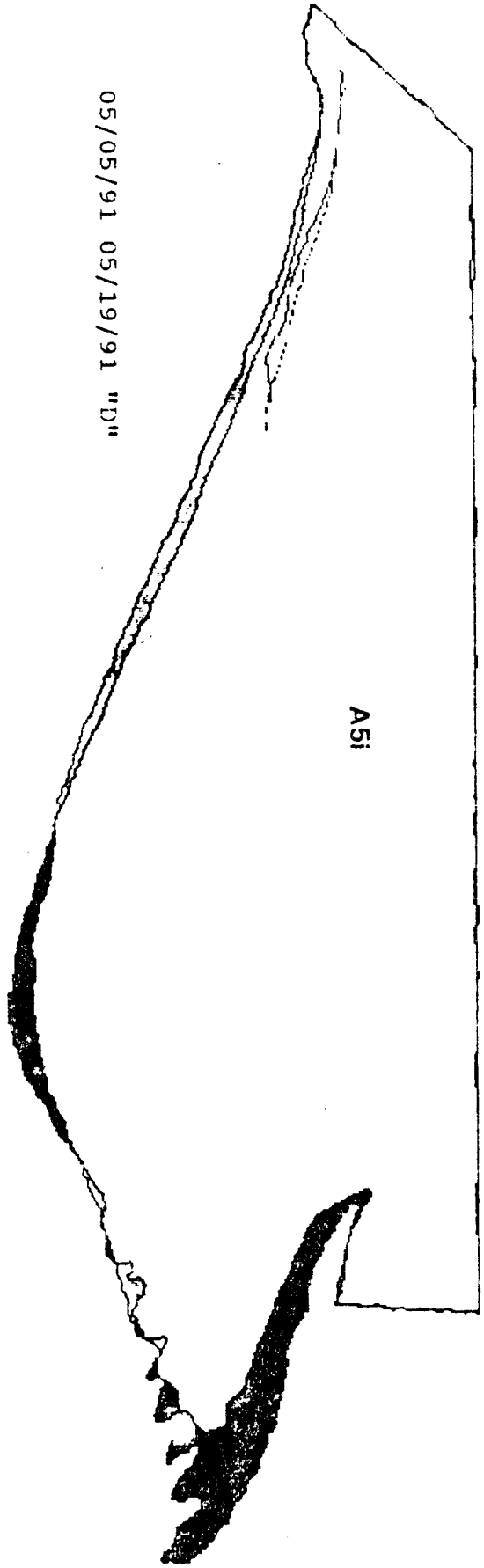
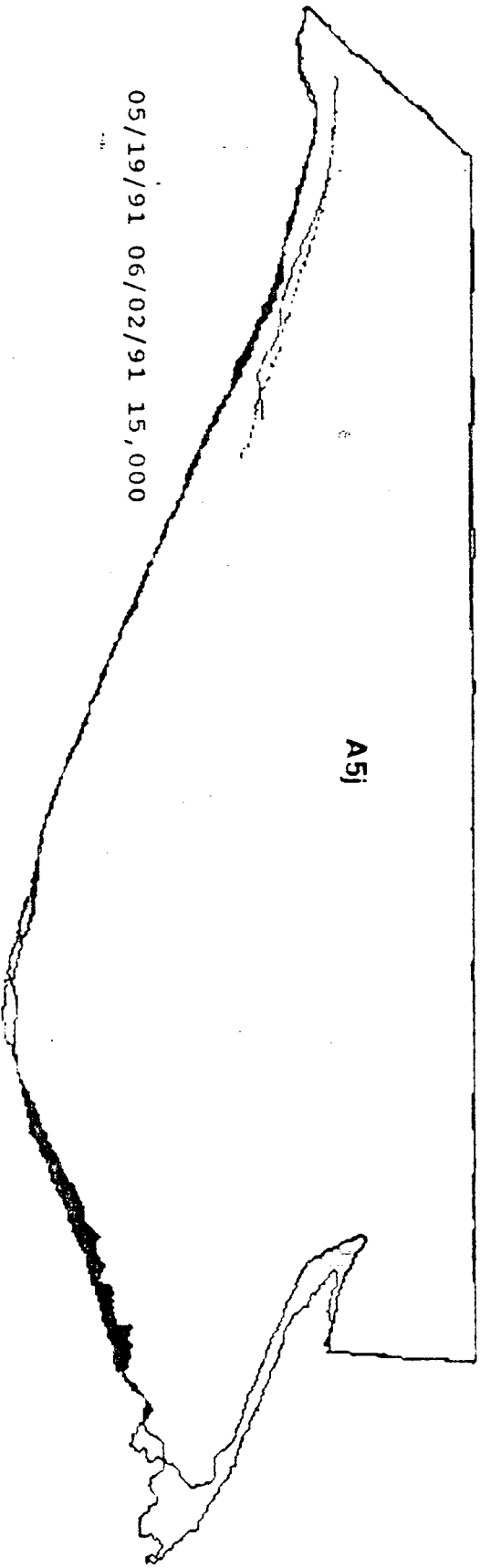
11/11/90 NORMAL
 12/30/90 11,000

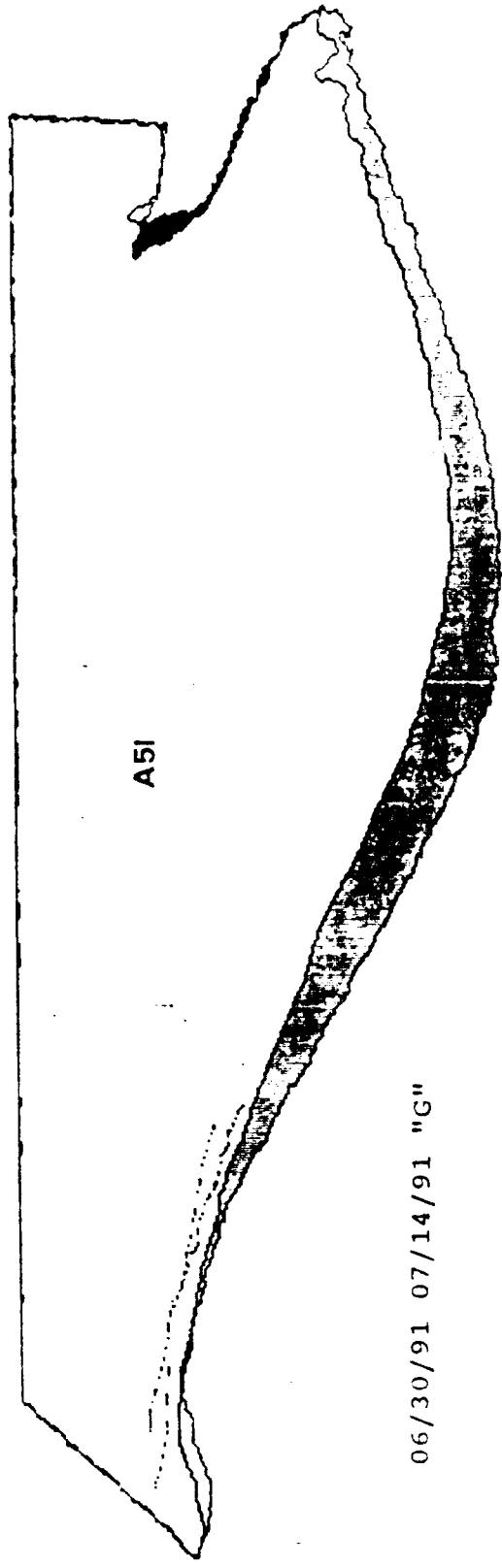
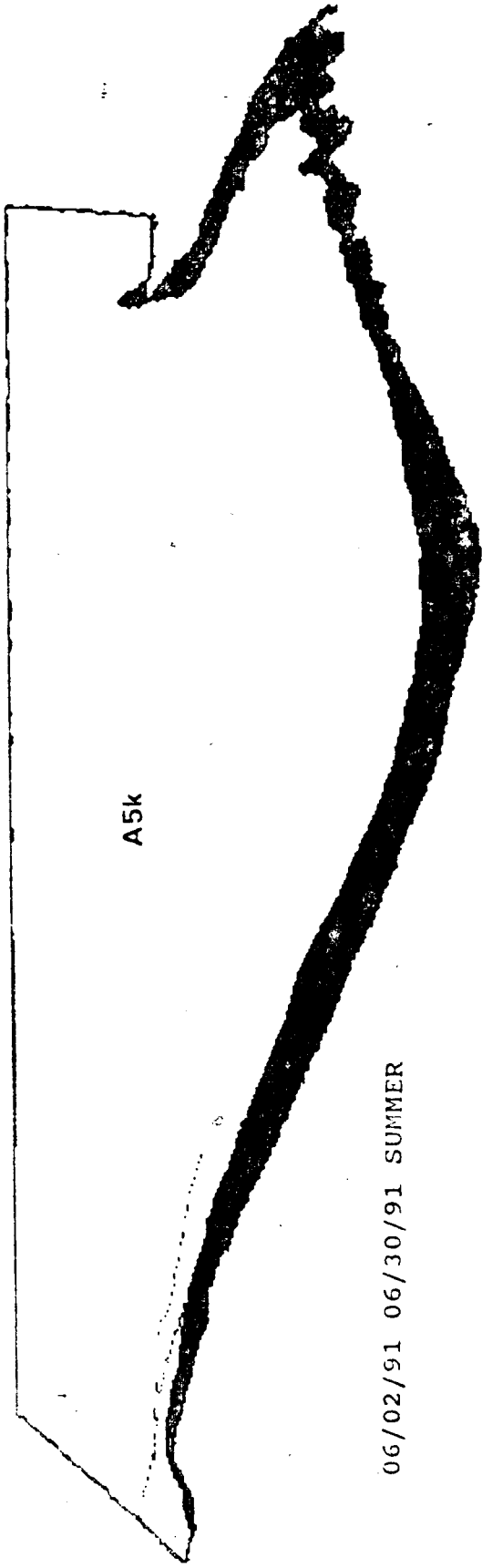


12/30/90 01/12/91 "C"



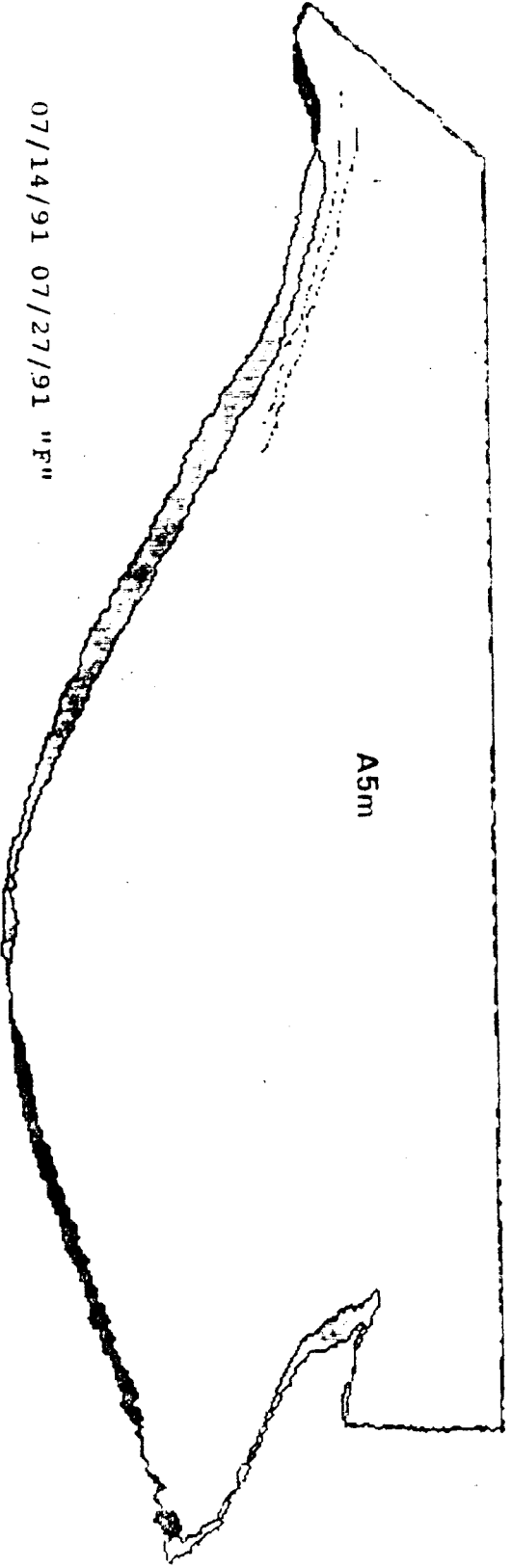






07/14/91 07/27/91 "F"

A5m



SITE 51 LEFT

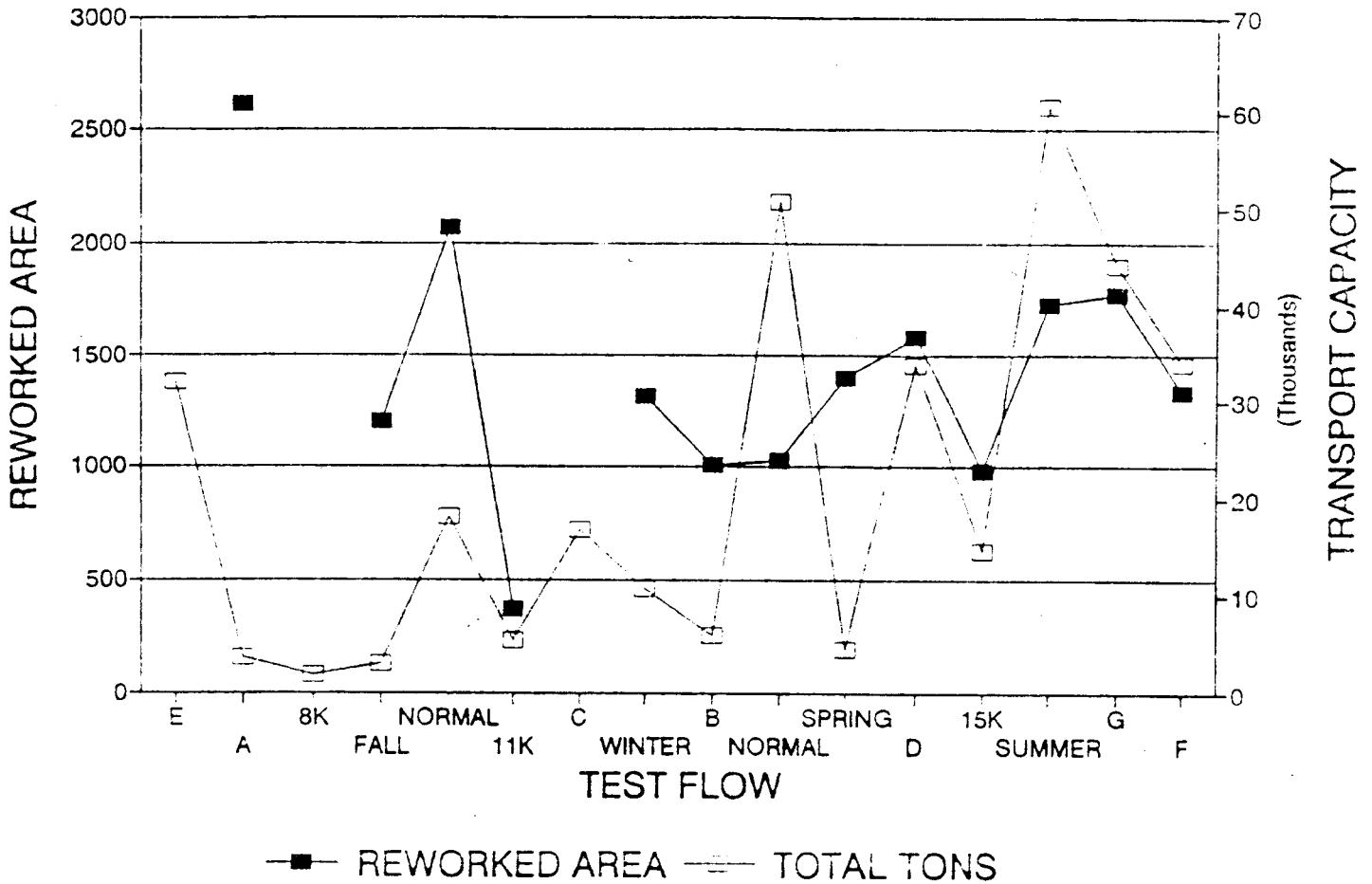


Figure A6. Time-series plot of reworked area and sediment transport capacity for site CR 51 L.

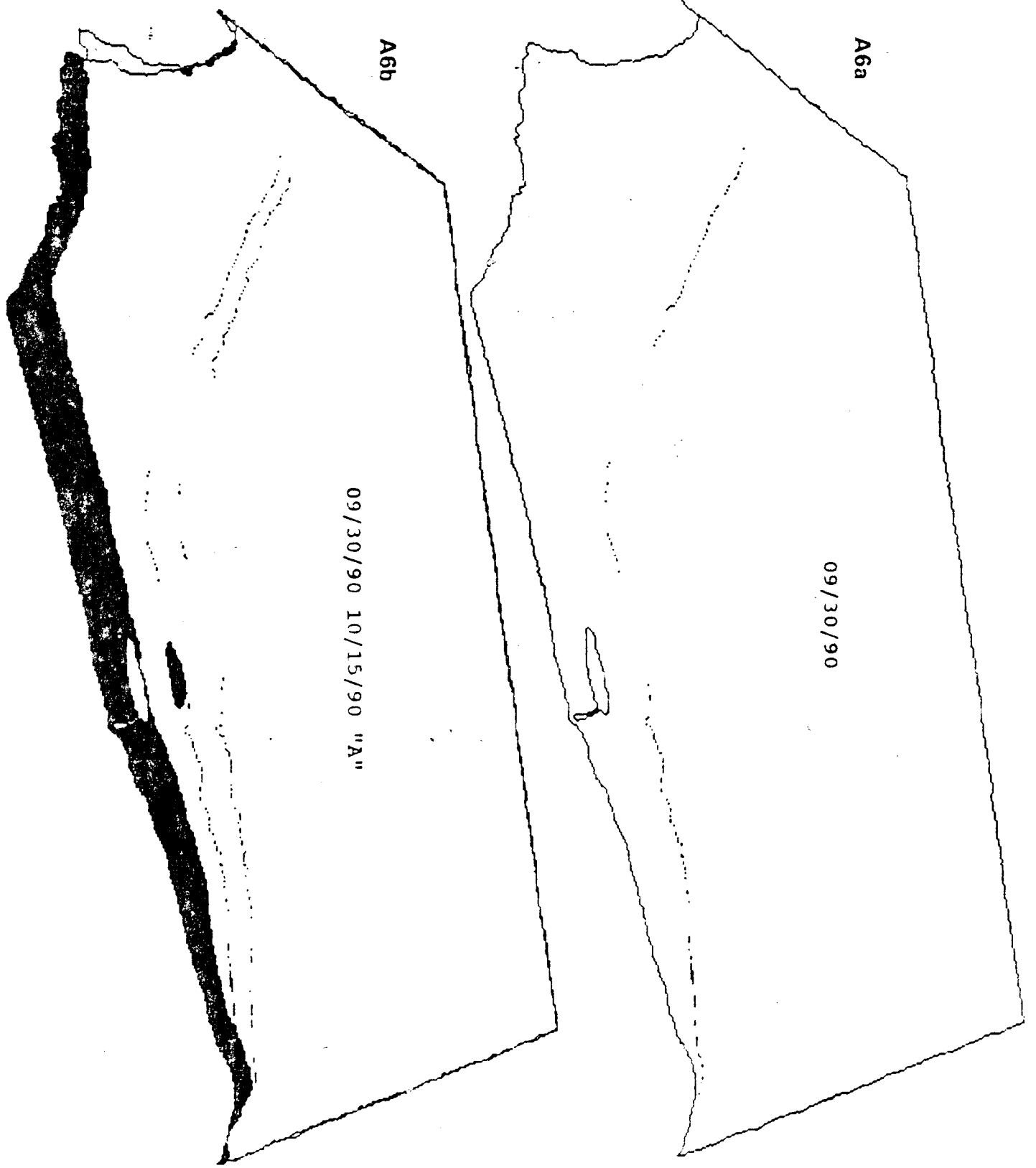
Figures A6a-A6n. Original planimetric outlines and subsequent comparisons of bracketing outlines. Dark shaded areas were eroded. Light shaded areas were aggraded.

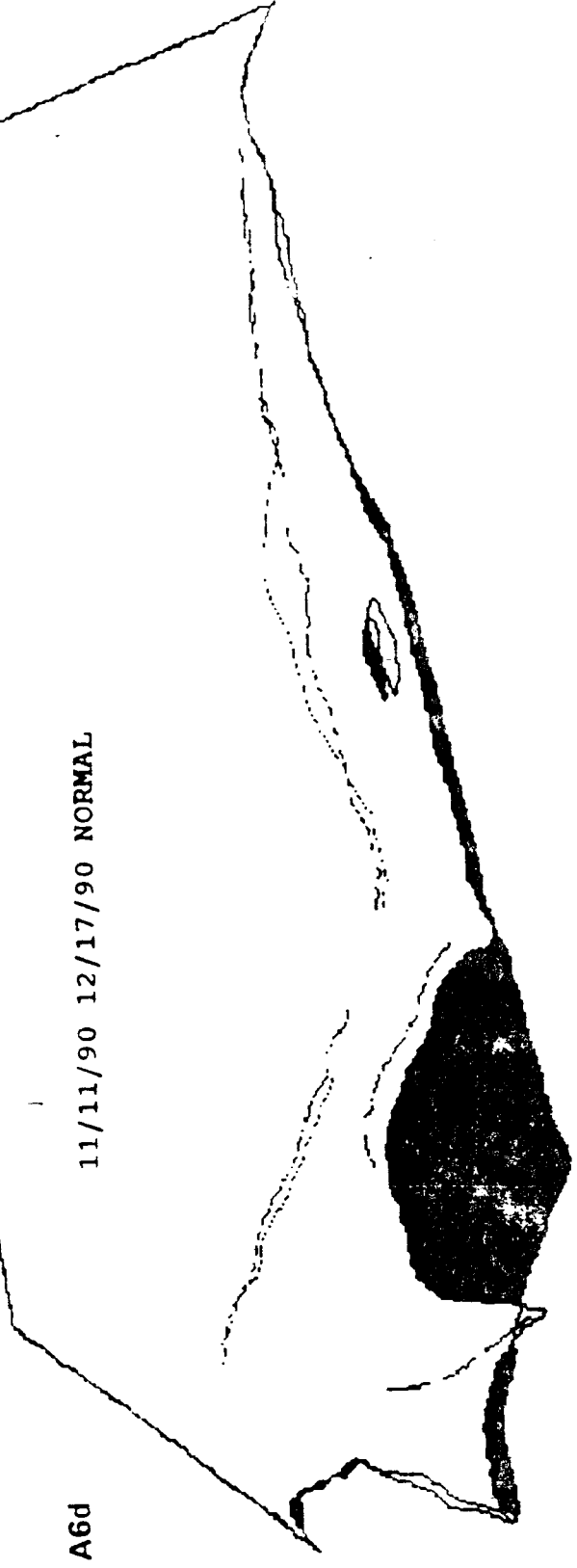
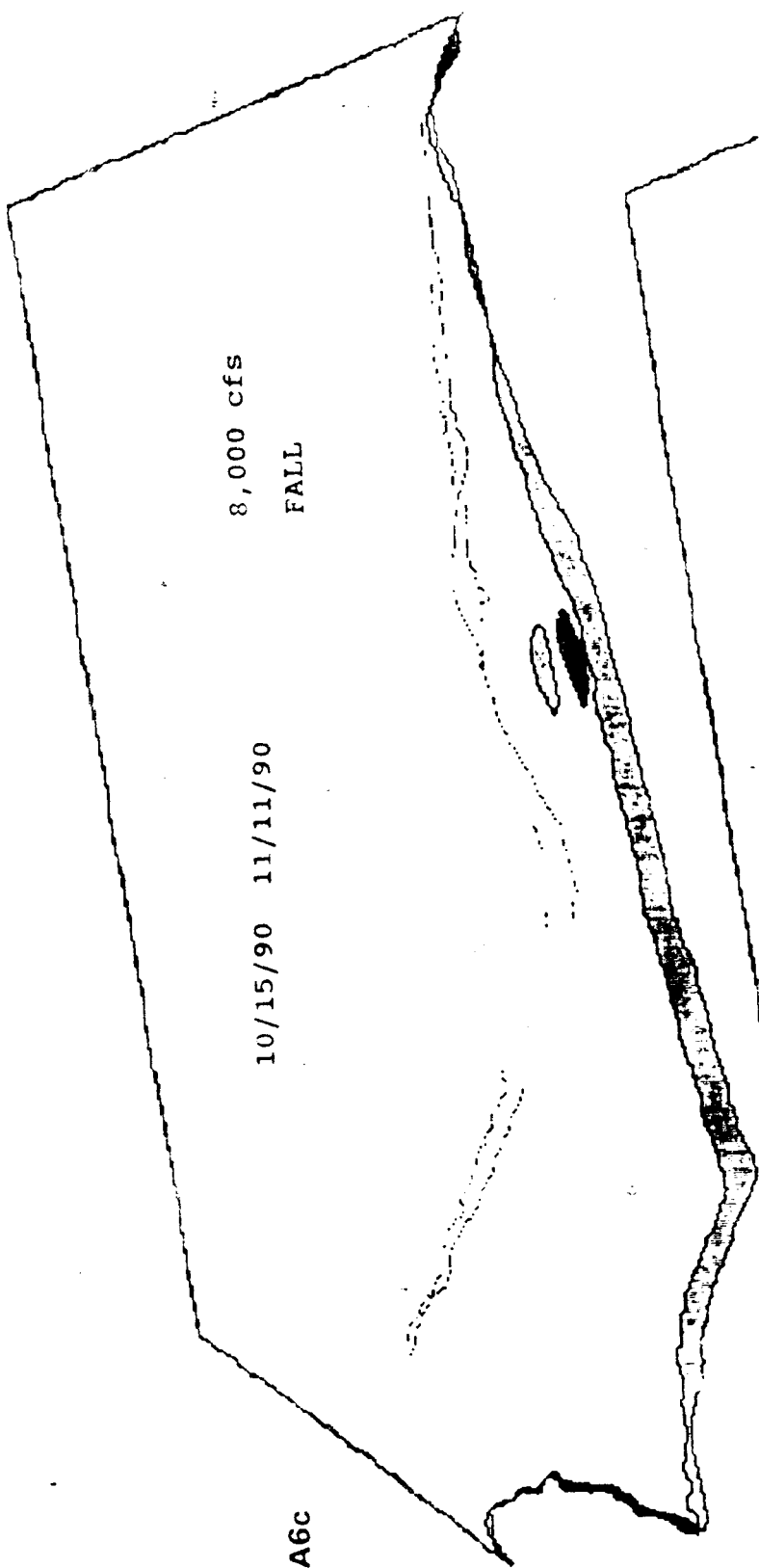
A6a

09/30/90

A6b

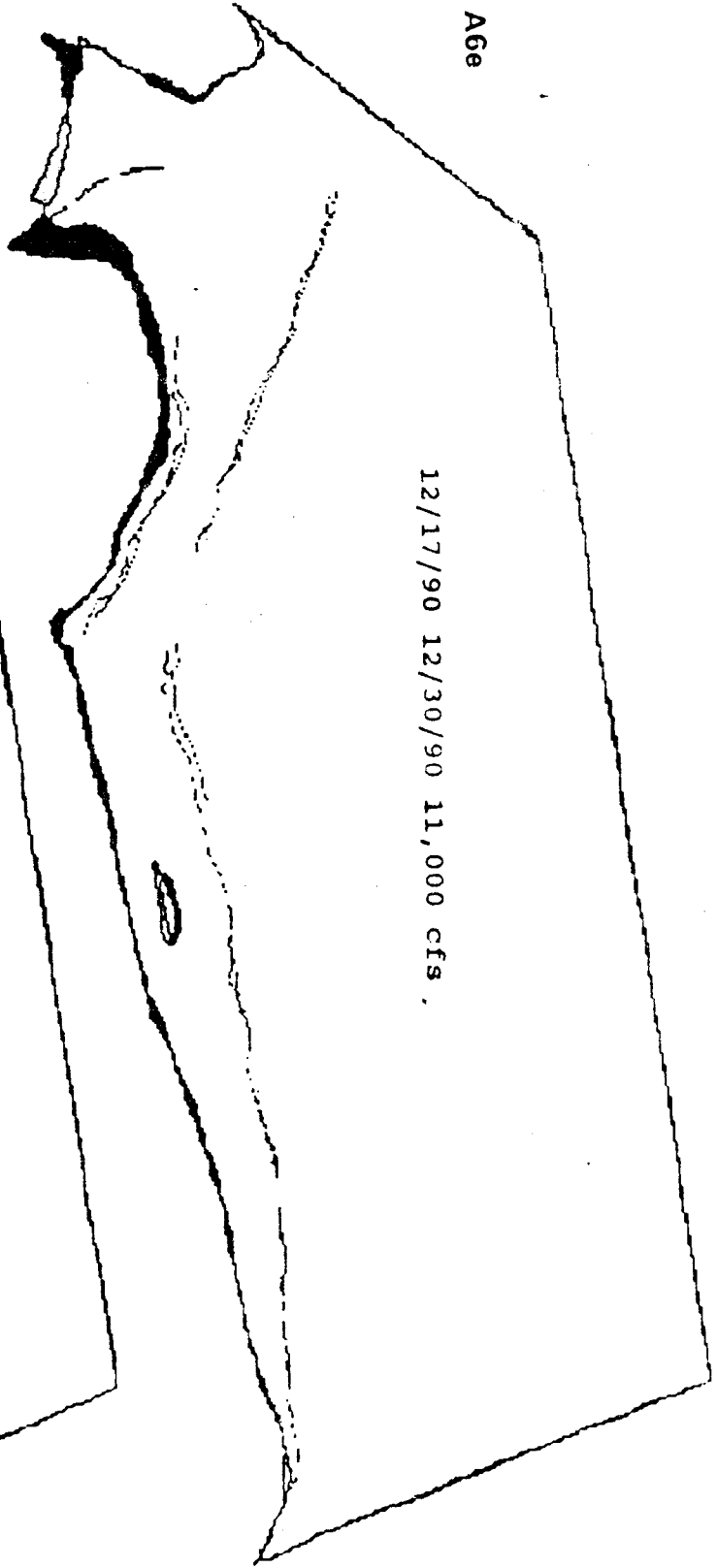
09/30/90 10/15/90 "A"





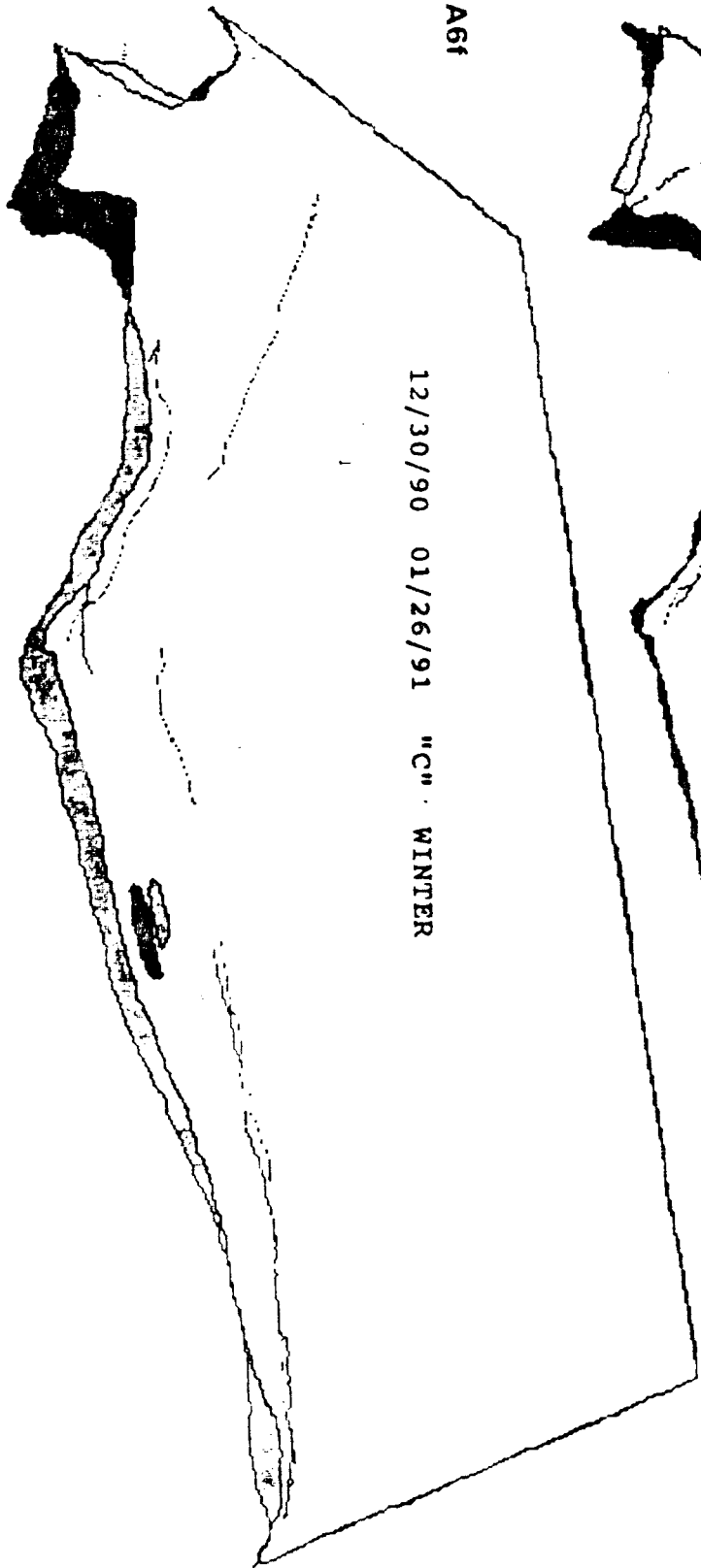
A6e

12/17/90 12/30/90 11,000 cfs .



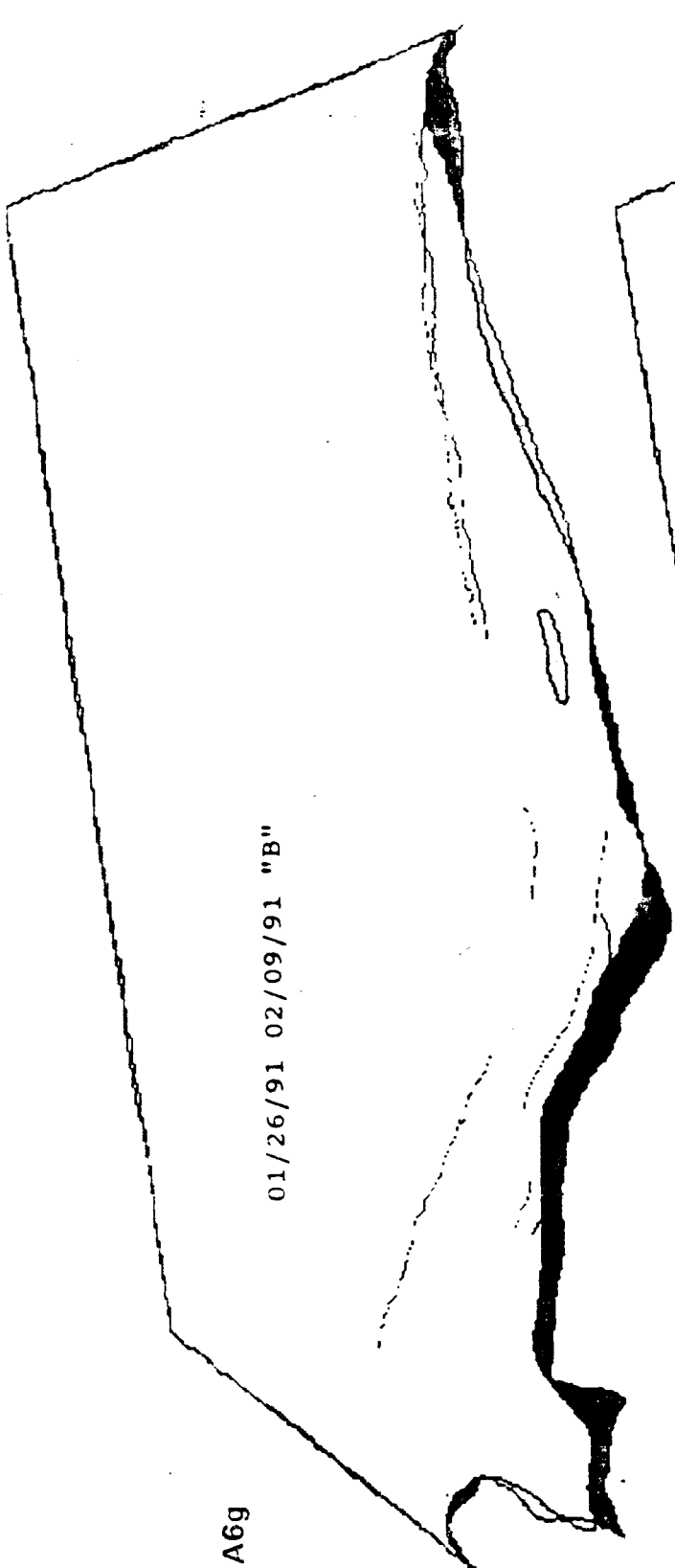
A6f

12/30/90 01/26/91 "C" WINTER



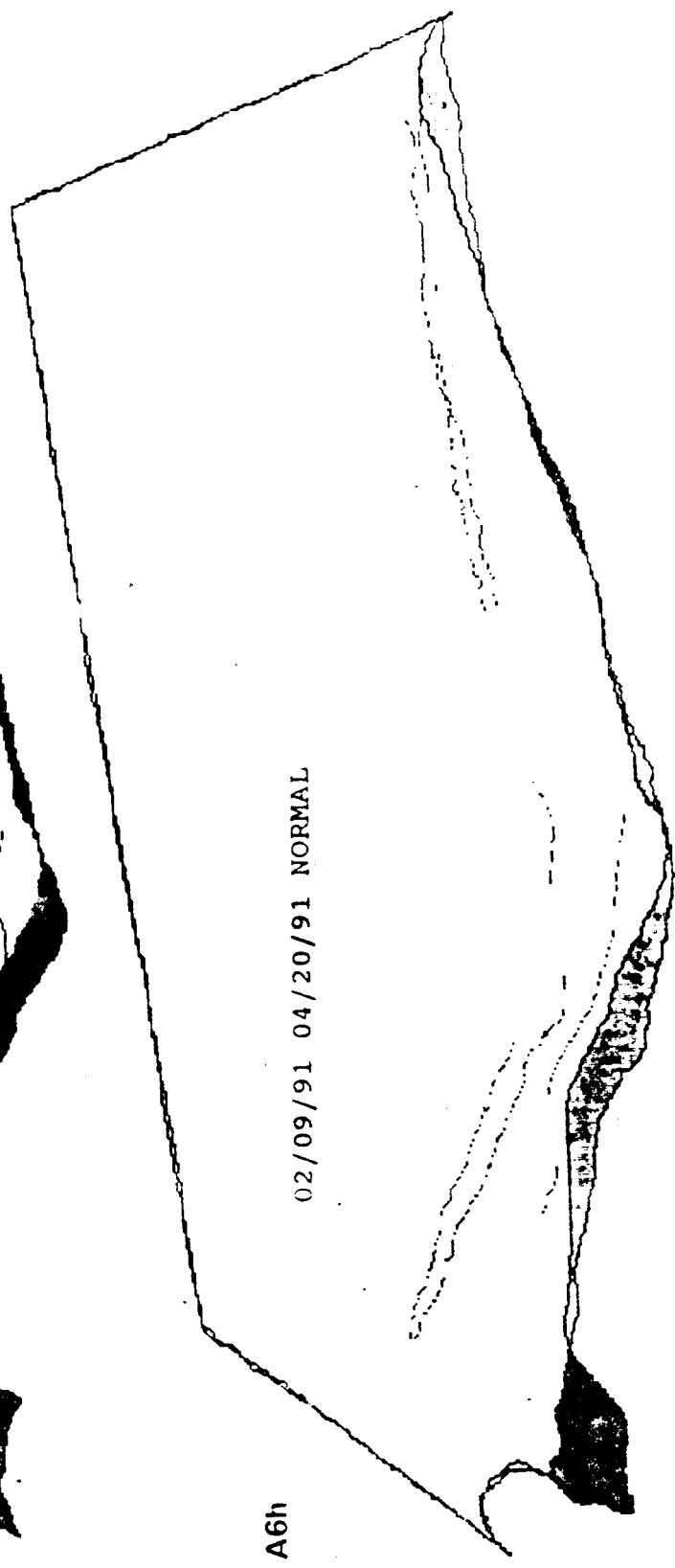
A6g

01/26/91 02/09/91 "B"



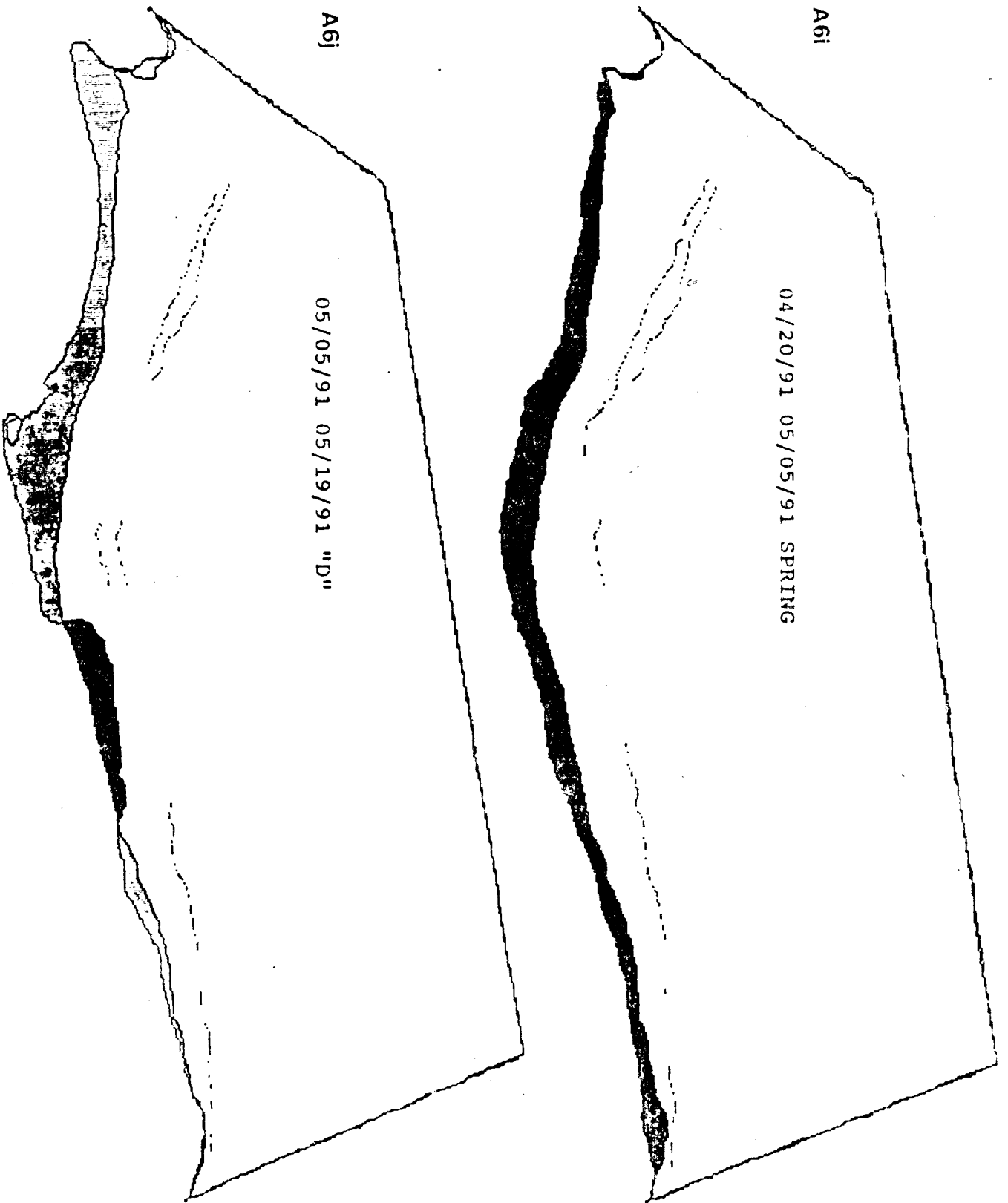
A6h

02/09/91 04/20/91 NORMAL



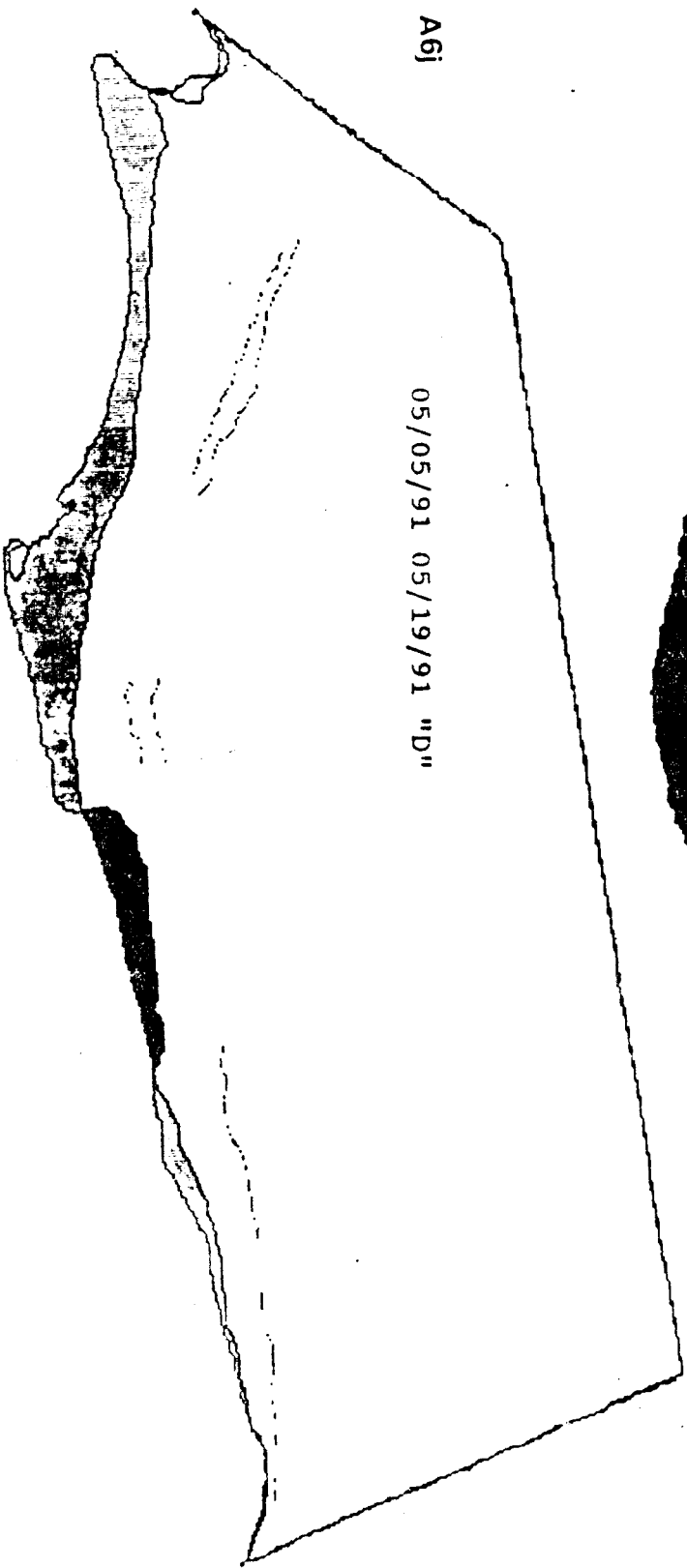
A6i

04/20/91 05/05/91 SPRING



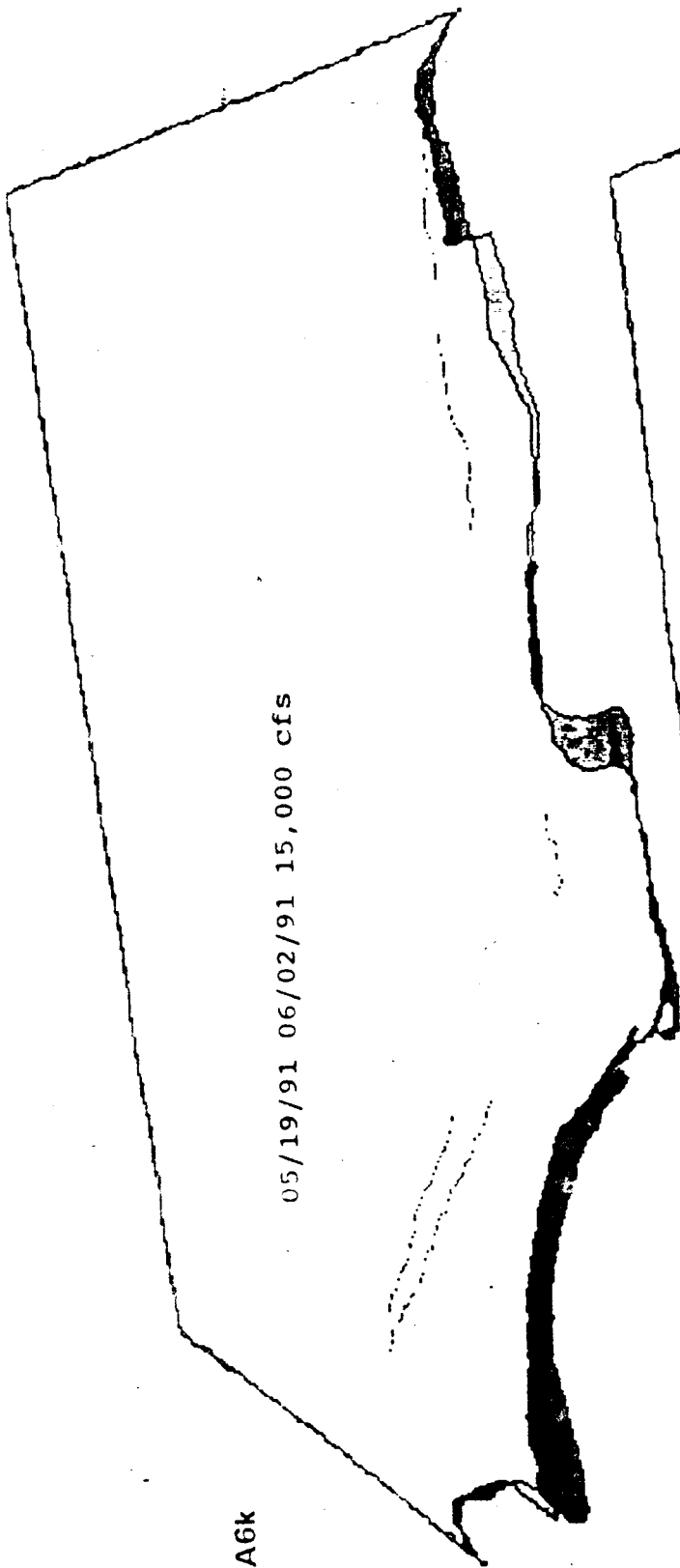
A6j

05/05/91 05/19/91 "D"



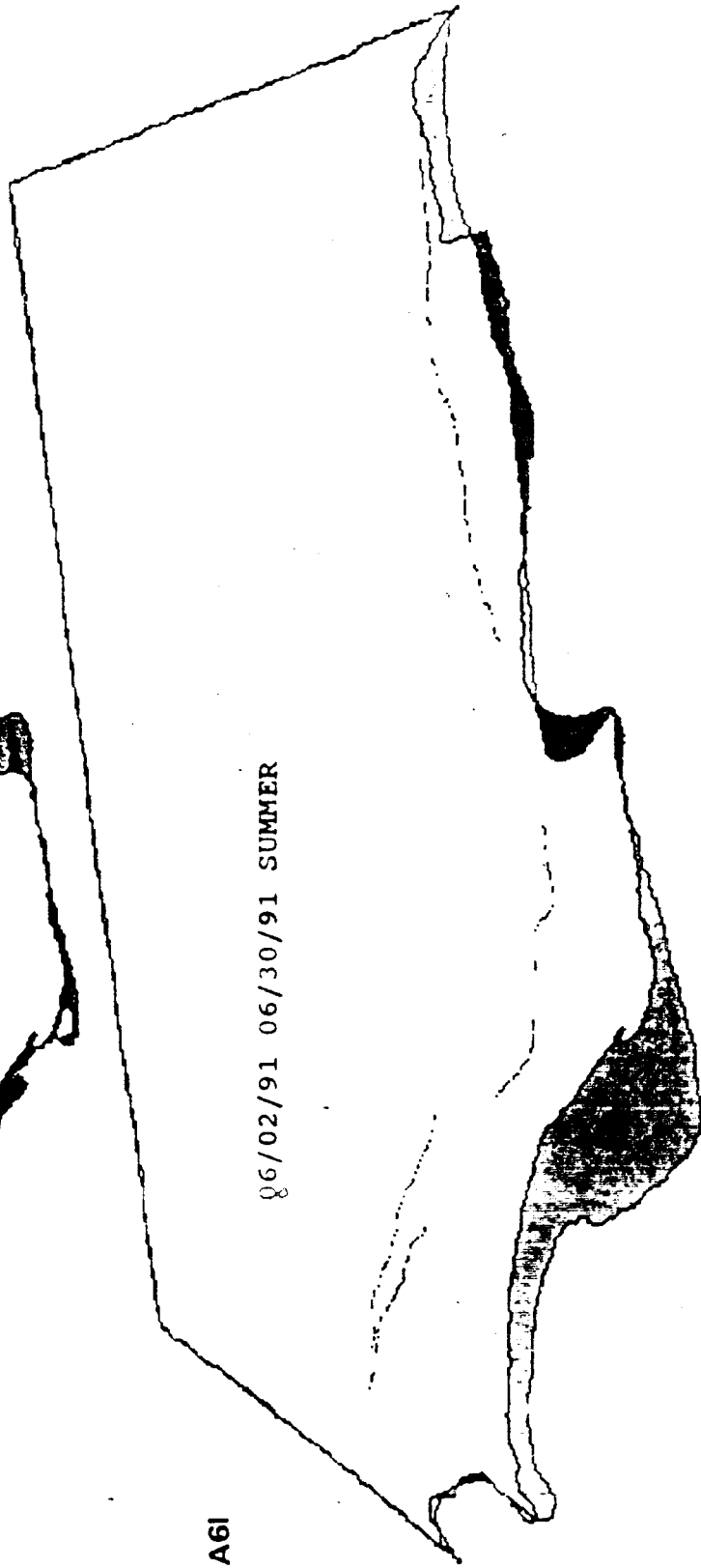
A6k

05/19/91 06/02/91 15,000 cfs



A6I

06/02/91 06/30/91 SUMMER

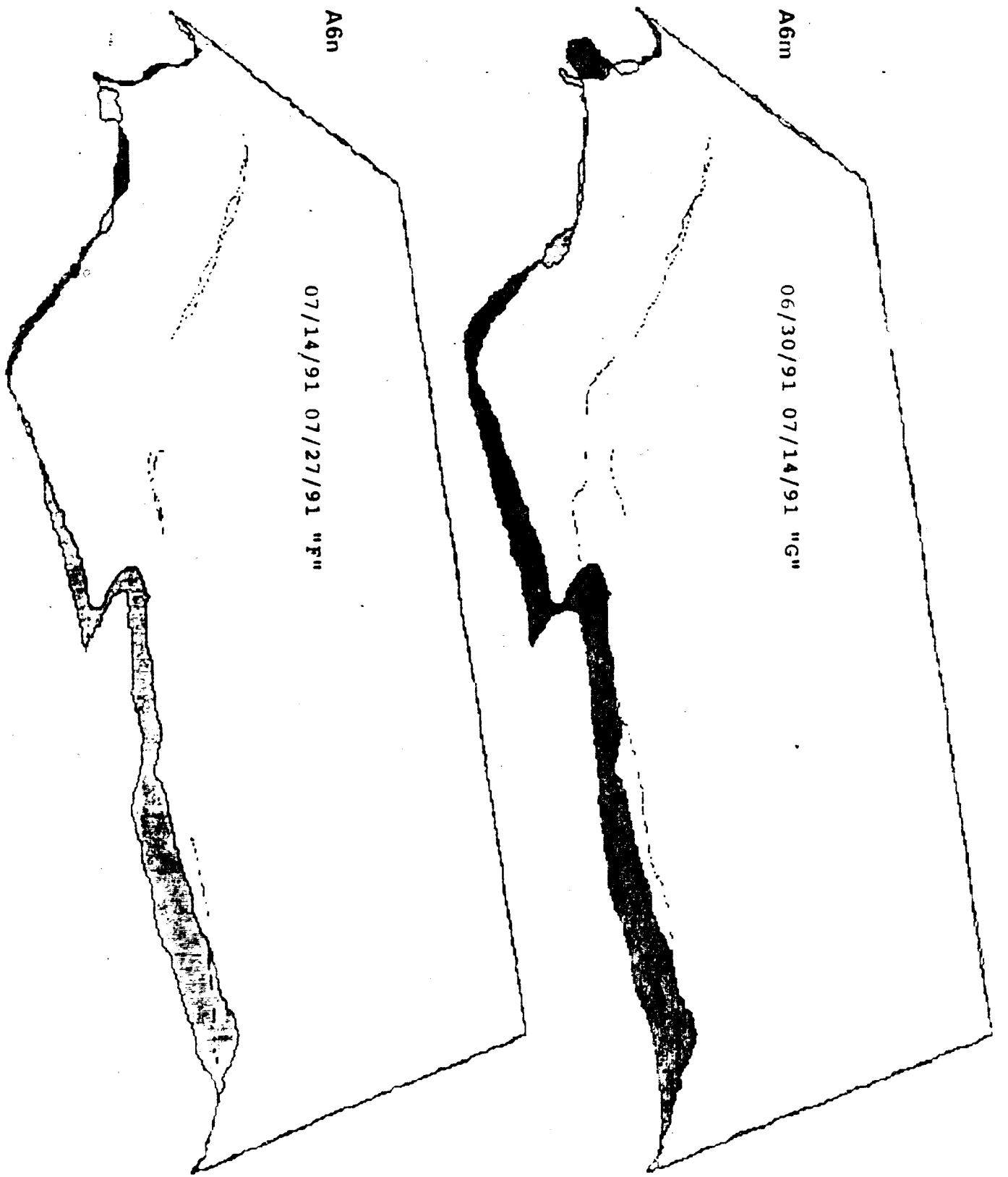


A6m

06/30/91 07/14/91 "G"

A6m

07/14/91 07/27/91 "F"



SITE 66 LEFT

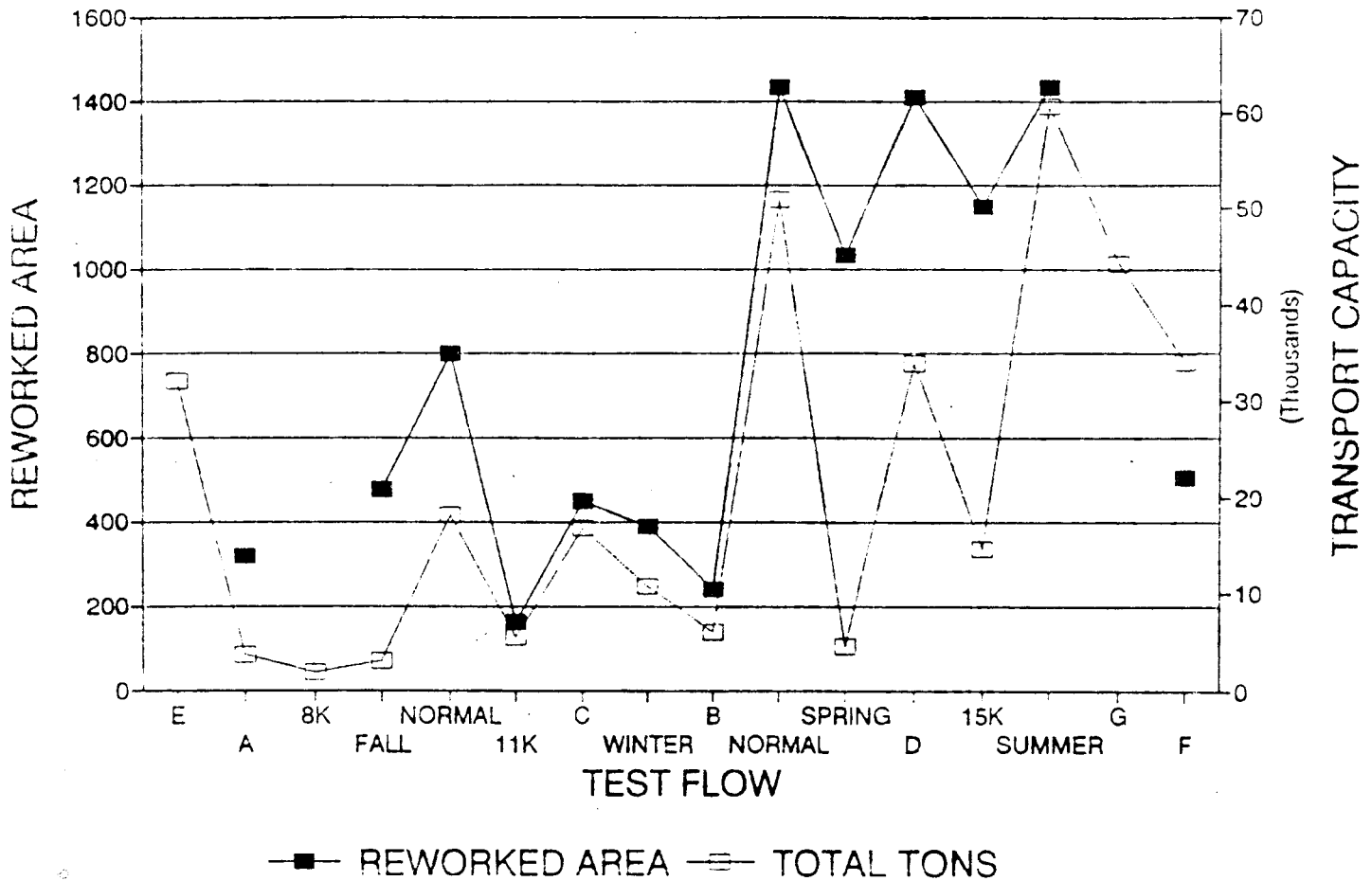
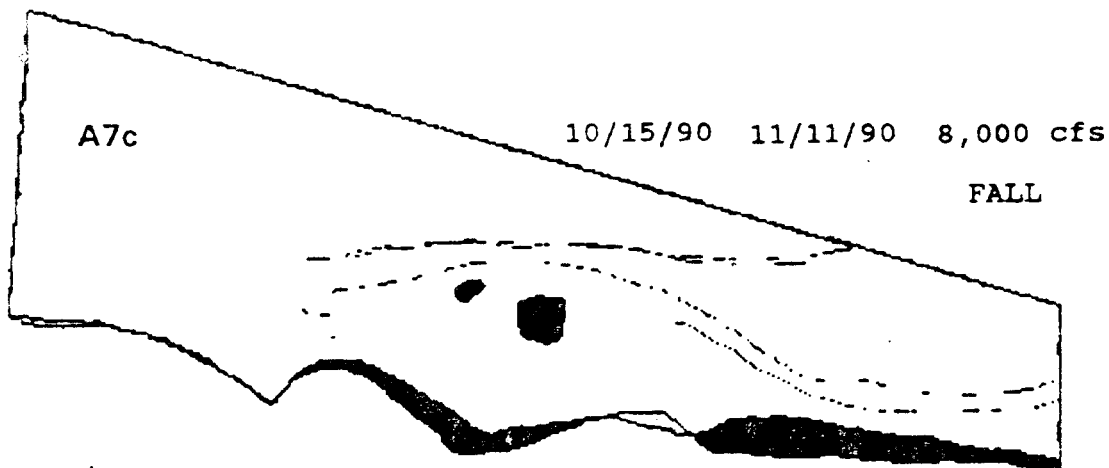
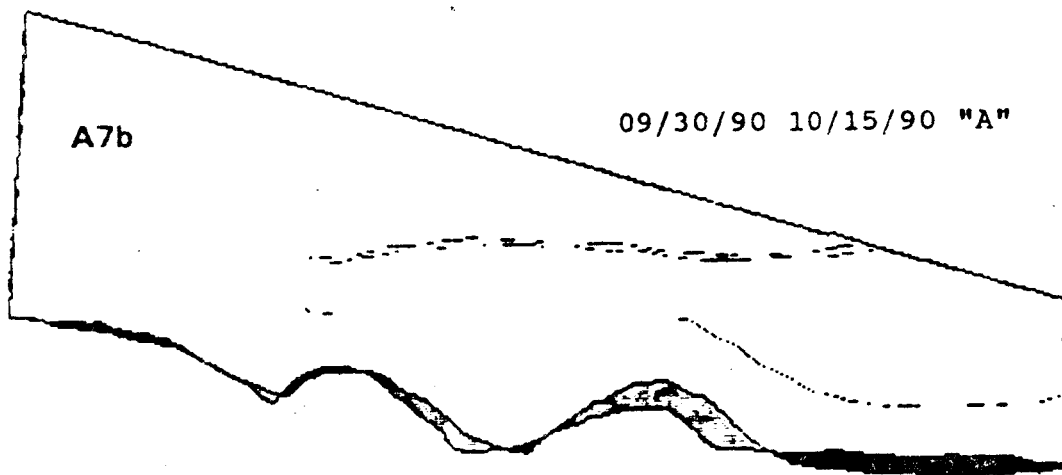
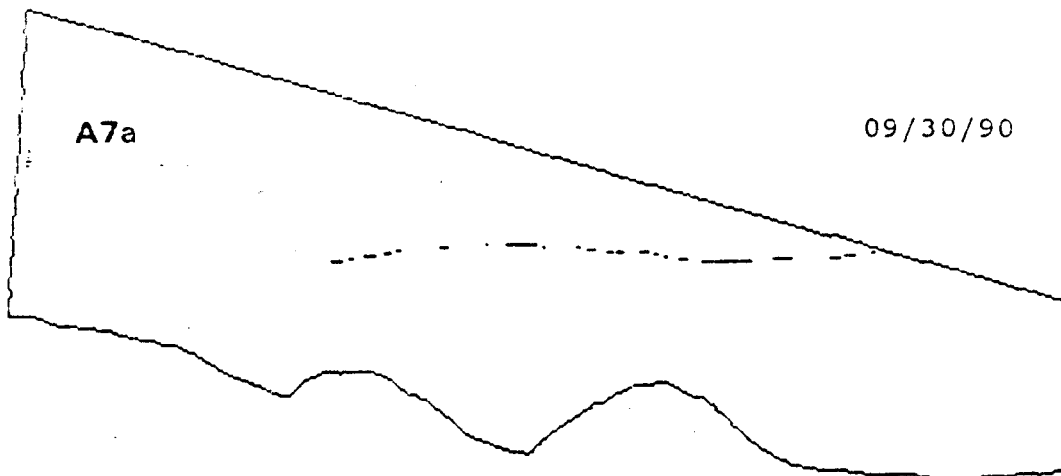
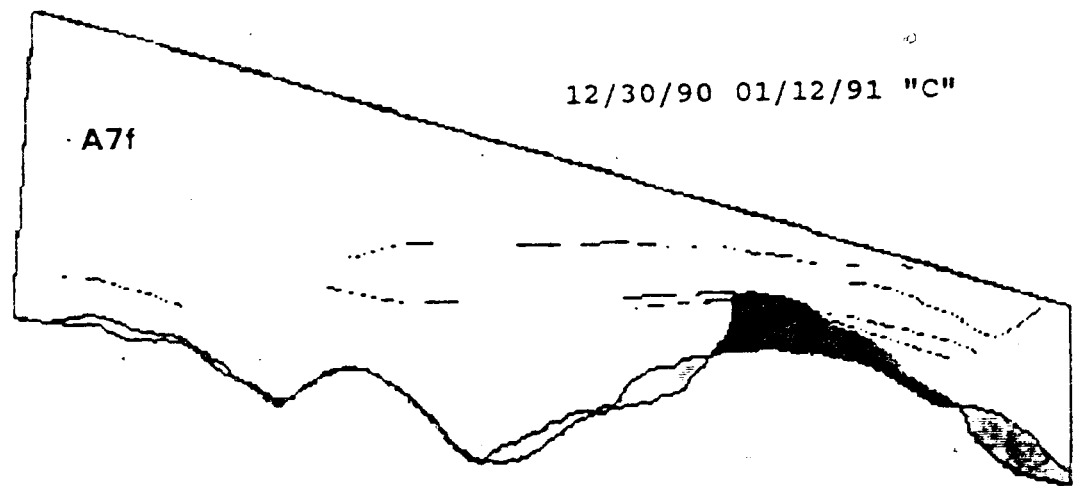
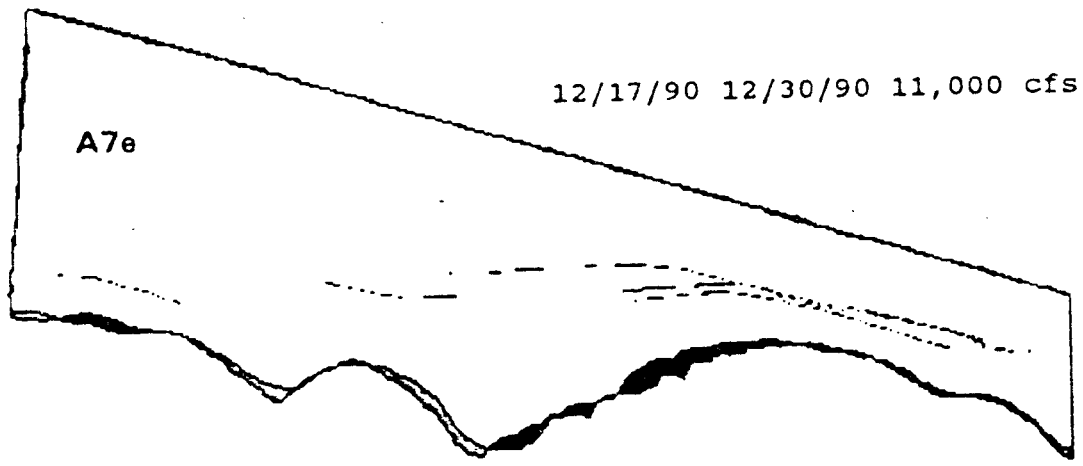
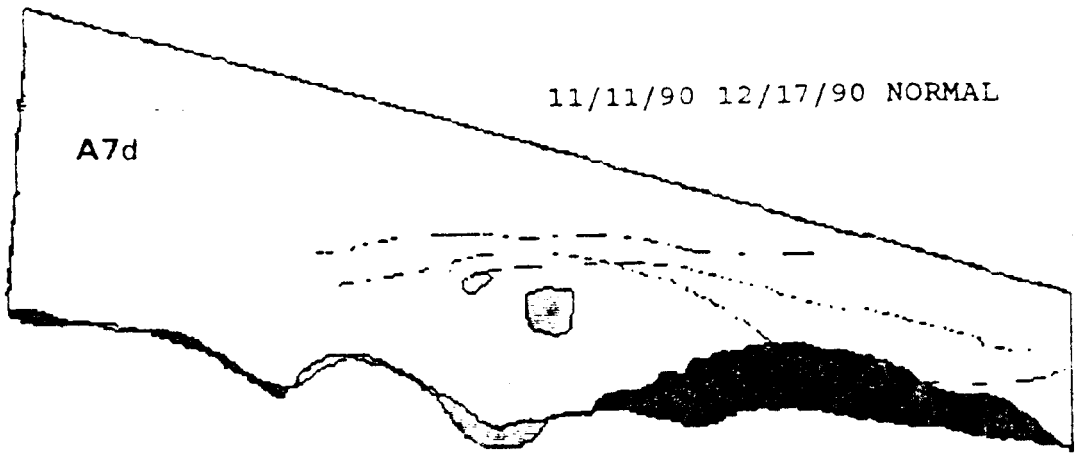


Figure A7. Time-series plot of reworked area and sediment transport capacity for site CR 66 L.

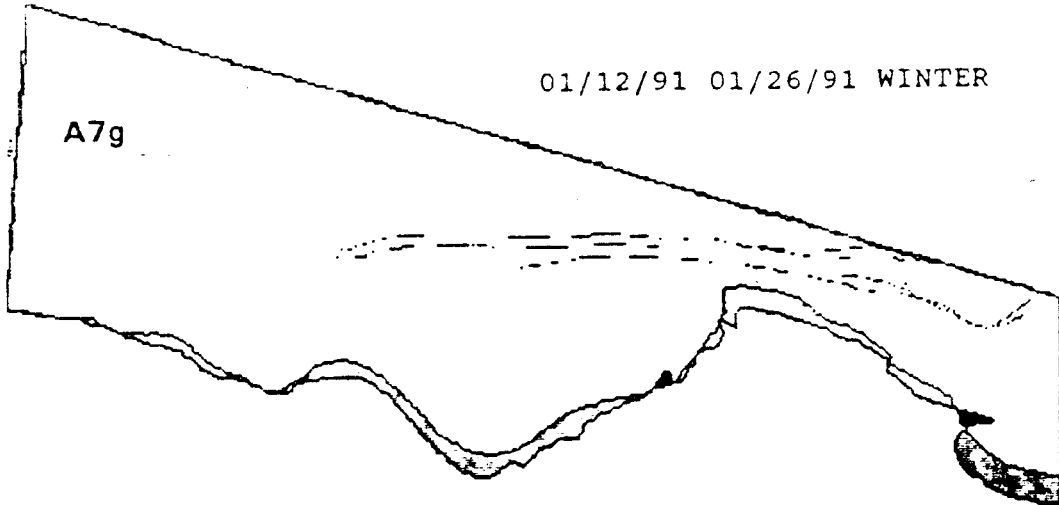
Figures A7a-A7n. Original planimetric outlines and subsequent comparisons of bracketing outlines. Dark shaded areas were eroded. Light shaded areas were aggraded.





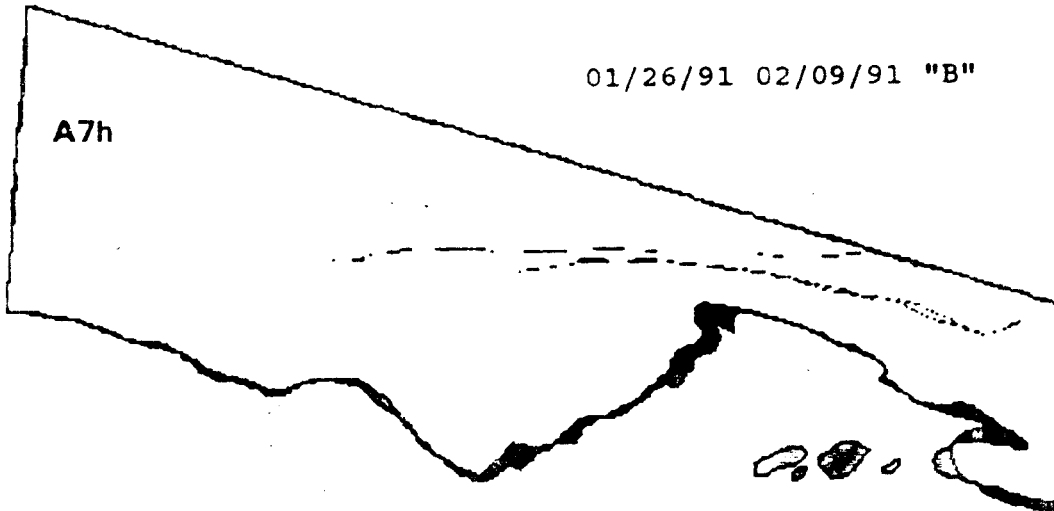
01/12/91 01/26/91 WINTER

A7g



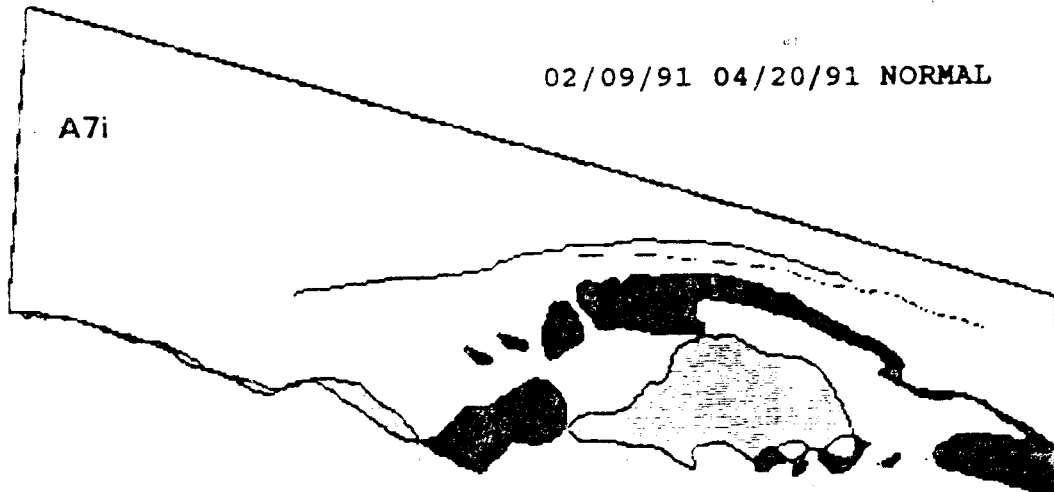
01/26/91 02/09/91 "B"

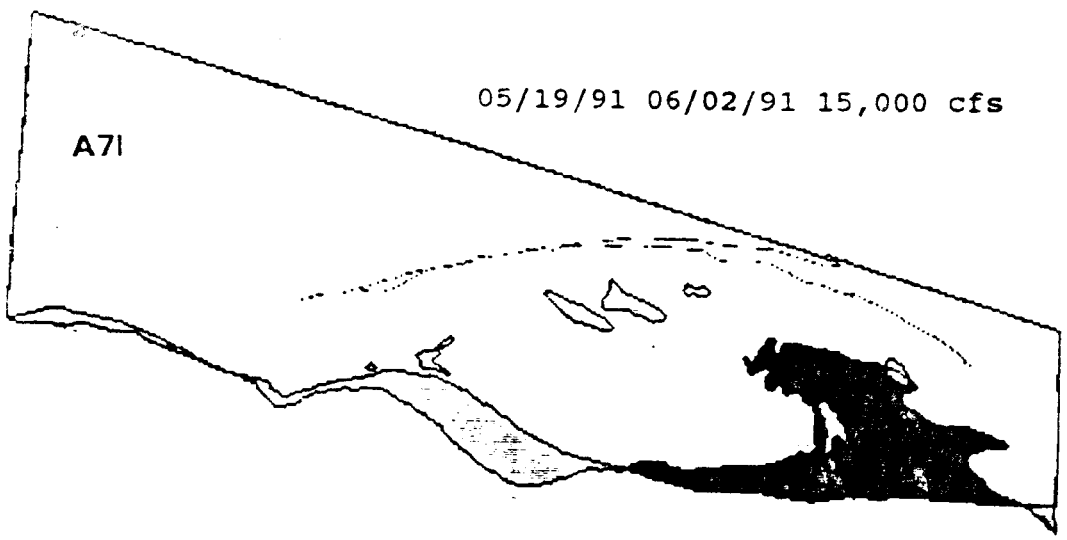
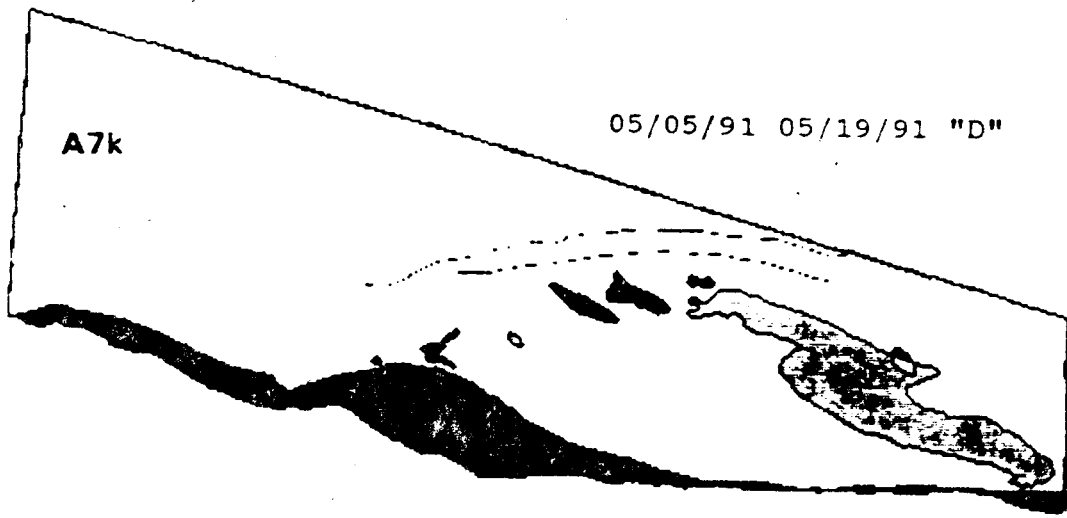
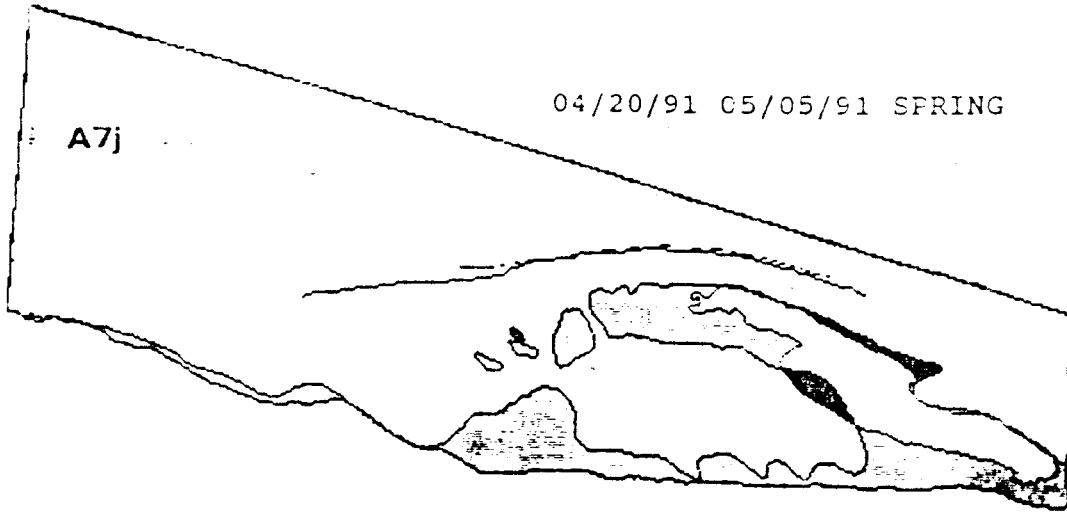
A7h

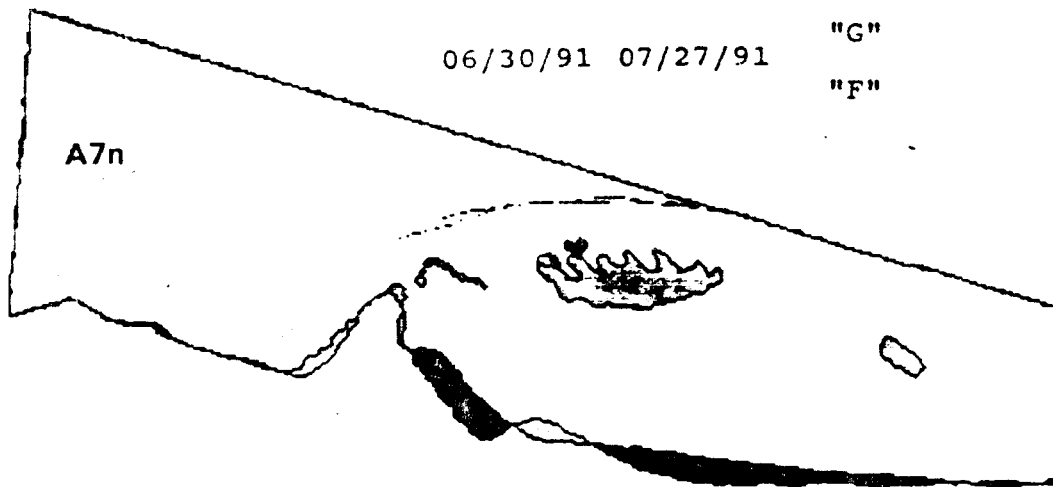


02/09/91 04/20/91 NORMAL

A7i







SITE 68 RIGHT

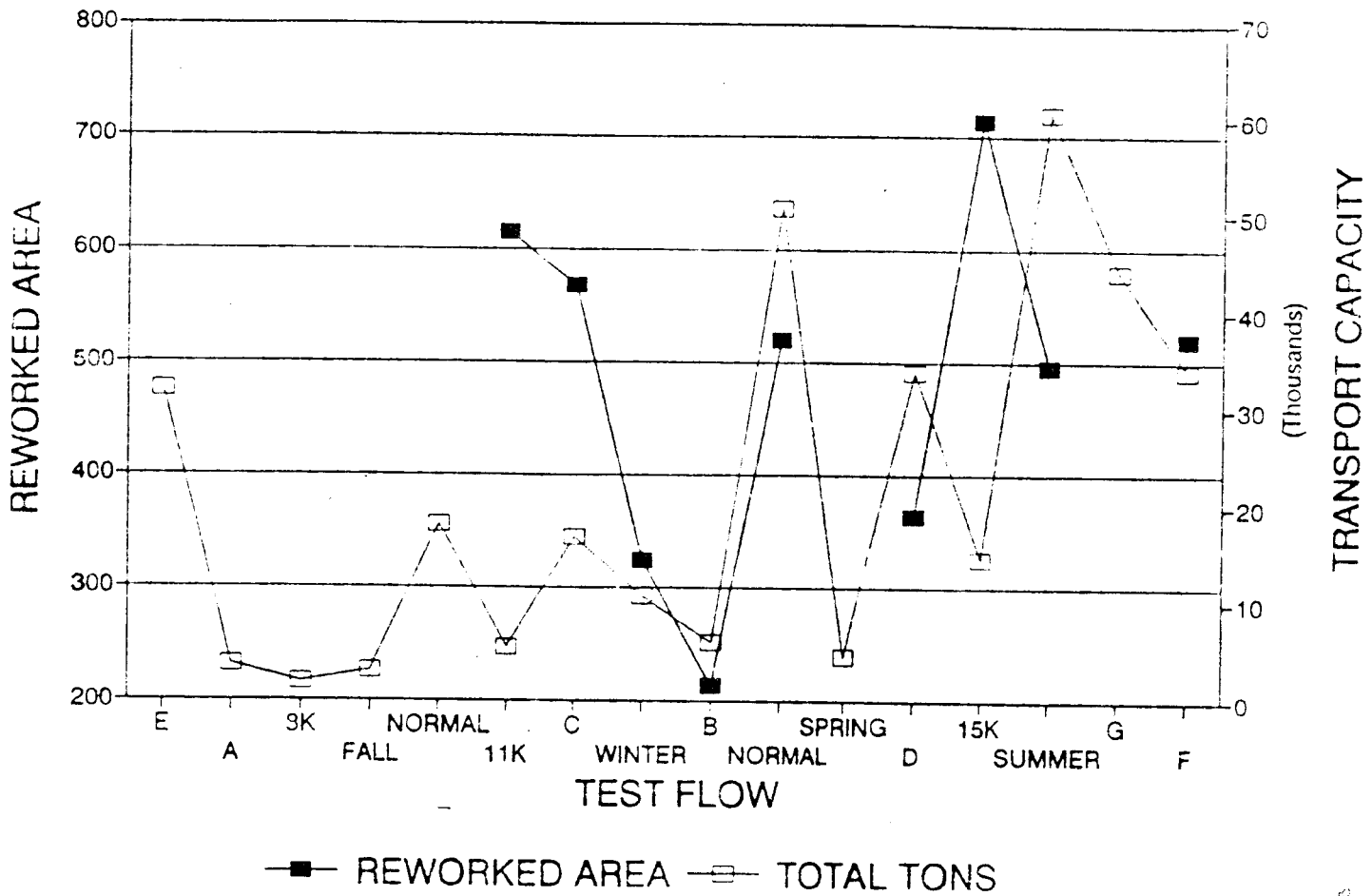
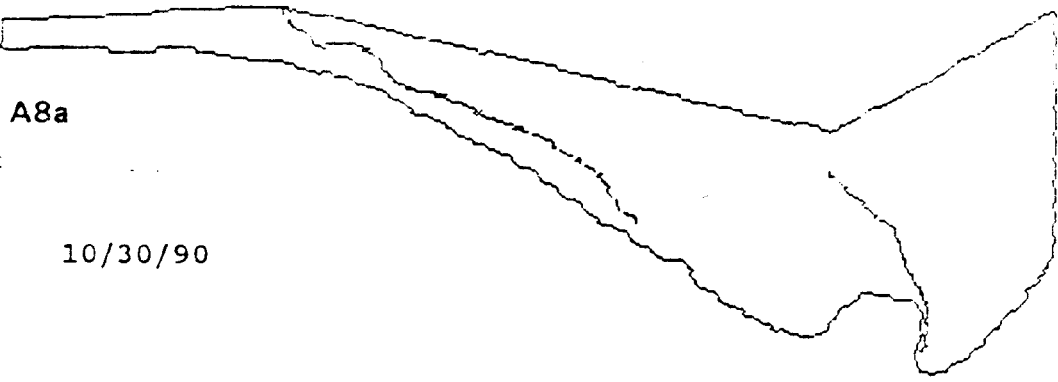


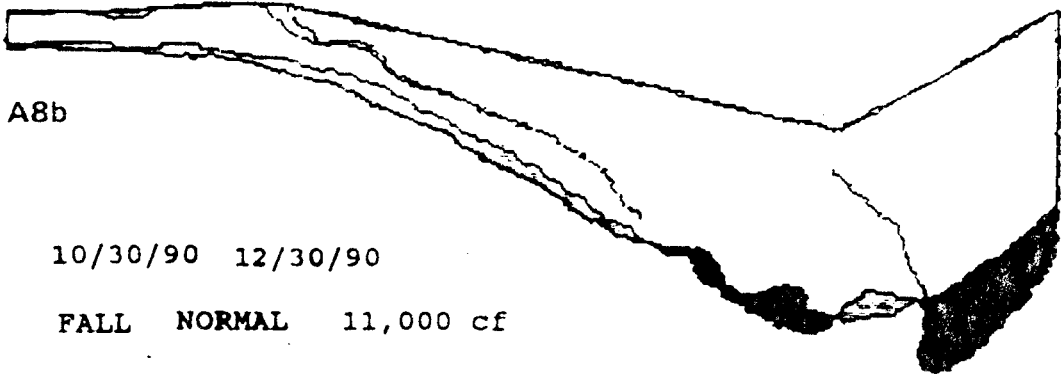
Figure A8. Time-series plot of reworked area and sediment transport capacity for site CR 68 R.

Figures A8a-A8j. Original planimetric outlines and subsequent comparisons of bracketing outlines. Dark shaded areas were eroded. Light shaded areas were aggraded.



A8a

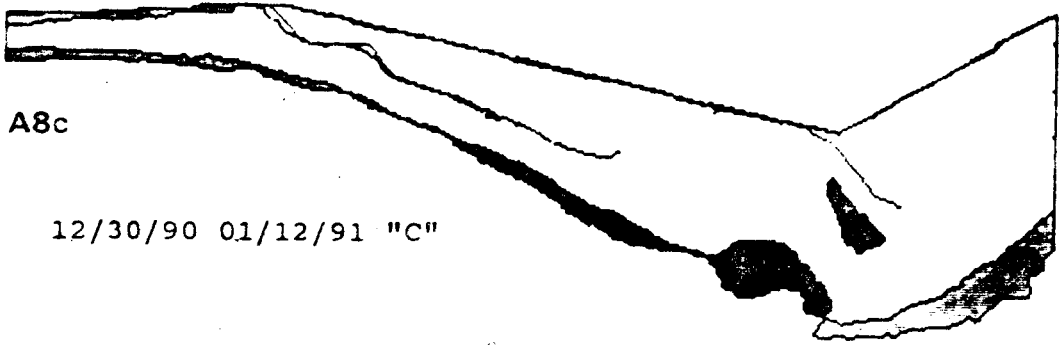
10/30/90



A8b

10/30/90 12/30/90

FALL NORMAL 11,000 cf



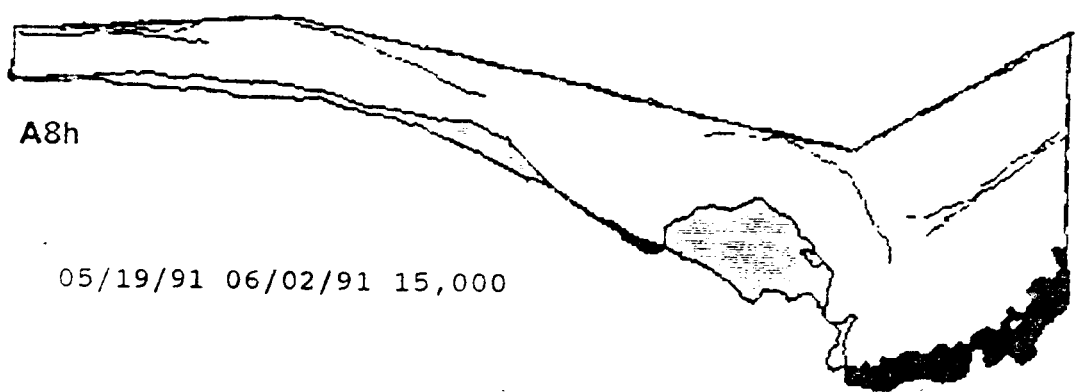
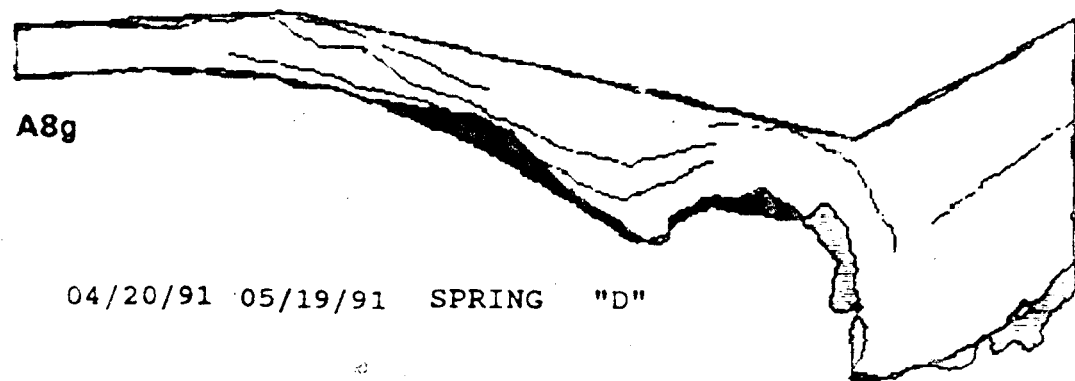
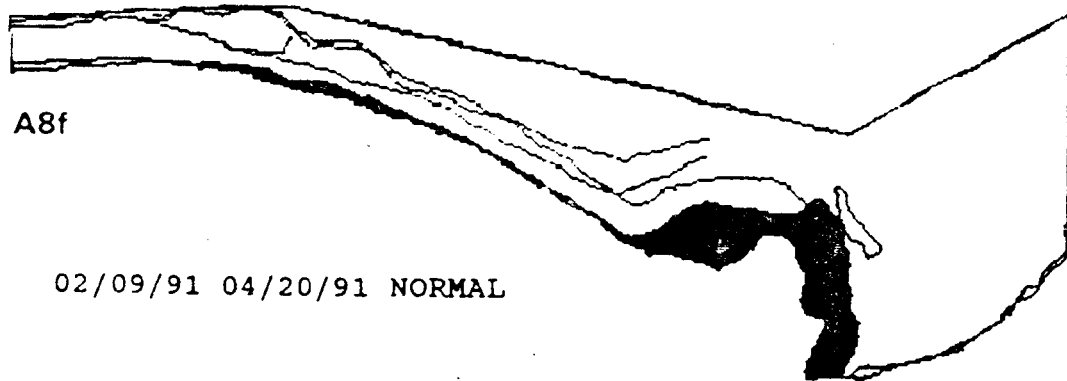
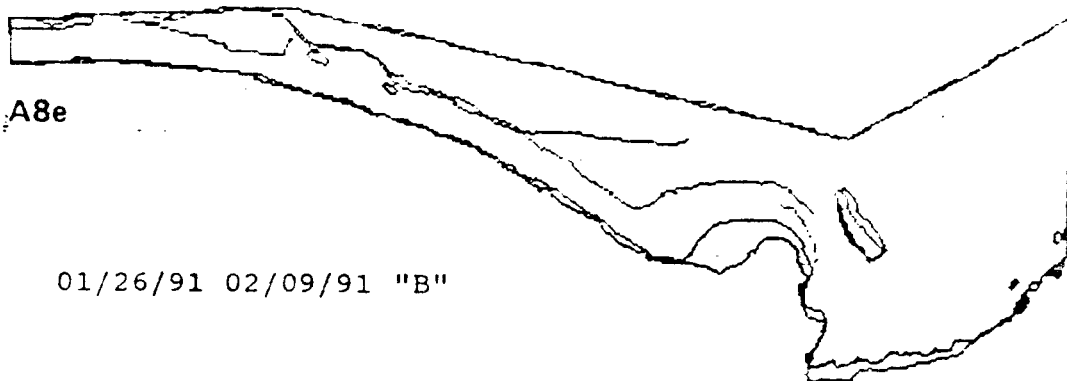
A8c

12/30/90 01/12/91 "C"



A8d

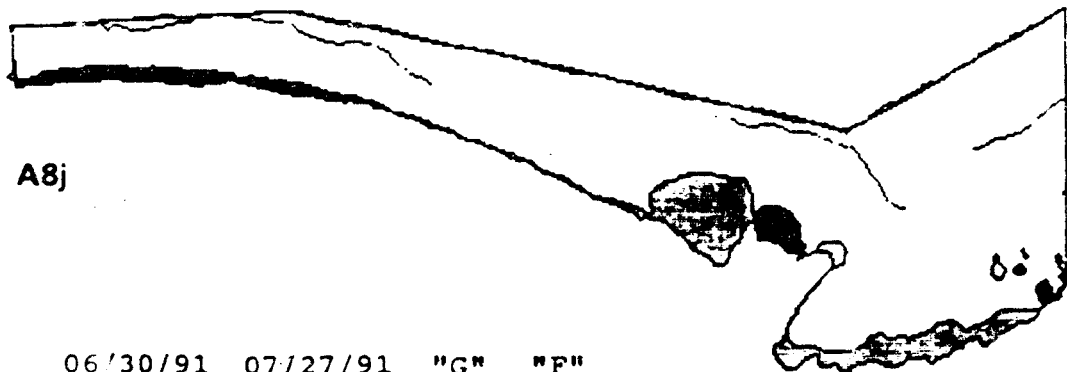
01/12/91 01/26/91 WINTER





A8i

06/02/91 06/30/91 SUMMER



A8j

06/30/91 07/27/91 "G" "F"

SITE 81 LEFT

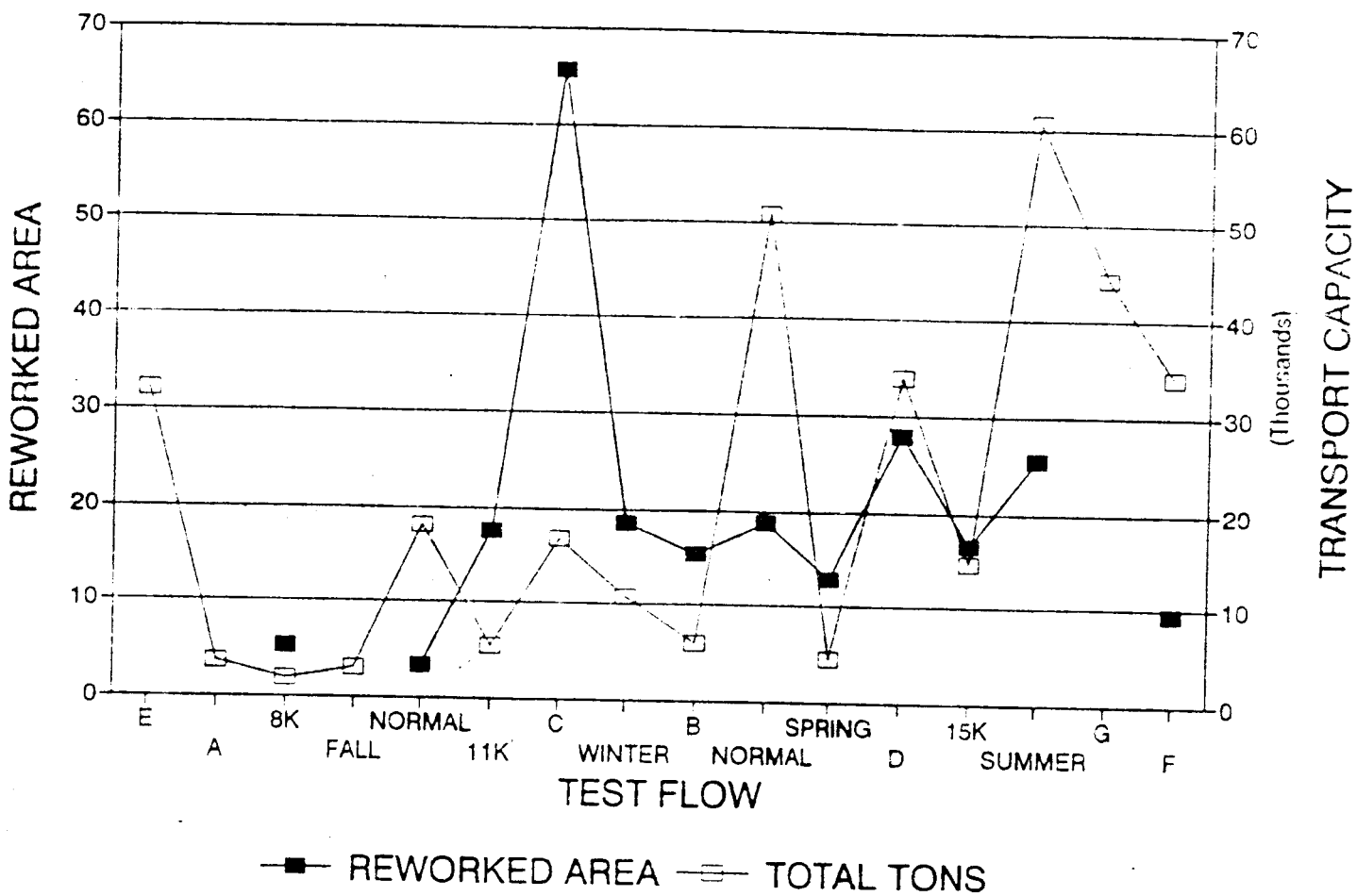


Figure A9. Time-series plot of reworked area and sediment transport capacity for site CR 81 L.

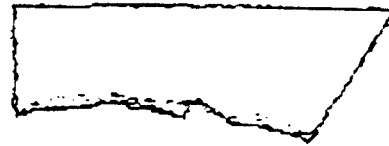
Figures A9a-A9m. Original planimetric outlines and subsequent comparisons of bracketing outlines. Dark shaded areas were eroded. Light shaded areas were aggraded.

A9a



10/15/90

A9b



10/15/90 10/30/90 8,000 cfs

A9c



10/30/90 12/17/90 FALL
NORMAL

A9d



12/17/90 12/30/90 11,000 cfs

A9e



12/30/90 01/12/91 "C"

A9f



01/12/91 01/26/91 WINTER

A9g



01/26/91 02/09/91 "B"

A9h



02/09/91 04/20/91 NORMAL

A9i



04/20/91 05/05/91 SPRING

A9j



05/05/91 05/19/91 "D"

A9k



05/19/91 06/02/91 15,000 cfs

A9i



06/02/91 06/30/91 SUMMER

A9m



06/30/91 07/27/91 "G" "F"

SITE 172 LEFT

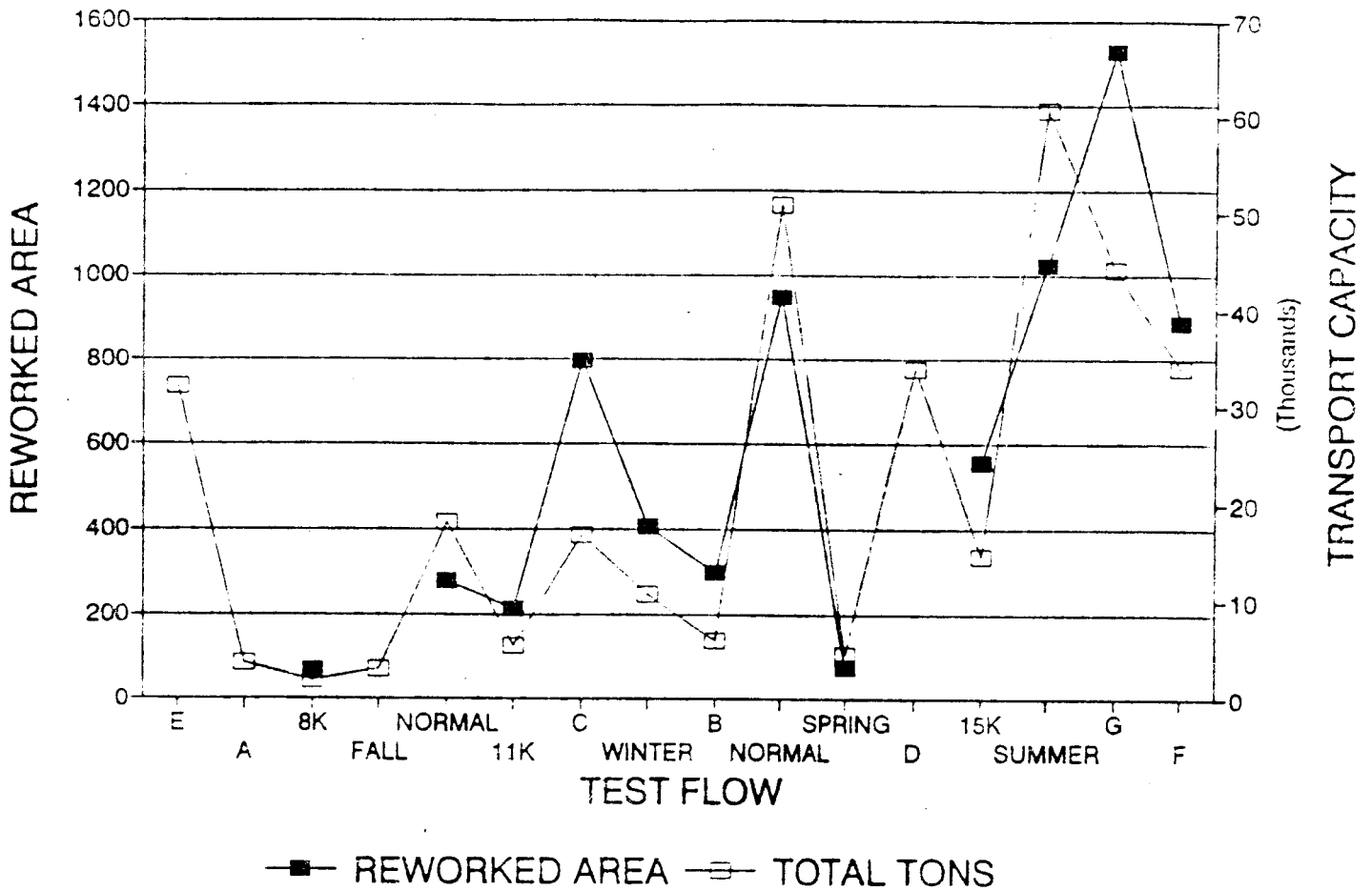
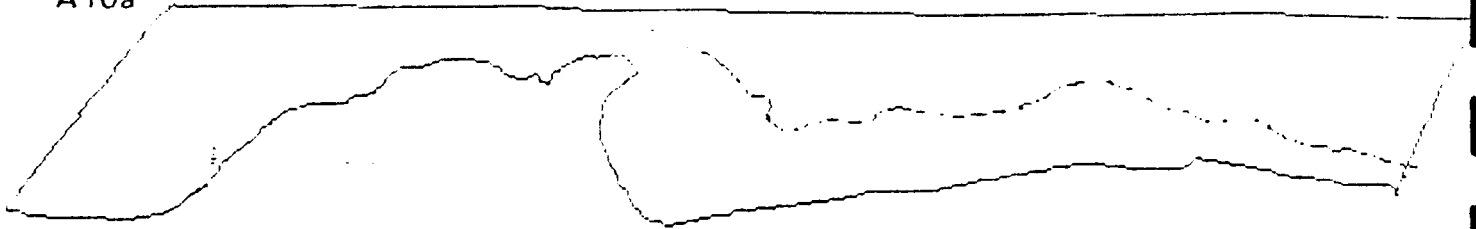


Figure A10. Time-series plot of reworked area and sediment transport capacity for site CR 172 L.

Figures A10a-A10m. Original planimetric outlines and subsequent comparisons of bracketing outlines. Dark shaded areas were eroded. Light shaded areas were aggraded.

A10a



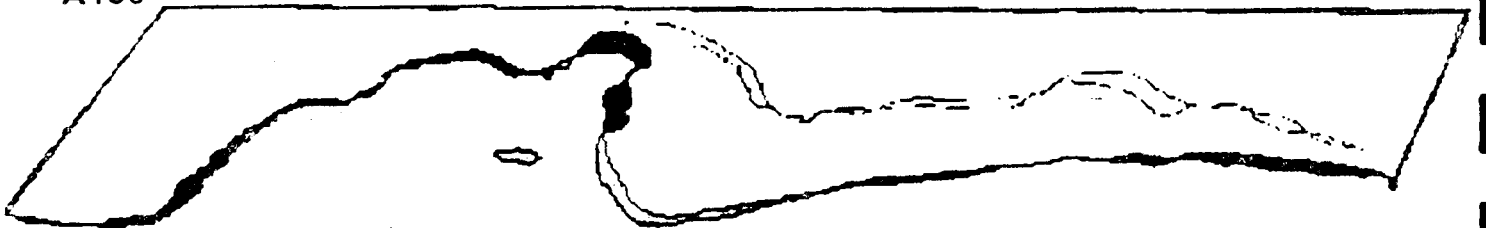
09/30/90

A10b



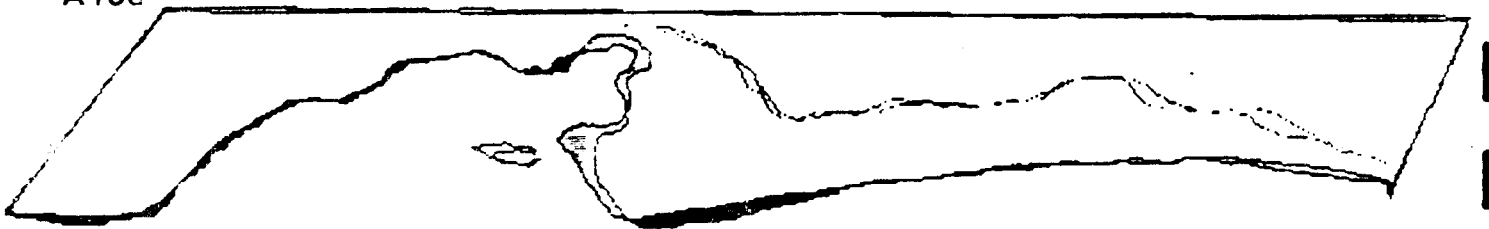
09/30/90 10/30/90 "A" 8,000 cfs

A10c



10/30/90 11/11/90 FALL NORMAL

A10d



12/17/90 12/30/90 11,000 cfs

A10e



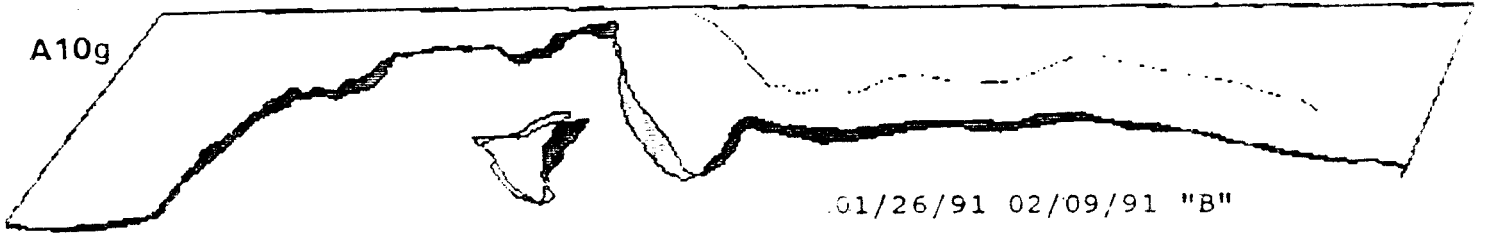
12/30/90 01/12/91 "C"

A10f



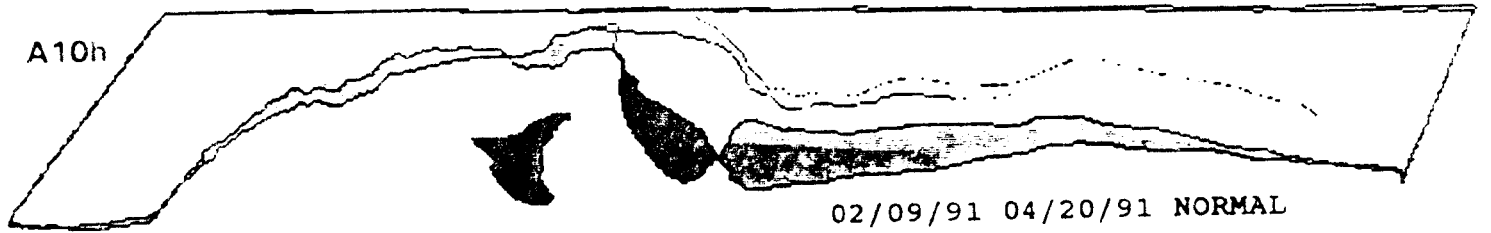
01/12/91 01/26/91 WINTER

A10g



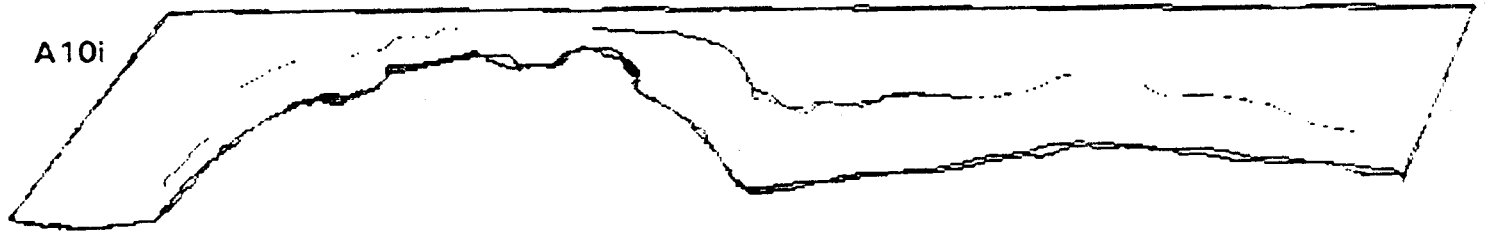
01/26/91 02/09/91 "B"

A10h



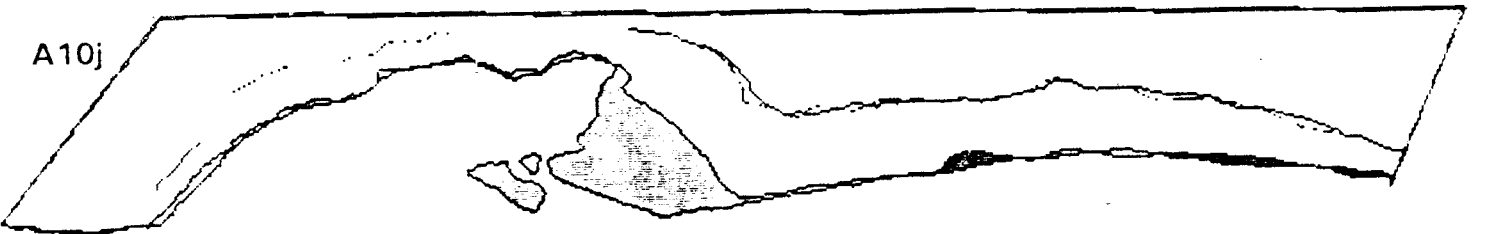
02/09/91 04/20/91 NORMAL

A10i



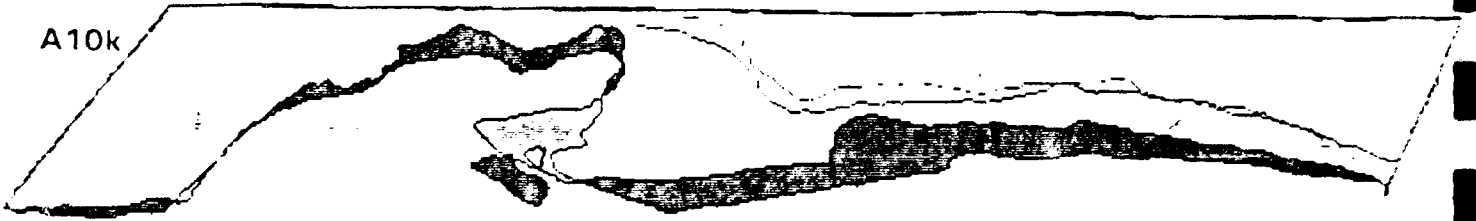
04/20/91 05/05/91 SPRING

A10j



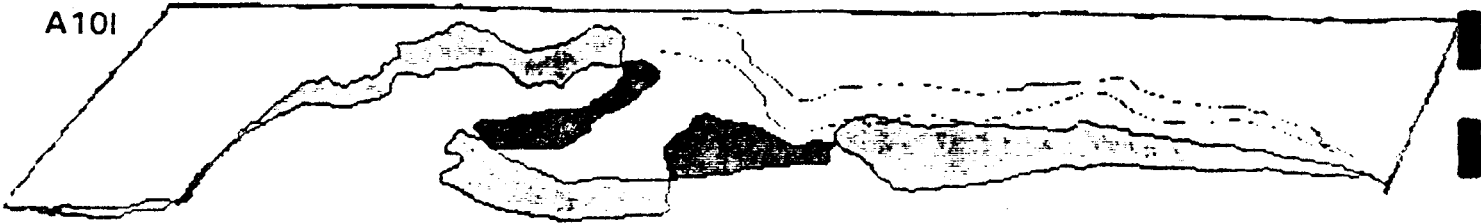
05/05/91 06/02/91 "D" 15,000 cfs

A10k



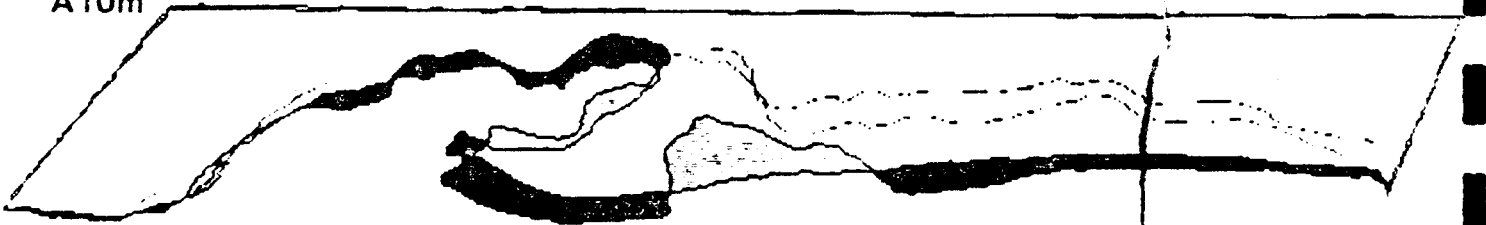
06/02/91 06/30/91 SUMMER

A10l



06/30/91 07/14/91 "G"

A10m



07/14/91 07/27/91 "F"

CHAPTER 8

**TEMPORAL AND SPATIAL CHANGES IN SEDIMENT STORAGE IN
GRAND CANYON**

**John C. Schmidt
Department of Geography and Earth Resources
Utah State University
Logan, Utah 84322-5240
July 1992**

ABSTRACT

Comprehensive mapping of the surficial geology of the Colorado River corridor in selected reaches of Grand Canyon at 8 different times between 1965 - 90 and compilations of sand-bar profile change between 1965 - 90 at 7 sites was completed in order to evaluate the spatial and temporal variability of sediment-storage changes. Results show that between 1965 - 82, a period when annual peak discharges were low, channel banks in wide reaches aggraded while high-elevation sand bars used as campsites eroded. Erosion rates declined with time. Between 1983 - 86 when annual peak discharges were at least twice that of the previous period, reattachment bars throughout Grand Canyon eroded but high-elevation bars used as campsites aggraded. Since 1987, low-elevation sites have aggraded, and high-elevation sites have eroded. Aggradation rates during this latter period are about the same as during the 1966 - 82 period, but erosion rates have been about twice that of the previous period. The variability in response of bars to changes in flow regime are such that (1) the entire record of temporal and spatial change must be considered in order to fully interpret short-term measurements of bar change, and (2) bar-building floods must be carefully designed lest they cause net campsite erosion.

INTRODUCTION

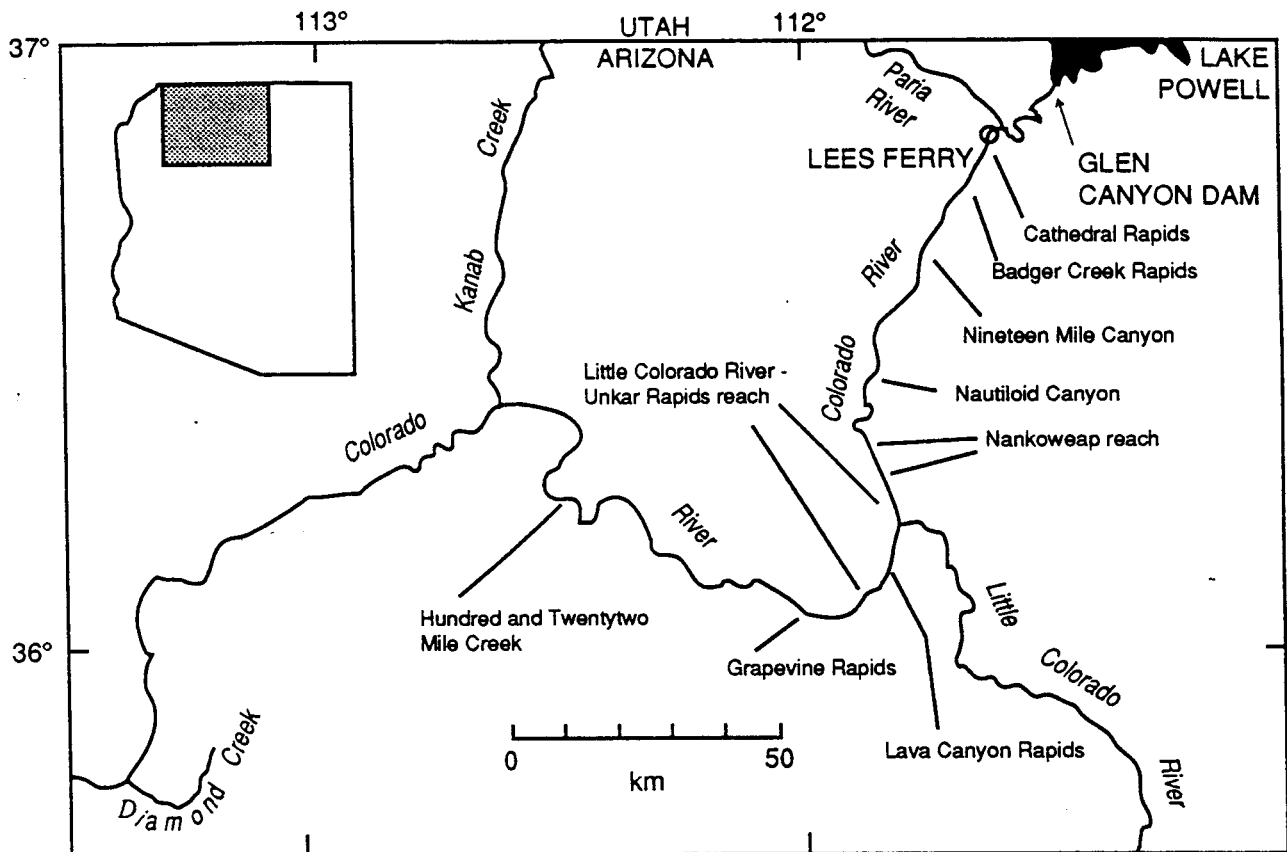
Long-term environmental change caused by large dams occurs upstream and downstream from every impoundment. In the case of the Colorado River in Grand Canyon downstream from Glen Canyon Dam (Fig. 1), the frequency and magnitude of flooding and the mass of sediment transported into Grand Canyon have been greatly reduced (Andrews, 1991; Laursen and others, 1976). Alluvial banks and sand bars are among the geomorphic resources of the Grand Canyon river corridor that have responded to these hydrologic and sediment-transport changes.

Since the days of early river runners, boaters have been impressed by the extensive open sand bars which intermittently form the river's banks at low discharge. These bars are commonly referred to as "beaches" by the 20,000 persons who annually travel by boat downstream from Lees Ferry and who use the bars as campsites. These bars are an integral physiographic component of the river corridor and of the national park itself. Bars are also substrate for riparian communities; higher and older alluvial deposits contain archaeological remains. Kearsley and Warren (1992) showed that campsites along the river, nearly all of which occur on these sand bars, greatly decreased in number and size between 1973-91.

River discharge within Grand Canyon National Park is nearly completely controlled by Glen Canyon Dam, officially completed in 1963. In fact, the Colorado River is the most highly regulated large river in North America (Hirsch and others, 1990, fig. 17). The downstream effects to Grand Canyon National Park were recognized by Dolan and others (1974) and first quantified by Turner and Karpiscak (1980) and Howard and Dolan (1981). Proposed revision of the hourly reservoir release pattern in the early 1980's and the occurrence of unusually high runoff between 1983-86 led to funding of multi-disciplinary research beginning in 1983 (Water Science and Technology Board, 1987, 1991).

One component of the research program has focused on understanding the relation between reservoir operations and geomorphic stability of alluvial deposits. Geomorphic research concerning alluvial deposits has focused on documentation of the history of bar aggradation and degradation (Beus and others, 1985; Schmidt and Graf, 1990), on bar sedimentology (Rubin and others, 1990), and on the general relation between sand bars and recirculating flow (Schmidt, 1990). Other research concerning hydraulics and sediment transport of the main channel are summarized by the U. S. Department of the Interior (1988) and reviewed by the Water Science and Technology Board (1987).

Figure 1. -- Study area and study sites.



Because studies conducted between 1983-86 occurred during a period of unusually high and steady reservoir release, another phase of research was initiated in 1990 specifically focused on the relation between hourly discharge patterns during hydroelectric peak-power generation and downstream environmental change. Research during the second phase has included calculations of bar deposition rates (Andrews, 1991), numerical modeling of recirculating flow (Nelson, 1991), studies of bank stability due to ground-water fluctuations (Bhudu and Contractor, 1991; Carpenter and others, 1991; Carruth and others, 1991; Werrell and others, 1991), and surveying and photography of topographic changes during periods of controlled water release (Beus and others, 1991; Cluer, 1991).

The research results presented here are another part of the second phase program. This project was initiated because development of any revised plan of dam operations must rely in part on (1) a detailed understanding of the volume and geography of changes in sediment deposits that have occurred in Grand Canyon since dam closure, and (2) analysis of the relation between those changes and the history of water release from the dam. Another reason for undertaking this study arises from the need to evaluate the spatial and temporal variability of sand-bar change, especially as an aid in interpretation of the results of Beus and others (1992). Interpretation and extrapolation of measured changes at selected sites and for relatively short time periods is partly dependent on the assumption that study sites are representative of reach-scale changes and that measured changes can be extrapolated in time.

This report summarizes (1) the results of Clark (1992) and Kyle (1992), each an undergraduate thesis in the Geology Department, Middlebury College, and funded by this project, and (2) other original studies. The two theses are included as Appendices A and B of this report. The reader is referred to each of these studies concerning the details of methodology and results.

BACKGROUND

Turner and Karpiscak (1980) demonstrated that riparian vegetation colonized low-elevation sediment deposits throughout Grand Canyon before 1975. Sediment-deposit change in Grand Canyon was first quantified by Howard (1975) and Howard and Dolan (1979, 1981), who evaluated sand-bar aggradation and degradation between 1963-80 based on analysis of aerial photographs and analysis of repeated surveys of sand-bar profiles. Although Dolan and others (1974) suggested that widespread erosion of sediment deposits might result from dam operations and Laursen and others (1976) had estimated

that there was a large deficit in the regulated sediment budget for Grand Canyon, Howard and Dolan (1981) found that sediment deposits had "suffered only a very slight erosion" after dam closure.

Inventories of the size and number of sand bars used as campsites were made in 1973 (Weeden, 1975), 1983 (Brian and Thomas, 1984), and 1991 (Kearsely and Warren, 1992). Schmidt and Graf (1990) and Zink (1989) inventoried the size and frequency of all sand bars, regardless of size or use, based on interpretation of 1973 and 1984 aerial photography. These inventories are valuable in assessing the history of sediment-storage change because sand-bar area, volume, and frequency likely reflects the overall condition of sediment storage in bedrock canyons. In these canyons, bar location is fixed over periods between decades and centuries, being controlled by the geometry of flow separation. In turn, flow separation is controlled by the geometry and location of constrictions, expansions, and mid-channel bars. Sand bars that form within flow-separation zones do not migrate in the manner of bars in alluvial channels, and it is reasonable to assume that changes in the size of sand bars reflect changes in the total volume of stored sediment in canyons. The validity of this assumption is discussed in this report.

The other primary method of evaluating sand-bar change has been repeated surveying of profiles or surveys of the entire topography of selected campsites. These monitoring studies were initiated by Howard (1975), resumed by Beus and others (1985) in 1983, expanded by Schmidt and Graf (1990), and continued by Beus and colleagues at Northern Arizona University (surveys every summer), Schmidt and colleagues at Middlebury College (surveys in January 1989 and January 1990), and Graf and colleagues at the U. S. Geological Survey (surveys in September 1988 and September 1989). There has been no comprehensive interpretation of area or volume changes that have occurred since 1986, and not integration of the results from these different survey groups.

On the basis of an inventory of sand-bar campsites, Brian and Thomas (1984) concluded that high discharges in 1983 had caused net erosion of these deposits in the first 290 km downstream from Lees Ferry. They also concluded that a net increase in the same type of sand deposits had taken place farther downstream. Beus and others (1985) evaluated the history of change of 20 major sand deposits between 1974-84 by repeating topographic surveys of profiles established by Howard (1975). Beus and others (1985) concluded that "a substantial net gain of sand [due to high discharges in 1983 and 1984] ... more than compensated for the previous 8-year loss."

Schmidt and Graf (1990) and Schmidt (1990) developed a classification of sediment deposits in Grand Canyon and a reach-length classification of the river corridor. Schmidt and Graf (1990) concluded that the set of beaches monitored by Howard (1975) and Beus and others (1985) was a set that typically aggraded or remained stable despite the fact that overall erosion of the entire population of bars occurred in the same reaches; by implication they argued that most bars used as campsites are the most stable subset of the entire population of sand bars. Schmidt and Graf (1990) inventoried sand bars in 400 large persistent eddies between Lees Ferry and river-mile 118 near Elves Chasm and concluded that high discharges in 1983 and 1984 had eroded sediment from those eddies located in narrow reaches, such as Supai Gorge, Redwall Gorge, Upper Granite Gorge. They concluded that net change of sediment storage in eddies in wide reaches (river-miles 36-77) was slightly positive. Zink (1989) found that there had been no significant changes in eddies downstream from river mile 118 between 1973 - 84. The dual effects of downstream changes in sediment budget and reach-scale hydraulic differences between narrow and wide reaches resulted in a pattern where downstream erosional effects did not decay exponentially, as suggested by Williams and Wolman (1984). In fact, the greatest erosion to eddy sand bars between 1973-84 occurred in Upper Granite Gorge, a narrow reach beginning at river-mile 77 and located downstream from the Little Colorado River, a major sediment source to the regulated Colorado River (Schmidt and Graf, 1990). The implications of these results are that individual study sites may be representative of a class or type of deposits, but not necessarily representative of overall behavior of sand bars in all reaches of Grand Canyon.

METHODS

Historical Change along Profiles

This study (1) integrated the results of previous topographic surveys of profile lines or general bar topography of seven longterm monitoring sites, (2) mapped spatial changes of bars using historical aerial photography, (3) replicated historical oblique photography and quantified observed changes at Badger Creek Rapids, and (4) calculated a long-term sediment budget for the Colorado River between Lees Ferry and the U. S. Geological Survey gaging station near Grand Canyon. Integration of previous studies (Table 1) necessarily included different measurement and sampling strategies. Profile data were adjusted to the same elevation datum, typically permitting development of topographic histories for the period 1975-91. Computations of volume change at these sites were

Table 1. -- Data sources and methods of evaluating sand-bar change in Grand Canyon

<u>Source</u>	<u>Period Evaluated</u>	<u>Techniques Used</u>
Howard (1975)	sites established	profiles, engineer's level and tape
Howard and Dolan (1979)	1962 - 75	air photos using zoom-transfer scope
Howard and Dolan (1981)	1962 - 80	profiles
Brian and Thomas (1984)	1974 - 83	campsite inventory
Beus and others (1985)	1974 - 84	profiles, engineer's level and tape
Schmidt and Graf (1990)	1965 - 86	profiles, topographic maps, inventory,

other survey data available:

1. Beus and others (1984, 1985, 1986, 1987, 1988, 1989, reports of Northern Arizona University to National Park Service)
2. Graf (1988, 1989, unpublished topographic maps)
3. Schmidt and others (1989)

developed by (1) comparing volume changes for the relatively few surveys of the entire bar topography, or (2) comparing volume changes by estimating the proportion of a sand bar represented by each profile and developing area-weighted average values for the relatively greater number of surveys that include such surveys. This report shows that the two methods yield comparable results. Kyle (1992) also computed weighted hypsometric integrals for five bars to quantify changes in the elevation distribution of sand deposits. Stage-to-discharge relations were developed at each study site in order to report change relative to the stage of particular discharges. More detailed descriptions of the methods employed by Kyle (1992) are included in Appendix B.

Alluvial-deposit mapping was undertaken in parts of two reaches where 1:2400 scale topographic maps are available (U. S. Bureau of Reclamation -- Nankoweap reach and Little Colorado River to Unkar Rapids reach). This mapping was undertaken (1) to evaluate whether the classification proposed by Schmidt (1990) is sufficiently comprehensive such that it includes all existing deposits, (2) to determine if the aggregate change in the exposed area of alluvial deposits is similar to the pattern determined from profile data of specific study sites, and (3) because the results of Schmidt and Graf (1990) concerning the historical pattern of change in wide reaches is uncertain.

Historical Changes Determined from Aerial Photography

Surficial geologic maps of the river corridor were made for each aerial photo series available between 1965 - 1990; 20 mapping units were used and are listed in Table 2. Air photos exist at many scales, and all data were transferred to the common topographic base using a stereo-zoom transfer scope. Field work in the Nankoweap reach was conducted in May, August, and September 1991; field work in the reach between the Little Colorado River and Unkar Rapids was conducted in September and October 1991. Completed maps were digitized into an Arc-Info database by the Geographic Information Systems laboratories at Utah State University and the U. S. Bureau of Reclamation, Denver.

Because the mapped area of sand bars and other sediment deposits is greatly dependent on river stage, this bias must be considered when evaluating change in area and volume of sediment deposits. For a particular reach, a linear least-squares relation between discharge and exposed area was used to compute residuals, which were considered representative of the temporal trends in sediment storage in each reach.

Use of aerial photography for interpretation of change in exposed sediment-deposit area permits assessment of aggradation and degradation of low-elevation areas along the

Table 2. -- Mapping units used in surficial geologic mapping

Reattachment bar (vegetated)
Reattachment bar (bare sand)
Reattachment bar (submerged)
Separation bar (vegetated)
Separation bar (bare sand)
Separation / reattachment bar, undifferentiated (vegetated)
Separation / reattachment bar, undifferentiated (bare sand)
Margin deposit (vegetated)
Margin deposit (bare sand)
Margin deposit (submerged)
High terrace
Debris fan
Debris fan / sand and boulders undifferentiated
Talus and bedrock
Aeolian sand
Sand and boulders, undifferentiated
Boulder or cobble bar
Gravel bar
Gravel bar (submerged)
Sand and gravel, undifferentiated

river shoreline, but is less valuable for assessing changes in high-elevation parts of bars. Changes at high elevation can only be detected if sequential photographs at high-discharge are available. Methods employed for this part of the study, as well as a complete analyses of changes between river-miles 52-56 are described by Clark (1992).

Long-Term Change Determined at Badger Creek Rapids

In addition, historical oblique photography of Badger Creek Rapids since 1923 was compiled in order to evaluate the relation between pre-dam and post-dam variability in sediment storage at one sand bar. Photographs of this site have been matched by R. H. Webb, U. S. Geological Survey, during the past 2 yrs. In October 1991, we made estimates of the topography of Jackass Creek beach, a separation bar located on river left, by (1) locating the point of sand-and-talus contact at several locations, (2) overlaying matched photographs from different years and determining those rocks that have been exposed during the intervening period, and (3) estimating the overall shape of the bar. These data were compiled and topographic maps were developed for each year where photographic coverage was sufficient. These maps were digitized into the same Arc-Info (geographic information system) coverage as were survey data from the period 1985-91. Geographic information system software was used to determine the volume differences between different years.

Long-Term Sediment Storage Computation

An order-of-magnitude sediment budget for the reach between Lees Ferry and the Grand Canyon gage was computed using published sand load rating relations (Randle and Pemberton, 1987). The sediment budget equation for this reach is:

$$Q_{SCR/LF} + Q_{SPR} + Q_{SLCR} = Q_{SCRGC} + \Delta S \quad (1)$$

where, Q_s = sediment discharge;

ΔS = change in storage;

CR/LF = Colorado River at Lees Ferry (station number 09380000);

PR = Paria River at Lees Ferry (station number 09382000);

LCR = Little Colorado River near Cameron (station number 09402000); and,

CR/GC = Colorado River near Grand Canyon (station number 09402500).

This budget was calculated by multiplying mean daily discharge data for each gage for each day between October 1, 1962 - September 30, 1989, by the appropriate sediment rating relation. Annual values of transported load were computed for each station, and annual

change in storage computed as the residual from these computed values (Appendix C). Equation (1) yields an order-of-magnitude estimate of cumulative sediment storage because of several errors. Although Randle and Pemberton (1987) argued that there is no evidence for shifts in rating relations, it is reasonable to expect that transport relations respond to bed aggradation. Continuity principles dictate that as cross-section area decreases due to bed aggradation, mean-section velocity, and sediment-transport, will increase if there is no great change in water-surface elevation. Also, actual data that are used to calculate transport relations have an order-of-magnitude error, and the significance of these errors is magnified by the exponential nature of the sediment-transport relation.

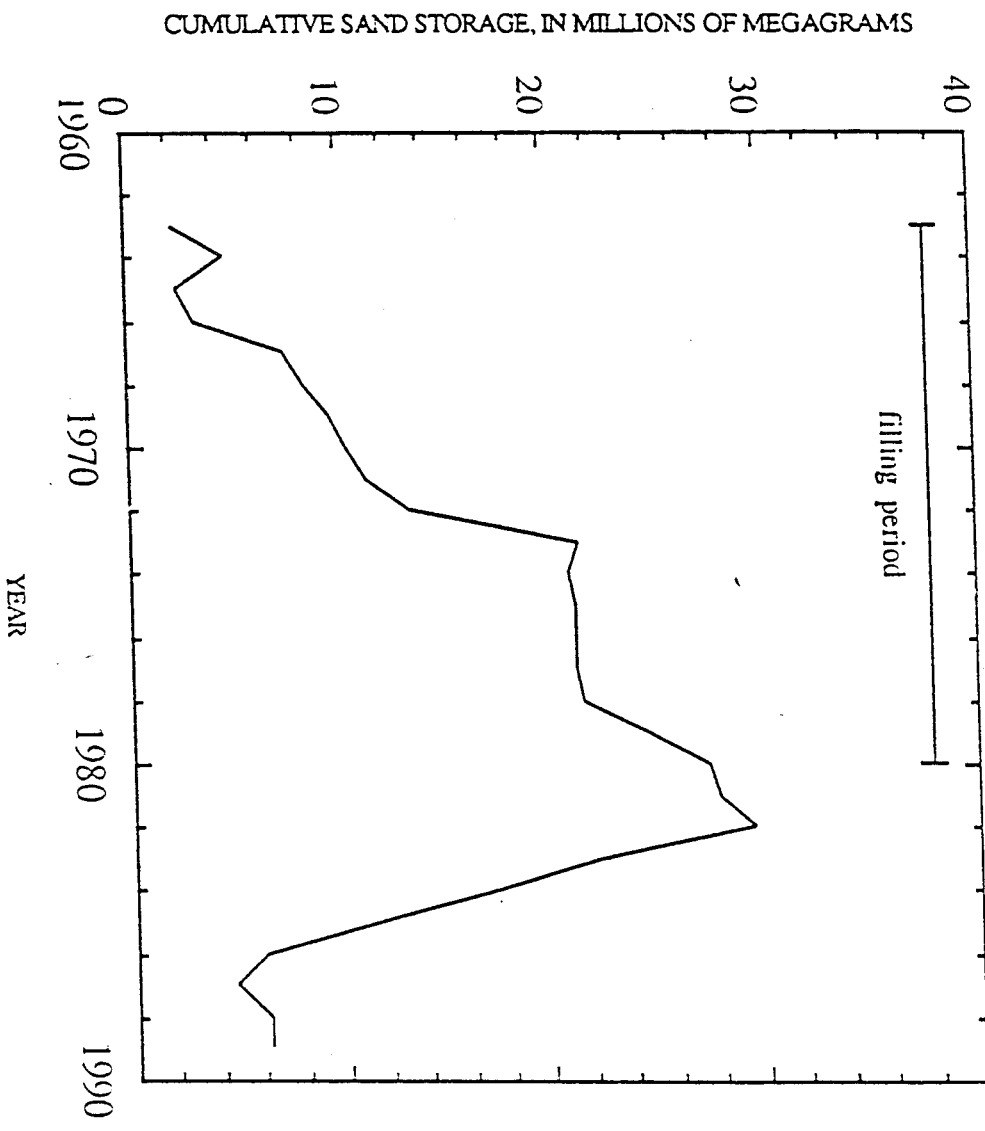
RESULTS

Changes in Sediment Storage

Figure 2 shows that cumulative storage steadily increased between 1966-73 and 1978-82 during the period when reservoir releases were almost always less than powerplant capacity. Between 1973-78, there was little accumulation even though reservoir releases were little different from other years of the 1966-82 period. The low accumulation rates are due to low tributary inflows during those years. High peak discharges between 1983-86 removed about the same mass of sediment as had previously accumulated.

The total range in change in sediment storage was about 30 million Mg, the same order of magnitude value as the 38-million-Mg estimate of the total mass of sand stored on the bed and in eddies of the Colorado River in the same reach in 1984 (U. S. Department of the Interior, 1988). The latter estimate was made by Schmidt (1987, U. S. Geological Survey, written commun.) and is included as Appendix D. This estimate is based on analysis of Wilson's (1984) interpretation of side-scan sonar data and estimates of the proportion of sand in each of Wilson's mapping units. The near equality of the two estimates may be coincidental, but the values are certainly of the same order of magnitude. Thus, the volume of sediment stored in the river between 1965-82 may have doubled the volume of sand that was in storage in the channel at the time of closure of Glen Canyon Dam. The sequence of high annual peak floods between 1983-86 effectively removed this accumulated mass.

Figure 2 - Cumulative sand storage in Colorado River near Grand Canyon following closure of Glen Canyon Dam



Bed Response

Clark (1992) measured bed-elevation change of 8 pools between river miles 52-56 between 1975-84. He determined that the average change in pool depth was -2.4 m; 7 of the 8 pools experienced some degradation. The difference between 1974 and 1984 bed elevation is significant at the 95-percent confidence level (paired t-test, $p = 0.049$, $n = 8$). These results are consistent with the unpublished results of S. Rathburn (1991, U. S. Geological Survey, Tucson, written commun.), who measured pool elevation changes in two reaches -- between river miles 62.4 - 64.0 and between 85.0 - 87.5. She showed that the average pool bed-elevation change was -3.5 m and -1.5 m, respectively.

Changes in Alluvial Deposits

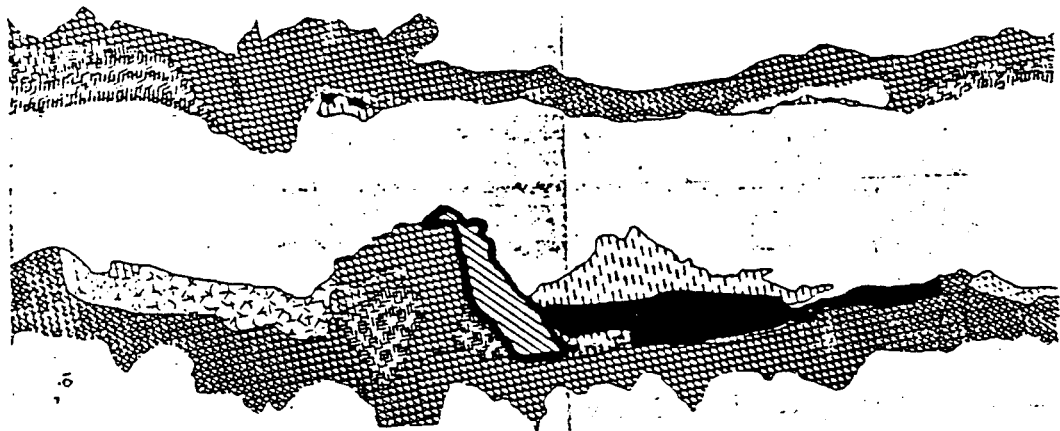
Reach-Scale Changes

Clark (1992) mapped the surficial geology of the river corridor between river miles 52-56. Figure 3 shows an example of this mapping for the reach between river miles 55 - 56; other maps are included as Appendix E. Descriptions and photographs of each mapping unit are included in Appendix A. Table 3 lists the area of different mapping units in reaches mapped by Clark (1992) and in the Little Colorado River - Unkar Rapids reach.

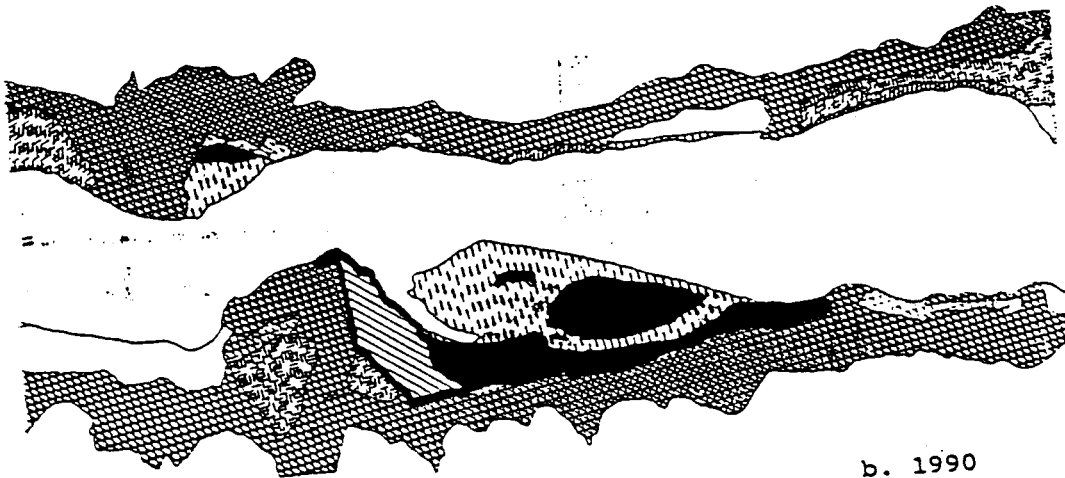
Figure 4 shows the area of different types of alluvial deposits between river miles 55-56 (Nankoweap reach, map 4) in different years and at different discharges. Best-fit linear regression relations were computed for these data, and residual values from these relations were calculated -- years when the surface area of sand was greater or less than average long-term values.

Time-series plots of residuals for statistically-significant relations show that the area of sand bars in this reach increased at least to 1980, and probably to spring 1982 (Fig. 5). During the period of high annual peak discharge between 1983-86, sand bar area decreased greatly, but area increased between 1987-89. Sand-bar area decreased from 1989-90.

Data for the Nankoweap reach also indicate that (1) reattachment bars have been subject to a greater range of aggradation and degradation than separation bars or margin deposits, (2) that all deposits increased in area from 1965 - 80, (3) that reattachment bars decreased in area during the period of high discharges from 1983 - 86, (4) that the decrease in area was greater for the period of high discharges in 1985 and 1986 than for the period of high discharges in 1983 and 1984, and (5) that the area of reattachment bars has increased since the cessation of high discharges in 1986.



a. 1965



b. 1990

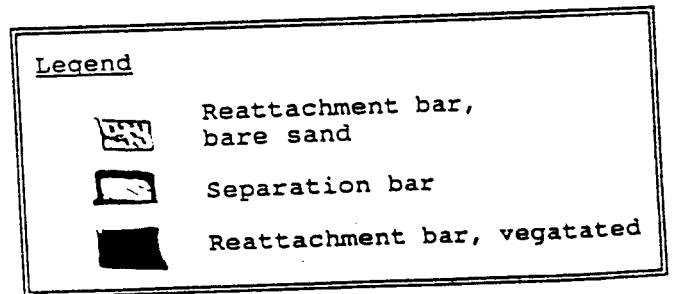


Figure 3 Example of surficial geologic map of Colorado River near 55-mile bar. River flows from left to right.
 A. May 14, 1965, discharge 792 m³/s.
 B. June 3, 1990, discharge 141.5 m³/s.

Table 3. -- Area of sand exposed in indicated years in study reaches

Year	Discharge, in cubic meters per second	Area of sand exposed in indicated year, in cubic meters									
		Reattachment bars		Separation bars		Margin deposits		All sand bars		Total	
		Map 2	Map 4	Map 2	Map 4	Map 2	Map 4	Map 2	Map 4	Map 2	Map 4
1965.4	792	13731	24379	4709	5117	9826	3179	10470	29816	39866	69782
1973.5	210	19740	39046	5673	5052	10725	4501	13889	34629	57987	92616
1980.5	767	16628	31056	5470	6069	11539	3879	12946	26953	50071	77024
1983.4	141.5	31395	43890	9565	6535	16100	6895	13599	72211	64024	136235
1984.8	979										
1985.4	239										
1987.4	477	28206		6508	6415	12923	3484	18435	64363	43102	128579
1988.4	141.5	33715	42227	6154	5925	12078	3499	16137	53921	64216	110052
1989.8	141.5	29258	36741								
1990.4	141.5										

Year	Discharge, in cubic meters per second	Little Colorado River - Urkar Rapids Reach											
		Reattachment Bars		Submerged		Total above water		Separation Bars		Undifferentiated eddy bars		Margin Deposits	
		Active	Inactive	Submerged	Total above water	Active	Inactive	Active	Inactive	Active	Inactive	Active	Inactive
1965.4	792	4102	646	4748	4748	1369	6081	1185	184	12208	1445	0	1445
1973.5	210	7878	2441	10119	10119	3547	7639	516	885	19139	805	0	805
1980.5	767												
1983.4	141.5	9208	1070	10276	12913	3636	12850	2006	752	25884	1583	0	1583
1984.8	979												
1985.4	239	5295	1214	6509	6509	3608	7373	1310	616	15808	1055	0	1055
1987.4	477	4811	1198	6009	6194	3411	6600	1492	0	13901	1176	0	1176
1988.4	141.5	12387	1234	13621	20366	3836	10845	1758	527	28751	1574	0	1574
1989.8	141.5	6810	1285	10095	10095	5176	10414	1334	707	22550	1412	0	1412
1990.4	141.5												
		MAP 2		888	888					888	4162		4162
1985.4	792	615	253	868	868					868	4162		4162
1973.5	210												
1980.5	767												
1983.4	141.5	357	984	1321	1321					1321	3133		3133
1984.8	979												
1985.4	239	434	985	1429	1429					1429	5216	2283	7409
1987.4	477		1338	1033	2371					1033	4214	2448	6800
1988.4	141.5												
1989.8	141.5	622	1197	1819	2853					1819	3642	4579	8221
1990.4	141.5												
		MAP 2		888	888					888	4162		4162
1985.4	792	615	253	868	868					868	4162		4162
1973.5	210												
1980.5	767												
1983.4	141.5	357	984	1321	1321					1321	3133		3133
1984.8	979												
1985.4	239	434	985	1429	1429					1429	5216	2283	7409
1987.4	477		1338	1033	2371					1033	4214	2448	6800
1988.4	141.5												
1989.8	141.5	622	1197	1819	2853					1819	3642	4579	8221
1990.4	141.5												
		MAP 2		888	888					888	4162		4162
1985.4	792	615	253	868	868					868	4162		4162
1973.5	210												
1980.5	767												
1983.4	141.5	357	984	1321	1321					1321	3133		3133
1984.8	979												
1985.4	239	434	985	1429	1429					1429	5216	2283	7409
1987.4	477		1338	1033	2371					1033	4214	2448	6800
1988.4	141.5												
1989.8	141.5	622	1197	1819	2853					1819	3642	4579	8221
1990.4	141.5												
		MAP 2		888	888					888	4162		4162
1985.4	792	615	253	868	868					868	4162		4162
1973.5	210												
1980.5	767												
1983.4	141.5	357	984	1321	1321					1321	3133		3133
1984.8	979												
1985.4	239	434	985	1429	1429					1429	5216	2283	7409
1987.4	477		1338	1033	2371					1033	4214	2448	6800
1988.4	141.5												
1989.8	141.5	622	1197	1819	2853					1819	3642	4579	8221
1990.4	141.5												
		MAP 2		888	888					888	4162		4162
1985.4	792	615	253	868	868					868	4162		4162
1973.5	210												
1980.5	767												
1983.4	141.5	357	984	1321	1321					1321	3133		3133
1984.8	979												
1985.4	239	434	985	1429	1429					1429	5216	2283	7409
1987.4	477		1338	1033	2371					1033	4214	2448	6800
1988.4	141.5												
1989.8	141.5	622	1197	1819	2853					1819	3642	4579	8221
1990.4	141.5												
		MAP 2		888	888					888	4162		4162
1985.4	792	615	253	868	868					868	4162		4162
1973.5	210												
1980.5	767												
1983.4	141.5	357	984	1321	1321					1321	3133		3133
1984.8	979												
1985.4	239	434	985	1429	1429					1429	5216	2283	7409
1987.4	477		1338	1033	2371					1033	4214	2448	6800
1988.4	141.5												
1989.8	141.5	622	1197	1819	2853					1819	3642	4579	8221
1990.4	141.5												
		MAP 2		888	888					888	4162		4162

Figure 4. -- Discharge and area of exposed deposits in Nankoweap Reach, map 4 (55-56).

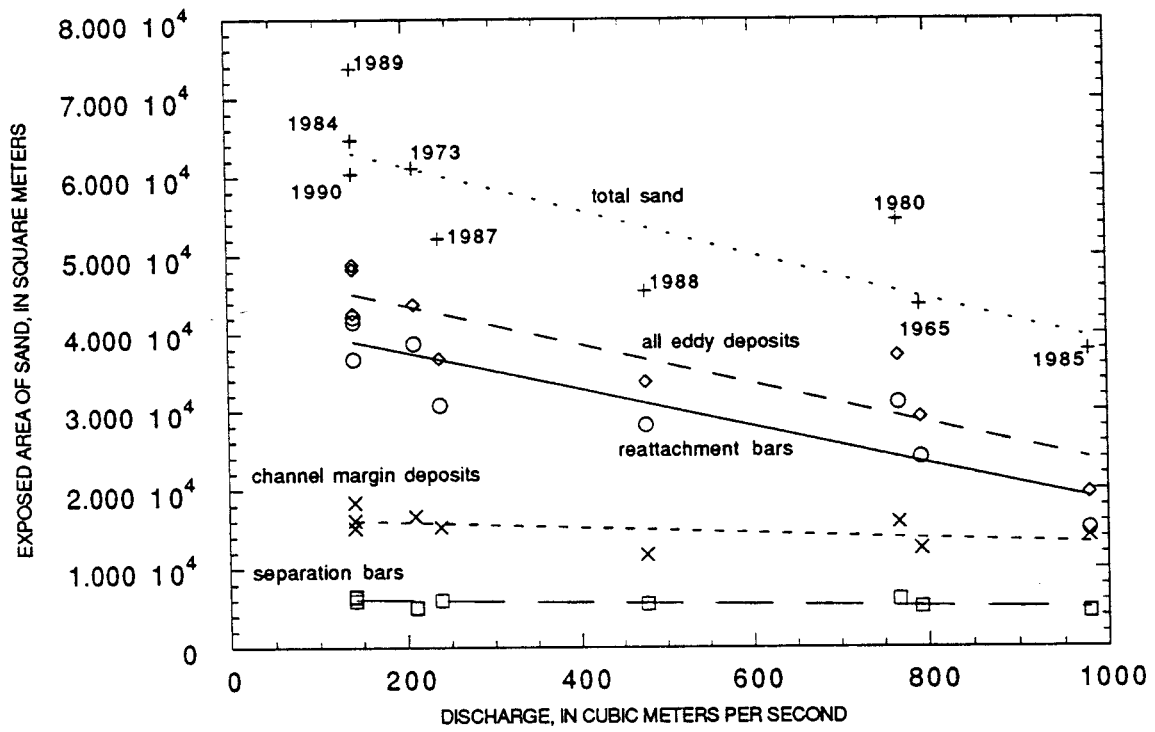
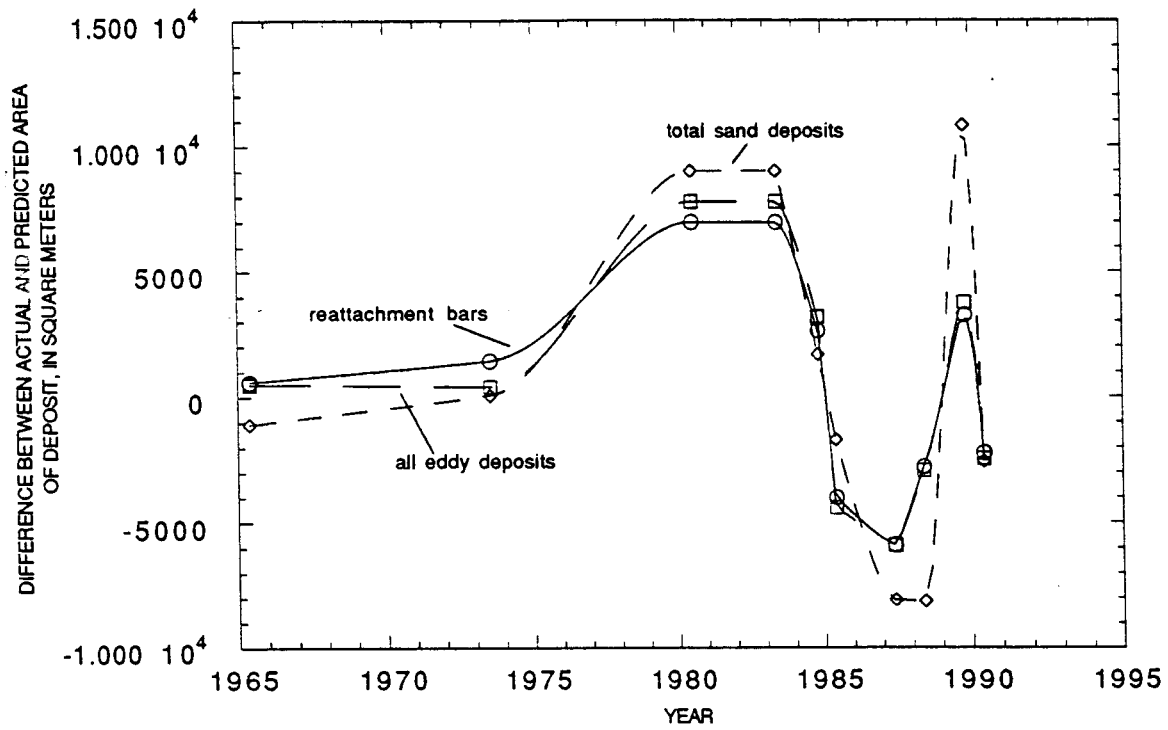


Figure 5. -- Time series change in residuals for Nankoweap reach, map 4 (miles 55 - 56).



It was not possible to obtain all years of aerial photography for the Little Colorado - Unkar Rapids reach, so best-fit linear regression relations for this reach can not be expected to be similar to those of the Nankoweap reach, even if both reaches behaved similarly. In order to overcome this limitation, area values for only 1965 and 1973 were used to compute regression relations for both reaches (Fig. 6); residuals were computed from these two-data-point relations and time-series plots were plotted (Fig. 7). The implicit assumption in this approach is that the style of bar change between 1965 and 1973 was similar between the two study reaches, and that residuals could validly be calculated from the relation, despite the fact that some other data points extend beyond the range of the 1965-73 relations.

These data show that the behavior of the downstream study reach was similar to the behavior of the Nankoweap reach. Sand-bar area in 1987 and 1988 was less than it had been in the 1965-73 period; sand-bar area also increased between 1987-88. Sand-bar area in 1989 and 1990 was greater than it had been in 1987-88. In both study reaches, residuals in 1990 were less than those calculated for 1989, reflecting the dynamic nature of the lowest-elevation parts of these bars.

Site-Specific Changes

Long-term change near Badger Creek Rapids

Oblique photographs of Badger Creek Rapids have been intermittently taken since 1889 (Table 4). The distribution of alluvial deposits near this rapid, and the patterns of flow at discharges between 140-2800 m³/s are discussed by Schmidt (1990). The difference in volume of the bar in different years was evaluated in two ways. Topographic changes were estimated for (1) a fixed area of the bar, mostly above the stage associated with discharges of about 710 m³/s and for which coverage was available in all years, and (2) variable areas of overlap between successive surveys. In the latter case, a relation was developed between area of overlapping coverage and volume change during that period, and residuals were calculated. Maps developed for these comparisons are included as Appendix F.

Figure 8 shows time-series plots of topographic change for the upper-elevation part of the bar (Fig. 8A) and for the entire bar (Fig. 8B). Figure 9 shows the elevation change at a fixed location on the upper part of the bar, and for which there is supplemental data. Figure 10 is a matched pair of photographs of the bar, showing these measurement sites. Also shown on Figure 8 are data points surveyed during the period evaluated by Beus and

Figure 6. -- Discharge and exposed area of sand in two reaches.

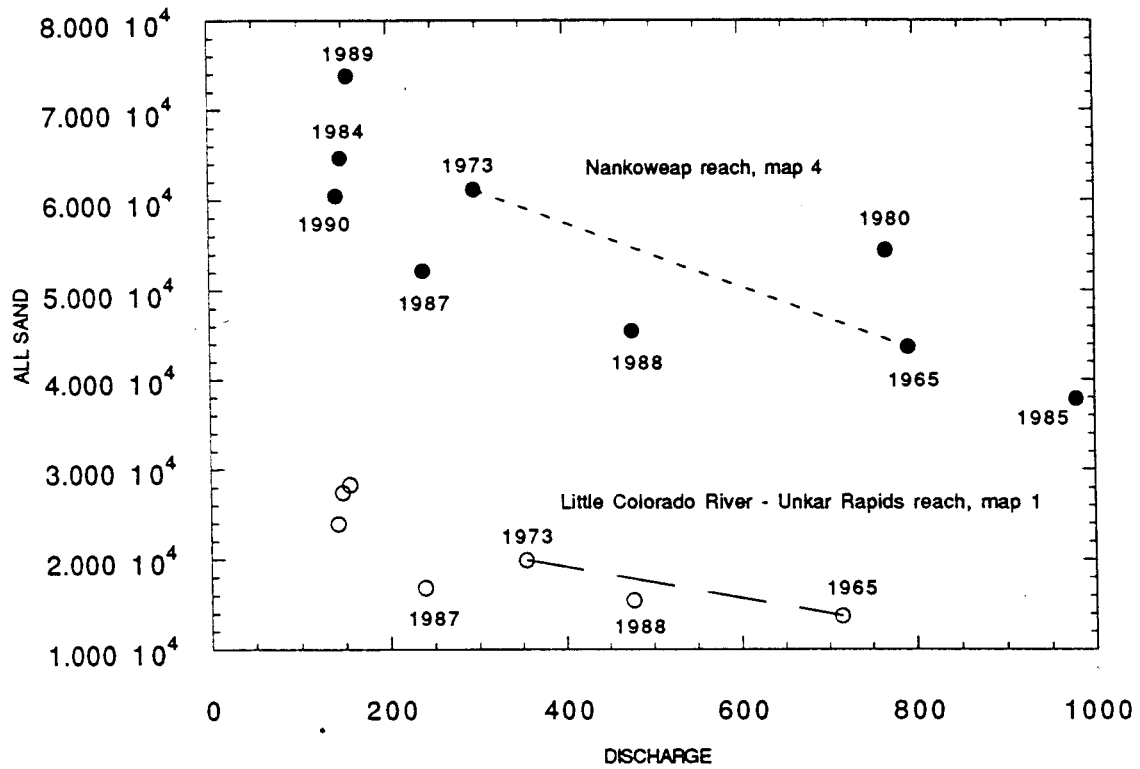


Figure 7. -- Time series of change in residuals for two study reaches.

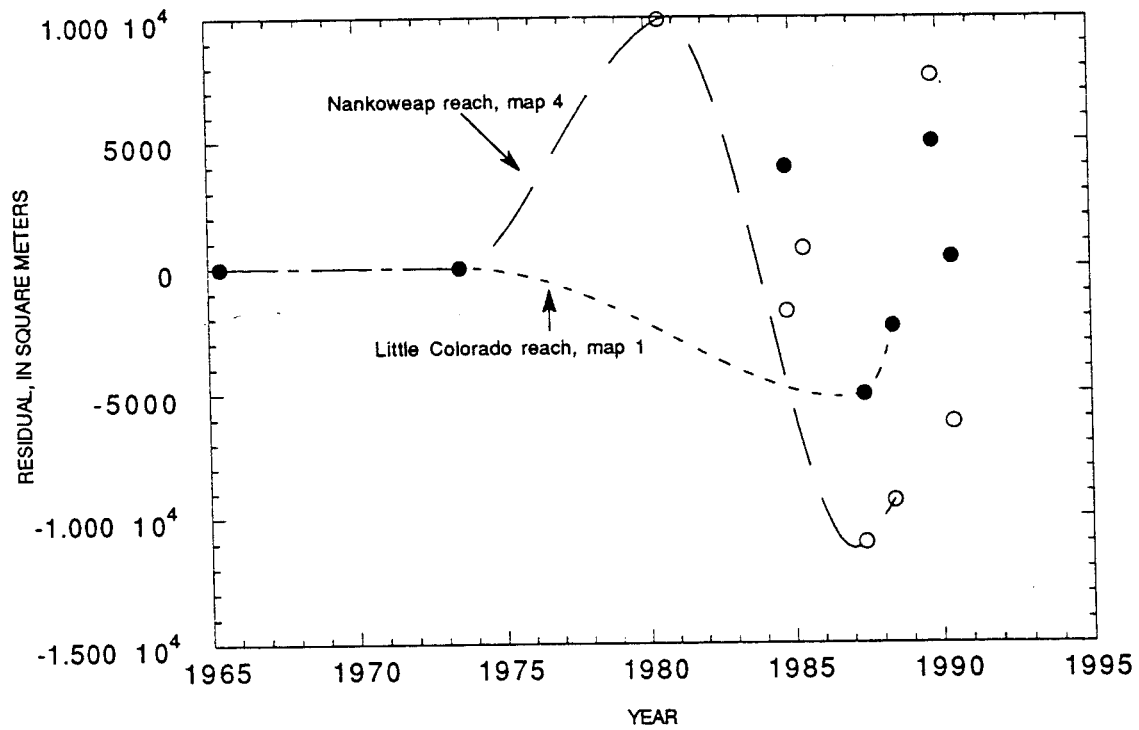


Table 4. List of photographs taken of Badger Creek Rapid, debris fans at the mouths of Jackass and Badger Canyons, and sand bars below the rapid (R.H. Webb, 1992, written commun.)

Year	Date	Photographer	Original number	Stake number	Side ¹	Dir- ection ²	Subject ³	Discharge ⁴ (ft ³ /s)
1889	Dec 28	Nims	277	1406a	R	US	R,DF,SB	~
1889	Dec 28	Nims	278	1403	L	US	R,DF	~
1897	Dec 1?	James	opp. p. 238 ⁵	2353	R	US	R,DF	
1909	Oct 28	Cogswell	plate 73A	2351	R	US	R,DF	
1911	Nov 8	Kolb	NAU 568- 1069	1401	R	US	R,DF	
1914	Dec 15?	Tadje		2354	R	US	SB, DF	
1923	Jul 22?	Freeman	16	1397	RR	DS	R,DF,SB	31,600
1923	Jul 22	LaRue	334	2057	RR	DS	R,DF,SB	31,600
1923	Aug 1	Kolb?	NAU 263- 3423	1404	L	US	R,DF	25,200
1927	Jul 18	Eddy	opp. p. 164 ⁶	1405a	L	AC	R,DF	25,100
1927	Dec 4	Eddy	--	1405b	L	AC	R,DF	9,730
1947	Jul 12	Marston	477 COLOR 1013	2019	L	US	SB,R	35,800
1952	Jun 19	Leding	NPS	705b	LR	DS	R,DF,SB	98,800
1952	Jun 19	Leding	NPS 2296	711	L	DS	SB	98,800
1952	Jun 19	Leding	NPS 2298	712a	L	AC	R,DF	98,800
1952	Jun 19	Leding	NPS 2299	712b	L	AC	R,DF	98,800
1952	Jul 11	Belknap	Vol 43(80)	2016	LR	AC	DF	34,000
1952	Jul 12	Belknap	Vol 43(88)	2048	LR	DS	R,DF,SB	31,400
1952	Jul 12	Belknap	Vol 43(90)	2017	LR	DS	R,DF,SB	31,400
1952	Jul 12	Belknap	Vol 43(91)	2017	LR	DS	R,DF,SB	31,400
1952	Sep 21	Leding	NPS 2333	2059	LR	DS	R,DF,SB	7,050
1954	Jan 2	Reilly	R 44-1	705b	LR	DS	R,DF,SB	4,440
1955	Mar 21	Reilly	L 12-00	----	AR	AC	R,DF,SB	10,400
1955	Sep 13	Marston	559 MECN 8.7	2012	LR	DS	R,DF,SB	3,140
1956	May 31	Atherton	Vol 43(103)	2064	LR	AC	R,DF,SB	55,400
1956	Jun 17	Marston	566 MECN 8.7	2013	LR	AC	R,DF,SB	40,600
1956	Jun 19	Rowlands	Vol 43(105)	2062	LR	DS	R,DF,SB	35,200
1956	Jul 1?	Nichols	--	2060	LR	AC	R,DF	~14,000
1956	Jul 1?	Nichols	--	2058	LR	DS	SB	~14,000
1957	May 6	Reilly	L 30-30	----	AR	AC	R,DF,SB	17,000
1957	May 6	Reilly	L 30-31	----	AR	AC	R,DF,SB	17,000
1957	Oct 27	Butchart	5710 MECN 8.8	----	AL	DS	R,DF,SB	12,900
1958	Oct 4	Reilly	L 42-17	----	AR	AC	R,DF,SB	5,700
1959	Jun 2	Marston	596 MECN 8.8	2015	LR	DS	R,DF,SB	19,300
1959	Aug 28	Marston	598 MECN 8.28.2.2	2014	LR	DS	R,DF,SB	7,010

1959	Aug 28	Marston	598 MECN 8.28.12	1787	L	AC	R,DF	7,010
1959	Aug 28	Marston	598 MECN 8.28.3	2352	L	AC	R,DF,SB	7,010
1959	Sep 26	Marston	599 MECN 8.11	1788	L	AC	R,DF,SB	7,010
1962	Jun 24	Reilly	L 56-02	2063	LR	DS	R,DF,SB	49,400
1963	Jun 17	Reilly	L 66-15	2061a	LR	AC	R,DF,SB	2,520
1963	Jun 17	Reilly	R 78-01	2061b	LR	AC	R,DF,SB	2,520
1964	Oct 31	Belknap	Koda 13	- - - -	AL	AC	R,DF,SB	
1965	May 14	USGS		- - - -	AV	- -	R,DF,SB	26,700
1972	Aug 21	Turner	NPS	705b	LR	DS	R,DF,SB	
1972	Aug 22	Turner	NPS 2296	711	L	DS	SB	
1972	Aug 22	Turner	NPS 2298	712	L	AC	R,DF	
1973	Jun 16	USGS		- - - -	AV	- -	R,DF,SB	3-14,000
1973	Jul 8	Weeden	I-5	2018a	L	AC	SB	
1973	Jul 8	Weeden	I-4	2018b	L	US	SB,DF	
1973	Jul 8	Weeden	I-7	1786a	R	US	R,DF,SB	
1973	Jul 8	Weeden	I-8	1786b	R	AC	SB	
1974		Howard	785-4	2355a	L	AC	SB	
1974		Howard	785-5	2355b	L	AC	SB	
1974		Howard	785-6	2355c	L	AC	SB	
1974		Howard	785-9	2356	L	AC	SB	
1974		Howard	786-1	2357	R	AC	SB	
1977?	- - - -	Blaustein	plate 10	2065	LR	DS	R,DF,SB	
1982	Oct 5	Turner	NPS 2298	712a	L	AC	R,DF	
1983	Oct 17	Turner	NPS 2296	711	L	DS	SB	
1983	Oct 17	Turner	NPS 2298	712a	L	AC	R,DF	
1984	Aug 12	Turner	NPS 2296	711	L	DS	SB	
1984	Oct 21	GOES	1-193	- - - -	AV	- -	R,DF,SB	

-
1. AV -- vertical aerial photography; AL - oblique aerial from left; AR - oblique aerial from right; LR - left rim; RR - right rim; L - river left; R - river right.
 2. US -- upstream; DS - downstream; AC - across the river; UC -- up tributary channel or away from the river.
 3. R - rapid, DF - debris fan(s), SB - sand bar(s).
 4. For photographs taken before 1921, the discharge is estimated from known stage-discharge relations at Badger Rapid. For photographs taken between 1921 and 1963, discharge is estimated from daily discharge records of the Colorado River at Lees Ferry. After 1963, discharge is estimated from known stage-discharge relations at Badger Creek Rapid. These estimates are perhaps accurate to $\pm 1,000$ ft³/s.
 5. James, G.W., 1900, In and around the Grand Canyon: Boston, MA, Little, Crown, and Company, 346 p.
 6. Eddy, C., 1929, Down the world's most dangerous river: New York, Frederick A. Stokes Company, 293 p.
 7. Blaustein, J., 1977, The hidden canyon, a river journey: New York, Penguin Books, 135 p.

Figure 8. -- Volume change at Jackass Creek camp. A. Average thickness of upper-elevation part of Jackass Beach, downstream from Badger Creek Rapids. B. Temporal change in residuals from post-1973 best-fit relation.

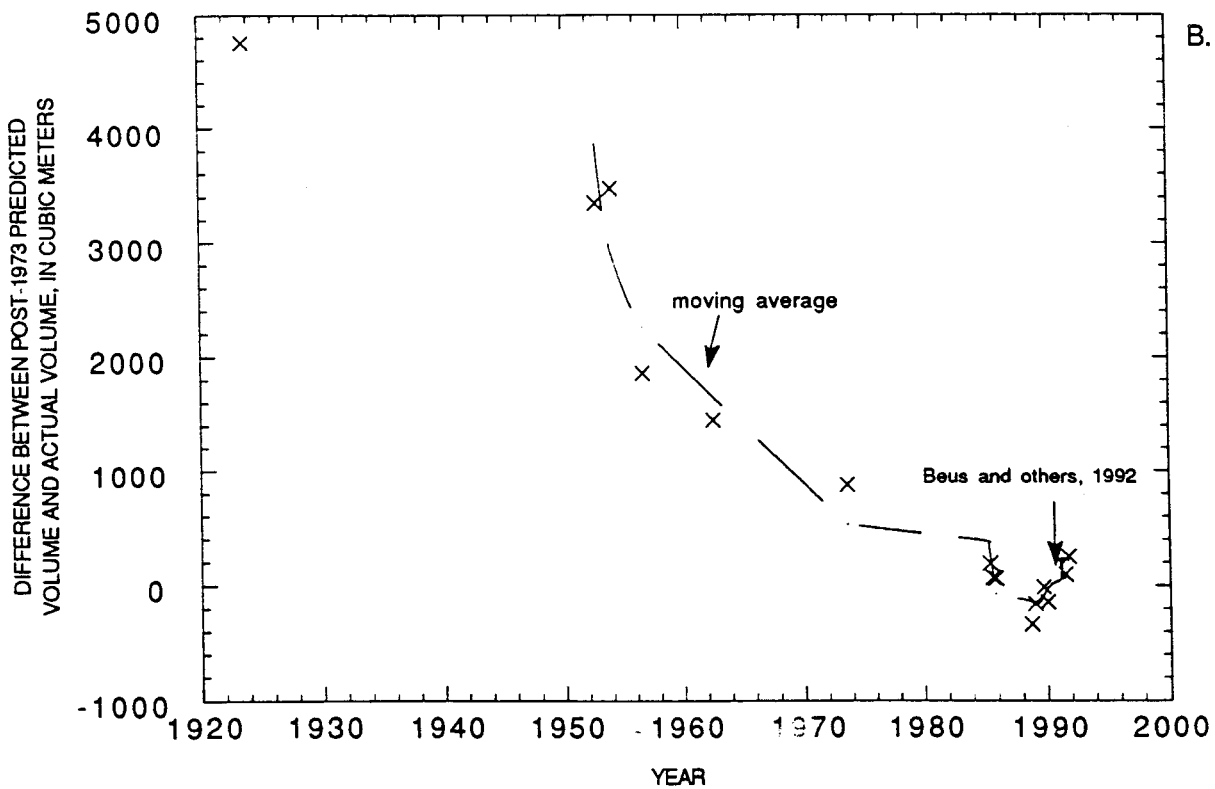
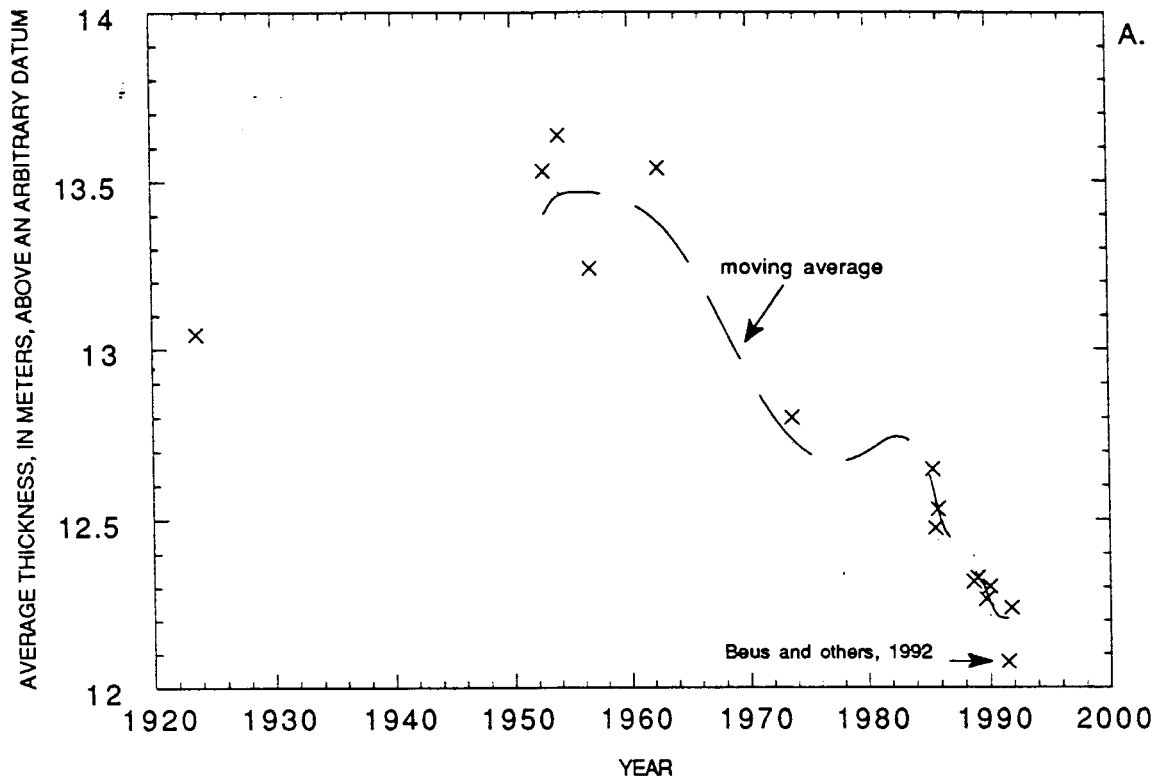


Figure 9. -- Elevation change at the turret rock, Jackass Beach downstream from Badger Creek Rapids.

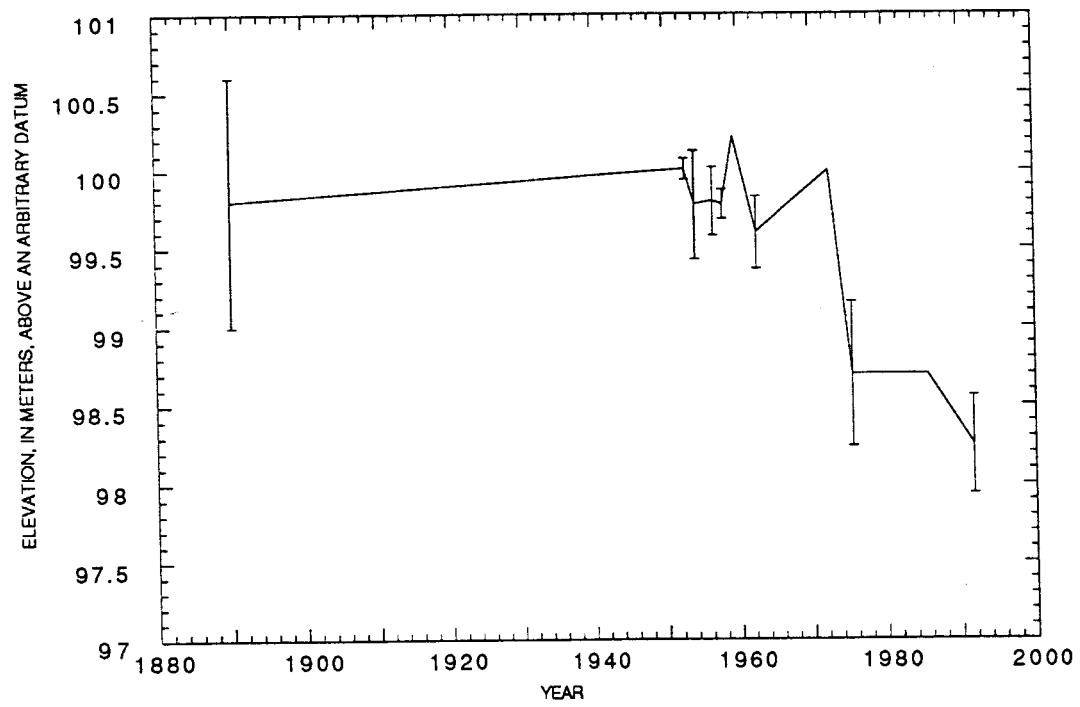
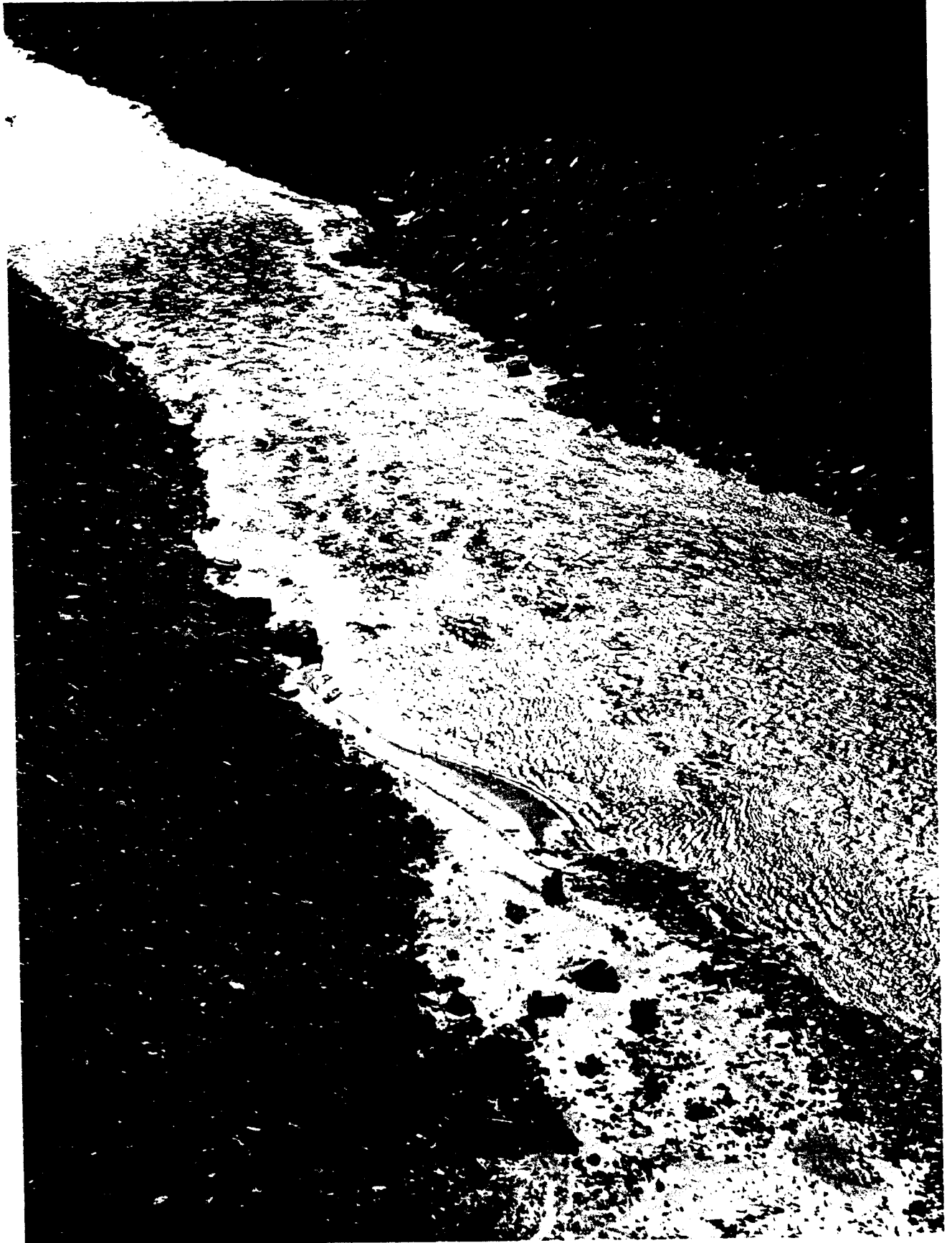


Figure 10. -- Camping beach at Jackass Creek, downstream from Badger Creek Rapids.
A. Photograph by T. Nichols, July 1956. B. Photograph by R. H. Webb,
October 5, 1991. Turret rock referred to in figure 9 is located in center of
lower part of photograph, to the left of the double-slabbed rock.

A.



B.



others (1992). The value shown in Figure 8A is outside the range of values measured between 1988-91. These differences are not real topographic changes because the upper-elevation part of the bar was never inundated during that period, and a subsequent measurement was similar to those that preceded the survey of Beus and others (1992). The differences between the volume estimate made from data provided by Beus and others (1992) and other available surveys is probably due to the fact that topographic contours by Beus and others (1992) were determined from software rather than field observation.

All figures show that there has been great change in the volume of sand stored since 1923, but that significant erosion occurred during the first 10 yrs of dam operations. Sand-bar volume changed little between 1923-54, and the upper-elevation part of the bar did not significantly change until after 1962. More than 0.5 m was eroded from this bar between 1962-73, and there was additional degradation, although of a lesser amount, from 1973-85. Since 1985, the bar has continued to degrade, but at a declining rate of change. The continuing decline in the volume of sand stored at high elevation (Fig. 8A) at this study site suggests that wind deflation is probably an important process at high elevation at this site. Some of the volume change in high-elevation parts of the bar has been compensated by increase in volume of low-elevation parts of the bar (Figure 8B). The total volume of the bar has changed little since 1985, and there has been a steady increase in the volume of low-elevation sand at this bar since September 1988.

Post-Dam Topographic Change at Grapevine Camp

Grapevine camp is a reattachment bar located at river mile 81.1 left, within Upper Granite Gorge, and located upstream from Grapevine Rapids (Fig. 1). It is the only large camp between Hance Rapids and Bright Angel Creek, and topographic changes have been monitored at this site since 1975. Kyle (1992) has discussed the geomorphic framework of this site, compiled all available profile data, and reported time-series changes along two profiles and area-weighted changes for the entire reattachment bar since 1975 (Fig. 11). Volume changes were computed at this site for those surveys between 1985-91 for which complete topographic maps were available, including one survey by Beus and others (1992) (Fig. 12). Although there are fewer data points in Figure 12, the trends are similar to those shown in Figure 11. Figure 13 shows topographic change along one of the profile lines between 1974-90.

Grapevine camp eroded between 1965-74, and that erosion was minimal between 1974-80. The greatest change at Grapevine occurred during the 1983 high discharges

Figure 11. -- Time sequence of volume changes at Grapevine Camp, river mile 81.1 left, determined from surveyed profiles.

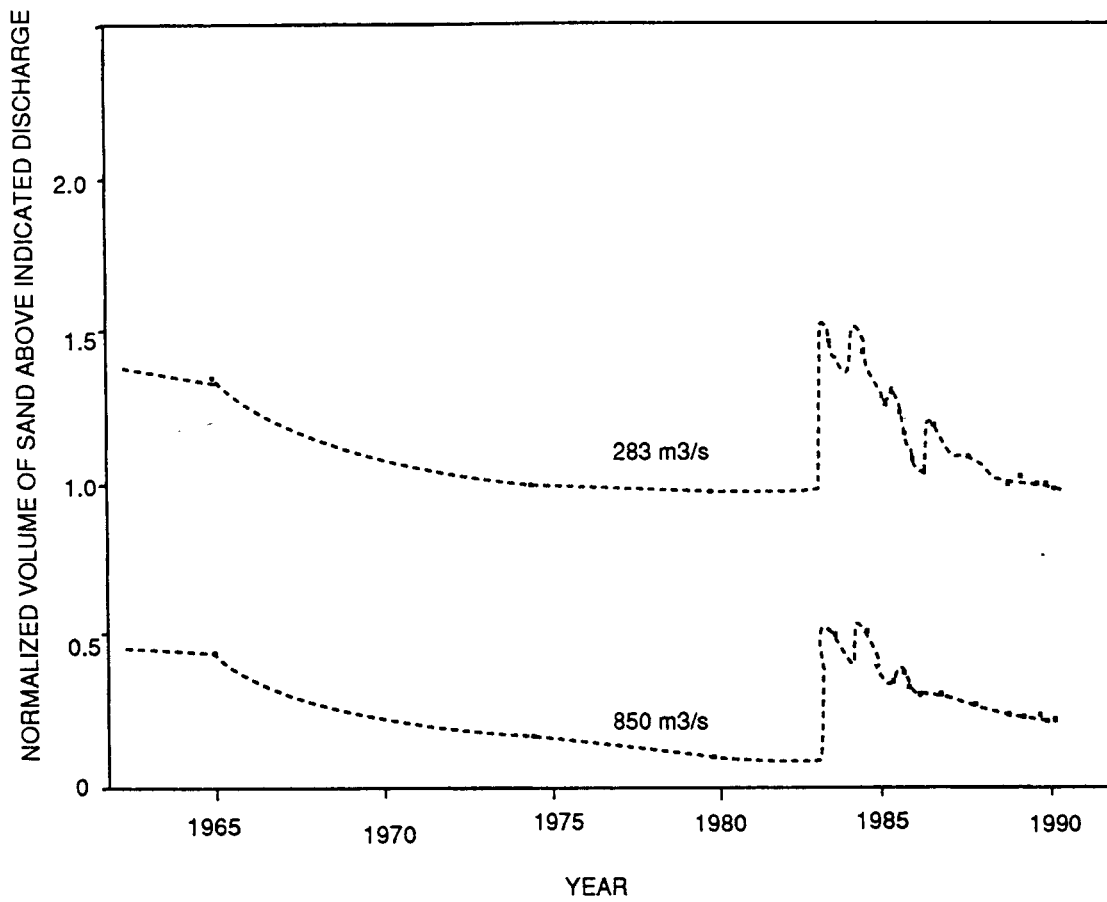


Figure 12. -- Change in volume of Grapevine Camp determined from comparison of topographic maps. A. Volume above an arbitrary datum associated with a discharge of 70 cubic meters per second. B. Change in average thickness.

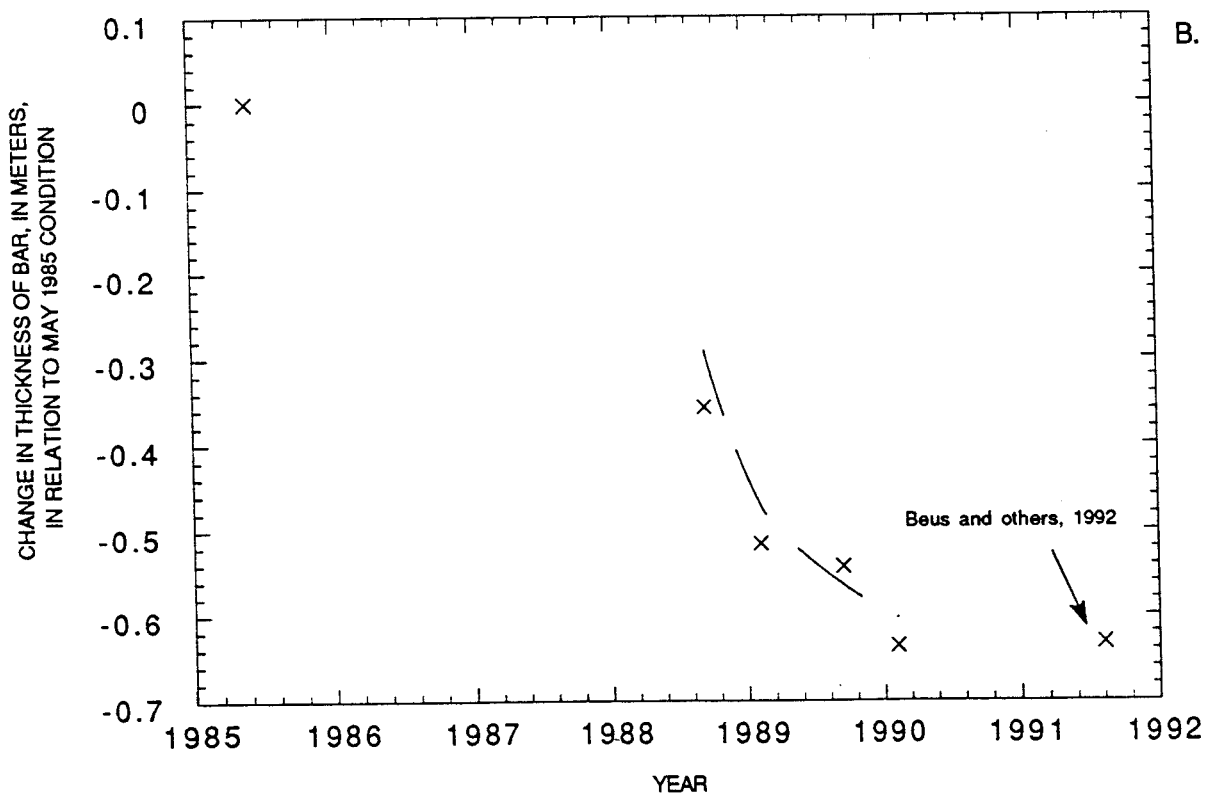
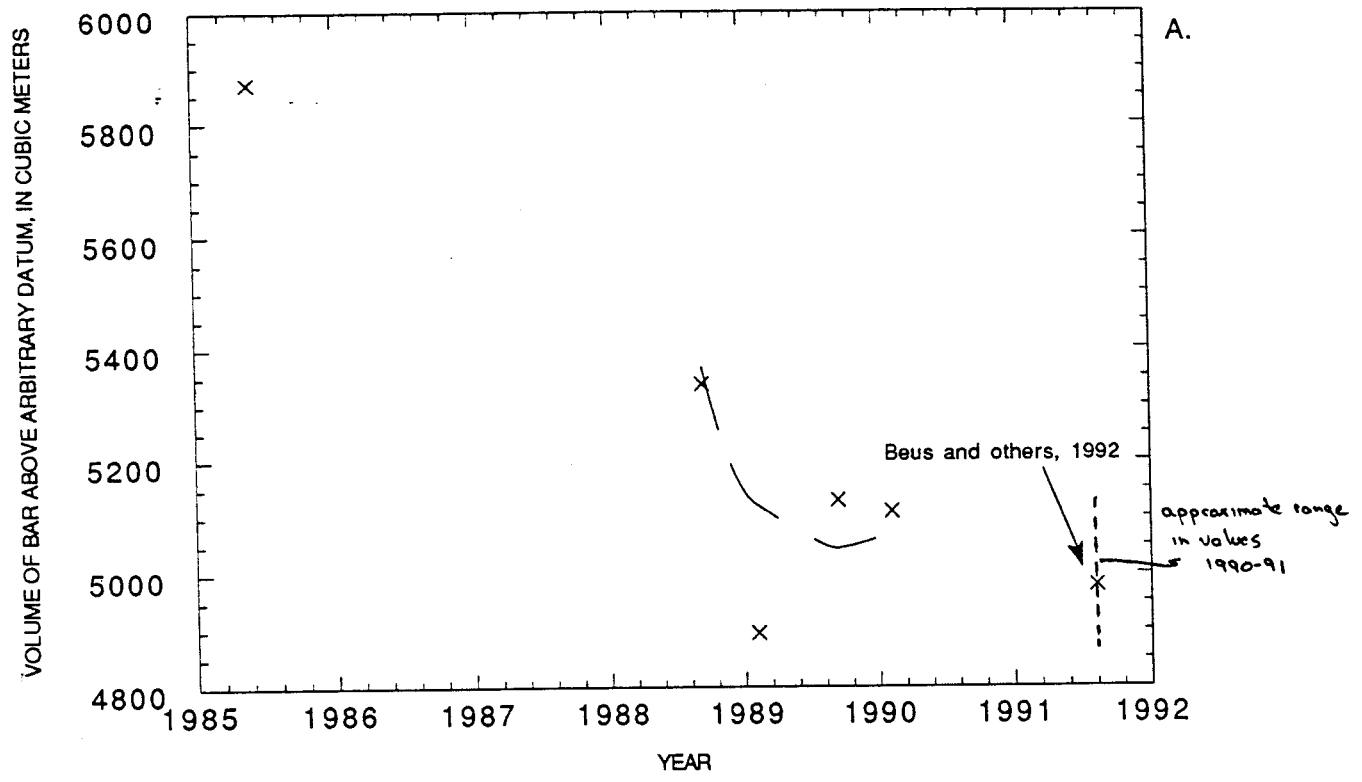
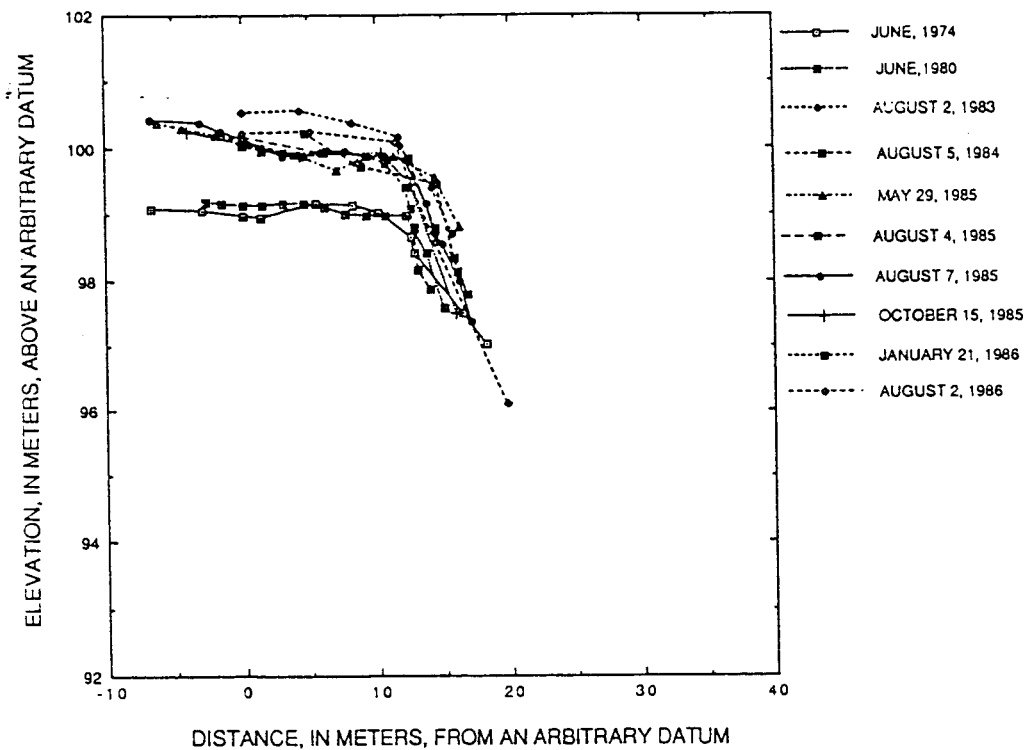
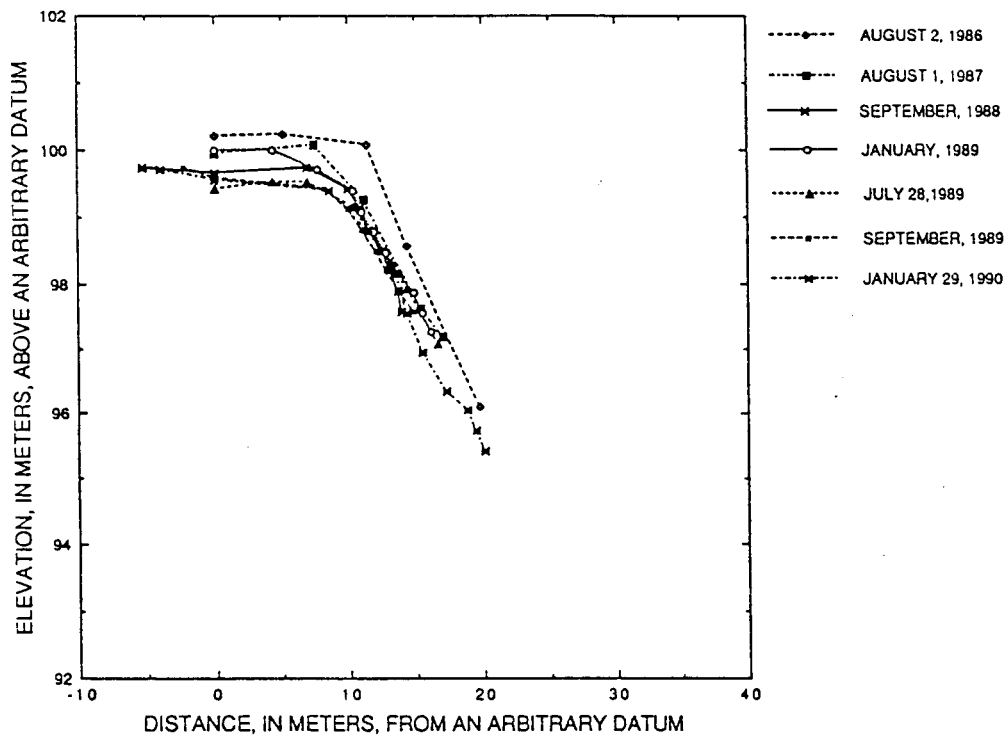


Figure 13. —

— Above Grapevine Rapids, profile 2, 1974-1986



— Above Grapevine Rapids, profile 2, 1986-1990



when about 3 m of sand aggraded on the upper bar surface; the bar reached a volume similar to that estimated for the site prior to completion of Glen Canyon Dam. Subsequent floods in 1984, 1985, and 1986 lowered parts of the upper bar surface, and the total volume of sand stored in the bar decreased during the 1985 flood. Subsequent change in volume of stored sediment at this site after recession of the 1986 peak flood has been by erosion of the steep face of the bar (fig. 12), probably by the seepage forces described by Bhudu (1992). The effect of this erosion has been to remove much of the sediment that had been deposited on the bar between 1983 - 86. Comparison of data for various years surveyed since 1975 indicates that Grapevine camp greatly resembles its topographic condition of the mid-1970's.

Although the topography of this bar in 1990 is similar to the condition in 1980, the rates of erosion in the few years preceding these two years is very different. During the period 1974-80, Kyle (1992) estimated that the erosion rate was less than 50 m³/yr, but the erosion rate between 1987-90 was about 150 m³/yr. Thus, Grapevine camp has returned to a condition similar to that which had existed in 1980, but the erosion rates associated with that topography are presently much greater.

Figure 13 also shows that the lateral extent of the bar changed remarkably little between 1974-90. The steep slope along the bar face, which includes the area defined as "hydrologically active" by Beus and others (1992), has varied over about a 5-m width during this period despite the occurrence of periods of high aggradation and degradation.

Other Study Sites

Time-series plots were developed at five other sites, and these data are summarized in figures 14-16. Although these data show substantial variability in bar behavior, two generalizations can be made that are consistent with those shown in the previous two study sites:

1. High annual peak discharges between 1983-86 caused significant change at each site.
2. Initially rapid, but temporally declining, rates of erosion occurred after recession from high discharges in 1986.

DISCUSSION

Bed-Elevation Changes

The results of Clark (1992) and Rathburn, in conjunction with other published results, indicate that bed scour during the 1983 high flow was typical of most pools,

Figure 14. -- Change in volume of reattachment bar above Cathedral Rapids.
 A. Volumes are computed above the arbitrary datum of 80 m for a fixed area. B. Change in average thickness.

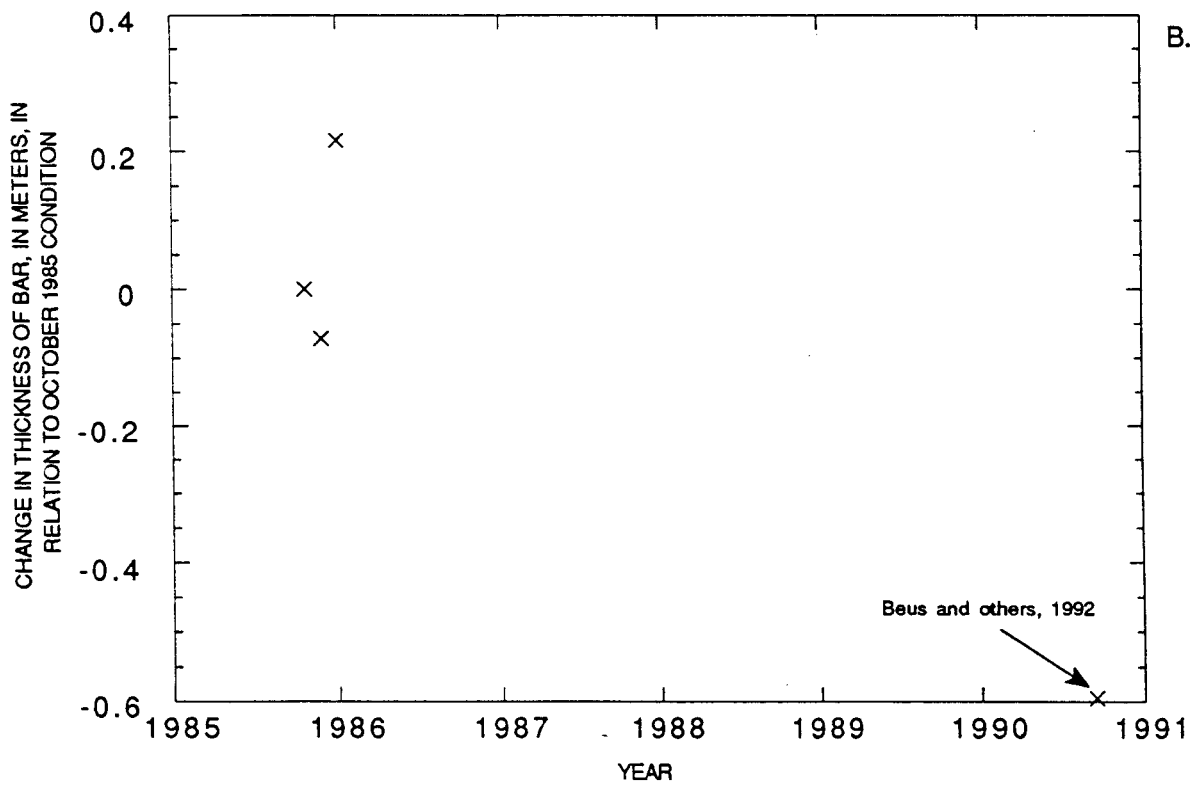
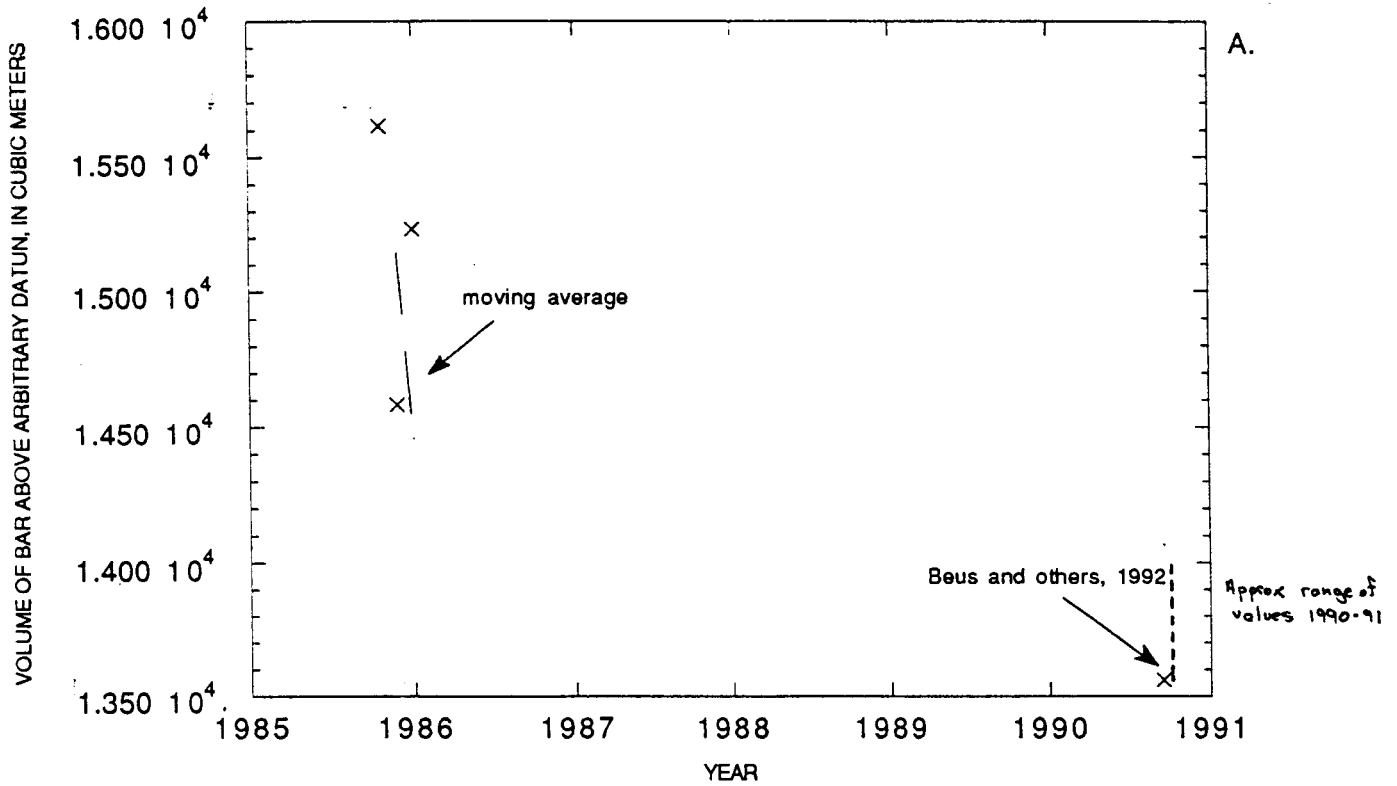


Figure 15. — Time series change of reattachment bars, Kyle (1992).

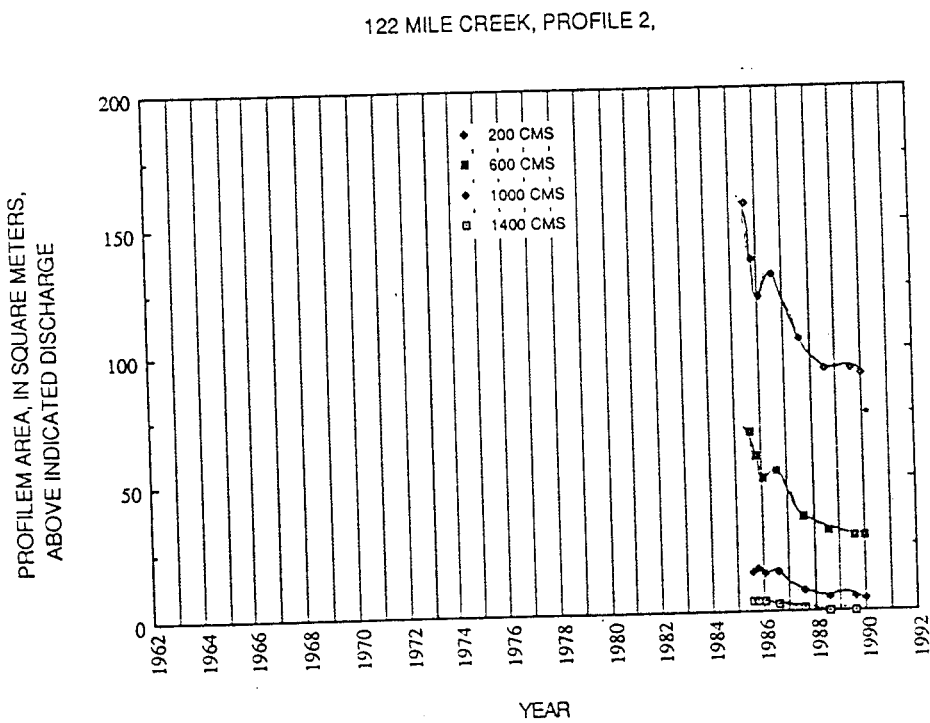
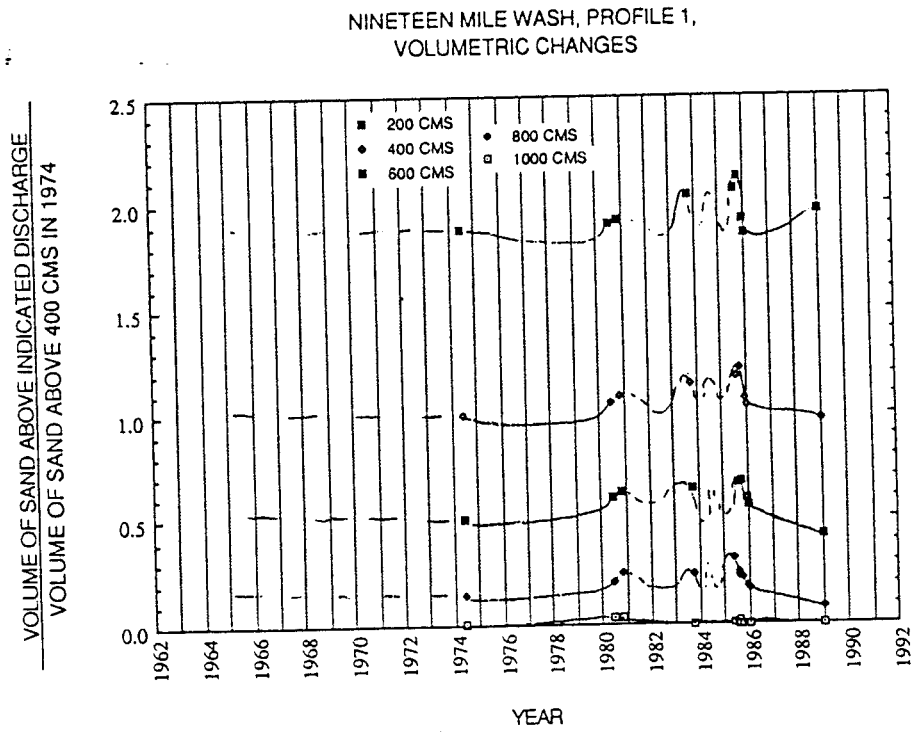
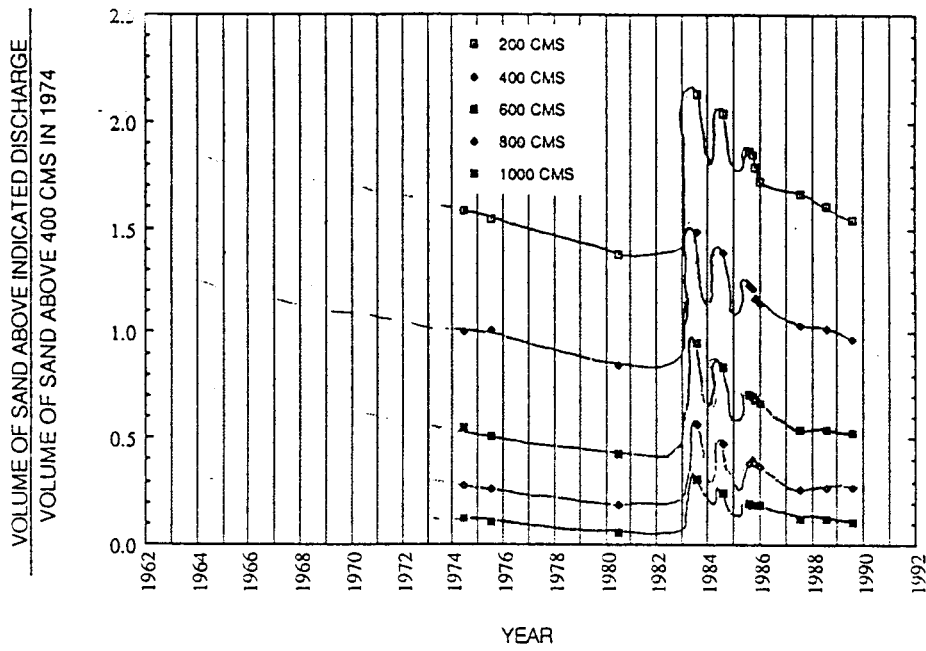
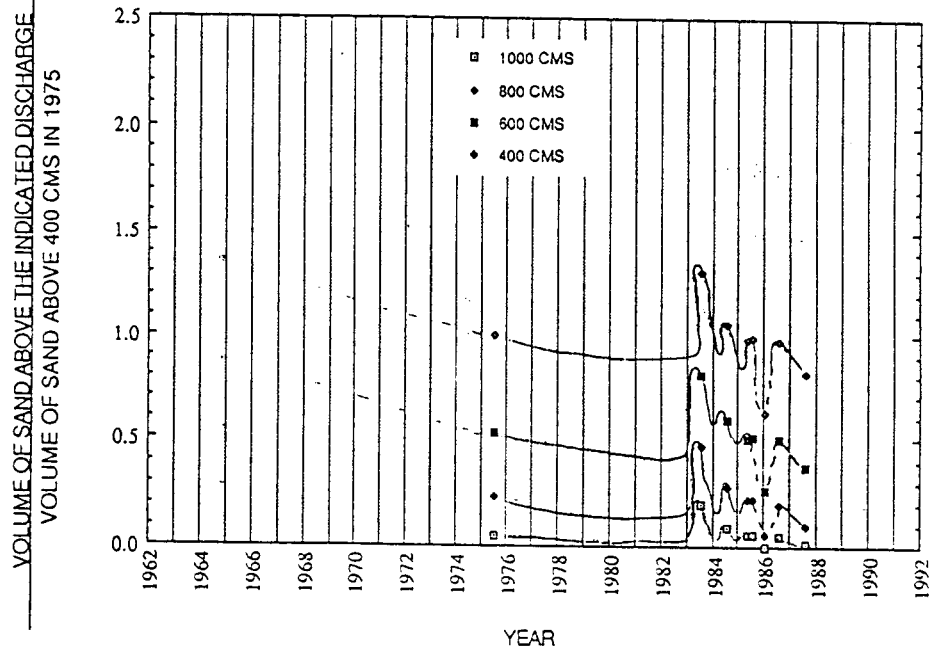


Figure 13. — Time series change at two separation bars, Kyle (1992).

NAUTILOID BEACH, RM 34.7L, PROFILE 2,
VOLUMETRIC CHANGES



BELOW LCR, MILE 61.8R, VOLUMETRIC CHANGES



regardless of channel width-to-depth ratio, downstream at least to the Grand Canyon gage. Irreversible bed degradation had reached Lees Ferry by 1965 (Pemberton, 1976), but the absence of long-duration high discharges between 1965-83 strongly suggests that the bed downstream from the Paria River had not irreversibly scoured prior to 1983.

Pemberton (1976) showed that erosion of bed sediment from the channel in the 25 km between Glen Canyon Dam and Lees Ferry had begun by 1959, 3 yrs after closure of the cofferdam. Pemberton (1976) also showed that most degradation was confined to the 10 km nearest the dam but that the first high release after the dam's official closure (1704 m³/s, June 15, 1965) extended degradation to Lees Ferry. Burkham (1987) showed that the cross-section at the U. S. Geological Survey gaging station at Lees Ferry annually scoured and filled, but that this cross-section did not refill after the 1965 high flow. Pemberton (1976) and Burkham (1987) both showed that the bed did not significantly change in elevation between 1965-82, presumably because of armoring (Fig. 17). Burkham (1987) showed that the high flow in 1983 caused bed scour below that of the 1965-82 elevation but that refilling took place upon flood recession.

There is much less data downstream from the Paria River, but available data suggest that this behavior may generally be represented by the behavior of the Grand Canyon gage. At the Grand Canyon cross-section, Burkham (1987) showed that the 1965 high flow degraded the bed to its historical low elevation, but that addition of coarse sediment to the rapid downstream from the gage and the supply of sediment from upstream caused subsequent bed aggradation of about 4 m by 1967. This higher bed elevation was maintained until 1980, but the bed was again scoured to its historical low elevation by the 1983 high flow. The status of the channel after recession of peak flows in 1986 can only be determined by continued monitoring.

Longitudinal Characteristics of Aggradation and Degradation of Bars and Banks

These results, combined with results of prior studies (Beus and others, 1985; Schmidt and Graf, 1990; Zink, 1989) show that different depositional environments located different distances downstream from Glen Canyon Dam in narrow and wide reaches of Grand Canyon responded differently to operations between 1965-90 (table 5). Schmidt and Graf (1990) showed that high discharges in 1983 and 1984 caused net erosion of bars within eddies occurred in narrow reaches downstream to river mile 118. Mapping by Clark (1992) and mapping near the Little Colorado River shows that erosion also

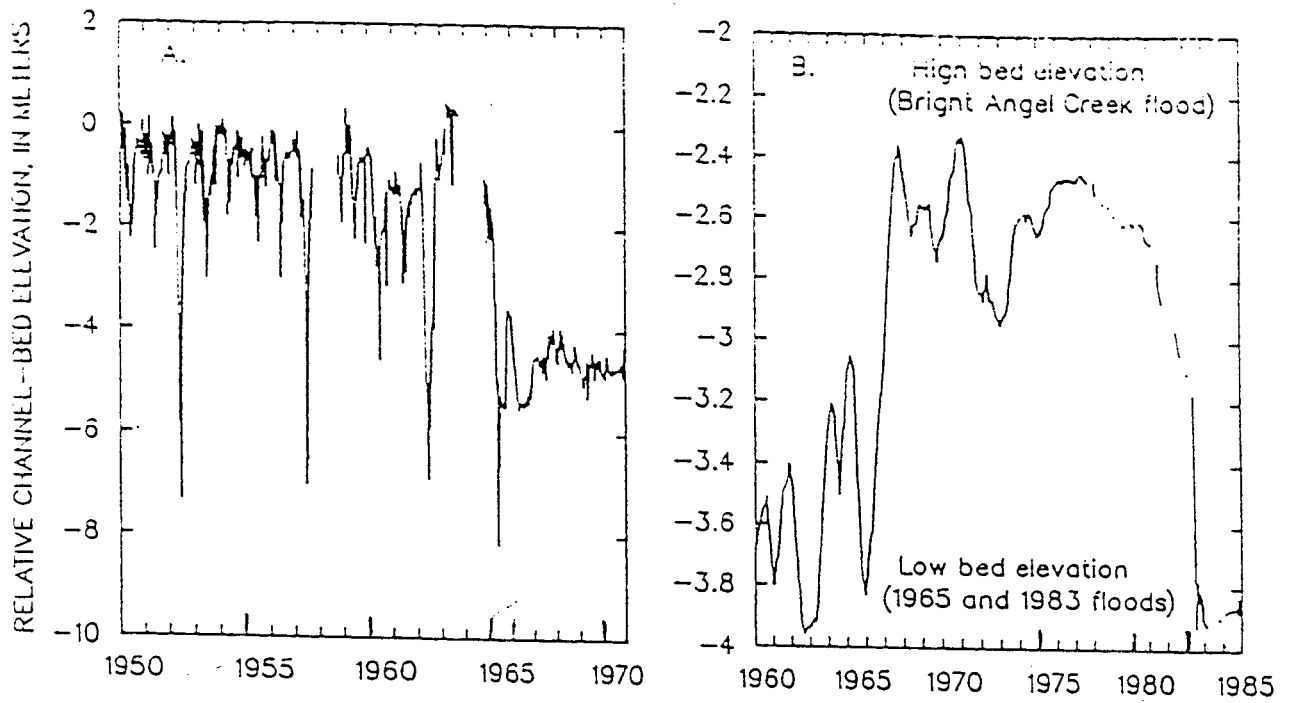


FIGURE 17 Bed elevation at (a) the U.S. Geological Survey gaging station, Colorado River at Lees Ferry (river mile 0), 1950-1970, and (b) at the U.S. Geological Survey gaging station, Colorado River near Grand Canyon (river mile 87.2, 139 km), 1960-1985. (From Kieffer and others, 1989)

occurred in the wide reach of Lower Marble Canyon. Zink (1989) showed that there were no clear degradation trends downstream from river mile 118.

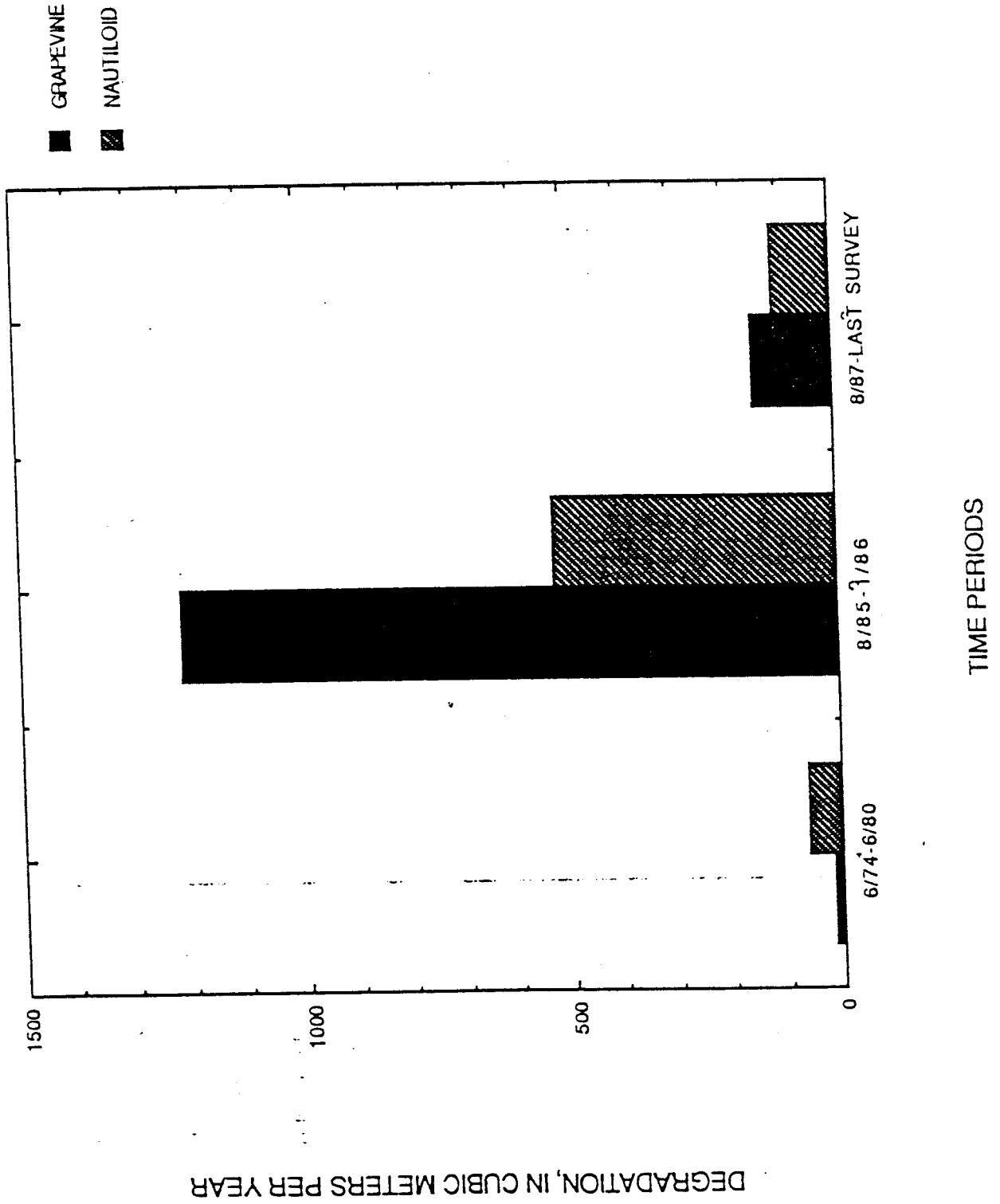
At the same time that there was net erosion from eddy systems throughout these most upstream 225 km, some sand bars used as campsites were aggraded. The response of Grapevine camp is representative of this response, and Schmidt and Graf (1990) documented similar behavior of a separation bar only 55 km downstream from the dam. Beus and others (1985) reported that some bars used as campsites were scoured greatly by these same high discharges, and in some cases, scoured sites were rendered unusable.

Resumption of fluctuating discharges in summer 1986 caused widespread erosion throughout Grand Canyon. The data presented in this report for 7 sites is consistent with the widespread erosion documented by Schmidt and Graf (1990) throughout Grand Canyon that occurred between October 1985 - January 1986 during a short period of fluctuating flows. These changes indicate that erosion is characteristic of the entire Grand Canyon corridor when river regime changes greatly, such as occurred in 1985 when flows changed from high steady discharge to lower fluctuating discharges.

Temporal Characteristics of Aggradation and Degradation of Bars and Banks

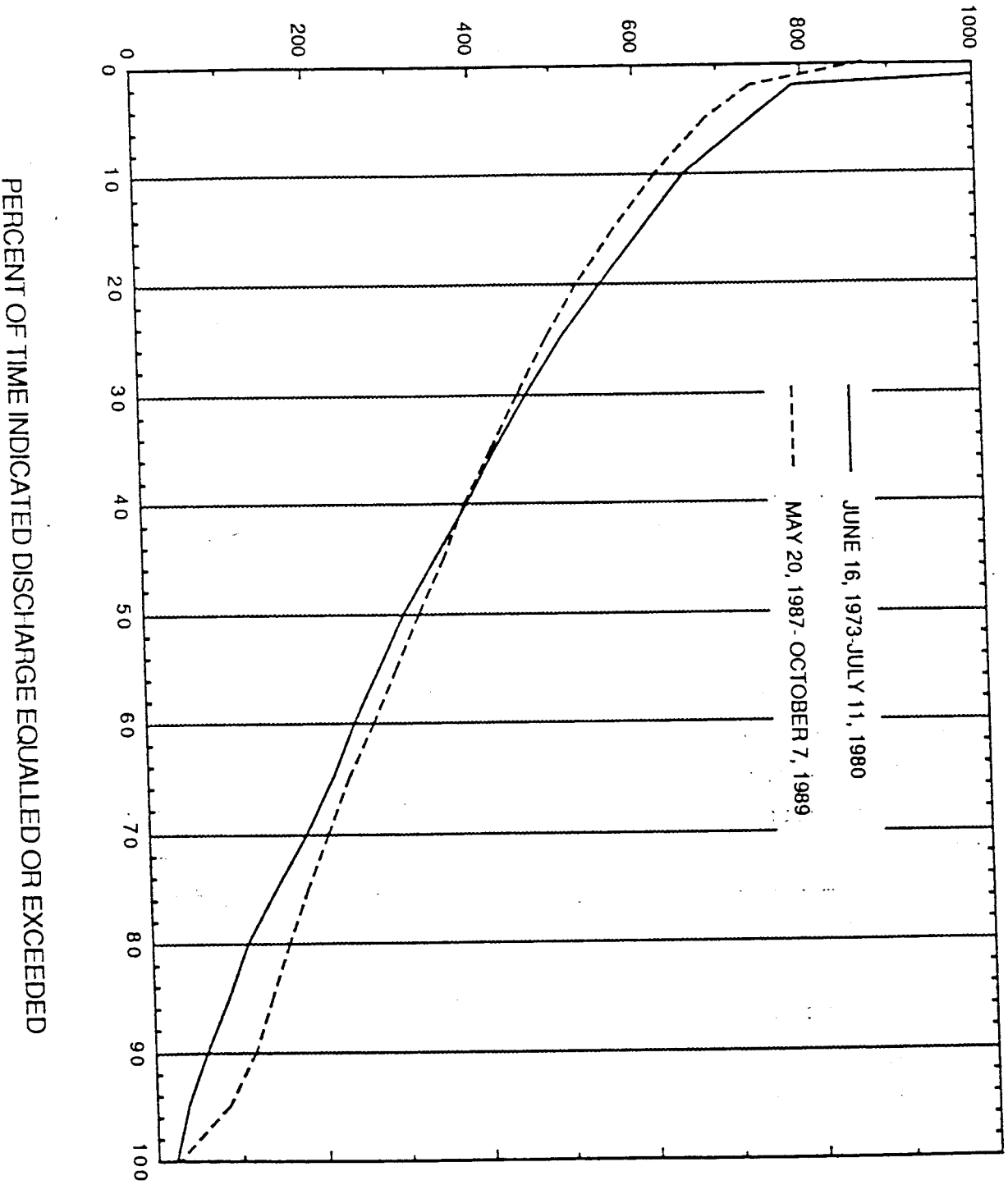
Each sand bar studied in this report experienced different erosion rates during different parts of the period 1965-91. The highest erosion rates at the five camping study sites studied by Kyle (1992) occurred in the 5-mth period of 1985-86 when fluctuating flows immediately followed recession from high discharges (Fig. 18). Erosion rates of less than half this rate were measured between August 1987 and 1990, and even lower rates were measured between 1974 - 80. Discharge characteristics during the latter two periods were compared by calculating flow-duration curves of hourly water release from Glen Canyon Dam (figure 19). The difference between discharge values for high and low durations (for example, the difference between the 10- and 90-percent duration values) shows that the range of discharge was greater for the 1973-1980 period than for the 1987-89 period; erosion rates were greater in the latter period, however. This comparison suggests that erosion rates are at least partly time dependent. Erosion rates were probably greatest between 1985-87 because there were newly deposited and unstable sand deposits at high elevation throughout Grand Canyon. These deposits eroded quickly during the onset of fluctuating flows between October 1985 - January 1986. However, these rates cannot be sustained; sediment eroded from high elevation may build low elevation subaqueous deposits that stabilize the remaining high-elevation deposits. Also, as high elevation deposits flatten in slope, they achieve a more stable form. Bhudu (1992) showed

Figure 10 RATES OF DEGRADATION FOR BEFORE, DURING AND AFTER THE HIGH FLOW PERIOD



HOURLY DISCHARGE, IN CUBIC METERS PER SECOND,
AT GLEN CANYON DAM

Figure 19
GLEN CANYON DAM HOURLY RELEASES
FREQUENCY ANALYSIS OF DISCHARGE



that where seepage-driven erosion dominates erosion processes, bars can achieve stability at angles of about 11 degrees. The implications of this time-dependence are that interpretation of the significance of any short-term measurements of erosion rates must be made within an historical context. The availability of erodible sediment largely determines sand-bar erosion rates. The time-dependence of erosion rates must also affect the relative importance of different erosional processes at bars. Seepage-driven erosion can be expected to be most important in the first few years after recession from one operating regime to a lower regime. Once such deposits have experienced erosion for a few years, the progressive movement of sediment from high elevation to low elevation must result in a decrease in the importance of this process. Further removal of sediment from bar surfaces must occur due to other processes.

Relation of Long-Term Measurements to Short-Term Studies of the 1990-91 Period

Figures 8, 12, and 14 show the estimated total range in values determined by Beus and others (1992) within the context of the long-term record. At each of these sites, the range in values measured during the 1990-91 period was at the low end of the range of values measured since recession of high discharges in 1986. Total range in fluctuation in volume of sediment stored in the hydrologically active zone were never more than 800 m³ at any site. These data are consistent with the findings of Bhudu (1992) that typical sand-bar behavior is for relatively minor adjustments to occur in a limited part of the entire bar.

Managing the River for Sediment Mass Balance

There has been much discussion about management of the Colorado River for sediment mass balance (T. Randle, 1992, U. S. Bureau of Reclamation, Denver, 1992, oral commun.). Comparison of Figures 2 and 17 with those describing change in alluvial deposits demonstrate clearly that (1) erosion of bars and banks can occur when mass accumulation is occurring in the system, and (2) removal of sediment from the system (Fig. 2) occurs by both bed scour and net scour from low-elevation bars in eddies. During the floods that cause such scour, some sediment is deposited at high elevations. Such sediment typically is removed in a decade.

Managing for sediment mass balance is no guarantor of the long-term stability of sediment deposits in Grand Canyon. Quasi-equilibrium of bars may develop at times when sediment accumulates in the system, but research has yet to demonstrate that the degree of

accumulation affects the nature of this equilibrium. It is only clear that mass accumulation will make more sediment available for transport during the next high discharge event.

Implications of Long-Term Trends

These data show that quasi-stability can occur at some sand bars in Grand Canyon. In some cases, such as Grapevine camp, bars are little different today than they were in the mid-1970's. In other cases, large-scale erosion has occurred in the past, but present erosion rates are much less because there is relatively little sand now available for erosion, as in the case of Jackass Creek camp. One must be cautious, however, in concluding that long-term stability to the sediment-depleted fluctuating flow regime of the regulated Colorado River can be achieved.

Other processes occur at Grand Canyon sand bars besides seepage-driven erosion. Cluer (1992) demonstrated that bank failure involving large areas of the bar, but of unknown thickness, can occur during a few hour period. Webb and others (1987) have demonstrated that debris flows can completely destroy sand bars during one catastrophic event. Kearsely and Warren (1992) show that vegetation invades some campsites, especially in wide reaches, and limits the longterm recreational use of these sites. Each of these processes leads to long-term decrease in bar and campsite availability.

In terms of recreational utility, the question is what is the duration of "usable life" of each site. There are two possible conditions which define end-member answers to this question:

1. The long-term rates of change exceed the interval of expected uncontrolled flooding from Glen Canyon Dam, or
2. The long-term rates of change are less than this interval.

It appears that the second case is the more probable, based on the relatively slow loss of campsites documented by Kearsely and Warren (1992). Only in the former case would intentional high discharges, such as those termed "habitat-building", be reasonable for management purposes.

Research in Hells Canyon of the Snake River (Grams, 1991) suggests that frequent high discharges can cause significant sediment depletion and large net scour in eddies. Data in this report shows that high floods between 1983-86 were the most significant geomorphic event in the last 30 yrs at most sites. These data also suggest that sediment availability decreased between 1983-86 because of transport out of the system (Fig. 2). The nearly complete absence of new deposits associated with discharges between 1984-86

(Rubin and others, 1992) and the fact that deposition to new topographic levels in 1985 and 1986 did not occur suggests that habitat-building floods should only occur when there is sufficient sediment stored in the channel or is available from other sources.

CONCLUSIONS

Net sediment storage in Grand Canyon has been greatly influenced by operations of Glen Canyon Dam. Although periods of powerplant discharge, such as between 1965 - 82, are periods of net sediment accumulation in Grand Canyon, these also represent periods when local readjustments transfer sediment from high- to low-elevation. The rate of these transfers depends on the availability of potentially erodible sediment, and has therefore been greatest immediately after deposition of high-elevation deposits.

High discharges, such as those that occurred annually between 1983-86 erode sediment from the channel and transfer sediment to some high-elevation sites. However, the particular sequence of high discharges that occurred between 1984 - 86 (in terms of magnitude and duration) successively depleted the high-elevation deposits created in 1983, and the entire sequence of high discharges between 1983-86 removed sediment from most eddies upstream from river-mile 118.

Therefore, it is not enough to develop bar-building flow scenarios based on sediment budget calculations and the knowledge that some sites will aggrade during those floods. It is possible for floods to be of too long a duration, too high a magnitude, and too frequent in occurrence for net system-wide campsite aggradation under the sediment regime of the present regulated river system. The net effect of such floods could be to scour many low-elevation eddies and to also degrade many campsites. Beus and others (1985) showed that high discharges in 1983 and 1984 actually completely eroded a number of former campsites. The reason why the net effect of floods can range between net erosive to net aggradational is that there are no accurate estimates of the volume of sand in storage in Grand Canyon. If the primary reservoir of sediment is the river channel, than bar-building floods can be more closely spaced in time. However, if the primary reservoir of sand is reattachment bars, then floods have a great potential to be net erosive.

The dilemma for river management is that erosion is an irreversible process of transferring sand from high to low elevation. Although these rates decline with time, erosion cannot be stopped. The plan for maintenance of sand bars in Grand Canyon must be based on precise understanding of the long-term, reach-scale erosion rates of campsite beaches, the accumulation rate of sediment in the main channel during times of low peak

discharge, the availability of accumulated sediment for deposition in eddies during bar-building flows, the necessary duration of bar-building events, the geography of depositional sites during such an event, the duration of such deposits once flows have receded, and the net trade-off between aggradation that will occur at some sites and irreversible erosion that will occur at other sites. If insufficient sediment is available to strike such a balance, then the only strategy to reverse the trend of long-term erosion will be to supplement Grand Canyon with sediment from some source not presently accessible by the regulated river.

REFERENCES CITED

- Andrews, E. D., 1991, Sediment transport in the Colorado River basin, *in* Committee to Review the Glen Canyon Environmental Studies, eds., Colorado River Ecology and Dam Management: Washington, D. C., National Academy Press, p. 54 - 74.
- Beus, S. S., Avery, C. C., Stevens, L. E., Kaplinski, M. A., and Cluer, B. L., 1992, The influence of variable discharge regimes on Colorado River sand bars below Glen Canyon Dam, *in* S. S. Beus and C. C. Avery (eds.), The Influence of Variable Discharge Regimes on Colorado River Sand Bars below Glen Canyon Dam: report to the National Park Service.
- Beus, S. S., Avery, C. C., and Cluer, B. L., 1991, Beach erosion studies under discrete controlled releases, Colorado River through Grand Canyon National Park: *Eos*, v. 72, p. 223.
- Beus, S. S., Carothers, S. W., and Avery, C. C., 1985, Topographic changes in fluvial terrace deposits in Grand Canyon: *Journal of the Arizona - Nevada Academy of Science*, v. 20, p. 111 - 120.
- Bhudu, M., 1992, Mechanisms of erosion and a model to predict seepage-driven erosion due to transient flow, *in* S. S. Beus and C. C. Avery (eds.), The Influence of Variable Discharge Regimes on Colorado River Sand Bars below Glen Canyon Dam: report to the National Park Service.
- Brian, N. J. and Thomas, J. R., 1984, 1983 Colorado River beach campsite inventory, Grand Canyon National Park, Arizona: Grand Canyon National Park Division of Resources Management report, 56 p.
- Clark, J. J., 1992, Analysis of sediment storage changes of the Colorado River near Nankoweap Rapids in Grand Canyon: unpublished Middlebury College senior thesis.

- Cluer, B. L., 1992, Analysis of sand bar response along the Colorado River in Glen and Grand Canyons to test flows from Glen Canyon Dam, using aerial photography, in S. S. Beus and C. C. Avery (eds.), *The Influence of Variable Discharge Regimes on Colorado River Sand Bars below Glen Canyon Dam: report to the National Park Service*.
- Committee to Review the Glen Canyon Environmental Studies, 1987, *River and dam management*: Washington, D. C., National Academy Press, 152 p.
- Dolan, R., Howard, A. D., and Gallenson, A., 1974, Man's impact on the Colorado River in Grand Canyon: *American Scientist*, v. 62, p. 393 - 401.
- Grams, P. E. and Schmidt, J. C., 1991, Response of recirculating-current alluvial sand bars to operations of Hells Canyon Complex dams, Snake River, Idaho and Oregon: *Eos*, v. 72, p. 219.
- Hirsch, R. M., Walker, J. F., Day, J. C., and Kallio, R., 1990, The influence of man on hydrologic systems, in Wolman, M. G. and Riggs, H. C. (eds.), *Surface Water Hydrology*: Boulder, Geological Society of America, *The Geology of North America* vol. O-1, p. 329 - 359.
- Howard, A. D., 1975, Establishment of benchmark study sites along the Colorado River in Grand Canyon National Park for monitoring of beach erosion caused by natural forces and human impact: *University of Virginia Grand Canyon Study Technical Report no. 1*, 182 p.
- _____ and Dolan, R., 1979, Changes in the fluvial deposits of the Colorado River in the Grand Canyon caused by Glen Canyon Dam, in Lin, R. M., ed., *First Conference on Scientific Research in the National Parks*, v. 2, New Orleans, November 9 - 12, 1976, *Proceedings: National Park Service Transactions and Proceedings Series*, no. 5, p. 845 - 851.
- _____, 1981, Geomorphology of the Colorado River in Grand Canyon: *Journal of Geology*, v. 89, p. 269 - 298.
- Hughes, T. C., 1991, Reservoir operations, in *Committee to Review the Glen Canyon Environmental Studies*, eds., *Colorado River Ecology and Dam Management*: Washington, D. C., National Academy Press, p. 207 - 225.
- Kyle, E. L., 1992, Temporal changes in sediment storage at longterm sand-bar monitoring sites in Grand Canyon: unpublished Middlebury College senior thesis.

- Laursen, E. M., Ince, S., and Pollack, J, 1976, On sediment transport through Grand Canyon: Third Federal Interagency Sedimentation Conference Proceedings, p. 4-76 to 4-87.
- Pike, R. J. and Wilson, S. E., 1971, Elevation-relief ratio, hypsometric integral, and geomorphic area - altitude analysis: Geological Society of America Bulletin, v. 82, p. 1079 - 1084.
- Schmidt, J. C. and Graf, J. B., 1990, Aggradation and degradation of alluvial sand deposits, Colorado River, Grand Canyon National Park: U. S. Geological Survey Professional Paper 1493, 74 p.
- Schmidt, J. C., Kepes, A. J., and Hanson, M. A., 1989, Topographic changes of sand bars, Lees Ferry to Bright Angel Creek: Middlebury College Grand Canyon Study Technical Report 89-1, 58 p.
- Turner, R. M. and Karpiscak, M. M., 1980, Recent vegetation changes along the Colorado River between Glen Canyon Dam and Lake Mead, Arizona: U. S. Geological Survey Professional Paper 1132, 125 p.
- Williams, G. P. and Wolman, M. G., 1984, Downstream effects of dams on alluvial rivers: U. S. Geological Survey Professional Paper 1286, 83 p.
- Zink, L. L., 1989, Effects of Glen Canyon Dam on sand bars of the Colorado River in Grand Canyon: unpublished Middlebury College senior thesis, 53 p.

Working copy for publication —

CHAPTER 9
ANALYSIS OF SAND BAR RESPONSE ALONG THE
COLORADO RIVER IN GLEN AND GRAND CANYONS
TO TEST FLOWS FROM GLEN CANYON DAM,
USING AERIAL PHOTOGRAPHY

by:

Brian L. Cluer
Resource Management Division
Grand Canyon National Park

*Sherman: repeatability of areas?
accuracy of areas?*

ABSTRACT

This investigation presents the first analysis of aerial photography captured during the GCES Phase II test flow program. Seventy four sites were photographed 17 times from September 30, 1990 to July 27, 1991. Sixteen test flows were bracketed with before and after photography. The ten sites presented in this report were analyzed using a new technique developed to obtain two-dimensional measures from images that were designed with stereo overlap and intended for three-dimensional analysis. True scale area measurements and comparison plots resulted in measures of; whole deposit area, area of aggradation; and area of degradation for each photo epoch. The combination of aggraded and degraded area yields a measure of the minimum area that was reworked during bracketed test flows.

Sediment transport capacity calculations for each of the test flows provided an index of relative hydraulic energy for the individual flows. This index correlates well with measurements of reworked area. The total area results were however not strongly correlated, indicating the natural variability in the fluvial system, and a combination of immediate and delayed responses to changes in flow regimes. Overall, flows with reduced energy following high energy flows resulted in increased area. Consequent return to a higher energy flow resulted in decreased deposit area. This generality held until the last two test flows where aggradation during the high energy "G" test flow was followed by degradation during the subsequent "F" test flow (with slightly lower energy). However, further sediment transport capacity modeling may show that there was little difference between the "G" and "F" test flows at some distance downstream.

Several hydrogeomorphic features were captured during this investigation. At two sites, secondary recirculation eddies formed during a normal flow period in November and December, 1990. The secondary eddy features persisted and ultimately eroded large percentages of the two deposits. Seepage of ground water during highly fluctuating flows produced rills and larger tunnel scours. At one site, the large tunnel scour features were associated with an aggradational period. Consequently, it appears that there is a well developed linkage between erosional and depositional processes affecting sand bars along the Colorado River in Grand Canyon. The two polarized processes operate together at all sites, but certain hydraulic perturbations allow one process to temporarily overpower the other. Understanding these linkages and the responses to hydraulic changes will require full development of sand bar monitoring techniques (and existing databases) that will provide the highest temporal and spatial resolutions possible.

In general, during the test flow program, reductions in stream energy and range of daily fluctuations following flows with higher energy and fluctuation ranges resulted in increased area. This was due to reworking of over-steepened deposits created during highly fluctuating flows. Conversely, flows with increased energy and fluctuation ranges following low energy low fluctuation range flows resulted in decreased area. This is due to reworking of sediments that were previously shifted to lower positions and deposition at higher positions. The long term effects of this type of deposit increase are not clear, and should be studied further.

Overall, this investigation concludes that regularly fluctuating flows were less damaging than the irregularly fluctuating "Normal" flows that included weekend low fluctuation periods.

*Background
Previous Investigations*

INTRODUCTION

It was recognized early in the NPS/GCES beach erosion project that a large sample size was necessary to adequately constrain sand bar responses to multiple variables. These variables include; test flow hydraulics, variations in sedimentologic and geomorphic environments, sediment inputs from tributaries, and distance from Glen Canyon Dam. Aerial photogrammetry offered a method that could capture a large number of subjects during the short three day evaluation periods between test flows.

Between August 1990, and July 1991, aerial photographs were taken of 75 sand bars in Glen and Grand Canyon located between 5 miles below Glen Canyon Dam and 240 miles down river at Diamond Creek. Seventeen photo epochs were completed which bracket 16 different test flows. The photographs captured a variety of sand bars at a low and constant river level at 5,000 cfs. A contract with the Photogrammetric Mapping Division-USGS in Flagstaff, Arizona, allowed for development of a two-dimensional analysis method that was applied to overlapping stereo imagery.

The objective of this study was to develop planimetric maps of 10 sand deposits along the Colorado River in order to analyze the affects of test flows from Glen Canyon Dam. Each photo epoch resulted in complete photographic coverage of selected sand deposits exposed at a constant low river level of 5,000 cfs. Subsequent planimetric plots were overlaid with the prior plot to discern the areas that changed during the test flow. These areas were digitally compared also, resulting in calculated areas of erosion and deposition associated with each test flow.

This paper presents the results of analysis of 10 out of 75 sites photographed through the test flow period from September 1990 to July 1991. It includes 17 planimetric analyses for each of the 10 sites, bracketing 16 unique test flows.

METHODS

Site Selection

Sites were selected for the original investigation to provide continuity with ^{*previous*} ~~historical~~ data, sufficient size for continued measurement throughout the test period, wide dispersion from the ~~Dam to Diamond Creek~~, and adequate variety of geomorphic and sedimentologic type. The 10 sites selected for this report were at Colorado River miles (CR): CR CR -6.5 R, CR CR 8 L, CR CR 43 L, CR CR 45 L, CR CR 47 R, CR CR 51 L, CR CR 66 L, CR CR 68 R, CR CR 81 L, and CR CR 172 L. Throughout this report sites are described by Colorado River mile from Lees Ferry and side of river looking downstream, left (L), or right (R). See Figure 1 for general locations of study sites. Schmidt and Graf (1988) categorized depositional environments and deposit types in Grand Canyon. Their nomenclature is used in this report (Fig. 2).

Site Description

The site at CR -6.5 R is located in Glen Canyon, in the Ferry Swale area. The sand bar is upstream of a minor channel constriction in a very quiet reach. Recirculation in the local eddy often changes direction rapidly, however, the recirculating current is usually very slow. This site is heavily impacted by motor boat wakes.

Site CR 8 L is located at Badger rapid, immediately downstream of Jackass Canyon. The sand bar is within a recirculation zone, but waves from the nearby rapid probably mask other fluvial processes on this deposit.

Down river is the Anasazi Bridge site, at CR 43 L. This sand bar is immediately upstream of a channel constriction, thus it is an upper pool deposit. It has two persistent recirculation eddies, but they are generally slow velocity and the deposit is probably dominated by seepage processes.

CR 45 L, at the Eminence Break trail is the next site. A major channel constriction from river left and the sweeping right turn of the canyon around Hansbrough Point have developed a large separation and reattachment bar environment at this site. Recirculating currents are swift in this eddy, and high river stages impinge on the separation deposit.

The next site down river is CR 47 R, where Saddle Canyon enters from the right. Here only the reattachment deposit was consistently photographed. This eddy has strong recirculating currents that often form sand waves on the platform deposit.

Site CR 51 L is another reattachment bar formed down stream of a minor channel constriction in a relatively calm reach. Strong recirculation currents exist in this eddy at high river stages.

Downstream from Palisades Creek, at CR 66 L is the next site. This sand bar is located immediately upstream of a large mid-channel gravel bar where high flows split and flow around both sides of the island. At the upstream end of the sand bar there is a minor channel constriction from a tributary on the left. This combination of channel conditions creates a strong recirculating eddy. A combination of separation and reattachment deposits was captured here.

Site CR 68 R is a large sand bar across from the Tanner trail. This site is located on the inside of a large right bend in the river, downstream of a long shallow riffle, and upstream of Tanner rapid. Both the separation and reattachment deposits were consistently photographed.

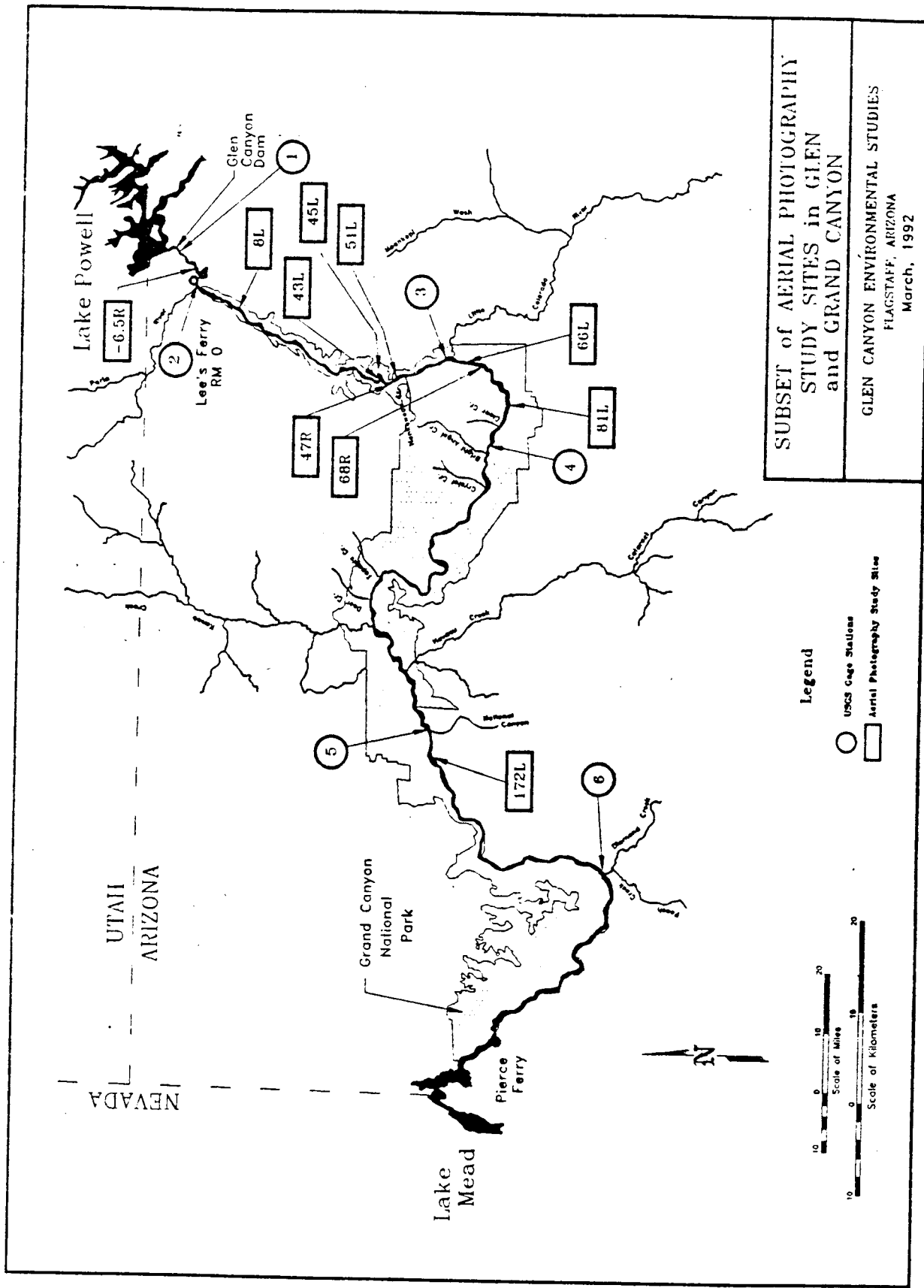


Figure 1. Location map of study sites along the Colorado River in Glen and Grand Canyons, Arizona.

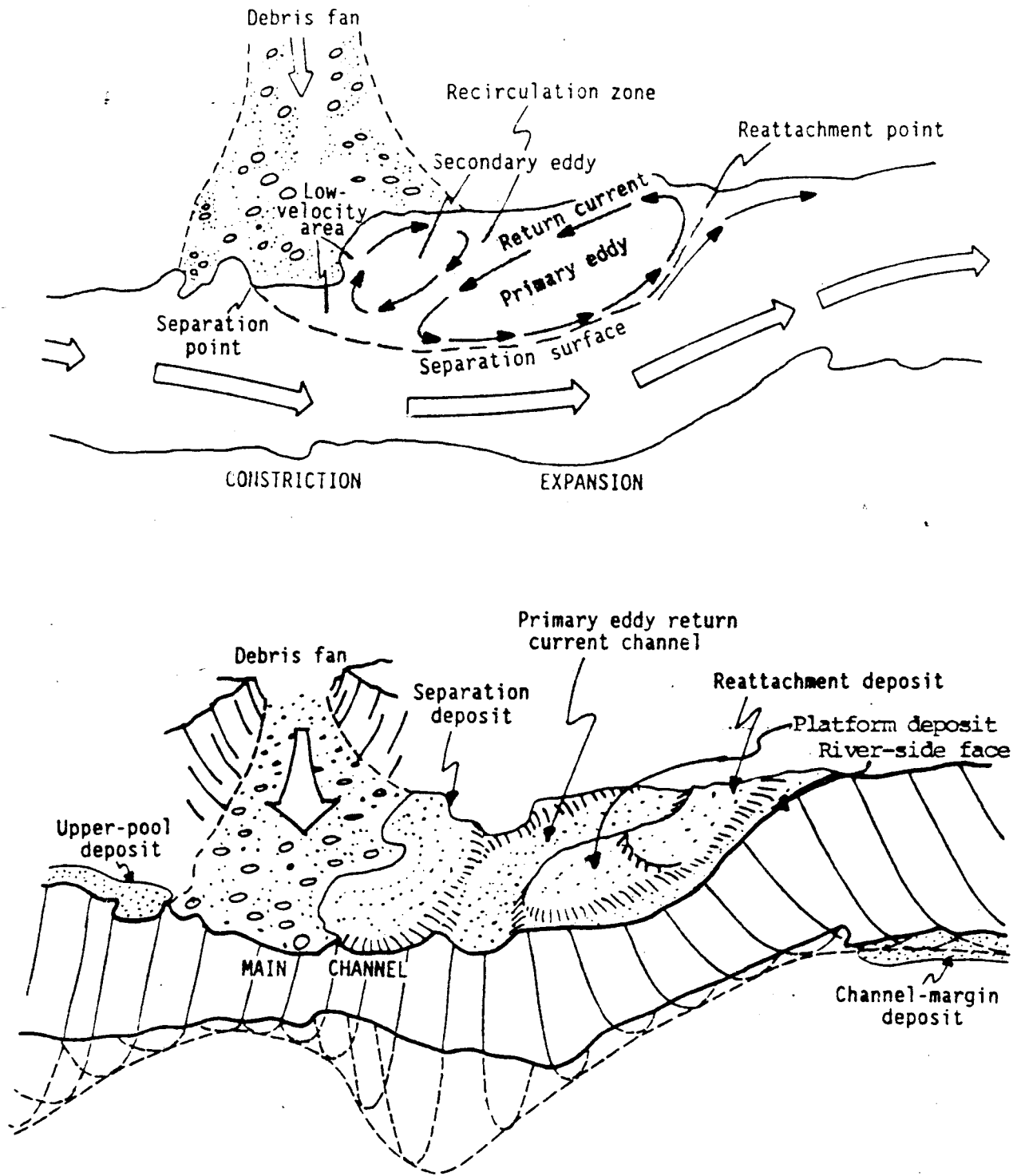


Figure 2. Diagram of deposit types and sedimentary environments in the Grand Canyon, with nomenclature used in this report. Modified from Schmidt and Graf, 1988 (Fig. 3).

Site CR 81 L is at Grapevine camp. This sand bar is located between two small side channel constrictions in the narrow and swift Inner Gorge reach. At high river stages, main channel flow affects the face of the sand bar. At lower river stages, small recirculation eddies form along the bar face.

Sand bar CR 172 L is below Mohawk rapid. This site is located immediately down stream of a secondary channel constriction below Mohawk and Gateway canyons. Strong recirculation currents exist in this eddy under a wide range of river stages. Both separation and reattachment deposits were consistently photographed at this site.

Site Preparation

During November and December, 1990, survey crews placed aerial photo panels on the sites selected for this investigation. All panels were surveyed to local datum and benchmark references using state-of-the-art equipment and techniques. Photographs taken during the ensuing evaluation period in mid-December, 1990, captured the surveyed photo panels. This photography provided photo scale and orientation for all prior and subsequent photography through analytical techniques that relate features with known locations to natural features with unknown locations.

Two-dimensional analysis development

Original black and white negatives were mechanically fitted under magnification to carefully align water edge at the front of the sand bar and immobile rocks at the back and edges of the sand bar. The aligned overlapping images were fixed onto a stable transparency base to create a composite full coverage image for each photo epoch. The composite images were then digitized, bounded by the water's edge and between repeatable rocks outside the fluctuating zone to enclose a perimeter that defined an area. A technique was developed to digitally process the perimeter on a video monitor, and a computer program counted the number of pixels filling the perimeter, applied scaling factors, and calculated the area within the perimeter in meters².

Additional corrections were made to rectify angular variations between photographs taken at different epochs and develop common photo scales. By choosing one composite image as the base, all other photo epochs were manually adjusted on the color video monitor to align at common rock points. With common immobile points aligned, the differences in area between epochs were visually obvious, and attributable to hydraulic processes operating during the preceding test flows. Areas of sand bar aggradation and degradation were distinguished by assigning individual layers unique colors.

Quality Control

The quality of the digitally derived area values was checked by carefully examining each photo epoch to verify areas of aggradation and degradation between test flows and water level for

each epoch. Photo epochs that captured subjects at water levels visually differing from the normal 5,000 cfs stage were removed from the data base. This process also resulted in description of fluvial geomorphic processes that left evidence on the surface of sand bars.

RESULTS

The results from two-dimensional analysis of the aerial photography are: perimeter plots of each epoch; area calculations of each epoch; comparison plots of contiguous epochs, with differently shaded areas of aggradation and degradation; calculations of area of aggradation and degradation; and descriptions of fluvial evidence preserved on the surface of deposits.

Table 1. Summary of photography captured for each site and each test flow.

SITE/ FLOW	DATE	CR - 6.5 R	CR 8 L	CR 43 L	CR 45 L	CR 47 R	CR 51 L	CR 66 L	CR 68 R	CR 81 L	CR 172 L
"E"	9/30/90			x	x	x	x	x			x
"A"	10/14/90			x			x	x		x	
8,000	10/30/90		x	x					x	x	x
Fall	11/11/90		x	x	x	x	x	x			x
Normal	12/17/90	x	x	x	x		x	x		x	x
11,000	12/30/90	x	x	x	x	x	x	x	x	x	x
"C"	1/12/91	x	x	x	x	x		x	x	x	x
Winter	1/28/91	x	x	x	x	x	x	x	x	x	x
"B"	2/9/91	x	x	x	x	x	x	x	x	x	x
Normal	4/20/91	x	x	x	x	x	x	x	x	x	x
Spring	5/5/91	x	x	x	x	x	x	x		x	x
"D"	5/19/91	x	x	x	x	x	x	x	x	x	x
15,000	6/2/91	x	x	x	x	x	x	x	x	x	x
Summer	6/30/91	x	x	x	x	x	x	x	x	x	x
"G"	7/14/91	x	x			x	x				x
"F"	7/27/91	x	x	x	x	x	x	x	x	x	x

MAP PRODUCTS

Planimetric Maps Each photo epoch resulted in complete photographic coverage of selected sand deposits exposed at a constant low river level of 5,000 cfs. Subsequent planimetric maps were overlaid with the prior map to discern the areas that changed during the test flow. These areas were digitally compared to calculate areas of erosion and deposition associated with each test flow. The results of this process are included in Appendix A, this report. In these maps, eroded areas are shown with dark shading and deposited areas are lightly shaded.

Calculated Areas Photographs of each epoch were digitized and corrected for angular variation. The area of each sand bar was calculated for each epoch using a computer program that counted the number of pixels within the perimeter. Areas of erosion and deposition were also calculated between photo epochs. These results are presented in table 2. Table 2 lists the total area of each site at each photo epoch, or between test flows. Also listed are the areas that were eroded or deposited during test flows. These are listed as -area and +area respectively. Flows that reworked large areas will have high -area and +area values. Flows that were erosive will have a correspondingly high -area value and show a decreased overall area value. Flows that were depositional have large +area and increased overall area values.

SEDIMENT TRANSPORT CAPACITY

A method of providing unique measures of the hydraulic effects for individual test flows was needed in order to compare the field results against the potential sediment transport of each test flow. Sediment transport capacity of each test flow was calculated to compare potential sediment movement in the main channel with measures of changes in sediment stored in channel margin depositional environments. A computer program was used to calculate sediment discharge using water discharge treated with sediment transport functions (Smilie et al, 1992, and this report). The equation used was:

$$Q_s = aQ_w^b \quad (1)$$

where Q_s is sediment discharge, Q_w is water discharge, a is $0.46047(10)^{-10}$, and b is 3.2228. The transport functions a and b were derived from measured values at the USGS gaging stations (Fig. 1) at Grand Canyon above the Little Colorado River, Grand Canyon Gage at Phantom Ranch, and Grand Canyon Gage at Diamond Creek. Inputs for Q_w were taken from mean daily values at the Lees Ferry Gage, for each test flow.

The results of sediment transport modeling are presented in Figure 3. This exercise was intended to provide an index of relative stream energy associated with each of the test flows. It is not intended that the calculations of sediment transport capacity represent transport through the system.

The resulting sediment transport capacity values range from a low of about 2,000 tons for the 11 day 8,000 cfs constant flow during the period October 15-25, 1990, to a high of over 135,000 tons for the 46 day "Normal Flow" test that lasted February 11-April 17, 1991. Daily sediment transport values range from a low of 174 tons per day for the 8,000 cfs

constant flow to a high of 4021 tons per day for the "G" flow in July 1991. In general, it is the duration at peak discharge that controls the sediment transport capacity of particular flows. The test flows had various peak discharges, and various up and down ramping rates, resulting in different peak and durations at peak discharge. Consequently, the test flows with large fluctuation ranges and high discharges had the greatest sediment transport capacity. Conversely, test flows with small fluctuation ranges and low peak discharges had low sediment transport capacities. The pattern of variability (Fig. 3) on a daily basis indicates that there was not much difference between many of the test flows. For instance the "A", 8,000 cfs constant, "Fall", "Normal", and 11,000 cfs constant flows varied little from the subsequent "B", "Normal", and "Spring" test flows. The fourth test flow, "Normal" is greatest in overall sediment transport capacity because of its high peak discharges and 46 day duration.

SITE	EPOCH	CR 51 L		CR 66 L - HOM SALT MARNE		CR 68 R - TANNER		CR 81 L - GRAPEVINE		CR 172 L - BELOW MOHAWK		
		AREA m2	+ AREA	AREA m2	+ AREA	AREA m2	+ AREA	AREA m2	+ AREA	AREA m2	+ AREA	% AREA
E	09/20/90	28692.79		8313.27						8319.56		
A	10/15/90	26921.41	101.86	8334.48	-139.08			1588.67				
B	10/30/90					4378.61		1695.29	4.97	-0.26	14.67	50.93
Fall	11/11/90	27115.29	1080.89	7893.47	-448.49				0.00			0.00
Normal	12/17/90	25120.42	106.80	7507.33	-880.61			1684.58	1.06	-2.35	72.33	-203.72
C	11/23/90	24705.63	58.87	7323.83	-81.54	4198.42	222.31	1559.75	2.87	-14.83	117.12	95.12
Winter	01/26/91	25112.07	890.82	7370.19	236.52	4216.43	287.13	1656.39	85.89	0.00	5483.47	675.58
B	02/09/91	24571.63	184.33	7711.79	89.40	4387.81	223.32	1831.35	0.00	-18.85	108.67	298.87
Normal	04/20/91	25019.97	673.08	7780.56	-11.78	4598.18	197.45	1877.52	0.00	-15.47	80.66	-210.41
C	05/05/91	21447.66	0.47	8828.53	968.42	4188.32	88.00	1823.51	18.55	0.26	5644.13	-253.07
D	05/19/91	24510.80	1304.33	8289.45	581.02			1824.03	23.52	-4.44		0.00
Spring	06/07/91	24893.77	289.46	7987.94	-730.54	4443.19	483.13	1621.66	3.40	-13.07	614.68	30.16
Summer	06/30/91	25410.48	1494.87	8110.35	785.96	4279.08	187.84	1652.78	20.78	2.35	525.87	889.61
G	07/14/91	21722.24	1.80.80							0.00		318.09
F	07/27/91	24871.82	1218.28	8109.76	-238.08	4489.37	370.25	1648.12	8.01	3.40	5687.30	561.03

Table 2b. Data from two-dimensional analysis of aerial photography from sites CR 51 L, CR 66 L, CR 68 R, CR 81 L, and CR 172 L. All values reported in meters². Values of erosion and deposition area shown as -area and +area respectively. Total area is shown as area.

SEDIMENT TRANSPORT CAPACITY

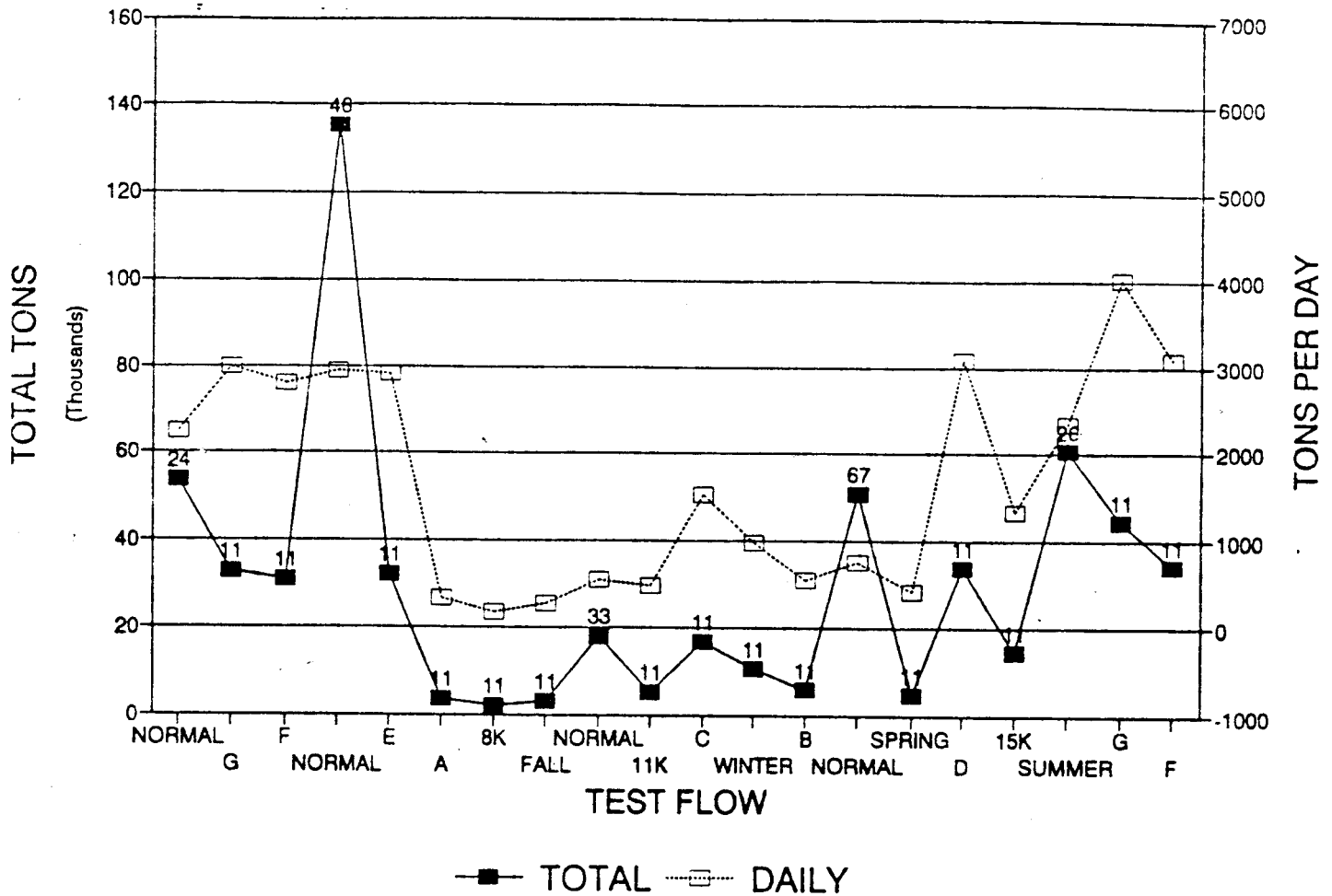


Figure 3. Graph of sediment transport capacity results for each test flow and daily values for each test flow. The numbers over the solid blocks indicate the duration in days of each test flow.

DISCUSSION

Comparison of Field Measurements and Sediment Transport Capacity

Reworked sediment area was derived from adding area of sediment increase to area of sediment decrease, or cut plus fill. A strong correlation was found between the area of reworked sediment and sediment transport capacity (Fig 4). This relationship is particularly well represented at site CR 66 L (Fig. A7), where the trends between reworked area and sediment transport capacity follow closely. The relationship is also evident at sites CR 45 L, CR 47 R, CR 51 L, CR 68 R, and CR 172 L (Figs. A4, A5, A6, A8, and A10 respectively, in appendix A). Overall, the composite of reworked area follows the sediment transport trends remarkably well (Fig. 5) where increased sediment transport results in increased reworked sand bar area.

The important metric to the fluvial sediment resource is the amount of reworked sediment that remains stored in the eddy following a particular test flow. The comparison of reworked area and resulting sand bar area is less clear (Fig. 6). The resulting total sand bar area, following each test flow, is plotted with reworked area during each test flow in figure 6. This comparison shows mixed results that are explored in the following section on flow pattern changes and geomorphic results.

A principal use of aerial photography is for describing surficial hydraulic features and general geomorphology. The photographs reveal some very interesting cause and effect relationships. During the course of this study several interesting hydrogeomorphic features developed and disappeared while others developed and persisted. This paper presents some of the geomorphic observations. Each observation is related to a particular test flow. The reader is advised to referred to Appendix I of this document for details of each test flow throughout the following discussion.

Photography recorded most of the sites during the September 28-30, 1990 evaluation period. Sand bar area at that time was used as the baseline value to compare subsequent changes to. The consistency of photo capture increased steadily as the study progressed (Table 1). Eight out of ten sites were captured on September 30, 1990 prior to the "A" test period. Discussion of sand bar area and changes relating to ground water and stream hydraulics begins with this flow.

Flow Pattern Changes and Geomorphic Results

In some of the photography it was obvious that main channel flow or eddy flow patterns had changed during the previous test flow. Notable occurrences were at sites CR 45 L, CR 51 L, CR 66 L, CR 68 R, and CR 172 L.

"A" test flow The "A" test flow fluctuated daily from 3,000-13,000 cfs for 11 days in early October 1990. On the 5 sand bars sampled, about 5% of the total area was reworked and there was a slight total gain in area of about 0.5% (Fig. 6). The CR 51 L site underwent a remarkable change during the "A" test flow (Fig. A6b). The sand bar retained all of its prior geomorphic features, including a small pond along the down stream end, but rather significant

TRANSPORT AND REWORKED AREA

N = 10

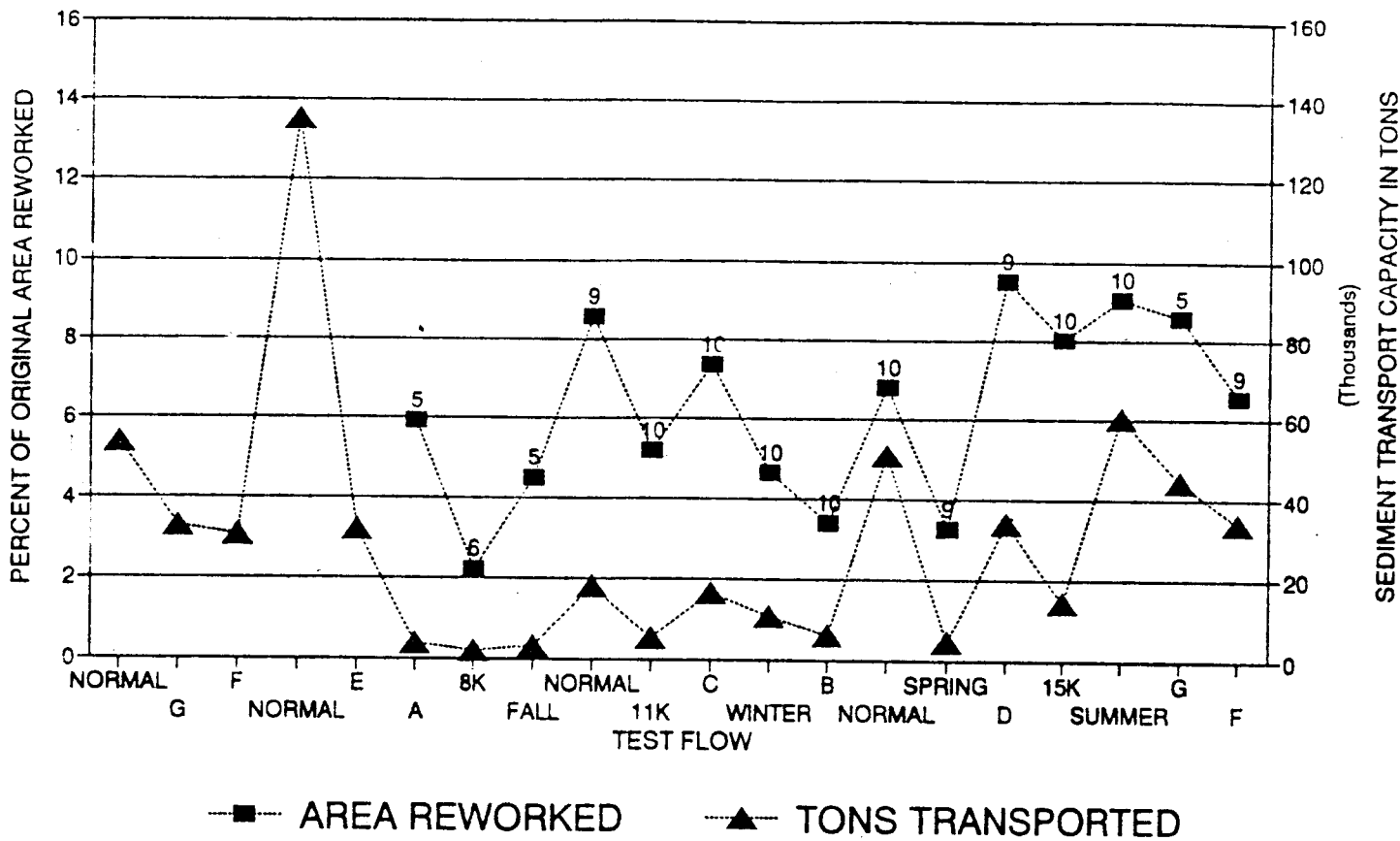


Figure 4. Graph of sediment transport capacity and reworked area for the study period. Numbers above solid blocks indicate sample size out of 10 sites chosen for this report.

REWORKED AREA VS TRANSPORT

N = 10

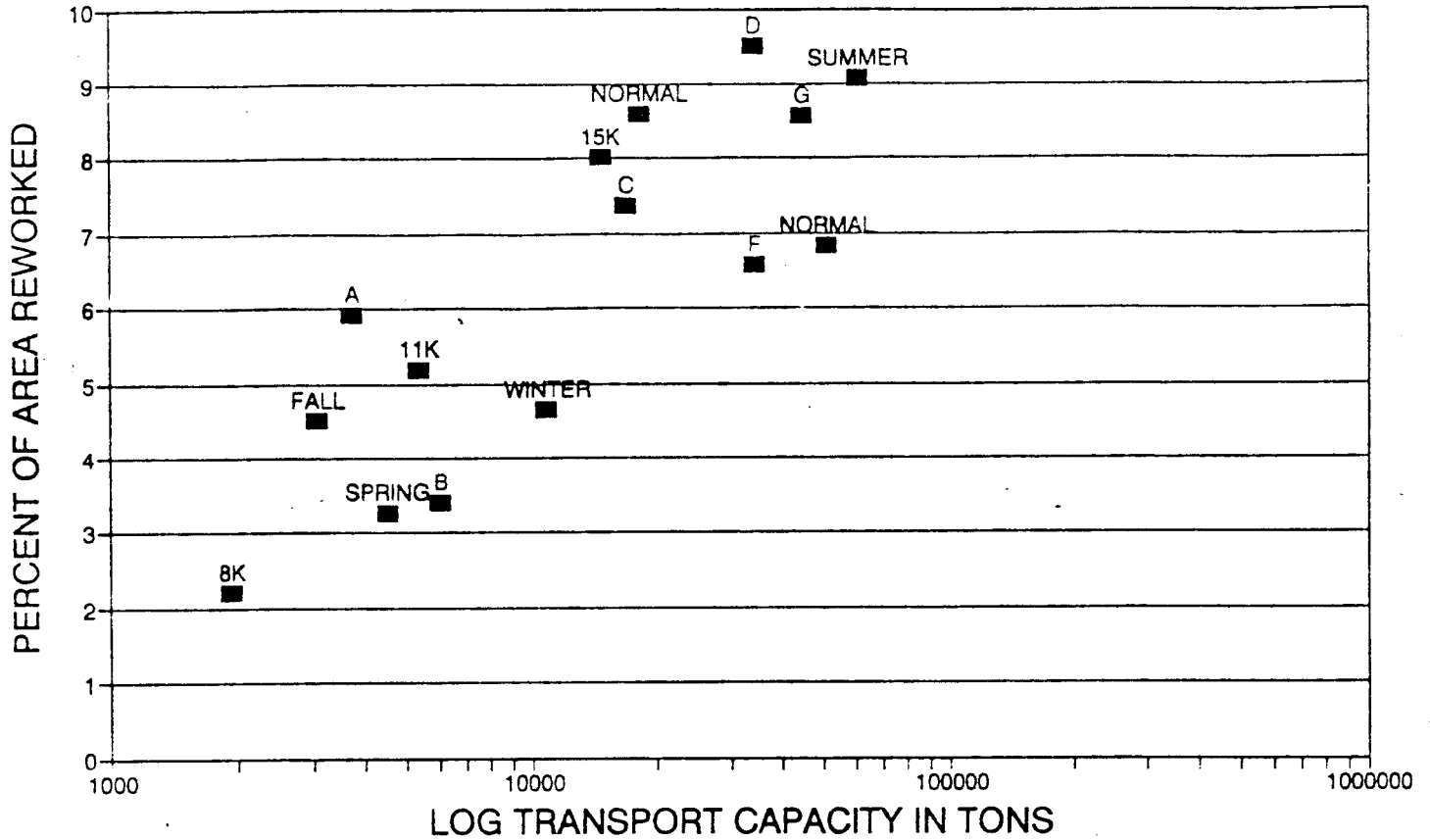


Figure 5. Graph of log transport capacity and percent of area reworked for the test flows included in this report.

REWORKED AND NET AREA

N = 10

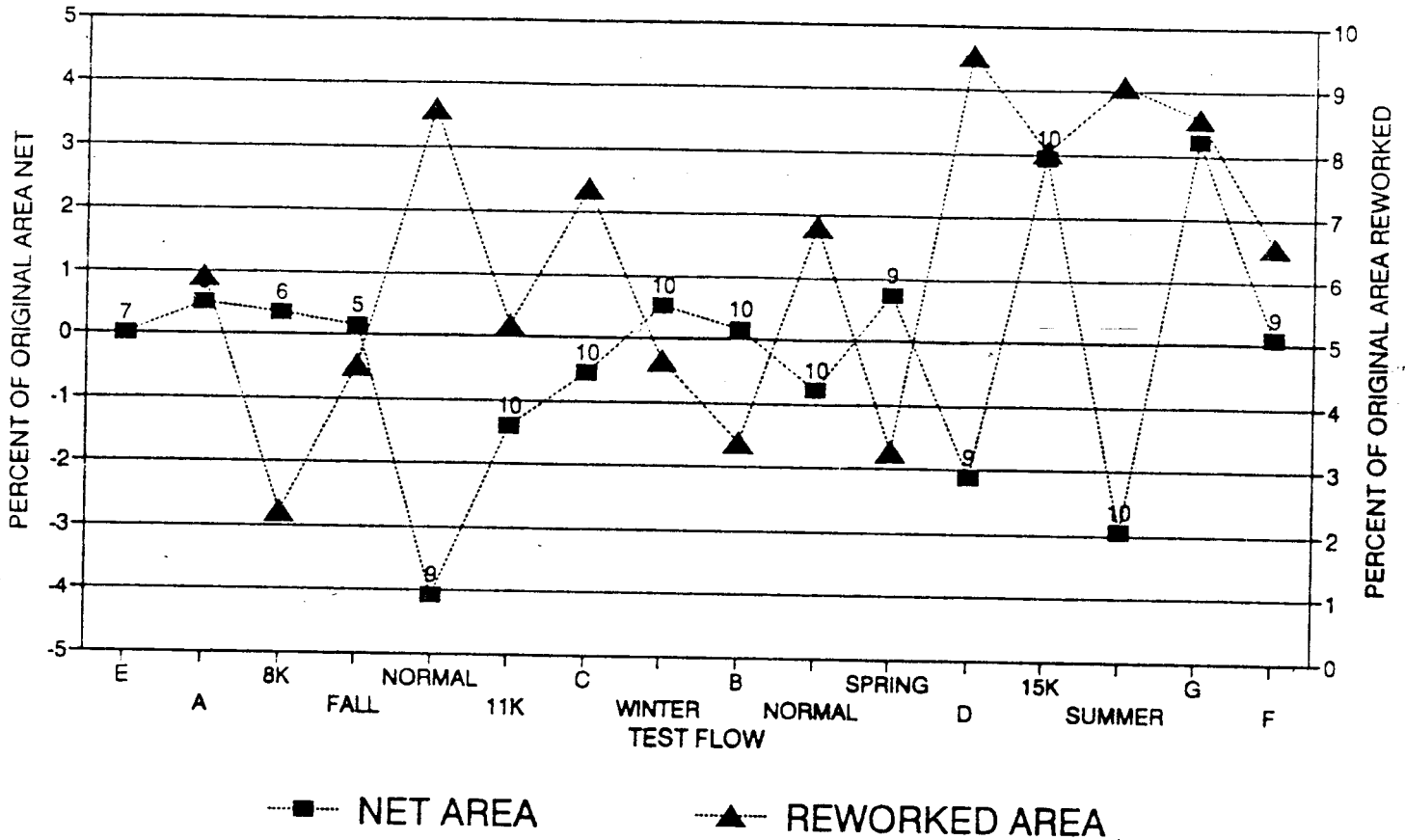


Figure 6. Graph of reworked and total areas for each of the test flows studied in this report. The numbers over the solid blocks indicate the number of sites measured, out of ten possible.

erosion occurred along the whole river side of the deposit involving 2,440 meters², 10% of the total area. This change would probably be unnoticed by any casual observer. The CR 66 L site also underwent erosion localized at the down stream end, accompanied by deposition within preexisting erosion features (Fig. A7b). The total result was enlarged area of about 30 meters². There were no other photos captured that allow analysis of sand bars for the "A" test flow.

This pattern of change, at two sites, indicates that the "A" test flow concentrated its energy on the lower portions of the deposits, and although it fluctuated from 3,000-13,000 cfs, it eroded materials that were probably deposited or stable during the previous "E" test flow that fluctuated from 3,000-26,000 cfs.

"8,000" cfs constant test flow This test was the least energetic of any of the test flows (Fig. 3) and reworked about 2% of total sand bar area for the 6 sites sampled. Overall, it resulted in about 1% decreased area (Fig. 6). This constant flow created minor cut banks at most sites. However, the low constant flow test resulted in significant sand bar change at only one site. At CR 43 L 215 meters² (0.5%) were aggraded during the 11-day test period (Fig. A3d).

The "8,000" cfs constant flow created minor cut banks along the bars either from direct stream scouring or simply from surface waves that were concentrated at the constant river stage. The slight area loss associated with cut bank formation is probably due to the prior steepness of slopes created during the highly energetic "E" (Fig. 3) test flow in September 1990.

"Normal Fall" test flow The "Normal Fall" test flow fluctuated irregularly from about 2,000-14,000 cfs on average for 11 days. Overall the "Fall" test reworked about 4.5% of the sand bar area and slightly decreased total area by about 0.25% (Fig. 6). The notable results were erosion of about 330 meters² at CR 43 L (0.8%) (Fig. A3e). This involved material that was deposited during the previous 8,000 cfs constant flow.

Although the fluctuations were small, the "Fall" test reversed the trend of deposition that occurred locally at CR 43 L. This may be due to renewed rill formation and seepage erosion (Table 3).

"Normal Flow" test The "Normal Flow" period lasted for 33 days, and fluctuated daily from about 2,000-15,000 cfs on average. There were discharge spikes to over 20,000 cfs and weekend low flows during this test flow. There was also twice daily discharge peaking. The overall effects of this test were increased reworking (about 8.5%) and decreased total area (about 4%) (Fig. 6). The results of this flow were discretely measured at sites CR 51 L and CR 66 L. At CR 51 L a large semi-circular area (about 1,800 meters²) was eroded from the bar near the reattachment point (Fig. A6d). This was probably due to development of a secondary recirculating eddy. At CR 66 L a similar semi-circular area was eroded, also near

the reattachment point, that involved about 660 meters² (Fig. A7d). This event was also probably due to development of a secondary eddy.

The overall total area loss associated with the "Normal Flow" test is probably a response to increased energy and daily fluctuation range acting upon materials that were shifted to lower positions during the prior low energy "A", "8,000", and "Fall" test flows (Fig. 3). Development of secondary recirculating eddies indicates that the change to higher flow regime scoured some deposits through main channel processes that were not measured.

"11,000 cfs constant" test flow This 11-day constant flow test produced cut banks at all deposits and reworked sediment on most. The overall results were reworking of about 5% of the sand bar area and an increase in total area of about 2.5% from the previous test flow (Fig. 6). The greatest changes were at CR -6.5 R, CR 45 L, CR 47 R, and CR 51 L. At CR -6.5 R about 130 meters² of material eroded from the low elevation portion of the bar (Fig. A1e). At CR 45 L an apron of sediment was deposited around the entire eddy, indicating a general lowering and reduction of slope of the previous deposits (Fig. A5c). At the CR 51 L site the secondary eddy that formed during the previous flow test continued to erode material from that part of the bar (Fig. A6e).

The mixed results from the "11,000" cfs test were a combination of cut bank development and deposition of cut bank derived materials at lower positions, thus increasing sand bar area exposed at 5,000 cfs. The previous test flow had a higher peak discharge than the preceding 3 tests and probably formed over-steepened deposits at many locations. These deposits responded rapidly to the fairly energetic "11,000" cfs constant flow (Fig. 3), and any surface waves would have concentrated at the river stage corresponding to 11,000 cfs.

"C" test flow The "C" test flow was for 11 days and involved regular fluctuations from 8,000-20,000 cfs daily. Overall the "C" test reworked about 7.5% of the original area and increased total bar area by about 1% over the previous area (Fig. 6). Specifically, CR 43 L increased in area, especially at the upstream end where sediment is scoured from the base of the large rock (Fig. A3g). At CR 47 R the reattachment platform was eroded, but the downstream end of the reattachment bar was widened (Fig. A5g). The platform deposit at CR 51 L was further eroded, but deposition occurred over most other area along the bar face (Fig. A6f). The semi-circular secondary eddy feature at CR 66 L eroded deeper into the deposit and impinged on the vegetated portion (Fig. A7f). At CR 68 R erosion in the return flow channel enlarged this scour feature, but the separation bar experienced deposition (Fig. A8c). Deposition also occurred at CR 81 L along most of the upstream end (Fig. A9e). At CR 172 L, the reattachment bar eroded significantly (675 meters², 11%) while minor aggradation occurred along the bank within the eddy zone and along the separation deposit (Fig. A10e).

In general, this test flow deposited material on separation bars and eroded material from reattachment bars. This indicates that the stagnation areas at separation bars and reattachment bars were generally enlarged. Sediment that was deposited at higher positions

during the "C" test had been moved to lower positions during the prior "11,000" cfs test flow.

"Normal Winter" test flow The 11-day "Normal Winter" test flow fluctuated daily from about 2,500-18,000 cfs in an irregular fashion with daily double peaks. It produced a small amount of deposit reworking (about 4.5%) and resulted in a slight (1%) increase of total sand bar area (Fig. 6). Individually, at CR -6.5 R deposition covered the area that had eroded during the 11,000 constant and "C" flows (Fig. A1g). At CR 45 L erosion occurred over the whole perimeter except for the slip face of the reattachment platform (Fig. A4f). The river-side face of the reattachment bar at CR 47 R lost the material previously deposited (Fig. A5e). At CR 51 L more of the platform deposit eroded, but the river-side face was widened, and the small pond was retained in a new position (Fig. A6f). The entire perimeter of CR 66 L received a narrow band of newly deposited material (Fig. A7g). At CR 68 R the return flow channel eroded, but the river-side face of the reattachment and separation bars built up (Fig. A8d). The entire perimeter of CR 172 L eroded during this test with deposition of an island in the eddy zone (Fig. A10f).

The pattern of area changes during the "Winter" test flow was similar to the patterns during the preceding "C" test flow. This indicates that most sand bars responded positively to decreased energy (Fig. 3), although the daily double peak may have actually increased the peak flow duration from the prior "C" test flow. At some distance downstream of the Dam, there may have been little difference between the "C" and "Winter" tests.

"B" test flow The "B" test flow fluctuated daily from 5,000-15,000 cfs on a regular schedule for 11 days. Overall it resulted in reworking about 3.5% of all sand bar area, and the total result was negligible area change (-0.25%) (Fig. 6). Locally, the "B" test flow eroded the face of CR 43 L (Fig. A3i) about 134 meters², deposited material around the perimeter of CR 45 L (Fig. A4g), continued to erode the platform deposit at CR 51 L (Fig. A6g), and eroded most the perimeter of CR 172 L except for minor deposition on the reattachment platform (Fig. A11g).

The comparatively small fluctuations of the "B" test, following the much greater fluctuations of the preceding "C" and "Winter" tests apparently resulted in little overall effect on the sand bars.

"Normal Flows" period The 67-day "Normal Flow" period fluctuated irregularly daily from average lows of about 3,000 cfs to average highs of about 17,000 cfs, with weekend low flows that fluctuated much less. Each daily fluctuation was usually double peaked. The overall result was a large reworked area (about 7%) and a total decrease (1%) in total area (Fig. 6). Specifically, at CR 8 L the upstream portion eroded about 35 meters² (Fig. A2i). At CR 45 L the perimeter of the reattachment deposit eroded about 860 meters², but the separation deposit aggraded about 250 meters (Fig. A5g). Erosion removed the remaining platform deposit at CR 51 L (Fig. A6h). The eddy at CR 66 L underwent major rearrangement with erosion along the main deposit body and deposition of a large island in the eddy zone

(Fig. A7i). At CR 68 R the whole reattachment deposit face eroded about 460 meters² and the separation bar changed little (Fig. A8f). At CR 172 L the reattachment deposit aggraded considerably (about 550 meters²) as did the banks within the eddy zone (Fig. A10h). However, the platform deposit and eddy island were eroded about 250 meters². The separation bar aggraded slightly.

This pattern of sand bar change is highly random, and reflects the randomness of pattern in the "Normal Flow". The pattern also suggests that individual sand bars may be subjected to different flow dynamics from the same release patterns depending on local channel geometry or flow routing characteristics as flows migrate downstream.

"Normal Spring" test flow The "Normal Spring" test ran for 11 days and fluctuated on average from about 3,000 cfs to 12,000 cfs with a weekend period of fluctuations from 3,000-8,000 cfs. The overall result of this test flow was a very small reworked area (about 3.5%) and a slight increase in total area (about 1%) (Fig. 6). The CR 51 L site eroded during this test period by about 1,400 meters² along the whole perimeter (Fig. A6i). The CR 66 L site aggraded about 900 meters² during the same period mostly within the eddy zone (Fig. A7j). Reworking with little total area change was the norm at all other sites.

The "Spring" test flow was not much different in range or daily energy from the preceding "Normal" test flow (Fig. 3). Consequently, sand bar responses were similarly random.

"D" test flow The "D" test flow fluctuated daily and regularly from 3,000-26,000 cfs for 11 days. This was a high energy test flow (Fig. 3) and resulted in the highest amount of reworked area during the study period (about 9.5%). The total result was a slight decrease (2.5%) in sand bar area (Fig. 6). Aggradation resulted on the CR -6.5 R, CR 8 L, and CR 43 L sites (Figs. A1k, A2k, and A3l). Mixed erosion and deposition occurred on the other sites. At CR 45 L erosion occurred everywhere except at the platform deposit which lengthened (Fig. A4j). At CR 47 R erosion occurred on the platform deposit and a thin deposit was laid down along the river-side face (Fig. A5i). At CR 51 L the platform enlarged as did the downstream river-side face, but another secondary eddy formed that eroded a semi-circular area along the middle of the bar (Fig. A6j). At CR 66 L the return flow channel aggraded but the upstream face eroded (Fig. A7k). CR 81 L also increased in size through deposition of about 20 meters² (Fig. A9j). Photography was missed at CR 68 R and CR 172 L for this epoch.

This pattern of area change resulting from the "D" test flow indicates that in general flow separation points moved downstream and recirculation zones were larger and probably of greater velocity than during the preceding "Normal" and "Spring" fluctuating flows. The resulting sand bar morphologies reflect the general response to enlargement of recirculation zones from a high fluctuation test flow.

"15,000" cfs constant test flow The "15,000" cfs constant flow lasted 11 days. Overall it reworked about 8% of the total sand bar area and resulted in an increase in total area (5%)

(Fig. 6). CR -6.5 R responded with erosion of about 140 meters² (Fig. A1l) while CR 8 L aggraded by about 170 meters² (Fig. A2l). CR 45 L responded to the "15,000" constant flow with aggradation over most of the perimeter by about 2,800 meters² (Fig. A4k). The platform deposit shortened slightly. The platform deposit at CR 51 L eroded as did the extreme downstream end of the river-side face (Fig. A6k). At CR 66 L the eddy zone eroded while the upstream portion aggraded (Fig. A7l). Reversal of the previous behavior occurred at CR 68 R, with erosion of the return flow channel and deposition on the separation bar (Fig. A8h). CR 81 L remained much as it was before the test flow (Fig. A9k). Sometime during the "D" or 15,000 cfs tests the CR 172 L site aggraded by deposition on the platform deposit of about 500 meters² of sediment.

The pattern of sand bar changes resulting from the "15,000" cfs constant flow indicates that at sites with low separation bars (ie, CR 68 R), the 15,000 cfs constant flow provided sufficient current of sufficient duration to scour sediment. This material was however probably redeposited in the reattachment environment. Generally, the "15,000" cfs flow following the high fluctuation "D" test flow redistributed sediments that were reworked during "D", and deposited them at lower positions along the toes of reattachment bars to increase area exposed at 5,000 cfs.

"Normal Summer" test flow The "Normal Summer" test was for 26 days in June 1991, and fluctuated daily from about 5,000 cfs to about 25,000 cfs on average. Each daily fluctuation was unique, often with double peaks. Three weekend low fluctuations occurred that ranged from 5,000 to about 16,000 cfs. This was a high energy flow test (Fig. 3) that reworked about 9% of the sand bar area on average and decreased overall total area by about 6% (Fig. 6). The upstream end of CR 43 L eroded about 125 meters² around the large rocks (Fig. A3n). At CR 45 L significant erosion occurred around the reattachment deposit (about 1,800 meters², 0.8%) (Fig. A4n). The whole perimeter of CR 47 R eroded, involving about 1,900 meters² of sediment (Fig. A5k). CR 51 L however aggraded by about 1,200 meters² (Fig. A6l). The CR 66 L site showed mixed results, both aggradation and erosion, largely reversing the prior events during the "15,000" flow. Photography was not captured at CR 68 R. Aggradation occurred at CR 81 L even though tunnel scour features were present (Fig. A9l) (see next section). At CR 172 L nearly the whole perimeter eroded (about 890 meters²) but the platform deposit lengthened.

This pattern of sand bar morphology change indicates that the "Summer" test flow disrupted the deposits that were enlarged during the preceding "15,000" cfs constant flow test. This may be a response to the duration of the test, the range of fluctuations, or the weekend low fluctuation periods. Carpenter and Carruth (1992) showed that bank failure events often occurred following weekend low-flow periods at CR 172 L. Cluer (1992) documented bank failures at four other sites that occurred immediately after weekend low flow periods.

"G" test flow The "G" test flow involved 11 days of regular fluctuations from 8,000 cfs to 27,000 cfs daily. Overall, "G" reworked about 8.5% of the sand bar area and resulted in a dramatic total increase of area by about 6% (Fig. 6). Many of the sites are not represented by photographs for this test flow. However, the prior trends of aggradation and erosion were

largely reversed at sites CR 47 R, CR 51 L, and CR 172 L. At CR 47 R the whole perimeter aggraded by about 1,925 meters² (Fig. A5l). CR 51 L eroded over its whole perimeter, about 1,690 meters² (Fig. A6m). Deposition occurred at CR 172 L along the river-side face, around the eddy zone, and on the separation deposit. Some erosion on the platform area created an island of the platform deposit (Fig. A10l).

The mixed results of the "G" test flow may in part be due to the smaller than normal sample size. The pattern of changes indicates that the high energy flow test (Fig. 3) resulted in highly erratic responses. Because of the smaller than normal sample size, the aggradation measured at CR 47 L dominates the analysis.

"F" test flow The "F" test flow had the same daily fluctuation range as "G", 8,000-27,000 cfs, but with a lower ramping rate. This resulted in shorter duration at peak discharge and consequently was a low energy flow (Fig. 3). It reworked about 6.5% of the sand bar area and were eroded in total area by about 3% (Fig. 6). The entire perimeters of CR 8 L and CR 43 L were eroded (Figs. A2o and A3o). CR 47 L was slightly enlarged by deposition along the downstream river face and in the eddy zone (Fig. A5m). Aggradation also increased the size of CR 51 L along most of its perimeter (Fig. A6n). Minor reworking occurred at CR 66 L with little total change in area (Fig. A7n). The prior trends at CR 172 L were reversed during the "F" flow. Erosion occurred along the downstream river-side face, within the eddy zone, on the platform deposit, and on the separation bar.

The pattern of change associated with the switch from "G" to "F" test flows indicates that a flow with the same range but shorter duration at peak results in total loss of sand bar area. This suggests that duration at peak discharge is an important variable in sand bar response. This is illustrated in the sediment transport model comparing test flows "G" and "F" (Fig. 3). Conversely, the comparison may also indicate that the "G" and "F" flows were not all that different, especially at some distance downstream, only that there was insufficient sediment stored for aggradation to continue during the "F" test flow as it had during the "G" test flow. Further sediment transport modeling should clarify this issue as would a larger sample size for analysis.

Seepage Related Features

Seepage of residual bank-stored water following river stage lowering causes a spring line to develop at the contact point of sand bar surface and ground water surface (Werrell et al, 1992). Below this line erosion features often developed when residual head was great enough. The most common features were rills and rill totalworks, and occasionally larger scale tunnel scour (Howard and McLain, 1988) features developed. Residual head increases where daily stage fluctuation is high and where sand bar slope is great. Sites where these features commonly developed along the river-side face were CR 43 L and CR 81 L. At other sites rills commonly developed along the steep slip faces of return flow channels (Fig. 2). Werrell et al (1992) showed that deposition and seepage erosion operate simultaneously on Grand Canyon sand bars, but that either process may dominate given certain flow conditions.

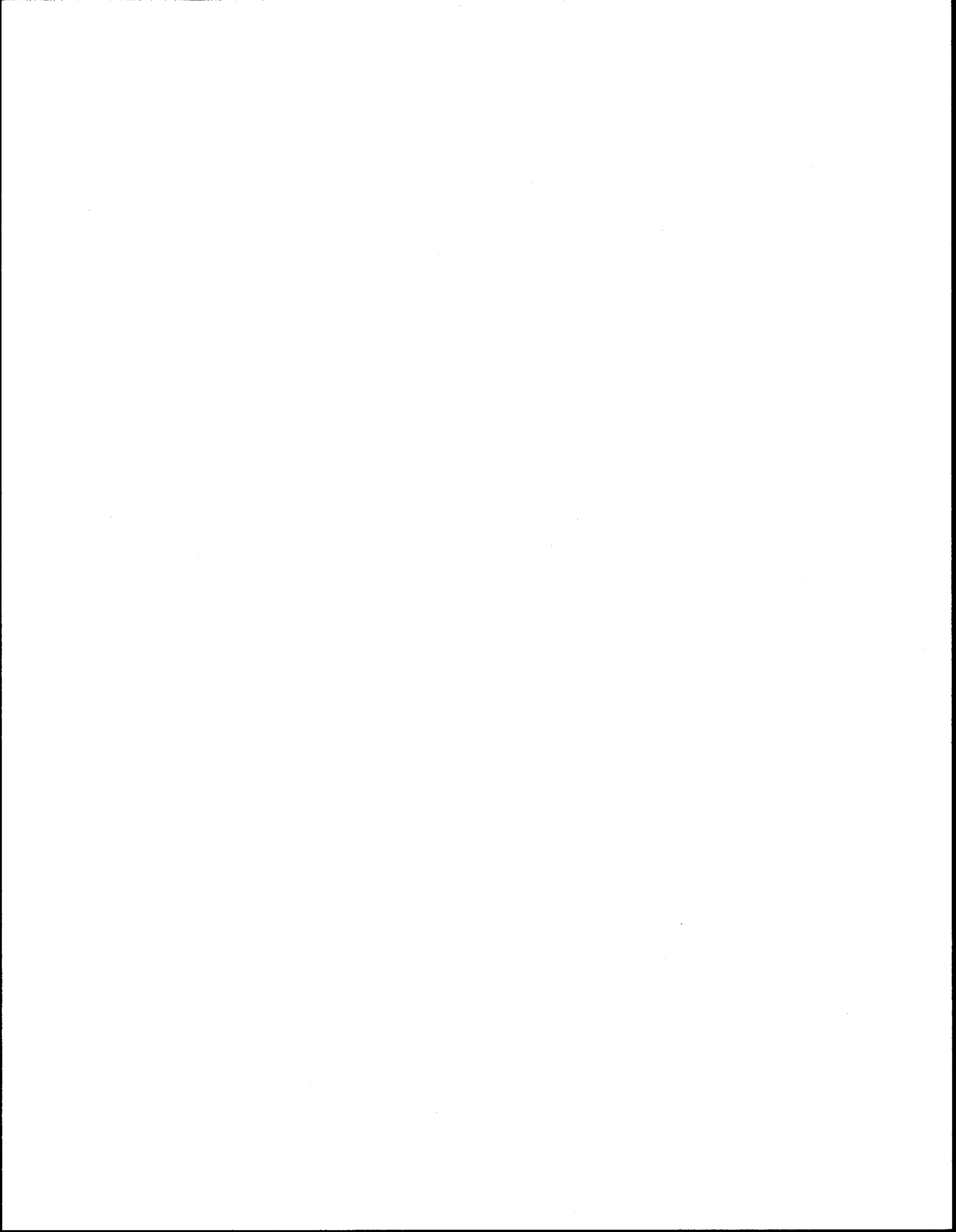
The test flows that resulted in seepage processes were generally those with high stage fluctuations. However, every fluctuating flow resulted in rills at sites CR 43 L, CR 45 L, and CR 81 L. These observations are summarized in table 3.

Table 3. Summary of seepage features and associated test flows.

SITE/ FLOW	CR - 6.5 L	CR 8 L	CR 43 L	CR 45 L	CR 47 R	CR 51 L	CR 66 L	CR 68 R	CR 81 L	CR 172 L
"A"			r	r				r	r	
8,000 c										
Fall			r	r					r	
11,000 c										
"C"			r	r		r	r		r	
Winter			r	r			r	r	r	
"B"			r	r					ts	
Normal			r	r					ts	
Spring			r	r					r	r
"D"			r	r					r	r
15,000 c										
Summer			r	r					r	r
"G"			r	r					ts	r
"F"			r	r					ts	r

Key: r = rills, ts = tunnel scour

Formation of seepage features often accompanied deposition of new sediment along the face of sand bars. Site CR 81 L was unique in the size of tunnel scour features that developed (Figs. 7 and A9I). The "B", "Normal", "G", and "F" test flows all resulted in tunnel scour at CR 81 L, and were all high energy flows. The "C" and "Normal Winter" test flows resulted in rill development at five out of ten sites. The "A", "Normal Spring", and "D" test flows produced rills at four out of ten sites.



CONCLUSIONS

The strong correlation between calculated sediment transport capacity and reworked area for the test flows during the study period indicates that this method of comparison may result in an accurate tool for predicting sand bar responses to alternative flow regimes. This would require completing development of the aerial photography database. Currently, the sample size is too small to allow confident prediction.

The changes documented at CR 51 L suggest that major sediment erosion or deposition can occur while leaving almost imperceptible change in overall geomorphology. Even subtle features such as the small pond on the river-side face were retained during large changes in area. This suggests that sand bars may appear stable when in fact they are dynamic. CR 47 R and CR 51 L responded to the test flows most often by erosion, and ultimately were 11% and 13% smaller, respectively, than in the beginning. Total area changes at the other sites were: -3% at CR -6.5 R; -2% at CR 8 L; no change at CR 43 L; +7% at CR 45 L; -2% at CR 66 L; +3% at CR 68 R; +4% at CR 81 L; and -6% at CR 172 L. The large losses at CR 47 R and CR 51 L are unique for the test flow period, and may indicate a local deficiency of sediment storage in the main channel, resulting in reductions of storage from eddy deposits.

In general, during the test flow program, reductions in stream energy and range of daily fluctuations following flows with higher energy and fluctuation ranges resulted in increased area. This was due to reworking of over-steepened deposits created during highly fluctuating flows. Conversely, flows with increased energy and fluctuation ranges following low energy low fluctuation range flows resulted in decreased area. This is due to reworking of sediments that were previously shifted to lower positions and deposition at higher positions. The long term effects of this type of deposit increase are not clear, and should be studied further.

The "15,000" cfs constant flow following the high energy "D" test flow produced the largest total gain in area. This was due to reworking sediments that were deposited at higher positions and steep slope angles by the "D" flow. This observation has implications for planning bar building test flows.

Overall, this investigation concludes that regularly fluctuating flows were less damaging than the irregularly fluctuating "Normal" flows that included weekend low fluctuation periods. The flows that most positively increased sand area were the "15,000" cfs constant and the "G" test. The flows that most obviously resulted in total erosion were the "Normal" flow in November and December 1990, and the "Summer" flow test.

RECOMMENDATIONS

The potential benefits of completing the development of the aerial photography database are significant. A large sample size is necessary to understand the range of effects particular flow regimes have on the wide variety of fluvial deposits along the Colorado River. This report includes analyses for 10 out of 75 sites photographed during the test flow program. Full development of this database is strongly recommended. With this database as background, the current interim flow period should be evaluated by similar methods, provided that periods of 5,000 cfs constant discharge are possible for photo capture.

The response rates of sand bars to the particularly highly erosive and gaining test flows need to be understood. Similarly, the long-term effects of the clearly aggradational or degradational test flows need to be understood before the full range of flow alternatives can be evaluated. There is a need for daily evaluation of a large sample of sand bars to determine short-term temporal and spatial responses, so that prediction of responses at longer temporal scales may become possible. Further modeling of the test flow dynamics is suggested. One interesting question is how sediment transport capacity changes with distance downstream in this system.

REFERENCES CITED

- Carpenter, M.C., and Carruth, R.L., 1992. Hydrogeology of beaches 43.1L and 172.3L and the implications on flow alternatives along the Colorado River in the Grand Canyon. *in* Beus, S.S., and Avery, C.C., 1992. The influence of variable discharge regimes on Colorado River sand bars below Glen Canyon Dam: 1991 Annual Report.
- Cluer, B.L., 1992. Daily responses of Colorado River sand bars to Glen Canyon Dam test flows, Grand Canyon, Arizona. *in* Beus, S.S., and Avery, C.C., 1992. The influence of variable discharge regimes on Colorado River sand bars below Glen Canyon Dam: 1991 Annual Report.
- Howard, A.D., and McLain, C.F., III, 1988. Erosion of cohesionless sediment by groundwater seepage. *Water Resources Research*, v.24, n.10, p.1659-1674.
- Schmidt, J.C., and Graf, J.B., 1988. Aggradation and degradation of alluvial sand deposits 1965 to 1986, Colorado River, Grand Canyon National Park, Arizona. U.S. Geological Survey, Open-File Report 87-555.
- Smillie, G., Jackson, W.L., and Tucker, D., 1992. Colorado River sand budget: Lees Ferry to Little Colorado River including Marble Canyon. *in* Beus, S.S., and Avery, C.C., 1992. The influence of variable discharge regimes on Colorado River sand bars below Glen Canyon Dam: 1991 Annual Report.
- Werrell, W., Inglis, R., Jr., and Martin, L., 1992. Beach face erosion in Grand Canyon National Park. *in* Beus, S.S., and Avery, C.C., 1992. The influence of variable discharge regimes on Colorado River sand bars below Glen Canyon Dam: 1991 Annual Report.

ACKNOWLEDGMENTS

Bill Jackson and Gary Smillie of the National Park Service Water Resources Branch provided valuable direction and support in modeling the test flows to determine sediment transport capacity. Tim Randle of the Bureau of Reclamation in Denver provided updated transport functions and necessary discussion prior to modeling. John Rote and Don Bills at the Flagstaff Field Office USGS provided the basic hydrographic information that was input to the sediment transport model. Certainly not least, Sherman Wu and his staff at the USGS Platotalary Mapping Division in Flagstaff provided unending creativity and persistence in utilizing the flawed images, and made the aerial photography analysis possible.

APPENDIX A

**RESPONSE CURVES OF INDIVIDUAL SITES AND
PLANIMETRIC OUTLINES ARRANGED BY TEST FLOW**

SITE -6.5 RIGHT

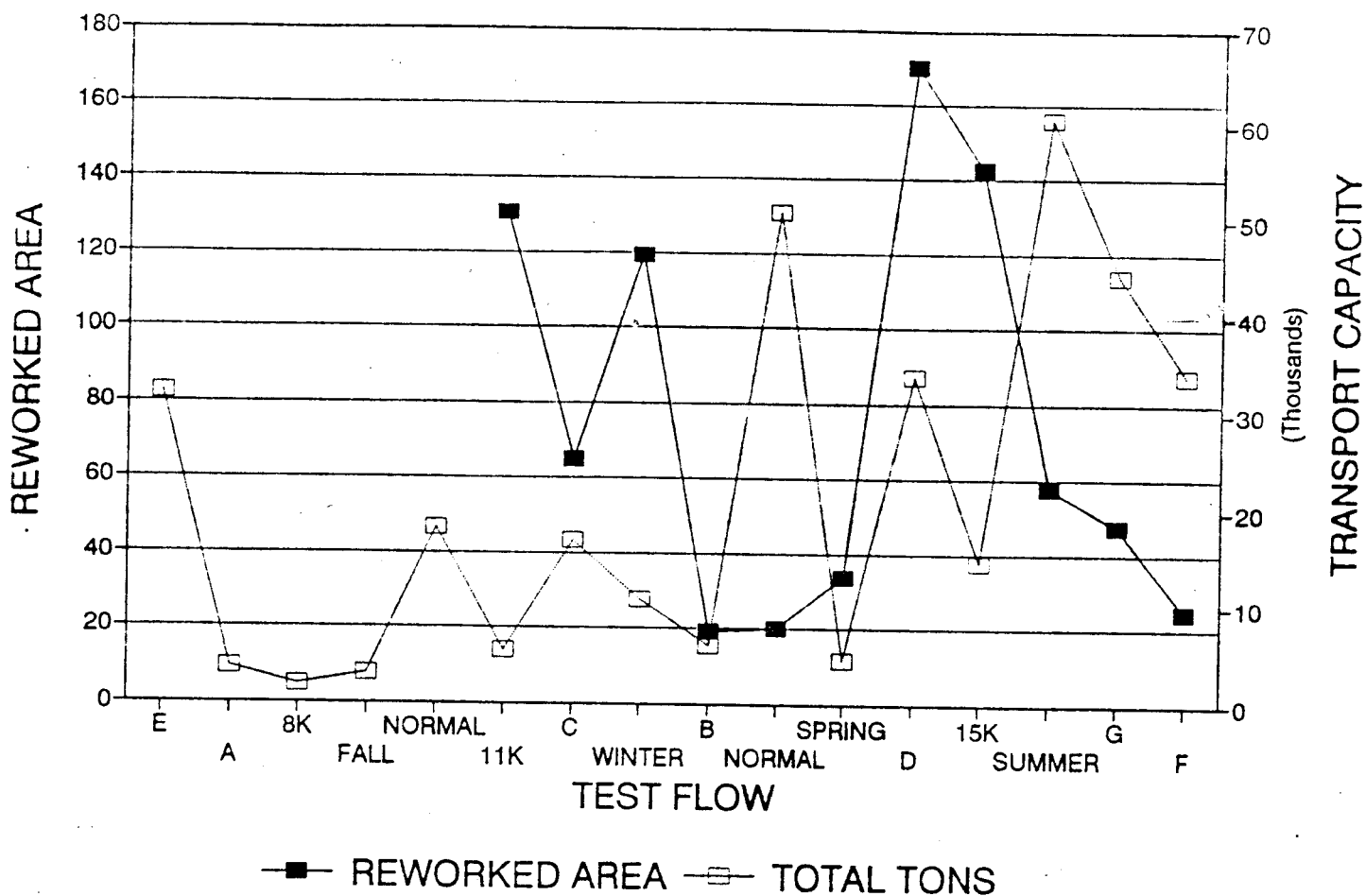


Figure A1. Time-series plot of reworked area and sediment transport capacity for site CR -6.5 R.

Figures A1a-A1i. Original planimetric outlines and subsequent comparisons of bracketing outlines. Dark shaded areas were eroded. Light shaded areas were aggraded.

A1a



12/17/90

A1b



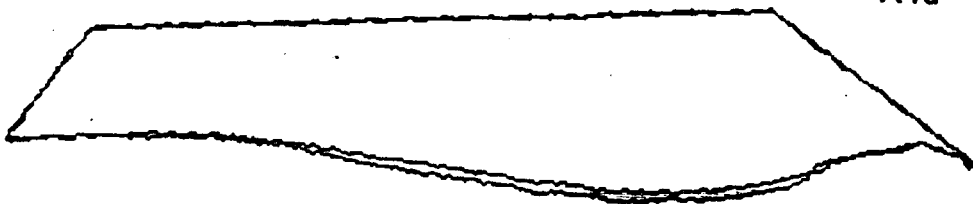
12/17/90 12/30/90 11,000 cf

A1c



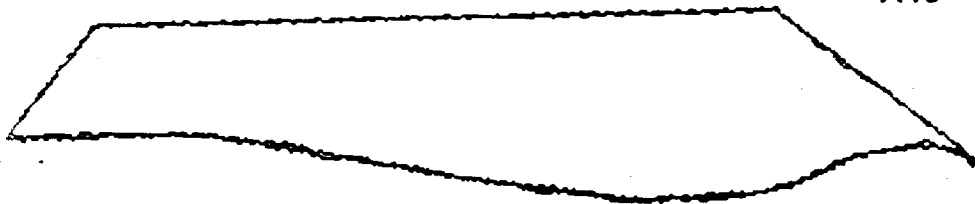
12/30/90 01/12/91 "C"

A1d



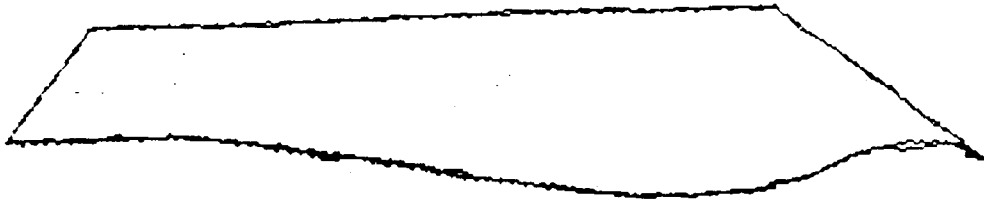
01/12/91 01/26/91 WINTER

A1e



01/26/91 02/09/91 "B"

A1f



02/09/91 04/20/91 NORMAL

A1g



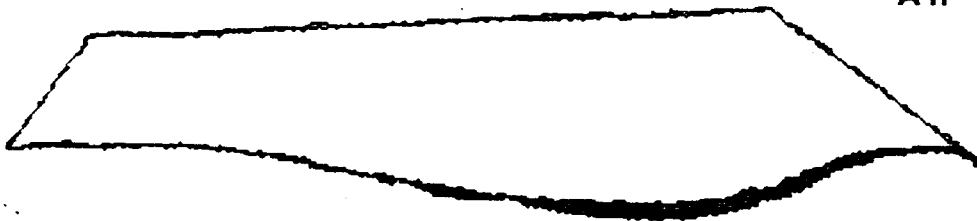
04/20/91 05/05/91 SPRING

A1h



05/05/91 05/19/91 "D"

A1i



05/19/91 06/02/91 15,000 cf

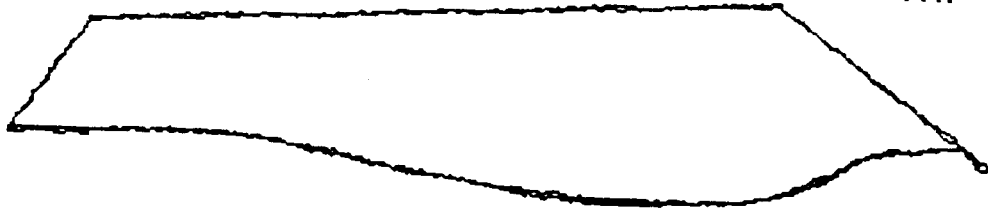
A1j



06/02/91 06/30/91 SUMMER



06/30/91 07/14/91 "G"



07/14/91 07/27/91 "F"

SITE 8 LEFT

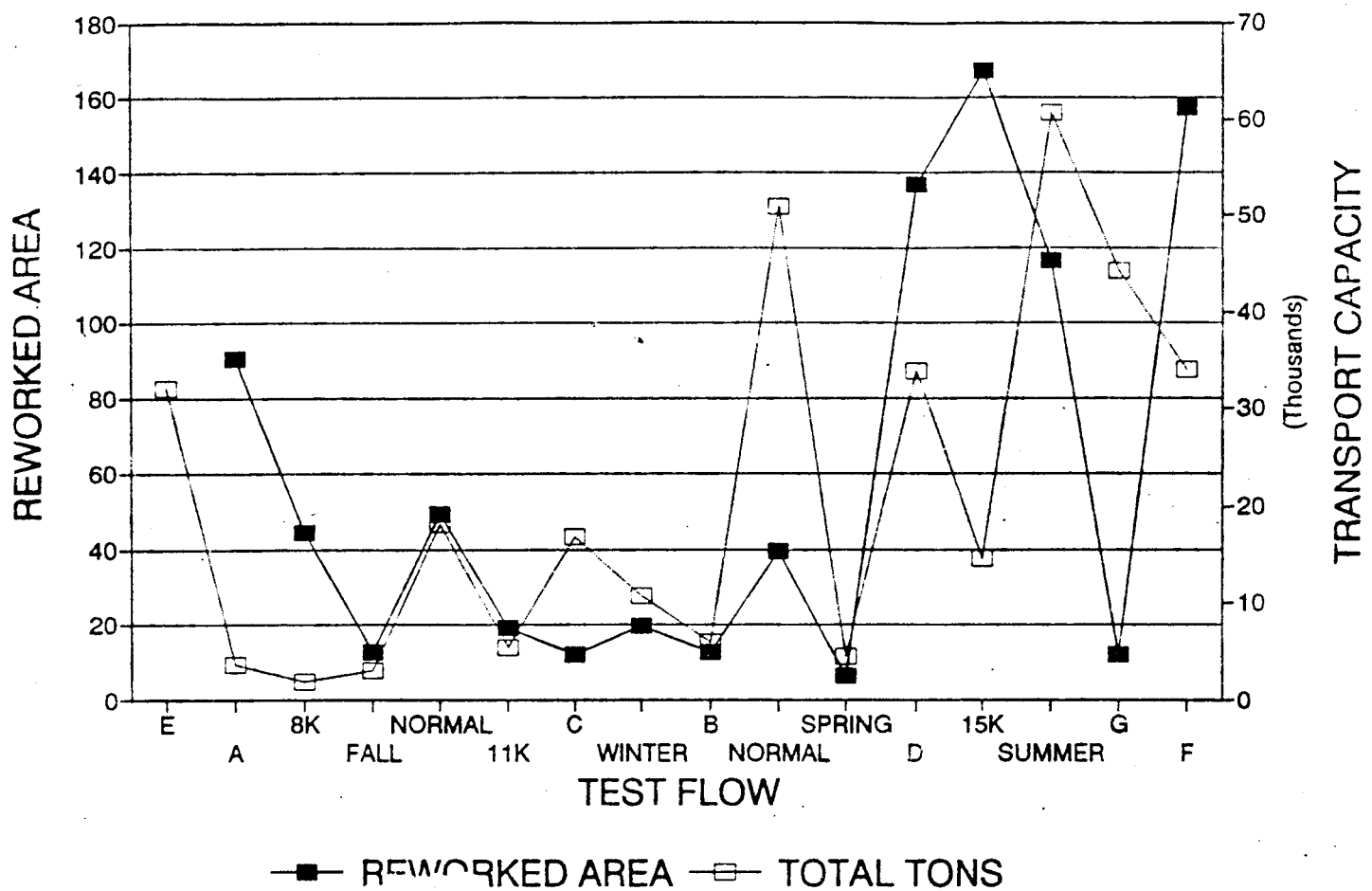
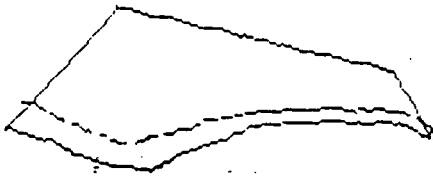


Figure A2. Time-series plot of reworked area and sediment transport capacity for site CR 8 L.

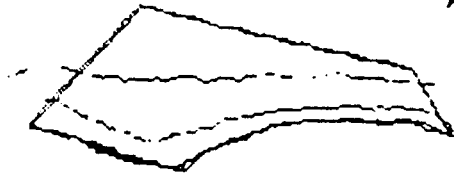
Figures A2a-A2n. Original planimetric outlines and subsequent comparisons of bracketing outlines. Dark shaded areas were eroded. Light shaded areas were aggraded.

A2a



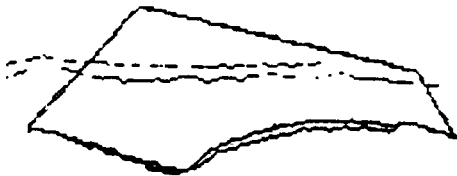
10/30/90

A2b



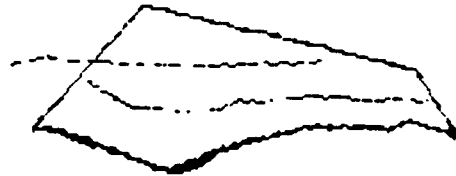
10/30/90 11/11/90 FALL

A2c



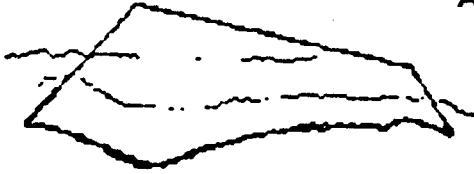
11/11/90 12/17/90 NORMAL

A2d



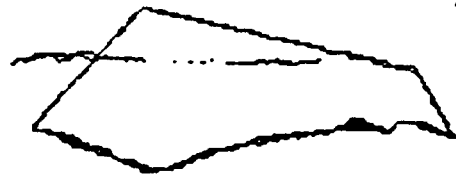
12/17/90 12/30/90 11,000 cfs

A2e



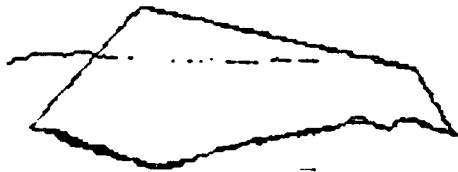
12/30/90 01/12/91 "C"

A2f



01/12/91 01/26/91 WINTER

A2g



01/26/91 02/09/91 "B"

A2h



02/09/91 04/20/91 NORMAL

A2i

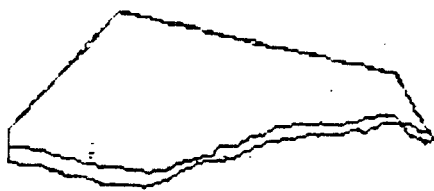


04/20/91 05/05/91 SPRING

A2j



05/05/91 05/19/91 "D"



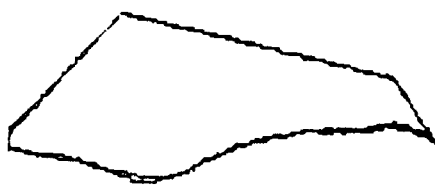
A2k

05/19/91 06/02/91 15,000 cfs



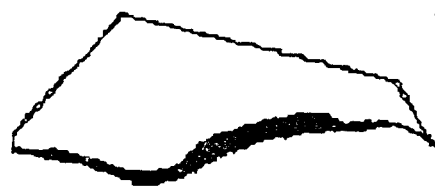
A2l

06/02/91 06/30/91 SUMMER



A2m

06/30/91 07/14/91 "G"



A2n

07/14/91 07/27/91 "F"

SITE 43 LEFT

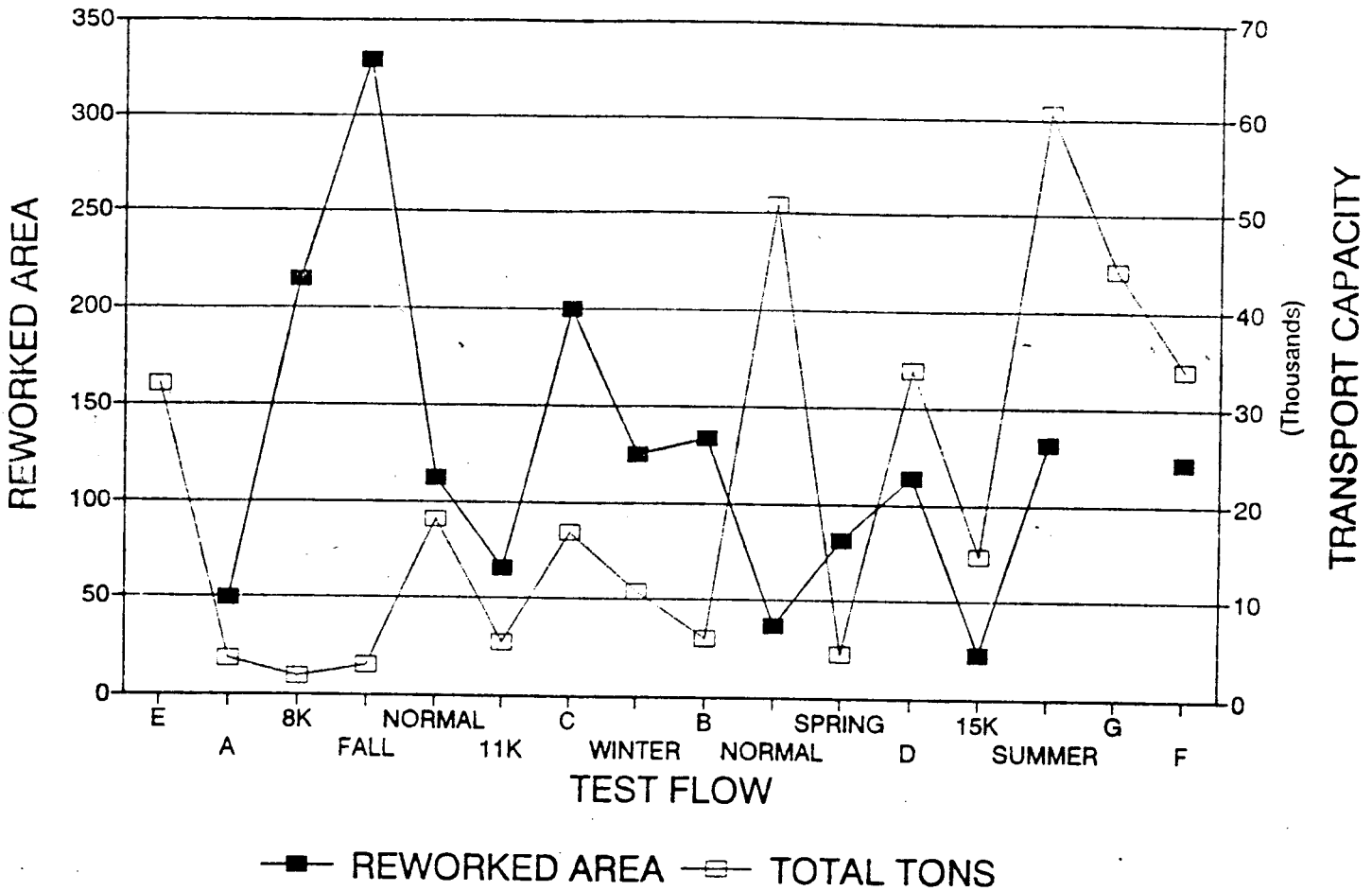
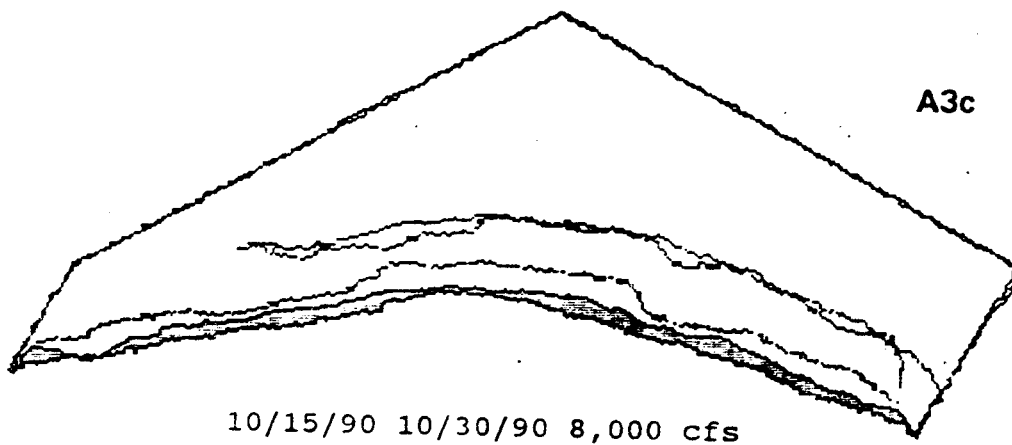
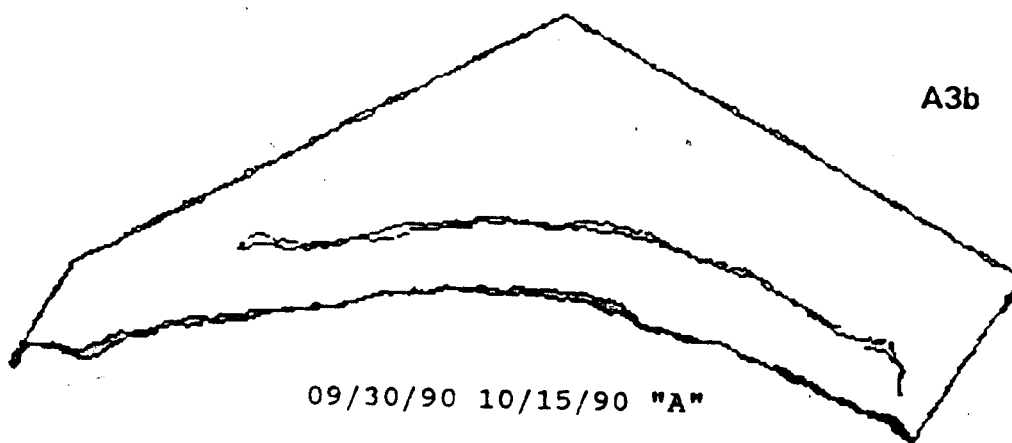
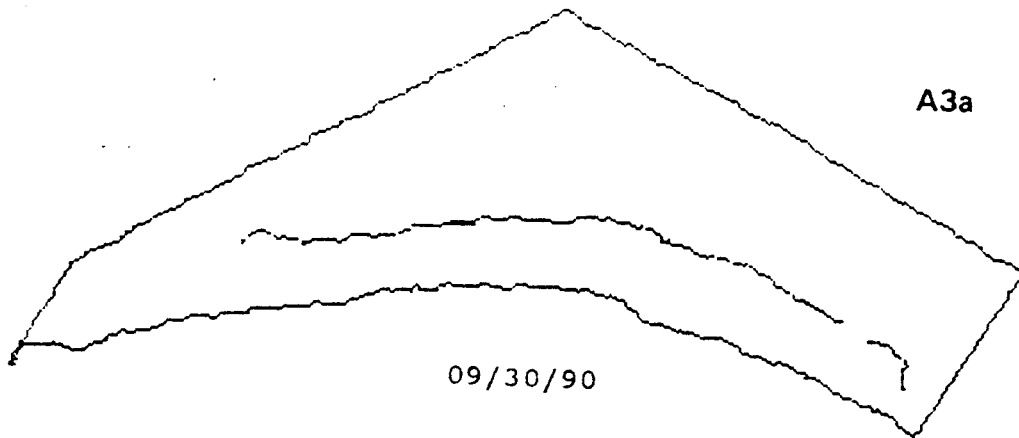
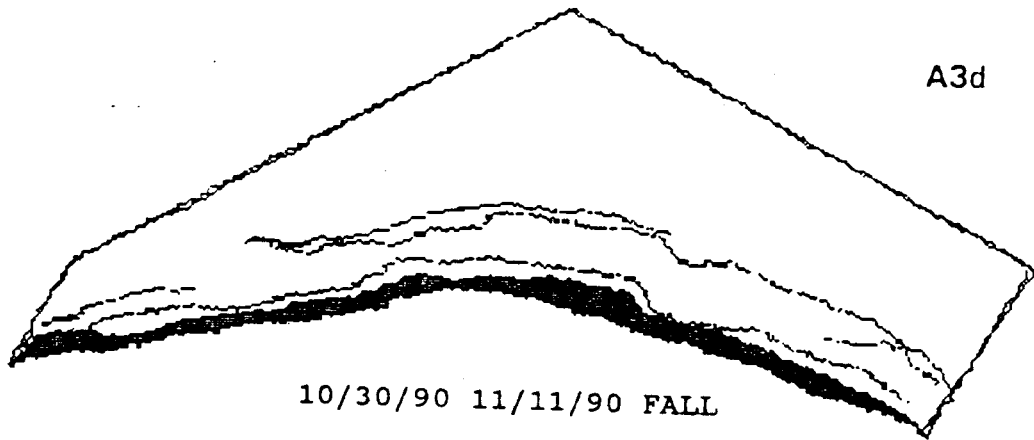


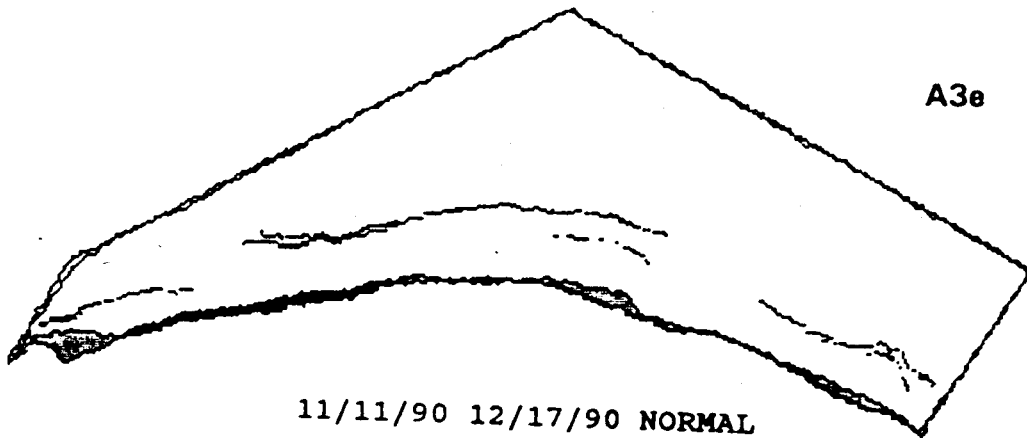
Figure A3. Time-series plot of reworked area and sediment transport capacity for site CR 43 L.

Figures A3a-A3o. Original planimetric outlines and subsequent comparisons of bracketing outlines. Dark shaded areas were eroded. Light shaded areas were aggraded.

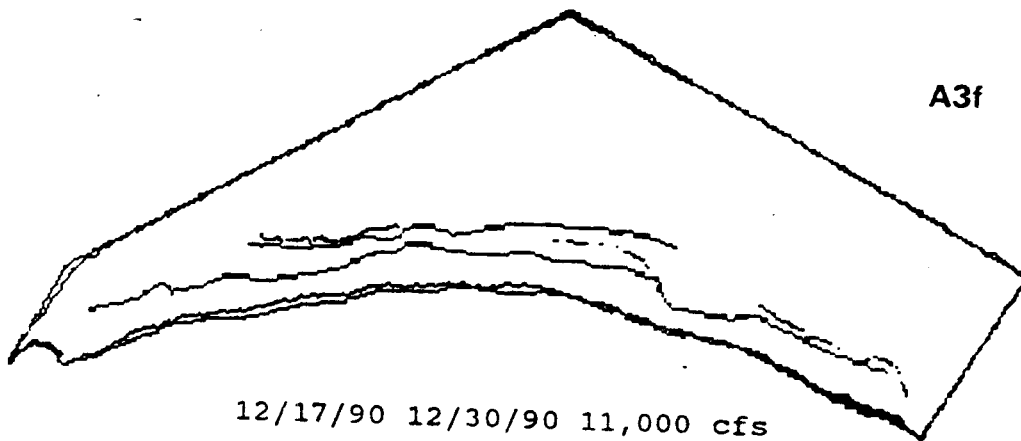




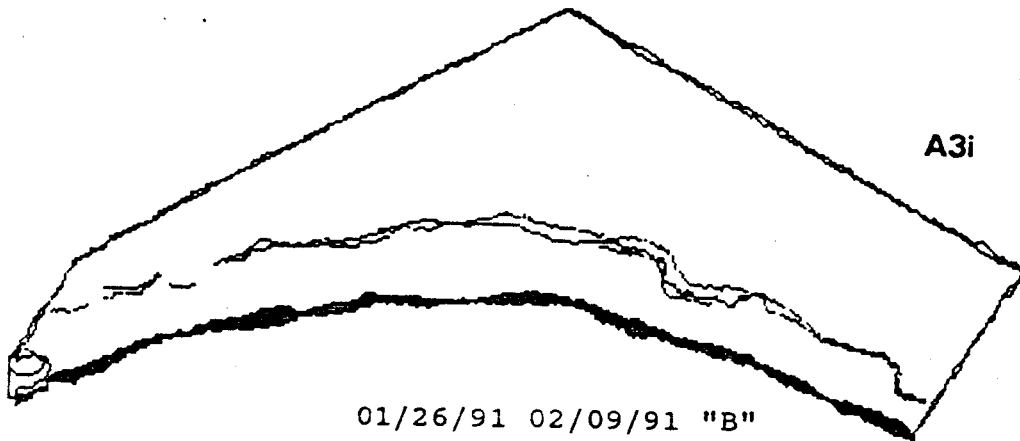
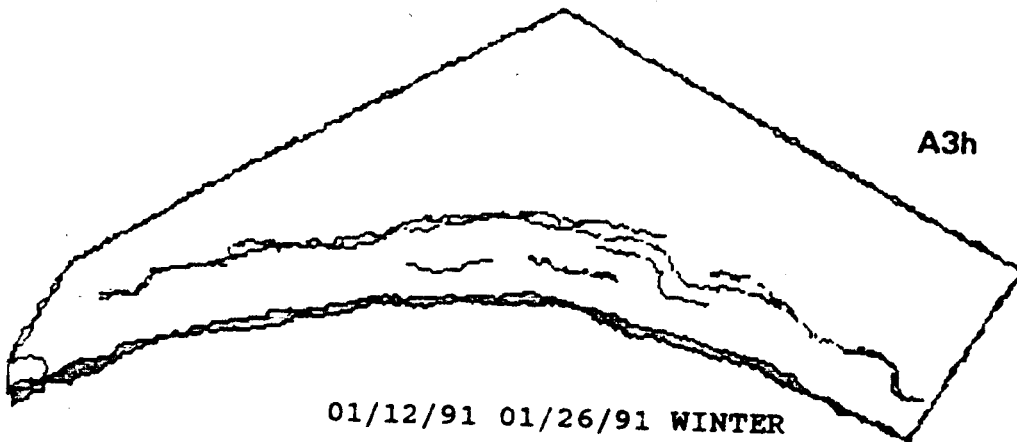
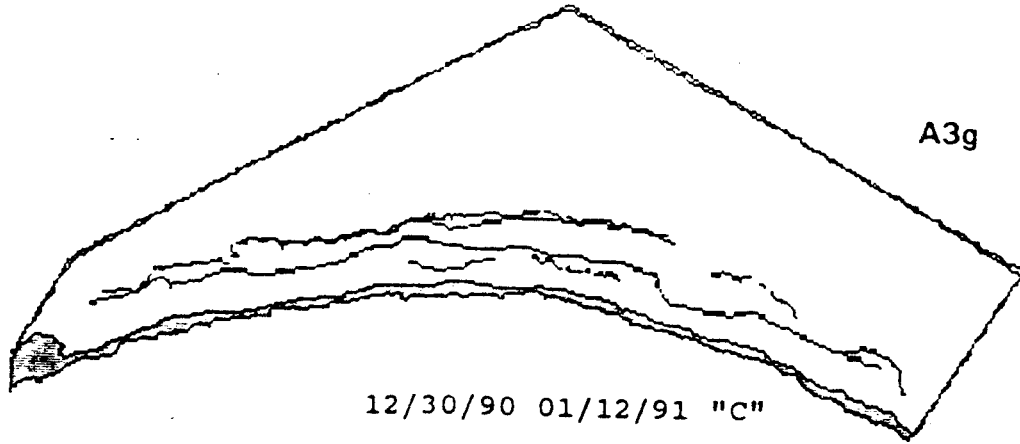
10/30/90 11/11/90 FALL

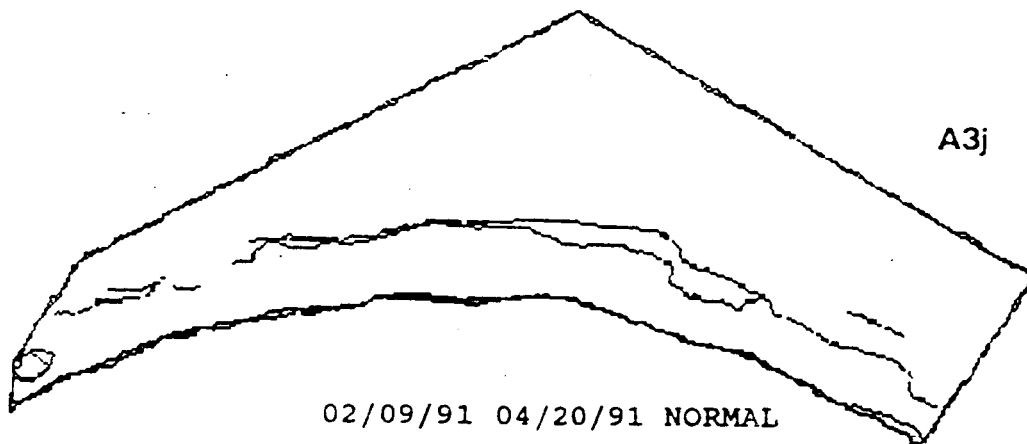


11/11/90 12/17/90 NORMAL

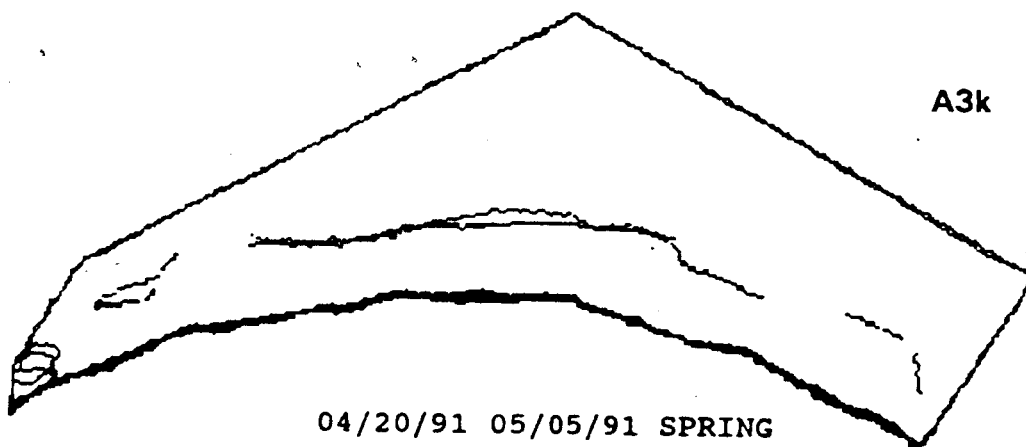


12/17/90 12/30/90 11,000 cfs

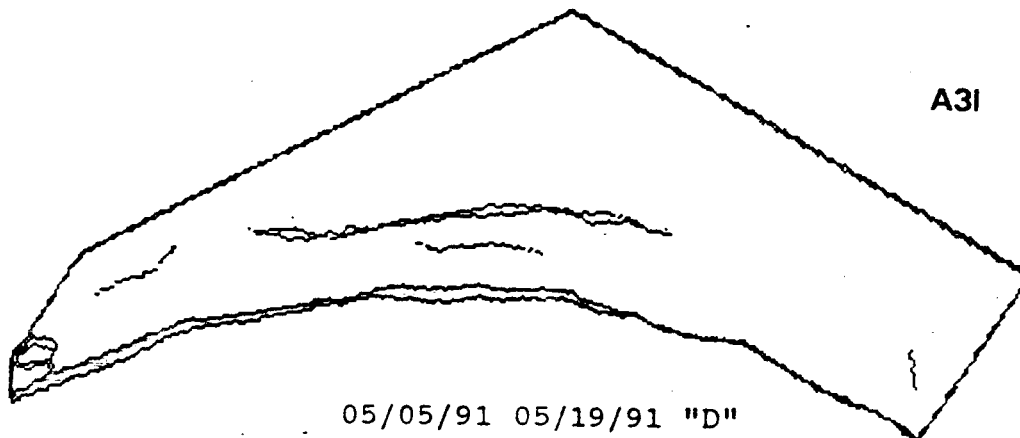




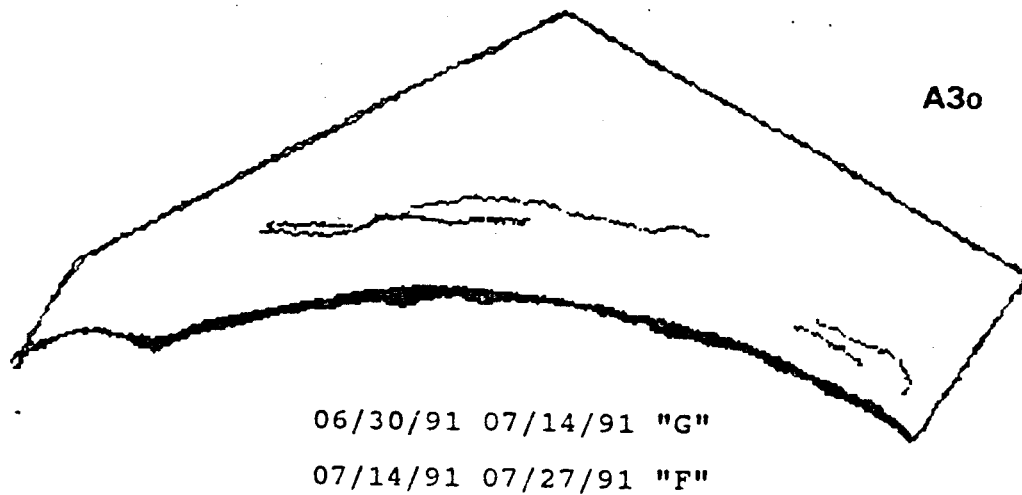
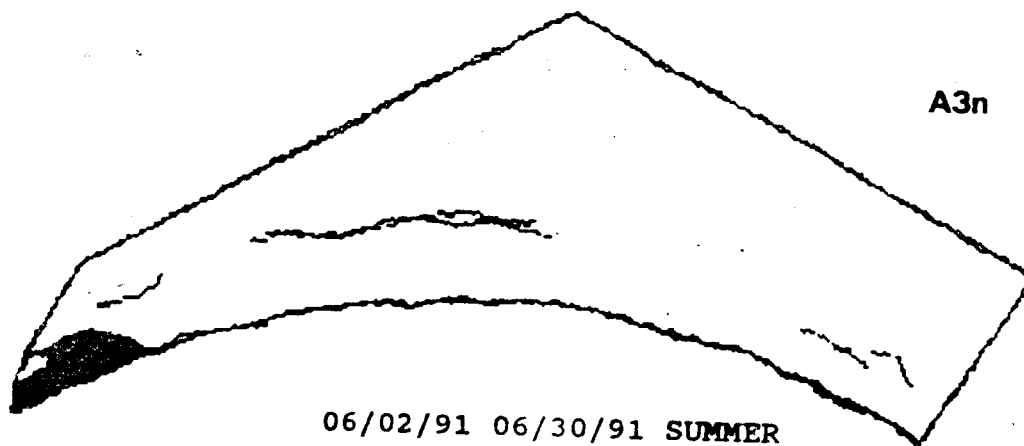
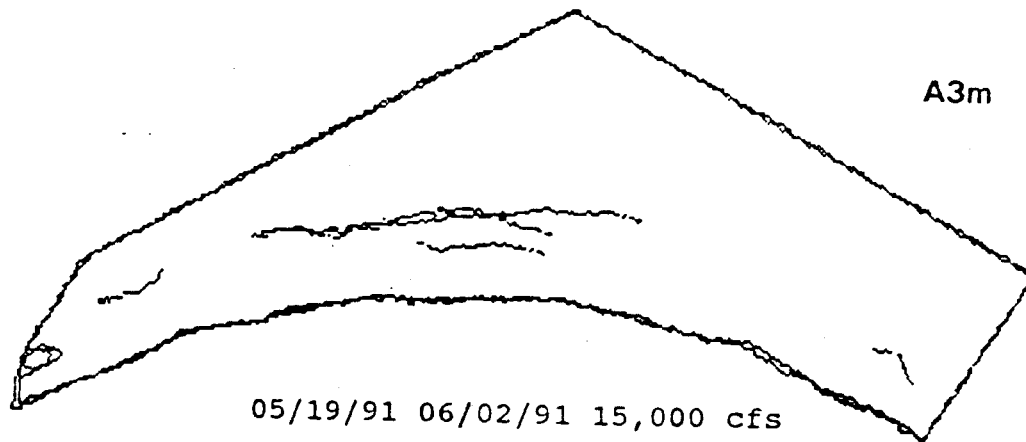
02/09/91 04/20/91 NORMAL



04/20/91 05/05/91 SPRING



05/05/91 05/19/91 "D"



SITE 45 LEFT

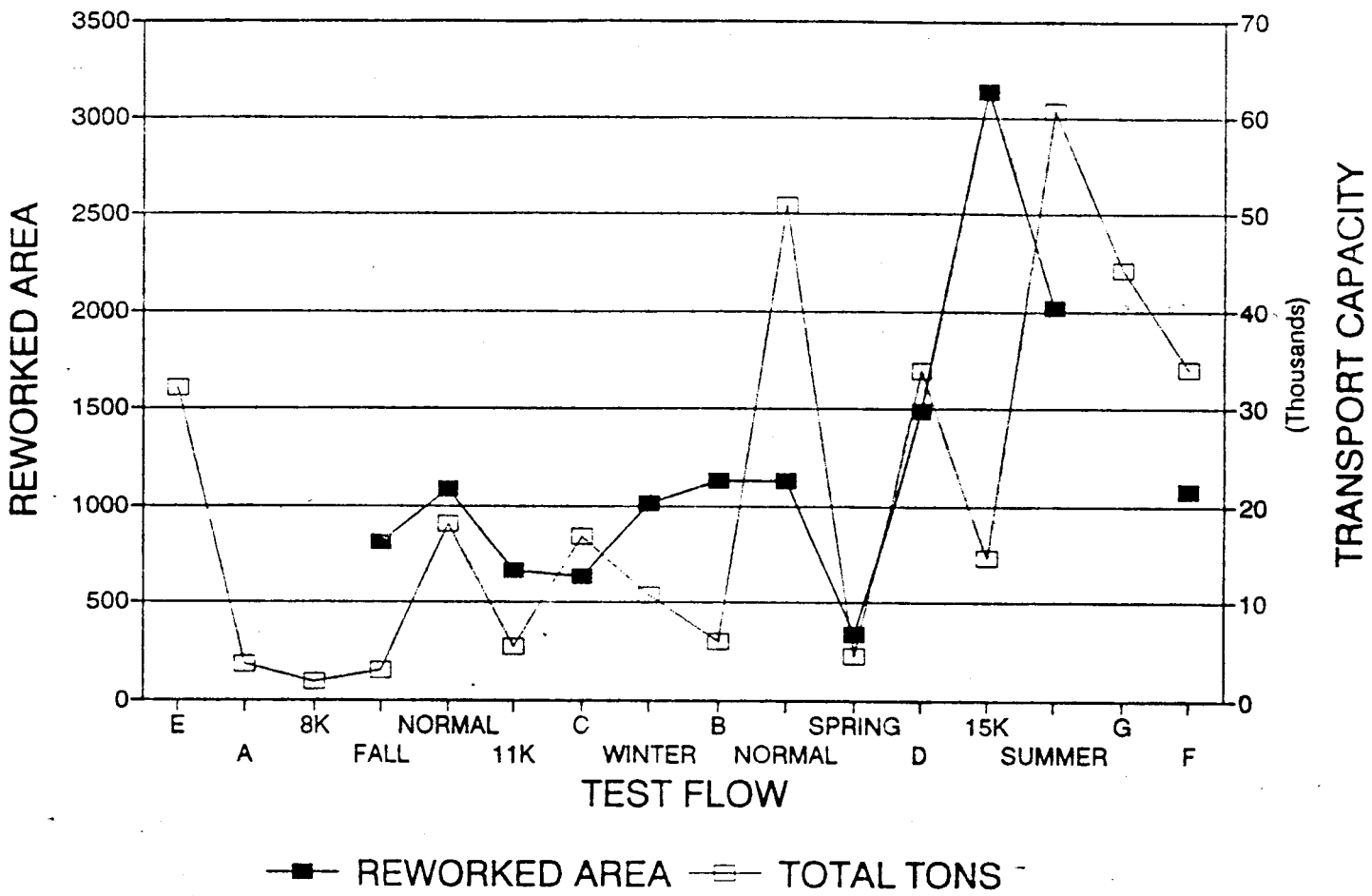
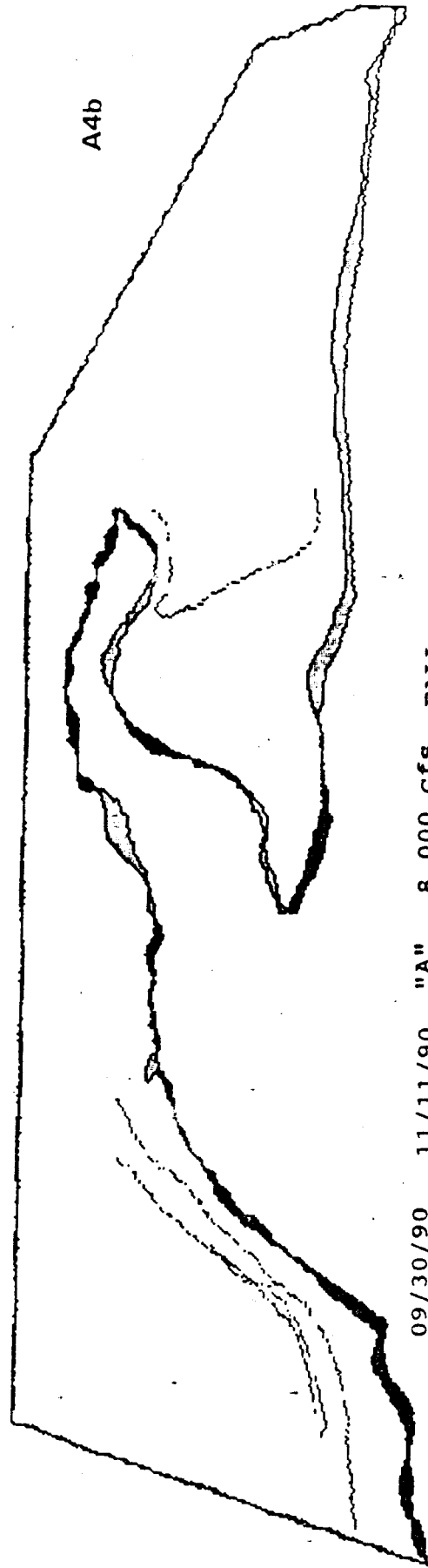
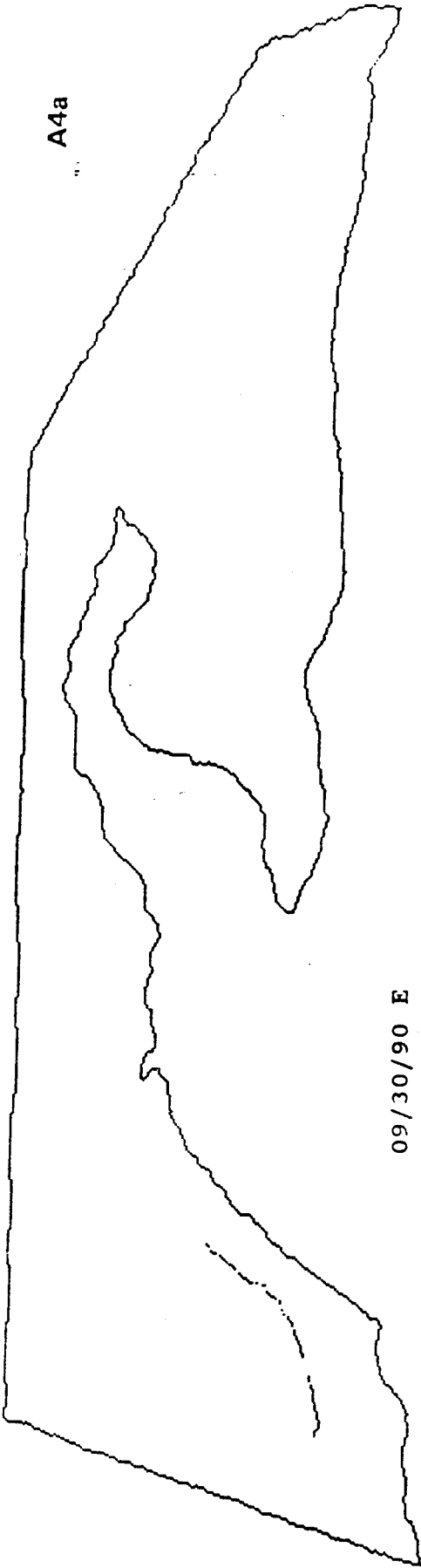
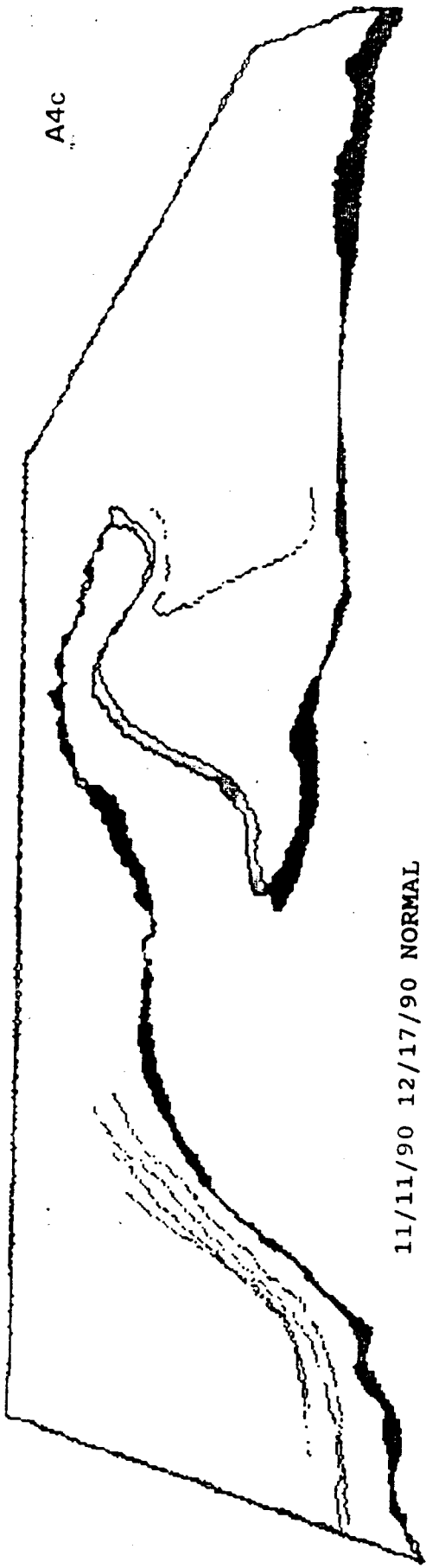


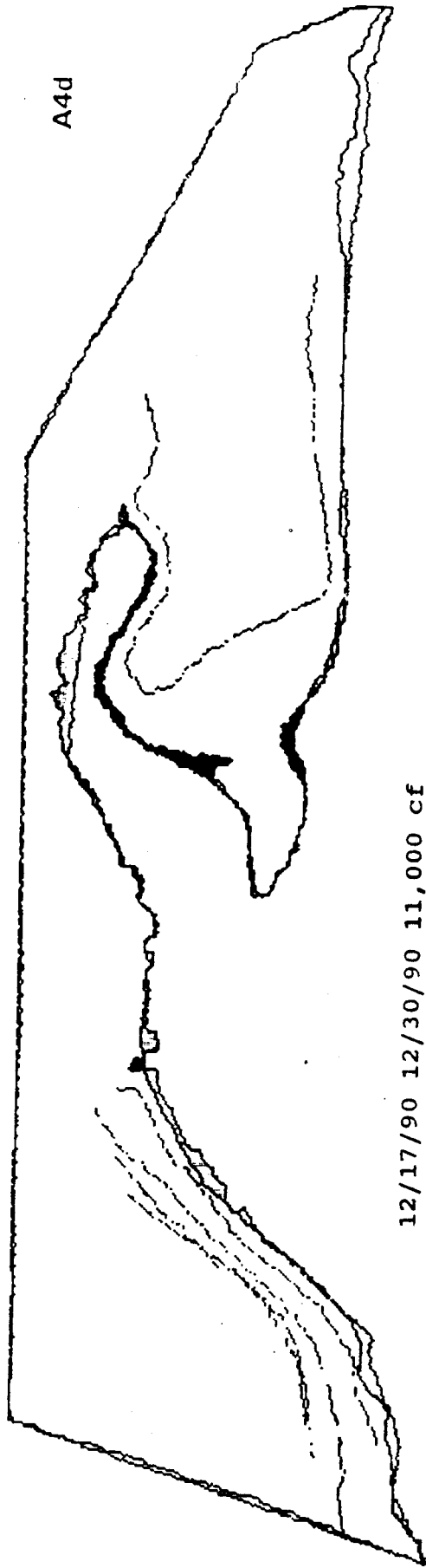
Figure A4. Time-series plot of reworked area and sediment transport capacity for site CR 45 L.

Figures A4a-A4m. Original planimetric outlines and subsequent comparisons of bracketing outlines. Dark shaded areas were eroded. Light shaded areas were aggraded.

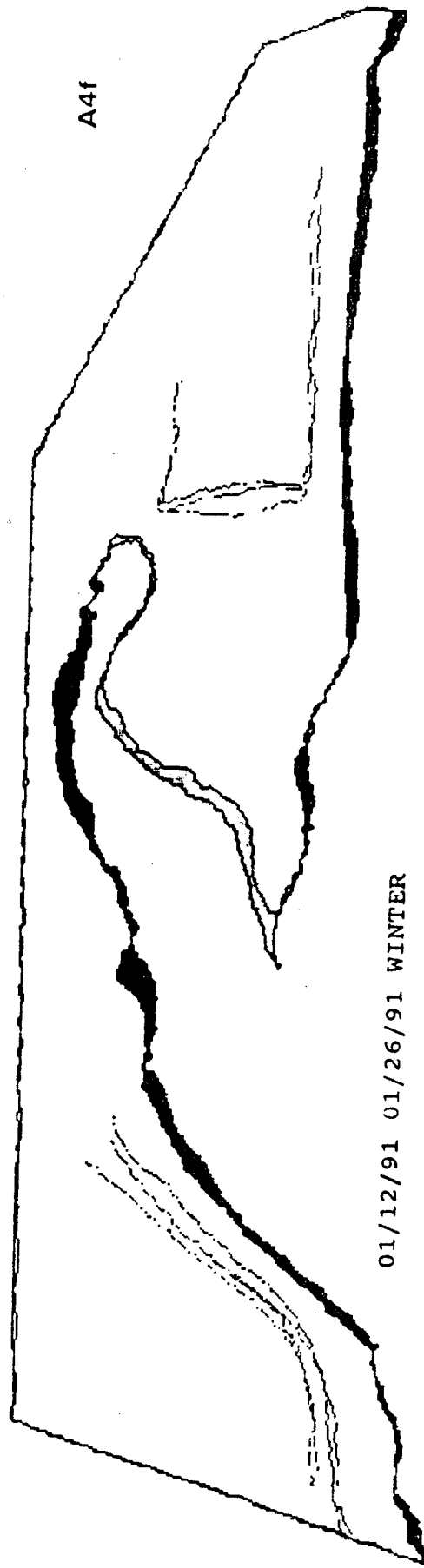
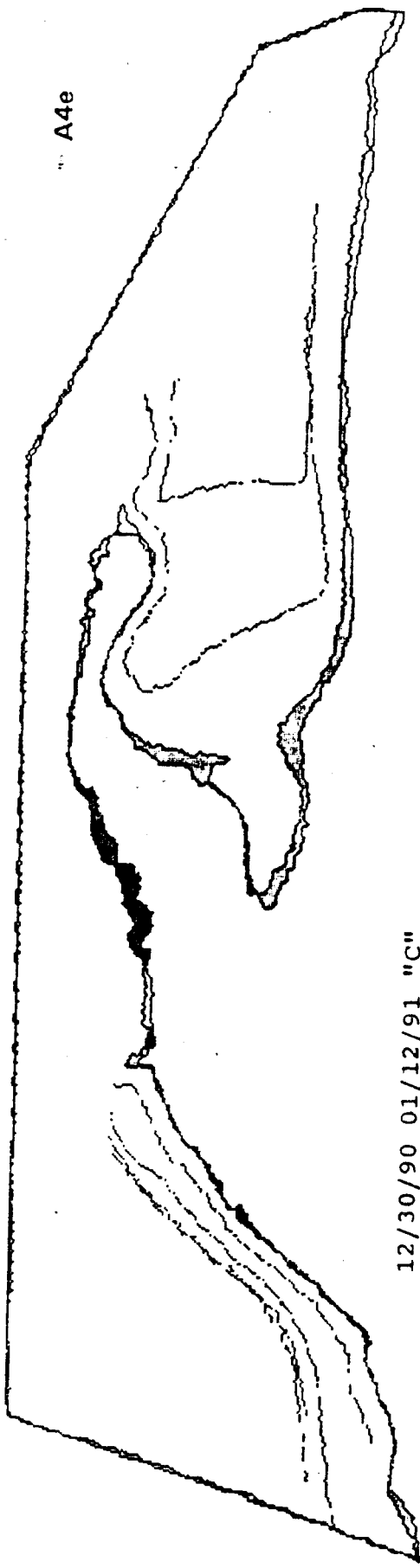


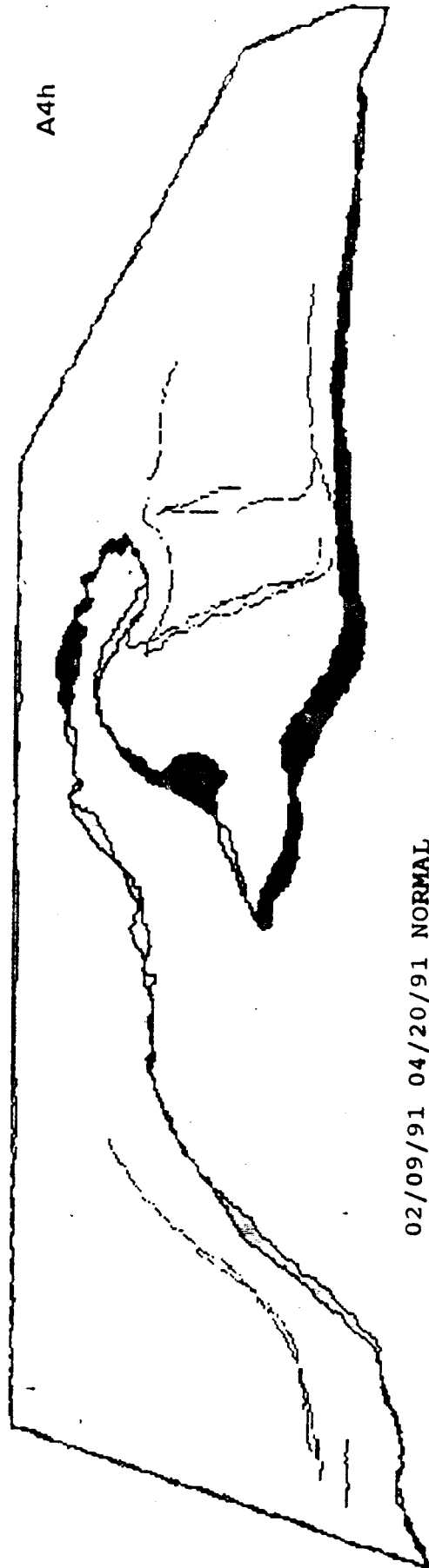
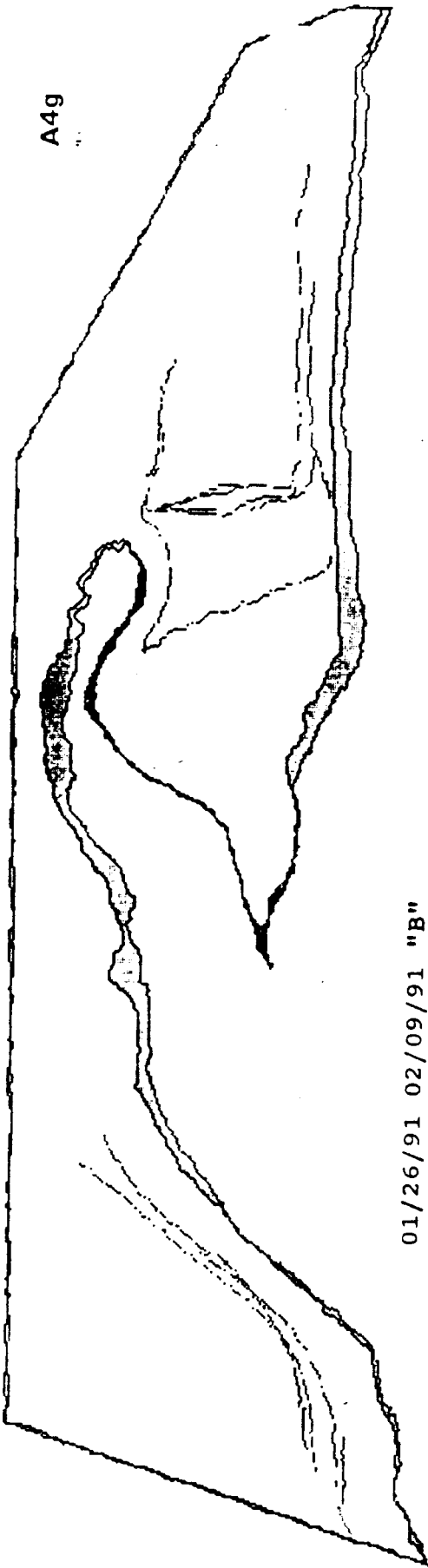


11/11/90 12/17/90 NORMAL

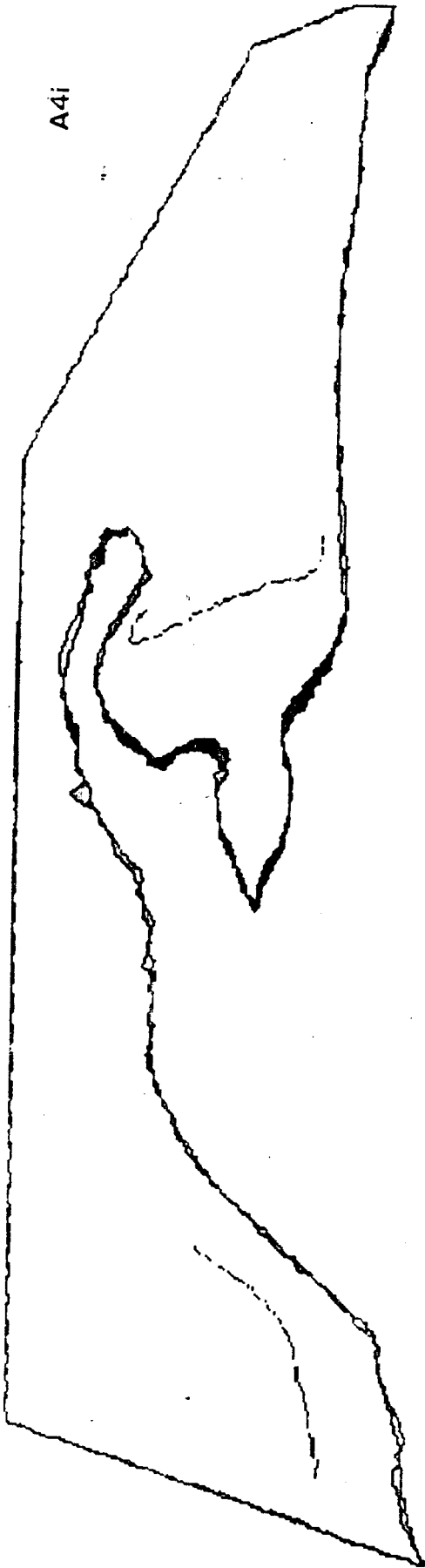


12/17/90 12/30/90 11,000 cf





A4i

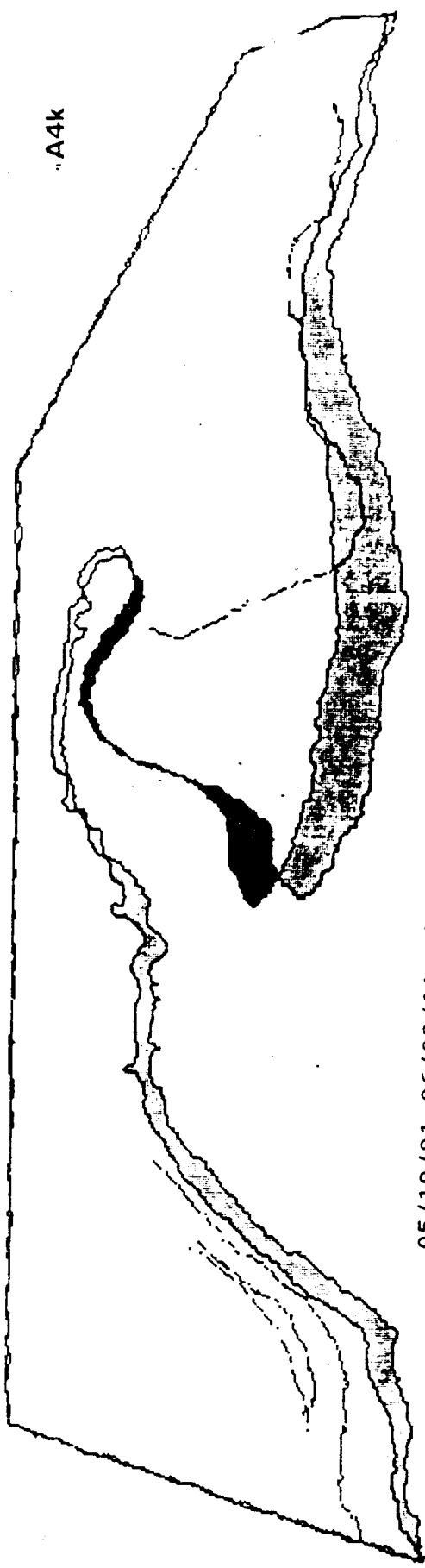


04/20/91 05/05/91 SPRING

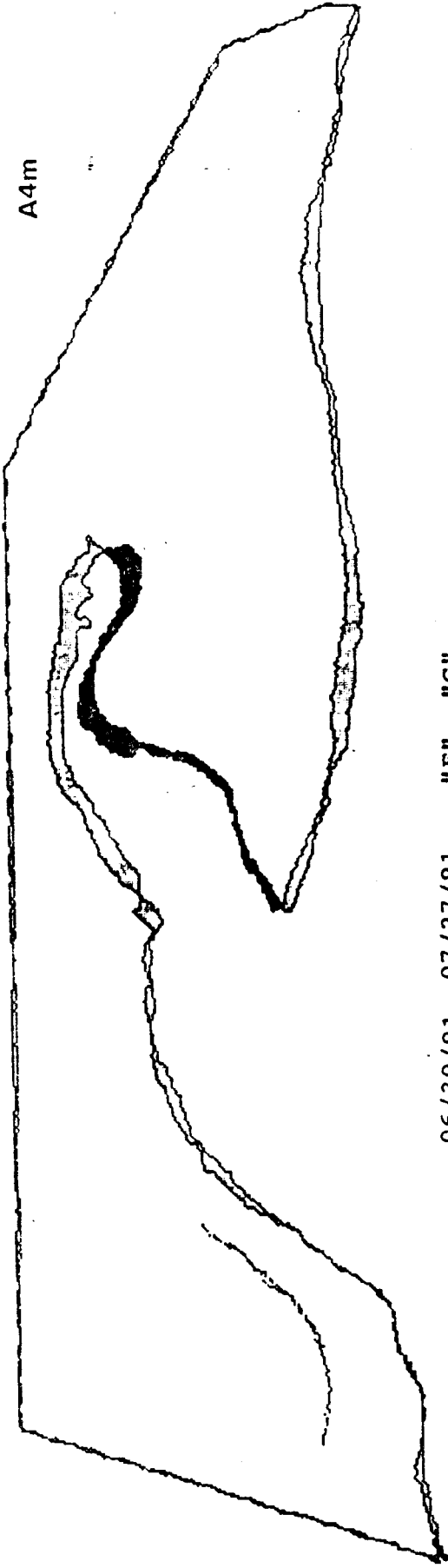
A4j



05/05/91 05/19/91 "D"



A4m



06/30/91 07/27/91 "F" "G"

SITE 47 LEFT

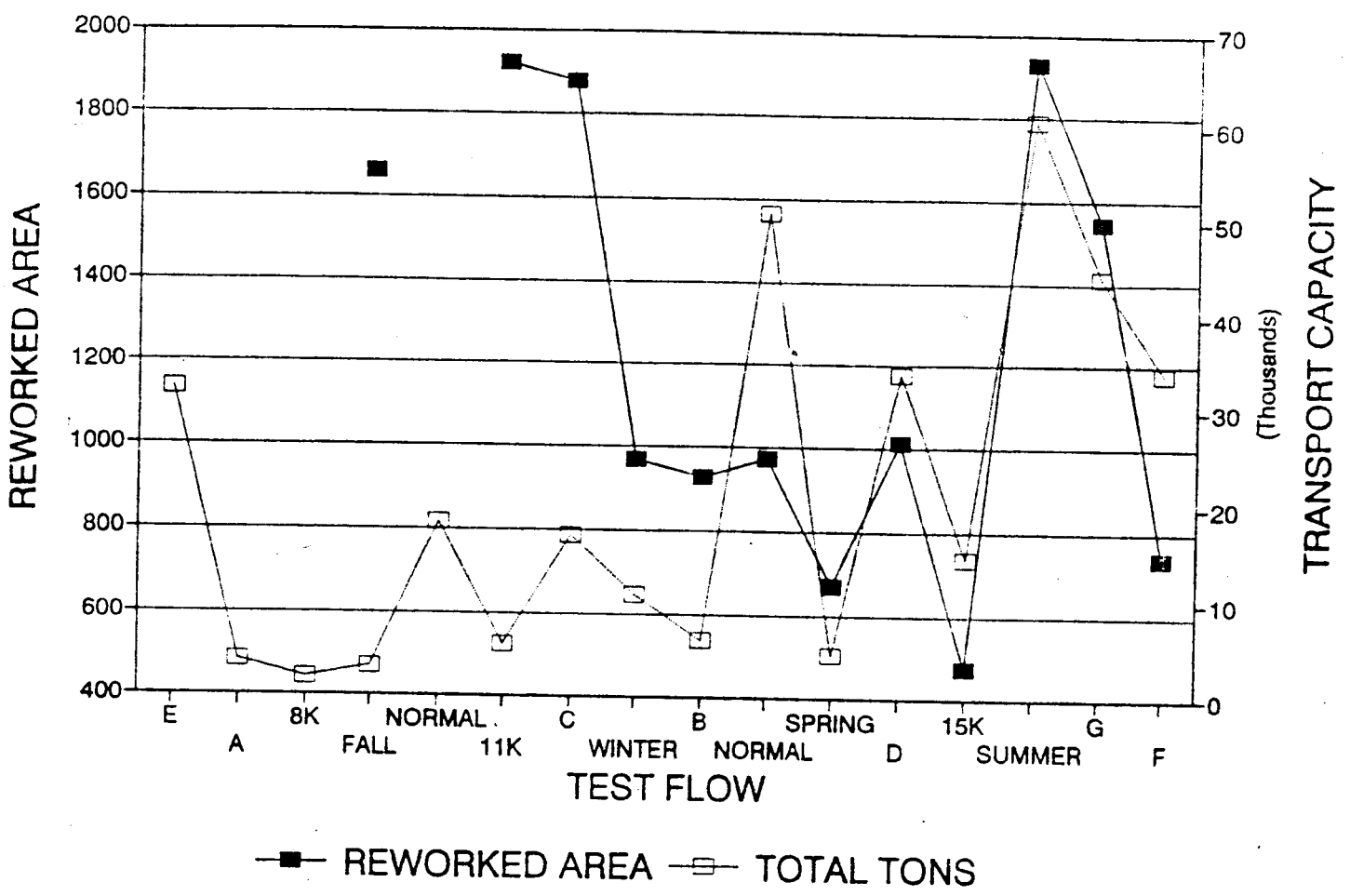
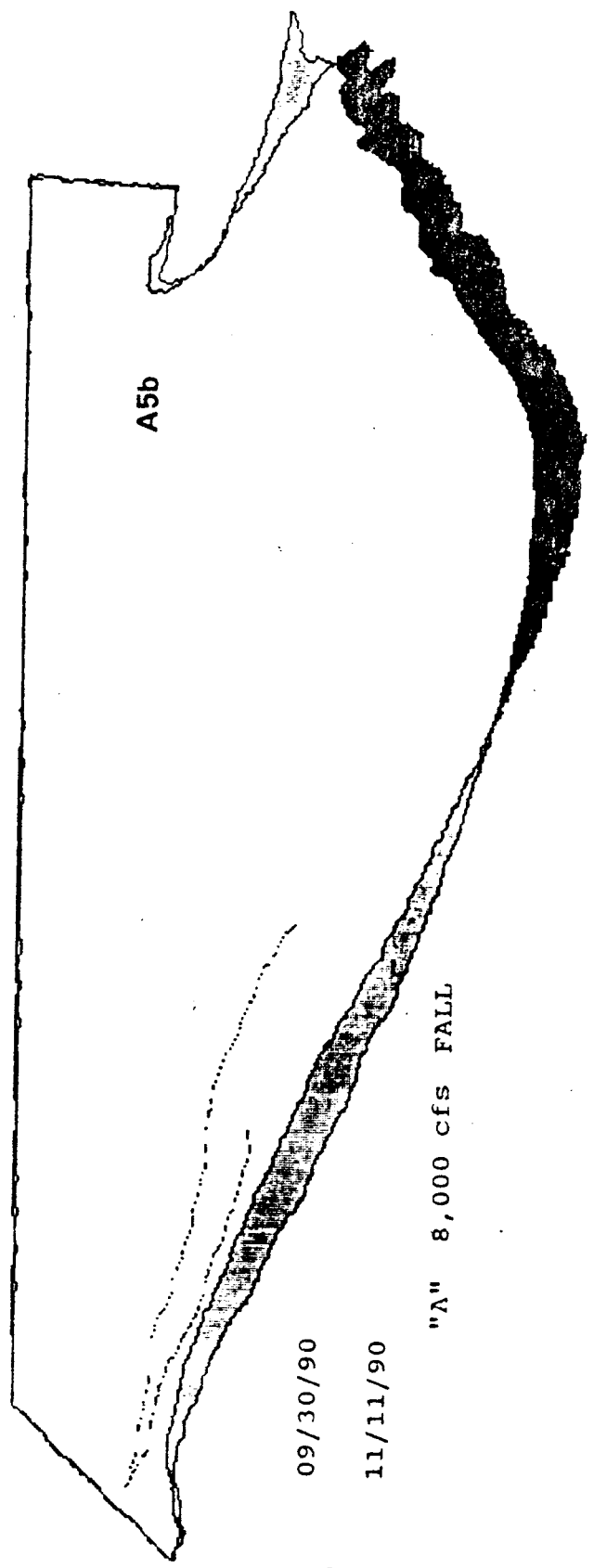
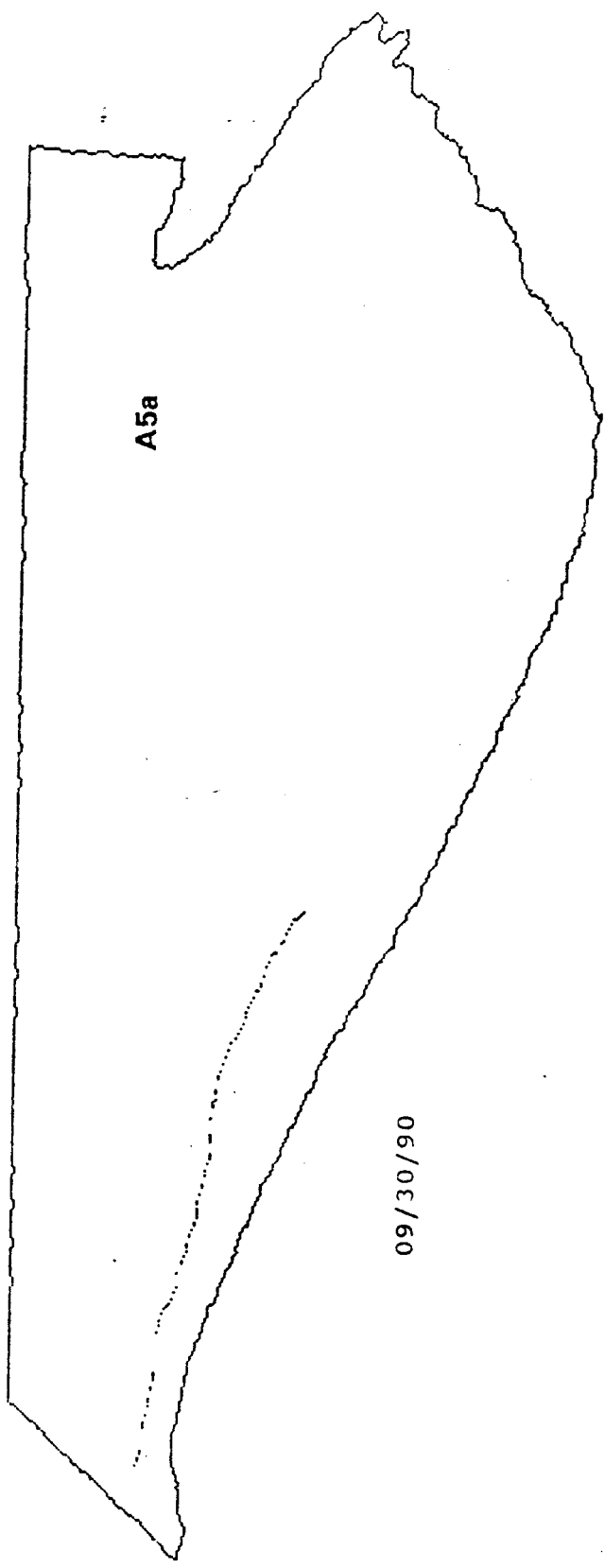
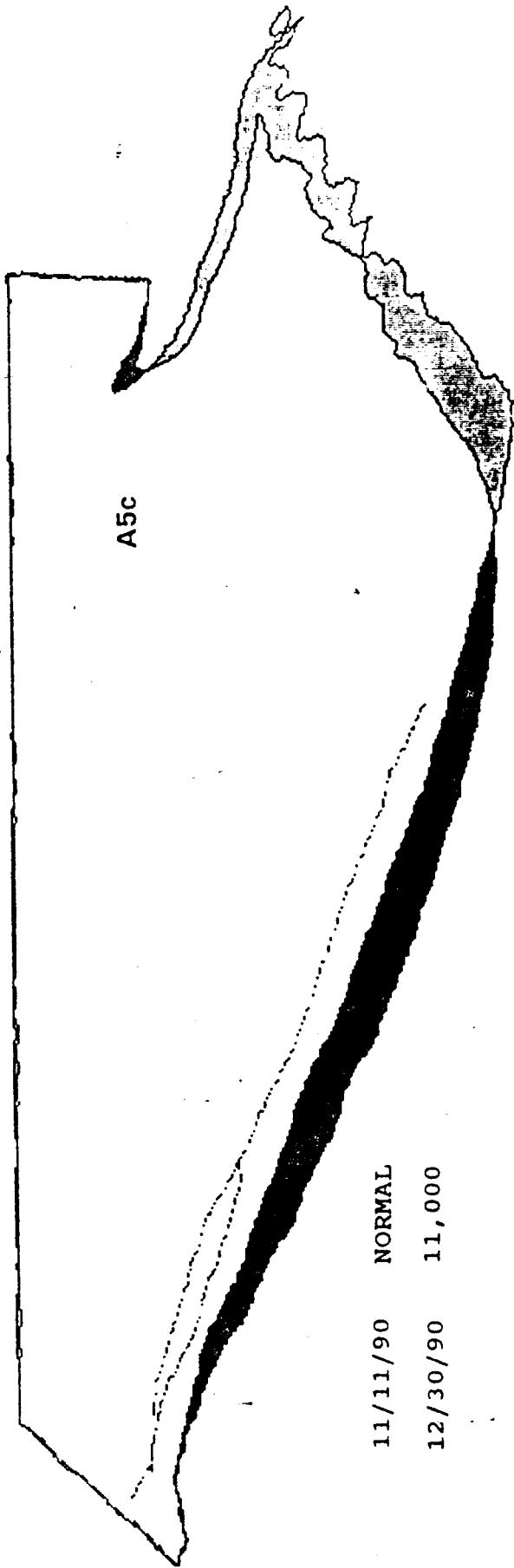


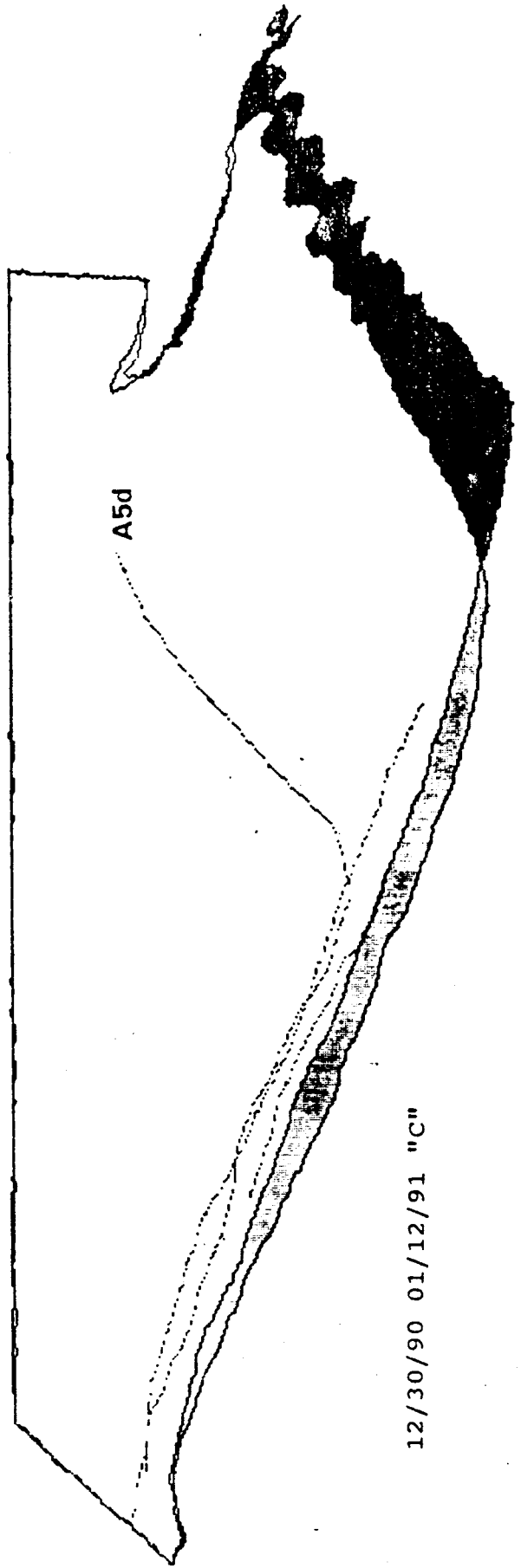
Figure A5. Time-series plot of reworked area and sediment transport capacity for site CR 47 R.

Figures A5a-A5m. Original planimetric outlines and subsequent comparisons of bracketing outlines. Dark shaded areas were eroded. Light shaded areas were aggraded.



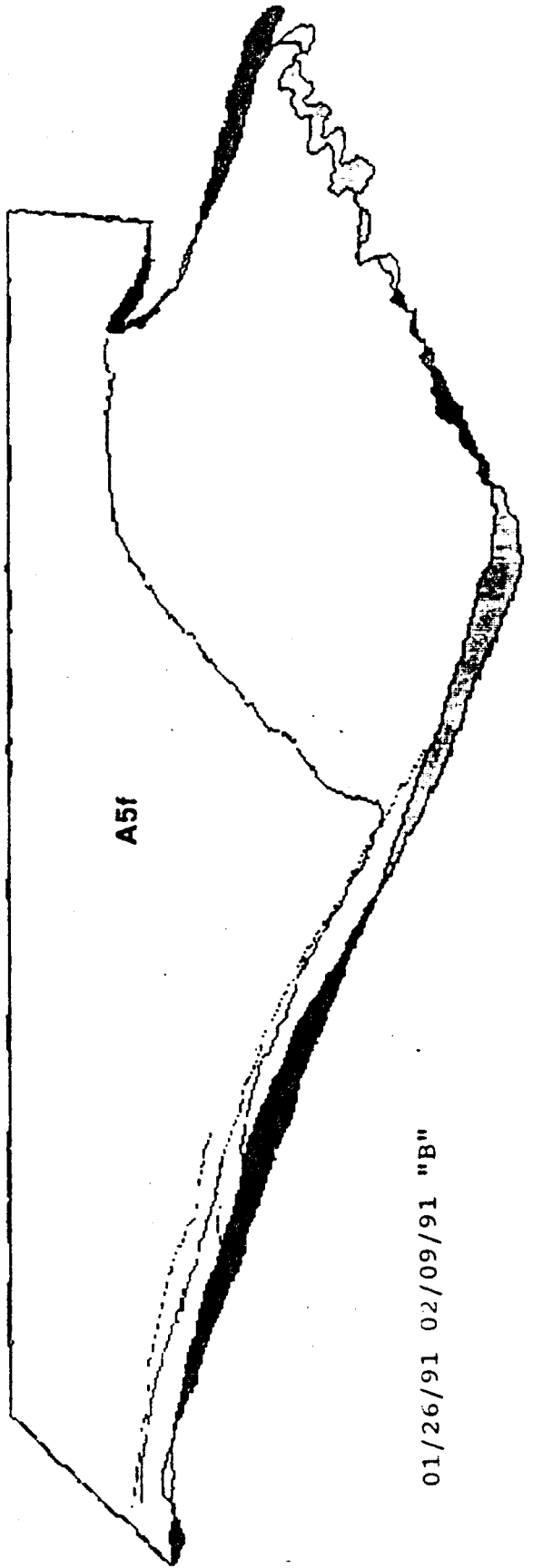
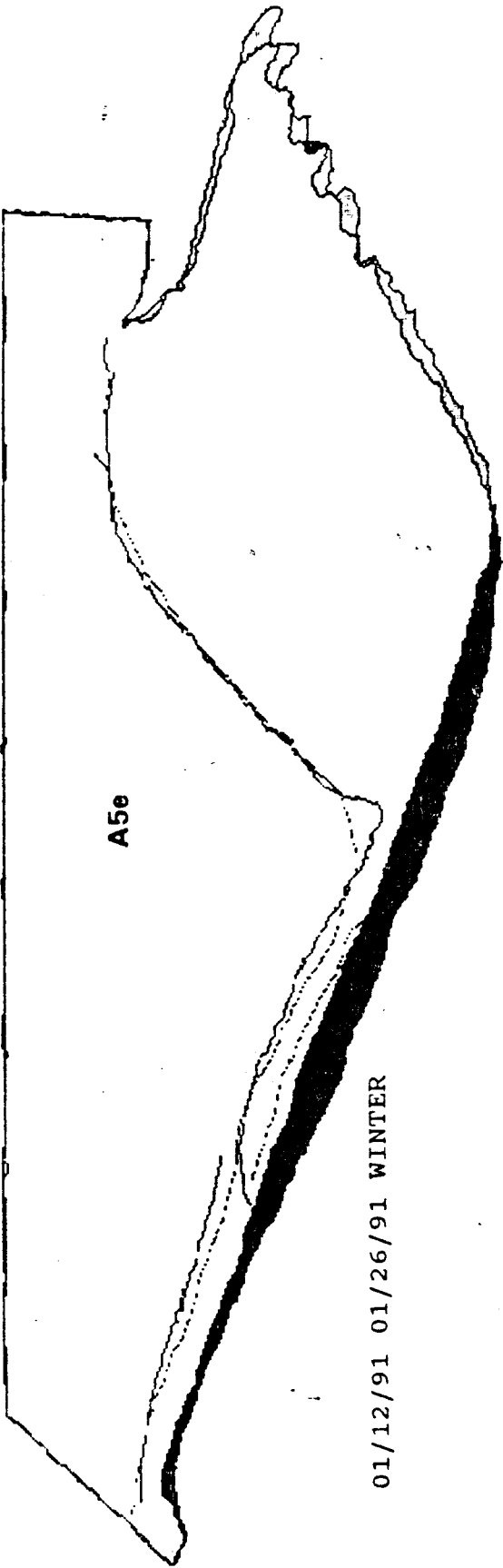


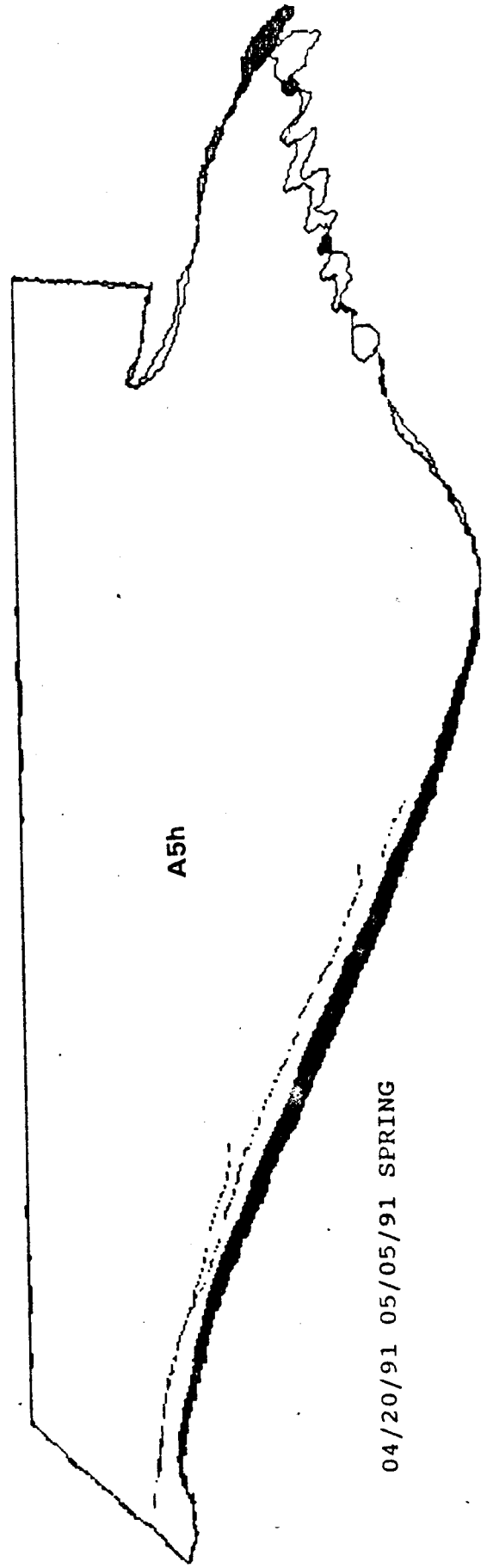
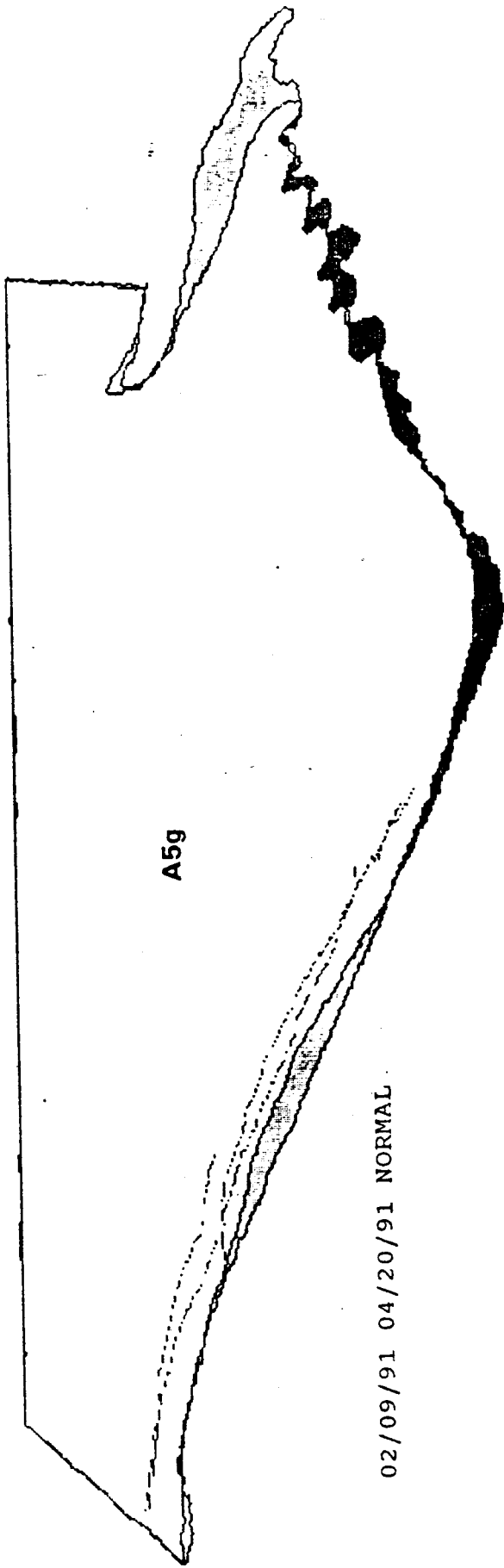
11/11/90 NORMAL
 12/30/90 11,000

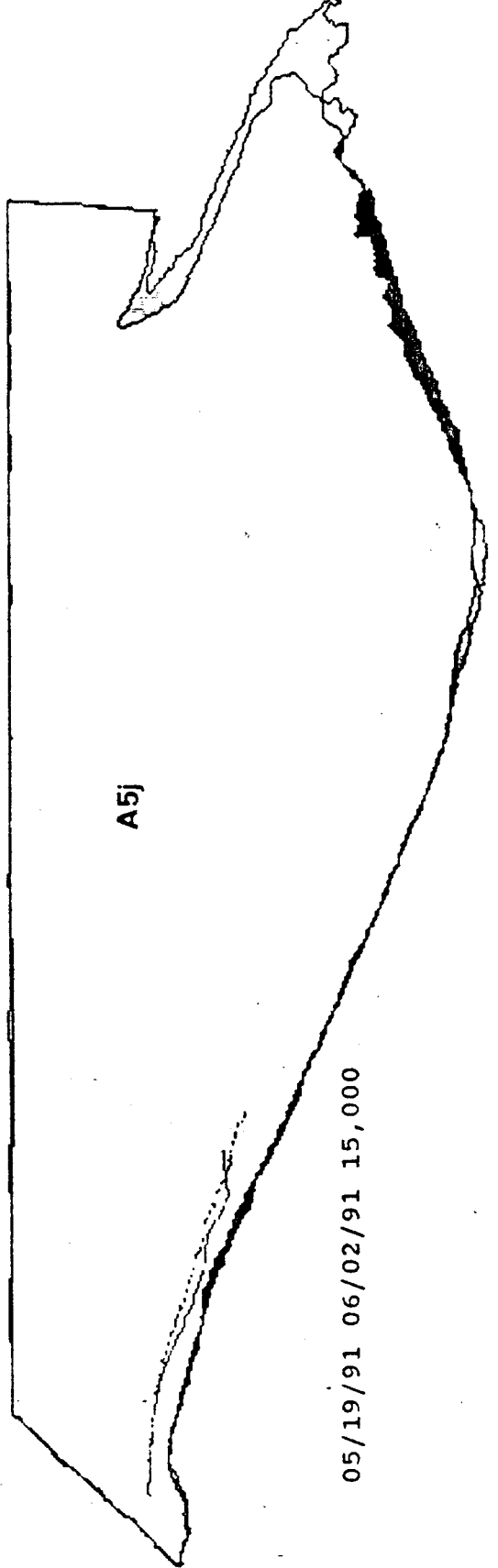
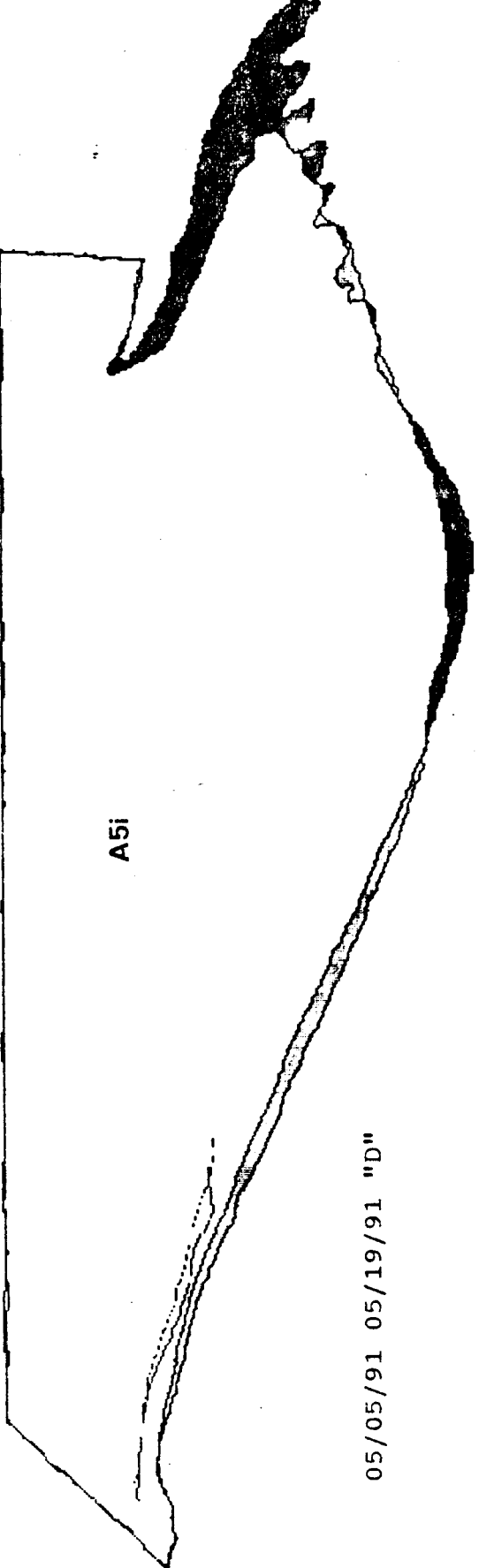


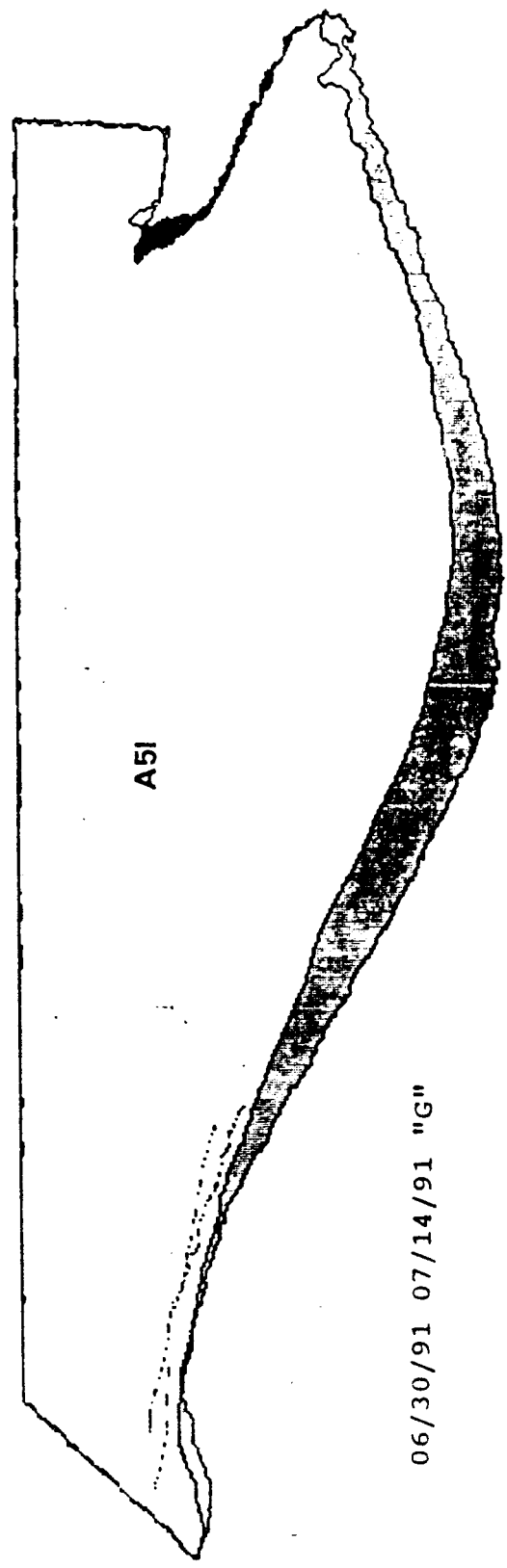
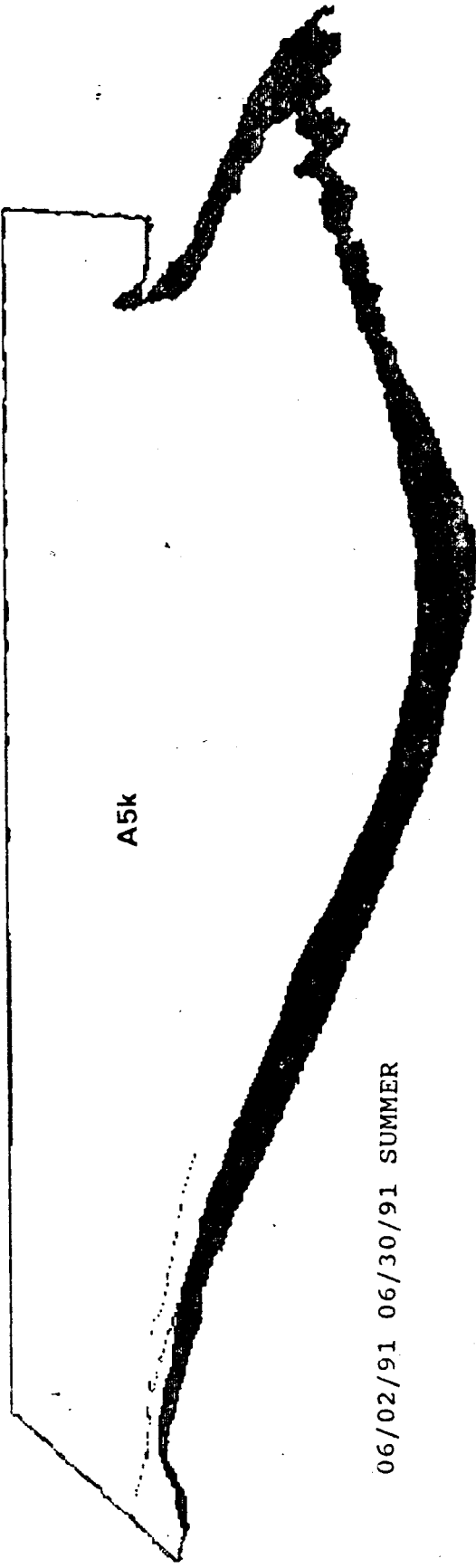
12/30/90 01/12/91 "C"

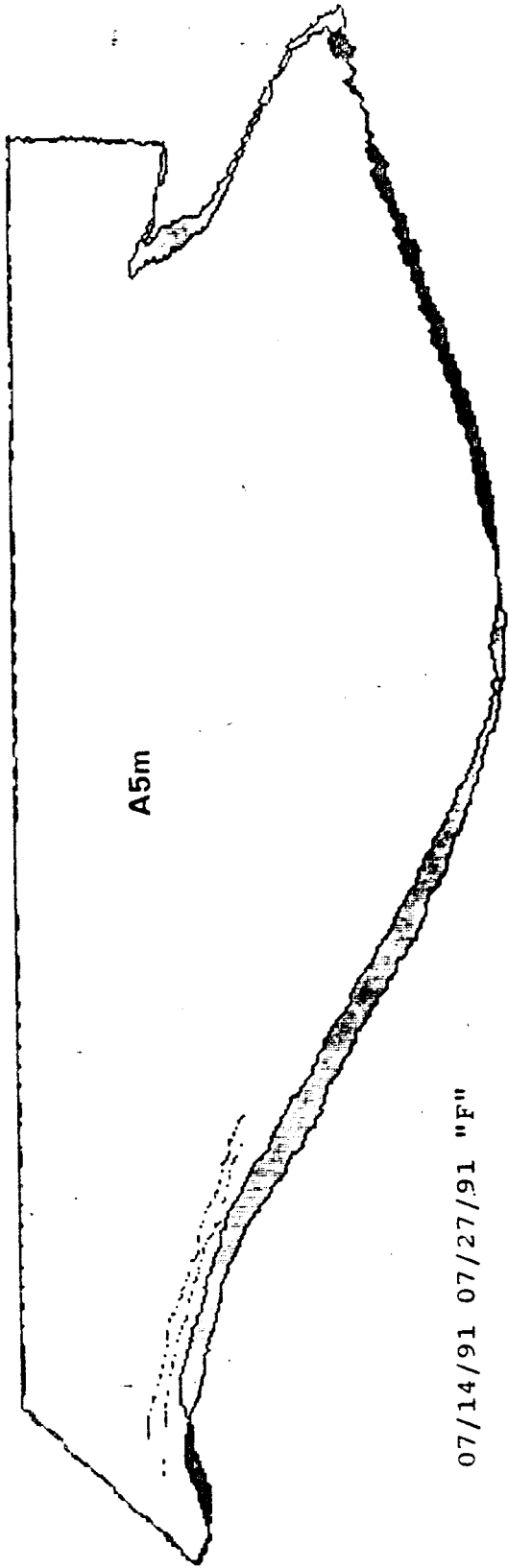












07/14/91 07/27/91 "F"

SITE 51 LEFT

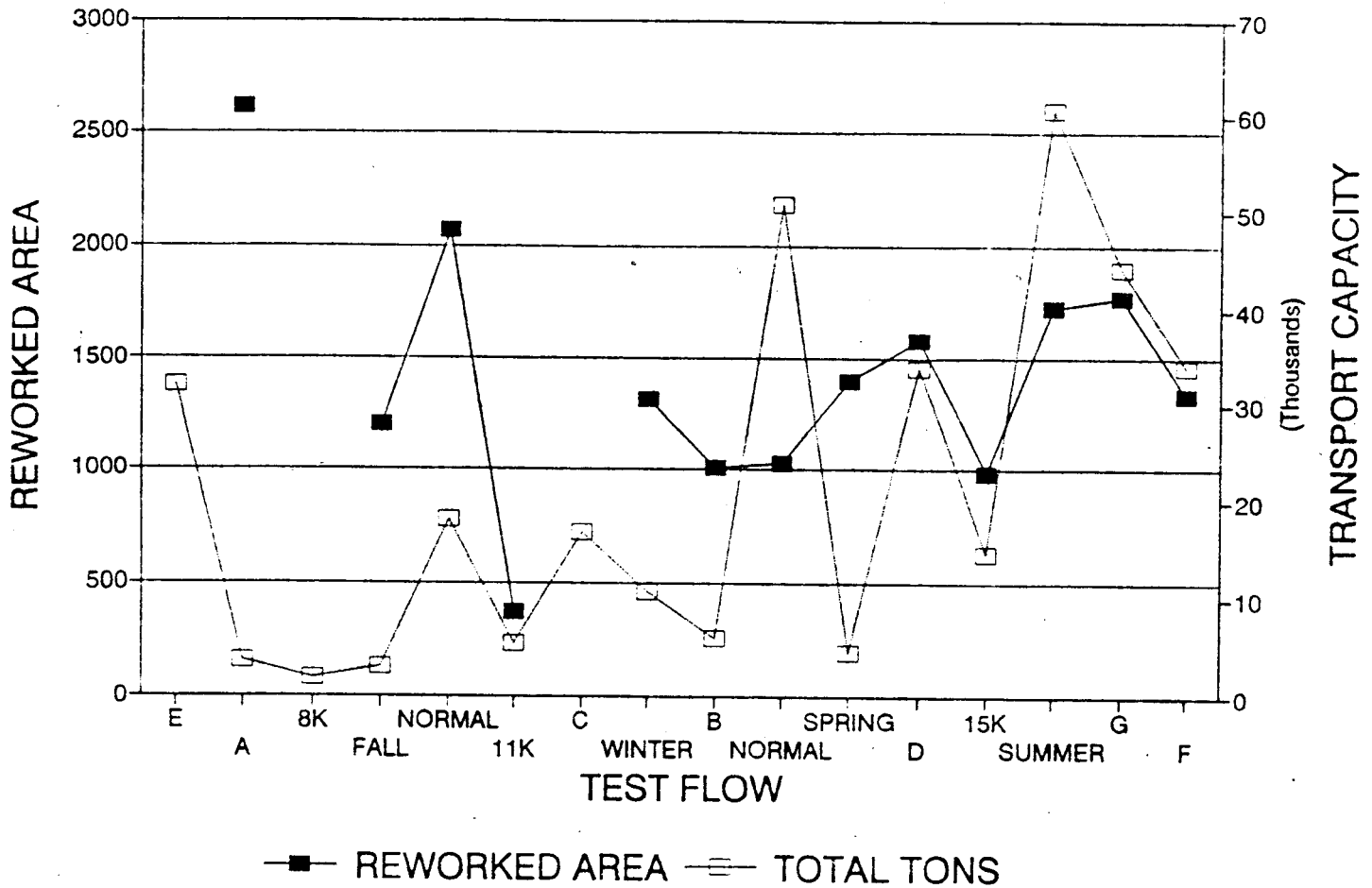
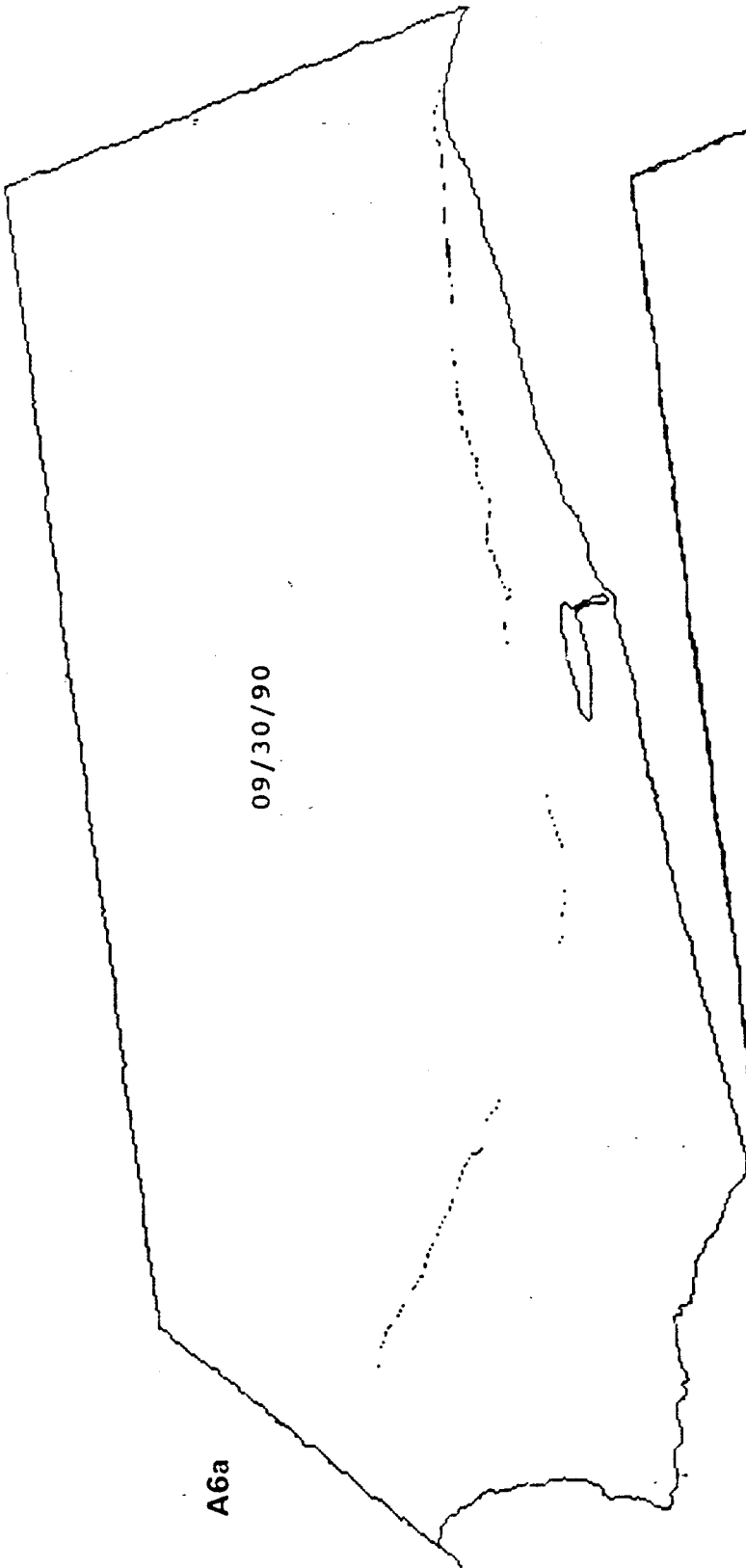


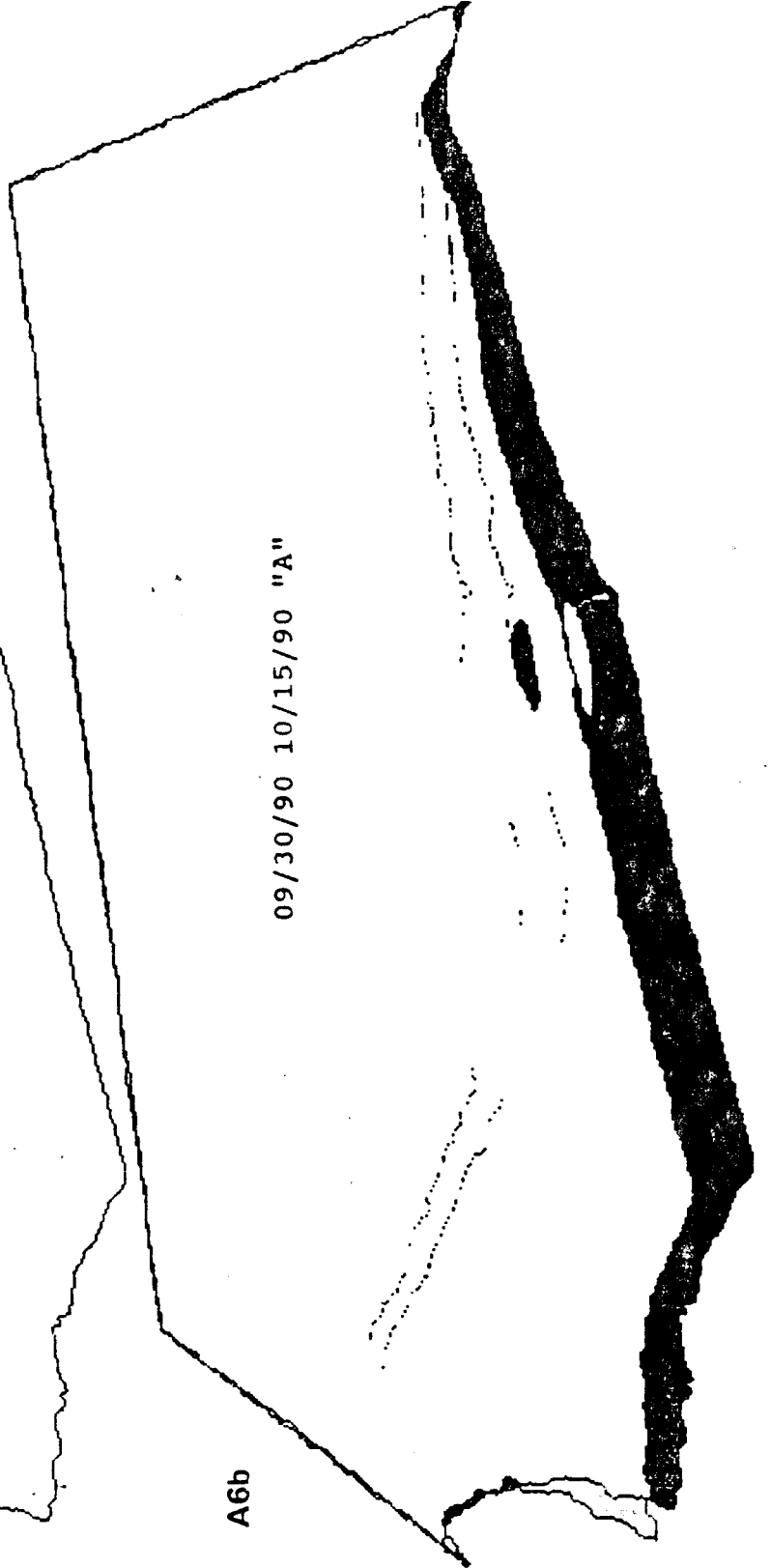
Figure A6. Time-series plot of reworked area and sediment transport capacity for site CR 51 L.

Figures A6a-A6n. Original planimetric outlines and subsequent comparisons of bracketing outlines. Dark shaded areas were eroded. Light shaded areas were aggraded.



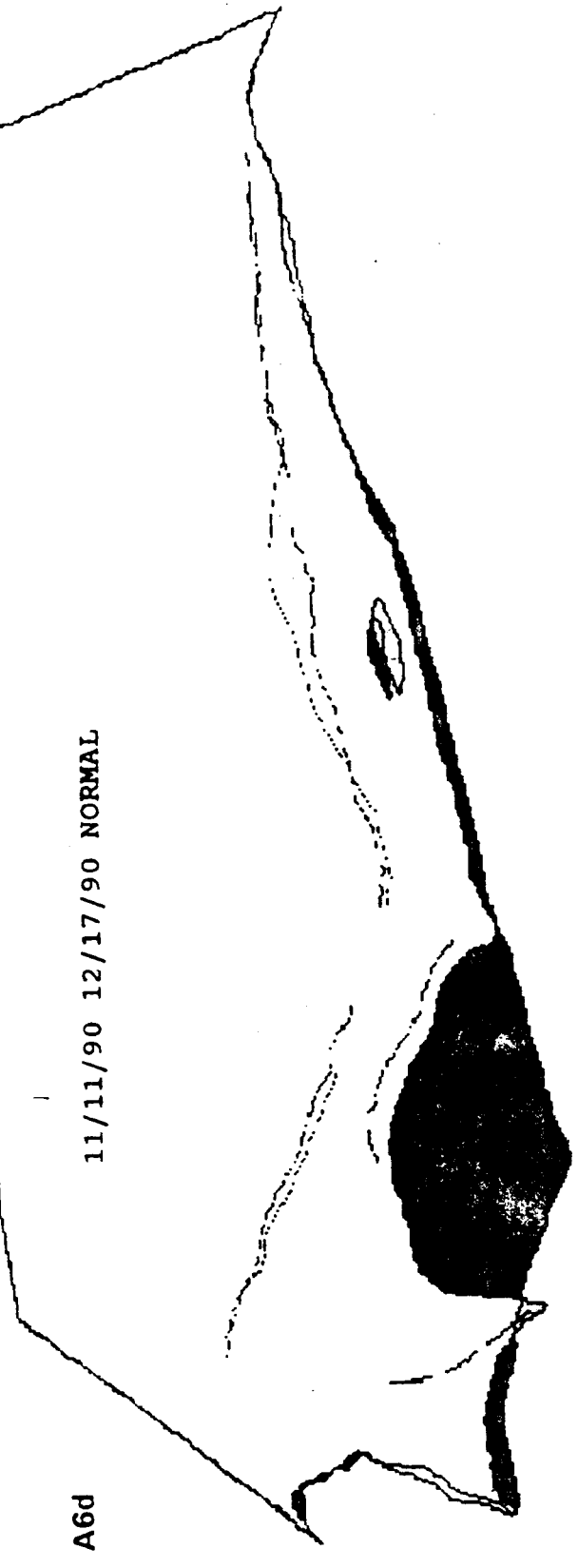
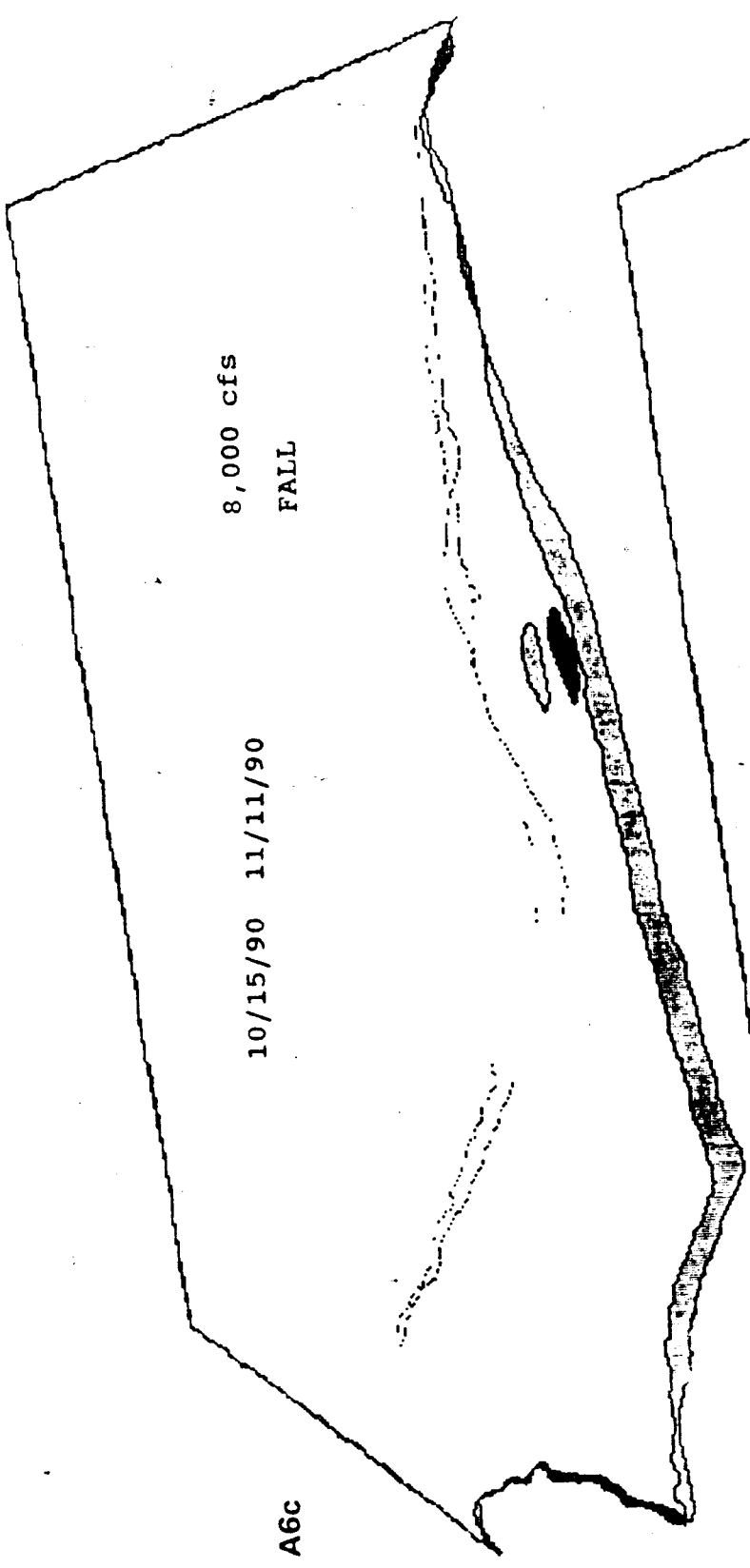
09/30/90

A6a



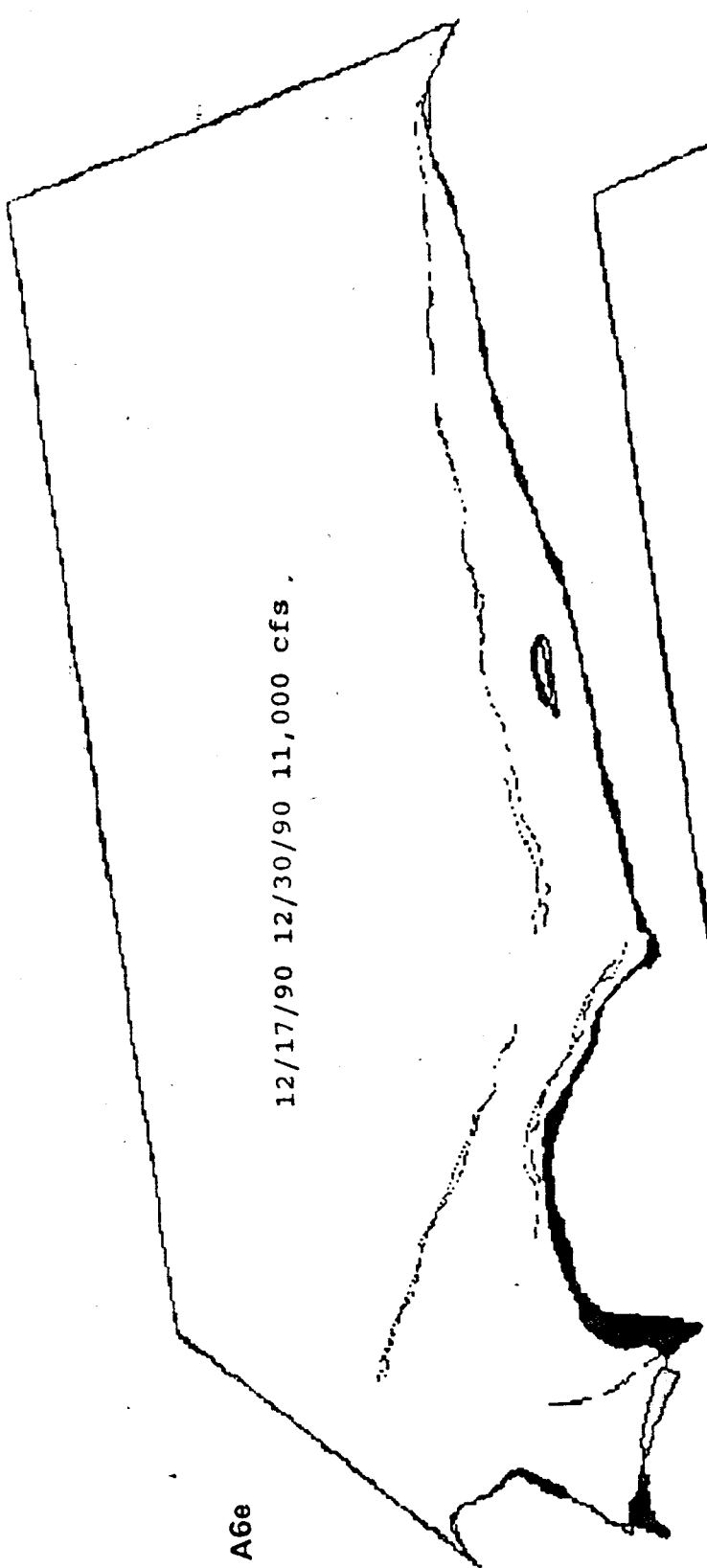
09/30/90 10/15/90 "A"

A6b



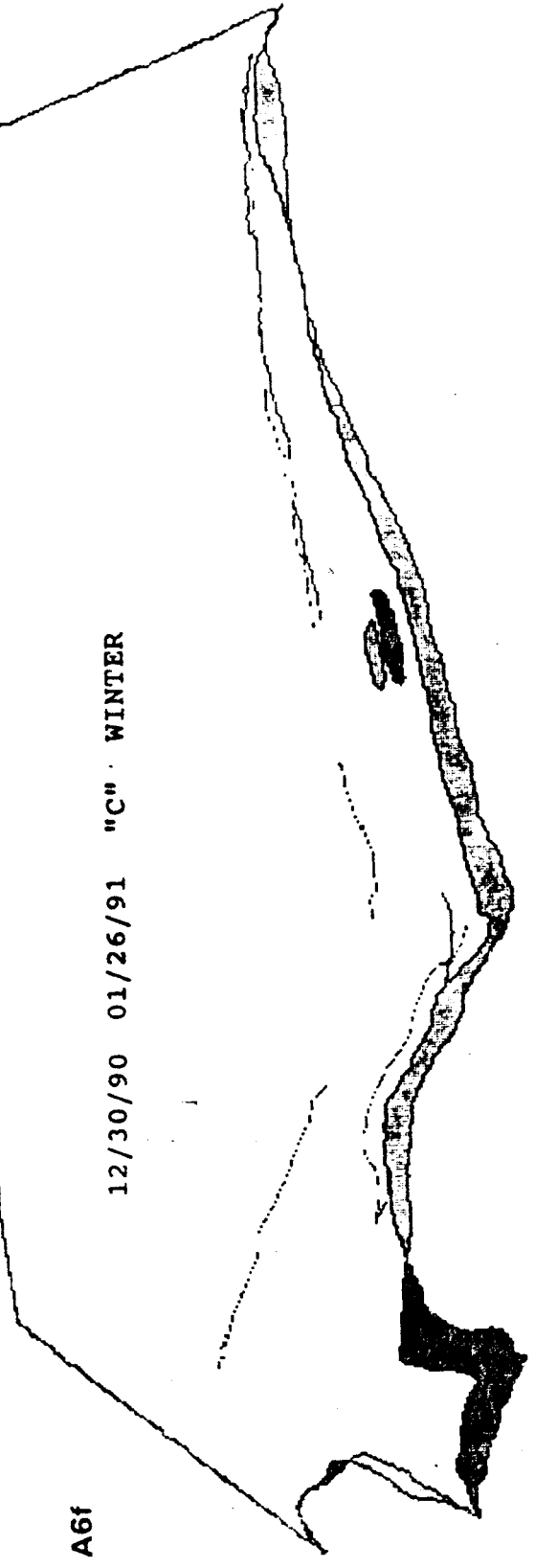
A6e

12/17/90 12/30/90 11,000 cfs .



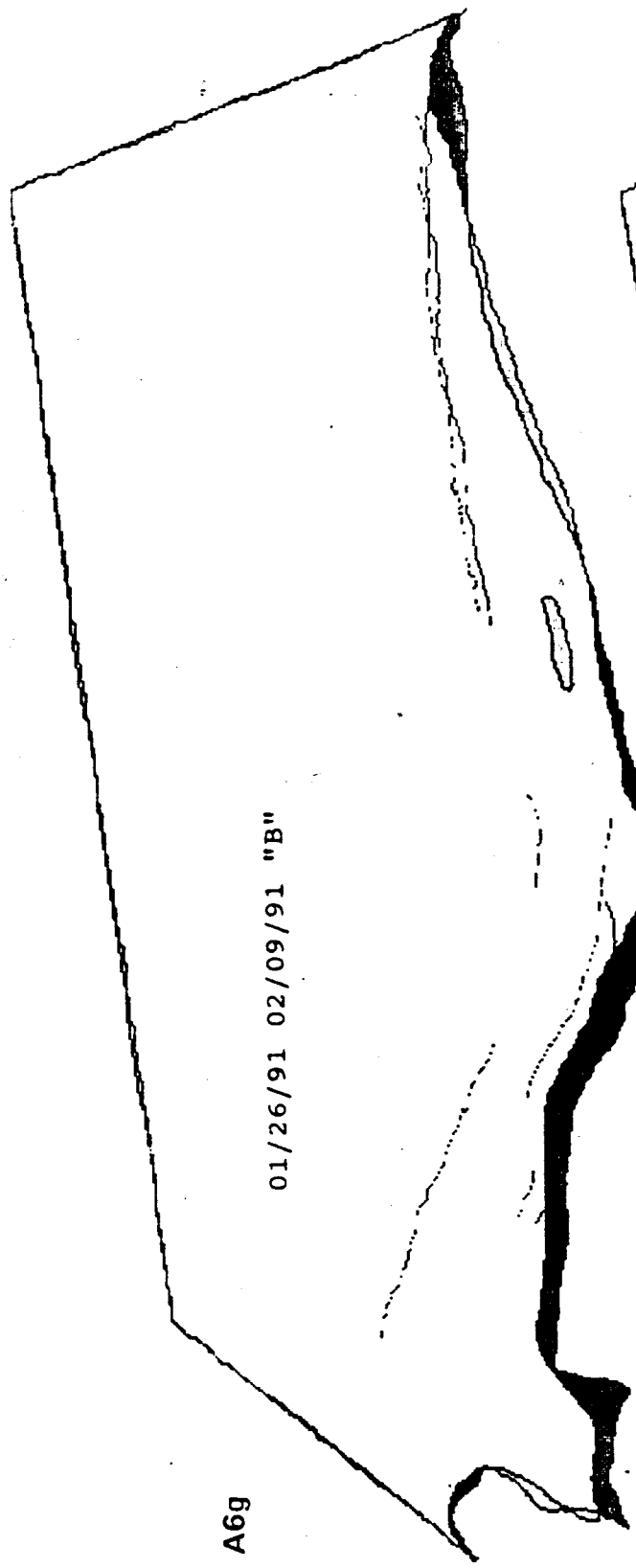
A6f

12/30/90 01/26/91 "C" WINTER



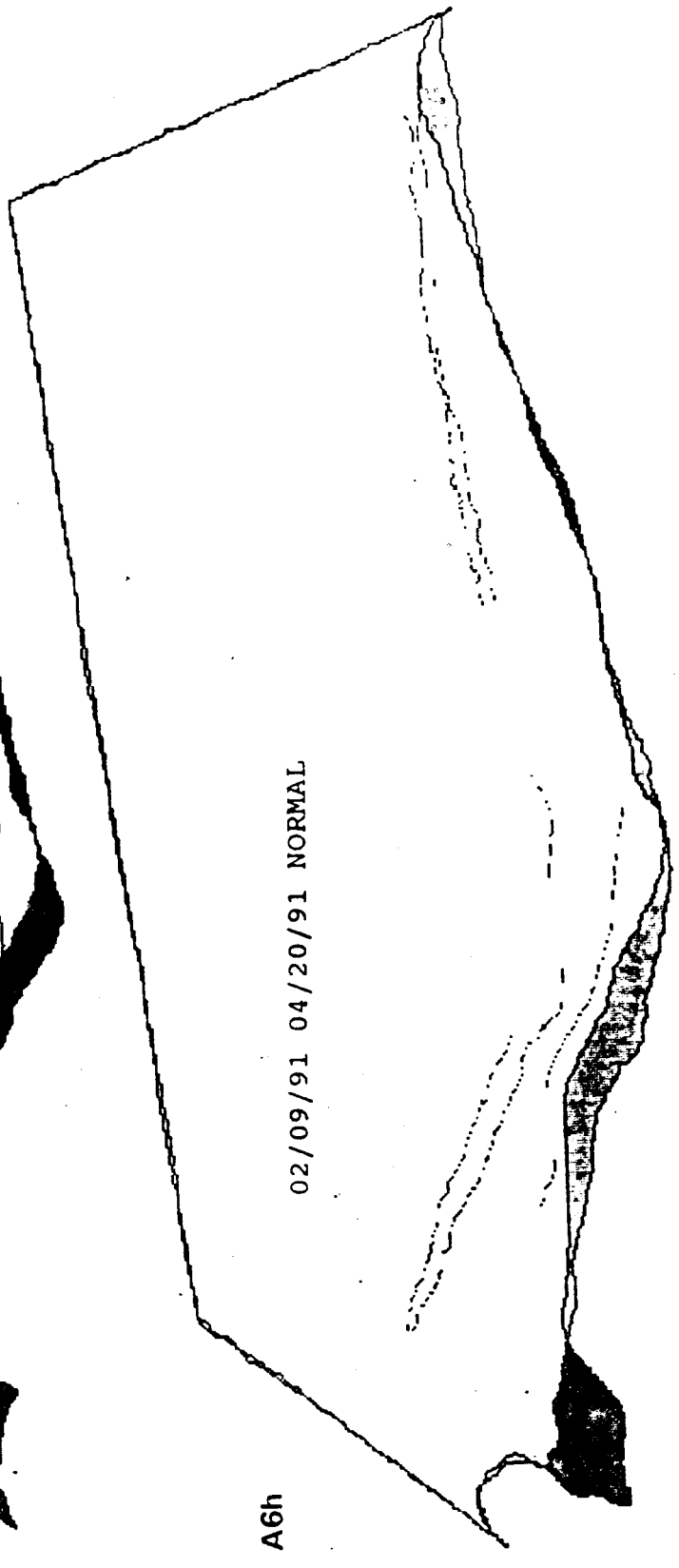
A6g

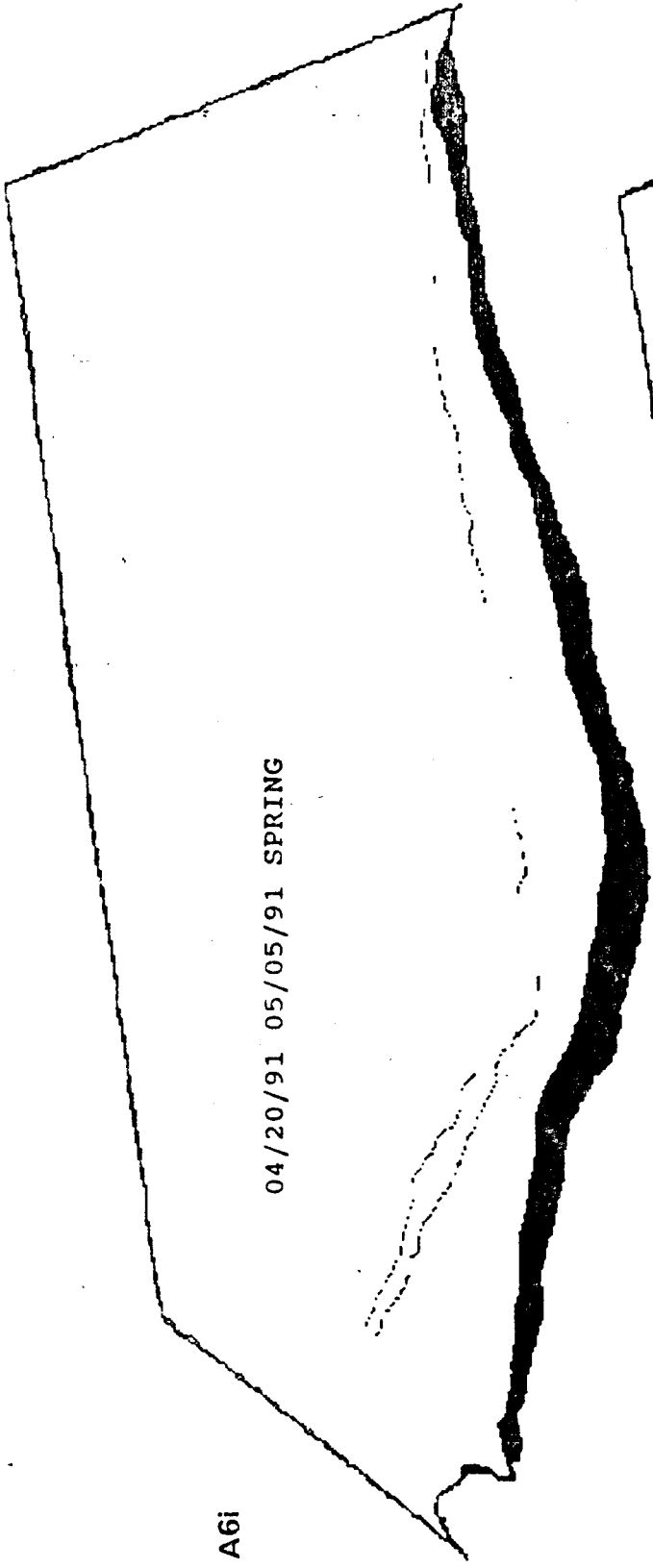
01/26/91 02/09/91 "B"



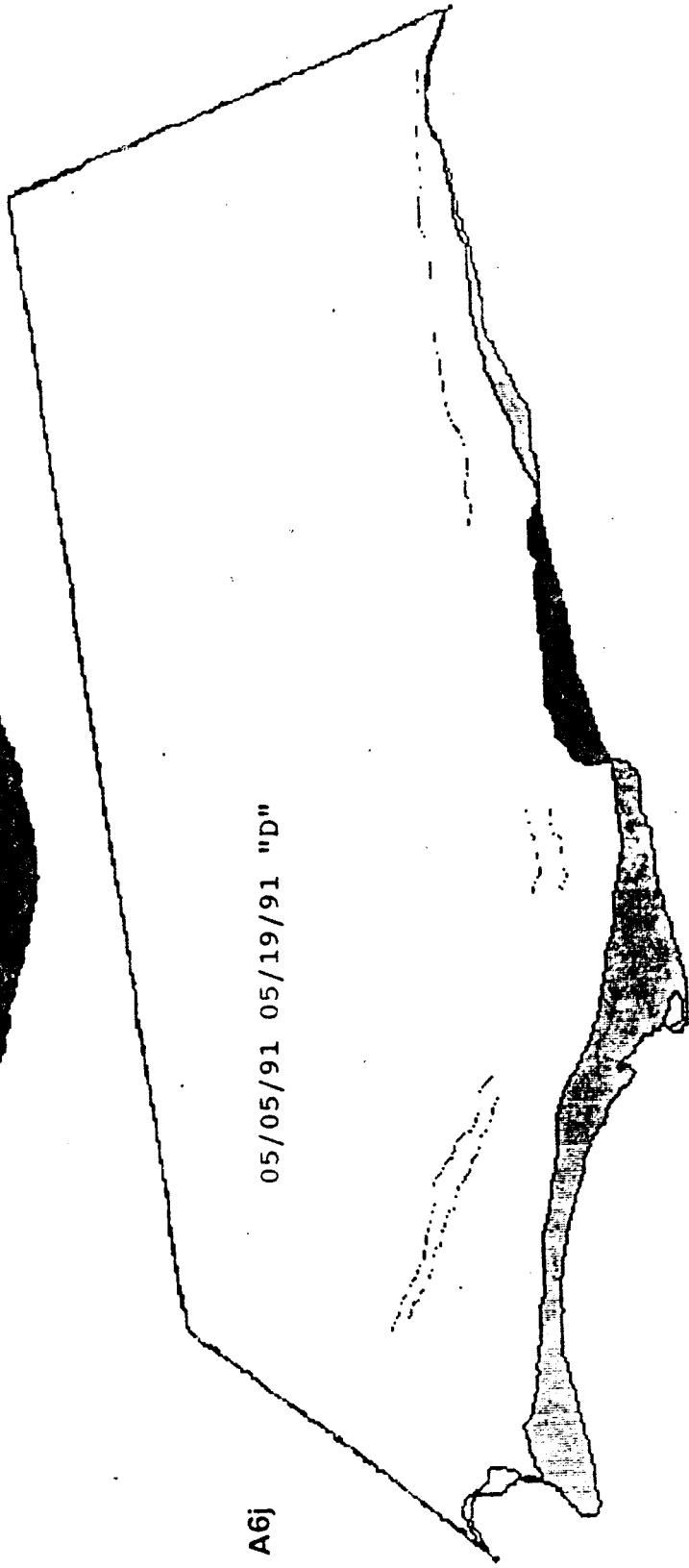
A6h

02/09/91 04/20/91 NORMAL





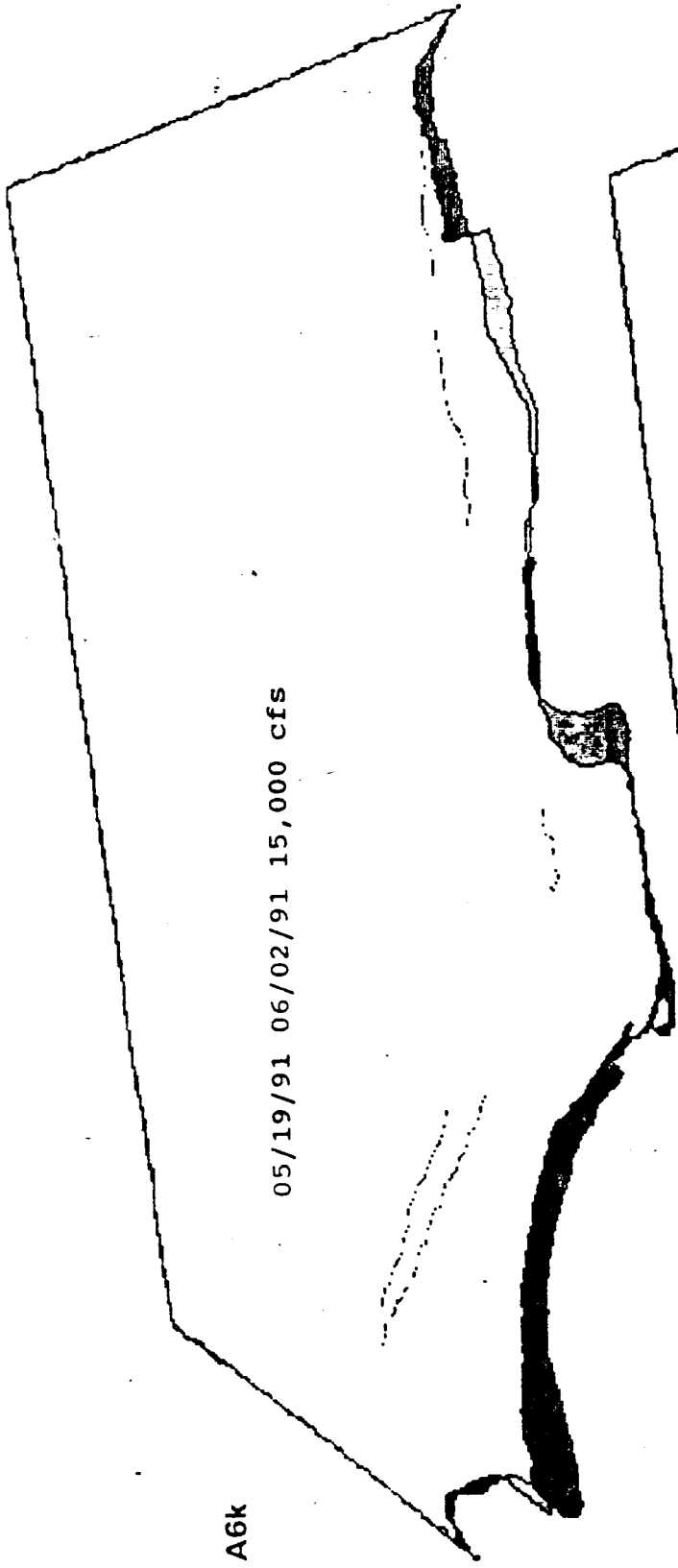
A6i



A6j

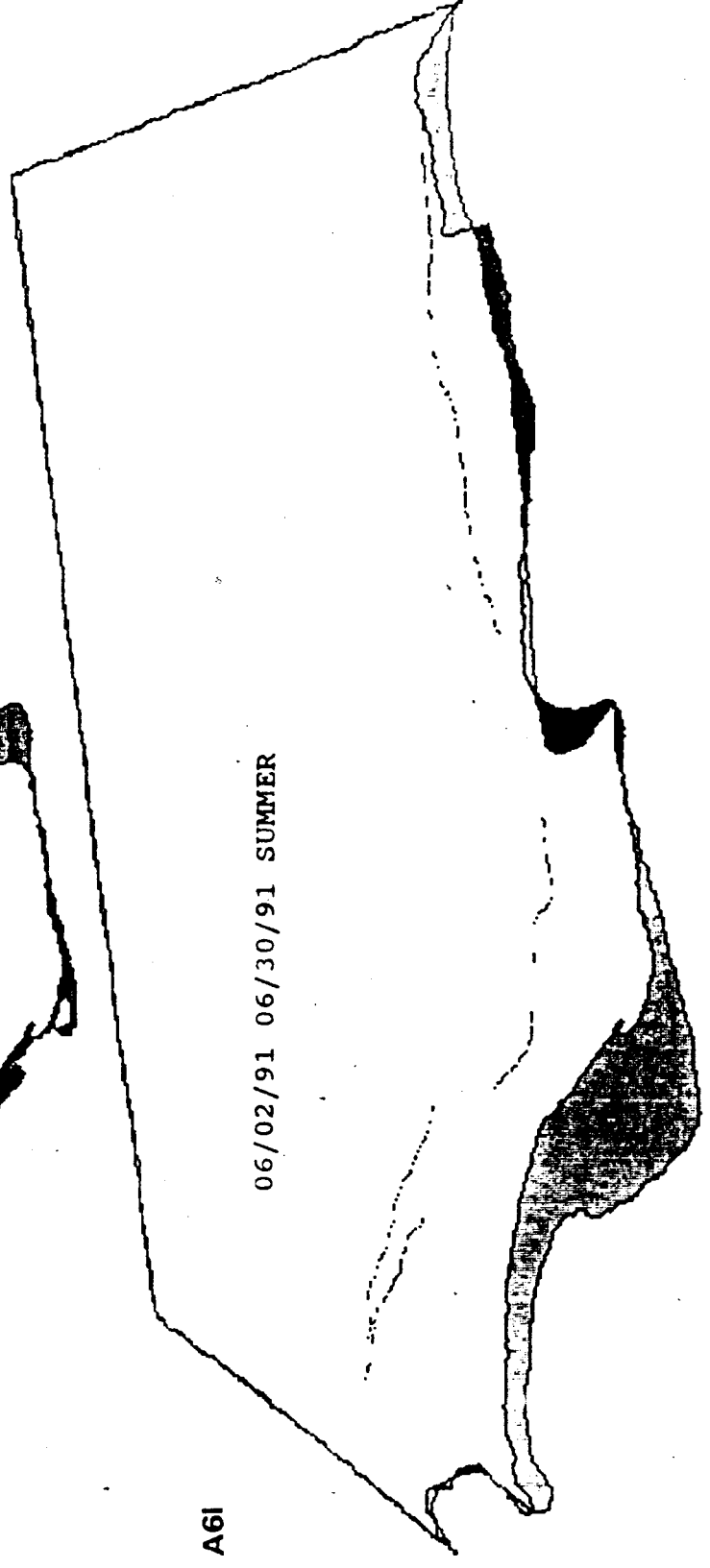
A6k

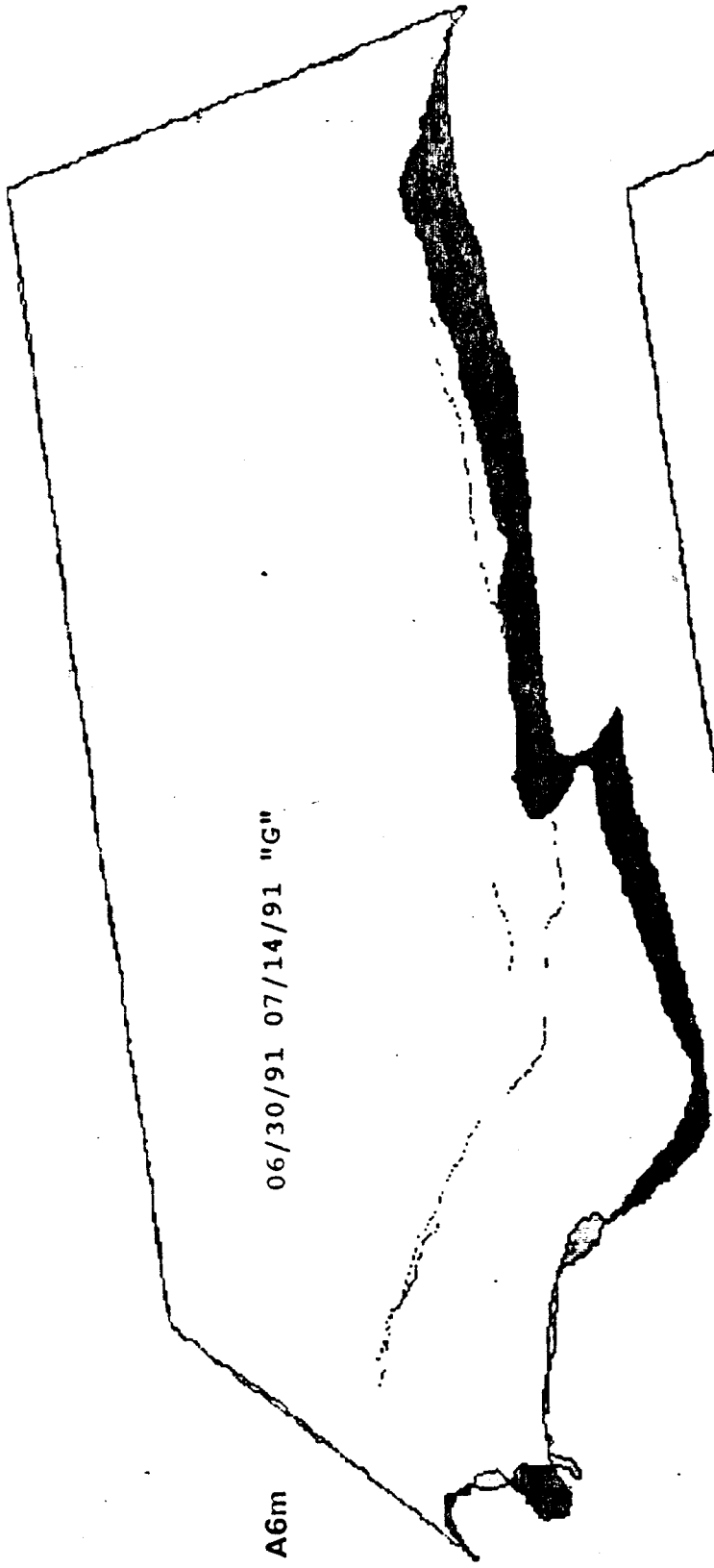
05/19/91 06/02/91 15,000 cfs



A6l

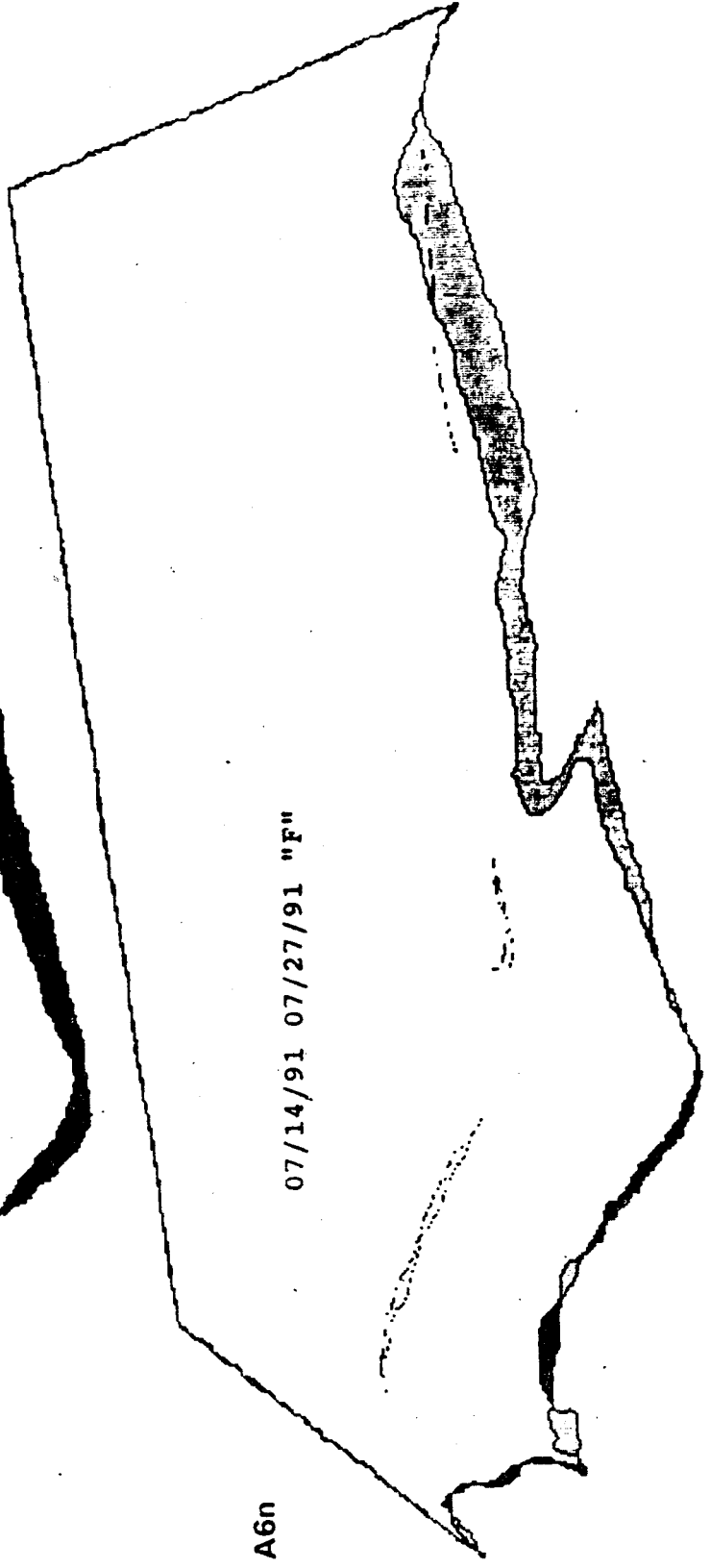
06/02/91 06/30/91 SUMMER





06/30/91 07/14/91 "G"

A6m



07/14/91 07/27/91 "F"

A6n

SITE 66 LEFT

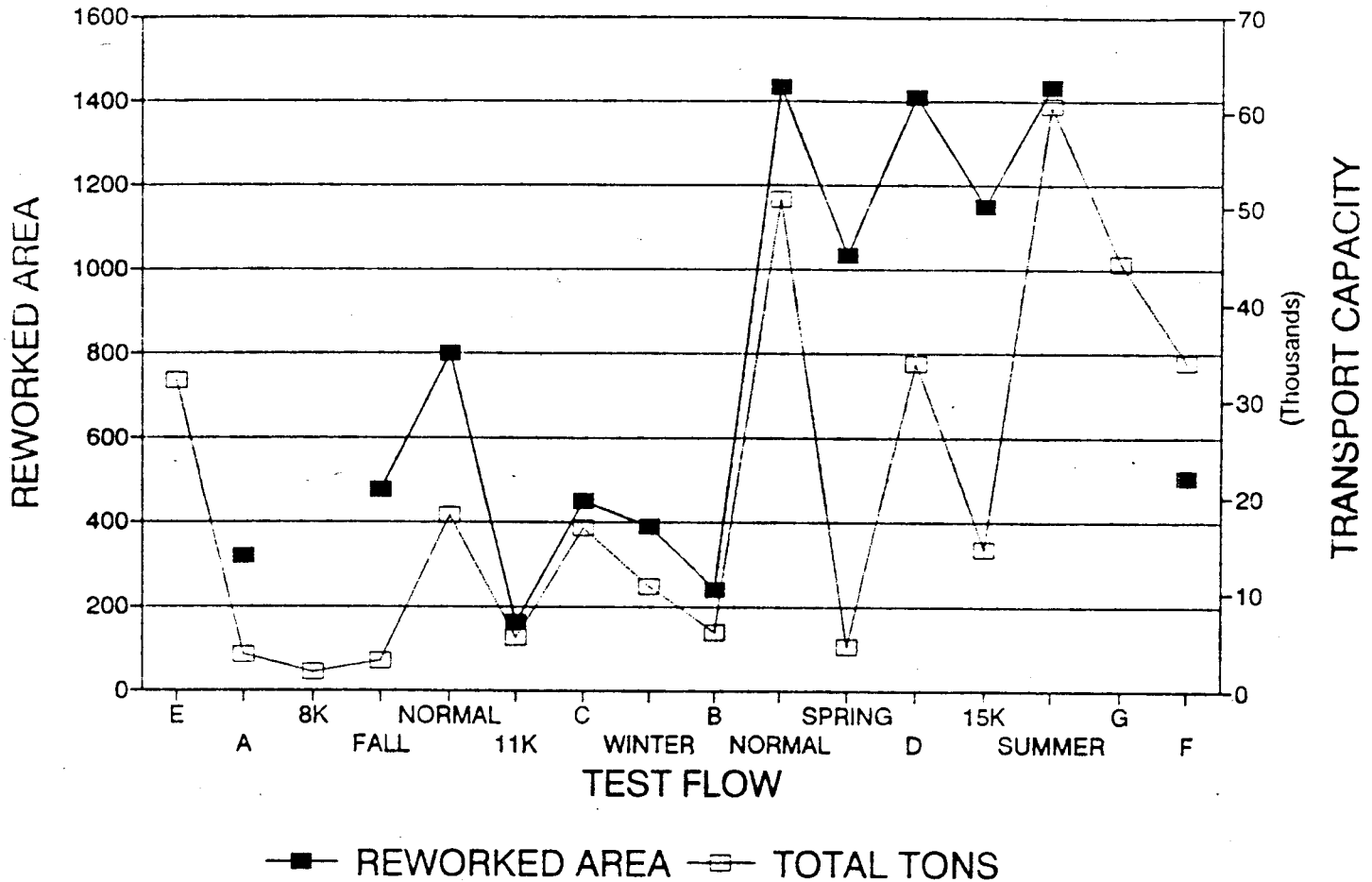
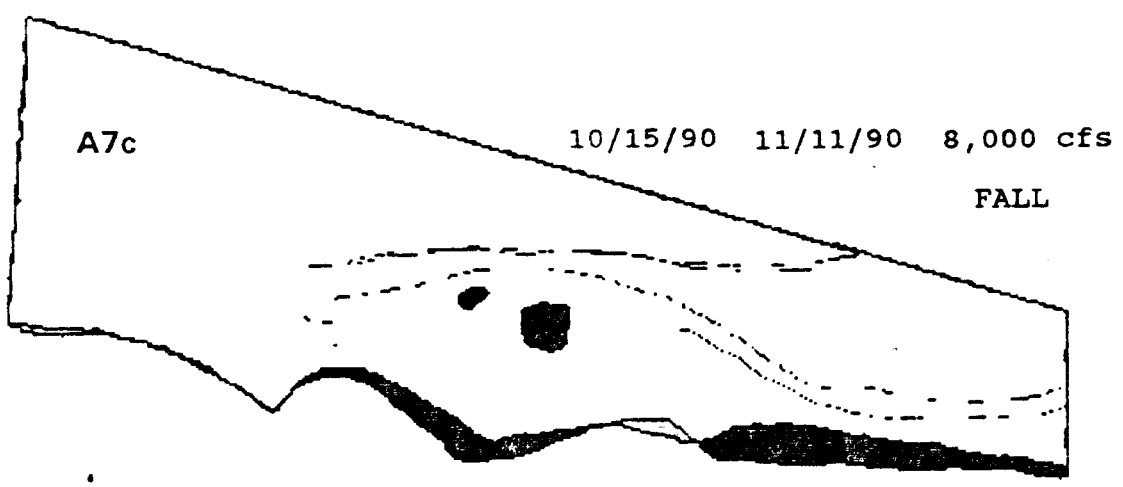
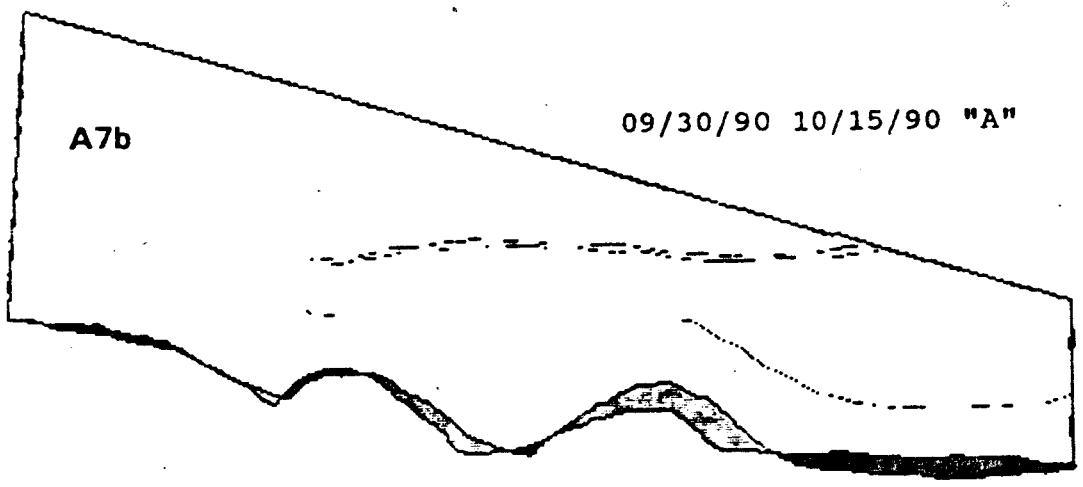
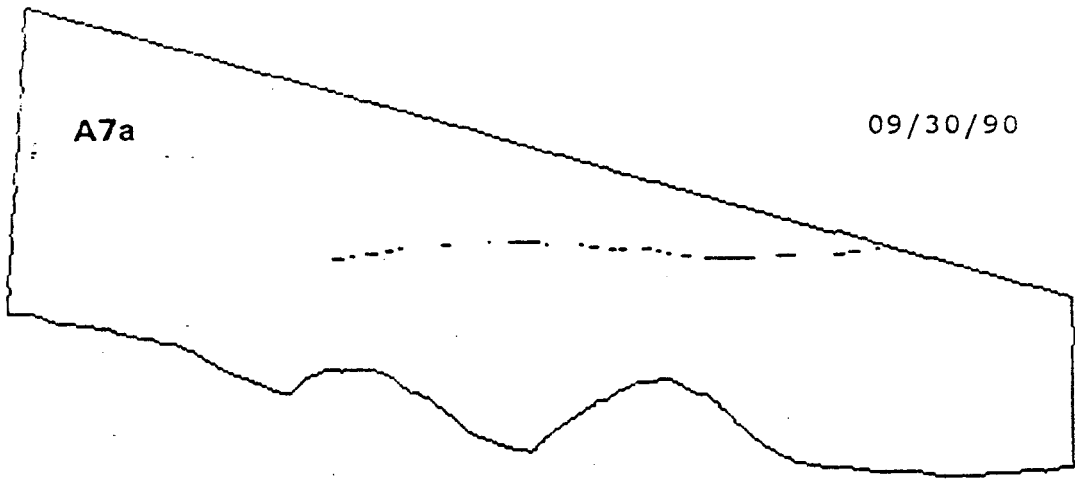
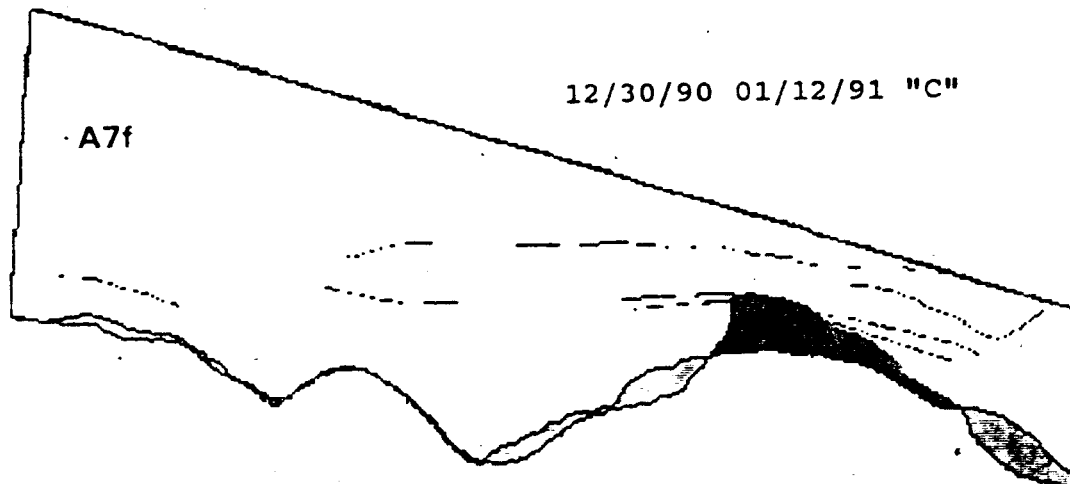
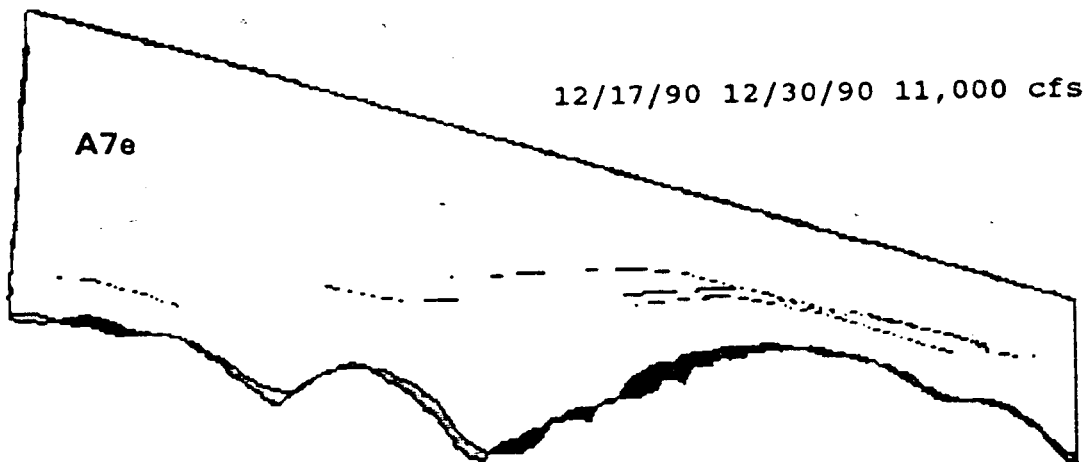
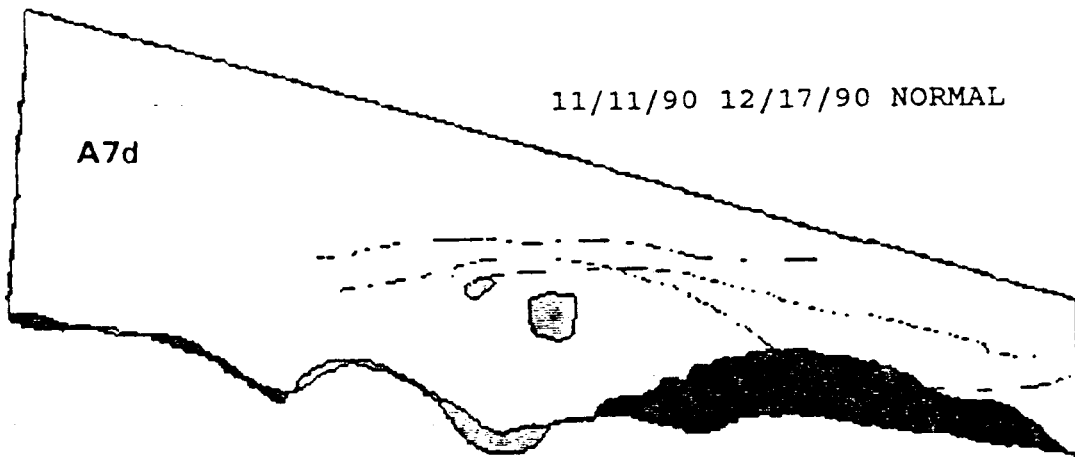


Figure A7. Time-series plot of reworked area and sediment transport capacity for site CR 66 L.

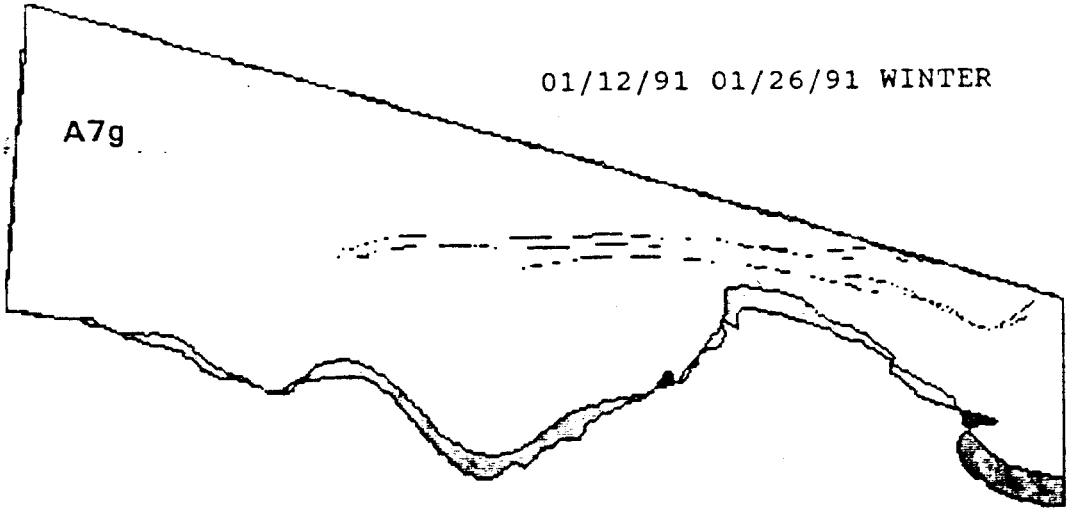
Figures A7a-A7n. Original planimetric outlines and subsequent comparisons of bracketing outlines. Dark shaded areas were eroded. Light shaded areas were aggraded.





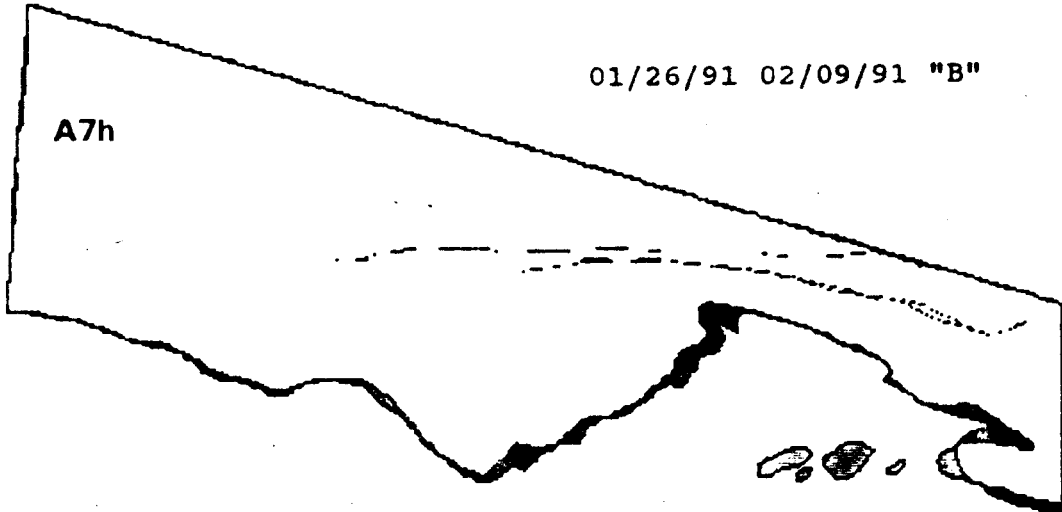
01/12/91 01/26/91 WINTER

A7g



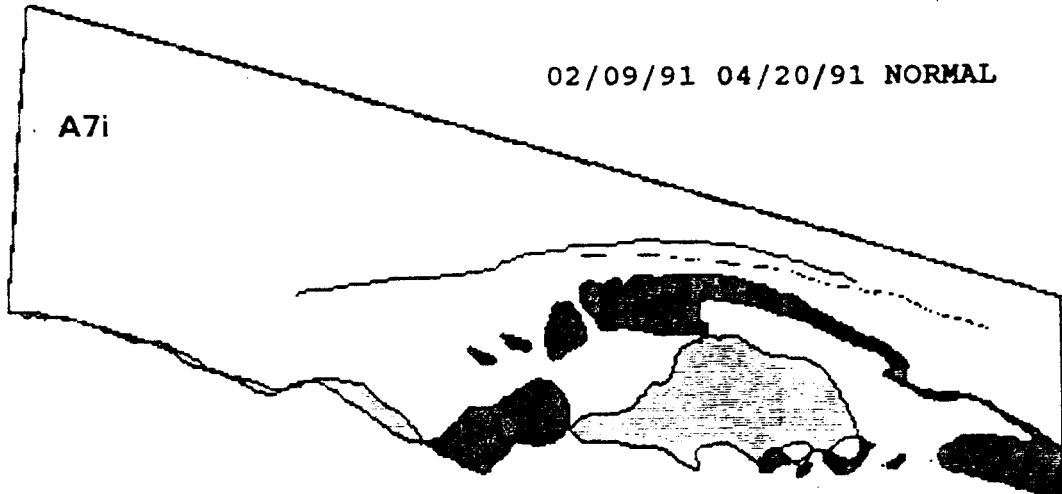
01/26/91 02/09/91 "B"

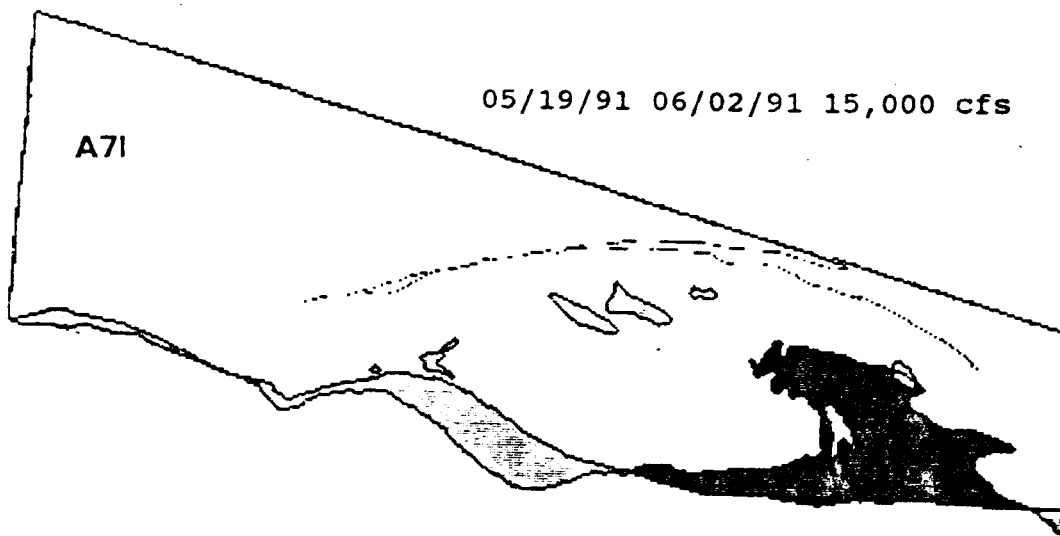
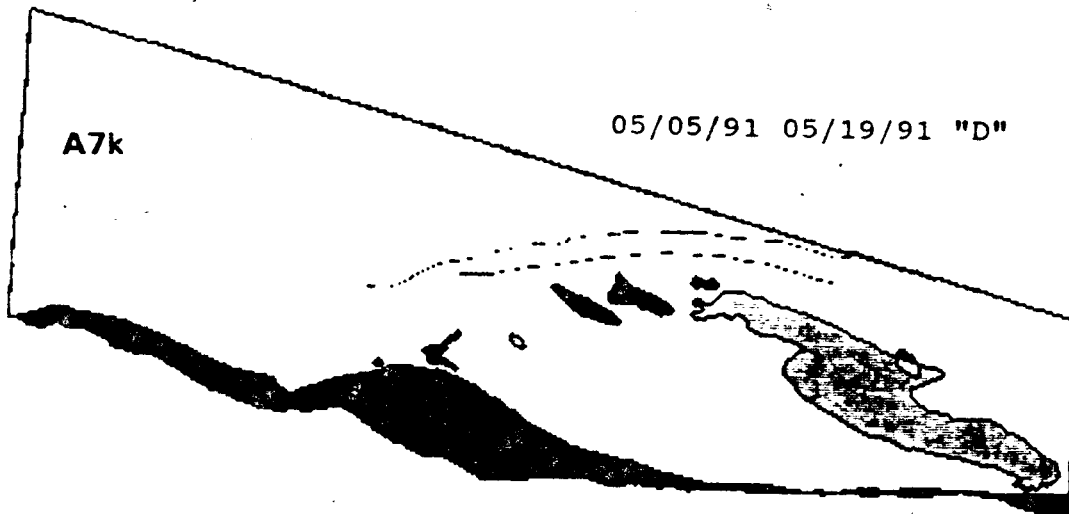
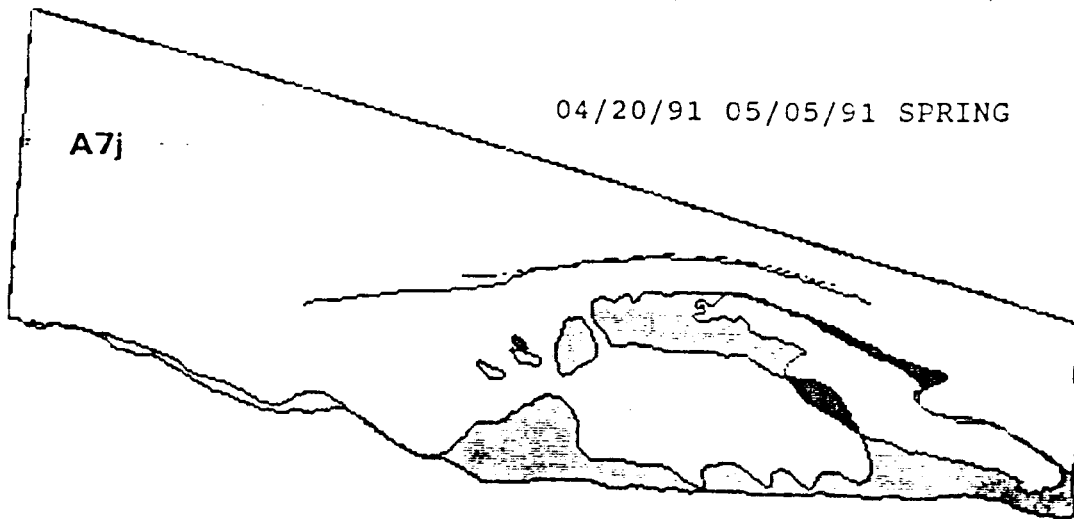
A7h

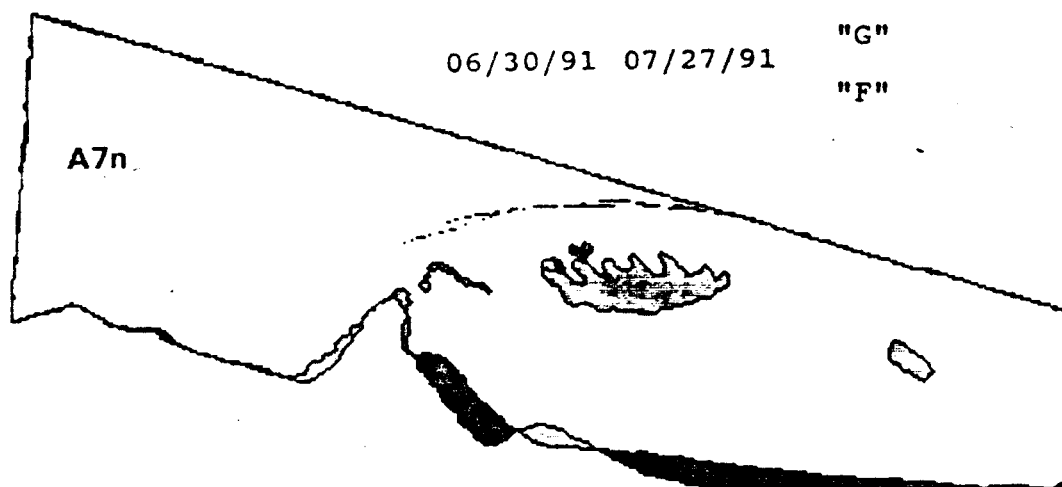
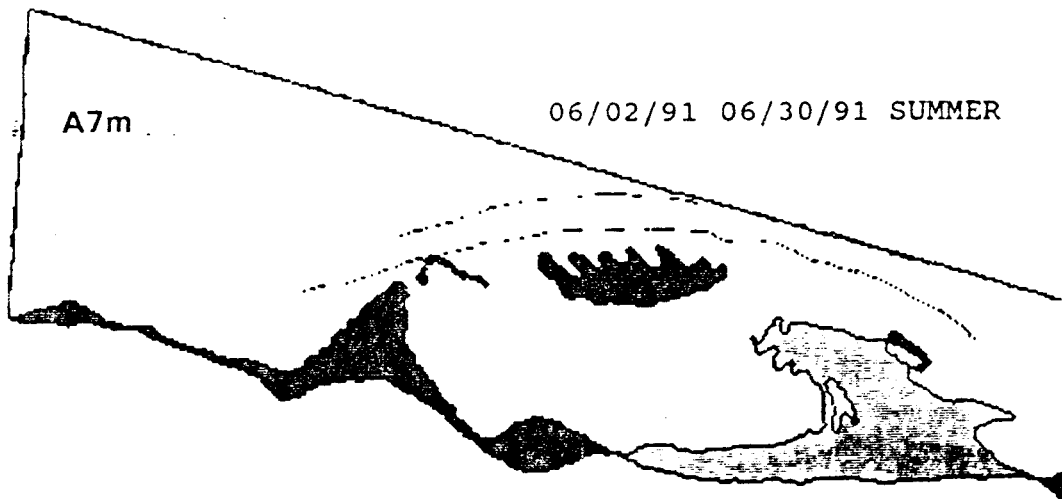


02/09/91 04/20/91 NORMAL

A7i







SITE 68 RIGHT

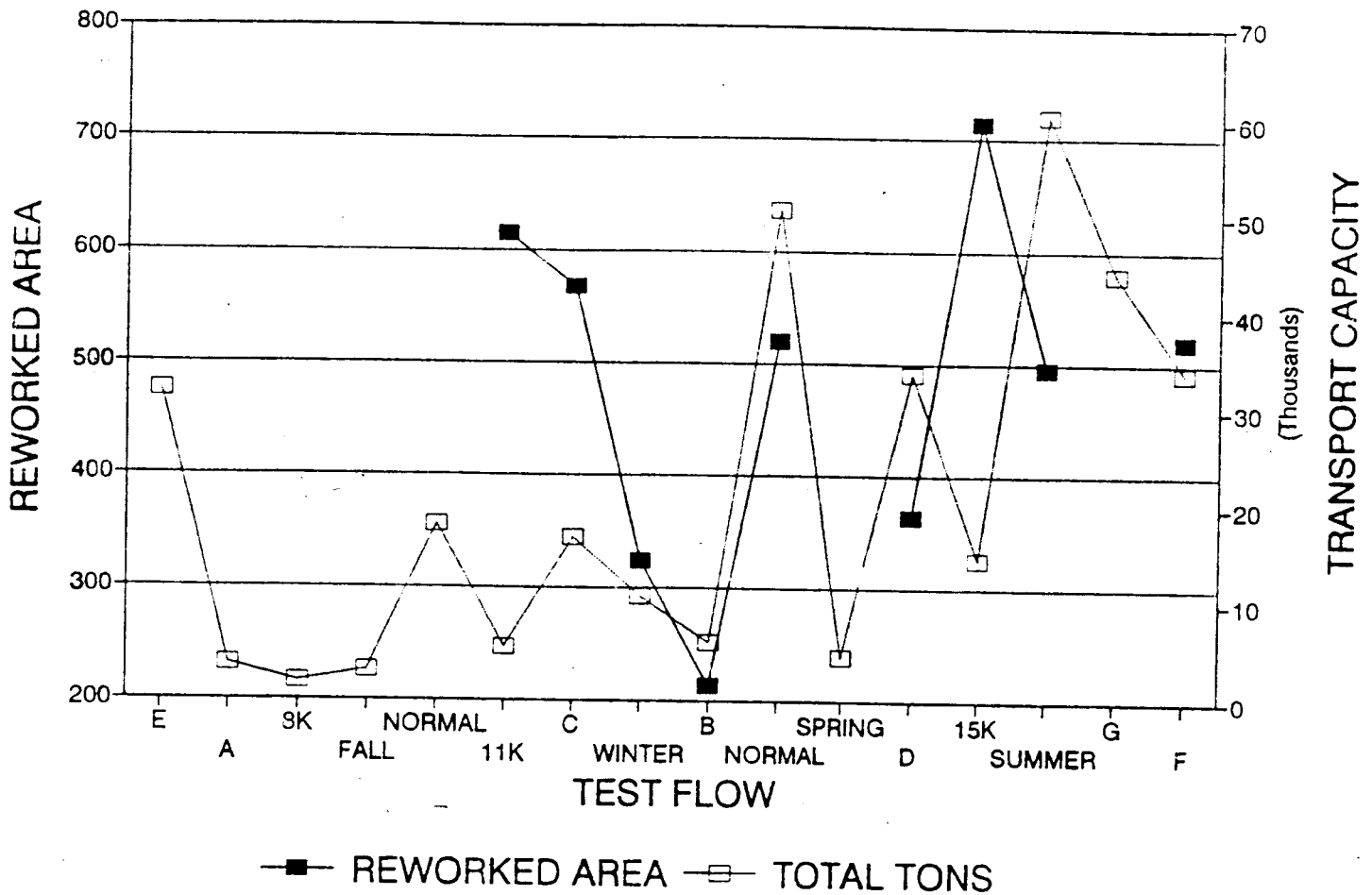
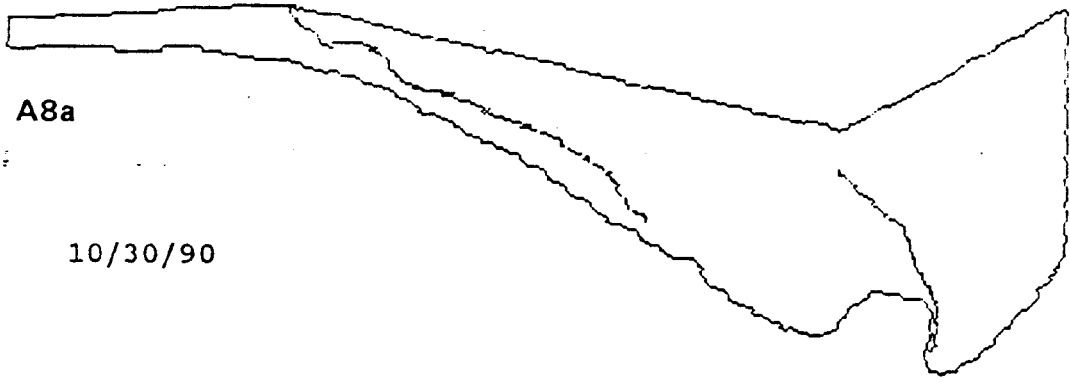


Figure A8. Time-series plot of reworked area and sediment transport capacity for site CR 68 R.

Figures A8a-A8j. Original planimetric outlines and subsequent comparisons of bracketing outlines. Dark shaded areas were eroded. Light shaded areas were aggraded.

A8a

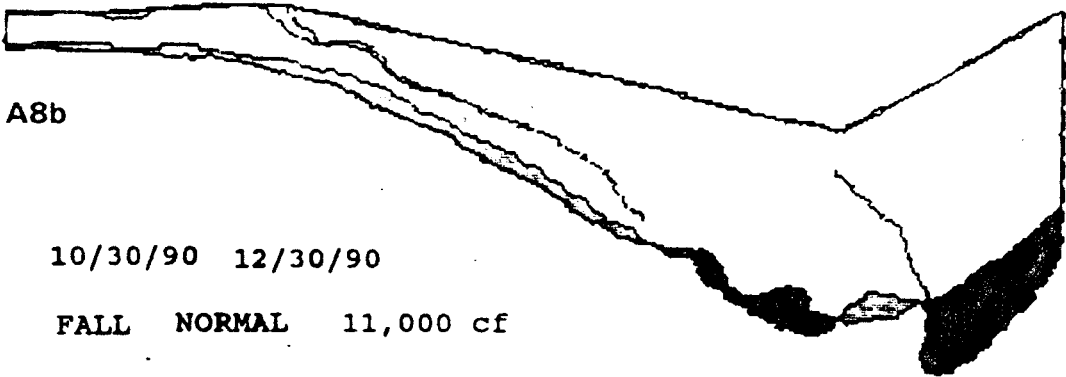
10/30/90



A8b

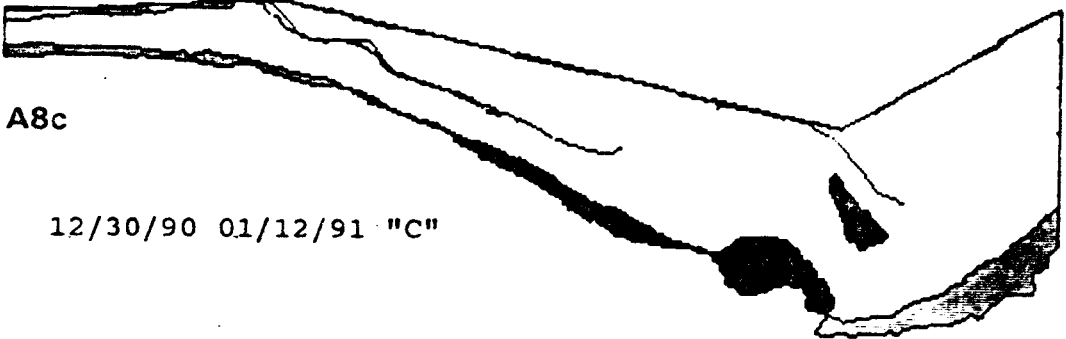
10/30/90 12/30/90

FALL NORMAL 11,000 cf



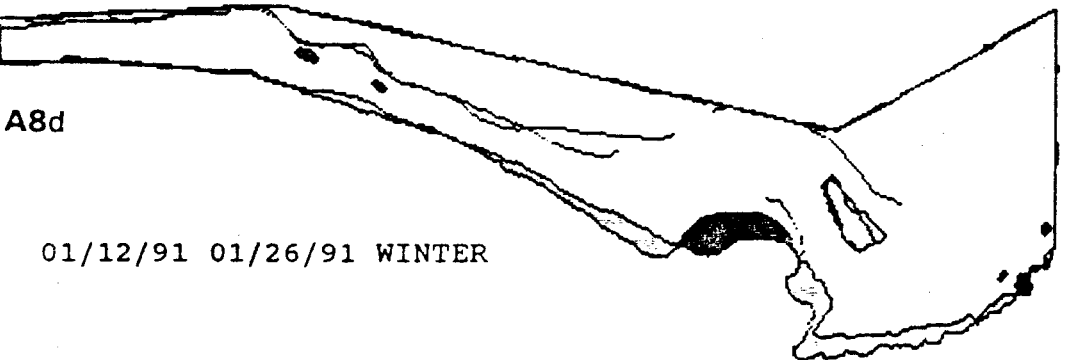
A8c

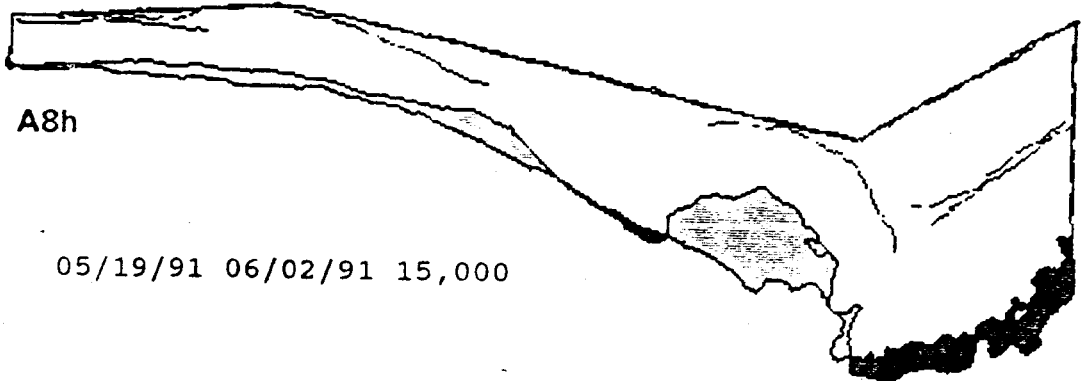
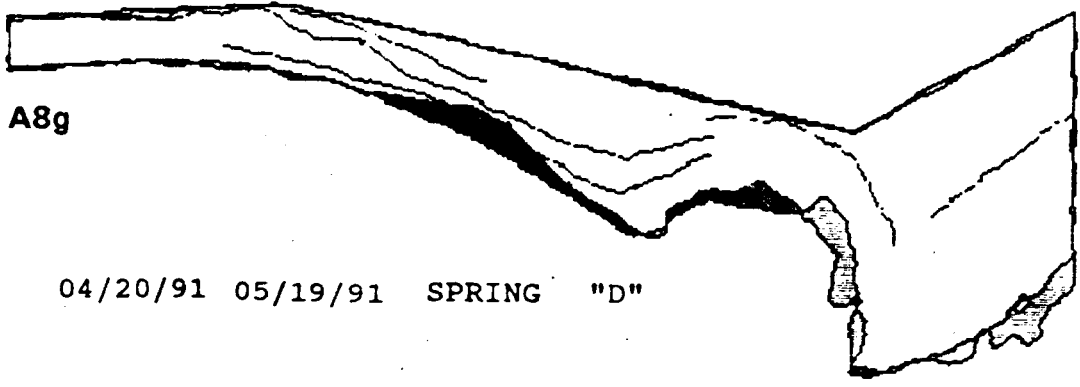
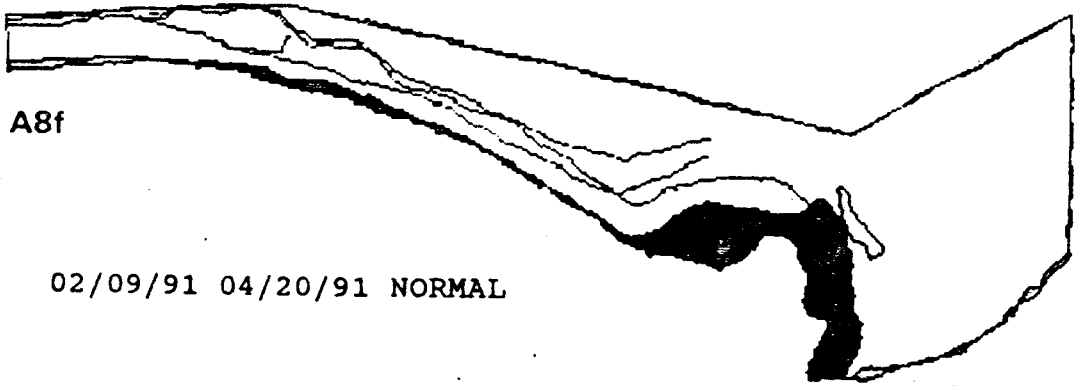
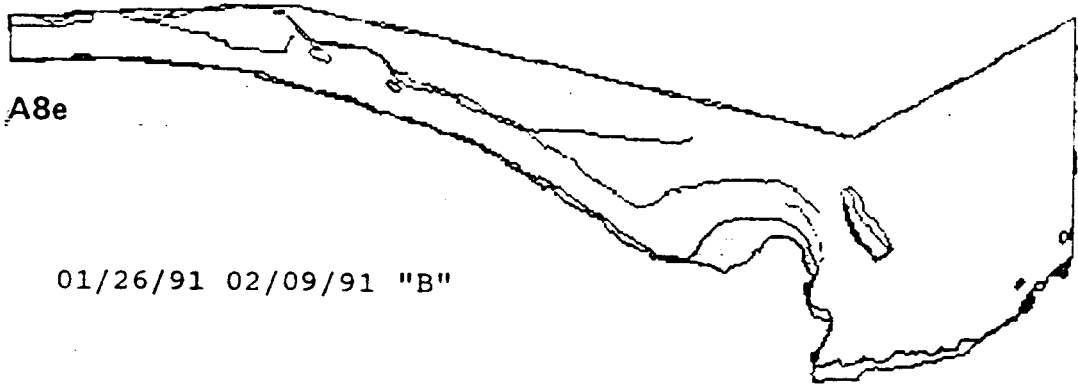
12/30/90 01/12/91 "C"

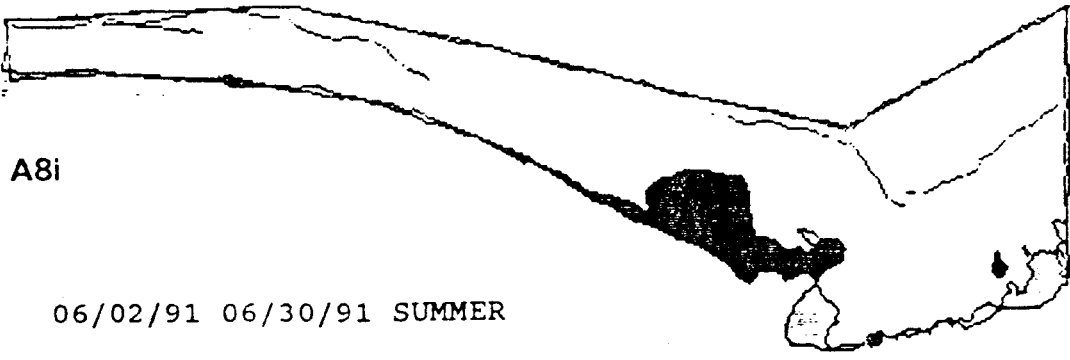


A8d

01/12/91 01/26/91 WINTER

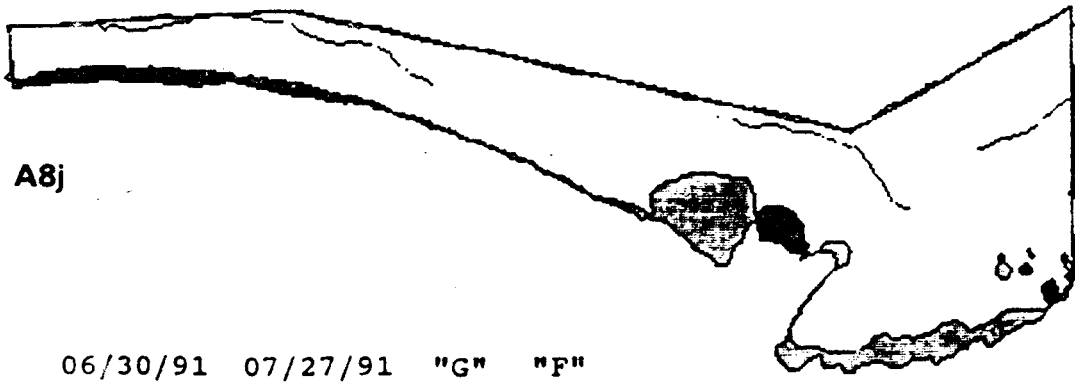






A8i

06/02/91 06/30/91 SUMMER



A8j

06/30/91 07/27/91 "G" "F"

SITE 81 LEFT

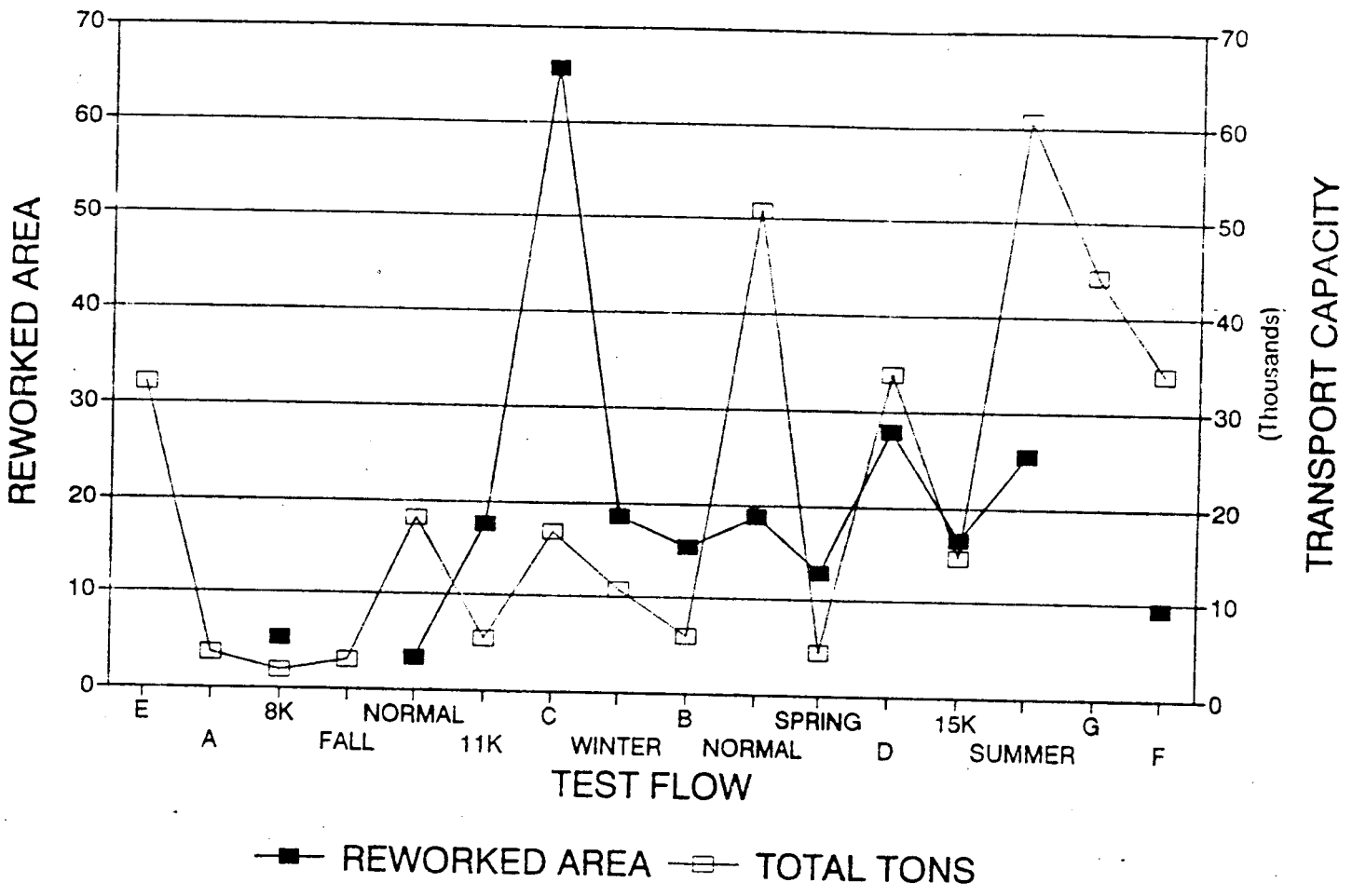


Figure A9. Time-series plot of reworked area and sediment transport capacity for site CR 81 L.

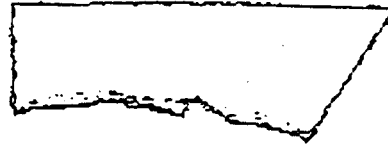
Figures A9a-A9m. Original planimetric outlines and subsequent comparisons of bracketing outlines. Dark shaded areas were eroded. Light shaded areas were aggraded.

A9a



10/15/90

A9b



10/15/90 10/30/90 8,000 cfs

A9c



10/30/90 12/17/90 FALL
NORMAL

A9d



12/17/90 12/30/90 11,000 cfs

A9e



12/30/90 01/12/91 "C"

A9f



01/12/91 01/26/91 WINTER

A9g



01/26/91 02/09/91 "B"

A9h



02/09/91 04/20/91 NORMAL

A9i



04/20/91 05/05/91 SPRING

A9j



05/05/91 05/19/91 "D"

A9k



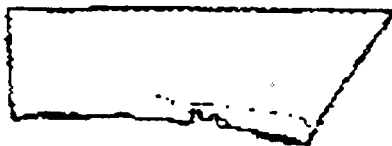
05/19/91 06/02/91 15,000 cfs

A9l



06/02/91 06/30/91 SUMMER

A9m



06/30/91 07/27/91 "G" "F"

SITE 172 LEFT

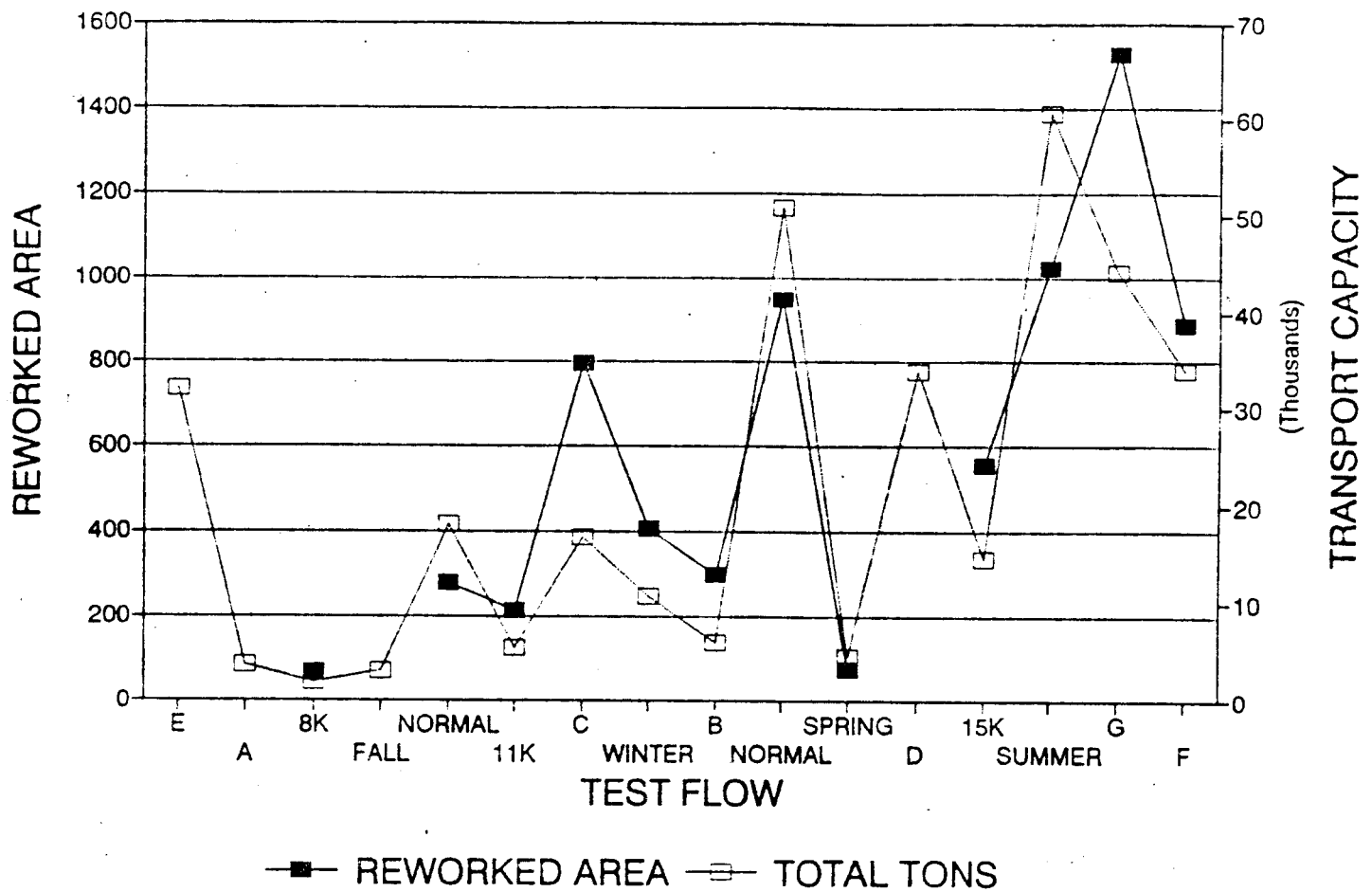
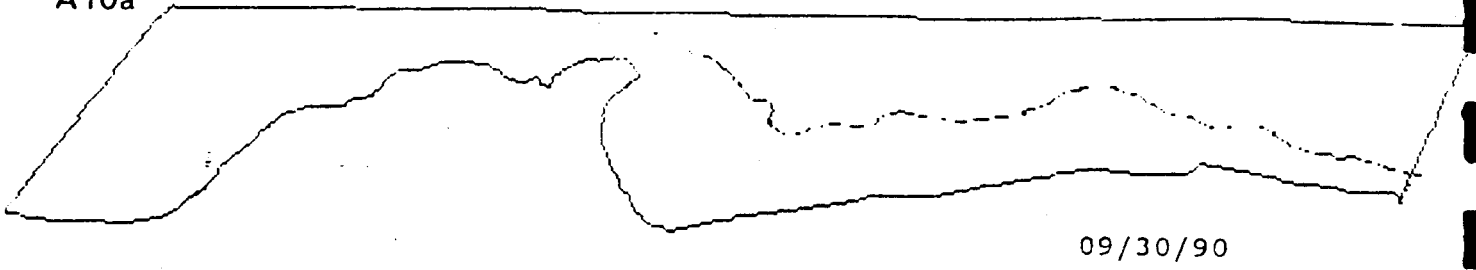


Figure A10. Time-series plot of reworked area and sediment transport capacity for site CR 172 L.

Figures A10a-A10m. Original planimetric outlines and subsequent comparisons of bracketing outlines. Dark shaded areas were eroded. Light shaded areas were aggraded.

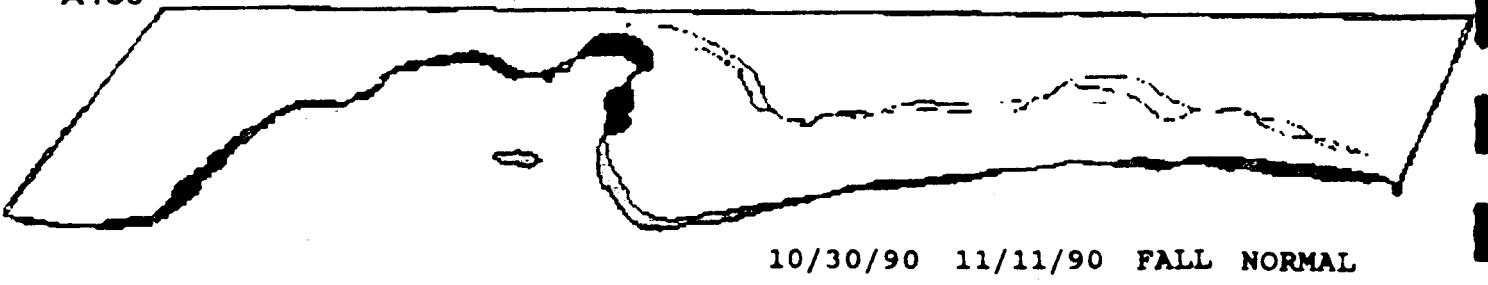
A10a



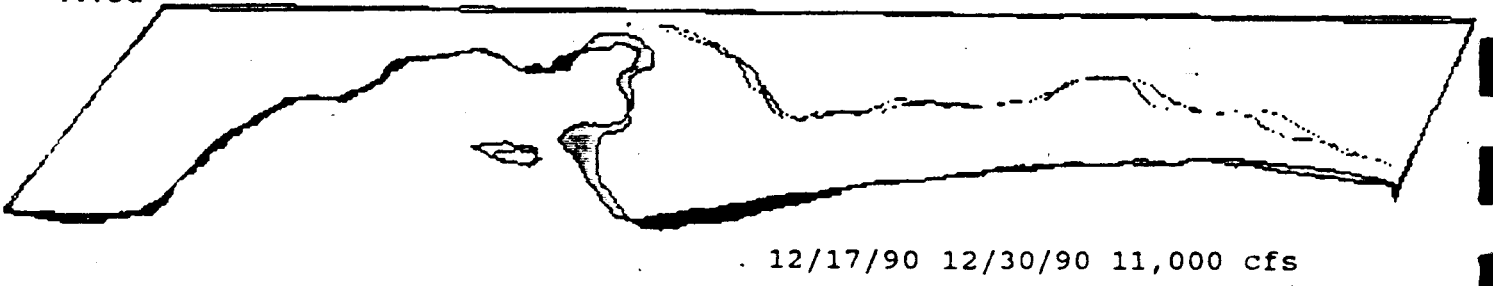
A10b



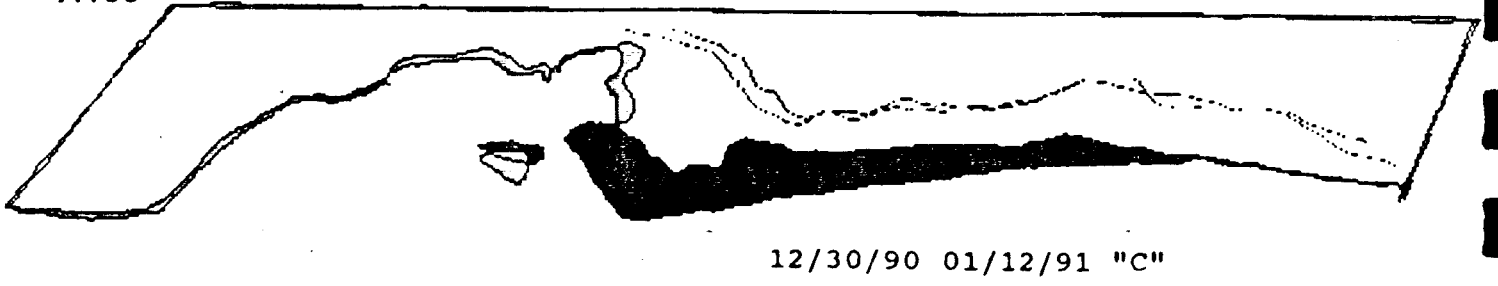
A10c

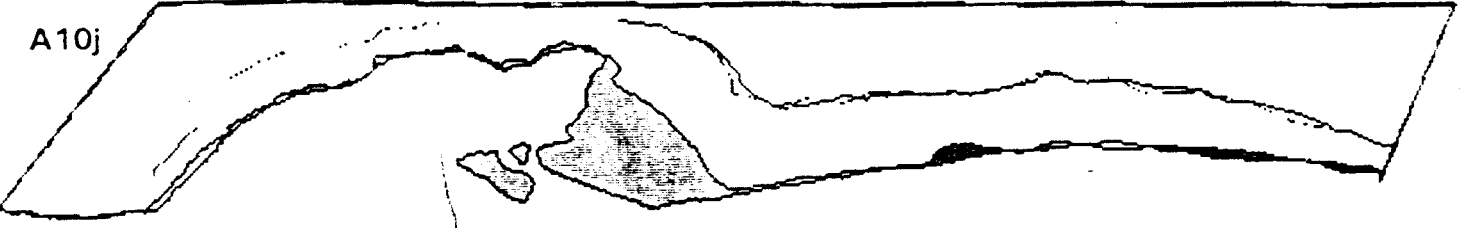
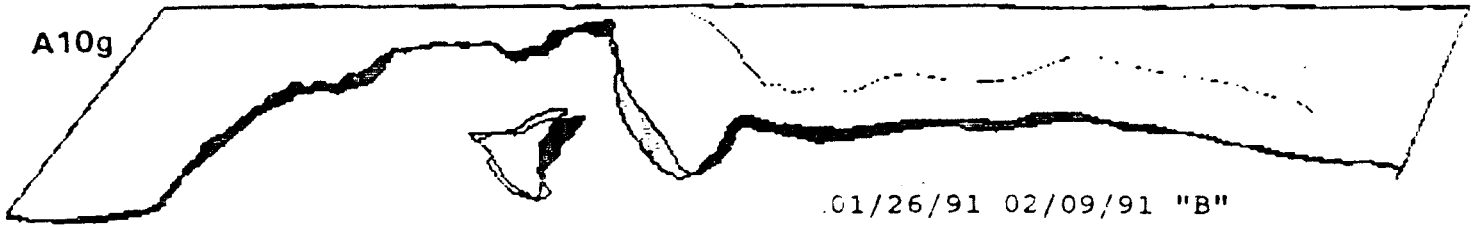
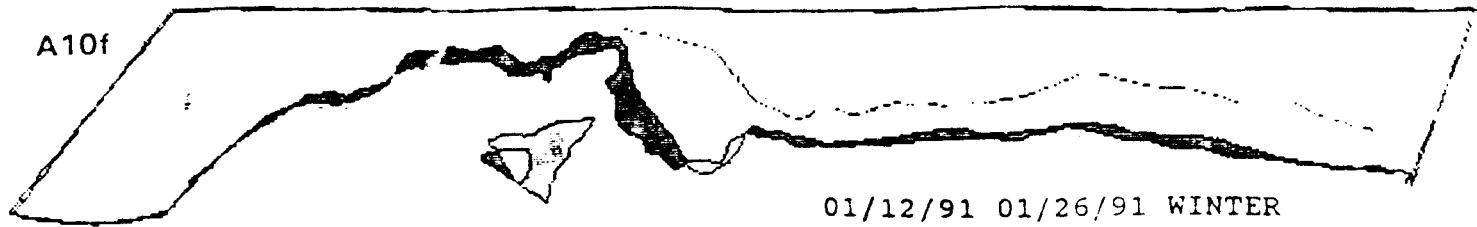


A10d

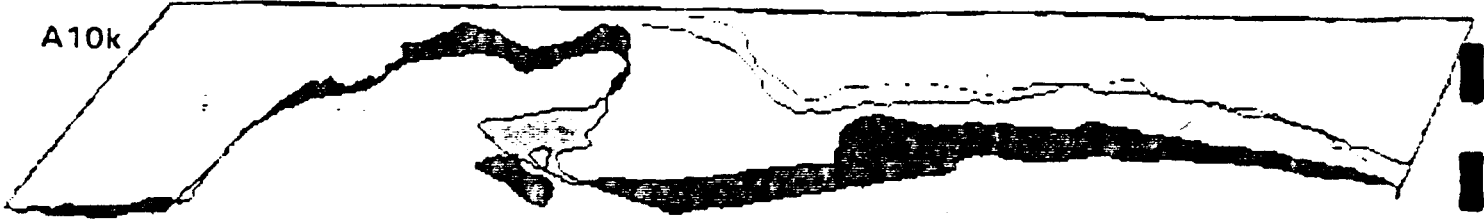


A10e



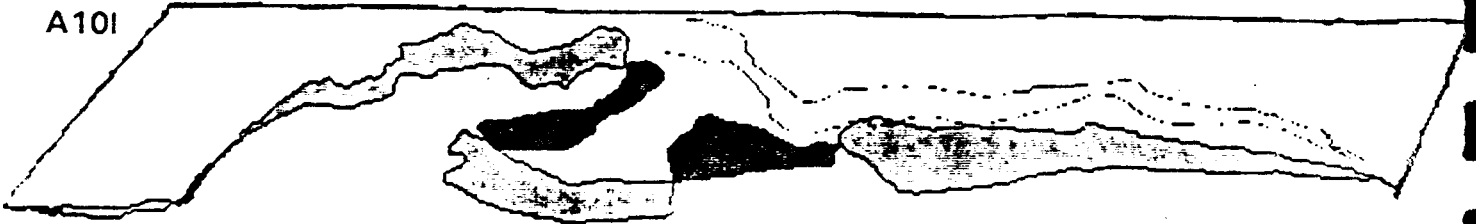


A10k



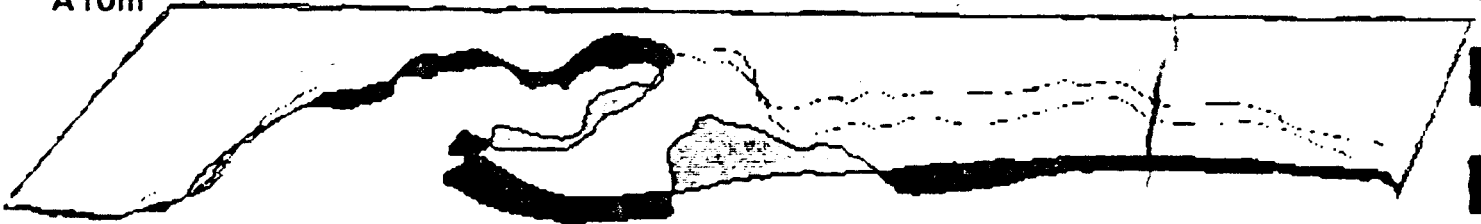
06/02/91 06/30/91 SUMMER

A10l



06/30/91 07/14/91 "G"

A10m



07/14/91 07/27/91 "F"

CHAPTER 9:

**COLORADO RIVER SAND BUDGET:
LEES FERRY TO LITTLE COLORADO RIVER
INCLUDING MARBLE CANYON**

Gary M. Smillie
William L. Jackson
and
Dean Tucker

National Park Service
Water Resources Division
Fort Collins, CO 80521

July 1992

United States Department of the Interior
National Park Service
Washington, D.C.

TABLE OF CONTENTS

OBJECTIVES / 1

BACKGROUND / 1

Flow Fluctuations and Sand Transport / 2

Ramping Rates, Stage Fluctuations and Beach Erosion / 2

METHODS / 2

RESULTS / 3

Figures 1 and 2. Sand delivery from the Paria River into the
Colorado River / 4

Figure 3. Sand budget Colorado River cumulative surplus/deficit / 5

Effects of Alternative Dam Operations on Main Channel Sand
Transport / 6

DISCUSSION AND RECOMMENDATIONS / 6

Figure 4. Sand transport examples / 7

REFERENCES / 8

OBJECTIVES

The objective of this analysis is to determine how annual variations in sand input from the Paria River affect the balance of river-stored sand in the Colorado River between Lees Ferry and the Little Colorado River under alternative conditions of annual sand transport capacity in the Colorado River. It will be shown that if flow fluctuations in the Colorado River are managed to achieve a balance with long-term average annual sand inputs from the Paria River, there will inevitably be periods of fairly substantial deficits in river-stored sand. Therefore, it may be prudent to select a somewhat more conservative objective for annual sand transport in the Colorado River. While certain assumptions in this analysis may need to be refined in the EIS process, we believe the analytical approach presented here should be useful in addressing the "river-reach" sand balance issue associated with EIS alternatives.

BACKGROUND

The operation of Glen Canyon Dam has altered the natural flow and sediment transport regimes of the Colorado River in the Grand Canyon. The natural unimodal spring runoff peak regime has been replaced by a regime characterized by a series of lesser and more frequent peak discharges that are intentionally sized and timed for the production of hydroelectric power. Additionally, Lake Powell is an efficient sediment trap and effectively removes all inorganic matter from the Glen Canyon Dam to the Paria River confluence, these clear water releases have stripped the channel of stored sand deposits. Below the confluence, however, sand supplied by the Paria is available to the Colorado River and under certain circumstances can be stored along the river margin as beach deposits.

In this analysis, a distinction is made between sediment management impacts associated with the range of flow fluctuations and those associated with ramping rates (especially "down-ramps"). Next, sand inputs from the Paria River are evaluated with an emphasis on annual variability. The implications of annual variations in sand input on long-term sediment balances in the Colorado River through Marble Canyon are described. Finally, implications for the management of flows are presented. Specifically, the implications of six hypothetical flow release regimes on annual sediment transport are evaluated. The reach between Lees Ferry and the Little Colorado River is the focus of this analysis, because this reach is most susceptible to management-induced reductions in sand storage.

Objectives for sediment management along the Colorado River in the Grand Canyon were developed by scientists affiliated with the Glen Canyon Environmental Studies Program (GCES). Those objectives are 1) to maintain a positive sand balance, and 2) to maintain the range of morphologic features associated the temporary storage of sediment in the river system (e.g., beach deposits, high-flow terrace deposits, return channels, etc.).

Flow Fluctuations and Sand Transport

It is determined elsewhere that sand transport, Q_s (in tons/day), in the Grand Canyon can be estimated by the relationship

$$Q_s = (2.84 \cdot 10^{-12}) Q_w^{3.53} \quad (1)$$

Where Q_w is stream discharge (E. Andrews, US Geological Survey, Boulder, CO, personal communication). This power function relationship means that sand transport through the Grand Canyon can be minimized for any given annual release by releasing water at a constant rate. As flow fluctuations are introduced to the system (both the range of fluctuation and the period of time during which flows deviate from the annual mean) annual sand transport rates increase. If annual sand transport is increased by highly fluctuating flows above a certain point, a long-term reduction of stored sand will result in the subject river reach.

When the amount of stored river sand is decreased, there is less sand available for deposition in backwaters and eddies, less sand available to "nourish" beaches during periods of high flow (flows in excess of normal operations), and a greater likelihood that the bases of margin deposits (including beaches) will be eroded. Because tributary sand inputs are highly variable on an annual basis, simply managing main channel sediment transport to achieve a balance with long-term (mean) sand inputs will not avoid periodic (and sometimes fairly large) periods of deficit in river-stored sand in critical river reaches. This situation will be further described and quantified in the analysis which follows.

Ramping Rates, Stage Fluctuations and Beach Erosion

While flow fluctuations influence sediment conditions in the Grand Canyon through their affect on sand transport quantities in the Colorado River (and the consequent effects on the balance of river-stored sand), stage fluctuations and ramping rates also influence sediment conditions through their effect on the stability of sediment margin deposits, including beaches (Bhudu 1992; Werrell, et al. 1992). Thus, the range (and duration) of flow fluctuations affect *both* sediment transport and the balance of river-stored sand, *and* the stability of stored sand on river margins.

METHODS

Daily (mean) flow and suspended sediment transport data are available for the Paria River at Lees Ferry streamgage for the 1949-1976 period. Daily sediment loads were then summed to determine annual sediment yields for each year of record. Sand loads were approximated by assuming that 20% of the total suspended sediment load was sand and that 20% of the total sand load occurred as unmeasured bedload (Randle, and others, 1991). Using the derived values for Paria River sand transport, annual sand

inputs to the Colorado River were plotted over time and summary statistics were generated (annual means, annual medians, and sand-flux duration curves).

To describe the effects of annual variations in sand input on the balance of stored sand in the Colorado River, we assumed three alternative annual sand transport rates for the Colorado River (565,000 tons/yr, 790,000 tons/yr, and 1,000,000 tons/yr) and tributary sand inputs which corresponded to the measured inputs for the 27-year period of record on the Paria River. All changes in stored river sand were expressed as deviations from 1949 amounts (the first year of record). The low Colorado River transport rate equates to the median annual sand input from the Paria River; the medium transport rate corresponds to the mean annual sand input from the Paria River; and the high sand transport rate corresponds to approximately the 30% transport rate on the Paria River sand flux duration curve (Figure 1).

Finally, to evaluate the effects of alternative dam operations on main-channel sand transport, we developed a computer program which developed annual flow-duration curves for alternative operations and applied the sand transport function in Equation 1, above, to calculate annual sand transport for alternative daily flow regimes (this program has a user-interface which permits alternative sand-transport functions to be evaluated).

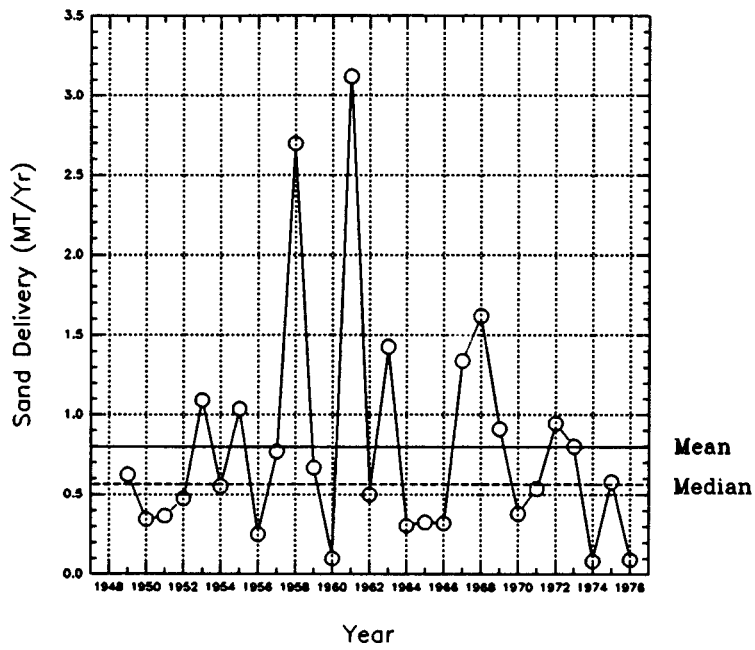
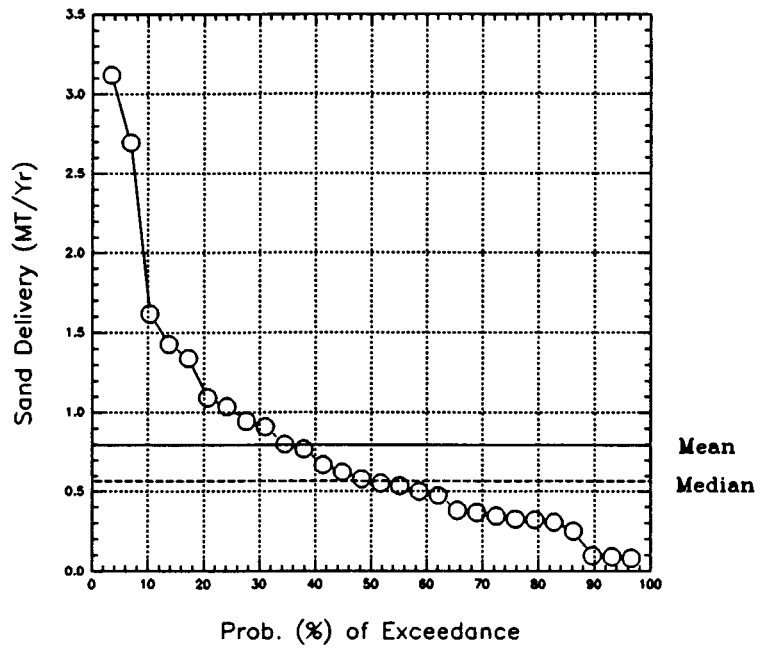
RESULTS

The distribution of annual sand inputs from the Paria River to the Colorado River is positively skewed. Thus, the mean annual sand input (790,000 tons) is considerably larger than the median annual sand input (565,000 tons) (Figure 2). A constant year-around release of 11,200 cfs from Glen Canyon Dam would result in approximately 200,000 tons/year of sand transport in the Colorado River. This value is far less than the mean annual supply from the Paria River and corresponds to approximately the 87% rate on the sand flux duration curve (i.e., 87 % of the time, annual sand input equals or exceeds 200,000 tons).

At the other end of the spectrum, nearly 1.5 millions tons/year of sand is predicted to be transported with a daily fluctuating flow of 3000 to 30,000 cfs (this regime also averages 11,200 cfs). This magnitude of transport is far in excess of the mean annual supply from the Paria. This result is very significant because it strongly suggests that a given long term mean flow in the Colorado River is 11,200 cfs, it is possible to operate the Glen Canyon Dam in a manner that will result in surplus, deficit, or balance of sediment transport relative to supply.

In examining the effects of annual sand input variations on the balance of river-stored sediment in the Colorado River, several interesting points can be observed (Figure 3).

First, if the sand transport capacity of the Colorado River is set to equate exactly to the long term average annual input of sand from the Paria River, fluctuations in river-



FIGURES 1 and 2 (respectively). Sand delivery (million tons/yr) from the Paria River into the Colorado River (1948 - 1975).

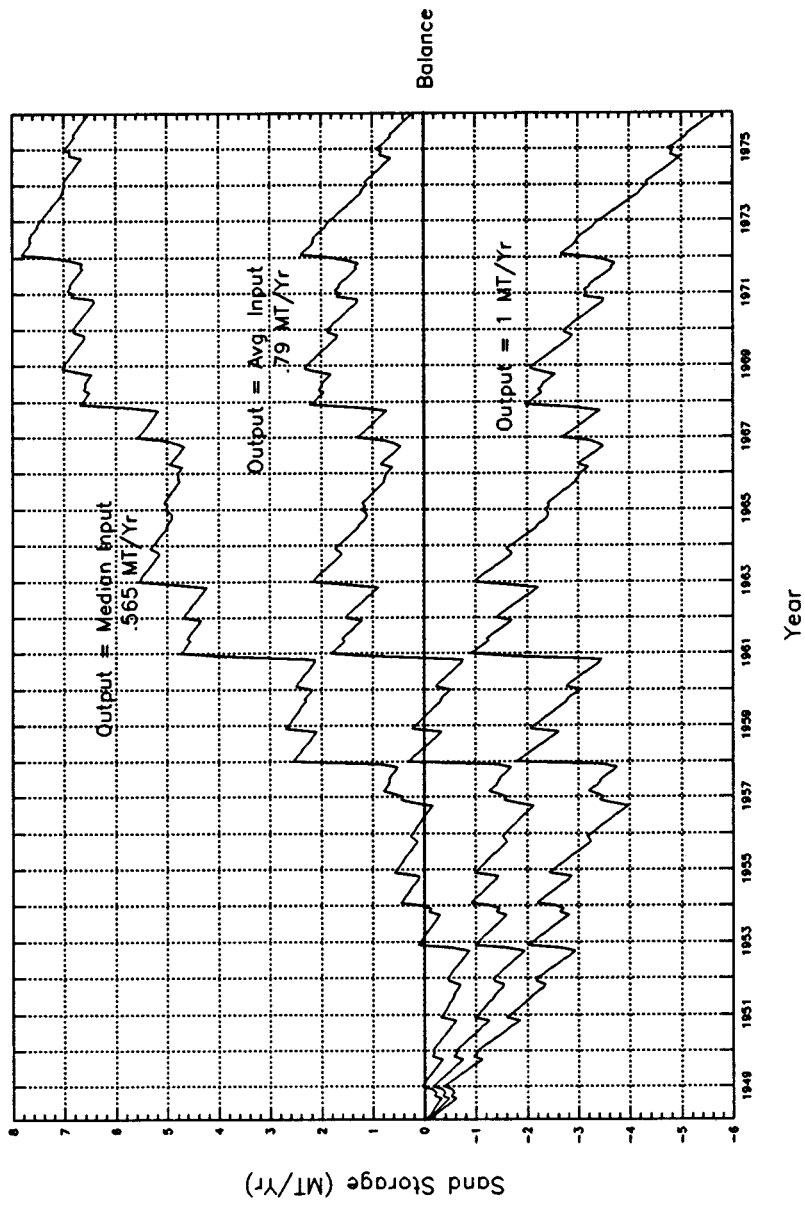


Figure 3. Sand budget Colorado River cumulative surplus/deficit (million tons).

stored sediment occur, even though a long-term balance is achieved. In fact, for the simulated period of record, there was an 11-year period (1949-1960) when a deficit in stored river sediment was realized. The maximum deficit during this period would have been about 2.1 million tons of sand. This deficit equates to approximately three times the annual mean input from the Paria River, or approximately four times the median sand input from the Paria River. Following this period of sand deficit, there was approximately a 15-year period of stored sand surplus. Over a longer period of record, continued periods of deficit and surplus would continue to occur. Over any relatively short time period (several years) there is a very real probability that managing for a balance with *mean* sediment inputs might result in a substantial sand deficit in critical river reaches.

Of course, if main channel transport capacities are less than the long-term mean sand inputs, there will be less chance for near-term periods of sand-storage deficits and there will be a long-term trend towards sand accumulation. Conversely, if sand transport rates in the Colorado River are greater than the mean sand inputs from tributaries, there will be a long-term trend of sand depletion from storage.

Effects of Alternative Dam Operations on Main Channel Sand Transport

To illustrate how alternative dam release regimes affect main channel sand transport, and thus the long-term balance of sand in the subject river reach, we modeled six different hypothetical release regimes including the two cases previously mentioned (Figure 4). In all cases the maximum discharge was maintained for four hours daily. Discharges were distributed over the rest of the period to minimize daily ramping rates and to achieve the required volume water delivery on a monthly and annual (11,200 cfs) basis. The results suggest that when daily fluctuations exceed roughly 18,000 cfs on an annual basis, long-term sand deficits will occur in the subject river reach. If periodic higher flows are desired to help build beaches, daily fluctuations in excess of 15,000 cfs on an annual basis result in long-term sand storage deficits (Figure 4).

DISCUSSION AND RECOMMENDATIONS

This analysis does not enable us to predict whether any particular operating regime for Glen Canyon Dam will cause significant short-term deficits in Colorado River sand storage in the Lees Ferry to Little Colorado River reach. Furthermore, a longer simulation period would have produced a much wider range in the amount and duration of fluctuations in sand storage. However, it does suggest that if Colorado River sediment transport is managed to achieve a balance with long-term average annual sediment inputs, there is a chance that a sand storage deficit of some magnitude and some duration will occur over the short-term. Conversely, there is a chance that a positive sand accumulation will occur.

SAND TRANSPORT EXAMPLES

	Tons of Sand/year
Steady, year-round flows	204,000
Daily Fluctuations:	
8,000-13,000 cfs	218,000
5,000 - 20,000	470,000
5,000-25,000	821,000
3,000-30,000	1,470,000
5,000 - 20,000 (11 months)	716,000
31,500 (2-weeks)	

* Avg. Annual Sand Input (Paria River): 790,000 tons/year

$$Q_s + (2,84 \cdot 10^{-12}) Q_w^{3.53}$$

All daily peaks were held for four hours.

FIGURE 4.

This analysis also does not consider that over the long term spills from Glen Canyon Dam will occur, resulting in potentially large-scale depletions of sand from the Lee's Ferry to LCR reach. Therefore, periodic, or even modest long-term sand accumulations in storage are of less concern than periodic depletions from storage. In fact, given both the unpredictability of spills, and the need for periodic beach nourishment above the normal flow zone, it may be wise policy to manage for modest long-term accumulations of sand in river storage. In this case, there would be some rationale for managing flows to achieve sand transport capacities less than the long-term mean annual sand input for this critical river reach, and using periods of sand surplus as times to generate "beach building" flows (or to provide "insurance" against spills).

Finally, this analysis does not attempt to place significance on any particular level or duration of stored-sand depletions, although additional work may permit such an analysis to be made. This would further contribute to determining if temporary sand depletions associated with managing flows to achieve a long-term sediment balance should be a concern to resource protection and management agencies.

REFERENCES

- Buddu, M. 1992. Mechanisms of erosion and a model to predict seepage-driven erosion due to transient flow. Department of Civil Engineering and Engineering Mechanics, University of Arizona. Tucson, Arizona.
- Randle, T.J., and E.L. Pemberton. 1987. Results and analysis of the STARS modeling efforts of the Colorado River in Grand Canyon. *Glen Canyon Environmental Studies Technical Report*. USDI Bureau of Reclamation, Salt Lake City, Utah.
- Werrell, W., R. Inglis, and L. Martin. (In press). Beach face erosion in Grand Canyon National Park. *Natural Resources Technical Report*. National Park Service, Water Resources Division. Fort Collins, Colorado.

CHAPTER 10:

**AN INTEGRATION OF RESULTS FROM THE GCES
SAND BAR STABILITY RESEARCH PROJECT**

**COLLECTIVELY PREPARED BY
THE SAND BAR STABILITY TEAM**

TABLE OF CONTENTS

List of Tables	i
List of Figures	i
Abstract	ii
Introduction	1
An overview of Sand Bar Dynamics	1
Mechanisms of Erosion	2
Empirical Results	5
Conclusions	14
Management Considerations and EIS Alternatives	15

LIST OF TABLES

Table 1: A summary of conclusions from this report.

LIST OF FIGURES

Figure 1: Effects of river stage fluctuation on water tables in sand bars.

Figure 2: A conceptual model illustrating the relationship between discharge parameters and erosion.

Figure 3: Equilibrium slope and transient sediment in the hydrologically active zone of Grand Canyon sand bars.

Figure 4: A conceptual model of sand bar responses to flood perturbation under different flow regimes.

Figure 5: A response curve analysis of discharge parameters on five sedimentological processes and patterns.

ABSTRACT

In this chapter we present an integrated overview of sediment storage and sand bar dynamics, measured over a variety of temporal and spatial scales. Maintenance of sand bars was found to be a dynamic process driven between interacting erosional mechanisms, including seepage-driven erosion, wave action and tractive erosion. We examined the role of seepage-driven erosion from theoretical and empirical perspectives. Although seepage-driven erosion was ubiquitous in Colorado River sand bars in Grand Canyon, wave, tractive forces, and interactions between erosional mechanisms were also influential. From the conceptual model developed and field validated here, we predicted that sand bars subject to daily discharge fluctuations achieved a condition of dynamic equilibrium in which the slope of the sand bar face could shift between a subaerial minimum of 11° and a subaqueous maximum of 26° . Down-ramping rate was positively correlated with seepage erosion, but up-ramping rate was not correlated in this seepage erosion model. High stages were positively correlated with increased sediment transport, and determined the maximum elevation of hydraulic deposition. The lowest stage determined the lowest level of seepage erosion and the base of the equilibrium slope; however, subaqueous bar changes related to tractive processes may continue to influence the slope and equilibrium condition.

Empirical studies demonstrated that sand bars were influenced by antecedent conditions and flow parameters. Although a near-equilibrium condition existed system-wide, individual sand bars were highly variable in their responses to the GCES-II test flows.

1. Short time-scale studies (hourly, daily) showed that seepage-induced erosion, slumping, and fissuring decreased as the range of daily river stage fluctuations decreased. Under fluctuating river stage conditions, the potential for seepage-induced erosion processes decreased as down-ramping rates decreased. Large mass wasting events were associated with up-ramping after "weekend" type low flows, with gradual bar rebuilding.

2. Bi-weekly time-scale studies showed that low, slow-fluctuation and constant flows resulted in no net change or were slightly erosive due to cutbank formation. Aggradation occurred most often under high-fluctuation flows associated significant tributary inflow, but aggradation was otherwise unpredictable. The variability of sand bar responses to test flows increased downstream of the Little Colorado River, where sediment availability was greater. A significant aggradation/degradation cycle was observed among most of the sand bars studied.

3. Longer time-scale studies (annual, multi-annual) showed that antecedent sediment storage strongly influenced erosional patterns. Sediment storage increased during the post-dam period between 1965 and 1982. Aggradation occurred on many, but not all, sand bars during flooding in 1983-1984, but erosion rates following that flooding were rapid. Height of the debris fan levee may be largely responsible for a sand bar's susceptibility to erosion under flood flows. Short-term measurements of sand bar erosion cannot be extrapolated for long-term estimates of change, but must be viewed in the context of sediment storage patterns.

Effective management may include maintaining a mass sand balance coupled with appropriate flow variability to maintain individual sand bars. Without bar building flows, the dynamic equilibrium condition achieved through seepage-driven erosion will minimize sand bar area and volume in this system.

Large fluctuations or bar building flows may be used to maintain or rebuild some sand bars in this system, provided that an adequate sediment supply is available. In situations where sediment supplies are low or unknown, a general strategy of sediment storage is recommended. This strategy may include low ramping rates, low range of daily flows and low maximum flows.

INTRODUCTION

Sand bar morphology and sediment storage in the Colorado River downstream from Glen Canyon Dam are products of complex interactions between dam discharge, tributary flows, weather, sand bar type, and antecedent conditions. Prior to impoundment, the morphology of Colorado River sand bars was attributable to conditions of abundant sand supply (mean annual sediment transport in excess of 60 million metric tons) and a long-term balance of sand storage under large seasonal fluctuations. None of these conditions obtain in the present dam-regulated environment. Large annual discharge fluctuations have been replaced by daily fluctuations in response to hydroelectric power generation. Sediment supply has been reduced by more than 90 percent and is restricted to erratic tributary contributions. Sand stored in the system has declined during the post-dam period to a near-minimum condition. The maintenance of sand bars, banks and a mass balance of sediments in the Colorado River downstream from Glen Canyon Dam are now major concerns to resource managers in the Bureau of Reclamation, the National Park Service, and other federal and state agencies because: (1) they are an essential characteristic of the river corridor; (2) they provide components of aquatic and terrestrial habitats on which the riverine and riparian ecosystem are based; (3) they may serve as a protective barrier which preserves cultural resources from erosion; and (4) they constitute a significant recreational resource to visitors in this large, desert ecosystem. Optimal management of this system may provide maximum discharge variability for power production within the constraints of maintenance of a long-term balance of sediments and associated resources.

The present research effort employed theoretical and empirical approaches at several temporal and spatial scales to evaluate the responses of sand bar stability to the operations of Glen Canyon Dam. Here we synthesize our observations and conclusions concerning the erosional processes observed in this system to assist cooperators prepare the Glen Canyon Dam Environmental Impact Statement. We first review the conceptual basis for a model of dynamic equilibrium of sand bar topography based on seepage driven erosion. We review information on ground-water responses to discharge fluctuations measured on 20-minute intervals during the GCES test flow period and integrate these results with the modeling effort. This information is subsequently related to daily changes in sand bar topography, determined through daily assessment of seepage and rilling, as well as daily photographs taken with fixed cameras. These short-interval studies demonstrate the highly dynamic nature of sand bars and responses to dam operations on a daily basis. Survey results at the bi-weekly time scale of the GCES-II test flows evaluated the effects of discharge regimes, distance from Glen Canyon Dam, geomorphology and sediment availability on sand bar stability throughout the river corridor. At the largest temporal scale studied here, we describe rates of sand bar change observed in this river system during the post-dam period (1965-1990). We further discuss these results in relation to a sediment transport model for the reach above the Little Colorado River confluence (Mile 61), which has the least available sediment. These results are summarized in a table of flow parameters and impacts on sand bars. Lastly, we present an integrated perspective on resource and process responses to discharge regimes, summarized by a response curve analysis.

AN OVERVIEW OF SAND BAR DYNAMICS

From a sedimentological perspective, sand bars along the Colorado River in the Grand Canyon represent temporary, or ephemeral, storage sites for sediments in transport through the river system. Sand bars are deposited in low velocity environments along the channel margin and in recirculation zones, up to just below the maximum elevation of river stage. They subsequently are eroded and redeposited, in continuing sequence over a variety of time scales. While sand transport and deposition processes are strictly controlled by flow hydraulics, erosion may occur by several processes as discussed below.

The sand bar morphology of the pre-dam river in Grand Canyon stemmed from 1) conditions of abundant sand supply and a long-term balance between sediment delivered to and transported through the river corridor, and 2) a very large range of discharges over the course of a year. In a typical year, sediments were deposited in eddies and along river margins during the spring snowmelt runoff up to the approximate elevation of the annual peak river stage. Those deposits were subsequently eroded, in part, as the river receded. Leroux (1925), Hereford (1984), Schmidt and Graf (1990) and Graf et al. (1991) document and conclude that summer monsoon floods from tributaries contributed substantial flows and equal or greater sediment concentrations as compared to the spring floods in this system. Sand bars were scoured and reworked as they were subjected to rising river stages the following spring, prior to undergoing a subsequent aggradational episode.

This annual sequence of sand bar deposition and erosion still occurs along less-regulated river reaches upstream from Lake Powell (W. Jackson and G. Smillie, National Park Service Water Resources Division, personal communication). It also occurred in a somewhat altered fashion between 1983-1990 in the post-dam period in Grand Canyon (Schmidt, Chapter 8). Although sand bar location may not shift as in other river systems, sand bars in this system are dynamic, but not necessarily stable, features over long time periods. As with all alluvial features on rivers, a "dynamic equilibrium" condition is achieved which reflects a long-term balance between the river's sediment and hydrologic regimes. Habitat features associated with sand bar morphology are dependent on conditions associated with sand bar dynamics.

In the post-dam Colorado River in Grand Canyon, flow and sediment regimes have been altered. By definition, alluvial features such as sand bars must evolve to a new dynamic equilibrium condition. As described by Smillie et al. (Chapter 9), releases from Glen Canyon Dam can still be managed to achieve conditions of abundant sand supply and a long-term balance between sand delivered to and transported from the Grand Canyon. While the large range of pre-dam discharges no longer occurs, significant flow variations may take place during the course of a year. Thus, the main ingredients remain for maintaining sand bar dynamics representative of (but different from) those experienced pre-dam. One factor which distinguishes pre- and post-dam sand bar processes is the fact that many higher-elevation pre-dam deposits are no longer subject to periodic reworking and are consequently vulnerable to irreversible erosion. This study presents substantial evidence that 1) a new post-dam dynamic equilibrium condition is being approached with regard to the sand bar resources along the Colorado River in Grand Canyon, and 2) that sand bars undergo substantial alteration on short time scales of hours, days and weeks, as compared to the same sequences of deposition and erosion that occur on unregulated rivers on an annual basis. In this study we present a conceptual model of the dynamic sand bar zone influenced by sediment deposition and erosion under regulated discharges. The existence of unvegetated sand bars, such as existed pre-dam, represents a continual sequence of sediment deposition and erosion.

MECHANISMS OF EROSION

Our field observations suggest that three proximal mechanisms interact with discharge to influence sedimentation in this system: sediment transport, wave-induced erosion, and ground-water seepage erosion (Budhu, Chapter 2). Sediment transport involves the entrainment, transport and deposition of bed sediments by tractive forces. Together with wave and seepage-induced erosion, these processes interact to cause changes in the size, shape and sediment composition of sand bars. This project was designed to quantify changes in sand bar volume in relation to different discharge regimes over a range of time-scales. In addition, the process of ground-water seepage-induced erosion was investigated in depth.

Seepage Erosion

Unlike wave and tractive effects, seepage-driven erosion is a ubiquitous phenomenon associated with daily discharge fluctuations downstream from Glen Canyon Dam. Seepage-driven erosion results when river stage falls faster than the rate at which the water table can be lowered by gravity drainage through the sand bar face, creating an excessive exit hydraulic gradient (Budhu, Chapter 2). This results in fluidization of the sediments at the sand bar face. Water seeping from the saturated sand bar face forms rivulets that move sand particles down the sand bar face, and deposit sand in areas of lower gradient or at the river's edge (Figure 1, from Werrell et al., Chapter 4). Seepage forces may also induce mass failure events, as described in this report (Budhu, Chapter 2; Carpenter et al. Chapter 3; Cluer, Chapter 5).

Seepage-driven erosion is manifested in many ways along the Colorado River downstream from Glen Canyon Dam. Observations reveal that the major seepage-driven processes are rilling, formation of rivulets, slumping and rotational features, bank failures (mass wasting), and piping or tunneling (Carpenter et al. Chapter 3; Werrell et al., Chapter 4). Seepage erosion was a significant form of erosion at the Mile 43 study site (Budhu, Chapter 2; Werrell et al. Chapter 4), and probably occurs on most sand bars downstream from Glen Canyon Dam. While many of the sand bar volume changes documented in this study stemmed from seepage-induced processes, other changes may have been attributable to wave action or tractive-based sediment transport, including the scour and deposition of sand in the subaqueous environments.

The factors investigated in this study which appear to affect seepage-driven erosion include:

Bank steepness: Sand bars with steeper slopes are more susceptible to seepage erosion.

Downramping rate: Higher downramping rates cause increased amounts of seepage-driven erosion.

Amplitude of discharge: Larger drops in river stage result in a larger saturated seepage face for a given down-ramping rate.

Duration of drainage: Increasing the period of time during which river stage is held below the seepage line enhances rilling and may increase the probability of bank failure.

A finite-element model of seepage-driven erosion was developed and field validated at three sites (Budhu, Chapter 2). The main purpose of the model was to predict seepage-driven erosion under alternative dam discharge regimes. The model predicted sand bar water table fluctuations and resulting seepage-driven erosion extremely well. Model results suggest that the downramping rate, duration and elevation of minimum flow are the primary dam operation factors that influence seepage-driven erosion. This is consistent with field observations of erosion discussed in this report (Carpenter et al. Chapter 3; Cluer, Chapter 5).

The seepage erosion model was calibrated using topographic, ground-water and stratigraphic data from the three validation sites. The effects of the GCD/EIS flow alternatives were investigated using this model. Steady flow alternatives would essentially eliminate seepage erosion as an erosional mechanism. Of the fluctuating flow alternatives, the moderate fluctuations alternative would limit seepage erosion. This finding is due, in part, to the limited duration of the flow peak, which would limit recharge to sand bar ground water.

Seepage-driven erosion is largely independent of upramping rates; however, other processes may be enhanced by higher upramping rates (e.g. sediment transport). Two studies here document rising limb

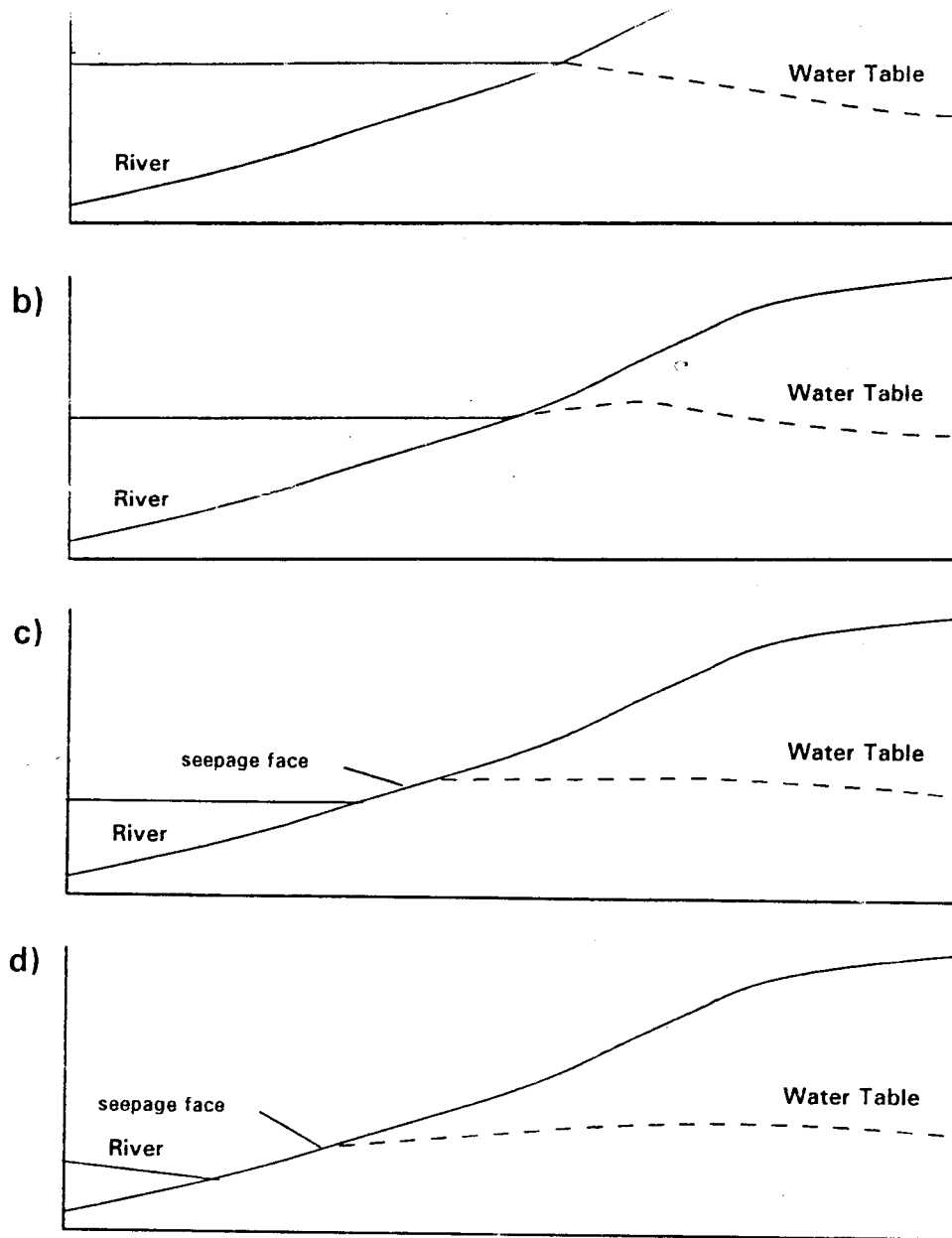


Figure 1. Effect of river stage fluctuation on water table in sand bars:
 a) highest river stage; b) falling river stage - Phase I;
 c) falling river stage - Phase II;
 d) falling river stage - Phase III

(after Werrell et. al., Figure 16, Chapter 4)

bank failure -- mass wasting that takes place during rapid upramping following prolonged periods of drawdown (Carpenter et al., Chapter 3; Cluer, Chapter 5). The causal mechanism for this form of mass wasting may be related to development of a failure plane during declining stage and tractive scouring of the deposit toe on rising stage, either in the subaqueous zone or at the surface. Most, but not all, of the erosion associated with major failure events documented in this study subsequently aggraded; however, more study on failure associated with rising hydrographs, their frequency and relationships to flow and groundwater parameters is recommended.

Interactions Between Discharge Parameters and Erosional Mechanisms

Erosion processes vary as a function of discharge and time, and are conceptually illustrated in Figure 2 (from Budhu, Chapter 2). Under fluctuating flows, seepage-driven erosion and rilling predominates at low rates of discharge, while tractive erosion predominates at higher rates of discharge. Wave-induced erosion is influenced not only by discharge parameters, but also wind and motor boat wakes. These three mechanisms interact with discharge parameters, local and system-wide antecedent conditions, and channel geometry to influence sand bar stability. Aggradation on eroded bars is only possible if discharges are sufficiently high and if sufficient sand is available for redistribution; however, fluctuating discharge regimes may limit sand storage in this system (Smillie et al., Chapter 9).

The importance of tractive and wave erosion mechanisms varies in relation to discharge parameters and over time. These forces are likely to erode sand bars rather quickly after a bar building event, as was reported after the 1983 flooding event (Kearsley et al., 1992). Seepage-driven erosion is a ubiquitous, persistent consequence of fluctuating discharge that interacts with wave and tractive forces under fluctuating flows until a stable slope is achieved. We propose that many sand bars develop a zone of reworked sediment under fluctuating discharges (Figure 3). Seepage erosion may affect sand bar topography above the minimum stage elevation until the bar reaches a subaerial equilibrium slope between 11° and 13° . Subaqueous slopes of up to 26° are stable. Under fluctuating flows, these two equilibria may shift back and forth. Approximately half of the sand bars under study here had reached that equilibrium slope (Beus et al., personal communication). This shallow slope will remain in a state of dynamics equilibrium until readjustment of topography is induced by other forces. Dynamic equilibrium is likely to be one in which subaerial sand bar area and volume above the lowest stage elevation are minimized.

EMPIRICAL RESULTS

Short-term Responses

This conceptual approach was evaluated using empirical results from several field studies. Carpenter et al. (Chapter 3) examined changes in ground-water head gradients and sandbar topographic responses at three sites instrumented with stage, pore pressure and tilt sensors. Their data were collected at 20 minute intervals. They concluded that highly predictable changes in head gradients occur under fluctuating flows. Head gradients and ground-water elevations rise quickly in response to increases in river stage, but sand bar drainage may not keep pace with daily declines in the hydrograph. This condition produced the characteristically elevated water table left by the rapidly falling river, that results in seepage erosion and rilling described by Budhu (Chapter 2) and Werrell et al. (Chapter 4).

Tilt sensors at the 43.1L site showed that bank deformation takes place on the declining limb of the daily hydrograph as effective stress increases and outflowing bank stored water erodes and oversteepens the lower portion of the slope. In contrast, bar deformation events occurred on the rising limb of the daily

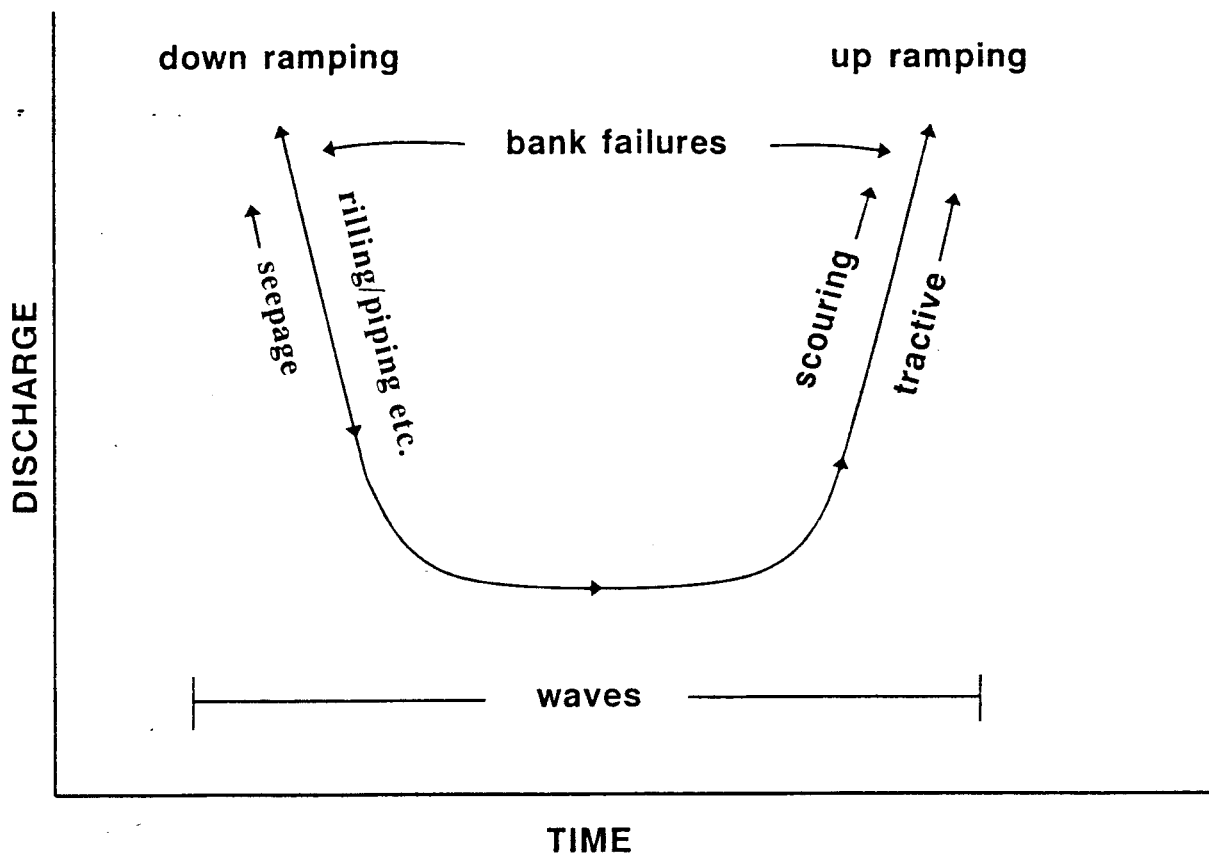


Figure 2. A conceptual model illustrating the relationship between discharge parameters and erosion.

(after Budhu, Figure 22, Chapter 2)

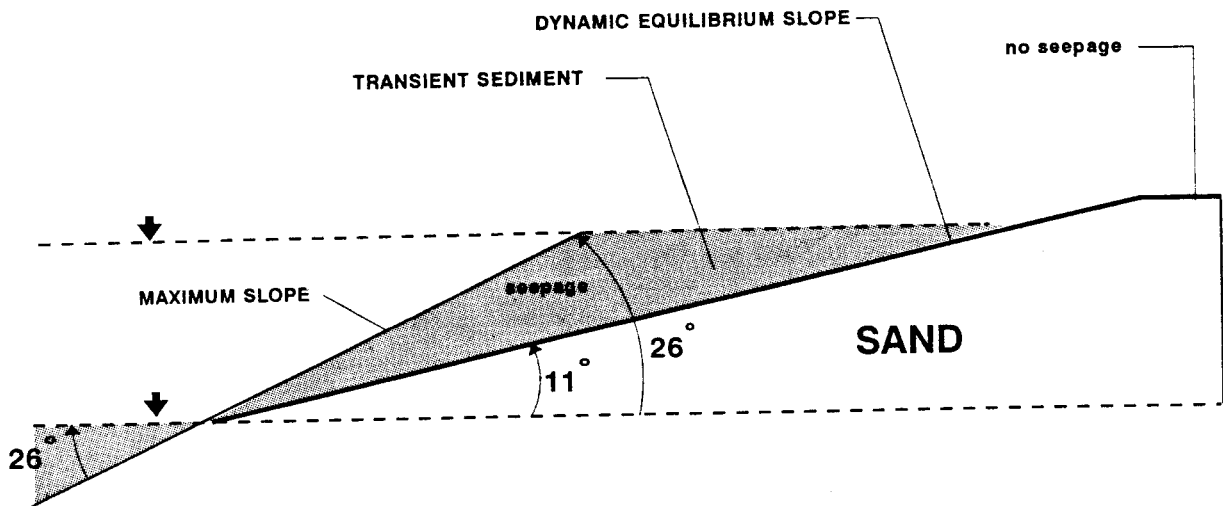


Figure 3. Equilibrium slope and transient sediment in the hydrologically active zone of Grand Canyon sand bars.

(after Budhu, Figure 11, Chapter 2)

hydrograph at the 172.1L site, probably in response to scour. The greater instability of sand bars in the lower end of Grand Canyon was attributable, at least in part, to greater sediment availability as suggested by Beus et al. (Chapter 6).

Werrell et al. (Chapter 4) explored daily topographic change accompanying fluctuating flows. Their data were collected on a daily basis at Mile 43 using a micro-topographic measurement device during two periods. The April 3-9, 1991 period sustained moderately fluctuating, "normal" flows. During periods with rapid daily drawdown and under the normal fluctuations, seepage and rilling/erosion exert conspicuous impacts on the hydrologically active zone. Werrell et al. experimentally tested the effects of seepage forces by installing drain pipes into the lower sand bar face. They reported that drain pipes significantly reduced rilling. The August 8-26, 1991 period was characterized by the limited fluctuations associated with interim flows. Werrell et al. reported a daily interaction between aggradational and degradational forces when downramping rates are reduced, in combination with increased mean river discharge. Cyclic deposition during higher stages was sufficient to temper and even overcome seepage/rilling erosion that takes place during drawdown.

Cluer (Chapter 5) examined daily fixed-camera photographs of seven sand bars and correlated oblique areal change with flow conditions. He documented daily responses of sand bars to flow regime changes. In particular, he reported that bank failure, the most sudden, large-scale process affecting sand bars, took place during both falling and rising hydrographs. The incidence of bank failure was closely related to "weekend" type flows, in which stage rises quickly after a several-day period of low flows. Furthermore, he reported that "normal" (highly fluctuating) flows were more likely to erode sand bars and less likely to rebuild those bars than were regulated flows, such as the GCES test flows. Large fluctuation flows without substantial tributary inflow, such as "G" and "F" in 1991, were degradational, while those associated with high tributary inflow could be aggradational (Beus et al. Chapter 6). The magnitude and timing of these events were in agreement with the findings of Carpenter et al. (Chapter 3) and are consonant with the failure/rebuilding cycle at the 45 Mile site reported by Beus et al. (Chapter 6).

Sand Bar Responses to Bi-weekly Test Flows

Beus et al. (Chapter 6) evaluated the effects of bi-weekly 1990-1991 GCES test flows on sand bar dynamics on 29 sand bars. They observed the following:

- 1) Most topographic changes occurred in a relatively narrow zone on the sand bar face (HAZ) sand bar face, a finding consistent with those of Budhu (Chapter 2), Carpenter et al. (Chapter 3), Werrell et al. (Chapter 4) and Cluer (Chapters 5, 7).
- 2) Sand bar area and volume were closely, but not perfectly, positively correlated. Because flooding and high flows tend to steepen sand bar faces, aerial photogrammetric analyses were likely to be conservative estimates of initial sand volume following major flooding events, such as occurred in 1983, and may change in accuracy through the long-term erosional decay curve following such events in this system.
- 3) HAZ volume change rate (%VCR) and HAZ areal change rates varied on a bi-weekly basis between the 29 study sites for which sufficient data were available and between the 16 test flows. From late summer, 1990 through July, 1991, three bars (10.3%) sustained significant net losses of HAZ sand, eleven bars (37.9%) remained relatively unchanged, and 15 bars (51.7%) gained sand. The 29 sand bars under study sustained a mean aggradation of 2.9% by volume (s.e. = 2.6%) between 27 October, 1990 (the first run for which survey coverage was virtually complete) and 31 July, 1991. During this time the

total 87,435 m³ of HAZ sand under study decreased by 1,034 m³ (1.2%) because several large losses occurred at a few sites in contrast with the general condition of near-equilibrium observed on most sites.

4) Test flows strongly affected bar volume and area, but no two test flows affected all sand bars in a similar fashion. Low, low-fluctuation and constant flows resulted in little change or in slight net degradation of 29 sand bars under study, while net aggradation occurred during periods of high fluctuation and significant tributary sediment input. Large fluctuation flows without tributary input often resulted in system-wide degradation.

5) Bar instability was, in part, attributable to bar type. Although mean rates of change were equivalent between separation and reattachment bars, the latter were more susceptible to aggradation or degradation as compared to the former. These results support a similar conclusion reached by Schmidt and Graf (1990).

6) Sand bars were remarkably dynamic and many bars displayed a significant cycle of erosion and re-deposition. Short time scale topographic changes, similar to those discussed above, were observed during periods of low flow.

7) Sand bars are more dynamic downstream of the Little Colorado River confluence, probably in response to increased sediment availability there.

8) Human recreational use intensity was not significantly correlated with bar stability, suggesting that recreational use has little effect on sand bars in comparison with dam operations.

Cluer (Chapter 7) further examined the utility of remote sensing images in determining sand bar responses to flow during the bi-weekly test flows. He analyzed two-dimensional aerial photogrammetry of 10 sand bars. He used Smillie et al.'s model (Chapter 9) to evaluate estimated sediment transport capacity of each test flow. This small sample set of bars suggested cyclical bar erosion and decay between the test flows. Flows with reduced energy following high energy flows resulted in increased bar area; but consequent return to a higher energy flow resulted in decreased deposit area. Cluer also reported interaction between hydraulic erosion mechanisms, with high energy processes (e.g. traction) overpowering seepage effects. These observations are supported by Budhu (Chapter 2), Werrell et al. (Chapter 4), and Beus et al. (Chapter 6).

Annual and Longer Term Patterns

Studies of post-dam changes in sand bars and sediment storage indicated that changes have been consistent over periods of years (Schmidt et al., Chapter 8). Aerial and oblique photography showed that bars eroded between 1965 and the mid-1970's, although data for this period were limited. High peak discharges between 1983 and 1986 caused aggradation at many sand bars, although the net change in sand bar area in both narrow and wide reaches was erosional. At sites that aggraded during this period, subsequent high discharges and normal fluctuating discharges (1986 to 1990) caused rapid, widespread erosion, with erosion rates declining with time.

These data showed that the highest sustained erosion rates measured in Grand Canyon occurred between October 1985 and January 1986. During this period, erosion was ubiquitous throughout Grand Canyon's length (Schmidt and Graf, 1990) because unconsolidated, well-sorted sand bars that had adjusted to high steady discharges greater than 700 m³/s were exposed to lower, widely fluctuating discharges. Cutbanks retreated on both separation and reattachment bars.

Schmidt and Graf (1990) argued that the erosion rates observed from August 1985 to January 1986 could not be sustained over a period of years and may represent a negative feedback mechanism. Subsequent measurements between 1987 and 1990 confirmed that erosion rates throughout Grand Canyon declined after that period. The time dependence of sand bar erosion complicates interpretation or extrapolation of short-term measurements, as illustrated at two study sites.

The Jackass camp (Mile 8.0L) has been under study since the early 1970's and has been repeatedly photographed during the past century. This large separation deposit has gradually lost sand without replenishment. Post-dam sand volume losses were greatest during the 1983 flood and this sand bar has not regained lost sand. The sand loss at Jackass Camp was probably attributable to a low debris fan levee that is overtopped by flows in excess of $2100 \text{ m}^3/\text{sec}$, scouring the camp area. Jackass Camp is a prime example of a sand bar that may not reacquire sand under any presently possible flow regime.

In contrast, Grapevine camp (Mile 81L) is far more dynamic. Erosion rates there between 1974 and 1980 were very low, about $20 \text{ m}^3/\text{yr}$. Erosion rates between August 1985 and January 1986 were about $1,200 \text{ m}^3/\text{yr}$, and declined to about $160 \text{ m}^3/\text{yr}$ between 1987 and 1990. Although local aggradation occurred at low elevations in some time periods, significant aggradation never occurred except during high floods when new sediments were deposited on the bar platform. During the GCES test flow period short-term erosion rates of the hydrologically active zone (HAZ) were measured for periods between 14 and 49 days at Grapevine camp (Beus et al., Chapter 6). These data revealed a wide range of values, with the highest erosion rates during a 14-day period equivalent to an annual rate of about $5,100 \text{ m}^3/\text{yr}$, four times greater than the maximum rates measured between 1965 and 1990. Erosion rates equal to the maximum historical rates were measured during two 14-day periods. During seven measurement periods net aggradation occurred at this site, despite the fact that historically-sustained deposition has occurred at this site only during flood discharges.

These analyses suggest that the relative magnitudes of short term erosion rates may serve as a basis for evaluating the erosional and depositional effects of different operational schemes; however, short-term measurements should not be extrapolated to longer term patterns. The maximum aggradation and degradation rates reported here appear to be associated with short-term adjustment processes. For example, Cluer (Chapter 5) showed that episodic degradation could occur within a few hours, involving as much as 50% of the bar area. Bar re-building took place over several days to weeks. Cluer correlated these mass wasting events with prolonged drawdown and subsequent rapid increase in stage, typical "weekend type" flows under normal dam operations. Short-term sand bar dynamics of this magnitude may characterize the lower reaches, but Schmidt et al. (Chapter 8) concluded that the overall system may be nearing its long term equilibrium (minimum) condition. Interim flows monitoring studies should reveal the direction of change in this system.

Dynamic Equilibrium of Sand Bars

Stable sand bar faces shifted in steepness over periods of hours to years (Budhu, Chapter 2; Carpenter et al., Chapter 3; Werrell et al. Chapter 4; Cluer, Chapters 5,7; Beus et al., Chapter 6; Schmidt et al., Chapter 8). The range in stable profile steepness varied between the angle of repose of the sediments and the stable angle of the bar undergoing seepage stresses. Seepage modeling predicted that subaerial sand bar faces subjected to seepage achieved equilibrium slopes of 11° to 13° (a very shallow bar slope; Figure 2 from Budhu, Chapter 2; Figure 11). When wave and tractive forces were unimportant, subaqueous sand deposition achieved an angle of repose of approximately 26° . Under fluctuating flows without other factors operating, a range of slopes between 11° to 26° should obtain. The "wedge" of sediment defined between these two slopes comprised a zone in which bar change may be expected to operate in the context of a cyclic, negative feedback mechanism (Figure 3). Under this mechanism, short-term aggradation could occur in the HAZ, especially in areas of lowest nearshore

velocity (Rubin et al. 1990), but such aggradation lead to oversteepened slopes that were susceptible to greater seepage stresses and possibly to greater tractive forces, and subsequent and conspicuous degradation. Erosional or depositional processes beyond this range of change constituted significant (longer duration) changes. Changes within this range may be simply short-term fluctuation and adjustment. Increased volume fluctuations within this zone of change or mass wasting events (Cluer, Chapter 5) may have resulted in either shoreward or riverward migration of this zone. Beus et al. (Chapter 6) concluded that cyclic aggradation and degradation of this zone was a general characteristic of the more dynamic sand bars.

Historical studies by Schmidt et al. (Chapter 8) suggested that, under "normal" dam operations, sand storage in the Colorado River corridor increased from 1965 to 1982, and subsequent high flows removed that stored sand. Recirculation zones still containing sufficient sand to maintain subaerial bars were likely to be those with sufficiently low velocity and appropriate channel geometry to effectively retain sand lost during the seepage-induced aggradation/degradation cycles described above. Flow regime changes at stable bars may create the appearance of erosion, but little net change occur. However, numerous sand bars diminished or disappeared in this system since 1983 (Kearsley et al. 1992; Schmidt, Chapter 8), and approximately 10% of the bars examined by Beus et al. (Chapter 6) sustained continued degradation throughout the test flow period. Without management concern for the timing of fluctuation and sediment input/storage, the equilibrium toward which the system is moving will be one in which sand bar volume and area will be minimized. Whether or not equilibrium is achieved, sand bars will be lost to debris flows, weather and other factors. While the role of bar building flows requires further examination, floods may rebuild some bars but erode others.

Bar-Building Flows

Several bar-building flows were observed during the GCES-II test flow period. Bar building was associated with higher ($600 \text{ m}^3/\text{sec}$ to $850 \text{ m}^3/\text{sec}$), fluctuating discharges during periods of sediment inflow from tributaries. During these periods, depositional processes tended to out-compete the enhanced seepage erosion processes, resulting in net sand accumulation. Although bar-building was observed during the GCES-II test flow period, those deposits were ephemeral and predictably eroded on return to lower discharge levels.

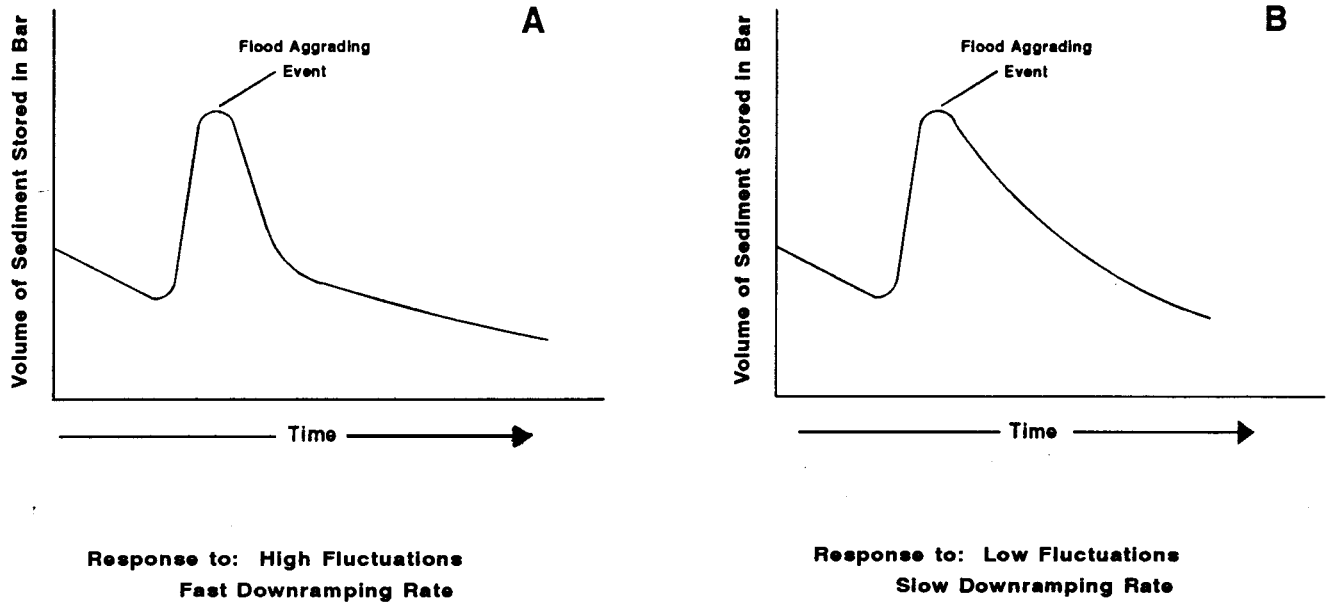
Bar-building flood flows may be considered as a management tool for restoring sand volume at higher elevations in this system. A conceptual model of temporal responses of sand bars to short term high discharges is presented in Figure 4. Such discharges have been shown to cause localized aggradation at some sites (e.g. Mile 81) but degradation at other sites (e.g. Mile 8; Beus et al., 1984; Schmidt and Graf, 1990; Schmidt et al., Chapter 8; Schmidt and Webb, personal communication; Kearsley et al. 1992).

Sites that aggraded during a flood will subsequently erode after recession of the flow; however, subsequent discharge parameters may influence the time of adjustment, or subsequent erosion, of newly re-formed bars (Budhu, Chapter 2, Beus et al. Chapter 6). Some bar responses may be consistently related to discharge parameters, such as range of fluctuations and down-ramping rates (Figure 4). Thus, a dam operations strategy that limits bank erosion processes will increase the longevity of these flood-formed deposits (Figure 4A). Conversely, an operational strategy that increases bar reworking and erosion may decrease the time during which an aggradational event has a net positive effect (Figure 4B).

It is important to re-emphasize that not all sites can be expected to aggrade during floods. For example, the Jackass camp (Mile 8) was eroded by the 1983 spillover flooding event and has not rebuilt (Figure 4C; Schmidt and Webb, personal communication). The height of the upstream debris fan levee

Aggradational Site

(e.g. RM81L - Schmidt et al., this report)



Degradational Site

(e.g. RM8L Jackass Camp - Schmidt et al., 1992)

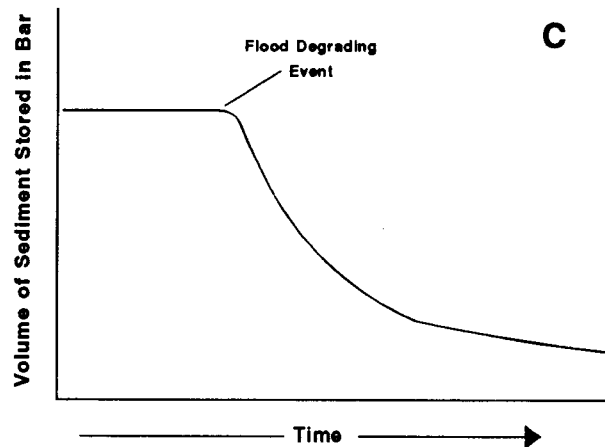


Figure 4. A conceptual model of sand bar responses to flood perturbation under different flow regimes.

determines whether and how much of a sand bar will be subjected to scouring flow during a flood. The Jackass Camp (Mile 8L) is protected by a low debris fan levee and has consistently eroded during the post-dam period. Flood-induced erosion is likely to occur on such sites and may dominate over erosion induced by normal dam operations. Such sites may not be sensitive to discharge parameters; but stage-to-discharge relationships are known for relatively few bars in this system at present.

Elements of Sand Bar Dynamics Requiring Further Study

There are several outstanding elements of sand bar dynamics that require further study and which would aid in the development of a sound management program.

1. What are the mechanisms by which stream sediment is moved to sand bar faces, in and through eddies, and in rapids?
2. What is the relationship between bottom channel sediments and subaqueous extension of sand bar materials as related to the stability of the subaqueous equilibrium slope?
3. What are the interactions between seepage forces, tractive forces and wave action?
4. How much sediment is required for a bar building flow to be effective; and if sediment availability is adequate, what duration and magnitude of flow is sufficient to result in meaningful aggradation?

CONCLUSIONS

These studies provided a surprisingly dynamic picture of sand bar changes and sediment storage in the Colorado River downstream from Glen Canyon Dam. Taken in concert, these studies concluded that sand bar topography was affected by discharge, geomorphology, sediment supply and antecedent conditions. Schmidt et al. (Chapter 8) portrayed a system which experienced a major perturbation in the mid-1980's, followed by a period of rapid and ubiquitous erosion, with erosion rates decaying up to the period of the GCES-II test flows. Despite the apparent near-equilibrium state of this system, these studies showed that the GCES-II 11-day test flows exerted significant effects on sand bars. The shortest-term studies demonstrated that sand bars adjusted to flow regime changes over as little as a few hours time.

Slight net aggradation occurred during the GCES test flow period; however, that process was not uniform and was strongly affected by discharge, geomorphology and tributary inflow. Approximately 10% of the sand bars under study continued net degradation, and these losses were considered unrecoverable under present dam operations. Several relationships were apparent. First, the total amount of sand bar instability, both aggradational and degradational, increased with distance downstream from Glen Canyon Dam. Second, major periods of erosion followed periods of aggradation suggesting that antecedent conditions influenced subsequent changes in sand bar topography. Relatively rapid aggradational periods (days to weeks) typically followed periods of erosion. The instantaneous erosion measurements made during this study were not intended to be extrapolated to long periods of time (years). Third, periods of aggradation were associated with large-fluctuation flows coincident with significant tributary sediment inflow. High-fluctuation flows not associated with tributary inflows were generally degradational or resulted in little net change. Fourth, little change or slight net erosion prevailed during the three constant flows and the low-fluctuation test flows.

These observations suggest that several processes and conditions interacted to cause sand bar instability during periods of relative historic stability. In particular, both localized sand bar erosion and aggradation occurred throughout the Grand Canyon. Additionally, depending upon conditions, alternative erosion mechanisms (seepage force, tractive force, wave action) may predominate. Several examples of interacting processes were observed during this project. For example, Werrell et al. (Chapter 4) observed strong expressions of ground-water seepage-induced rilling at Mile 43 during August, 1991. However, other processes not associated with rilling may have resulted in net beach aggradation over the rillzone during the study period. Similarly, mass failure events at Mile 172 caused the largest sand bar erosion events measured during the study period, but many erosional losses were replenished during subsequent days or weeks (Cluer et al., Chapter 5). While the composite response of sand bars to flow regimes was found to be complex, Budhu (Chapter 2) suggested that seepage-induced erosion processes intensified as the range of daily stage fluctuations and down-ramping rates increased.

In summary, this project provided insights into the dynamics of sediment storage in sand bars during periods of low and fluctuating releases from Glen Canyon Dam. Sand bar topographic changes were dynamic, with some sand bars aggrading and others eroding during the GCES-II test flow period. We surmised that this dynamic condition resulted from interaction between degradational and aggradational processes. These processes depended on maintaining sufficient sand supplies in storage in the river channel and eddy systems. Smillie et al. (Chapter 9) demonstrated that alternative daily releases will affect the net volume of river system-stored sands.

MANAGEMENT CONSIDERATIONS AND EIS ALTERNATIVES

Visible erosion is an integral component of the Grand Canyon sand bars. Abundant sand supplies and periodic higher flows are required for sand bar aggradation to occur. A clear rationale exists for flow variability (as opposed to "steady" flows) at times when sufficient sediment supplies are available for bar building. The basic management issues include 1) managing flow releases to achieve a positive sand balance in critical reaches, and 2) maximizing flow variations within that constraint. The fundamental management question is, "given that adequate constraints are in place to protect sand supplies, how best are discharge fluctuations imposed on the river to support the processes of sand bar dynamics?" What, for example, are the benefits or drawbacks to sand resources of "annual" flow peaks as compared to "daily" or "weekly" flow peaks? Are higher-elevation pre-dam deposits that presently exist as historic terraces, affected by daily dam operations or are they largely unmanageable by post-dam discharge options? While some of the questions go beyond the scope of this study, we suggest that maintenance of a positive sand balance and optimum discharge variability are essential when considering the management issues associated with contemporary sand bar resources.

Effective sediment management may therefore include maintaining a mass sand balance coupled with appropriate flow variability to maintain individual sand bars. Without bar building flows, the dynamic equilibrium condition achieved through seepage-driven erosion will keep the system at or near the minimum sand bar area and volume for this system. Large fluctuations or bar building flows may be used to maintain or rebuild the remaining sand bars in this system, provided that adequate sediment supplies are available for bar-building. In situations where sediment supplies are low or unknown, a general strategy of sediment storage is recommended. This strategy may include low ramping rates, low range of daily flows and low maximum flows.

To summarize these observations and conclusions, we present the following response curve analyses and discussion for various physical processes examined in this study, including sand-bar stability and mass wasting, seepage erosion and gross sediment transport (Table 1; Figure 5).

Sand Bar Characteristics

1. Short-term sand bar change takes place in a narrow zone on the bar face, the hydrologically active zone.
2. Responses of sand bars to flow conditions varied between test flows and between sand bars. Separation bars were slightly more stable than reattachment bars, and instability (both aggradation and degradation) increased downstream of the Little Colorado River confluence.
3. The dynamic equilibrium seepage model (Budhu, Chapter 2) predicts that an 11° to 26° slope represents a range of stable face slopes above the minimum stage for Colorado River sand bars subjected to fluctuating flows. These slopes develop as an equilibrium adjustment to seepage driven erosion. Equilibrium slopes are predicted to develop from the lowest stage elevation reached, and thus the minimum flow exerts a significant influence on sand bar morphology. Achievement of this slope under daily fluctuations also represents the minimum subaerial sand bar area and volume for Colorado River sand bars.

TABLE 1: A SYNTHESIS OF CONCLUSIONS FROM THIS REPORT.

EFFECTS	SUPPORTING DOCUMENTATION* (CHAPTER OF REPORT)
SAND BAR CHARACTERISTICS	
Sand bar responses to flows are variable and occur over short-time intervals	2, 3, 4, 5, 6
Dynamic equilibrium bar face slope of 11° represents a stable but minimum subaerial bar area and volume	2, 4, 8
Sand bar change takes place in a narrow zone on the bar face	2, 3, 4, 5, 6, 7, 8
SEDIMENT AVAILABILITY	
Tributary input is associated with aggradation	6
Hydraulic sand bar instability increases downstream where sediment availability is greater	2, 3, 5, 6, 7
STAGE	
Stage correlates with bar area affected by hydraulics	2, 3, 5, 6, 7, 8
Lowest stage: Determines lowest level of seepage erosion	2, 4
Subaqueous bar changes co-occur with subaerial change.	3, 5
Higher stage: Positively correlated with increased sediment transport.	5, 9
Determines the maximum elevation of hydraulic deposition and erosion.	6

RANGE OF FLOWS

Changes in operating regimes (e.g. weekend-type flows, floods, etc.) alter erosion rates	2, 3, 5, 6, 8
Constant flows resulted in no net change or were slightly erosive due to cutbank formation; equilibration time may involve months	2, 4, 6, 7
Low-fluctuation flows resulted in no net change or were slightly erosive due to cutbank formation	2, 6, 7
Short duration, high range flows limit seepage	2, 3, 4
High range flows increased seepage erosion	2, 3, 4
If suspended load is high, aggradation associated with high range flows can overcome erosional losses associated with seepage erosion	6

RAMPING RATES

Slow down-ramp rate lessens bank failure	2, 3, 4, 8
Up-ramp rate: Does not influence seepage erosion	2
Fast up ramp rates are positively correlated with bank failure, possibly as a result of scour	3, 5

FLOODS

High flood deposits are ephemeral (several years)	2, 6, 8
Deposition may occur at high stages if debris fan levees are high	Not studied here

*Supporting documentation in this report:

- Chapter 2. Budhu, M. Seepage erosion modeling.
- Chapter 3. Carpenter, M. et al. Groundwater studies.
- Chapter 4. Werrell, W. et al. Seepage erosion at 43L.
- Chapter 5. Cluer, B. Terrestrial photogrammetry.
- Chapter 6. Beus, S.S. et al. Sand bar surveys.
- Chapter 7. Cluer, B.C. Aerial photogrammetry.
- Chapter 8. Schmidt, J.C. et al. Historical change in sediment storage.
- Chapter 9. Smillie, G. et al. Estimated sediment transport capacity.

Dam Release Parameters

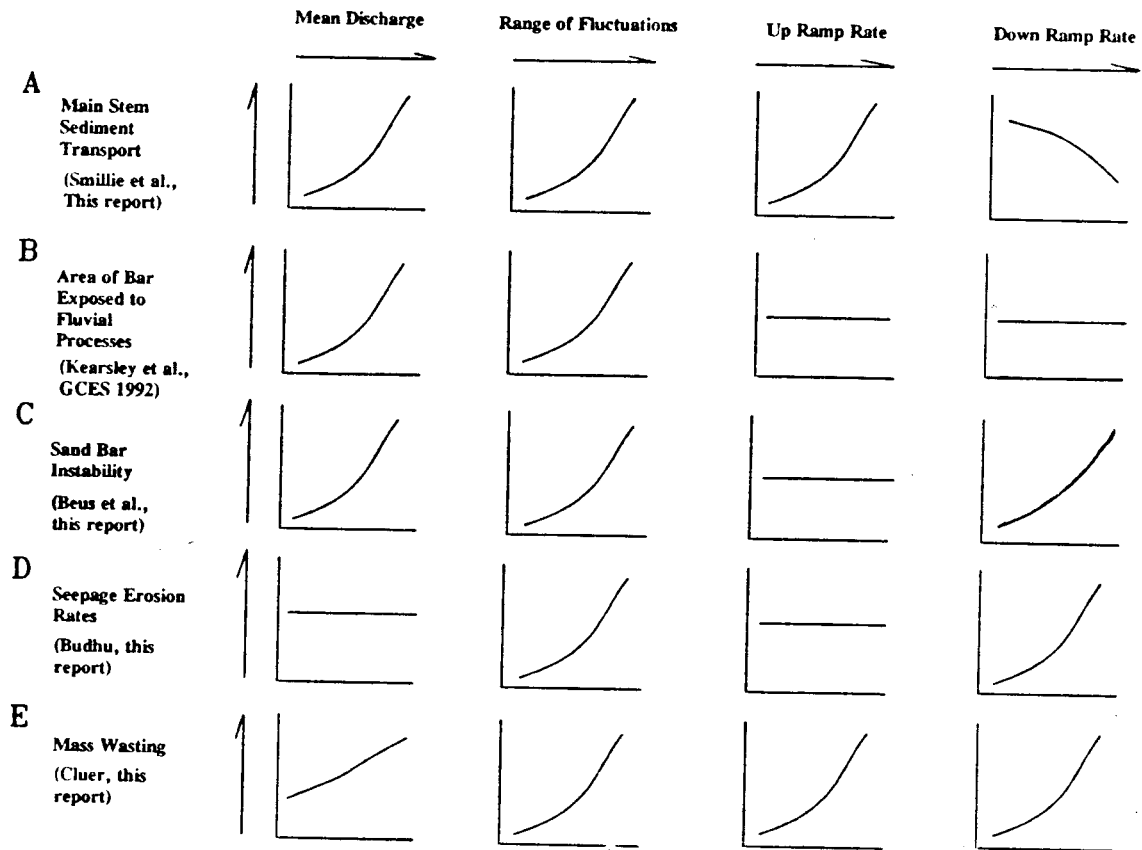


Figure 5. Response curves to dam-release parameters

Sediment Availability

1. Smillie et al. (Chapter 9) showed that mainstream sediment transport increased with increasing mean discharge, increasing range of daily fluctuations, increased up-ramping rate, and decreases with increased down-ramping rates. Using Smillie et al.'s model, Cluer (Chapter 7) and Beus et al. (Chapter 6) showed demonstrated that system-wide aggradation took place during GCES test flows with high estimated sediment transport capacity; however, some high transport/high fluctuation flows were aggradational. Beus et al. reported system-wide aggradation was often associated with large daily stage fluctuations during, or immediately following, periods of significant sediment input from tributaries.
2. Kearsley et al. (GCES 1992) showed that the area of bars available for camping (that is, not directly exposed to fluvial processes) increased with lower mean discharge and lower range of fluctuations: any larger discharges or higher ebb of fluctuating discharge inundate increasingly larger areas of sand bars, subjecting those areas to fluvial processes.
3. Beus et al. (Chapter 6) demonstrated great variability in bar response during the study period. Their results suggested that sand bar instability (both aggradation and degradation) was a function of sediment supply. Sand bars in the lower reaches were far more dynamic (responsive to test flows) than were bars in the upper reaches. Attenuation of discharge parameters with distance means that lower canyon reaches may be subject to reduced sediment transport capacity; however, lower canyon reaches received far more tributary-derived sediment than do upper canyon reaches. Therefore, sand bar dynamics were positively correlated with sediment availability.

Discharge Effects on Sand Bar Stability

1. Seepage induced erosion, slumping, and fissuring decrease as the range and ramping rate of daily river stage fluctuations decreases. Under fluctuating river stage conditions, the potential for seepage induced erosion processes decrease as down-ramping rates decrease (Budhu, Chapter 2). Longer duration of drainage at low river stage increases seepage erosion. Thus, increasing weekend peaks to approximately mid-week values would avoid the "weekend" drawdown phenomenon and should decrease the extent of seepage induced erosion, but would increase minimum weekend flows.
2. Large mass wasting events were associated with up-ramping after "weekend" type low flows (Cluer, Chapter 5). Seepage-induced mass wasting increases as down-ramping rates increase. Seepage cannot induce mass wasting under constant flows, but wave action may produce bank failure at any discharge regime through undercutting and over-steepening bar faces (Cluer, Chapter 5).
3. The lowest stage determines the lowest level of seepage erosion and the base of the equilibrium slope (Budhu, Chapter 2); however, subaqueous bar changes were also observed to accompany subaerial change. Higher stages were positively correlated with increased sediment transport (Smillie et al. Chapter 9), and determines the maximum elevation of hydraulic deposition and erosion.
4. Changes in operating regimes (e.g. weekend-type flows, floods, etc.) increased erosion. Low fluctuation at slow rates, and constant flows resulted in no net change or were slightly erosive due to cutbank formation. Short duration, high range flows limited seepage erosion by limiting bank storage. High range flows increased seepage erosion; however, aggradation occurred under high fluctuation flows if those flows co-occurred with significant tributary inflow. This aggradation was apparently sufficient to temporarily overcome seepage-induced erosion.
5. Slow down-ramping rates reduces seepage-induced bank failure. Although up-ramping rate does not influence seepage erosion, fast up-ramping rates were associated with bank failure, possibly from scour.

GLOSSARY

Antecedent. Prior, preceding.

Mass wasting. Downslope movement of material at the earth's surface under influence of gravity; in this case, bank failure or collapse of a riverside sand bar face.

Discharge. A flux of water (volume per unit of time; $1000 \text{ ft}^3/\text{sec} = 28.31685 \text{ m}^3/\text{sec}$)

EIS. Environmental Impact Statement

Fluctuating zone. Synonymous with the HAZ

GCES, GCES-II. Glen Canyon Environmental Studies Phase II, a Bureau of Reclamation research program designed to evaluate the impacts of Glen Canyon Dam discharge parameters on downstream riverine resources.

HAZ. The volume or area of a sand bar that is within the hydrologically active zone between low ($850 \text{ m}^3/\text{s}$) and high ($141.5 \text{ m}^3/\text{s}$) flows.

Photogrammetry. The science of data collection from photographic images.

Reattachment deposit. A sand bar deposit located near the point of flow reattachment that typically projects upstream beneath the primary eddy.

Sand bar. A body of sand deposited by moving water; in this case, a beach or channel margin deposit.

Seepage erosion. Degradation of a sediment deposit through outflowing ground water.

Scour. Erosion due to tractive forces.

Separation deposit. A sand bar deposit located near the point of flow separation that typically mantle large debris fans and extend to the edge of the primary-eddy return-current channel.

Stage. Elevation of a particular discharge, measured from an arbitrary datum.

Total station. An integrated theodolite and EDM (electronic distance measurement) surveying system.

Purpose

This section includes plots of instantaneous discharge from Colorado River Gage, one mile downstream of Glen Canyon Dam, for the test flow period June 1, 1990 through July 28, 1991. These plots are included for reference to the preceding technical reports and to aid the GCES EIS team in understanding the general characteristics of given Research Discharges referred to in this report. Additional hydrologic data are available from the temporary network set up by the USGS that established stage recording stations every five miles between the Glen Canyon Dam (RM -15) and Diamond Creek (RM 225). All discharge values are plotted in cubic feet per second. The following table may be used to convert cfs to cubic meters per second (m^3/s) (Table 1). Statistical analyses on the test flows are included in table 2. Sediment transport capacity was calculated for each test flow based on discharges from Lees Ferry.

Table 1. Conversion of metric to english discharge values common to the test flows.

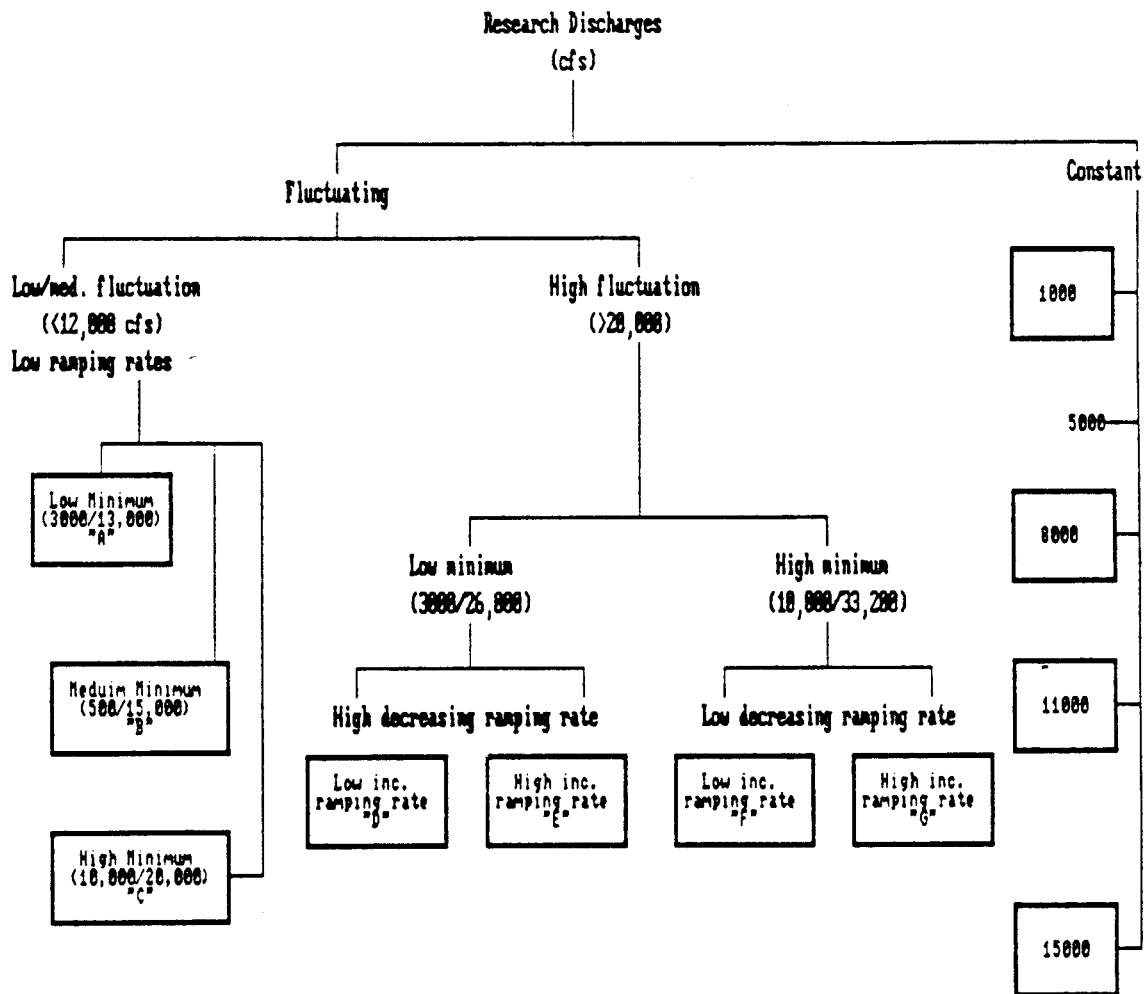
CUBIC FEET PER SECOND (cfs)	CUBIC METERS PER SECOND (m^3/s)
3,000	85
5,000	142
8,000	227
10,000	283
11,000	311
15,000	425
20,000	566
25,000	708
26,200	742
28,000	793
30,000	850
33,200	940

CONVERSION FORMULAE:

To convert: cfs to m^3/s , multiply cfs by 0.0283

m^3/s to cfs, multiply m^3/s by 35.313

Dendrogram of research discharges.
 Fluctuating discharges have approximately the same value
 as constant discharges on the same level.

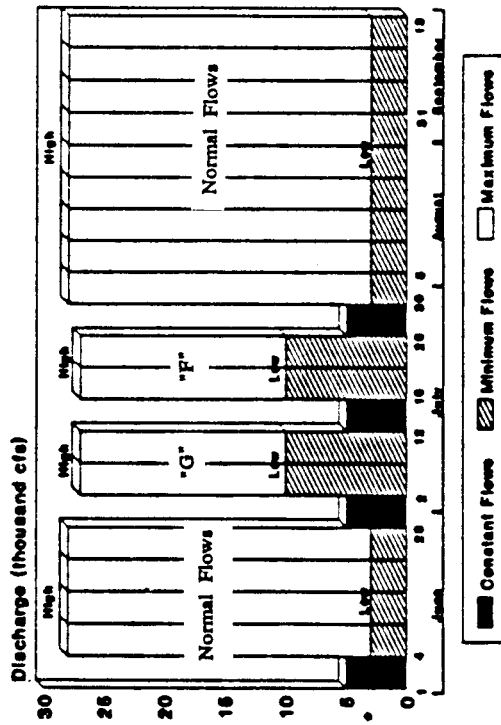


GLEN CANYON ENVIRONMENTAL STUDIES

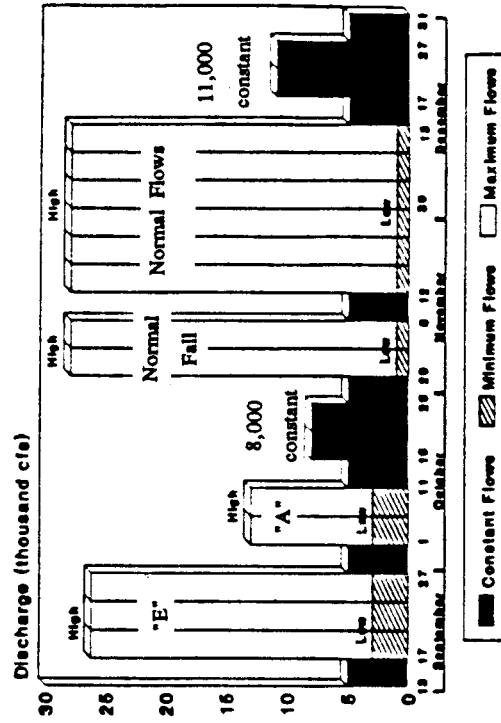
RESEARCH FLOW SCHEDULE

Calendar Year 1990

June - September, 1990



September - December, 1990



- The 3-day 6,000 cfs constant flows are scheduled to begin at 12:01 a.m. on Friday and conclude at 12:01 a.m. on Monday
- The 8,000 cfs and 11,000 cfs constant flows will last 11 days each

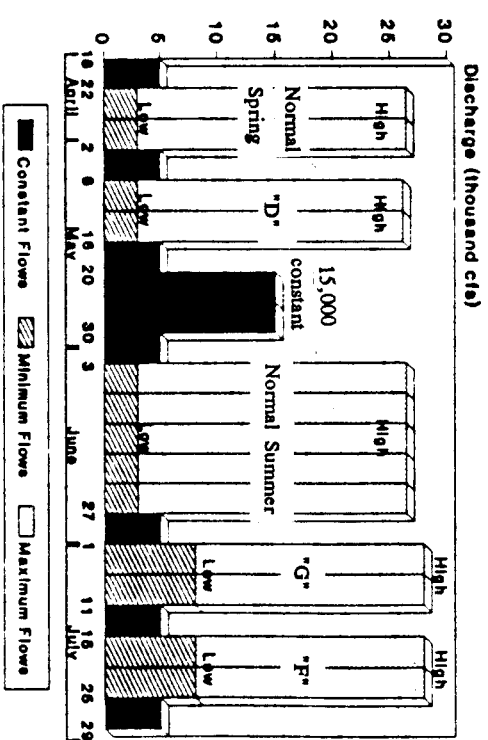
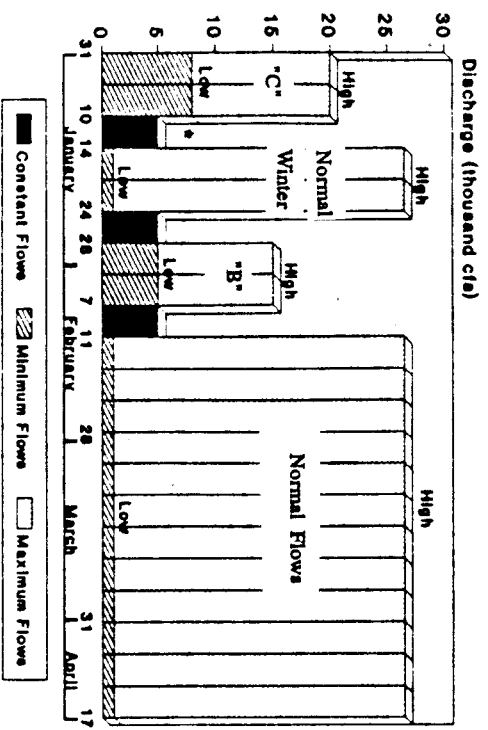
GLEN CANYON ENVIRONMENTAL STUDIES

Research Flow Schedule

Calendar Year 1991

January - April, 1991

April - July, 1991



* The 3-day 5,000 cfs constant flows are scheduled to begin at 12:01 a.m. on Friday and conclude at 12:01 a.m. on Monday

+ The 15,000 cfs constant flows will last 11 days

Glen Canyon Dam Research Flows
Statistical Analysis by Flow Period

flow period	begin date	julian date	research flow description	number obs. discharge	mean discharge (cms)	range of discharge (cms)	std. dev. discharge (cms)	number obs. upramp	mean upramp (cms/hr)	maximum upramp (cms/hr)	std. dev. upramp (cms/hr)	number obs. downramp	mean downramp (cms/hr)	maximum downramp (cms/hr)	std. dev. downramp (cms/hr)	range	discharge volume (cubic km)
01JUN90	152	5000	cfs	96	142.253	3.710	0.634	29	1.0907	2.973	0.5777	30	1.1034	2.973	0.6061	5.95	0.04916
05JUN90	156	non-research		576	413.286	817.653	216.123	292	51.9010	347.450	53.7073	279	54.3135	248.567	51.6414	596.02	0.85699
29JUN90	180	5000	cfs	72	143.460	84.413	9.715	29	4.0357	78.466	14.3501	26	1.3385	5.182	1.0036	83.65	0.03718
02JUL90	183	Discharge	"g"	264	425.180	658.568	233.867	122	53.2471	207.762	80.7108	132	49.7978	129.097	46.3607	336.86	0.40409
13JUL90	194	5000	cfs	72	143.596	89.029	10.275	29	4.3237	87.556	16.0301	32	1.3539	5.210	0.9615	92.77	0.03722
16JUL90	197	Discharge	"f"	264	439.606	663.637	225.894	130	49.7758	114.486	46.2432	118	55.5433	133.316	46.7597	247.80	0.41780
27JUL90	208	5000	cfs	72	142.142	29.053	3.422	32	1.6946	8.184	1.8333	28	2.9743	25.315	4.8864	33.50	0.03684
30JUL90	211	non-research		1104	433.094	856.080	243.472	579	52.4700	308.231	53.9071	518	58.5938	295.969	61.7508	604.20	1.72129
14SEP90	257	5000	cfs	72	141.334	60.627	6.821	29	1.9636	9.090	1.7354	27	4.3262	51.537	9.6453	60.63	0.03663
17SEP90	260	Discharge	"e"	264	414.262	682.751	297.840	122	62.5420	227.867	84.3487	123	61.6061	214.954	84.3833	442.82	0.39371
28SEP90	271	5000	cfs	72	141.259	56.974	6.550	27	1.9497	5.324	1.2887	33	3.1372	52.415	8.8917	57.74	0.03661
01OCT90	274	Discharge	"A"	264	239.390	302.312	130.566	122	28.4488	112.418	39.9420	121	28.2295	110.125	40.4352	222.54	0.22752
12OCT90	285	5000	cfs	72	133.565	140.792	23.648	30	6.5412	79.911	16.5177	29	3.9068	54.793	9.9101	134.70	0.03462
15OCT90	288	8000	cfs	264	226.529	88.292	5.449	114	2.8344	14.470	2.4030	122	3.2848	75.352	6.9332	89.82	0.21529
26OCT90	299	5000	cfs	72	141.957	6.088	1.195	25	1.7817	4.559	1.1730	35	1.4684	3.823	0.8476	8.38	0.03680
09NOV90	302	"Normal"	Fall	264	200.988	475.726	125.879	125	36.1248	267.171	46.4473	135	33.6293	155.262	32.6021	422.43	0.19102
12NOV90	313	5000	cfs	72	142.401	11.412	1.480	36	2.0593	26.618	4.4391	27	1.9570	9.118	1.9304	35.74	0.03691
14DEC90	348	5000	cfs	768	270.133	607.400	165.733	347	57.3219	275.524	62.3685	412	48.3382	266.010	48.2488	541.53	0.74686
17DEC90	351	11,000	cfs	264	142.158	11.468	1.773	30	2.9308	29.818	5.3087	27	2.3220	9.175	2.0171	38.99	0.03685
28DEC90	362	5000	cfs	72	311.150	64.195	6.230	128	5.8118	155.149	14.4451	121	4.7849	35.170	5.1775	190.32	0.29572
31DEC90	365	Discharge	"C"	264	412.469	363.477	155.852	123	34.0617	131.249	46.9794	122	33.6629	144.303	48.0445	275.55	0.39201
11JAN91	376	5000	cfs	72	142.661	13.082	2.186	33	2.0234	7.674	1.5478	30	5.2698	79.797	14.2085	87.47	0.03698
1-JAN91	379	"Normal"	Winter	264	330.607	614.337	165.569	125	56.4057	269.181	60.4263	135	51.5804	231.973	45.7913	501.15	0.31421
25JAN91	390	5000	cfs	72	141.713	11.553	2.040	31	2.1101	6.938	1.7464	29	5.0726	80.137	14.6191	87.07	0.03673
28JAN91	393	Discharge	"B"	264	295.083	295.969	129.724	124	27.3378	114.287	39.6191	118	28.7449	111.994	40.2210	226.28	0.28045
08FEB91	404	5000	cfs	72	141.696	14.583	2.098	32	2.0999	10.732	2.2121	26	2.5551	8.410	2.0598	19.14	0.03673
11FEB91	407	non-research		1608	293.205	708.916	172.065	735	52.1166	552.295	64.9160	851	45.0125	397.741	53.1937	950.04	1.69731
19APR91	474	5000	cfs	72	142.361	11.638	1.614	31	2.0050	6.201	1.5866	26	2.1216	6.994	1.8579	13.20	0.03690
22APR91	477	"Normal"	Spring	264	254.665	462.756	126.457	139	32.4930	241.657	34.5173	117	38.6849	167.835	39.6070	409.49	0.24203
03MAY91	488	5000	cfs	264	141.273	61.250	6.665	31	3.0683	10.845	2.7496	31	4.6440	46.525	8.3799	57.37	0.03662
06MAY91	491	Discharge	D	264	423.745	676.182	279.448	141	53.2846	132.580	46.8251	94	79.3825	212.462	90.4419	345.04	0.40273
17MAY91	502	5000	cfs	72	146.343	298.461	33.802	25	13.8708	275.496	54.6473	23	2.6396	29.478	5.9499	304.97	0.03793
20MAY91	505	15,000	cfs	264	424.987	296.394	17.494	121	3.9770	18.491	3.8466	115	5.8163	72.435	13.2258	120.72	0.40391
31MAY91	516	5000	cfs	72	139.930	95.740	12.587	33	5.4412	48.280	10.9079	30	58.6809	782.540	81.6738	1050.53	0.92627
03JUN91	519	"Normal"	Summer	600	426.536	788.374	245.509	319	50.3852	267.992	51.3788	274	1.6019	6.060	1.1136	88.69	0.03718
28JUN91	544	5000	cfs	72	143.450	87.188	9.891	30	4.1230	82.629	14.8498	28	48.8252	143.567	46.0241	368.69	0.49471
01JUL91	547	Discharge	"G"	264	520.527	669.697	249.164	112	59.9420	225.120	82.9133	139	2.6003	11.412	2.7052	87.36	0.03729
12JUL91	558	5000	cfs	72	143.867	84.300	9.662	31	4.7107	75.946	13.3722	29	54.0393	157.527	47.5302	275.52	0.46306
15JUL91	561	Discharge	"F"	264	487.226	674.851	234.840	134	48.6093	117.997	46.7882	122	1.5564	3.823	1.0708	54.93	0.03712
26JUL91	572	5000	cfs	72	143.205	53.406	6.038	27	3.4222	51.112	9.5825	28					

Table 2a. Summary statistics for each test flow by flow period

Glen Canyon Dam Research Flows
Daily Statistical Analysis

flow period begin date	julian date	research flow description	mean daily discharge (cms)	std. dev. daily discharge (cms)	mean daily max upramps (cms/hr)	std. dev. daily max upramps (cms/hr)	mean daily max downramps (cms/hr)	std. dev. daily max downramps (cms/hr)	mean daily range of discharge (cms)	std. dev. daily range of discharge
01JUN90	152	5000 cfs	141.919	0.789	1.685	0.926	1.495	0.908	1.495	1.385
05JUN90	156	non-research	162.879	95.610	169.239	74.128	162.581	47.695	538.012	168.491
29JUN90	180	5000 cfs	162.828	41.018	21.655	37.894	3.105	1.806	3.157	2.455
02JUL90	183	Discharge "G"	403.009	80.599	204.680	2.103	108.022	12.257	527.753	166.293
13JUL90	194	5000 cfs	164.109	43.431	24.119	42.309	3.474	1.548	2.485	1.886
16JUL90	197	Discharge "F"	416.190	85.128	108.941	3.841	107.059	12.942	531.689	167.609
27JUL90	208	5000 cfs	136.110	12.774	6.938	1.140	11.546	9.770	6.513	4.728
30JUL90	211	non-research	427.275	93.627	164.631	57.985	183.969	55.540	581.005	161.442
14SEP90	257	5000 cfs	128.002	28.229	4.550	4.003	17.627	22.626	5.302	3.813
17SEP90	260	Discharge "E"	392.267	80.111	196.161	46.454	207.412	5.388	611.994	192.826
28SEP90	271	5000 cfs	128.357	27.334	4.568	1.308	15.765	4.326	3.809	2.979
01OCT90	274	Discharge "A"	231.665	28.214	98.871	13.605	103.936	24.443	267.711	84.387
12OCT90	285	5000 cfs	155.625	48.296	35.198	36.879	21.559	28.785	19.029	28.139
15OCT90	288	8000 cfs	220.235	22.856	7.131	3.049	12.247	20.066	9.330	4.838
26OCT90	299	5000 cfs	141.687	0.624	4.049	0.441	2.789	1.264	3.228	2.182
29OCT90	302	"Normal" Fall	194.155	58.836	142.960	68.103	101.295	33.963	285.055	143.363
09NOV90	313	5000 cfs	141.293	2.359	12.686	12.356	5.508	2.874	4.559	4.933
12NOV90	316	non-research	265.522	61.740	192.373	56.732	153.872	42.075	435.896	131.929
14DEC90	348	5000 cfs	141.247	1.928	12.743	15.028	5.352	2.861	6.116	5.442
17DEC90	351	11,000 cfs	310.525	2.579	29.753	42.761	14.284	8.599	22.439	14.646
28DEC90	362	5000 cfs	143.064	2.149	4.014	1.306	54.888	89.784	22.439	2.933
31DEC90	365	Discharge "C"	397.844	53.229	125.818	5.408	121.504	37.542	322.911	101.769
11JAN91	376	5000 cfs	141.470	2.558	5.125	2.336	23.220	37.720	6.152	4.862
14JAN91	379	"Normal" Winter	322.168	65.682	188.877	33.796	147.945	37.667	420.819	138.351
25JAN91	390	5000 cfs	142.107	0.888	5.196	2.037	32.111	41.593	6.555	4.648
28JAN91	393	Discharge "B"	282.822	44.588	103.854	5.289	94.829	28.983	265.720	83.712
08FEB91	404	5000 cfs	141.791	0.465	5.777	3.984	6.673	1.900	6.931	6.043
11FEB91	407	non-research	291.100	75.813	194.998	92.086	166.502	71.548	413.940	133.096
19APR91	474	5000 cfs	143.993	3.454	5.048	1.476	4.663	2.800	4.856	3.722
22APR91	477	"Normal" Spring	245.508	77.300	113.433	55.506	109.712	46.832	267.865	131.821
03MAY91	488	5000 cfs	129.163	25.630	7.230	3.889	18.222	19.384	9.883	9.647
06MAY91	491	Discharge D	401.233	81.675	107.229	19.496	204.616	3.375	609.741	192.072
17MAY91	502	5000 cfs	213.765	142.794	76.626	132.692	12.157	15.125	11.051	13.228
20MAY91	505	15,000 cfs	402.846	80.361	11.437	4.517	31.767	74.137	13.960	6.466
31MAY91	516	5000 cfs	143.021	7.015	17.061	20.965	28.761	37.831	27.198	45.850
03JUN91	519	"Normal" Summer	416.147	105.534	162.933	52.519	236.231	127.438	561.282	171.015
28JUN91	544	5000 cfs	163.187	41.799	23.128	39.679	4.040	1.898	2.839	1.993
01JUL91	547	Discharge "G"	491.192	106.654	209.536	8.673	112.440	20.545	534.000	168.360
12JUL91	558	5000 cfs	162.887	40.281	23.935	34.708	8.873	3.755	6.654	5.013
15JUL91	561	Discharge "F"	459.846	99.424	109.211	4.403	116.501	20.342	529.415	166.879
26JUL91	572	5000 cfs	155.123	25.239	15.454	23.808	3.313	0.441	3.632	2.448

Table 2b. Daily statistical analysis of test flows.

Sediment Transport Capacity

The sediment transport capacity of each test flow was calculated in order to compare potential sediment movement in the main channel with measures of changes in sediment stored in channel margin environments. A simple computer program was used that calculates sediment discharge using water discharge treated with sediment transport functions (Smilie et al, this report). The equation used was:

$$Q_s = aQ_w^b \quad (1)$$

where Q_s is sediment discharge, Q_w is water discharge, a is $0.46047(10)^{-10}$, and b is 3.2228. The transport functions a and b were derived from measured values at the USGS gaging stations at Grand Canyon above the Little Colorado River, Grand Canyon Gage at Phantom Ranch, and Grand Canyon Gage at Diamond Creek. Inputs for Q_w were taken from mean daily values at the Lees Ferry Gage, for each test flow.

The resulting sediment transport capacity values range from a low of about 2,000 tons for the 11 day 8,000 cfs constant flow during the period October 15-25, 1990, to a high of over 135,000 tons for the 46 day "Normal Flow" test that lasted February 11-April 17, 1991. Daily sediment transport values range from a low 174 tons per day for the 8,000 cfs constant flow to a high of 4021 tons per day for the "G" flow in July 1991. The results of sediment transport modeling are presented in Figure 3. This exercise was intended to provide an indication of the stream energy associated with each of the test flows, for comparative purposes only. It is not intended that the calculations of sediment transport capacity represent transport through the system. The results of this exercise are presented in table 3, and figure 1.

Table 3. Calculated sediment transport capacity for the test flows.

TEST FLOW	TEST FLOW NAME	DURATION IN DAYS	TOTAL TONS	TONS/DAY
1	NORMAL	24	53731	2239
2	G	11	32913	2992
3	F	11	30785	2799
4	NORMAL	46	135246	2940
5	E	11	32038	2913
6	A	11	3692	336
7	8K	11	1921	175
8	FALL	11	3058	278
9	NORMAL	33	18097	548
10	11K	11	5360	487
11	C	11	16804	1528
12	WINTER	11	10811	983
13	B	11	6014	547
14	NORMAL	67	50872	759
15	SPRING	11	4494	409
16	D	11	33900	3082
17	15K	11	14540	1322
18	SUMMER	26	60669	2333
19	G	11	44239	4022
20	F	11	34005	3091

SEDIMENT TRANSPORT CAPACITY

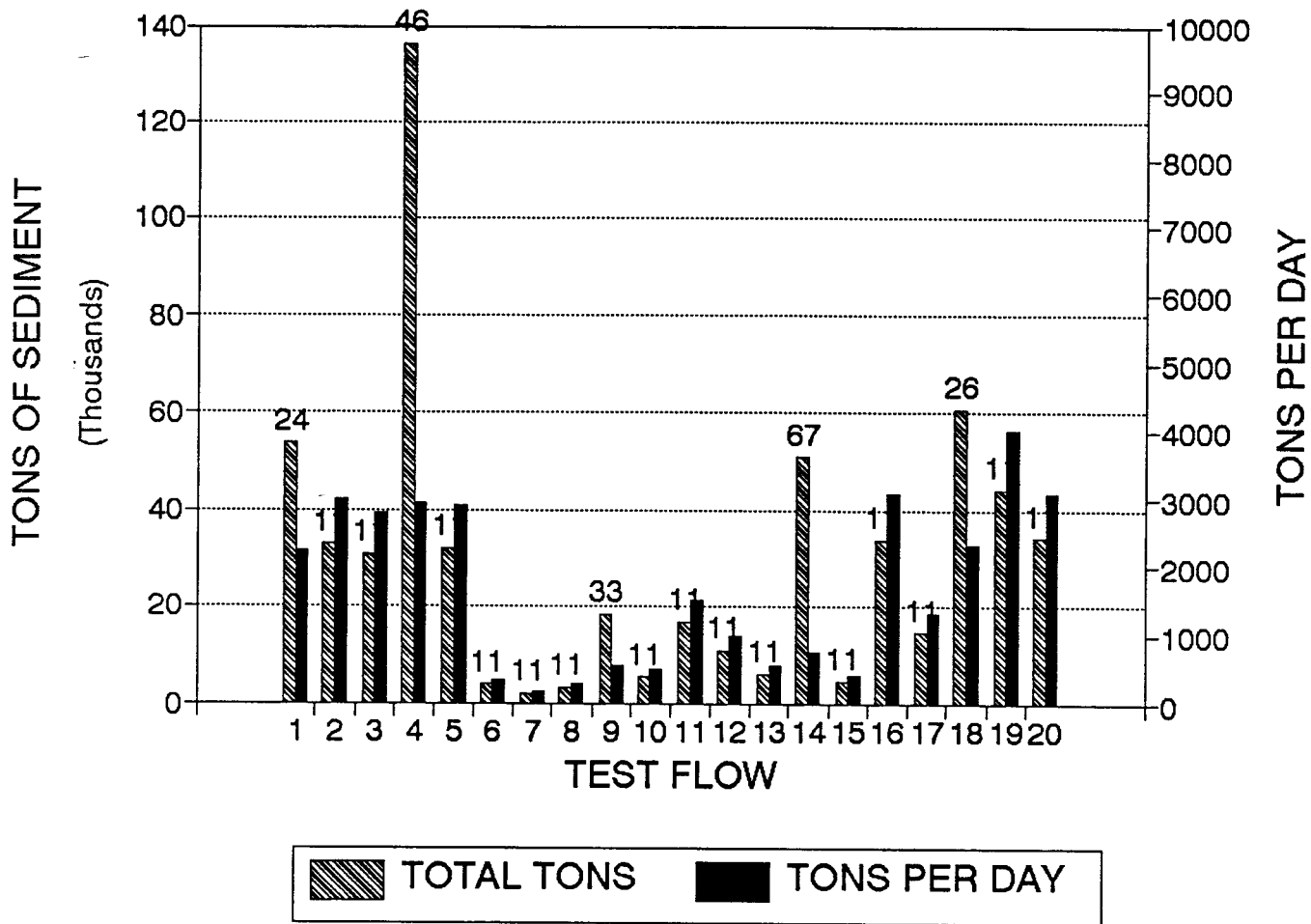


Figure 1. Histogram of calculated sediment transport capacity in tons per test flow, and tons per day. Numbers above blocks indicate duration of test in days.

**THE INFLUENCE OF VARIABLE DISCHARGE REGIMES ON
COLORADO RIVER SAND BARS BELOW GLEN CANYON DAM:
DRAFT FINAL ADMINISTRATIVE REPORT**

**Stanley S. Beus, Charles C. Avery,
and Kenneth A. Walters**

Northern Arizona University

NPS Cooperative Agreement Number: CA 8006-8-0002

Government Technical representative: Dr. Peter G. Rowlands

Effective Date of Cooperative Agreement: 27 August, 1990

Cooperative Agreement Expiration Date: 1 July, 1992

**Sponsored by: The U.S. Department of Interior National Park Service Cooperative Parks Study Unit
Northern Arizona University Flagstaff, AZ 86011**

ADMINISTRATIVE REPORT

Project Summary

This project involved three subcontractors and many personnel and was authorized by five purchase orders to NAU over the course of two years (Summary of Expenses). Of the allocated \$857,755, approximately 66% went to pay wages and salaries while overhead expenses claimed the next highest proportion (Account Summary). Management costs and travel were the least expensive categories, while supplies and materials consumed about 12% of the budget. The summary sheet indicates the partitioning of these funds and it is supported by both a budget and an expense break-out. Detailed worksheets are also on file in addition to the formal accounting documents retained by the university.

Because of the tremendous irregularity in the actual work assignments of most of the staff personnel, as well as in the travel costs associated with the surveys, it was necessary to maintain a management system separate from the traditional system used for most federal contracts. This proved invaluable as the work progressed towards completion and it was found necessary to request a modification to the original grant in order to finish the basic data reduction (Budget Summary). Between 65,000 and 75,000 work hours were dedicated to this effort, a figure that includes about 7,000 volunteer hours. Only one serious work-related accident occurred during a river survey in 1991.

The total productivity of the persons associated with this project was remarkable and the principal investigators are deeply appreciative of the dedication expressed. The formal acknowledgements in this report are but slight tribute: we trust satisfaction for a job well-done is more enduring.

GCES Beach Erosion Study

Administrative Report

Summary of Expenses

Inception to End

	Encumbered**	Paid	Total Expenses
Salaries			
Investigators	\$3,475.93	\$36,814.40	\$40,290.33
Sub-Contractors	\$19,259.61	\$172,905.38	\$192,164.99
NPS/Field Crews	\$1,062.14	\$333,719.72	\$334,781.86
Travel			
Investigators	\$0.00	\$2,733.11	\$2,733.11
Sub-Contractors	\$0.00	\$11,089.20	\$11,089.20
NPS/Field Crews	\$0.00	\$29,335.76	\$29,335.76
Equipment			
Investigators	\$0.00	\$15,782.39	\$15,782.39
NPS/Field Crews	\$0.00	\$38,827.36	\$38,827.36
Supplies			
NPS/Field Crews †	\$0.00	\$58,817.94	\$58,817.94
Lab Analysis			\$0.00
Management			
	\$1,290.84	\$23,660.96	\$24,951.80
Total	\$25,088.52	\$723,686.22	\$748,774.74

Money Awarded (less indirect costs)	Original	Fiscal Year 1	Fiscal Year 2	Fiscal Year 3	Total Awarded
Modification 3a					\$167,104.00
Modification 4					\$380,311.00
					\$108,761.00
					\$38,500.00
					\$54,099.00
					\$748,775.00

**as of 1 July 1992

† includes \$10,000 for photogrammetry

Amount Under Budget	\$0.26
---------------------	---------------

GCES Beach Erosion Study

Administrative Report

Account Summary

Inception to End

	Budgeted	Expensed	Difference	Difference as % of Total Budgeted *
Salaries				
Investigators	\$61,147.00	\$40,290.33	\$20,856.67	-2.43%
Sub-Contractors	\$184,918.00	\$192,164.99	(\$7,246.99)	0.84%
NPS/Field Crews	\$332,111.00	\$334,781.86	(\$2,670.86)	0.31%
Travel				
Investigators	\$7,840.00	\$2,733.11	\$5,106.89	-0.60%
Sub-Contractors	\$18,958.00	\$11,089.20	\$7,868.80	-0.92%
NPS/Field Crews	\$28,117.00	\$29,335.76	(\$1,218.76)	0.14%
Equipment				
Investigators	\$15,000.00	\$15,782.39	(\$782.39)	0.09%
NPS/Field Crews	\$19,135.00	\$38,827.36	(\$19,692.36)	2.30%
Supplies				
NPS/Field Crews	\$58,397.00	\$58,817.94	(\$420.94)	0.05%
Lab Analysis				
	\$3,410.00	\$0.00	\$3,410.00	-0.40%
Management				
	\$19,742.00	\$24,951.80	(\$5,209.80)	0.61%
NAU Indirect Costs				
	\$108,980.00	\$108,980.00	\$0.00	0.00%
Total	\$857,755.00	\$857,754.74	\$0.26	

*negative = under budget

Indirect Costs	NAU	\$108,980.00
	U of A	\$12,997.00
	Middlebury	\$3,475.00
	Utah State	\$6,677.00
	Total	\$125,452.00
Indirect Costs =	15%	of total budget

Salaries	Investigators	\$41,290.33
	Sub-Contractors	\$192,164.99
	NPS/Field Crews	\$334,781.86
	Management	\$22,527.00
	Total	\$589,764.18
	Work-hours @ \$8.60/hr =	68,577

GCES Beach Erosion Study

Administrative Report Budget Summary Inception to End

	Original	Mod 3a	Mod 4	Total Budget
Salaries				
Investigators	\$61,147.00			\$61,147.00
Sub-Contractors	\$184,918.00			\$184,918.00
NPS/Field Crews	\$262,612.00	\$15,400.00	\$54,099.00	\$332,111.00
Travel				
Investigators	\$7,840.00			\$7,840.00
Sub-Contractors	\$18,958.00			\$18,958.00
NPS/Field Crews	\$5,017.00	\$23,100.00		\$28,117.00
Equipment				
Investigators	\$15,000.00			\$15,000.00
NPS/Field Crews	\$19,135.00			\$19,135.00
Supplies				
NPS/Field Crews	\$58,397.00			\$58,397.00
Lab Analysis				
Management	\$3,410.00			\$3,410.00
Management	\$19,742.00			\$19,742.00
NAU Indirect Costs				
NAU Indirect Costs	\$90,460.00	\$7,700.00	\$10,820.00	\$108,980.00
Budget Totals	\$746,636.00	\$46,200.00	\$64,919.00	\$857,755.00